New Palladium Catalyzed Carbonylative Approaches to Heterocycle and Acid Chloride Synthesis

Gerardo Martin Torres

A thesis submitted to McGill University in partial fulfillment of the requirements of the degree of Doctor of Philosophy

Department of Chemistry

McGill University

Montreal, Quebec, Canada

H3A 0B8

August 2019

Abstract

Metal catalyzed carbonylation reactions are heavily exploited in synthetic chemistry. These include not only high volume industrial reactions (e.g. catalytic acetic acid synthesis or hydroformylations), but also a plethora of catalytic small molecule syntheses. These latter often exploit palladium catalysts. Nevertheless, there remain a number of important forums where carbonylations could play a useful role in providing more efficient access to products. This thesis will describe our efforts to develop such reactions. In these, palladium catalyzed carbonylations are exploited to build-up reactive products such as acid chlorides or carbonyl-containing 1,3-dipoles. Coupling this with the ability of the products undergo other spontaneous reactions can offer new routes to build up products from combinations of available reagents or be used to expand the scope of carbonylation chemistry.

In chapter 2, we describe how the palladium catalyzed carbonylation of aryl iodides in the presence of imines can allow the overall generation of a 1,3-dipole: a Münchnone. A variety of mechanistic studies were performed on this reaction and show that it proceeds via a tandem catalytic process: the first involving the $Pd(P^tBu_3)_2$ catalyzed coupling of aryl iodides with carbon monoxide and a chloride salt to form an acid chloride, which can react with an imine and then undergo a second spontaneous $Pd(P^tBu_3)_2$ catalyzed cyclocarbonylation to afford the Münchnone product. As Münchnones are reactive towards 1,3-dipolar cycloaddition with alkynes to form pyrroles, coupling their formation with alkyne cycloaddition can be used to develop a novel method to assemble broad families of pyrroles from aryl iodides, imines, carbon monoxide and alkynes.

In Chapter 3 we develop a strategy to apply our palladium catalyzed carbonylative synthesis of Münchnones to construct more complex pyrrole structures. In this, the combination of alkyne-

tethered imines, aryl iodides, and carbon monoxide generates a Münchnone that can undergo intramolecular 1,3-dipolar cycloaddition to generate polycyclic pyrroles. This approach allows the modular and regioselective synthesis of complex pyrrole structures, and is compatible with less activated alkynes than those typically used in Münchnone 1,3-dipolar cycloadditions. In addition, we show that this reaction can be used in tandem with the palladium catalyzed Sonogashira functionalization of terminal alkynes with aryl iodides. To create a modular route to fused-ring pyrroles from three diversifiable reagents.

In Chapter 4 we describe our efforts to take advantage of the ketene-like reactivity of Münchnones to generate β-lactams. This transformation occurs via the palladium catalyzed formation of Münchnones from imines, aryl iodides, and carbon monoxide, followed by a cycloaddition to a second equivalent of imine to afford amide substituted β-lactam products. Since this transformation required higher temperatures, we were also able to utilize aryl bromides as substrates. The latter are more widely available and inexpensive than aryl iodides. Moreover, applying the conditions described in Chapter 2 for the synthesis of Münchnones allowed us to construct more diversely substituted β-lactams by reacting the Münchnone with a different imine. Alternatively, the palladium catalyzed carbonylation of imine-tethered aryl iodides leads to the formation of isoindolinones with an exocyclic ketene group. The latter can react with an imine to produce novel spirocyclic β-lactams.

The palladium catalyzed synthesis of acid chlorides is a key component to the synthetic approaches to heterocycles presented in Chapters 2-4. However, the specific features that enable the catalyst to mediate the challenging reductive elimination of acid chlorides also inhibit the reverse oxidative addition step. These reactions are therefore limited to the use of relatively activated aryl iodide substrates. In Chapter 5 we address these limitations by approaching this

palladium catalyzed reaction from a different perspective. In this, visible light is used to drive both key steps in palladium catalysis: oxidative addition and reductive elimination. Analogous to other reports, we show that visible light excitation of a Pd(0)-carbonyl complex can drive oxidative addition of a wide variety of aryl and alkyl halides. In addition, we find that visible light can induce a new reaction step the reductive elimination of acid chlorides. The latter occurs via the excitation in this case of the palladium-acyl intermediate. Together, this offers a platform to perform palladium catalyzed carbonylations at ambient temperature, with a wide array of organic halide substrates that have proven to be challenging in traditional palladium catalysis, and form from these acid chloride electrophiles that can allow the use of nucleophiles that are typically incompatible with carbonylations. These results suggest that simple visible light excitation on palladium may offer a general approach to perform carbonylative coupling reactions.

Résumé

Les réactions de carbonylation catalysée métaux de transition sont parmi les plateformes synthétiques les plus exploitées en chimie. Elles incluent non seulement des réactions industrielles à grande échelle (e.g. synthèse catalytique de l'acide acétique ou d'hydroformylation), mais aussi un vaste éventail de synthèses catalytiques de petites molécules. Ces dernières utilisent parfois la catalyse palladium. Néanmoins, il reste d'important domaines les réactions de carbonylation pourraient jouer un rôle important, fournissant un accès efficace à des produits de synthèse. Cette thèse décrira nos efforts pour développer ce type de réactions. Dans celles-ci, les carbonylations catalysées palladium sont exploitées pour créer des composés réactifs tels que des chlorures d'acyles ou des dipôles-1,3 contenant une fonction carbonyle. Ceci peut offrir de nouvelles routes synthétiques pour la création de produits faits à partir de combinaisons de réactifs disponibles commercialement, ou être utilisé pour développer l'étendue de la chimie de la carbonylation.

Dans le deuxième chapitre, nous décrivons comment la carbonylation d'iodures d'aryle catalysée palladium en présence d'imines peut permettre la génération de dipôles-1,3 : des Münchnones. Une variété d'études mécanistiques ont été effectuées sur cette réaction, et montrent que la réaction fonctionne via un procédé catalytique tandem : le premier implique le couplage, catalysé par le $Pd(P^tBu_3)_2$, d'iodures d'aryle avec le monoxyde de carbone et d'un sel de chlorure pour former un chlorure d'acyle, qui peut réagir avec une imine et effectuer une deuxième carbonylation spontanée à l'aide du même catalyseur, $Pd(P^tBu_3)_2$, pour obtenir la Münchnone comme produit final. Comme les Münchnones sont des précurseurs de réaction dipolaire-1,3 en présence d'alcynes pour former des pyrroles, combiner leur formation avec la cycloaddition d'alcynes peut être utilisé pour développer une nouvelle méthode afin d'assembler une vaste famille de pyrroles à partir d'iodures d'aryle, d'imines, de monoxyde de carbone et d'alcynes.

Dans le troisième chapitre, nous développons une stratégie pour diversifier notre synthèse carbonylative de Münchnones catalysée palladium pour construire des pyrroles plus complexes. Dans cette stratégie, la combinaison d'imines possédant un alcyne, d'iodures d'aryle, et de monoxyde de carbone génère une Münchnone qui réagit de façon intramoléculaire par cycloaddition dipolaire-1,3 pour former des pyrroles polycycliques. Cette approche permet la synthèse modulaire et régiosélective de structures pyrrole complexes, et est compatible avec des alcynes moins activés que ceux typiquement utilisés dans les cycloadditions dipolaires-1,3 des Münchnones. De plus, nous montrons que cette réaction peut être utilisée en tandem avec la fonctionnalisation d'alcynes terminaux avec des iodures d'aryle par la réaction de Sonogashira catalysée au palladium. Cette approche fournit une route réactionnelle modulaire pour générer des pyrroles à cycles fusionnés avec une variété de substituants différents en une seule opération.

Dans le quatrième chapitre, nous décrivons nos efforts pour tirer avantage de la réactivité similaire au cétène des Münchnones pour générer des β-lactames. Cette transformation se produit via la formation de Münchnones en utilisant la catalyse au palladium à partir d'imines, d'iodures d'aryle, et de monoxyde de carbone. Elle est suivie par une cycloaddition d'un second équivalent d'imine pour fournir des β-lactames substituées avec un amide. Puisque cette transformation nécessite des températures élevées, nous avons également été capable d'utiliser des bromures d'aryle. Ceux-ci sont plus disponibles commercialement et moins cher que les iodures d'aryle. De plus, en appliquant les conditions décrites dans le chapitre 2 pour la synthèse de Münchnones, cela nous a permis de construire des β-lactames plus diversifiées en réagissant la Münchnone avec une imine différente. Alternativement, la carbonylation d'iodures d'aryle possédant une imine catalysée palladium mène à la formation d'isoindolinones avec un groupement cétène exocyclique.

Ce type de molécule peut réagir avec une imine pour produire de nouvelles β-lactames spirocycliques.

La synthèse de chlorure d'acyle catalysée palladium est la clé de l'approche synthétique d'hétérocycles présentée dans les chapitres 2 à 4. Cependant, les caractéristiques spécifiques qui permettent au catalyseur d'intervenir sur l'élimination réductrice difficile de chlorures d'acyle limite aussi la réaction inverse, l'addition oxydante. Ces réactions sont donc limitées à des iodures d'aryle relativement activés et exclus les halogénures d'alkyle. Dans le cinquième chapitre, nous adressons ces limitations en approchant cette réaction catalysée au palladium avec une perspective différente. Dans ce cas, la lumière visible est utilisée pour favoriser les étapes clés de la catalyse palladium : l'addition oxydante et l'élimination réductrice. En analogie aux autres rapports, nous montrons que l'excitation d'un complexe de Pd(0) par la lumière peut favoriser l'addition oxydante d'une grande variété d'halogénures d'aryle et d'alkyle. De plus, nous avons aussi trouvé que la lumière visible peut induire l'élimination réductrice de chlorures d'acyle en passant par un état excité de l'intermédiaire palladium-acyle. Cette méthodologie offre une plateforme pour effectuer des carbonylations catalysées palladium à température ambiante, avec un large éventail de substrats organiques halogénés qui sont difficiles à utiliser dans les réactions de catalyse palladium traditionnelles, et permet à partir de ces chlorures d'acyle électrophiles l'utilisation de nucléophiles qui sont typiquement incompatible avec les réactions de carbonylation. Ces résultats suggèrent que l'excitation du palladium par la lumière visible peut offrir une approche générale pour exécuter des réactions de couplage carbonylatives.

Acknowledgements

I would like to thank my supervisor, Professor Bruce Arndtsen, for his support during the course of my degree. I appreciate our insightful conversations that helped me stay on track and find creative ways to produce high quality research.

I would also like to thank past and present members of our research group. Firstly, I want to acknowledge Dr. Jeffrey Quesnel for providing useful advice and guidance during the first year of my PhD. Additionally, I want to mention past members of the Arndtsen group who I interacted with throughout this degree: Dr. Fabio Lorenzini, Dr. Laure Kayser, Dr. Boran Xu, Dr. Jevgenijs Tjutrins, Victoria Jackiewicz, Maximiliano De La Higuera Macias, Anthony Lau, Nigel Braun, Neda Firoozi, Alexander Fabrikant, and Oliver Williams. Likewise, I want to thank the current members of the lab for their friendship and support: Garrison Kinney, Huseyin Erguven, Yi Liu, Pierre-Louis Lagueux-Tremblay, Taleah Levesque, Sébastien Roy, Anthony Labelle, Angela Kaiser, and Jose Zgheib.

I want to thank members of the supporting staff at the Department of Chemistry. Firstly, I want to thank Dr. Robin Stein, the NMR facility manager, for being so supportive and proactive in helping setup complex NMR experiments. I would also like to acknowledge Dr. Nadim Saadeh and Dr. Alexander Wahba at the mass spectrometry facility for providing useful tips for challenging mass characterizations. I also want to extend this acknowledgement to the rest of the technical staff: Chantal Marotte, Rick Rossi, Weihua Wang, Jean-Philippe Guay, Mario Perone, Stephanie Trempe, Jean-Marc Gauthier, Sandra Aerssen, Linda Del Paggio, Jennifer Marleau, and Chelsea-Briand-Pitts.

I want to thank my mother for always encouraging me to pursue my life goals and strive for excellence. I also want to thank my sister, grandparents, aunts, uncles, and cousins for always believing in me. Without my family, none of this would have been possible.

Finally, I am very grateful for the financial support provided by the CONACyT (Mexican National Council of Science and Technology) throughout the duration of my degree.

Table of Contents

List of Schemes

List of Figures

List of Tables

List of Abbreviations

AcOEt	Ethyl Acetate
AcOH	Acetic Acid
Ac_2O	Acetic anhydride
Ad	Adamantyl
APCI	Atmospheric pressure chemical ionization
Ar	Aryl
ATR	Attenuated total reflectance
^{n}Bu	*n*-butyl
^{t}Bu	*tert*-butyl
BINAP	2,2′-Bis(diphenylphosphino)-1,1′-binaphthyl
BINOL	[1,1′-binaphthalene]-2,2′-diol
Bpy/Bipy	2,2,-bipyridine
Cat.	Catalyst
cataCXium A	di(1-adamantyl)-n-butylphosphine
COgen	9-methyl-9H-fluorene-9-carbonyl chloride
Collidine	2,4,6-trimethylpyridine

Cy	Cyclohexyl
DABCO	1,4-Diazabicyclo[2.2.2]octane
dba	Dibenzylideneacetone
DBU	1,8-Diazabicyclo[5.4.0]undec-7-ene
DCC	*N*,*N*'-dicyclohexylcarbodiimide
DCM	Dichloromethane
DCE	1,2-Dichloroethane
DIPEA	*N*,*N*-Diisopropylethylamine
DMA	Dimethylacetamide
DMAD	Dimethyl acetylenedicarboxylate
DMAP	4-dimethylaminopyridine
DMF	dimethylformamide
DMI	1,3-Dimethyl-2-imidazolidinone
DMSO	dimethylsulfoxide
dcpp	1,3-Bis(dicyclohexylphosphino)propane
dF(CF_3)ppy	2-(2,4-difluorophenyl)-5-(trifluoromethyl)pyridine
dippp	1,3-bis(diisopropylphosphino)propane
DPE-Phos	Bis[(2-diphenylphosphino)phenyl]ether

dppe	1,2-bis(diphenylphosphino)ethane
dppf	1,1′-ferrocenediyl-bis(diphenylphosphine)
dppp	1,3-bis(diphenylphosphino)propane
dtbbpy	4,4'-Di-tert-butyl-2,2'-bipyridine
Equiv.	Equivalent
ESI	Electrospray ionization
Et	Ethyl
FG	Functional group
Hantzsch's Ester	Diethyl 1,4-dihydro-2,6-dimethyl-3,5-pyridinedicarboxylate
HMPA	Hexamethylphosphoramide
HOTf	Triflic acid
IMes	1,3-Dimesitylimidazol-2-ylidene
^{i}Pr	Isopropyl
JosiPhos (Cy)	1-(Dicyclohexylphosphino)-2-[(1S)-1-(dicyclohexylphosphino)ethyl]ferrocene
L	Ligand
L_n	Unspecified number of ligands
mg	Milligram

mmol	millimole
mL	Milliliter
µL	Microliter
NMP	*N*-Methyl-2-pyrrolidone
NMR	Nuclear magnetic resonance
N. R.	No reaction
NuH	Nucleophile
OAc	Acetate
OTf	Triflate (trifluoromethanesulfonate)
Ph	Phenyl
PhH	Benzene
PhMe	Toluene
PMB	*p*-methoxybenzyl
PMP	*p*-methoxyphenyl
ppy	2-Phenylpyridine
p-Tol	*para*-Tolyl
PTSA	*para*-toluenesulfonic acid
SET	Single electron transfer

rt	Room temperature
TEMPO	(2,2,6,6-Tetramethylpiperidin-1-yl)oxyl
TFA	Trifluoroacetate
THF	Tetrahydrofuran
TMEDA	Tetramethylethylenediamine
TMU	Tetramethylurea
t	Ton
TON	Turnover number
Ts	*p*-toluenesulfonyl
Xantphos	4,5-bis(diphenylphosphino)-9,9-dimethylxanthene

Contributions and Co-Authors

This thesis consists of six chapters. Chapter 1 is an introduction to the work described in this thesis. Chapters 2-4 are published manuscripts, while Chapter 5 will be submitted for publication. Chapter 6 provides conclusions and suggestions for future work. The work presented in this thesis was carried out as part of my doctoral dissertation in chemistry under the supervision of Dr. Bruce Arndtsen. Thus, he is the corresponding author on all the manuscripts and assisted in editing this thesis. All the experiments reported in these manuscripts were performed by myself, except where noted below:

Chapter 2: "From Aryl Iodides to 1,3-Dipoles: Design and Mechanism of a Palladium Catalyzed Multicomponent Synthesis of Pyrroles." *J. Am. Chem. Soc.* **2016**, 138, 7315. Diane Bijou and Jeffrey Quesnel performed preliminary reaction and catalyst development.

Chapter 3: "Palladium Catalyzed, Multicomponent Synthesis of Fused-Ring Pyrroles from Aryl Iodides, Carbon Monoxide, and Alkyne-Tethered Imines." *J. Org. Chem.* **2016**, 81, 11145. Neda Firoozi performed preliminary catalyst development, synthesized the products in Scheme 3.5, developed the catalyst system for the tandem Sonogashira coupling of terminal alkyne tethered imines and aryl iodides, and synthesized the products in Scheme 3.6.

Chapter 4: "Palladium-Catalyzed, Multicomponent Approach to β-Lactams via Aryl Halide Carbonylation." *J. Org. Chem*. **2016**, 81, 12106. Veeranna Yempally and Jeffrey Quesnel performed preliminary reaction and catalyst development. Oliver Williams helped develop the synthesis of β-lactams with two different imines and synthesized some of the products in Table 4.4. Maximiliano De La Higuera Macias developed the reaction and catalyst system for the

synthesis of spirocyclic β-lactams, synthesized the products in Table 4.5, and obtained the crystal structure for product **4.9g**. Professor Ashfaq Bengali assisted in writing the manuscript.

Chapter 5: "A Dual Light Driven Approach to Palladium Catalysis and Carbonylation Reactions." Is a manuscript in preparation. Yi Liu and myself are listed as first authors, and contributed equally to this work.

Chapter 1. Introduction: Palladium Catalyzed Carbonylative Coupling Reactions

1.1. Perspective

The ability of transition metal catalysts to mediate the selective formation of new covalent bonds has become one of the fundamental driving forces in modern synthetic organic chemistry. In recent years, many novel catalytic approaches have been devised to activate classically inert bonds, manipulate functional groups, couple building blocks, and form products with high selectivity. This development has had an impact in diverse areas such as medicinal chemistry, materials science, agrochemical synthesis, and fine chemical production. Among these new technological achievements, metal catalyzed cross-coupling reactions have proven particularly useful. These reactions employ a metal catalyst to couple an organic electrophile (typically an aryl or vinyl halide) with a nucleophile to form a carbon-carbon or carbon-heteroatom bond.[1-5] Some examples of these reactions include Mizoroki-Heck, Suzuki-Miyaura, Migita-Kosugi-Stille, Kumada, Negishi, Hiyama-Denmark couplings, Buchwald-Hartwig aminations, and related approaches to C-O, C-S, and other bonds (Scheme 1.1a). A common element in these coupling reactions is the use of palladium, or sometimes nickel, as the catalyst. Through rational catalyst design, many reactions have been tuned to proceed with high efficiency and under mild conditions. A testament of this versatility was the 2010 Nobel Prize in Chemistry awarded to Richard F. Heck, Ei-ichi Negishi, and Akira Suzuki for the development of several of these palladium-catalyzed reactions.[6]

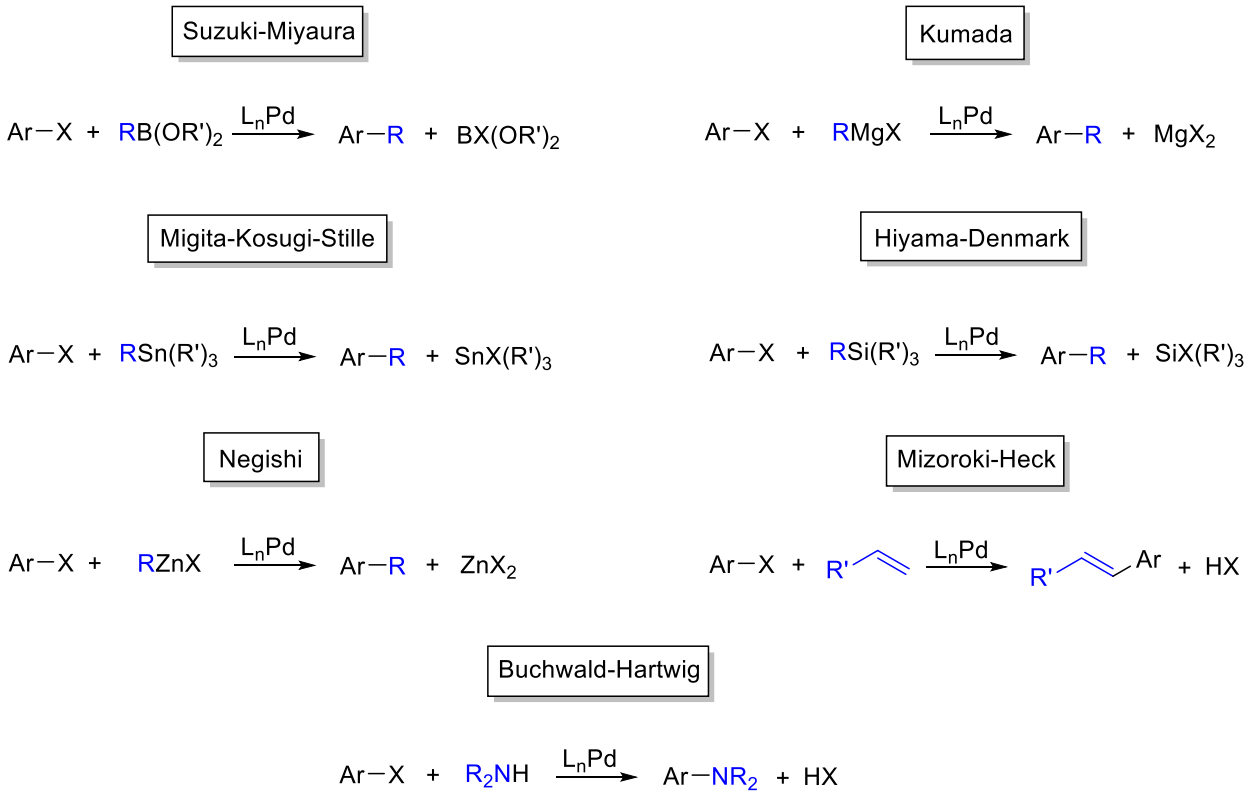

Scheme 1.1. Examples of Palladium Catalyzed Cross-Coupling Reactions.

Cross-coupling reactions, while extremely powerful, generally produce inert (hetero)aryl-(hetero)aryl or related bonds. These bonds are typically unreactive, and further manipulation of the product often requires the presence of reactive functionalities in other parts of the molecule. An important variant of cross-coupling reactions is palladium catalyzed carbonylations, in which an organic electrophile is coupled with carbon monoxide and a nucleophile to produce a carbonyl-containing product (Scheme 1.2a).[7-11] Such carboxylic acid derivatives are among the most common structures found in pharmaceuticals, agrochemicals, polymers, biomolecules, and other synthetic materials. In addition, the carbonyl group can be easily manipulated to access other functionalities. Carbonylation chemistry is attractive from an efficiency standpoint since carbon monoxide is an abundant and inexpensive feedstock. These features have made metal catalyzed

carbonylations amongst the core industrial technologies used for the efficient bulk production of chemicals. The most prominent examples of these include the Monsanto and Cativa acetic acid process (Scheme 1.2b) and hydroformylation for the production of aldehydes (Scheme 1.2c).[12-14]

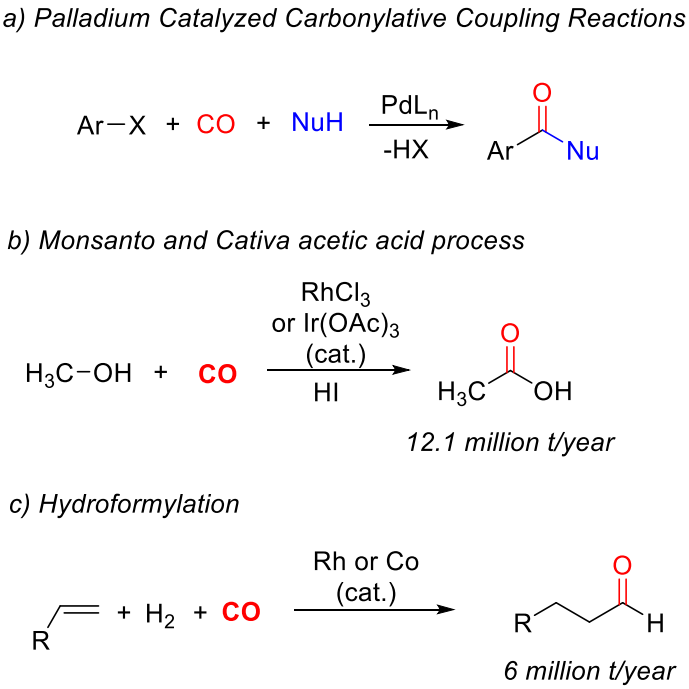

Scheme 1.2. Metal Catalyzed Carbonylations and Industrial Examples

While the large scale carbonylations shown above use non-group 10 metal catalysts, an attractive feature of palladium catalysts is their versatility in allowing access to products such as amides, esters, carboxylic acids, aldehydes, or ketones.[7-11] In contrast to classic approaches to synthesize these products with synthetic acylating agents, carbonylations simply require an organic electrophile, CO, and a nucleophile, all of which are stable and widely available. There is therefore a continued interest in developing more efficient, accessible, and reliable approaches to expand these reactions in key areas of research. This chapter will provide an overview of some of the

important advances in this area. This will focus first on developments in palladium catalyzed carbonylative couplings using aryl halide electrophiles (Section 1.2). In Section 1.3, the focus will shift to discussing the recent developments in alkyl halide carbonylation, especially unactivated alkyl halides, which have proven to be very challenging substrates for these transformations. Finally, Section 1.4 will highlight important strategies in the construction of heterocyclic products using palladium catalyzed carbonylations.

1.2. Aryl Halide Carbonylation

1.2.1. Early Development and Mechanism

Some of the first examples of aryl halide carbonylation were developed by R.F. Heck and co-workers.[15-17] In these seminal studies, aryl iodides and aryl bromides were carbonylated using $PdX_2(PPh_3)_2$ (X = I, Br) as catalyst in the presence of alcohols and amines to produce esters and amides (Scheme 1.3). The reactions proceeded at relatively elevated temperatures (60-100 ºC) but with only 1 atm CO, and were compatible with a range of substituted aryl and heteroaryl halide substrates.

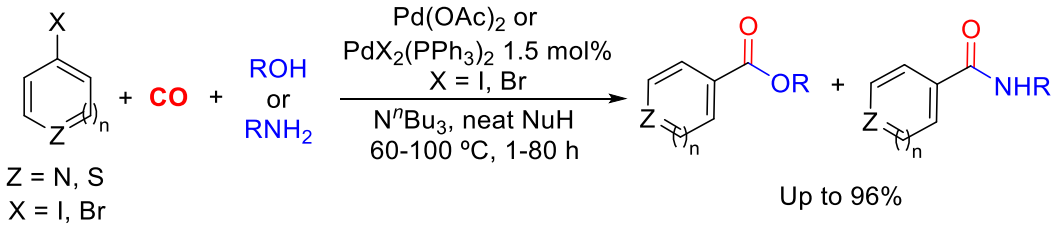

Scheme 1.3. Heck Carbonylation of Aryl and Heteroaryl Halides

Since these initial reports, many groups have studied this transformation to both expand upon its scope, and probe how the reaction proceeds.[18-22] The current understanding of the mechanism

of this reaction is presented in Scheme 1.4. As with many palladium catalyzed reactions, carbonylations often employ palladium(II) salts as the catalyst precursor. These salts are more air stable than Pd(0) sources, and can be reduced under the reaction conditions (e.g. by amine bases, phosphorus, CO itself) to generate *in situ* the active Pd(0) catalyst (Scheme 1.4a). Nevertheless, Pd(0) sources can also be employed. Common examples of these include $Pd_2dba_3 \cdot CHCl_3$ and $Pd(PPh_3)_4$.[23-25]

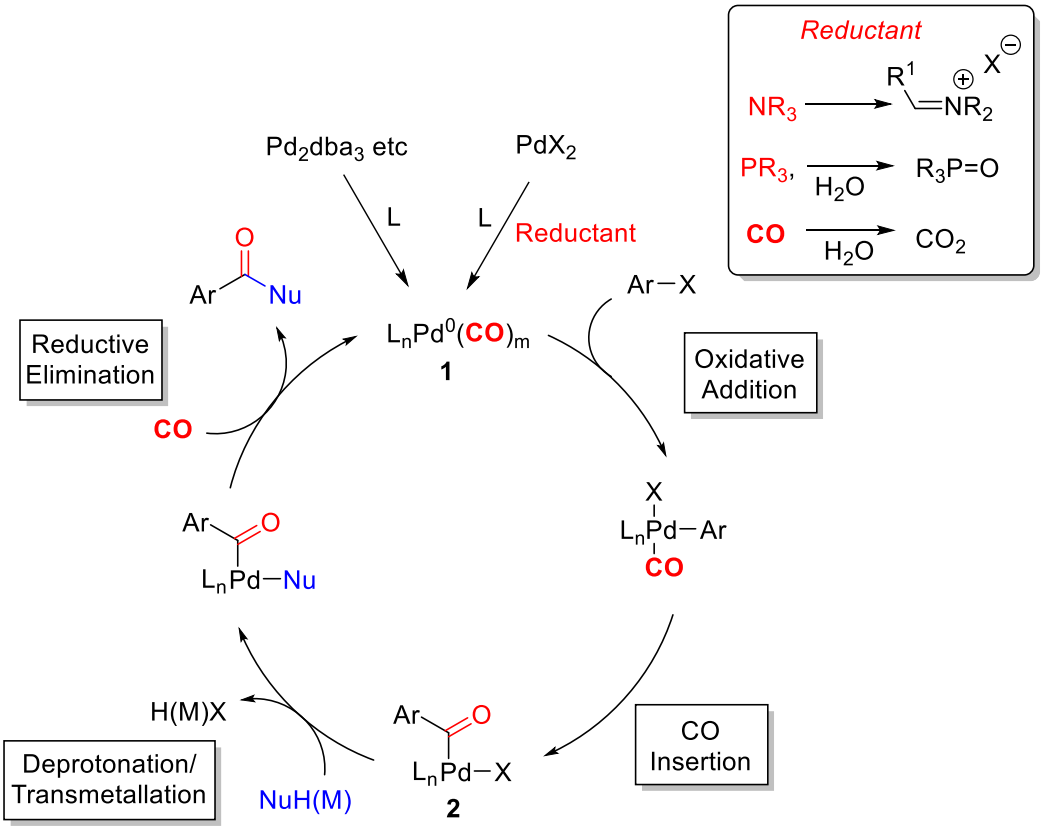

Scheme 1.4. General Mechanism for Palladium Catalyzed Carbonylation Reactions

Once the Pd(0) **1** catalyst forms, the first productive step in the catalytic cycle is oxidative addition of the aryl halide to produce a aryl-palladium complex. This step is common as well in most cross-coupling reactions, and its rate is dependent upon several factors. Firstly, the propensity

of aryl halides to undergo oxidative addition is typically related to the bond strength of the C-X bond that is cleaved in the process. The order of reactivity is thus: Ar-I > Ar-Br > Ar-Cl.[8] The ancillary ligands coordinated to palladium modulate its electronic properties, and also influence its ability to undergo oxidative addition. Perhaps the most common ligand for these transformations are phosphines, which are typically strong donors. These ligated palladium complexes typically have more electron density to backbond to the Ar-X σ* orbital, thereby weakening this bond and favoring the formation of the palladium(II) oxidative addition product. Since oxidative addition is often rate determining in coupling reactions, significant research efforts have been directed towards designing new phosphine ligands that can accelerate this step. For instance, while the relatively weak bond in aryl iodides can be cleaved with a variety of palladium catalysts, and even non-phosphine coordinated Pd(0) complexes, aryl chlorides have a much more robust bond, and therefore have commonly required strongly donating bidentate phosphine ligands to favor oxidative addition.[7, 26-29] Sterically encumbered ligands can also accelerate this step by creating empty coordination sites on palladium for oxidative addition. In this regard, one aspect that differentiates carbonylations from other types of cross-coupling reactions is the presence of carbon monoxide, which is: a) often present in excess relative to palladium, b) can coordinate to palladium, and c) is a strong π-acceptor. This coordination reduces the electron density on palladium and often slows oxidative addition relative to other cross-coupling reactions. Depending on the specific identity of the $L_nPd(0)$ species, there could be more than one CO ligand in **1**, which can further increase the barrier for this step.[30]

After oxidative addition, a coordinated carbon monoxide can undergo migratory insertion into the Pd-Ar bond to form acylpalladium complex **2**.[27] This step can be rapid, although there have been reports of slower insertion rates involving palladium-aryl groups with electron withdrawing

groups, and unfavorable insertion equilibria with certain Pd-bound ligands.[31-32] The final step in the mechanism involves the reaction of the palladium-acyl complex **2** with a nucleophile to form the product. This nucleophile can take several forms, with common examples including water (to form carboxylic acids), alcohols (alkoxycarbonylations), or amines (aminocarbonylations). Over time, other examples have emerged, such as alkynes to generate alkynones, reductive carbonylation reactions utilizing hydrogen gas to produce aldehydes, alkenes in carbonylative Heck reactions, and stoichiometric organometallic reagents for the generation of ketones (Scheme 1.5). Several pathways for the reaction of the nucleophile with the palladium-acyl complex have been put forward. In their initial work, Heck proposed a direct nucleophilic attack on the acyl ligand as this final step.[18] However, Yamamoto and others gathered kinetic data on alkoxy- and aminocarbonylations, and the results were instead consistent with an initial coordination of the nucleophile to Pd followed by deprotonation, and reductive elimination.[19, 21,33]

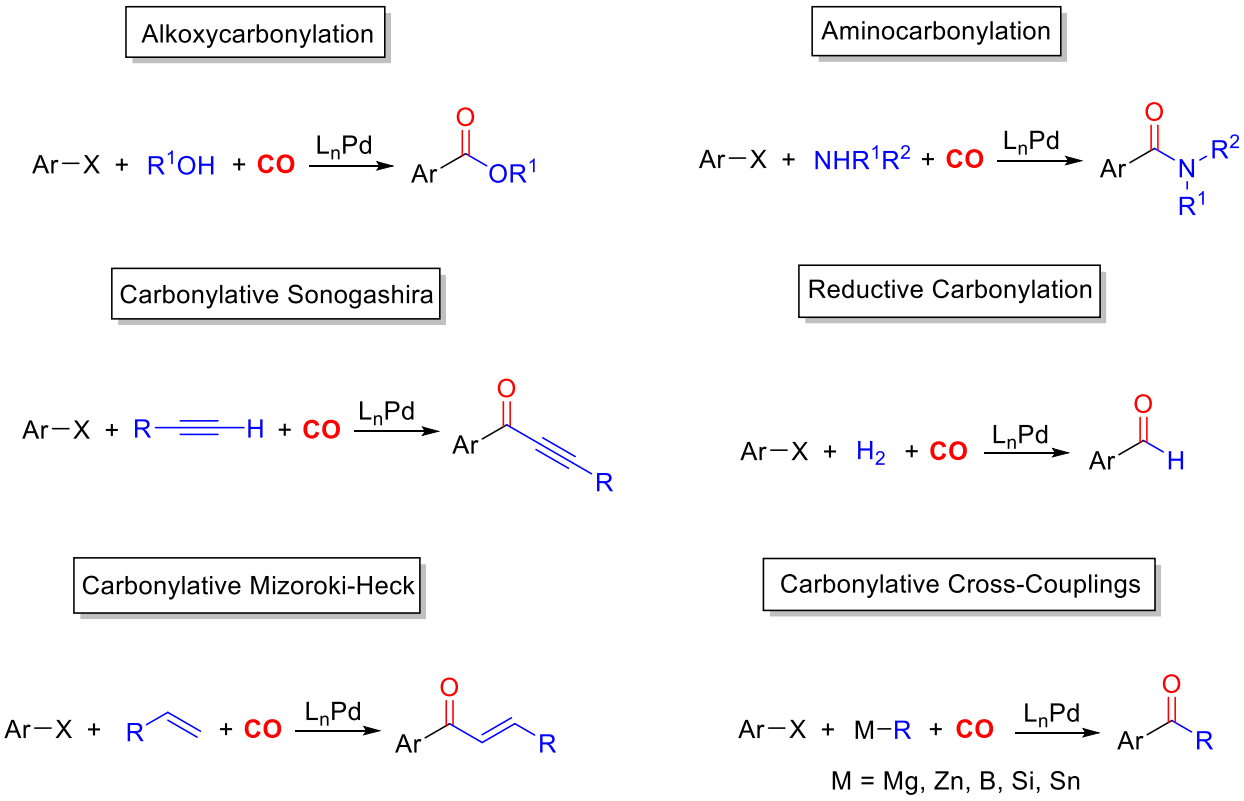

Scheme 1.5. Nucleophiles in Palladium Catalyzed Carbonylative Coupling Reactions

There have been a number of more recent theoretical and experimental studies on this reaction, and these generally support the mechanism outlined above.[22, 30, 34-35] One particularly insightful report has emerged from the Hartwig group in which the effect of bidentate phosphines in aryl chloride carbonylation was examined by synthesizing key intermediates and probing their reactivity (Scheme 1.6).[36] They showed that 1,3-bis(dicyclohexylphosphino)propane (dcpp) coordinated Pd(0) catalyst can bind to two CO ligands to form a stable 18 electron carbonyl complex, which they were able to isolate and characterize. Kinetic studies suggest that the active oxidative addition species in these reactions is a three-coordinate, monocarbonyl complex (dcpp)Pd(CO) formed via the initial dissociation of a CO ligand. The oxidative addition of aryl halide to this complex was found to be the rate determining step in catalysis. The latter was

attributed to the deactivating effect of CO coordination to palladium, as well as the barrier for CO loss from the stable (dcpp)Pd(CO)$_2$. Stoichiometric model studies and kinetics were also used to probe how the model nucleophile, ammonia, is incorporated. Their data is consistent with a pathway in which a chloride ligand in acyl complex **2** undergoes reversible ligand substitution with ammonia to generate a cationic palladium complex. In a subsequent step, the coordinated NH_3 ligand is deprotonated by a base to generate a palladium amido complex that can reductively eliminate the amide product.

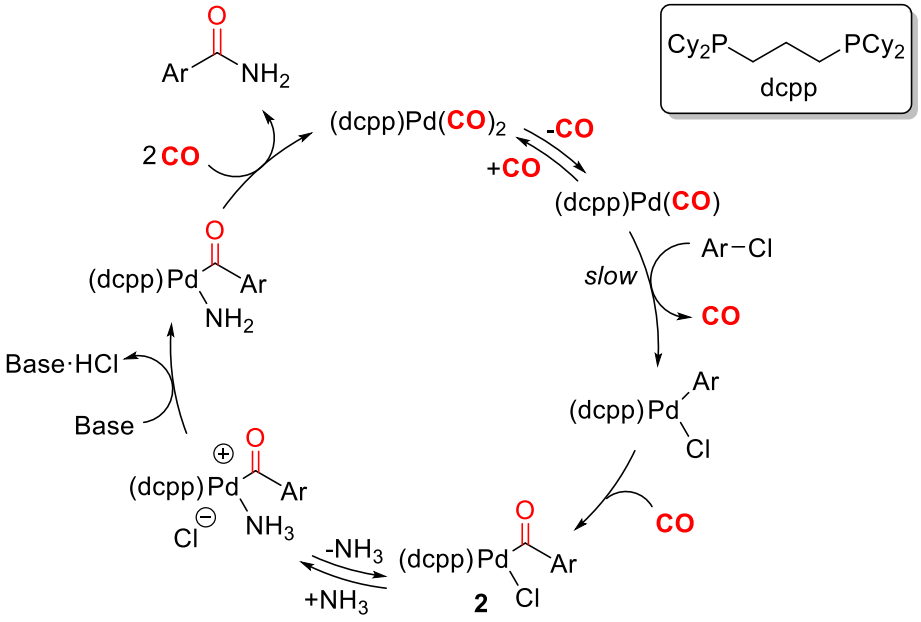

Scheme 1.6. Hartwig's Mechanistic Studies on the Palladium Catalyzed Carbonylation of Aryl Chlorides with dcpp as Ligand

1.2.2. Expanding the Breadth of Aryl Halide Electrophiles in Carbonylations

Since the advent of cross coupling reactions, aryl halides have become ubiquitous as starting materials and are increasingly available for commercial sources. However, the most reactive of these substrates (aryl iodides) are the most expensive. Conversely, the most economical and

readily available compounds (aryl bromides or chlorides) are more challenging to activate. While this issue is rapidly becoming solved in many cross coupling platforms, it remains problematic in carbonylations. As an example, in Heck's seminal work, aryl iodides could be carbonylated with simple $Pd(OAc)_2$ as the catalyst precursor with no added ligands, while the less reactive aryl bromides required a phosphine ligand (PPh_3) and elevated temperatures, and aryl chlorides were not employed (See Scheme 1.3). This has stimulated a number of efforts to create more active catalysts for aryl halide activation in the presence of carbon monoxide. A highlight of some of these efforts is described below.

The Beller group has been one of the leaders in developing more efficient catalyst systems for carbonylations. In 2006, they reported the use of a new class of monodentate phosphine ligand, cataCXium A or $(1\text{-adamantyl})_2P(n\text{-butyl})$, for use in aryl bromide carbonylation. This catalyst system allowed the carbonylation of a variety of aryl and heteroaryl bromides in very good yields and with low catalyst loadings (Scheme 1.7).[37-40] This ligand combines the electron donating capabilities of tri-alkylphosphines, but adds steric bulk. The latter presumably minimized the number of carbon monoxide ligands coordinated to palladium, and thereby accelerates oxidative addition. The ligand is also air stable, which eliminates the need for inert conditions to setup the reaction.

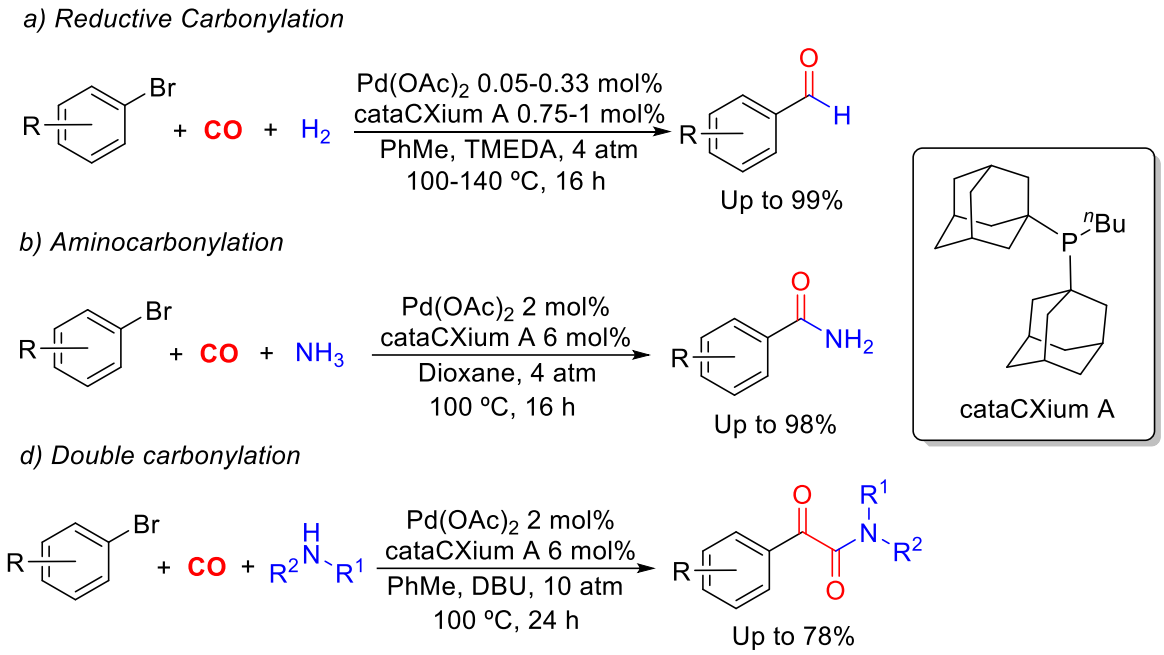

Scheme 1.7. Efficient Palladium Catalyzed Carbonylations Using cataCXium A

An alternative approach to active catalysts for aryl bromide carbonylation is to use bidentate ligands. For example, the Walker group reported the carbonylation of electron-rich aryl bromides, which are particularly hard to use in carbonylations due to their sluggish oxidative addition, using BINAP as a ligand (Scheme 1.8a).[41] In 2008, the Buchwald group reported an even more general system for amino- and alkoxycarbonylation of aryl bromides by exploiting the sterically encumbered, wide bite angle Xantphos ligand. Unlike many of the previous examples, these catalysts require only 1 atm CO, and can be used to generate an array of primary and second amides, Weinreb amides, or esters in good yield and at relatively mild temperature (Scheme 1.8b).[42]

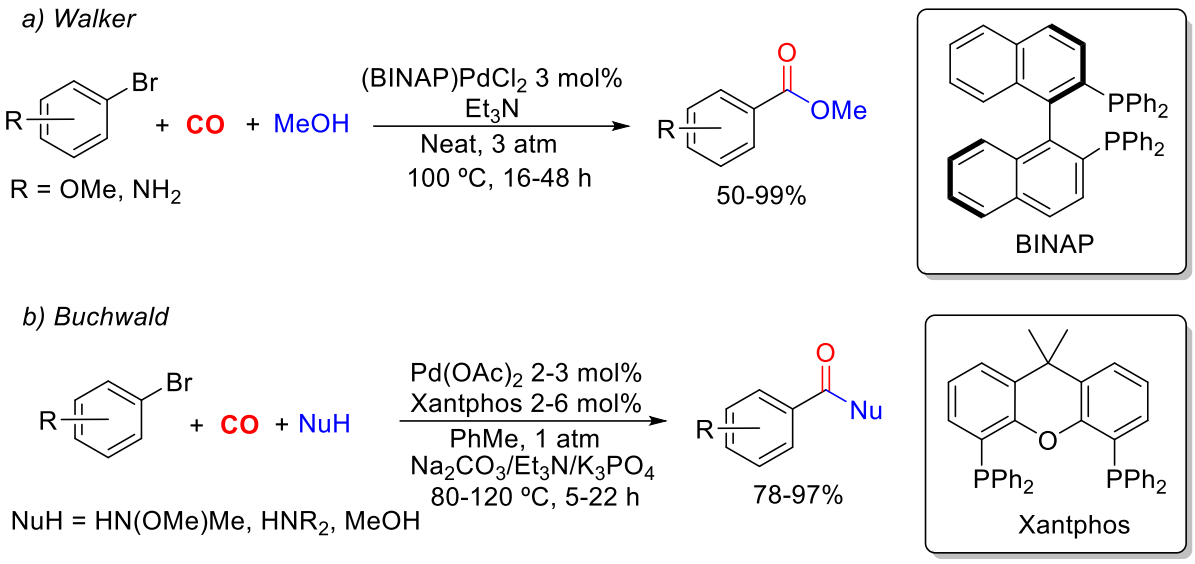

Scheme 1.8. Use of Bidentate Ligands in Aryl bromide Carbonylation

Compared to aryl bromides, aryl chlorides are significantly more challenging substrates to activate due to the strong C-Cl bond. In the context of carbonylation chemistry, aryl chlorides remain elusive substrates even to this day because they often require harsh reaction conditions and specialized catalysts. Alper reported a protocol for the hydroxycarbonylation of aryl chlorides in a biphasic system with a Pd/PCy_3 catalyst system (Scheme 1.9a). While the yields of carboxylic acids were low, the catalyst system showed relatively high TON.[43] One of the first general systems described for palladium catalyzed aryl chloride carbonylation came from the Milstein lab, who reported an alkoxycarbonylation of simple aryl chlorides using the large, strong donor, bidentate dippp ligand (Scheme 1.9b). The overall yields were very good, but the reaction did require elevated temperature (150 ºC).[44]

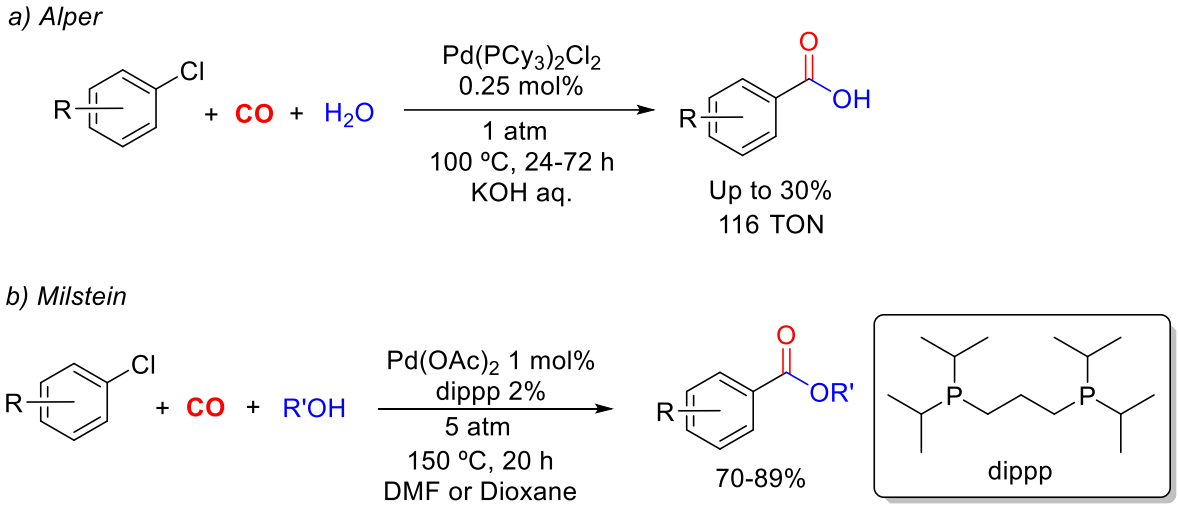

Scheme 1.9. Early Examples of Aryl Chloride Carbonylation

For years, Milstein's work remained one of the few viable protocols for chloroarene carbonylation. However, the use of this method was not widespread due to the difficulty associated with the synthesis of the dippp ligand and its high pyrophoricity.[8, 27] Later developments address some of these limitations. For example, Beller and Hamilton showed that a variety of chloroarenes can be carbonylated to form esters at low pressure (1 atm), but elevated temperature, using the large, monodentate JosiPhos ligand (Scheme 1.10a).[45-46] Alternatively, Buchwald developed an efficient aminocarbonylation reaction under milder conditions utilizing the dcpp (1,3-(bis(dicyclohexyl)phosphinopropane) ligand (Scheme 1.10b).[47] In contrast with Milstein's work, the dcpp ligand was used as its HBF_4 salt during reaction set-up, providing greater air stability. Catalysis with this system also proceeded with atmospheric CO pressure.

The use of bidentate ligands can also allow the carbonylation of even more challenging, yet valuable, substrates, such as heteroaryl chlorides. One example of the latter are chloropyridines, which can associate to palladium via nitrogen, and further inhibit oxidative addition. The Beller,[48]

Studer,[49] and Walker[41] groups have each shown that sterically hindered, electron rich bidentate phosphines can be used to activate chloropyridines towards carbonylation to form a range of ester or amide products (Scheme 1.10c).

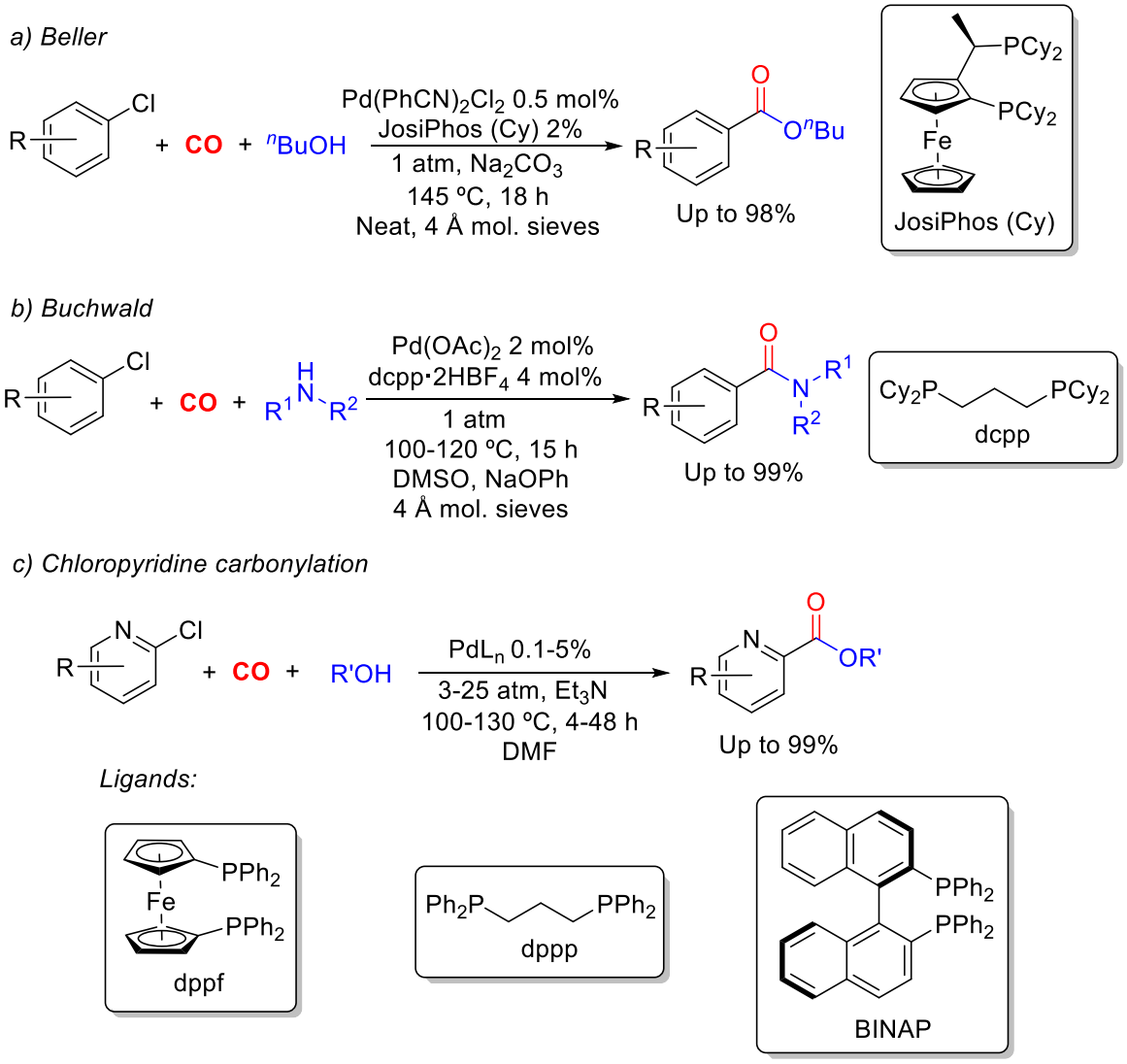

Scheme 1.10. Mild Methods for Aryl- and Hetero-Aryl Chloride Carbonylation

1.2.3. Expanding the Breadth of Nucleophiles in Carbonylations

In addition to the challenges regarding the scope of aryl halides in palladium catalyzed carbonylations, there are also significant limitations in the second component, the nucleophile, that can be employed. Since the nucleophile must associate to palladium prior to a reductive elimination step, carbonylations typically require nucleophiles that are strongly coordinating (e.g. negatively charged or with strong donor atoms) and are not sterically encumbered. This contrasts with the more classical synthesis of carbonyl-products with electrophilic acylating agents, which can often react with diverse array of nucleophiles.[50] One of the first studies to address this challenge came from the Buchwald lab, where they observed that bulky secondary amines can be used as nucleophiles in carbonylations, but only in concert with NaOPh as the base.[47] This was found to arise from the ability of NaOPh to coordinate better to palladium than the amine and thus form phenyl esters (Scheme 1.11a).[51] The latter are moderately electrophilic and can serve as *in situ* acyl transfer reagents. Buchwald elaborated on this concept to show it offers a more general platform to use nucleophiles that are typically incompatible with palladium catalysis, such as allyl alcohols and thiols.[51]

The formation of electrophilic acylating agents by carbonylation has since been expanded upon by several labs, including Grushin,[52] Skrydstrup,[53-54] and Manabe,[55] who showed that thioesters, aroyl azides, and acid fluorides, respectively, could be generated via palladium catalyzed carbonylation of aryl halides (Scheme 1.11b-d). These products could then react with challenging nucleophiles to access an unprecedented variety of carbonyl containing products.

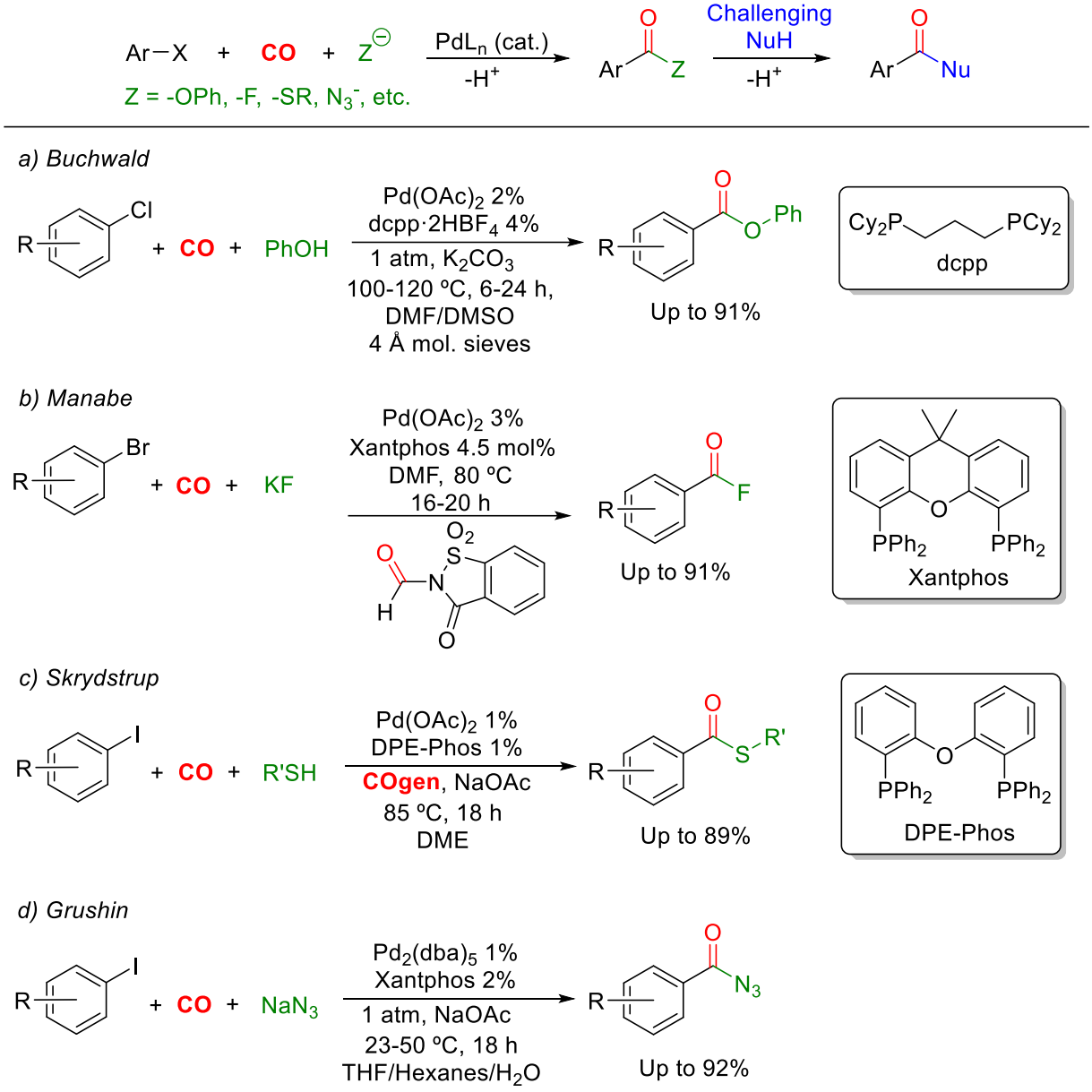

Scheme 1.11. Palladium Catalyzed Carbonylative Formation of Acylating Reagents

Recently, our laboratory has shown that it is possible to build up even more electrophilic species using palladium catalyzed carbonylations. For example, the palladium catalyzed carbonylation of various aryl and heteroaryl halides in the presence of a chloride salt was found to lead to the high yield formation of acid chlorides when using the sterically encumbered P^tBu_3 ligand.[56-59] The

formation of a highly electrophilic acid chloride in the presence of Pd(0) is an unusual observation, since these products commonly undergo facile oxidative addition to palladium.[58-59] Kinetic and computational studies suggest that the large P^tBu_3 ligand along with CO coordination to palladium generate a sterically destabilized palladium-acyl intermediate, and induces an equilibrium reductive elimination of acid chloride (Scheme 1.12a).[30] The generation of such a potent electrophile can be exploited to acylate an even wider selection of nucleophiles under mild conditions.

More recently, our lab showed that the carbonylation of aryl iodides can allow the *in situ* formation of acid iodides (Scheme 1.12b),[60] or when performed in the presence of AgOTf, form exceptionally electrophilic acid triflate products (Scheme 1.12c).[61] Interestingly, this latter reaction required the use of a non-phosphine coordinated palladium catalyst. The key intermediate in the reaction was proposed to be a highly electron-poor, CO-coordinated palladium-acyl complex that can readily reductively eliminate acid triflate. The generation of potent electrophiles with this approach allowed the formation of ketones via the C-H functionalization of simple arenes and heteroarenes.[61]

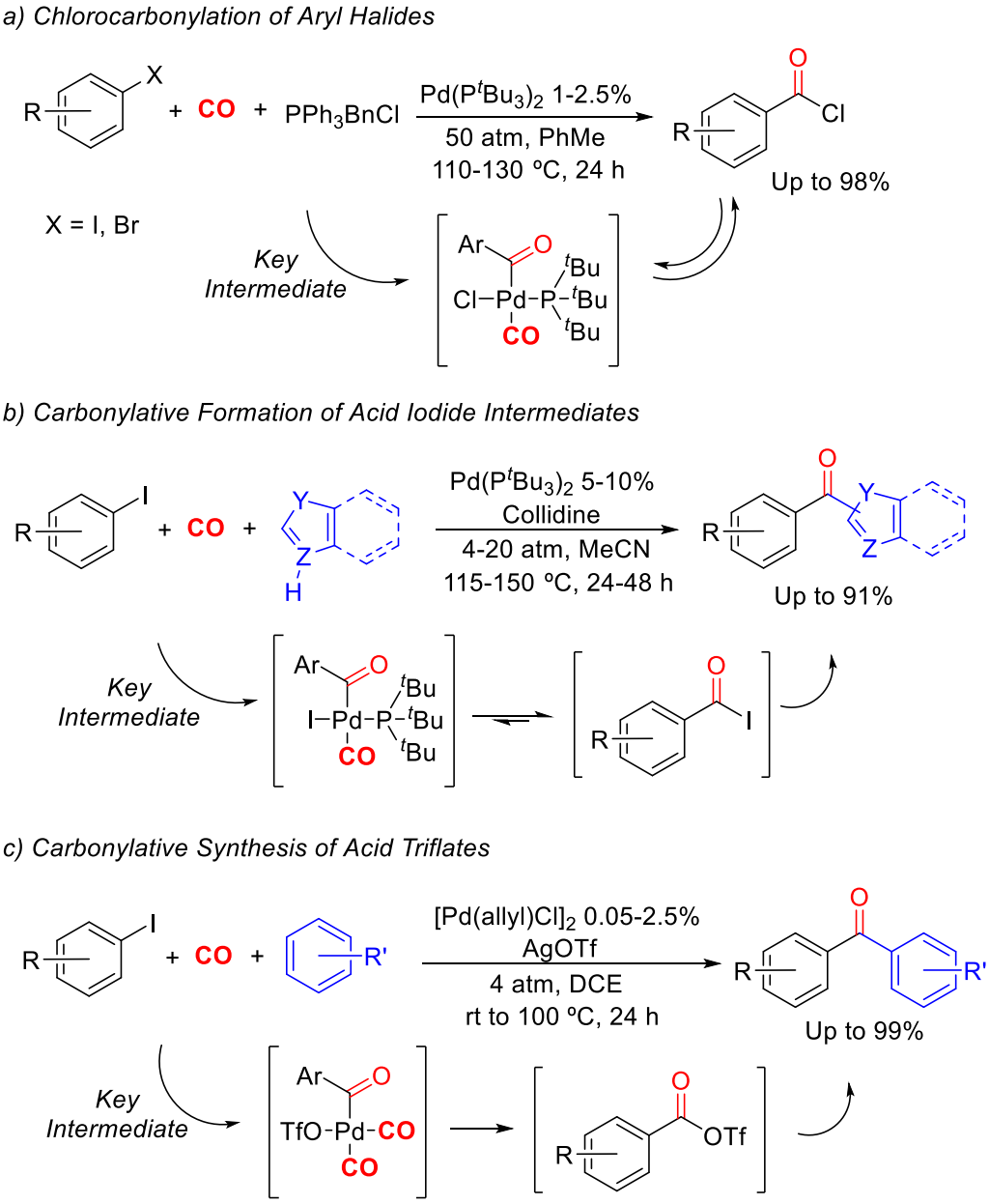

Scheme 1.12. Carbonylative Strategies for the Generation of Acid Chlorides and Related Electrophiles

Morandi and our lab have simultaneously reported another approach to acid chloride synthesis via the palladium catalyzed metathesis of aryl iodides and acid chlorides (Scheme 1.13).[62-63] In

this system, the dynamic nature of the oxidative addition/reductive elimination steps is exploited to activate both aryl iodides and acid chlorides, which can then undergo ligand exchange and eliminate to form a new acid chloride (and aryl iodide) products. Morandi had shown a related palladium catalyzed approach to alkyl acid chlorides via the reversible addition of HCl/CO across alkenes.[64]

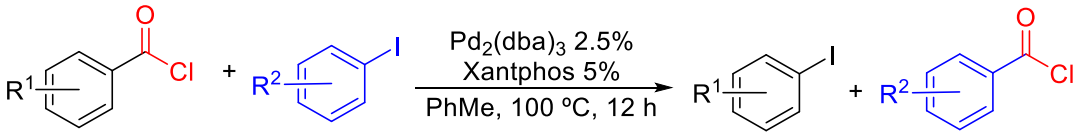

Scheme 1.3. Palladium Catalyzed Carbonyl Functional Group Metathesis for the Synthesis of Acid Chlorides

1.3. Alkyl Halide Carbonylation

1.3.1. Palladium Catalyzed Carbonylation of Alkyl Halides

While the field of palladium catalyzed coupling reactions has seen an incredible growth in the last several decades as a method to construct C-C and C-heteroatom bonds, one common criticism is that the field seems to be trapped in "flatland".[65] The majority of the catalytic cross-coupling reactions reported rely on the coupling of sp^2-hybridized substrates, particularly those with aryl units. This has exponentially increased the number of ways to construct aryl-, heteroaryl-, and vinyl-substituted products, which are valuable and relevant. However, many applications require a more comprehensive set of tools to construct products, and in particular C-sp^3 bonds, which are ubiquitous in natural products and pharmaceuticals.

Alkyl electrophiles, such as alkyl halides, are much less commonly used in cross-coupling chemistry. This is often attributed to the considerable challenges in activating these substrates towards oxidative addition to palladium; the first step in coupling reactions.[66-67] It has been proposed that alkyl halides lack key stabilizing interactions in the transition state for oxidative addition to palladium.[68] Aryl halides have a π-system that can coordinate to the palladium center, which contributes to the stabilization. Additionally, calculations have suggested that the metal can backbond better to a C-X σ* and π* orbital, both of which stabilize the transition state for oxidative addition.[68] In contrast, alkyl halides lack any π-system for pre-coordination to palladium, and the metal has no other choice but to backbond only to the C-X σ* orbital (Scheme 1.14a). This concerted oxidative addition pathway is therefore often high in energy for a large number of simple alkyl halides. Instead, the active mechanism for alkyl halide oxidative addition is believed to involve a polar mechanism, where the palladium center behaves as a nucleophile and displaces the halide similar to an S_N2 reaction.[66, 69] Experimental evidence for this pathway has been observed with anionic palladium complexes and chiral alkyl halides, which undergo stereochemical inversion upon oxidative addition (Scheme 1.14b).[70-71] Alternatively, there is also data suggesting that the oxidative addition of alkyl halides proceeds via alkyl radicals. In this, an initial single-electron transfer from palladium to the alkyl halide leads to a radical anion that can fragment into an alkyl radical and a halide anion. The resulting alkyl radical can then add to Pd(I) to generate the oxidative addition product (Scheme 1.14c).[72-73]

a) Concerted Oxidative Addition of Aryl Halides vs Alkyl Halides

b) Stepwise Mechanism for the Oxidative Addition of Alkyl Halides

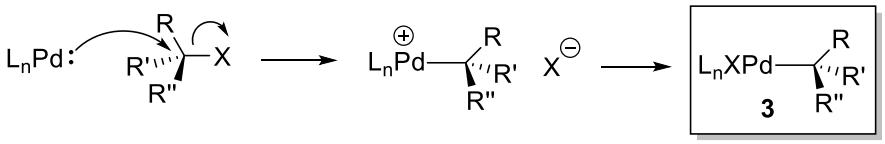

c) Single Electron Transfer Mechanism for the Oxidative Addition of Alkyl Halides

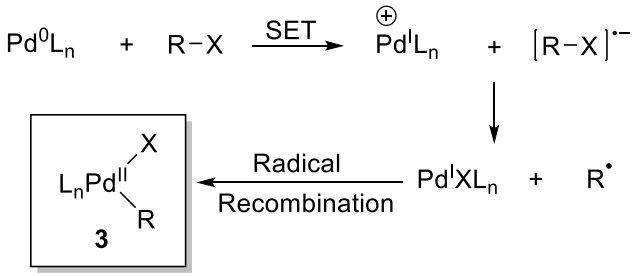

Scheme 1.14. Oxidative Addition of Alkyl Halides to Palladium

A second feature complicating the use of alkyl halides is the reactivity of the resultant alkyl-palladium complex **3**. The most important of these is β-hydride elimination. In this, if the alkyl group has a hydrogen in the β position, and the palladium center has an empty coordination site *cis* to the alkyl ligand, the complex can undergo rapid β-hydride elimination to form alkene-coordinated palladium-hydride complex **4** (Scheme 1.15a).[74-77] β-Hydride elimination is a useful step in many palladium catalyzed reactions (e.g. Heck couplings), but for carbonylation reactions it is often non-productive. There are several different strategies to inhibit β-hydride elimination (Scheme 1.15b). The simplest solution is to use substrates that have no β-hydrogens, but the

consequence of the latter is an extremely limited substrate scope.[78] Alternatively, steric bulk in the palladium-bound ligands can be used to slow the elimination step by inhibiting the β-hydrogen on the alkyl ligand from adopting an agostic interaction to palladium, which is key for elimination.[79] Chelating ligands can also sometimes be effective in limiting β-hydride elimination, since the elimination typically requires an empty coordination site on the catalyst.[80] Such coordination sites can be easy to form by ligand dissociation with monodentate ligands, but the chelation effect disfavors a partial ligand dissociation, thus often suppressing this pathway.[77, 81]

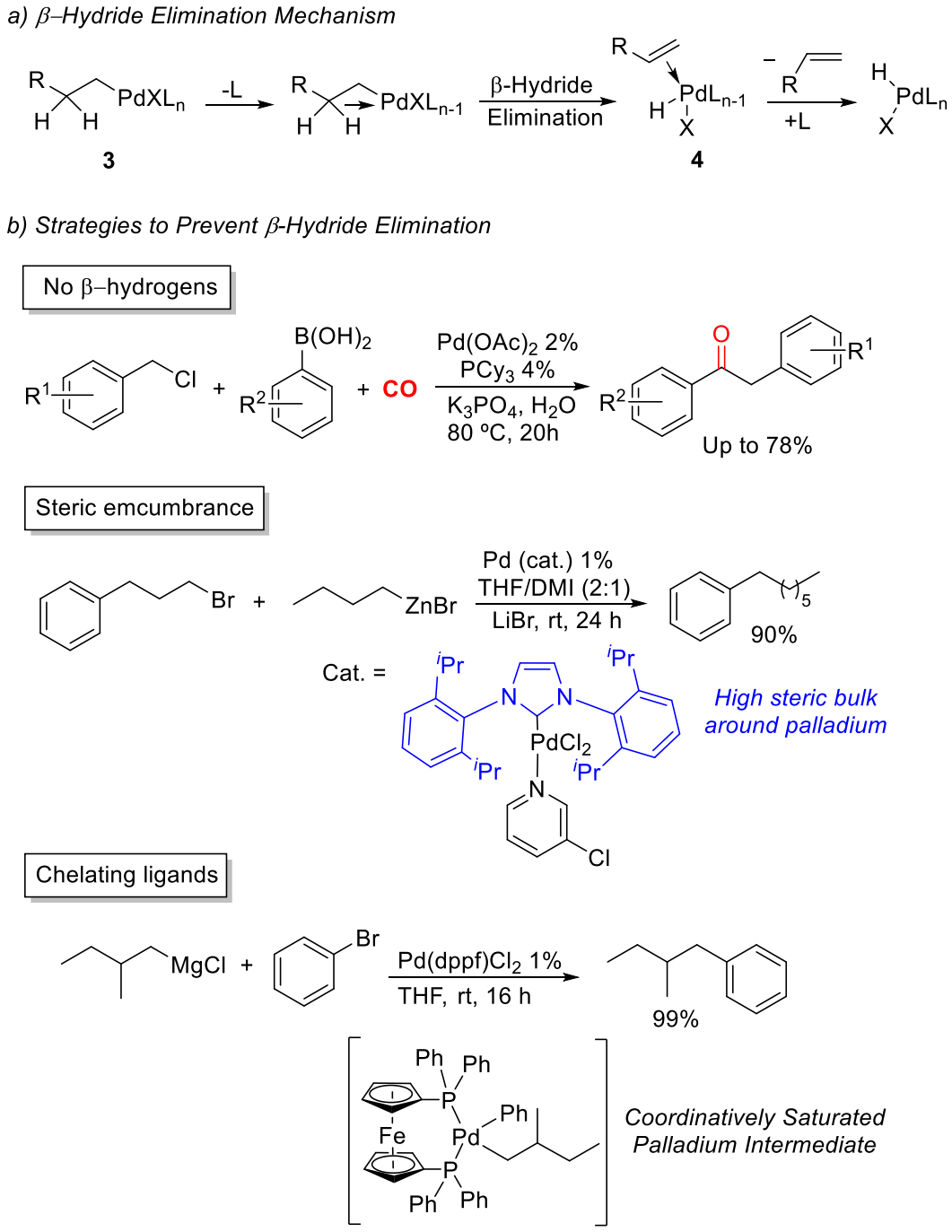

Scheme 1.15. β-Hydride Elimination from Alkyl-Palladium Complexes and Strategies to Overcome this Step

Interestingly, and despite these limitations, alkyl halide carbonylation also lies at the core of the key industrial processes for the conversion of methanol to acetic acid (Monsanto/Cativa), albeit with iridium and rhodium catalysts rather than palladium.[12-13] However, this involves the formation of particularly reactive primary methyl iodide (and one without β-hydrogens). Other classes of activated alkyl halides have also been shown to be viable substrates in palladium catalyzed carbonylations, including allyl halides, benzyl halides, and α-halo-ketones or -esters.[82] In general, these substrates are activated towards nucleophilic attack thus favoring the reaction, and lack β-hydrogens that can undergo facile elimination.

A particularly important use of activated alkyl halides in carbonylations involves the synthesis α-amino acid derivatives from amides, aldehydes, and carbon monoxide (Scheme 1.16a). The latter came to be known as the amidocarbonylation reaction, and is a powerful tool for the industrial synthesis of products used in specialty surfactants, artificial sweeteners, and food additives.[83] This reaction was first noted by the Ajinomoto Company as a minor side-product in the cobalt catalyzed reductive carbonylation of acrylonitrile to generate 3-cyanopropionaldehyde (Scheme 1.16b).[84] Wakamatsu would later report the low yield formation of *N*-acetylalanine from the cobalt-catalyzed reaction of acetonitrile, acetic anhydride, and synthesis gas (H_2/CO) (Scheme 1.16c).[85] The reaction required HCl, which led Wakamatsu to conclude that it proceeded via hydrolysis of the nitrile to produce acetamide. Moreover, the reduction of acetic anhydride to acetaldehyde was observed in the system, suggesting that the aldehyde also played a role in the reaction.[86] Wakamatsu went on to demonstrate that the cobalt-catalyzed reaction of acetaldehyde, acetamide, and H_2/CO led to *N*-acetylalanine in high yield.[85] Pino later showed that this reaction was generally applicable to a wide variety of amide and aldehyde substrates.[87]

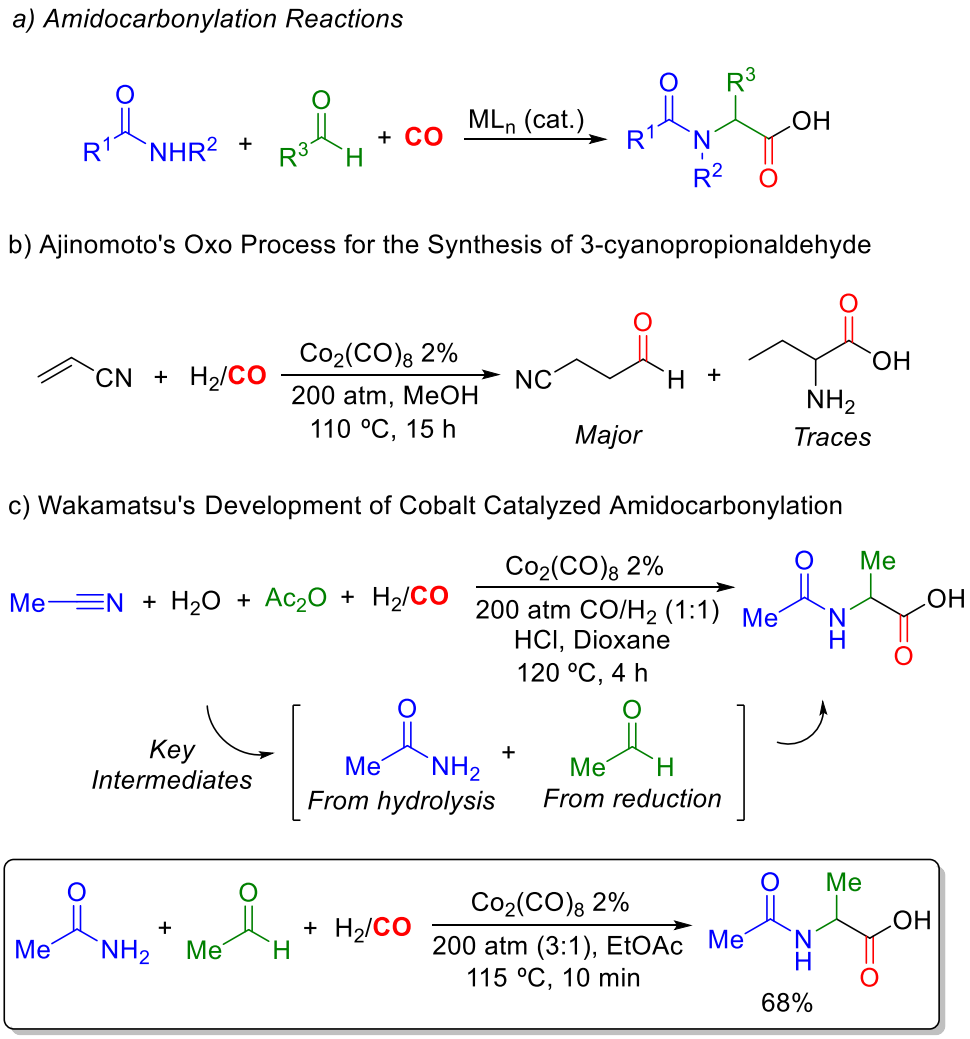

Scheme 1.16. Development of Metal Catalyzed Amidocarbonylation Reactions

Beller reported the first example of a palladium catalyzed amidocarbonylation to produce α-substituted *N*-acyl glycines.[84, 88-91] As in the cobalt chemistry above, the transformation is thought to proceed via the initial condensation of the aldehyde and amide under acidic conditions to form an α-bromoamide, which can oxidatively add to palladium to form a stabilized chelated intermediate (Scheme 1.17).[92-93] Subsequent CO insertion and hydrolysis affords the α-amino acid product. Of note, this palladium catalyzed reaction proceeds under milder conditions (e.g. 70-130

ºC and 10-60 atm) than the cobalt catalyzed variants.[84] In addition, this transformation has been applied to the synthesis of hydantoins,[94] functionalized arylglycines,[88] and chemoenzymatic synthesis of optically active natural and unnatural amino acids.[95] More recently, our laboratory has reported a variant of this reaction using acid chlorides and imines at much lower pressure and temperature (discussed in Section 1.4.3).

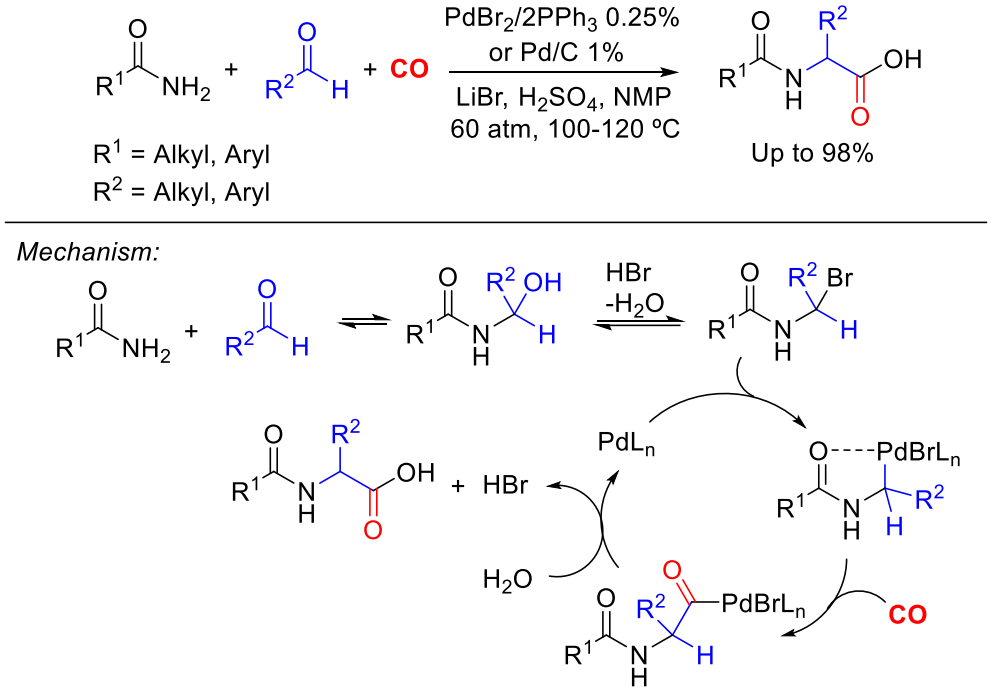

Scheme 1.17. Palladium Catalyzed Amidocarbonylation

In contrast to the examples above, the utilization of unactivated alkyl halides in palladium catalysis, and in particular carbonylations, remains challenging, and is an active developing field. Fuchikami reported one of the first examples of palladium catalyzed carbonylation of β-hydride containing alkyl halides. They showed that primary and secondary perfluoroalkyl iodides could be

transformed into esters and amides with a $PdCl_2(PPh_3)_2$ catalyst (Scheme 1.18a).[96-97] The authors proposed that the weak coordination of fluoride to palladium might be effective in suppressing β-hydride elimination. Notably, this reaction required very high CO pressure (30-50 atm), which presumably favors the CO insertion step and also inhibits β-hydride elimination. The same group later showed this carbonylation could also be applied to non-fluorinated alkyl iodides at 50 atm CO (Scheme 1.18b).[98-100] These reactions were carried out in weakly basic tetramethylurea (TMU) solvent to prevent the dehydrohalogenation of alkyl halides bearing sensitive functionalities.

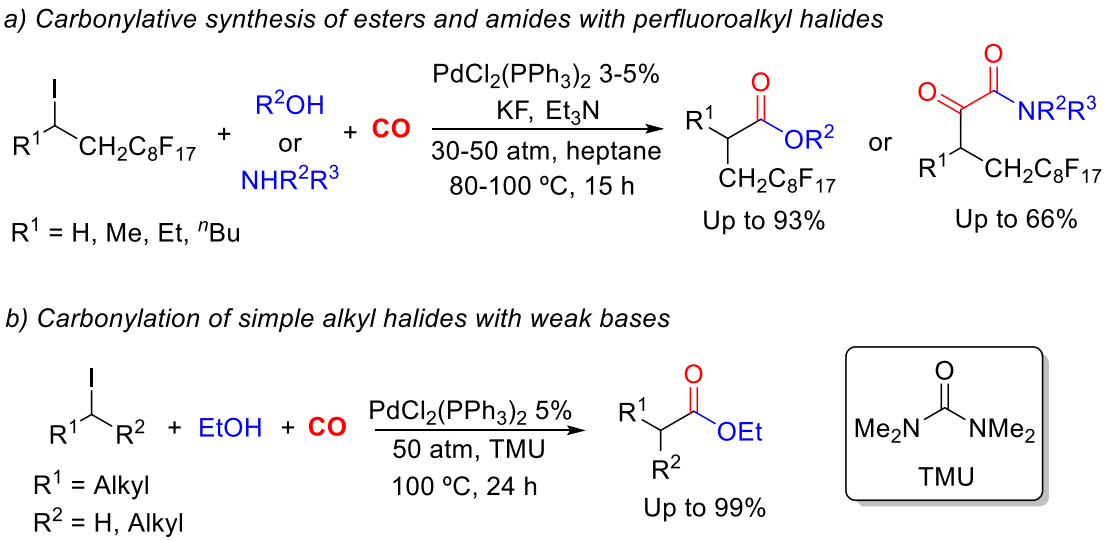

Scheme 1.18. Carbonylation of Unactivated Alkyl Iodides

The Alexanian group has made significant advances in utilizing unactivated alkyl halides in palladium catalyzed coupling reactions, including carbonylations.[101-102] They reported in 2010 an intramolecular alkyl Heck-type carbonylation to form cyclic products in good yields (Scheme 1.19a).[101] The reaction proceeded with commercially available $Pd(PPh_3)_4$ catalyst, and, as with

the previous work of Fuchikami, used elevated CO pressure (50 atm). The latter was also thought to be key to inhibit β-hydride elimination. Later, the same group reported an extremely mild alkoxycarbonylation of alkyl bromides by using a strong donor *N*-heterocyclic carbene ligand (IMes, Scheme 1.19b).[102] Unlike the alkyl halide carbonylation protocols described above, this reaction proceeded at low temperature and with only 1 atm of CO. Mechanistic evidence suggested the intermediacy of carbon-centered radicals in this reaction, hinting at an oxidative addition via an inner-sphere SET and bromide atom abstraction by palladium. This was supported by the lower efficiency of the reaction at higher CO pressure and the incompatibility of primary alkyl bromides. The former could indicate that excess CO can saturate the metal center and impede alkyl bromide coordination, while the latter relates to the decreased stability of the primary carbon radicals relative to secondary and tertiary alkyl substrates.

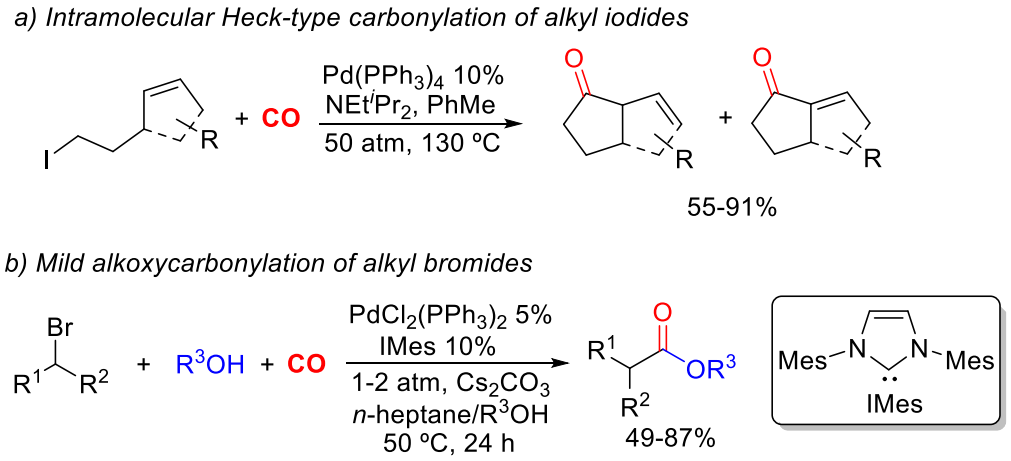

Scheme 1.19. Alexanian's Work on Carbonylation of Unactivated Alkyl Halides

1.3.2. Nickel Catalyzed Carbonylations of Alkyl Halides

There have recently been significant efforts directed towards using nickel catalysts in alkyl halide carbonylations. As with palladium, nickel is also a group 10 metal, but it has several different properties that distinguish it from palladium.[103-106] For example, nickel is a much more abundant and inexpensive metal than palladium or platinum. Moreover, nickel is a less electronegative element, which facilitates steps such as oxidative addition.[103-104] In the context of alkyl halide activation, alkyl-nickel complexes are also less prone to β-hydride elimination.[103-104] DFT studies have suggested that relative to palladium, nickel has an increased rotational barrier for the CH_α-CH_β bond in the alkyl ligand that is required to establish the agostic interaction leading to β-hydride elimination.[107] Finally, nickel more easily exists in stable odd electron configurations (Ni(I) or Ni(III)), which allows it to more easily engage in single electron transfer (SET), and therefore offers an alternative path for alkyl halide activation through radical intermediates. Nevertheless, nickel has a few major drawbacks. Firstly, the low electronegativity that facilitates oxidative addition also makes reductive elimination from Ni(II) complexes much more challenging. In addition, simple, unligated nickel is often avoided in carbonylations due to the potential formation of $Ni(CO)_4$, which is volatile and extremely toxic.[103]

One of the first general examples of nickel catalyzed carbonylations of alkyl halides was reported by the Troupel group. They developed an electrosynthesis of symmetrical ketones via the reductive carbonylative coupling of benzyl halides catalyzed by $NiBr_2$(bpy) (Scheme 1.19).[108] High pressures of CO were found to be detrimental to the process, presumably due to the formation of a stable $Ni(bpy)(CO)_2$ complex. They therefore resorted to the use of $Fe(CO)_5$ to slowly release CO during the reaction, which is believed to allow for the generation of the active Ni(0)(bpy)(CO) catalyst. The latter is postulated to undergo SET with an alkyl halide generating an alkyl radical,

which can combine with Ni(I) and then insert CO forming a nickel-acyl intermediate. The acyl complex is believed to engage in SET with a second alkyl halide to ultimately generate the product.

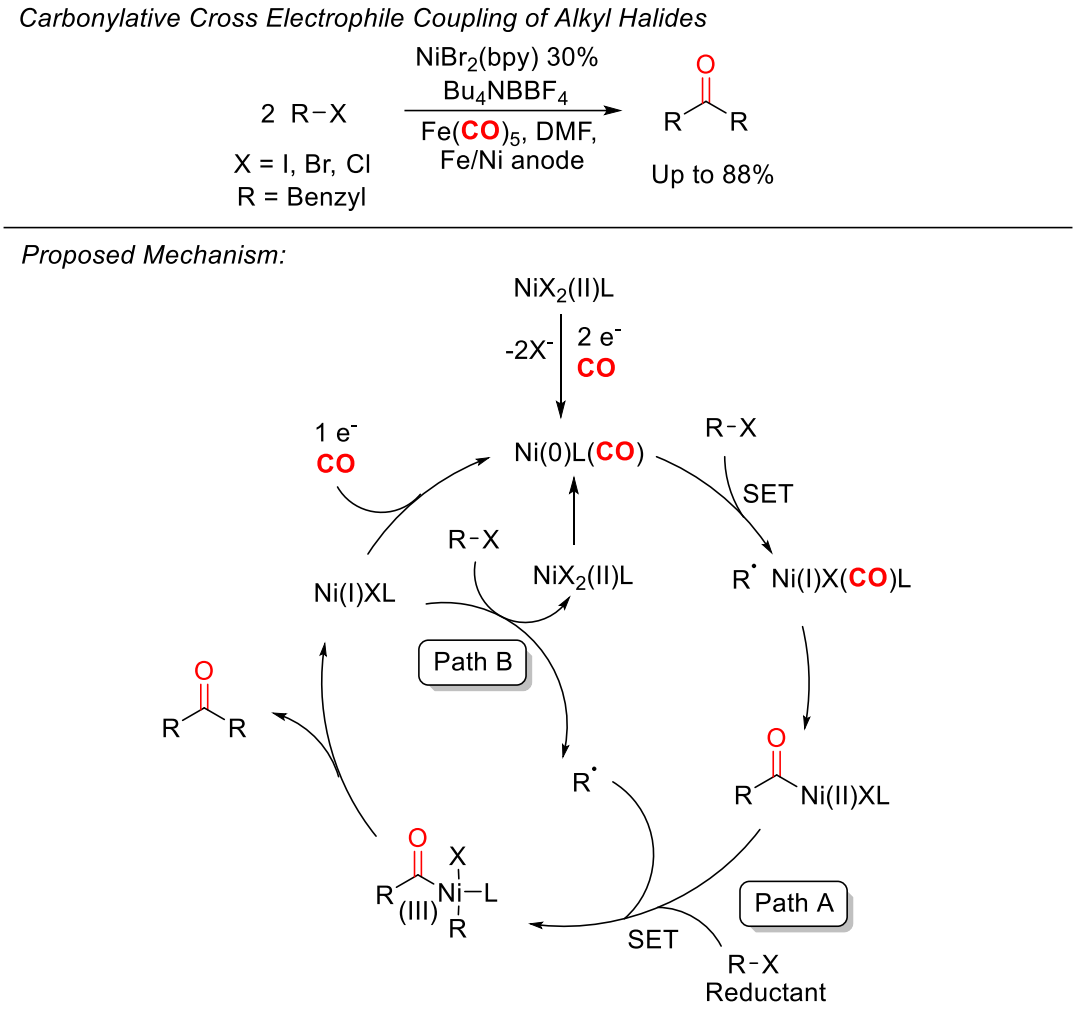

Scheme 1.20. Nickel Catalyzed Carbonylative Coupling of Alkyl Halides

The mechanism by which this Ni(II)-acyl complex reacts with alkyl halides has been probed by several labs. In Troupel's initial report, it was proposed that the second SET event might be facilitated by an initial reduction of the Ni(II)-acyl complex to a Ni(I)-acyl intermediate (Scheme

1.20, path A). However, in their study of a related system (*vide infra*), the Weix lab showed that the reaction between a Ni(II)-acyl complex and alkyl halides was largely unaltered in the presence of a reductant, implying that the Ni(II) intermediate could directly react with the alkyl halide.[109] Nevertheless, certain substrates (e.g. aryl bromides) did show enhanced reactivity and selectivity when a Zn reductant was added. Alternatively, Hu proposed in another related reaction (*vide infra*) a bimetallic mechanism, where an alkyl radical generated by another low-valent Ni complex adds to the Ni(II)-acyl complex to form a Ni(III)-acyl intermediate that can undergo facile reductive elimination (Scheme 1.20, path B).[110]

Nickel catalysts have been exploited by several other labs for the synthesis of unsymmetrical alkyl ketones with alkyl halides. For example, the Gong,[111-112] Weix,[113] and Reisman[114] groups have developed a non-carbonylative version of this reaction by coupling acid chlorides and related acyl electrophiles with alkyl halides to generate ketones (Scheme 1.21a). Alternatively, the Hu group demonstrated the cross-electrophile carbonylative coupling of unactivated alkyl bromides and iodides with *in situ* generated CO (Scheme 1.21b).[109-110] Weix also showed that aryl bromides can be coupled to unactivated alkyl iodides or bromides in the presence of CO to produce alkyl-aryl ketones (Scheme 1.21c).[109] Each of these reactions is also believed to generate a Ni(II)-acyl intermediate that reacts with alkyl halides.

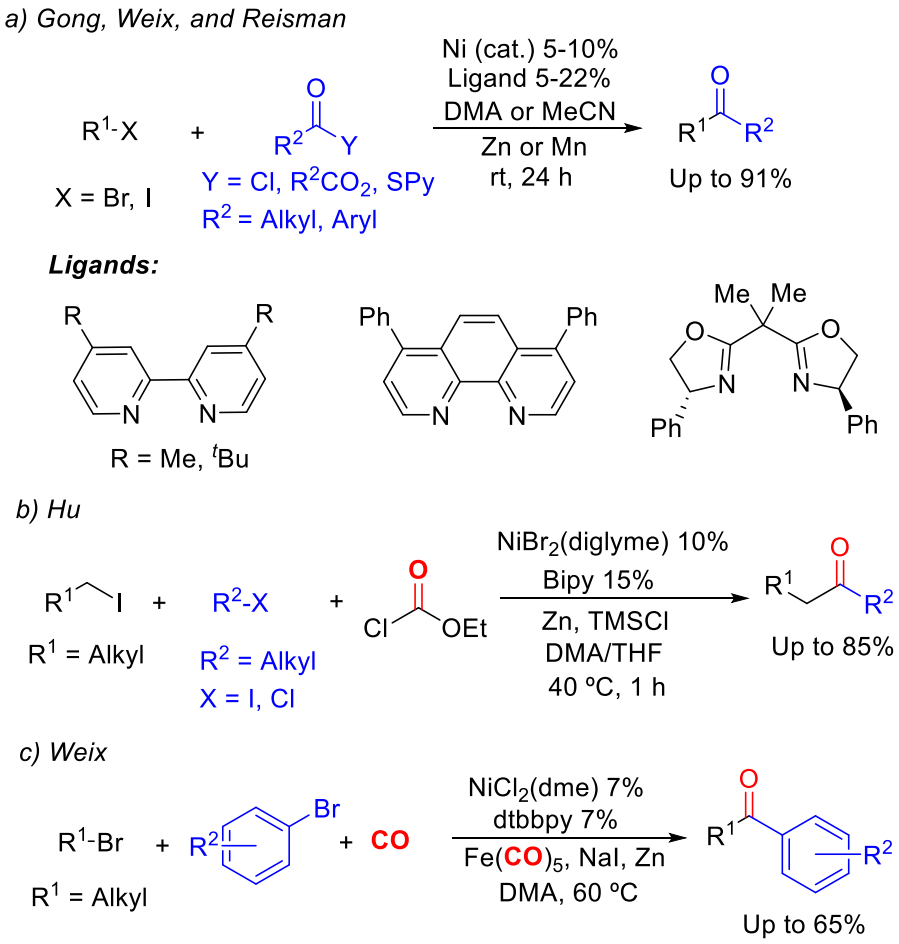

Scheme 1.21. Reductive Nickel Synthesis of Ketones from Alkyl Halides

Recently, the Skrydstrup group has shown that Ni-pincer complexes can be used as catalysts for the non-reductive carbonylative coupling of benzyl or alkyl bromides and alkylzinc reagents (Scheme 1.22).[115-117] Unlike classical carbonylative cross coupling chemistry, the alkyl-zinc reagent and CO are believe to react with the Ni(II)-halide catalyst to form a Ni(II)-acyl intermediate. Similar to above, this nickel-acyl complex is postulated to couple with alkyl halides via a bimetallic mechanism, where one Ni(II)-acyl complex abstracts a bromine atom from the alkyl bromide, while a second Ni(II)-acyl complex adds to the resulting alkyl radical. The latter

forms a Ni(III)-acyl complex that can reductively eliminate the product. The cycle is closed by a comproportionation between Ni(I) and Ni(III) to regenerate the Ni(II) catalyst.[117]

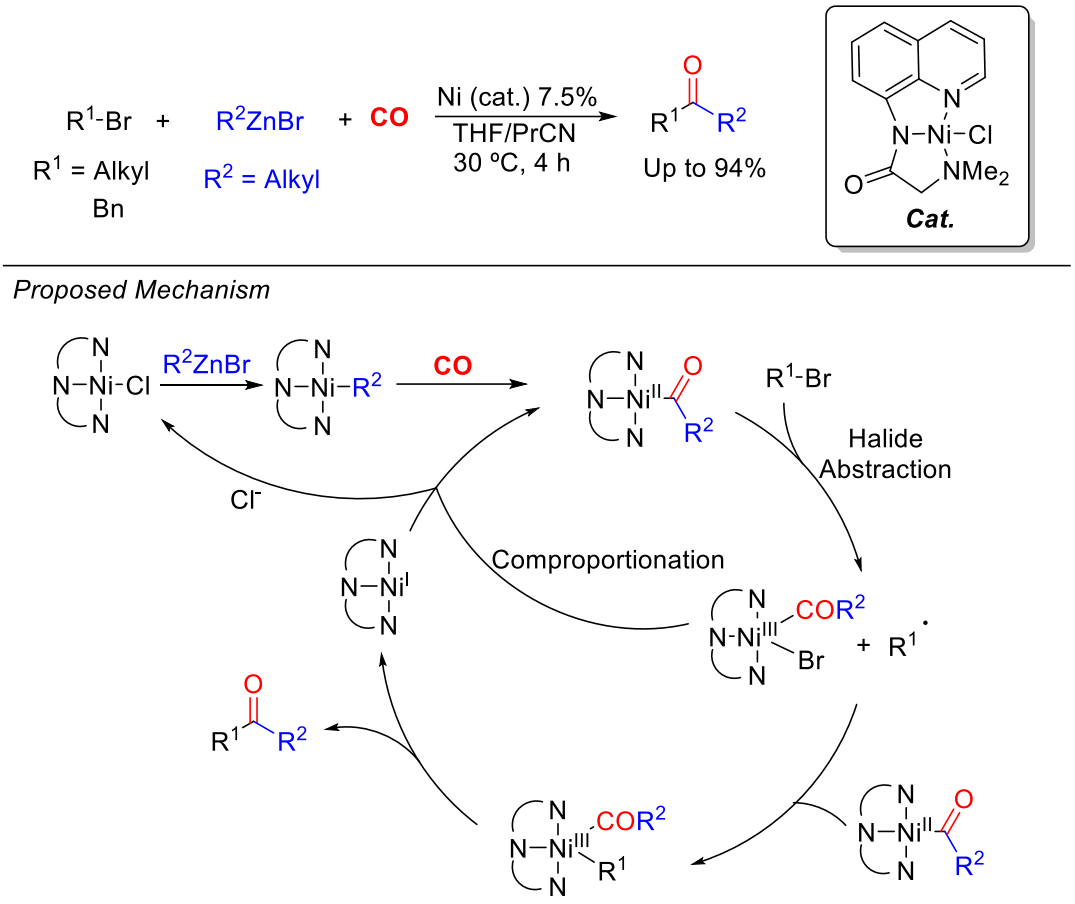

Scheme 1.22. Nickel-Pincer Complexes for Non-Reductive Carbonylative Coupling of Alkyl Halides and Alkylzinc Reagents

1.3.3. Palladium Catalyzed Carbonylation of Alkyl Halides Under UV-Irradiation

Alexanian's work described above (Scheme 1.19) represents an example of a palladium catalyzed carbonylation reaction involving a single electron transfer between the alkyl halide substrate and $L_nPd(0)$ in the ground state. This redox strategy is now commonly seen in photochemical reactions, where the interplay of light irradiation and transition metals can induce SET events. Ryu has done extensive research on developing palladium catalyzed carbonylations assisted by UV-light, in works dating back over a decade.[118-119] These reactions are thought to proceed through a photoinduced SET between the excited state of Pd(0) and an alkyl halide to generate Pd(I) and a radical anion that fragments into a halide anion and a carbon-centered radical (Scheme 1.23).[118] The carbon-halide bond in alkyl halides is relatively weak, and UV light is also established to itself lead to carbon-halogen bond homolysis without palladium.[120] Indeed, control experiments show that the reaction between an alkyl iodide, CO, and alcohol under UV light produces ester in moderate yields after 50 hours of irradiation (Scheme 1.22).[121] Nevertheless, the same reaction with a catalytic amount of palladium proceeds in very high yields and in only a fraction of the time. The noticeable rate enhancement is thought to be due to a photoinduced electron transfer step between $L_nPd(0)$ and the alkyl iodide that more efficiently generates alkyl radicals.[122]

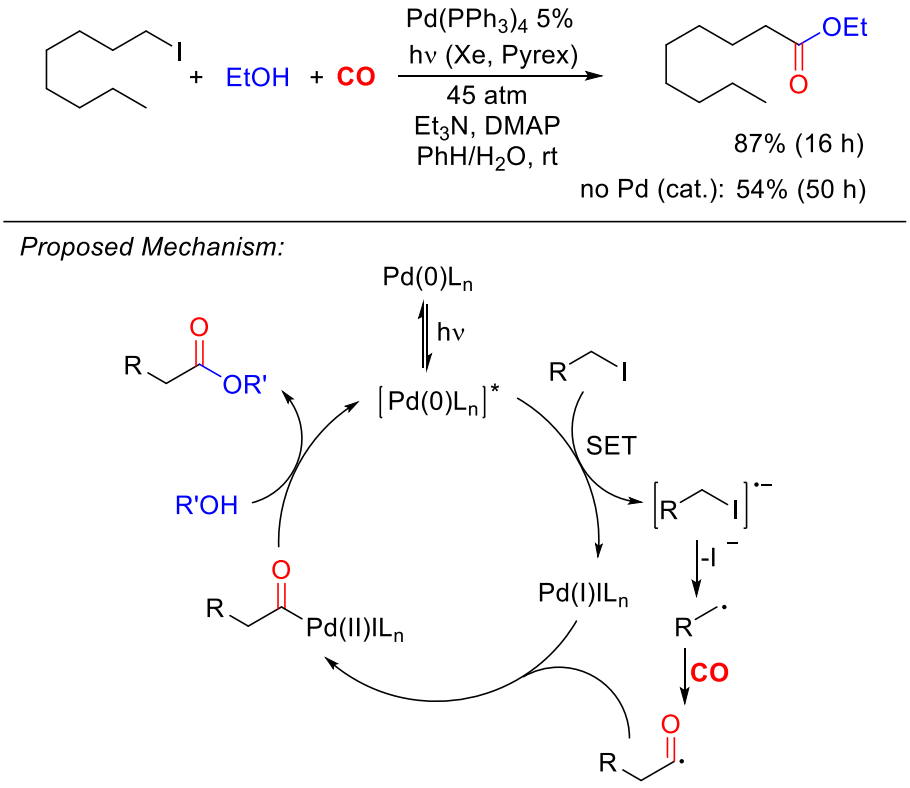

Scheme 1.23. Acceleration Effect of UV-Light on the Palladium Catalyzed Alkoxycarbonylation of Alkyl Iodides

The Ryu group has reported numerous applications of the UV-light assisted palladium catalyzed carbonylation of alkyl iodides. Examples are shown in Scheme 1.24, and include carbonylative coupling with alkynes to produce alkynones,[123] carbonylative Suzuki-Miyaura reactions to generate alkyl-aryl ketones,[124] carbonylative Mizoroki-Heck reactions to produce α,β-unsaturated ketones,[125] and aminocarbonylations to form amides.[126] In each of these, high CO pressures are employed and are thought to help favor the trapping of the alkyl radical.

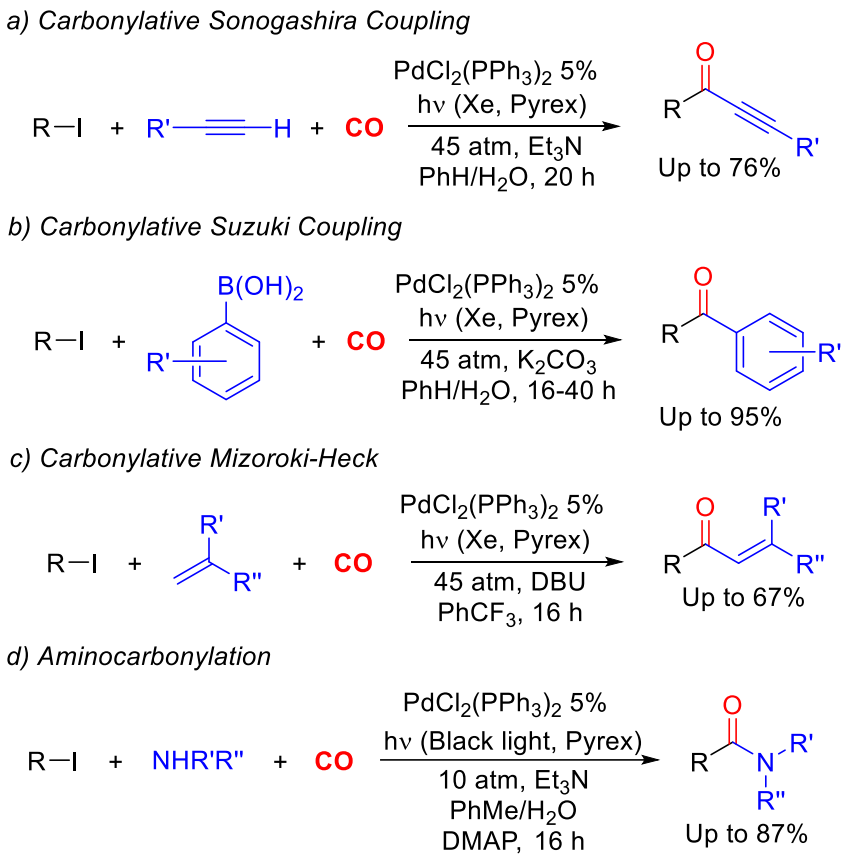

Scheme 1.24. Examples of UV-Light Assisted Palladium Catalyzed Carbonylations of Alkyl Iodides

1.3.4. Alkyl Halide Carbonylation with Visible Light Photoredox Catalysis

Although the use of UV-light in carbonylation reactions has been successful, there are also downsides to this strategy. UV light is sufficiently energetic that it can homolyze other covalent organic bonds, which limits functional group compatibility when applied to complex molecule synthesis.[127-129] Moreover, the equipment needed for of UV light experiments can be expensive, and often requires specialized apparatus. Nevertheless, the idea of using a light as a source of energy to aid carbonylations is very attractive. In recent years, the focus has shifted towards using

more benign light sources, such as compact fluorescent lamps (CFL) and LEDs, to work in tandem with metal and organic photocatalysts (i.e. photoredox catalysis).[130-132] Such systems can provide access to radical reactivity in a controlled, mild, and efficient fashion. In these systems, visible light absorption puts the photocatalyst in its long lived excited state, which can then engage in either single-electron oxidation or reduction with a substrate or co-catalyst. The photocatalyst can then go back to its original oxidation state by reacting with a stoichiometric oxidant/reductant or with a suitable reaction intermediate (Scheme 1.25).

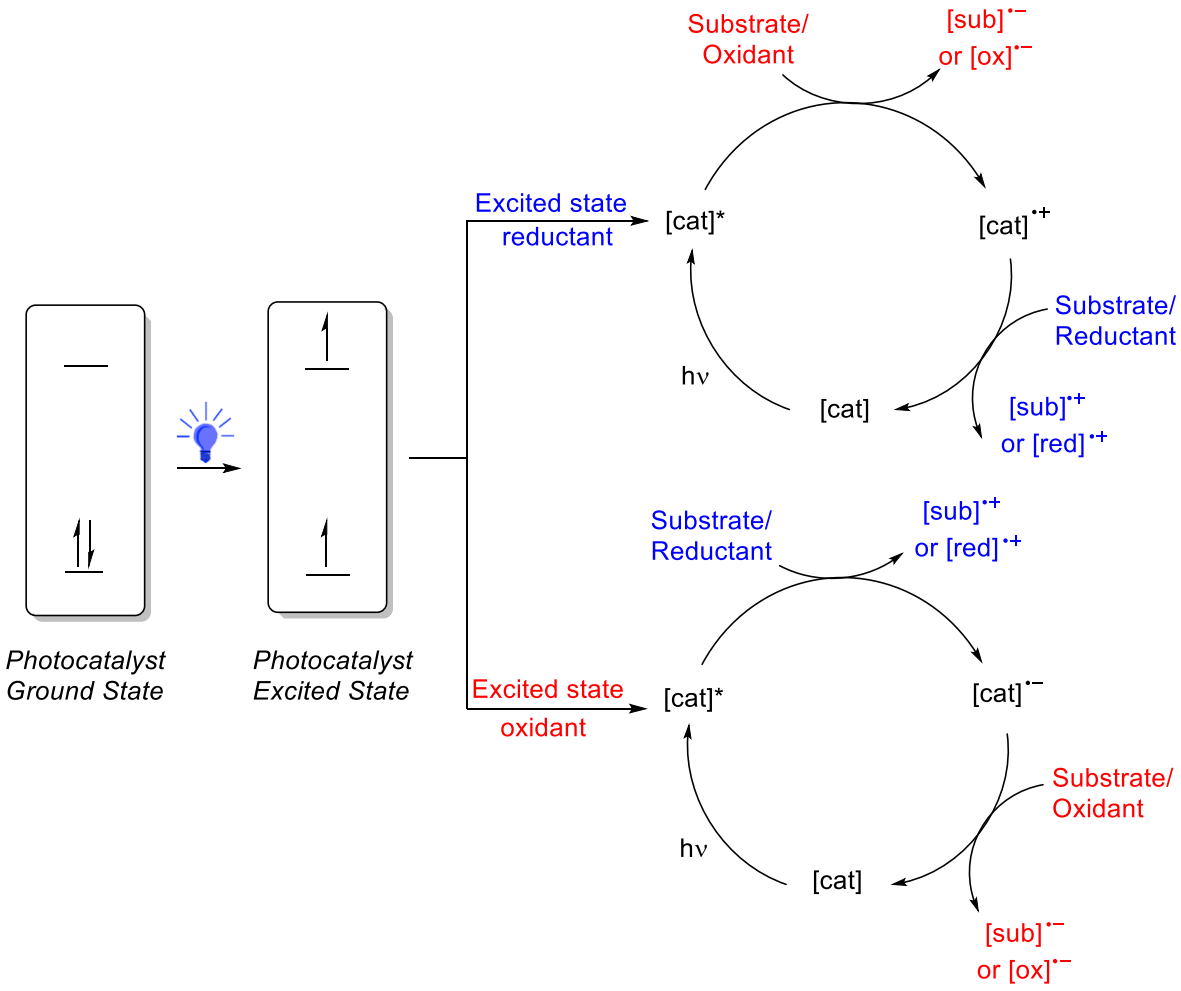

Scheme 1.25. General Mechanism for Visible Light Photoredox Catalysis

A number of laboratories have shown how coupling photocatalysis with traditional transition metal catalysis can be used to access unprecedented reactivity in cross-coupling chemistry.[133-135] These often do so by unlocking radical pathways. Group 10 metals, in particular nickel, have been used successfully in a variety of challenging coupling reactions using alkyl or aryl halides as reagents. However, examples of using visible light photoredox catalysts in carbonylation reactions are very limited. The Wangelin,[136] Xiao,[137] and Gu[138] groups have reported photoredox assisted carbonylation reactions without metals to produce esters and ketones from aryl diazonium salts (Scheme 1.26a). These substrates are easily reduced by common dye photocatalysts and generate aryl radicals that add to CO forming acyl radicals. The latter are believed to be ultimately oxidized by the photoredox catalyst (or substrate) to produce electrophilic acylium ions that react with alcohol or arene nucleophiles to form the product.

More recently, Odell reported the first example of unactivated alkyl iodide aminocarbonylation using photoredox catalysis.[139] Using an $Ir(ppy)_3$ photocatalyst and *ex situ* generated CO, they were able to carbonylate secondary and tertiary alkyl iodides to form amides with visible light (Scheme 1.26b). Notably, aryl iodides were not compatible with this protocol, presumably due to their considerably higher reduction potential.

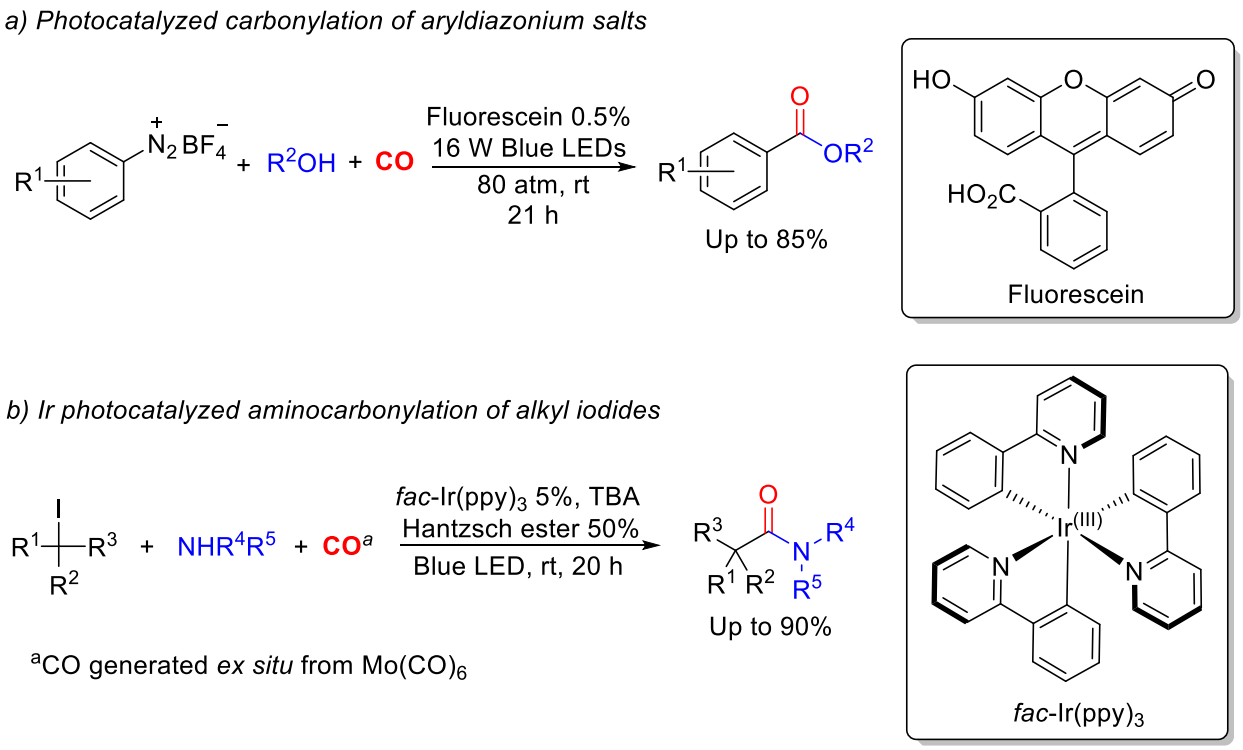

Scheme 1.26. Visible Light Photoredox Catalyzed Approaches to Carbonylation Reactions.

Recently, the Gevorgyan and a number of other labs have developed palladium catalyzed cross-coupling reactions driven by the direct visible light excitation of palladium.[140-142] This approach eliminates the need for the expensive Ir or Ru photocatalysts required in other metallaphotoredox protocols. These works posit that palladium serves two different roles: harvesting photons and mediating the bond forming and breaking steps. As with the UV chemistry of Ryu, the role of visible light is postulated to involve excitation of the Pd(0), which induces SET with the organic halide to favor oxidative addition.[143] Rueping has performed synthetic and DFT studies to support this role of light shown in Scheme 1.27.[144] These visible light/palladium catalyst systems can mediate cross-coupling and related reactions under mild conditions (ambient temperature) and with alkyl halides. Representative examples are shown in Scheme 1.27.[145-148]

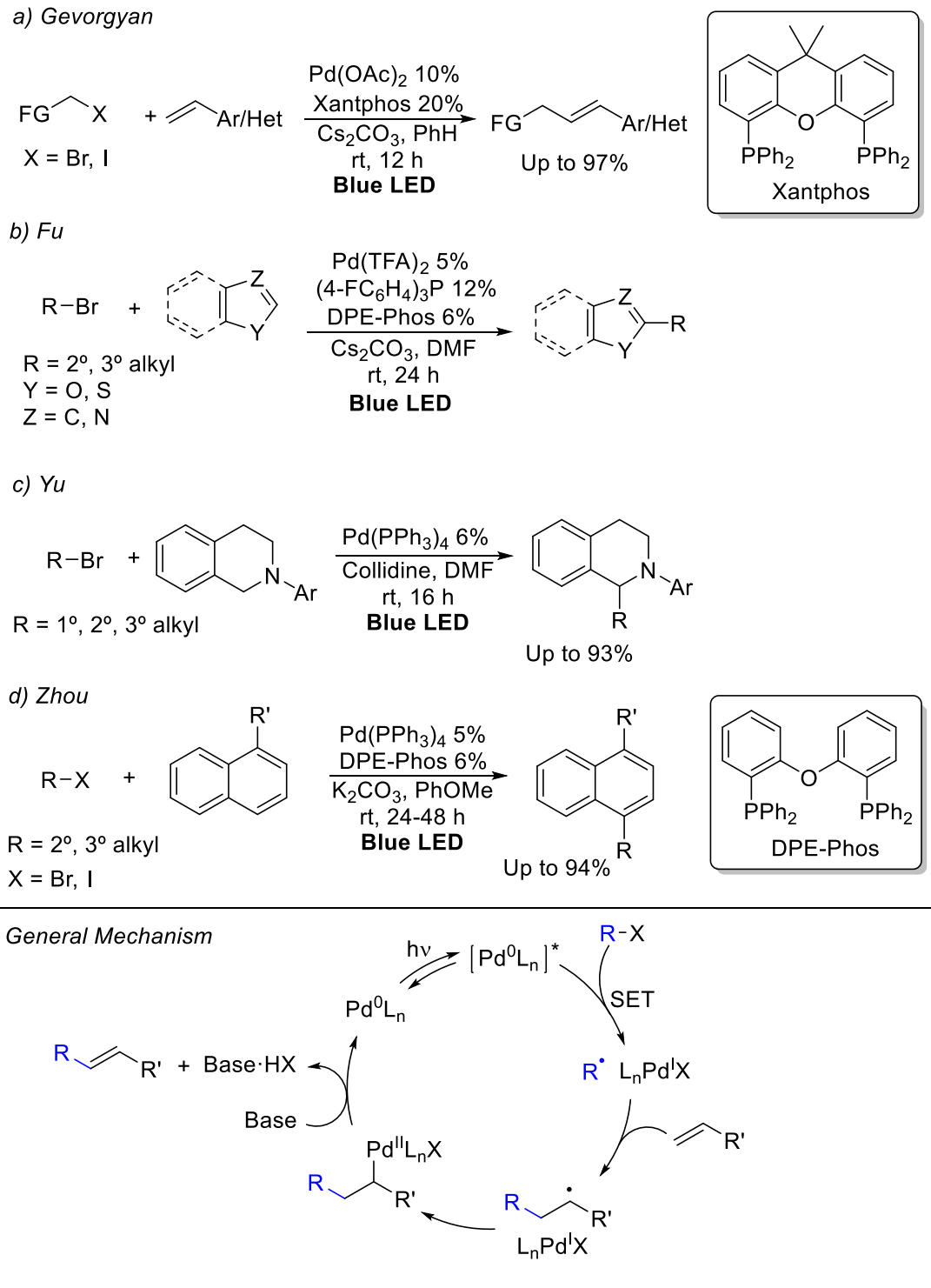

Scheme 1.27. Examples of Visible Light/Palladium Catalyzed Coupling Reactions of Alkyl Halides

The Odell group used this visible light driven strategy in the palladium catalyzed carbonylative Suzuki-Miyaura of alkyl halides (Scheme 1.28).[149] As described above, it was proposed that light induces electron transfer from palladium to the alkyl halide to generate an alkyl radical. They suggested two alternative pathways for the subsequent steps. One involved the addition of the alkyl radical to a Pd-CO bond to form an acyl ligand. The acyl complex could then undergo transmetallation with the aryl-boron reagent and reductively eliminate product (Scheme 1.28 Path A). Alternatively, the alkyl radical could instead add to free CO to generate an acyl radical, which could then activate a second alkyl halide by halogen atom abstraction (Scheme 1.28 Path B). However, no mechanistic evidence was provided for either pathway.

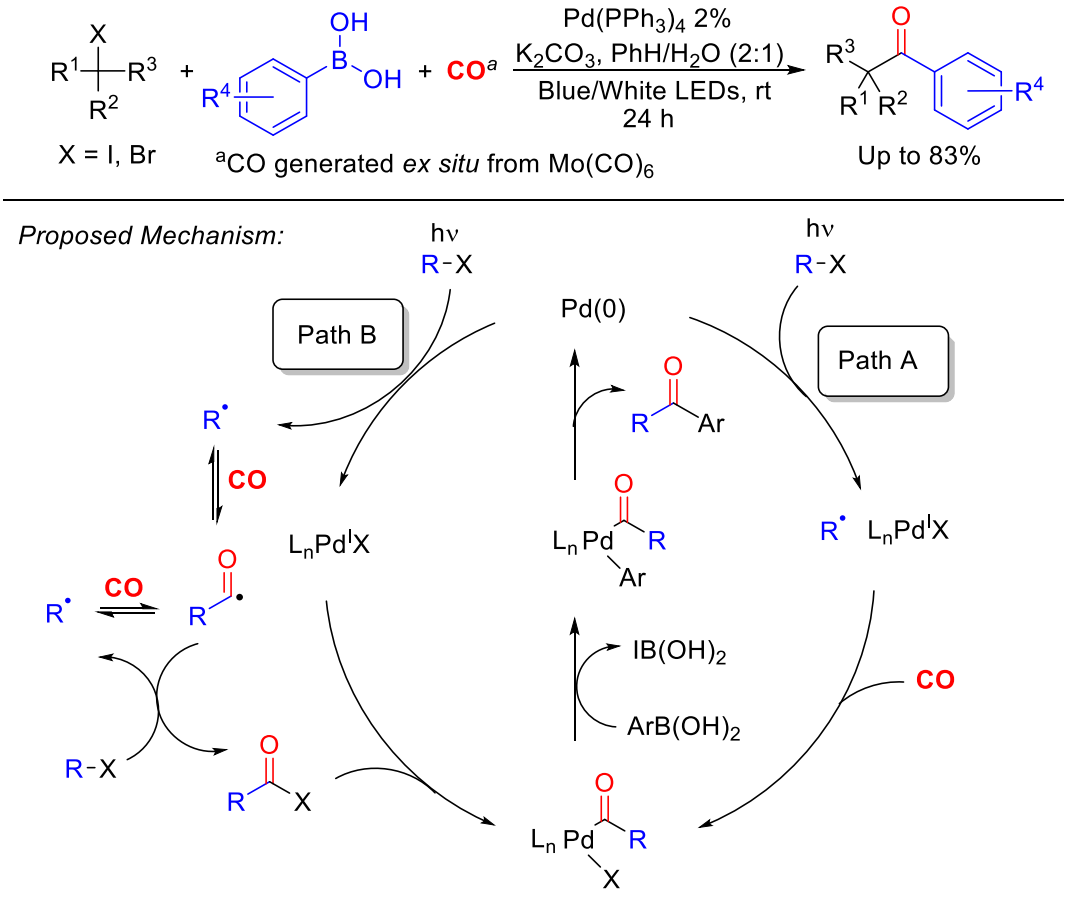

Scheme 1.28. Odell's Visible Light/Palladium Catalyzed Carbonylation of Alkyl Halides.

1.4. Palladium Catalyzed Strategies for the Carbonylative Synthesis of Heterocycles

Heterocyclic compounds are highly sought-after structures in synthetic organic chemistry, and are found in a diverse array of pharmaceuticals, natural products, agrochemicals, and electronic materials, among others (Scheme 1.29).[150-154] In light of the efficiency of carbonylations, there has been growing interest in the application of these reactions to heterocycle synthesis. This topic has been extensively reviewed, including by our own lab.[155-160] In this section, we will briefly discuss general approaches to these reactions, with a particular focus on those involving the use of carbon monoxide to access reactive intermediates, which is the focus of later work in the thesis.

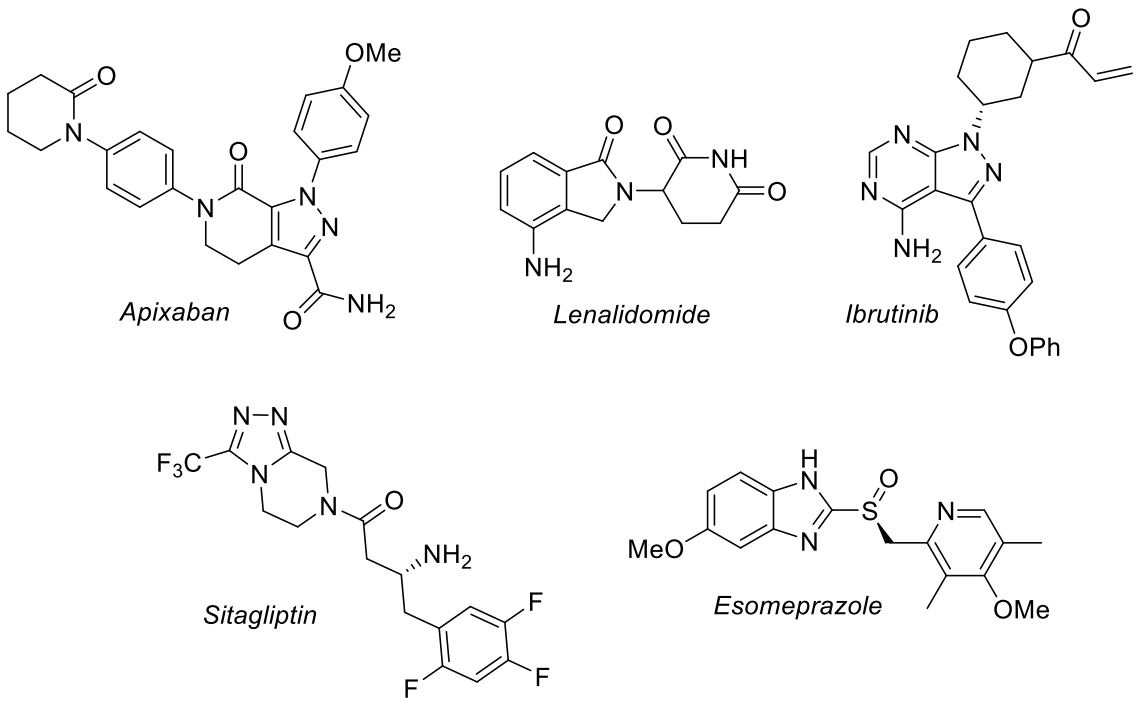

Scheme 1.29. Examples of Top-Grossing Heterocyclic Pharmaceuticals in 2018

1.4.1. Cyclocarbonylation Reactions

A common approach to form heterocycles with CO is via cyclocarbonylation reactions. A diverse range of these transformations have been reported (Scheme 1.30).[161-164] One of the most straightforward is via tethering a nucleophile in the ortho-position to aryl halides.[165-168] These can undergo cyclocarbonylation by themselves (Scheme 1.30a),[169] or in concert with insertion substrates (Scheme 1.30b).[162] Alternatively, cyclocarbonylations can also be performed with alkynyl- or alkenyl-tethered units on either the aryl halide or nucleophile component for carbonylations (Scheme 1.30c),[170] which undergo insertion during carbonylation to afford cyclized products. While the details of these reactions have been discussed elsewhere,[157, 171-172] it is notable that they all lead to the formation of carbonyl-containing heterocyclic products.

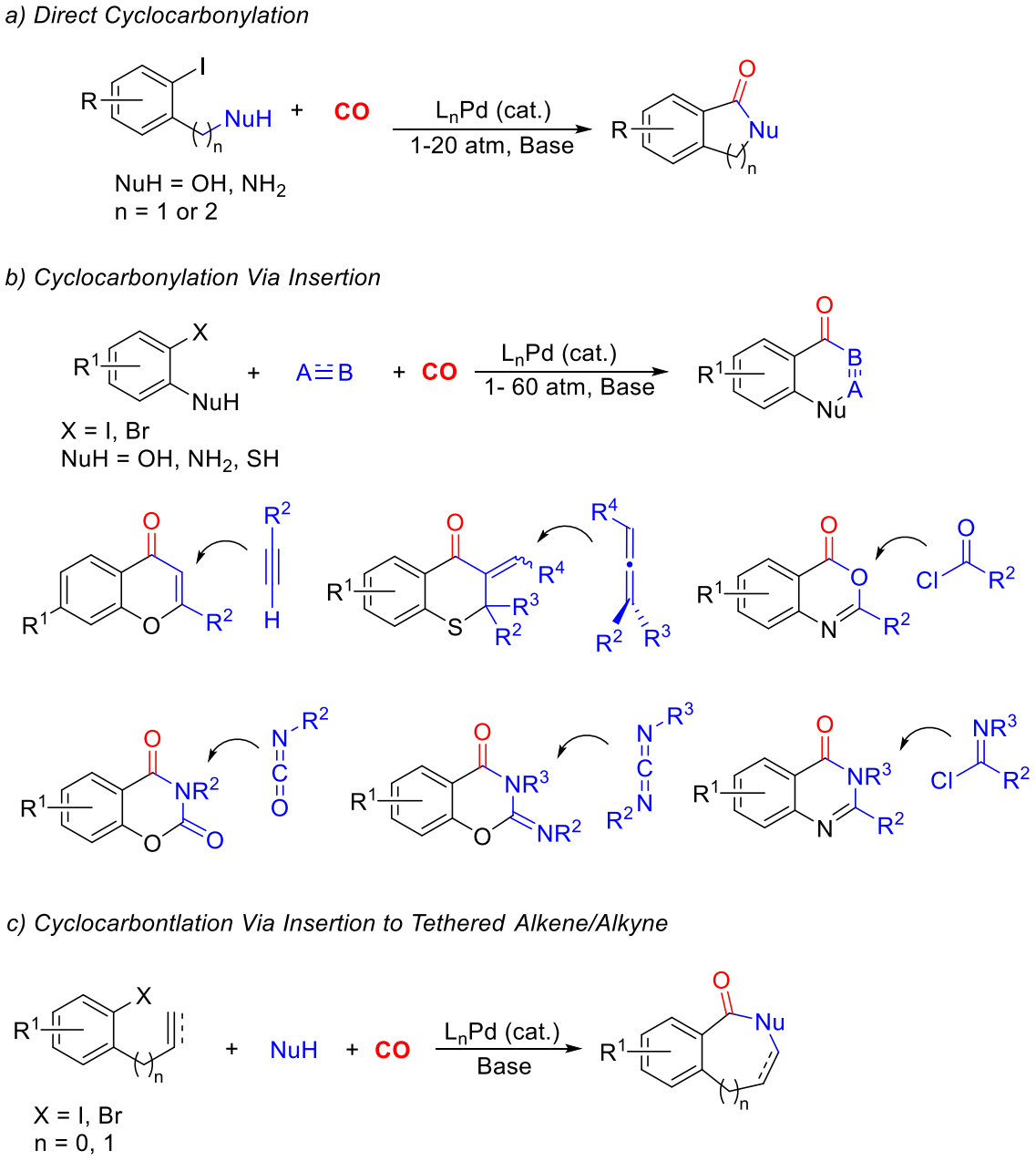

Scheme 1.30. Examples of Cyclocarbonylation Reactions

1.4.2. Carbonylative Ring Expansions

A second general approach to carbonylative heterocycle synthesis is via ring expansion chemistry. These commonly employ strained three or four-membered substrates, wherein CO

insertion into the ring produces a larger and more stable heterocycle. An early example of this approach was reported by Heck in 1963 in the stoichiometric reaction of $HCo(CO)_4$ with oxetane to produce a γ-lactone (Scheme 1.31a).[173] Years later, Alper, Drent, and Coates pioneered the use of various metal catalysts for the carbonylative ring expansion of epoxides and aziridines to form β-lactones and β-lactams, respectively.[174-176] One particularly active catalyst for the carbonylation of epoxides was described by Coates using a $Co(CO)_4^-$ ion paired with chiral aluminum lewis acid (Scheme 1.31b).[177] The latter can coordinate to the epoxide and activate it towards nucleophilic attack from the cobalt anion. This system allowed the ambient temperature enantioselective formation of *cis*-β-lactones.

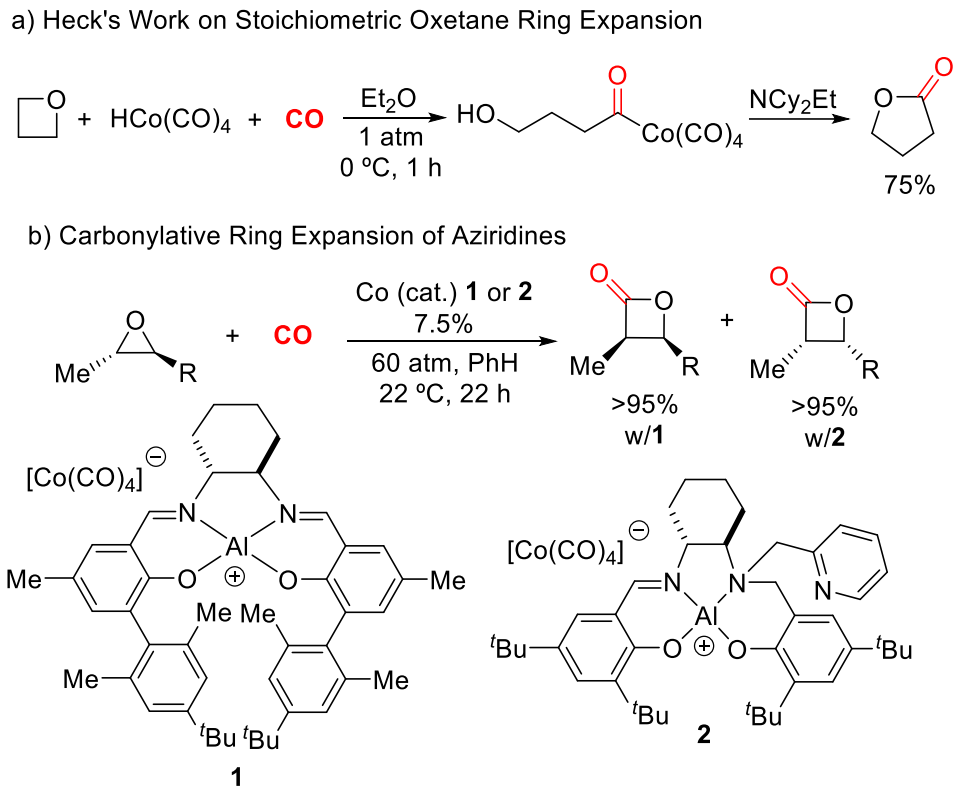

Scheme 1.31. Metal Catalyzed Carbonylative Ring Expansions of Epoxides and Oxetanes

While the above reactions exploit cobalt catalysts, a few palladium systems have also been reported. One example was described by Alper in the carbonylative expansion of 2-methylene or 2-vinyl substituted aziridines (Scheme 1.32a).[178] In these reactions, Pd(0) is postulated to play the role of a nucleophile in an attack on the C-N bond, opening the ring and generating a palladium-allyl intermediate. CO insertion forms a palladium-acyl complex that can ring-close via attack from the nitrogen atom.

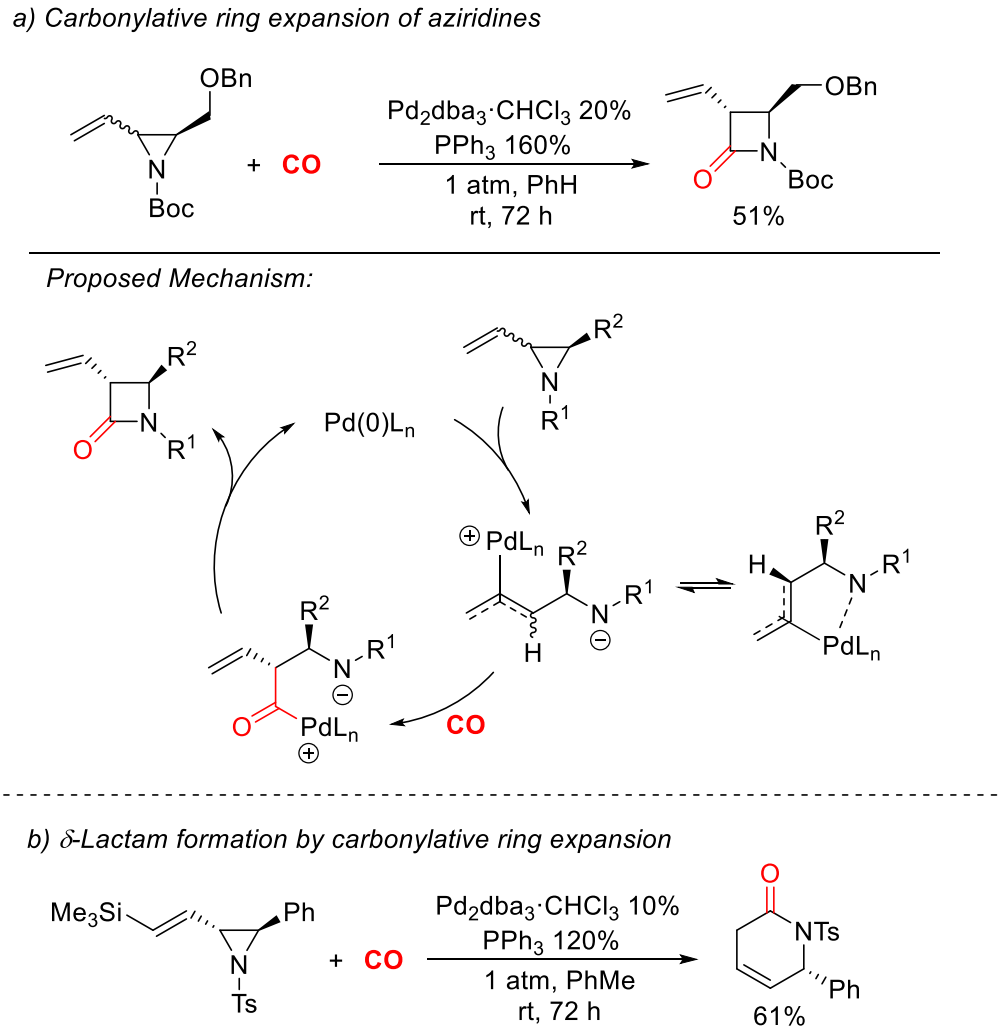

Scheme 1.32. Palladium Catalyzed Carbonylative Aziridine Ring Expansion

The palladium catalyzed carbonylative expansion of larger rings is less thermodynamically driven, and thus there are less examples in the literature. However, Aggarwal reported an unusual reaction of aziridines with CO to form δ-lactams (Scheme 1.32b).[178] This transformation was limited to TMS substituted vinyl aziridines, which undergoes protodesilylation under the reaction conditions.

1.4.3. Heterocycle Synthesis via Cyclization of Carbonylation Products

Another approach to heterocycle synthesis that is more relevant to the research described in this thesis involves exploiting palladium catalyzed carbonylations to build-up reactive products for subsequent cyclization. Among other features, these reactions are amenable to intermolecular reactions to form cyclized products, and therefore can offer more modular approaches to the heterocyclic core. Fewer methods like this have been described. One of the simplest strategies is to exploit the electrophilicity of the carbonyl product generated in carbonylations in coupling with nucleophiles. An example of this approach is the carbonylative buildup of alkynones by palladium catalyzed carbonylative Sonogashira coupling. The Müller group has developed numerous examples of this strategy via the combination of acid chlorides and alkynes, followed by cyclization with nucleophiles (e.g. amidines, hydrazines, hydroxylamines) (Scheme 1.33a).[179-183] The same group has also reported palladium catalyzed carbonylative variants of these reactions utilizing aryl halides, alkynes, and carbon monoxide to generate the intermediate alkynone (Scheme 1.33b).[184-187] In related works, the Mori,[188] Stonehouse,[189] and Beller[190] groups have also shown that these products can react with a variety of nucleophiles to generate nitrogen and oxygen-containing heterocycles (Scheme 1.33c). In each of these systems, the alkynone is postulated to react as an electrophile, leading to either cyclocondensation or 1,3-dipolar cycloaddition.

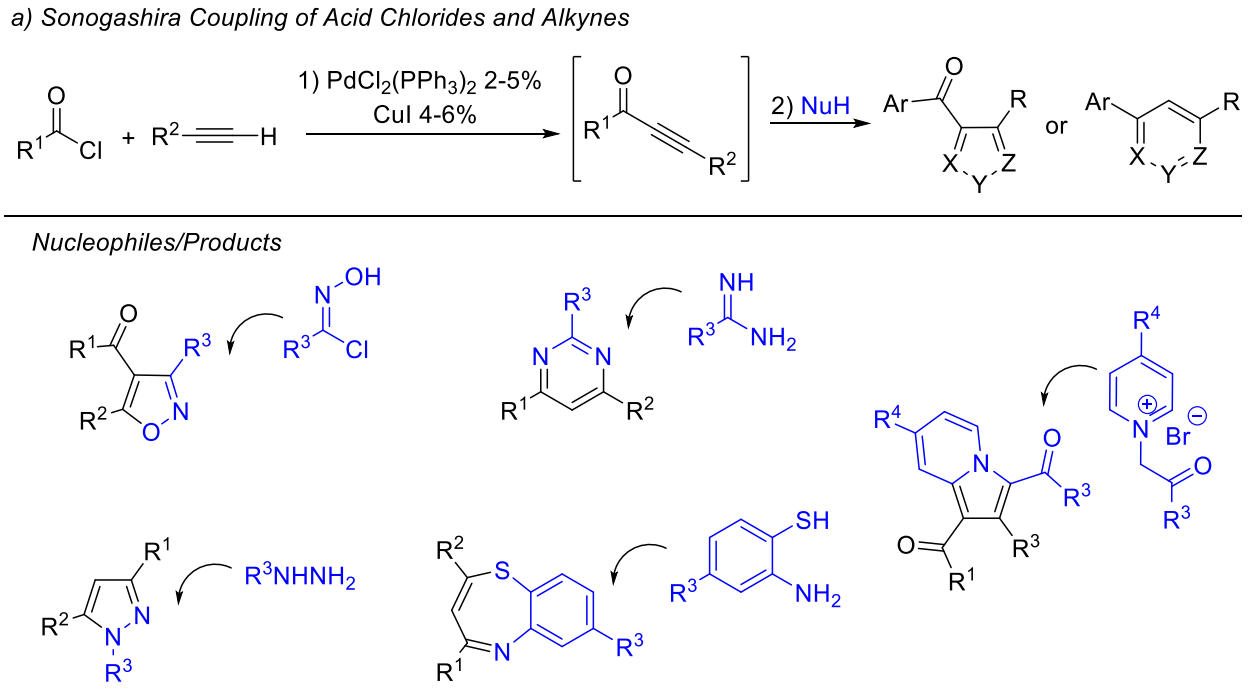

Scheme 1.33. Carbonylative Synthesis of Alkynones as Heterocycle Precursors

The palladium catalyzed formation of esters and amides has also been exploited for heterocycle synthesis. For example, the Meyers[191] and Perry[192-193] labs utilized an intramolecular cyclization

approach for the synthesis of benzoxazoles and benzothiazoles (Scheme 1.34). In these reactions, the carbonylative coupling of aryl halides and amino alcohol/thiols, initially produces an amide product. The later can spontaneously cyclize upon further heating or in the presence of dehydrating reagents to form the heterocyclic product.

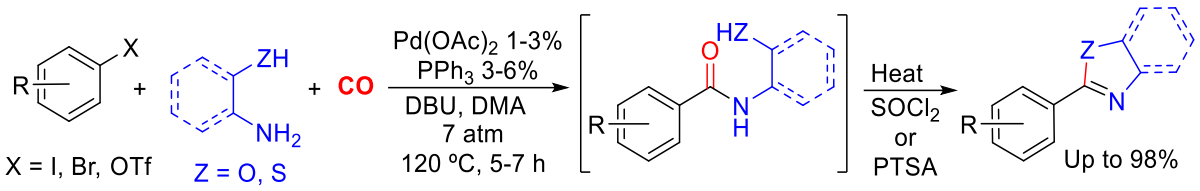

Scheme 1.34. Palladium Catalyzed Synthesis of Benzoxazoles and Benzothiazoles

A related approach to heterocycles was described by the Young group in the synthesis of oxadiazoles. In this transformation, the palladium catalyzed carbonylation of aryl iodide with amidoximes leads to an ester product. This intermediate can then cyclodehydrate to furnish the oxadiazole product (Scheme 1.35).[194]

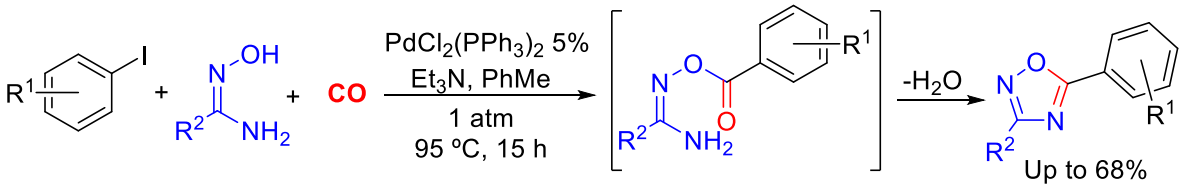

Scheme 1.35. Palladium Catalyzed Synthesis of Oxadiazoles

The Staben group at Genentech developed a similar approach for the synthesis of triazoles. This reaction proceeds through initial palladium catalyzed carbonylation to form an acylated amidine (Scheme 1.36).[195] The latter can react with a hydrazine in a second step to produce an Einhorn-Brunner intermediate.[196] These species are known to spontaneously cyclize to furnish the triazole product.

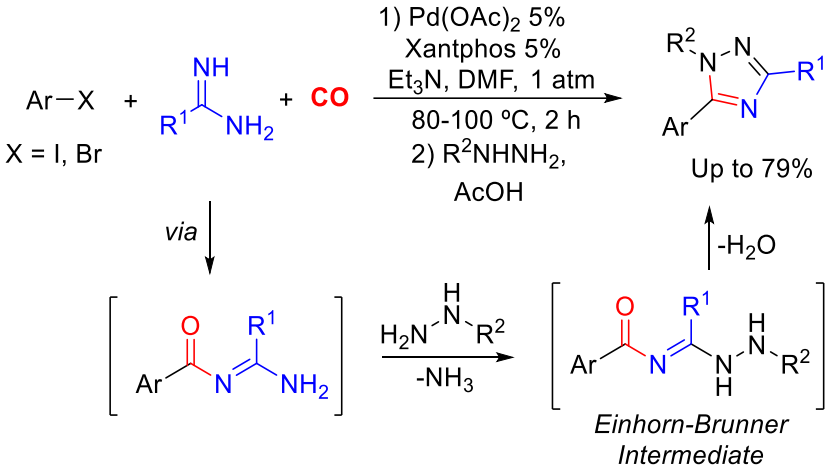

Scheme 1.36. Staben's Carbonylative Synthesis of Triazoles

Our group has reported a different carbonylative approach to heterocycle synthesis. This involves the use of palladium catalyzed carbonylations to generate 1,3-dipoles (i.e. Münchnones) as products. Münchnones, or 1,3-oxazolium-5-oxides, were first discovered in the 1960's,[197-198] and shown to undergo 1,3-dipolar cycloaddition with a variety of substrates by the Huisgen group.[199-200] Their classical synthesis involves the cyclodehydration of α-amido acids, which can limit their accessibility. We showed in 2003 that these dipoles can instead be generated by the palladium catalyzed coupling of imines, acid chlorides and CO (Scheme 1.37).[201] This

transformation can be considered as a variant of amidocarbonylations (Section 1.3.1), where in this case imine and acid chloride react to generate *N*-acyl iminium salt intermediates for carbonylation. However, since there is no water nucleophile present (as there is in amidocarbonylation), the palladium intermediate formed on CO insertion cyclizes upon loss of HCl to form the Münchnone product.

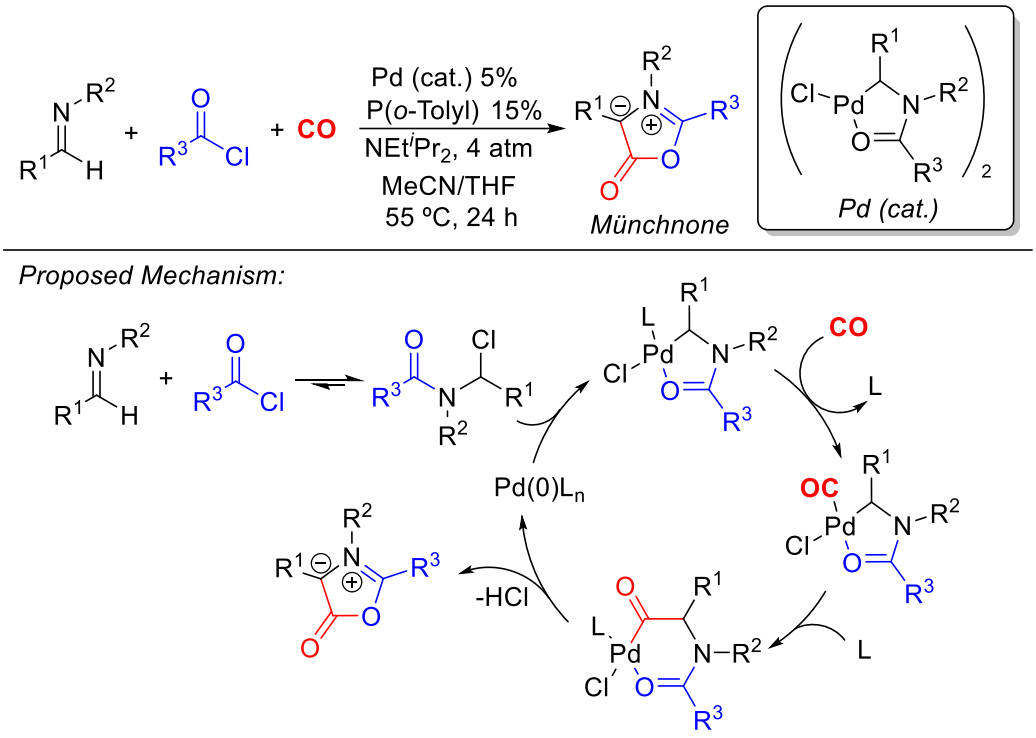

Scheme 1.37. Palladium Catalyzed Cyclocarbonylation of Imines and Acid Chlorides to Form Münchnones

Münchnones can undergo 1,3-dipolar cycloaddition with a range of reagents. The most common example is cycloaddition with alkynes to form pyrroles upon extrusion of CO_2 (Scheme 1.38a).[198] Coupling this step with the palladium catalyzed formation of the 1,3-dipole offers a modular and easily accessible approach to prepare pyrroles (Scheme 1.38b).[202]

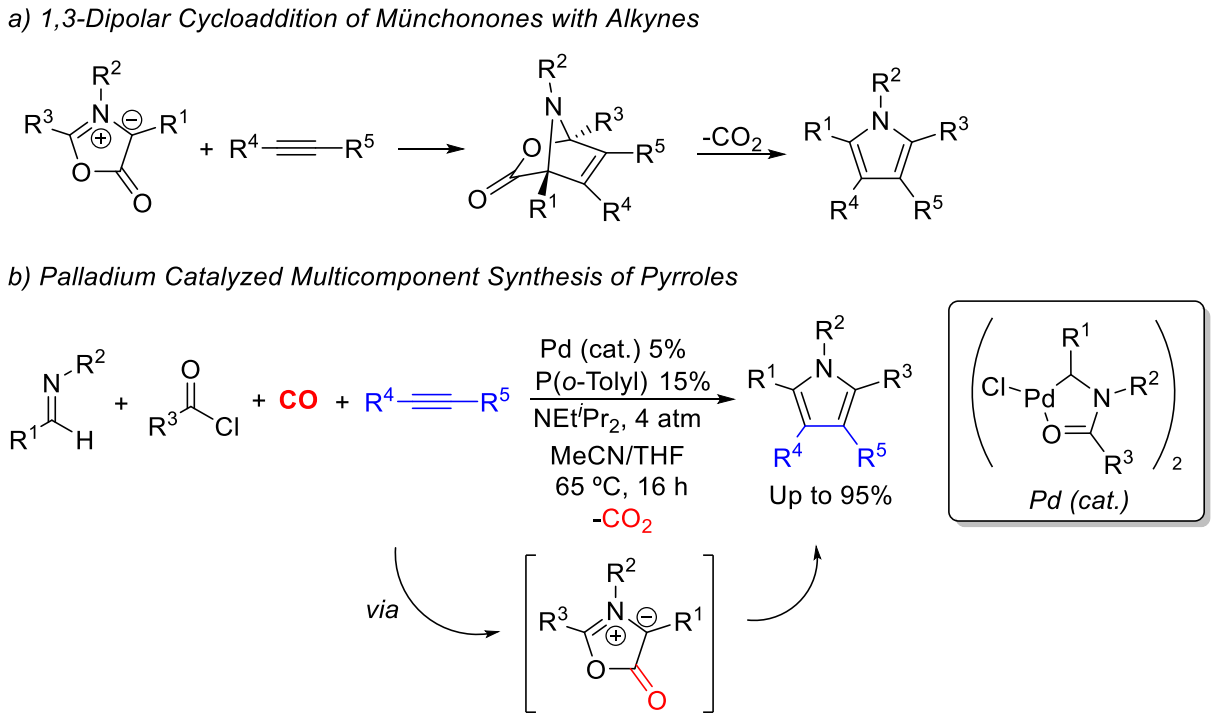

Scheme 1.38. Synthesis of Pyrroles via 1,3-Dipolar Cycloaddition of Münchnones and Alkynes

Building upon this concept, our lab has gone on to show how this strategy can open multicomponent routes to a range of heterocycles. Examples of these are highlighted in Scheme 1.36, and include the synthesis of imidazoles[203] and imidazolinium carboxylates (Scheme 1.39).[201] Alternatively, Münchnones are known to display ketene-like reactivity with imines. This has been exploited to generate multisubstituted β-lactams (Scheme 1.40).[204]

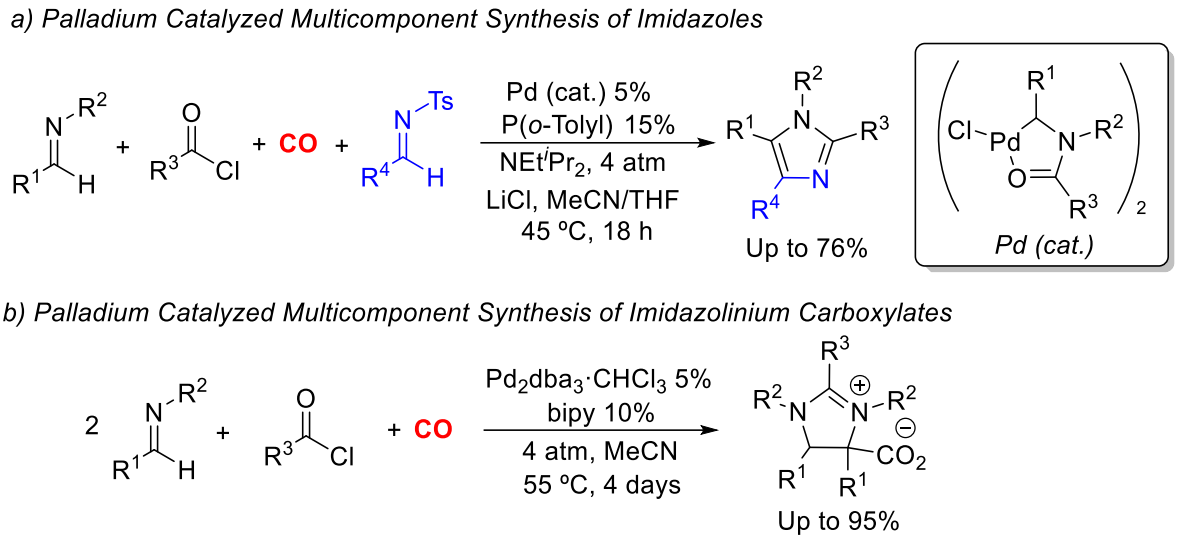

Scheme 1.39. Palladium Catalyzed Multicomponent Synthesis of Imidazoles and Imidazolinium Carboxylates

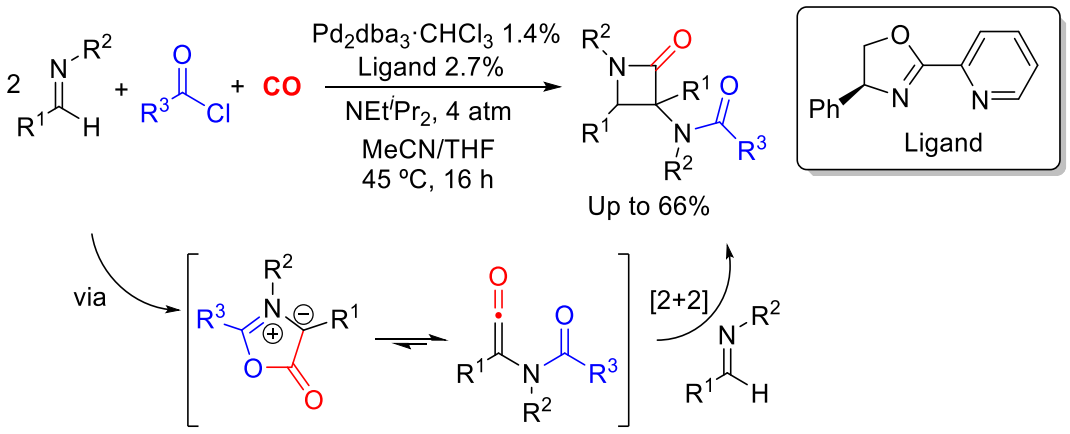

Scheme 1.40. Palladium Catalyzed Carbonylative Synthesis of β-Lactams

While effective, the approaches described above rely on the use of acid chlorides, which are both reactive and require synthesis with toxic and energetic reagents. As an alternative, we recently showed that imidazolinium carboxylates can instead be generated from aryl iodides, imines, and

carbon monoxide utilizing a Pd/P^{t}Bu$_3$ catalyst system (Scheme 1.41).[205] It was proposed that the palladium-acyl intermediate in carbonylations can behave as an electrophile, and thus serve the role of an acid chloride surrogate in the reaction with imines. However, as discussed in Section 1.2.3, our lab eventually found that the palladium catalyzed carbonylation of aryl halides in the presence of chloride can produce acid chlorides. The exact mechanism of this tandem multicomponent reaction is one of the topics discussed in Chapter 2 of this thesis.

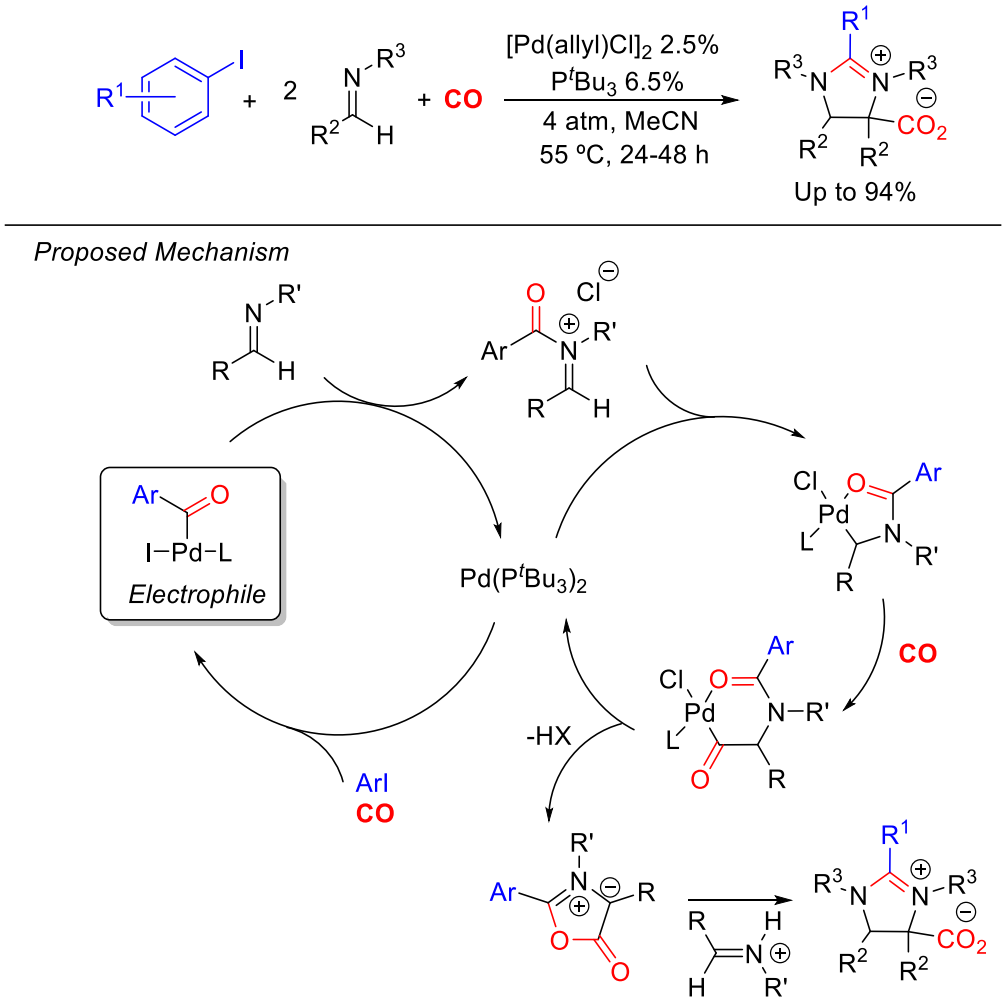

Scheme 1.41. Palladium Catalyzed Carbonylative Synthesis of Imidazolinium Carboxylates

1.5. Overview of the Thesis

Palladium catalyzed carbonylations offer a convenient approach to synthesize valuable carbonyl containing products. These utilize an inexpensive and abundant C1 source, carbon monoxide, and combine it with readily available substrates such as organic halides and nucleophiles. In addition to forming simple esters, amides, or ketones, efforts have been dedicated to exploiting the efficiency of these reactions to construct complex heterocyclic structures. Our laboratory has developed a number of these approaches via the palladium catalyzed coupling of imines, acid chlorides, and carbon monoxide to form 1,3-dipoles (Münchnones). Combining these syntheses with Münchnone cycloaddition can offer one-pot routes to various heterocycles (Section 1.4.3). However, one disadvantage of this approach is the use of acid chlorides, which are reactive and are typically prepared using high energy and toxic reagents (e.g. $SOCl_2$, oxalyl chloride, etc.). Our lab has recently developed a palladium catalyzed carbonylative synthesis of acid chlorides from aryl halides (Section 1.2.3). Considering the broad availability of aryl halides and carbon monoxide, we questioned whether we could couple this palladium catalyzed acid chloride formation with the carbonylative formation of Münchnones. The potential of this reaction was preliminarily developed in our group in the palladium catalyzed synthesis of imidazolinium carboxylates from aryl iodides, imines, and carbon monoxide (Scheme 1.41). However, the mechanism by which this reaction proceeds was unclear.

In Chapter 2, we explore this concept and show how a single $Pd(P^tBu_3)_2$ catalyst can couple aryl iodides, imines, and two equivalents of carbon monoxide to generate Münchonones in high yields. Mechanistic studies suggest that this reaction proceeds via two tandem catalytic reactions. The first produces acid chloride via the combination of aryl iodide, chloride, and CO. The acid

chloride product can then react with imine to produce an α-chloroamide that can then undergo a second carbonylation mediated by the same palladium catalyst to generate a Münchone. The formation of these reactive products was coupled with 1,3-dipolar cycloadditions with alkynes to generate a large variety of structurally complex pyrroles.

In Chapter 3 we elaborate on this concept and show how the palladium catalyzed coupling of aryl iodides, CO, and alkyne-tethered imines can produce fused-ring pyrroles via intramolecular 1,3-dipolar cycloaddition. This not only allows the formation of more complex pyrrole structures, but also eliminates the problems with regioselectivity that are commonly observed in Münchnone 1,3-dipolar cycloaddition. Moreover, combining the Sonogashira coupling of terminal alkynes and aryl iodides with this reaction offers a unique triple tandem catalytic reaction for the synthesis of structurally complex pyrroles.

Chapter 4 describes our efforts to apply this approach to the synthesis of β-lactams by exploiting now the ketene-like reactivity of Münchnones. The palladium catalyzed formation of Münchnone in the presence of excess imine was found to lead to the spontaneous formation of amide substituted β-lactam from aryl iodides, CO, and imines. The use of high temperatures can also allow the use of aryl bromides in this reaction, which are more readily available and inexpensive than aryl iodides. This reaction can also be used to form more complex β-lactam products. For example, using the conditions of Chapter 2 to form Münchnones followed by the addition of a second imine can allow the formation of β-lactams from two different imines. Alternatively, the use of aryl iodide-tethered imines can be used to generate an exocyclic ketene that can react with another imine to form novel spirocyclic β-lactams.

A key aspect of the success of these approaches is the *in situ* generation of acid chloride electrophiles using palladium catalysis. While effective, in order to build up these reactive

products, a palladium catalyst that strongly favors reductive elimination is required. This limits the ability of the system to undergo oxidative addition, and commonly requires reactive aryl iodides, or sometime aryl bromides at elevated temperatures. Aryl chlorides or alkyl halides are not viable substrates in this chemistry. Indeed, as noted in Section 1.3.1, the use of alkyl halides in palladium catalyzed carbonylations remains a challenge, and typically requires harsh reaction conditions and specialized catalysts that would be difficult to incorporate into our acid chloride platform.

In Chapter 5 we address these limitations by rethinking our approach to this palladium catalyzed reaction. Palladium catalyzed coupling reactions are traditionally constrained by conflicting ligand effects, since the factors that favor oxidative addition often inhibit the reverse reductive elimination. An alternative would be to decouple these steps, and instead use external factors to drive the reaction. We show that this can be accomplished with visible light. This exploits visible light excitation directly on palladium to drive oxidative addition of a diverse range of aryl or alkyl halides, in analogy to the research discussed in Section 1.3.4. In addition, we find that light can also drive the reductive elimination of acid chlorides through a new photoprocess: the excitation of the palladium-acyl intermediate. Together, this offers a unique platform to perform palladium catalyzed carbonylations in a general fashion, at ambient temperature, and with classically inaccessible substrates.

1.6. References

1. Miyaura, N., *Cross-Coupling Reactions: A Practical Guide*. Springer-Verlag Berlin Heidelberg: 2002.

2. *Metal-Catalyzed Cross-Coupling Reactions*. 2nd Edition ed.; WILEY-VCH Verlag GmbH & Co. KGaA: 2004.

3. Alberico, D.; Scott, M. E.; Lautens, M. *Chem. Rev.* **2007,** *107*, 174.

4. *New Trends in Cross-Coupling: Theory and Applications*. The Royal Society of Chemistry: 2015.

5. Ruiz-Castillo, P.; Buchwald, S. L. *Chem. Rev.* **2016,** *116*, 12564.

6. Johansson Seechurn, C. C. C.; Kitching, M. O.; Colacot, T. J.; Snieckus, V. *Angew. Chem. Int. Ed.* **2012,** *51*, 5062.

7. Barnard, C. F. J. *Organometallics* **2008,** *27*, 5402.

8. Brennführer, A.; Neumann, H.; Beller, M. *Angew. Chem. Int. Ed.* **2009,** *48*, 4114.

9. Wu, X.-F.; Neumann, H.; Beller, M. *Chem. Soc. Rev.* **2011,** *40*, 4986.

10. Beller, M.; Wu, X.-F., *Transition Metal Catalyzed Carbonylation Reactions*. Springer-Verlag Berlin Heidelberg: 2013.

11. Wu, X.-F.; Fang, X.; Wu, L.; Jackstell, R.; Neumann, H.; Beller, M. *Acc. Chem. Res.* **2014,** *47*, 1041.

12. Jones, J. H. *Platinum Metals Rev* **2000,** *44*, 94.

13. Beller, M.; Steinhoff, B. A.; Zoeller, J. R.; Cole-Hamilton, D. J.; Drent, E.; Wu, X.-F.; Neumann, H.; Ito, S.; Nozaki, K., Carbonylation. In *Applied Homogeneous Catalysis with Organometallic Compounds*, Cornils, B.; Herrmann, W. A.; Beller, M.; Paciello, R., Eds. Wiley-VCH Verlag GmbH & Co. KGaA: 2017.

14. Cornils, B.; Börner, A.; Franke, R.; Zhang, B.; Wiebus, E.; Schmid, K., Hydroformylation. In *Applied Homogeneous Catalysis with Organometallic Compounds*, Cornils, B.; Herrmann, W. A.; Beller, M.; Paciello, R., Eds. Wiley-VCH Verlag GmbH & Co. KGaA: 2017.

15. Schoenberg, A.; Bartoletti, I.; Heck, R. F. *J. Org. Chem.* **1974,** *39*, 3318.

16. Schoenberg, A.; Heck, R. F. *J. Org. Chem.* **1974,** *39*, 3327.

17. Schoenberg, A.; Heck, R. F. *J. Am. Chem. Soc.* **1974,** *96*, 7761.

18. Garrou, P. E.; Heck, R. F. *J. Am. Chem. Soc.* **1976,** *98*, 4115.

19. Ozawa, F.; Kawasaki, N.; Okamoto, H.; Yamamoto, T.; Yamamoto, A. *Organometallics* **1987,** *6*, 1640.

20. Moser, W. R.; Wang, A. W.; Kildahl, N. K. *J. Am. Chem. Soc.* **1988,** *110*, 2816.

21. Yamamoto, A.; Ozawa, F.; Osakada, K.; Huang, L. *Pure & Appl. Chem.* **1991,** *63*, 687.

22. Hu, Y.; Liu, J.; Lü, Z.; Luo, X.; Zhang, H.; Lan, Y.; Lei, A. *J. Am. Chem. Soc.* **2010,** *132*, 3153.

23. Amatore, C.; Carre, E.; Jutand, A.; M'Barki, M. A. *Organometallics* **1995,** *14*, 1818.

24. Johansson Seechurn, C. C. C.; Parisel, S. L.; Colacot, T. J. *J. Org. Chem.* **2011,** *76*, 7918.

25. DeAngelis, A. J.; Gildner, P. G.; Chow, R.; Colacot, T. J. *J. Org. Chem.* **2015,** *80*, 6794.

26. Parshall, G. W. *J. Am. Chem. Soc.* **1974,** *96*, 2360.

27. Portnoy, M.; Milstein, D. *Organometallics* **1993,** *12*, 1655.

28. Hamann, B. C.; Hartwig, J. F. *J. Am. Chem. Soc.* **1998,** *120*, 7369.

29. Qadir, M.; Möchel, T.; Hii, K. K. *Tetrahedron* **2000,** *56*, 7975.

30. Quesnel, J. S.; Moncho, S.; Ylijoki, K. E. O.; Torres, G. M.; Brothers, E. N.; Bengali, A. A.; Arndtsen, B. A. *Chem. Eur. J.* **2016,** *22*, 15107.

31. Milstein, D. *J. Chem. Soc., Chem. Commun.* **1986**, 817.

32. Huser, M.; Youinou, M.-T.; Osborn, J. A. *Angew. Chem. Int. Ed.* **1989,** *28*, 1386.

33. Gillie, A.; Stille, J. K. *J. Am. Chem. Soc.* **1980,** *102*, 4933.

34. Ragaini, F.; Cenini, S. *J. Mol. Catal. A: Chem.* **1996,** *109*, 1.

35. Ragaini, F.; Gasperini, M.; Cenini, S.; Arnera, L.; Caselli, A.; Macchi, P.; Casati, N. *Chem. Eur. J.* **2009,** *15*, 8064.

36. Wang, J. Y.; Strom, A. E.; Hartwig, J. F. *J. Am. Chem. Soc.* **2018,** *140*, 7979.

37. Wu, X.-F.; Neumann, H.; Beller, M. *Chem. Asian J.* **2010,** *5*, 2168.

38. Wu, X.-F.; Neumann, H.; Beller, M. *ChemCatChem* **2010,** *2*, 509.

39. Shen, C.; Fink, C.; Laurenczy, G.; Dyson, P. J.; Wu, X.-F. *Chem. Commun.* **2017,** *53*, 12422.

40. Klaus, S.; Neumann, H.; Zapf, A.; Strübing, D.; Hübner, S.; Almena, J.; Riermeier, T.; Groß, P.; Sarich, M.; Krahnert, W.-R.; Rossen, K.; Beller, M. *Angew. Chem. Int. Ed.* **2006,** *45*, 154.

41. Albaneze-Walker, J.; Bazaral, C.; Leavey, T.; Dormer, P. G.; Murry, J. A. *Org. Lett.* **2004,** *6*, 2097.

42. Martinelli, J. R.; Watson, D. A.; Freckmann, D. M. M.; Barder, T. E.; Buchwald, S. L. *J. Org. Chem.* **2008,** *73*, 7102.

43. Grushin, V. V.; Alper, H. *J. Chem. Soc., Chem. Commun.* **1992**, 611.

44. Ben-David, Y.; Portnoy, M.; Milstein, D. *J. Am. Chem. Soc.* **1989,** *111*, 8742.

45. Beller, M.; Mägerlein, W.; Indolese, A. F.; Fischer, C. *Synthesis* **2001,** *2001*, 1098.

46. Jimenez-Rodriguez, C.; Eastham, G. R.; Cole-Hamilton, D. J. *Dalton Transactions* **2005**, 1826.

47. Martinelli, J. R.; Clark, T. P.; Watson, D. A.; Munday, R. H.; Buchwald, S. L. *Angew. Chem. Int. Ed.* **2007,** *46*, 8460.

48. Mägerlein, W.; Indolese, A. F.; Beller, M. *Angew. Chem. Int. Ed.* **2001,** *40*, 2856.

49. Blaser, H.-U.; Diggelmann, M.; Meier, H.; Naud, F.; Scheppach, E.; Schnyder, A.; Studer, M. *J. Org. Chem.* **2003,** *68*, 3725.

50. Sonntag, N. O. V. *Chem. Rev.* **1953,** *52*, 237.

51. Watson, D. A.; Fan, X.; Buchwald, S. L. *J. Org. Chem.* **2008,** *73*, 7096.

52. Miloserdov, F. M.; Grushin, V. V. *Angew. Chem. Int. Ed.* **2012,** *51*, 3668.

53. Burhardt, M. N.; Taaning, R. H.; Skrydstrup, T. *Org. Lett.* **2013,** *15*, 948.

54. de Almeida, A. M.; Andersen, T. L.; Lindhardt, A. T.; de Almeida, M. V.; Skrydstrup, T. *J. Org. Chem.* **2015,** *80*, 1920.

55. Ueda, T.; Konishi, H.; Manabe, K. *Org. Lett.* **2013,** *15*, 5370.

56. Quesnel, J. S.; Fabrikant, A.; Arndtsen, B. A. *Chemical Science* **2016,** *7*, 295.

57. Lagueux-Tremblay, P.-L.; Fabrikant, A.; Arndtsen, B. A. *ACS Catalysis* **2018,** *8*, 5350.

58. Quesnel, J. S.; Arndtsen, B. A. *J. Am. Chem. Soc.* **2013,** *135*, 16841.

59. Quesnel, J. S.; Kayser, L. V.; Fabrikant, A.; Arndtsen, B. A. *Chem. Eur. J.* **2015,** *21*, 9550.

60. Tjutrins, J.; Arndtsen, B. A. *J. Am. Chem. Soc.* **2015,** *137*, 12050.

61. Garrison Kinney, R.; Tjutrins, J.; Torres, G. M.; Liu, N. J.; Kulkarni, O.; Arndtsen, B. A. *Nature Chemistry* **2017,** *10*, 193.

62. Lee, Y. H.; Morandi, B. *Nature Chemistry* **2018,** *10*, 1016.

63. De La Higuera Macias, M.; Arndtsen, B. A. *J. Am. Chem. Soc.* **2018,** *140*, 10140.

64. Fang, X.; Cacherat, B.; Morandi, B. *Nature Chemistry* **2017,** *9*, 1105.

65. Lovering, F.; Bikker, J.; Humblet, C. *J. Med. Chem.* **2009,** *52*, 6752.

66. Stille, J. K., Oxidative addition and reductive elimination. In *The Metal—Carbon Bond (1985)*, John Wiley & Sons, Inc.: 1985; Vol. 2.

67. Pearson, R. G.; Figdore, P. E. *J. Am. Chem. Soc.* **1980,** *102*, 1541.

68. Ariafard, A.; Lin, Z. *Organometallics* **2006,** *25*, 4030.

69. Straub, B. F., *Organotransition Metal Chemistry: From Bonding to Catalysis*. University Science Books: 2010.

70. Labinger, J. A.; Braus, R. J.; Dolphin, D.; Osborn, J. A. *J. Chem. Soc. D Chem Commun.* **1970**, 612b.

71. Griffin, T. R.; Cook, D. B.; Haynes, A.; Pearson, J. M.; Monti, D.; Morris, G. E. *J. Am. Chem. Soc.* **1996,** *118*, 3029.

72. Stille, J. K.; Lau, K. S. Y. *Acc. Chem. Res.* **1977,** *10*, 434.

73. Stadtmüller, H.; Vaupel, A.; Tucker, C. E.; Stüdemann, T.; Knochel, P. *Chem. Eur. J.* **1996,** *2*, 1204.

74. Hosokawa, T.; Maitlis, P. M. *J. Am. Chem. Soc.* **1973,** *95*, 4924.

75. Bryndza, H. E. *J. Chem. Soc., Chem. Commun.* **1985**, 1696.

76. Strömberg, S.; Zetterberg, K.; E. M. Siegbahn, P. *J. Chem. Soc., Dalton Trans.* **1997**, 4147.

77. Gøgsig, T. M., Background. In *New Discoveries on the β-Hydride Elimination*, Gøgsig, T. M., Ed. Springer Berlin Heidelberg: Berlin, Heidelberg, 2012; pp 1.

78. Wu, X.-F.; Neumann, H.; Beller, M. *Tetrahedron Lett.* **2010,** *51*, 6146.

79. Nasielski, J.; Hadei, N.; Achonduh, G.; Kantchev, E. A. B.; O'Brien, C. J.; Lough, A.; Organ, M. G. *Chem. Eur. J.* **2010,** *16*, 10844.

80. Hayashi, T.; Konishi, M.; Kobori, Y.; Kumada, M.; Higuchi, T.; Hirotsu, K. *J. Am. Chem. Soc.* **1984,** *106*, 158.

81. Lu, X., *Control of the β-Hydride Elimination Making Palladium-Catalyzed Coupling Reactions more Diversified*. Springer Science: 2005; Vol. 35, p 73.

82. Wu, L.; Fang, X.; Liu, Q.; Jackstell, R.; Beller, M.; Wu, X.-F. *ACS Catalysis* **2014,** *4*, 2977.

83. Lin, J. J.; Knifton, J. F., Amidocarbonylation. In *Homogeneous Transition Metal Catalyzed Reactions*, American Chemical Society: 1992; Vol. 230, pp 235.

84. Beller, M.; Eckert, M. *Angew. Chem. Int. Ed.* **2000,** *39*, 1010.

85. Wakamatsu, H.; Uda, J.; Yamakami, N. *J. Chem. Soc. D Chem Commun.* **1971**, 1540.

86. Wakamatsu, H.; Furukawa, J.; Yamakami, N. *Bull. Chem. Soc. Jpn.* **1971,** *44*, 288.

87. Parnaud, J.-J.; Campari, G.; Pino, P. *J. Mol. Catal.* **1979,** *6*, 341.

88. Beller, M.; Eckert, M.; Holla, E. W. *J. Org. Chem.* **1998,** *63*, 5658.

89. Beller, M.; Moradi, W. A.; Eckert, M.; Neumann, H. *Tetrahedron Lett.* **1999,** *40*, 4523.

90. Beller, M. *Synlett* **1999,** *1999*, 108.

91. Gördes, D.; Neumann, H.; von Wangelin, A. J.; Fischer, C.; Drauz, K.; Krimmer, H.-P.; Beller, M. *Adv. Synth. Catal.* **2003,** *345*, 510.

92. Freed, D. A.; Kozlowski, M. C. *Tetrahedron Lett.* **2001,** *42*, 3403.

93. Enzmann, A.; Eckert, M.; Ponikwar, W.; Polborn, K.; Schneiderbauer, S.; Beller, M.; Beck, W. *Eur. J. Inorg. Chem.* **2004,** *2004*, 1330.

94. Beller, M.; Eckert, M.; Moradi, W. A.; Neumann, H. *Angew. Chem. Int. Ed.* **1999,** *38*, 1454.

95. Beller, M.; Eckert, M.; Geissler, H.; Napierski, B.; Rebenstock, H.-P.; Holla, E. W. *Chem. Eur. J.* **1998,** *4*, 935.

96. Hisao, U.; Kosukegawa, O.; Ishii, Y.; Yugari, H.; Fuchikami, T. *Tetrahedron Lett.* **1989,** *30*, 4403.

97. Urata, H.; Ishii, Y.; Fuchikami, T. *Tetrahedron Lett.* **1989,** *30*, 4407.

98. Urata, H.; Maekawa, H.; Takahashi, S.; Fuchikami, T. *J. Org. Chem.* **1991,** *56*, 4320.

99. Urata, H.; Hu, N.-X.; Maekawa, H.; Fuchikami, T. *Tetrahedron Lett.* **1991,** *32*, 4733.

100. Urata, H.; Kinoshita, Y.; Asanuma, T.; Kosukegawa, O.; Fuchikami, T. *J. Org. Chem.* **1991,** *56*, 4996.

101. Bloome, K. S.; Alexanian, E. J. *J. Am. Chem. Soc.* **2010,** *132*, 12823.

102. Sargent, B. T.; Alexanian, E. J. *J. Am. Chem. Soc.* **2016,** *138*, 7520.

103. Tasker, S. Z.; Standley, E. A.; Jamison, T. F. *Nature* **2014,** *509*, 299.

104. Ananikov, V. P. *ACS Catalysis* **2015,** *5*, 1964.

105. Standley, E. A.; Tasker, S. Z.; Jensen, K. L.; Jamison, T. F. *Acc. Chem. Res.* **2015,** *48*, 1503.

106. Iwasaki, T.; Kambe, N. *Top. Curr. Chem.* **2016,** *374*, 66.

107. Lin; Liu, L.; Fu, Y.; Luo, S.-W.; Chen, Q.; Guo, Q.-X. *Organometallics* **2004,** *23*, 2114.

108. Dolhem, E.; Oçafrain, M.; Nédélec, J. Y.; Troupel, M. *Tetrahedron* **1997,** *53*, 17089.

109. Wotal, A. C.; Ribson, R. D.; Weix, D. J. *Organometallics* **2014,** *33*, 5874.

110. Shi, R.; Hu, X. *Angew. Chem. Int. Ed.* **2019,** *58*, 7454.

111. Wu, F.; Lu, W.; Qian, Q.; Ren, Q.; Gong, H. *Org. Lett.* **2012,** *14*, 3044.

112. Yin, H.; Zhao, C.; You, H.; Lin, K.; Gong, H. *Chem. Commun.* **2012,** *48*, 7034.

113. Wotal, A. C.; Weix, D. J. *Org. Lett.* **2012,** *14*, 1476.

114. Cherney, A. H.; Kadunce, N. T.; Reisman, S. E. *J. Am. Chem. Soc.* **2013,** *135*, 7442.

115. Andersen, T. L.; Donslund, A. S.; Neumann, K. T.; Skrydstrup, T. *Angew. Chem. Int. Ed.* **2018,** *57*, 800.

116. Neumann, K. T.; Donslund, A. S.; Andersen, T. L.; Nielsen, D. U.; Skrydstrup, T. *Chem. Eur. J.* **2018,** *24*, 14946.

117. Donslund, A. S.; Neumann, K. T.; Corneliussen, N. P.; Grove, E. K.; Herbstritt, D.; Daasbjerg, K.; Skrydstrup, T. *Chem. Eur. J.* **2019,** *25*, 9856.

118. Sumino, S.; Fusano, A.; Fukuyama, T.; Ryu, I. *Acc. Chem. Res.* **2014,** *47*, 1563.

119. Matsubara, H.; Kawamoto, T.; Fukuyama, T.; Ryu, I. *Acc. Chem. Res.* **2018,** *51*, 2023.

120. Kropp, P. J. *Acc. Chem. Res.* **1984,** *17*, 131.

121. Fukuyama, T.; Nishitani, S.; Inouye, T.; Morimoto, K.; Ryu, I. *Org. Lett.* **2006,** *8*, 1383.

122. Fusano, A.; Sumino, S.; Nishitani, S.; Inouye, T.; Morimoto, K.; Fukuyama, T.; Ryu, I. *Chem. Eur. J.* **2012,** *18*, 9415.

123. Fusano, A.; Fukuyama, T.; Nishitani, S.; Inouye, T.; Ryu, I. *Org. Lett.* **2010,** *12*, 2410.

124. Sumino, S.; Ui, T.; Ryu, I. *Org. Lett.* **2013,** *15*, 3142.

125. Sumino, S.; Ui, T.; Hamada, Y.; Fukuyama, T.; Ryu, I. *Org. Lett.* **2015,** *17*, 4952.

126. Sumino, S.; Fusano, A.; Fukuyama, T.; Ryu, I. *Synlett* **2012,** *23*, 1331.

127. Schwarzenbach, R. P.; Gschwend, P. M.; Imboden, D. M., Direct Photolysis. In *Environmental Organic Chemistry*, Schwarzenbach, R. P.; Gschwend, P. M.; Imboden, D. M., Eds. 2005; pp 611.

128. Schultz, D. M.; Yoon, T. P. *Science* **2014,** *343*, 1239176.

129. Raviola, C.; Protti, S.; Ravelli, D.; Fagnoni, M. *Green Chemistry* **2019,** *21*, 748.

130. Prier, C. K.; Rankic, D. A.; MacMillan, D. W. C. *Chem. Rev.* **2013,** *113*, 5322.

131. Shaw, M. H.; Twilton, J.; MacMillan, D. W. C. *J. Org. Chem.* **2016,** *81*, 6898.

132. Romero, N. A.; Nicewicz, D. A. *Chem. Rev.* **2016,** *116*, 10075.

133. Levin, M. D.; Kim, S.; Toste, F. D. *ACS Central Science* **2016,** *2*, 293.

134. Tellis, J. C.; Kelly, C. B.; Primer, D. N.; Jouffroy, M.; Patel, N. R.; Molander, G. A. *Acc. Chem. Res.* **2016,** *49*, 1429.

135. Twilton, J.; Le, C.; Zhang, P.; Shaw, M. H.; Evans, R. W.; MacMillan, D. W. C. *Nature Reviews Chemistry* **2017,** *1*, 0052.

136. Majek, M.; Jacobi von Wangelin, A. *Angew. Chem. Int. Ed.* **2015,** *54*, 2270.

137. Guo, W.; Lu, L.-Q.; Wang, Y.; Wang, Y.-N.; Chen, J.-R.; Xiao, W.-J. *Angew. Chem.* **2015,** *127*, 2293.

138. Gu, L.; Jin, C.; Liu, J. *Green Chemistry* **2015,** *17*, 3733.

139. Chow, S. Y.; Stevens, M. Y.; Åkerbladh, L.; Bergman, S.; Odell, L. R. *Chem. Eur. J.* **2016,** *22*, 9155.

140. Parasram, M.; Chuentragool, P.; Sarkar, D.; Gevorgyan, V. *J. Am. Chem. Soc.* **2016,** *138*, 6340.

141. Wang, G.-Z.; Shang, R.; Cheng, W.-M.; Fu, Y. *J. Am. Chem. Soc.* **2017,** *139*, 18307.

142. Parasram, M.; Gevorgyan, V. *Chem. Soc. Rev.* **2017,** *46*, 6227.

143. Chuentragool, P.; Kurandina, D.; Gevorgyan, V. *Angew. Chem. Int. Ed. 0*.

144. Kancherla, R.; Muralirajan, K.; Maity, B.; Zhu, C.; Krach, P. E.; Cavallo, L.; Rueping, M. *Angew. Chem. Int. Ed.* **2019,** *58*, 3412.

145. Kurandina, D.; Parasram, M.; Gevorgyan, V. *Angew. Chem. Int. Ed.* **2017,** *56*, 14212.

146. Zhou, W.-J.; Cao, G.-M.; Shen, G.; Zhu, X.-Y.; Gui, Y.-Y.; Ye, J.-H.; Sun, L.; Liao, L.-L.; Li, J.; Yu, D.-G. *Angew. Chem. Int. Ed.* **2017,** *56*, 15683.

147. Cheng, W.-M.; Shang, R.; Fu, Y. *Nature Communications* **2018,** *9*, 5215.

148. Wang, G.-Z.; Shang, R.; Fu, Y. *Synthesis* **2018,** *50*, 2908.

149. Roslin, S.; Odell, L. R. *Chem. Commun.* **2017,** *53*, 6895.

150. Baumann, M.; Baxendale, I. R. *Beilstein J. Org. Chem.* **2013,** *9*, 2265.

151. Degennaro, L.; Trinchera, P.; Luisi, R. *Chem. Rev.* **2014,** *114*, 7881.

152. Pitts, C. R.; Lectka, T. *Chem. Rev.* **2014,** *114*, 7930.

153. Rotstein, B. H.; Zaretsky, S.; Rai, V.; Yudin, A. K. *Chem. Rev.* **2014,** *114*, 8323.

154. Zhang, B.; Studer, A. *Chem. Soc. Rev.* **2015,** *44*, 3505.

155. Arndtsen, B. A. *Chem. Eur. J.* **2009,** *15*, 302.

156. Gabriele, B.; Mancuso, R.; Salerno, G. *Eur. J. Org. Chem.* **2012,** *2012*, 6825.

157. Wu, X.-F.; Neumann, H.; Beller, M. *Chem. Rev.* **2013,** *113*, 1.

158. *Transition Metal Catalyzed Carbonylative Synthesis of Heterocycles*. Springer International Publishing: 2016.

159. Allen, B. D. W.; Lakeland, C. P.; Harrity, J. P. A. *Chem. Eur. J.* **2017,** *23*, 13830.

160. Shen, C.; Wu, X.-F. *Chem. Eur. J.* **2017,** *23*, 2973.

161. Brunner, M.; Alper, H. *J. Org. Chem.* **1997,** *62*, 7565.

162. Acerbi, A.; Carfagna, C.; Costa, M.; Mancuso, R.; Gabriele, B.; Della Ca', N. *Chem. Eur. J.* **2018,** *24*, 4835.

163. Wu, X.-F.; Schranck, J.; Neumann, H.; Beller, M. *Chem. Eur. J.* **2011,** *17*, 12246.

164. Yang, Q.; Alper, H. *J. Org. Chem.* **2010,** *75*, 948.

165. Gabriele, B.; Salerno, G.; Veltri, L.; Costa, M.; Massera, C. *Eur. J. Org. Chem.* **2001,** *2001*, 4607.

166. Ma, S.; Wu, B.; Jiang, X. *J. Org. Chem.* **2005,** *70*, 2588.

167. Tang, S.; Yu, Q.-F.; Peng; Li, J.-H.; Zhong, P.; Tang, R.-Y. *Org. Lett.* **2007,** *9*, 3413.

168. Lu, S.-M.; Alper, H. *J. Am. Chem. Soc.* **2008,** *130*, 6451.

169. Kadnikov, D. V.; Larock, R. C. *J. Org. Chem.* **2003,** *68*, 9423.

170. Cao, H.; Vieira, T. O.; Alper, H. *Org. Lett.* **2011,** *13*, 11.

171. Omae, I. *Coord. Chem. Rev.* **2011,** *255*, 139.

172. Yan, D.-M.; Crudden, C. M.; Chen, J.-R.; Xiao, W.-J. *ACS Catalysis* **2019,** *9*, 6467.

173. Heck, R. F. *J. Am. Chem. Soc.* **1963,** *85*, 1460.

174. Alper, H.; Urso, F.; Smith, D. J. H. *J. Am. Chem. Soc.* **1983,** *105*, 6737.

175. Alper, H.; Hamel, N. *Tetrahedron Lett.* **1987,** *28*, 3237.

176. Piotti, M. E.; Alper, H. *J. Am. Chem. Soc.* **1996,** *118*, 111.

177. Mulzer, M.; Whiting, B. T.; Coates, G. W. *J. Am. Chem. Soc.* **2013,** *135*, 10930.

178. Fontana, F.; Tron, G. C.; Barbero, N.; Ferrini, S.; Thomas, S. P.; Aggarwal, V. K. *Chem. Commun.* **2010,** *46*, 267.

179. Karpov, A. S.; Müller, T. J. J. *Org. Lett.* **2003,** *5*, 3451.

180. D'Souza, D. M.; Müller, T. J. J. *Nature Protocols* **2008,** *3*, 1660.

181. Willy, B.; Frank, W.; Rominger, F.; Müller, T. J. J. *J. Organomet. Chem.* **2009,** *694*, 942.

182. Rotzoll, S.; Willy, B.; Schönhaber, J.; Rominger, F.; Müller, T. J. J. *Eur. J. Org. Chem.* **2010,** *2010*, 3516.

183. Rotaru, A. V.; Druta, I. D.; Oeser, T.; Müller, T. J. J. *Helv. Chim. Acta* **2005,** *88*, 1798.

184. Karpov, A. S.; Merkul, E.; Rominger, F.; Müller, T. J. J. *Angew. Chem. Int. Ed.* **2005,** *44*, 6951.

185. Merkul, E.; Boersch, C.; Frank, W.; Müller, T. J. J. *Org. Lett.* **2009,** *11*, 2269.

186. Denißen, M.; Nordmann, J.; Dziambor, J.; Mayer, B.; Frank, W.; Müller, T. J. J. *RSC Advances* **2015,** *5*, 33838.

187. Moni, L.; Denißen, M.; Valentini, G.; Müller, T. J. J.; Riva, R. *Chem. Eur. J.* **2015,** *21*, 753.

188. Mohamed Ahmed, M. S.; Kobayashi, K.; Mori, A. *Org. Lett.* **2005,** *7*, 4487.

189. Stonehouse, J. P.; Chekmarev, D. S.; Ivanova, N. V.; Lang, S.; Pairaudeau, G.; Smith, N.; Stocks, M. J.; Sviridov, S. I.; Utkina, L. M. *Synlett* **2008,** *2008*, 100.

190. Wu, X.-F.; Neumann, H.; Beller, M. *Chem. Eur. J.* **2010,** *16*, 12104.

191. Meyers, A. I.; Robichaud, A. J.; McKennon, M. J. *Tetrahedron Lett.* **1992,** *33*, 1181.

192. Perry, R. J.; Wilson, B. D. *Macromolecules* **1994,** *27*, 40.

193. Perry, R. J.; Wilson, B. D. *Organometallics* **1994,** *13*, 3346.

194. Young, J. R.; DeVita, R. J. *Tetrahedron Lett.* **1998,** *39*, 3931.

195. Staben, S. T.; Blaquiere, N. *Angew. Chem. Int. Ed.* **2010,** *49*, 325.

196. Atkinson, M. R.; Polya, J. B. *Journal of the Chemical Society (Resumed)* **1952**, 3418.

197. Huisgen, R.; Gotthardt, H.; Bayer, H. O. *Angew. Chem. Int. Ed.* **1964,** *3*, 135.

198. Huisgen, R.; Gotthardt, H.; Bayer, H. O.; Schaefer, F. C. *Angew. Chem. Int. Ed.* **1964,** *3*, 136.

199. Gingrich, H. L.; Baum, J. S., Mesoionic Oxazoles. In *Chemistry of Heterocyclic Compounds*, Turchi, I. J., Ed. John Wiley & Sons, Inc.: 2008; pp 731.

200. Lopchuk, J. M., Mesoionics. In *Metalation of Azoles and Related Five-Membered Ring Heterocycles*, Gribble, G. W., Ed. Springer Berlin Heidelberg: Berlin, Heidelberg, 2012; pp 381.

201. Dghaym, R. D.; Dhawan, R.; Arndtsen, B. A. *Angew. Chem. Int. Ed.* **2001,** *40*, 3228.

202. Dhawan, R.; Arndtsen, B. A. *J. Am. Chem. Soc.* **2004,** *126*, 468.

203. Siamaki, A. R.; Arndtsen, B. A. *J. Am. Chem. Soc.* **2006,** *128*, 6050.

204. Dhawan, R.; Dghaym, R. D.; St. Cyr, D. J.; Arndtsen, B. A. *Org. Lett.* **2006,** *8*, 3927.

205. Bontemps, S.; Quesnel, J. S.; Worrall, K.; Arndtsen, B. A. *Angew. Chem. Int. Ed.* **2011,** *50*, 8948.

Chapter 2: From Aryl Iodides to 1,3-Dipoles: Design and Mechanism of a Palladium Catalyzed Multicomponent Synthesis of Pyrroles

2.1. Preface

As described in Chapter 1, our laboratory found that the $[Pd(allyl)Cl]_2/P^tBu_3$ catalyzed coupling of aryl iodides, imines, and CO can allow the multicomponent formation of imidazolinium carboxylate products. In this work, it was proposed that the palladium-acyl intermediate generated in the carbonylation of aryl iodide behaves as an electrophilic acylating reagent in the reaction with imine, which then undergoes cyclocarbonylation to generate a Münchnone. However, we have also reported that the carbonylation of aryl iodides in the presence of chloride can lead to the formation of acid chlorides. This made us question if the mechanism of the reaction with aryl iodides, imines, and CO involved the *in situ* formation of acid chlorides. This chapter describes our efforts to elucidate the mechanism of this reaction. Moreover, it explores the conditions necessary to build-up Münchnone products and subsequently react them with alkynes to form pyrroles. This project was started by Dr. Jeffrey Quesnel and Diane Bijou (the latter a visiting student in our lab). They developed preliminary conditions to generate Münchnones. My contributions to this work include the synthesis and characterization of intermediate palladium complexes, performing stoichiometric control experiments with these complexes, kinetic studies on the catalytic reaction, catalyst development, and synthesis of the products in Tables 2.3 and 2.4. This work was published in *J. Am. Chem. Soc.* **2016**, 138, 7315.

2.2. Introduction

Palladium-catalyzed carbonylative coupling reactions with organic halides and pseudohalides have become an important tool in synthetic chemistry. Since its initial discovery by Heck in the mid-1970's, this reaction has been applied to the synthesis of a diverse range of carboxylic acid derivatives (esters, amides, aldehydes, ketones, etc.).[1-3] Carbonylations have also seen rapidly growing use in the assembly of more complex carbocyclic and heterocyclic scaffolds.[4] One approach developed by Alper, Coates, Drent, and others involves the ring expansion of heterocycles to form lactones or lactams.[5] Alternatively, a range of aryl halide carbonylations with intramolecular cyclization have been described,[6] as have sequential or cascade insertions,[7] and reactions involving the subsequent cyclization of the ester or amide products of carbonylation.[8] From a mechanistic perspective, metal-catalyzed carbonylations are typically postulated to involve the *in situ* formation of metal-acyl complexes (**2.1**) which subsequently undergo coupling with nucleophiles (Scheme 2.1a). The reactivity of **2.1** therefore shows similarity to that of activated carboxylic acid derivatives such as acid chlorides. In considering this analogy, and the broad utility of acid chlorides in synthesis, we recently became interested in the potential use of carbonylations to access products other than carbonyl-containing derivatives. As an initial study towards this reaction, aryl halide carbonylation in the presence of imines results in the generation of imidazolinium carboxylates **2.2** (Scheme 2.1b).[9] The latter is based upon the established generation of iminium salts from acid chlorides, and provides a rare example of a five-component coupling reaction, as well as a modular method to assemble these heterocycles.

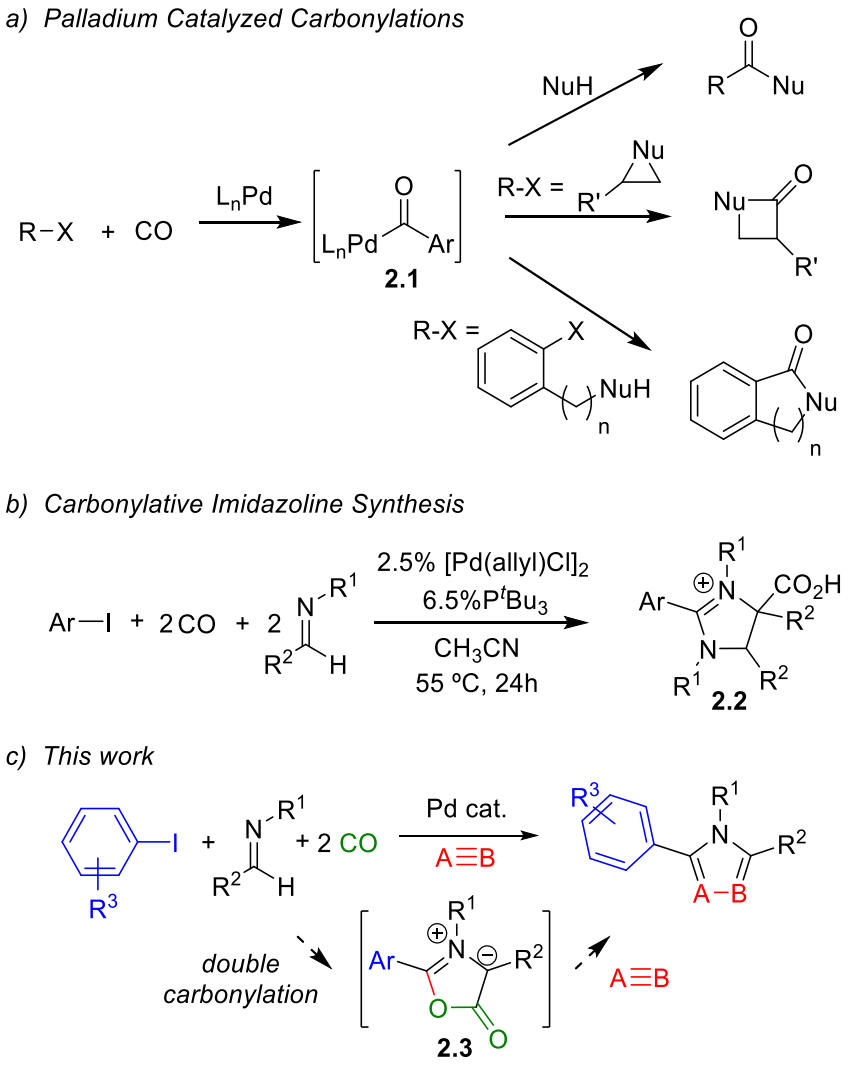

Scheme 2.1. Palladium Catalyzed Carbonylation and Heterocycle Synthesis

While the imidazolinium carboxylates formed above are limited to symmetrically substituted products, this reaction has prompted us to question if aryl halide carbonylation chemistry might open a more broadly applicable approach to construct heterocycles from fundamental building blocks. Polysubstituted heterocycles, and in particular the aryl-heteroaryl motif, are among the most common structural units found in pharmaceutical development. These products are typically generated via substitution chemistry on pre-synthesized heterocycles (e.g. cross coupling

reactions), or cyclization reactions, both of which require the multistep synthesis of substituted precursors.[10] In contrast, the transformation in Scheme 2.1b presumably involves the *in situ* generation of an interesting class of 1,3-dipole: Münchnones (**2.3**), although these intermediates are not observed. Münchnones are well-known 1,3-dipoles that have been exploited for the convergent synthesis of various classes of heterocycles.[11] One limitation to the use of **2.3** in heterocycle synthesis is their own formation, as these compounds are typically generated via the cyclization of α-amido acids, which can themselves require a multistep synthesis. While alternative approaches to Münchnones have been described,[12,13] including via the carbonylation of *N*-acyl iminium salts, these also rely upon the use of reactive (and synthetic) building blocks, such as acid chlorides or metal-carbenes. In contrast to each of these reactions, the palladium catalyzed formation of imidazolines suggests that Münchnones can be generated from the carbonylation of aryl iodides and imines. We therefore hypothesized that inhibiting imidazoline formation and generating **2.3** could provide a general platform to generate aryl-substituted heterocycles from simple combinations of available substrates (Scheme 2.1c). In addition to the synthetic chemistry, a notable feature of this system would be its use of CO not to generate a carbonylated product, but instead to drive the multicomponent assembly of fundamental building blocks via the ultimate liberation of CO_2.

One challenge to the use of this carbonylation chemistry to generate heterocycles is the lack of a complete understanding of how imidazolinium carboxylates are generated, and indeed if Münchnones are intermediates in this reaction. To address this, we have undertaken a series of studies to determine the mechanism of this catalytic transformation. These demonstrate the steps by which the multicomponent coupling occurs, and conditions that can favor the formation of 1,3-dipoles. Based upon this data, we have designed a palladium catalyzed dicarbonylative approach

for the synthesis of polysubstituted pyrroles. In contrast to typical procedures, this reaction provides a method to form a pyrrole unit at the same time as the aryl-pyrrole bond, in one pot, and from four simple components: aryl iodides, imines, CO, and alkynes or alkenes.

2.3. Results and Discussion

2.3.1. Stoichiometric Model Reactions

Our preliminary mechanistic postulate for the catalytic generation of imidazolines is shown in Scheme 2.2. Palladacycles of the general form of **2.4** have been established to undergo cyclocarbonylations to generate Münchnones.[14] We therefore hypothesized that an *in situ* generated palladium-aroyl complex **2.1** serves as a precursor to **2.4** by reacting with imine. In this scenario, the palladium catalyst would mediate both an initial carbonylation of aryl iodide to form **2.1**, followed by a subsequent cyclocarbonylation to form Münchnone **2.3** and liberate the catalyst. The bulky P^tBu_3 ligand is believed to facilitate catalysis due in part to its lability in palladacycle **2.4**, which can allow CO association and subsequent insertion. While Münchnones are not observed in the reaction, protonated imines are known to undergo rapid cycloaddition to **2.3**, and upon carbon-oxygen bond scission form imidazolinium salts.[14]

In order to further probe this mechanism, we first performed a series of model reactions for each of these individual steps.

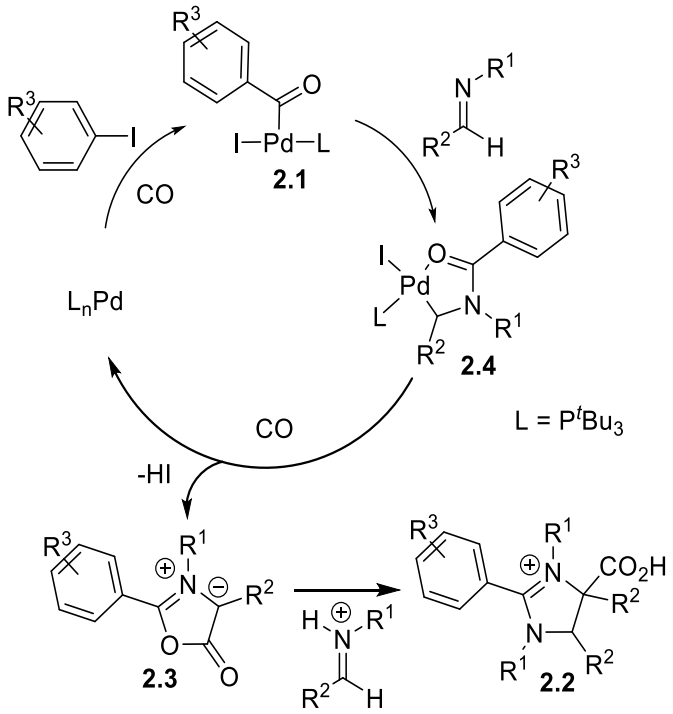

Scheme 2.2. Mechanistic Postulate for Catalysis

Reaction of Pd(P^{t}Bu$_3$)$_2$ Aryl Iodide, CO and Imine Our initial studies examined the putative first steps in the catalytic cycle: the formation of palladium-aroyl complex **2.1** and its reaction with imine. Similar to previous reports,[15] the addition of Pd(P^{t}Bu$_3$)$_2$,[16] as a model for the *in situ* generated Pd(0) catalyst, to aryl iodide and carbon monoxide leads to the rapid formation of the three-coordinate palladium-aroyl complex **2.1a** (Scheme 2.3). This complex can be easily isolated in high yield upon precipitation with pentane.[15a,b] Interestingly, control experiments show no reaction occurs between **2.1a** and imine, the postulated next step in catalysis, even upon prolonged heating at 55 °C. However, the addition of the other reagent present in catalysis, CO, initiates the slow disappearance of **2.1a** and generation of imidazolinium carboxylate **2.2a** (32% yield). We observe no intermediates in this reaction, indicating that subsequent steps leading to the formation of product are faster than the reaction of imine with palladium-aroyl complex. Although this data

demonstrates that **2.1a** is a viable intermediate in the formation of **2.2a**, it is notable that the stoichiometric reaction is low yielding and slow (2 days, 55 °C). This suggested that **2.1a** may not be an immediate precursor to imidazolines during catalysis.

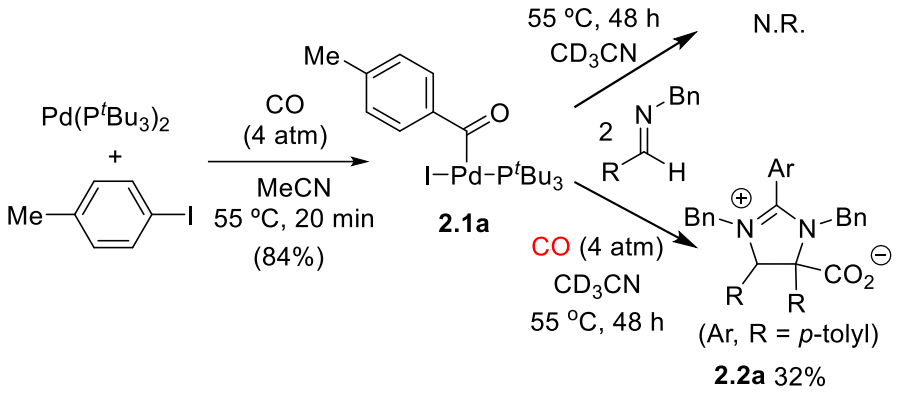

Scheme 2.3. Reactivity of Pd-Aroyl Complex 2.1a

Influence of Chloride In considering differences between the control experiments in Scheme 2.3 and catalysis, we noted that the catalytic synthesis of imidazolinium carboxylate employs [Pd(allyl)Cl]$_2$ / P^{t}Bu$_3$, rather than Pd(P^{t}Bu$_3$)$_2$, as the catalyst precursor. While both of these are expected to generate similar P^{t}Bu$_3$-coordinated Pd(0) catalysts, as shown in Scheme 2.4, the use of Pd(P^{t}Bu$_3$)$_2$ as catalyst results in minimal coupling under identical conditions. One potentially important difference between these two systems is the presence of chloride in the [Pd(allyl)Cl]$_2$ catalyst precursor. To examine the role of chloride in the reaction, 5 mol% Bu$_4$NCl was added to the catalytic reaction with Pd(P^{t}Bu$_3$)$_2$. This restores catalytic activity to the level noted with Pd(allyl)Cl]$_2$ / P^{t}Bu$_3$ (Scheme 2.4). Further, increased chloride concentration results in accelerated reaction.

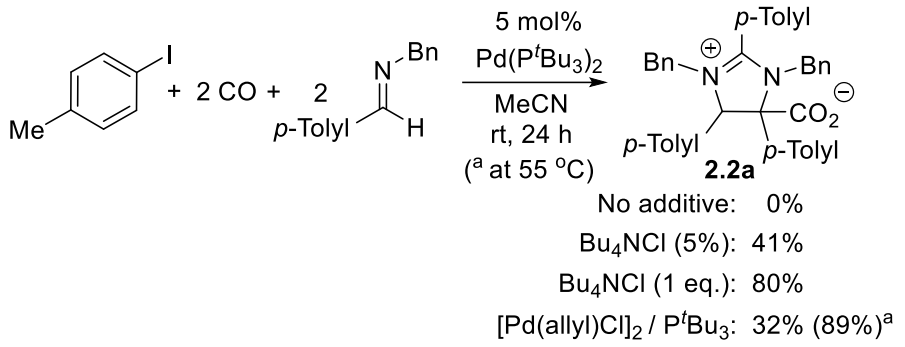

Scheme 2.4. Influence of Chloride on Catalysis

A plausible role of chloride in catalysis would be to exchange with iodide on palladium and therefore modulate reactivity.[17] To test this, the analogous chloride coordinated palladium-aroyl complex **2.1b** was generated by the oxidative addition of acid chloride to Pd(P^{t}Bu$_3$)$_2$ (Scheme 2.5). This chloride coordinated **2.1b** also does not directly react with imine. However, the addition of carbon monoxide results in the room temperature formation of imidazolinium carboxylate **2.2a** in high yield (90%). The latter transformation is much more rapid (6 h, rt) than that with the iodide complex **2.1a**, and of sufficient rate to be a viable step in the catalytic reaction.

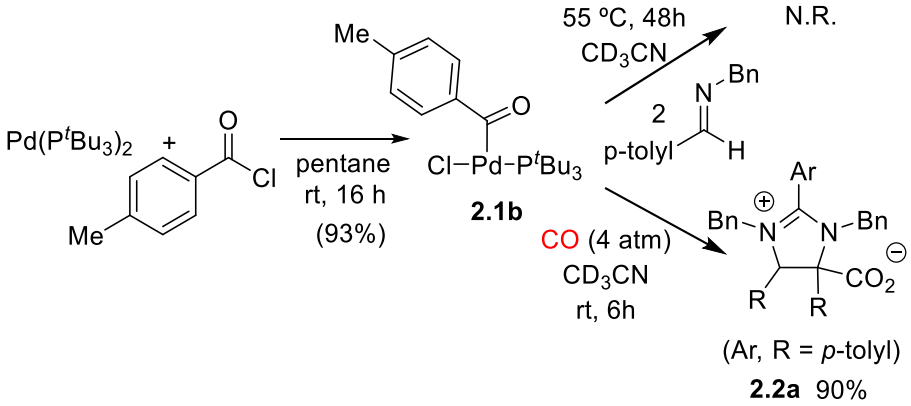

Scheme 2.5. Reactivity of Pd-Aroyl Complex 2.1b

Acid Chloride Intermediates The above data suggest that both chloride and carbon monoxide can facilitate the reaction of imines with palladium-aroyl complexes, and in particular carbon monoxide is required for any reaction to occur. One rationale for these effects is that chloride and/or carbon monoxide coordination exert an influence on the reaction of imine with the palladium-aroyl complex. The latter may occur via a direct nucleophilic attack on the electrophilic aroyl ligand (Scheme 2.6, path A), or, in analogy to previous reports with cationic palladium-acyl complexes, coordination and migratory insertion (path B).[18] However, we have recently noted that chloride and carbon monoxide in concert with the P^{t}Bu$_3$ ligand can accelerate palladium catalyzed aryl halide carbonylations by allowing the generation of acid chlorides.[19] As such, an alternative postulate for the influence of chloride is that it allows the *in situ* generation of acid chlorides for reaction with imine (path C).

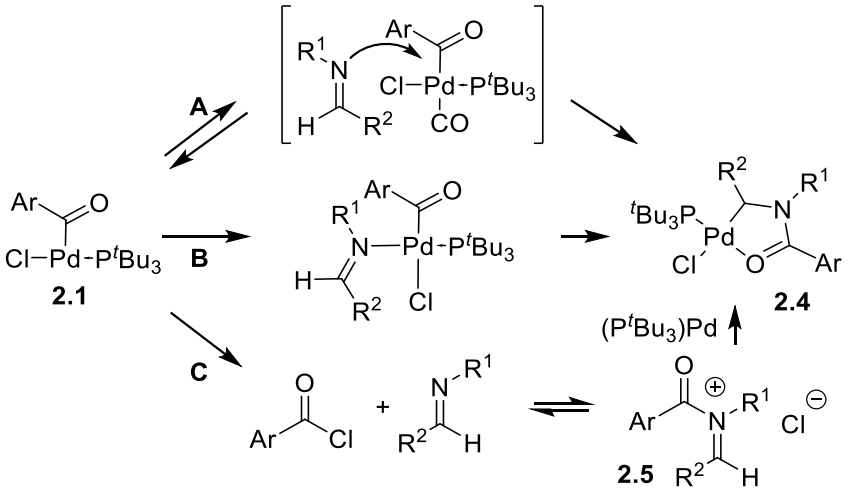

Scheme 2.6. Mechanism of Imine Reaction with 2.1

Insight into the pathway followed in this transformation can be obtained by simply omitting the addition of imine to the reaction of palladium-aroyl complex **2.1b**. The addition of CO to **2.1b**

leads to the rapid, equilibrium formation of acid chloride (Scheme 2.7a). Removal of CO from the reaction allows the quantitative re-formation of **2.1b**, while increasing CO pressure results in the further favored generation of acid chloride. A plot of the ratio of product vs. CO pressure provides a linear fit to $[CO]^2$ (Scheme 2.7b), implying that two CO ligands may bind to the Pd(0) complex. Notably, no reaction is noted for the analogous iodide complex **2.1a**, nor with **2.1b** in the absence of CO. The rapid formation of acid chloride from **2.1b** provides a rationale for the role of chloride in catalysis, and a reasonable pathway for coupling with imine, as acid chlorides are established to react rapidly with imines to form *N*-acyl iminium salts (**2.5**, path C).[20] The intermediacy of **2.5** in this chemistry is further examined below.

*a) Equilibrium Elimination of Acid Chloride from **2.1b***

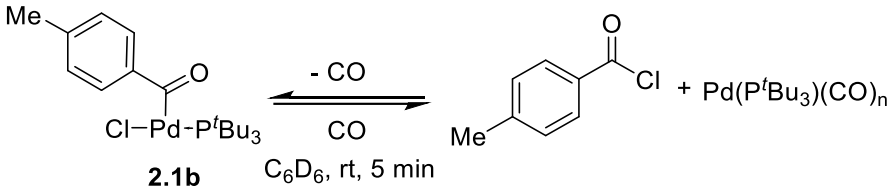

CO (atm)	**%** acid chloride
1	18%
2	30%
3	42%
4	52%

b) Plot of Acid Chloride Formation vs. [CO]^2

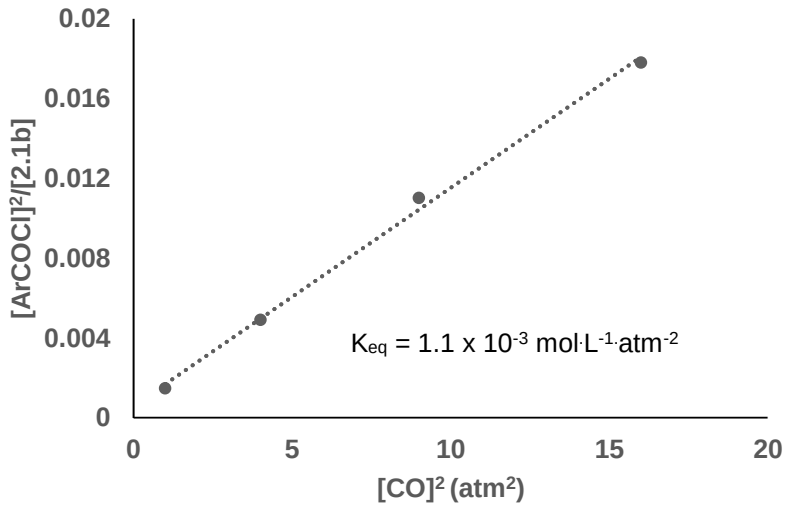

Scheme 2.7. Generation of Acid Chlorides from 2.1b

N-Acyl Iminium Salts We see no evidence for the formation of *N*-acyl iminium salts, or any intermediate, by monitoring the stoichiometric reaction of **2.1b**, imine, and carbon monoxide by ^{1}H NMR analysis. To probe for their intermediacy, we therefore employed scrambling experiments with a labelled iminium salt (**2.5b**, Scheme 2.8). The latter could exchange with any free iminium

salt generated from palladium complex **2.1b**, and may allow **2.5a** to build-up in solution. Monitoring the reaction of palladium-aroyl complex **2.1b** with imine and CO in the presence of an excess of **2.5b** by *in situ* ^{1}H NMR analysis reveals that iminium salt **2.5a** does indeed form in this reaction at short reaction times (50% at 35 min). Allowing the reaction to continue leads to the complete consumption of both iminium salts and generation of two separate imidazolines, **2.2b** and **2.2c**.

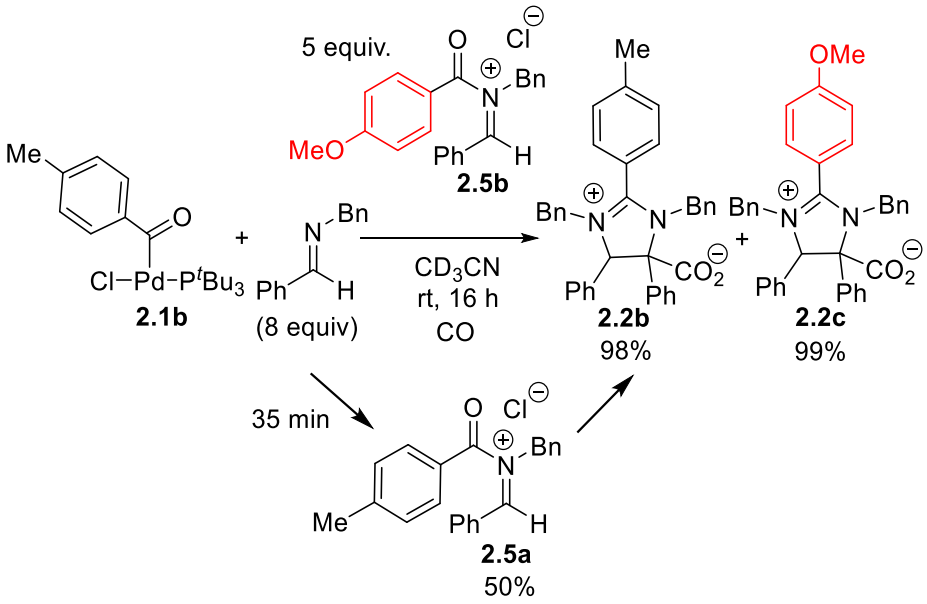

Scheme 2.8. Intermediacy of *N*-Acyl Iminium Salts

Palladacycle Formation. The generation of free *N*-acyl iminium salt **2.5** in this chemistry requires that this intermediate add to palladium for a second carbonylation to ultimately generate imidazolinium carboxylates **2.2**. Control experiments show that this step is also viable. The addition of *N*-acyl iminium salt **2.5b** to Pd(P^{t}Bu$_3$)$_2$ leads to the near quantitative formation of palladacyclic complex **2.4b** within 2 h (Scheme 2.9). This complex displays spectroscopic features similar to previously isolated amide-chelated palladacycles.[12a,18] Complex **2.4b** is also a viable

intermediate in catalysis: the addition of CO to this palladacycle results in its rapid (3h, rt) conversion into imidazolinium carboxylate in 89% yield.

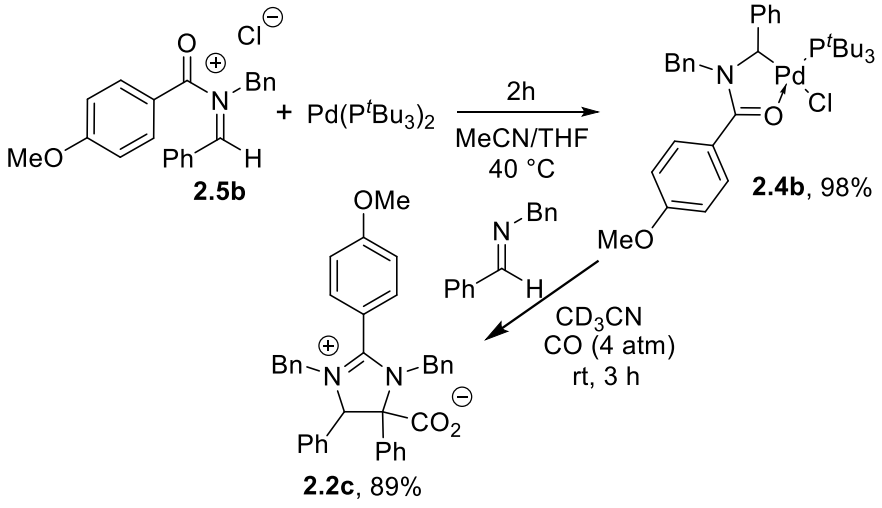

Scheme 2.9. Synthesis of Palladacyclic Intermediates

Münchnone Formation One intermediate not observed in the stoichiometric chemistry above is Münchnone **2.3**. Previous studies on 1,3-dipolar cycloadditions with Münchnones have demonstrated that protonated *N*-alkyl imines can undergo very rapid cycloaddition to generate imidazolinium salts.[14] In the chemistry above, acid is generated upon the cyclocarbonylation of palladacycle **2.4** (Scheme 2.2), and can presumably protonate imine to allow the generation of **2.2**. We therefore examined the effect of base on the stoichiometric reactions. As shown in Scheme 2.10a, the addition of NEt^{i}Pr$_2$ base to the reaction of palladium-aroyl complex **2.1b**, imine, and CO inhibits imidazolinium formation and leads instead to the formation of Münchnone **2.3a**. in 73% yield. A similar effect of base is noted on the reaction with palladacycle **2.4a** (Scheme 2.10b).

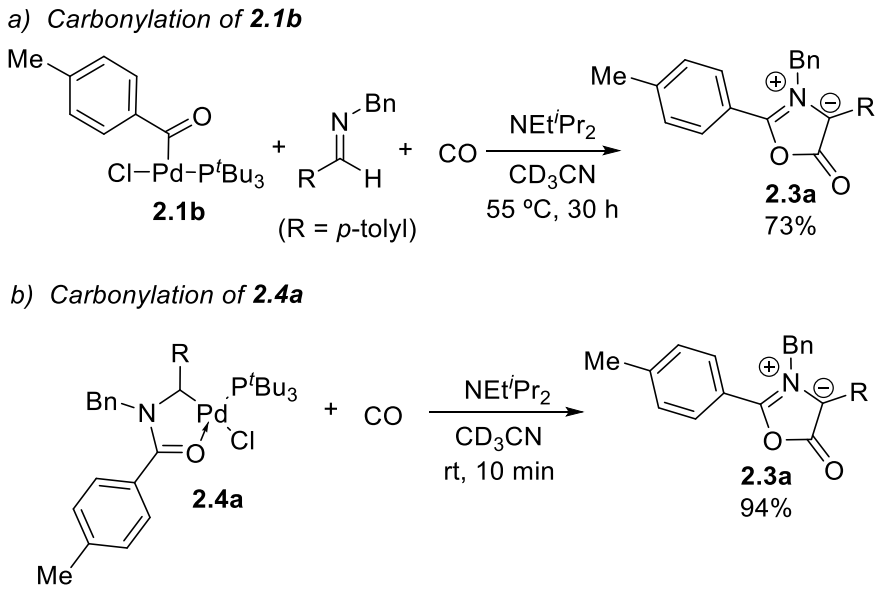

Scheme 2.10. Stoichiometric Münchnone Generation

2.3.2. Postulated Mechanism of Imidazolium Formation

The above studies show that several palladium complexes and organic products are each competent intermediates in catalysis: palladium-aroyl complexes (**2.1a** and **2.1b**), acid chlorides, *N*-acyl iminium salts **2.5**, palladacyclic complex **2.4** and Münchnones. Based upon this data, we can formulate a reasonable mechanism for the multicomponent formation of imidazolines (Scheme 2.11). In this, the oxidative addition of aryl iodide and CO insertion is rapid, and leads to the generation of the palladium-aroyl complex **2.1a**. Control experiments demonstrate that complex **2.1a** does not react rapidly with imine (e.g. Scheme 2.3). The latter is consistent with many examples in carbonylation reactions, which suggest that palladium-aroyl ligands are only moderately electrophilic, and typically require anionic nucleophiles that can first coordinate to palladium for more facile reductive elimination.[21] Instead, our data is consistent with the reductive

elimination of acid chloride from the chloride-coordinated complex **2.1b**, which can react with the weakly nucleophilic imine away from the palladium catalyst to generate free *N*-acyl iminium salts **2.5**. The role of CO and P^{t}Bu$_3$ in the formation of acid chloride is presumably similar to that we have previously noted, where coordination of CO to the T-shaped complex creates a sterically encumbered and electron-poor palladium intermediate **2.6** for the favored reductive elimination of acid chloride.[19] As such, both chloride and carbon monoxide are critical for the build-up of iminium salts. Once *N*-acyl iminium salt **2.5** is generated, control experiments suggest that it can undergo rapid oxidative addition to Pd(P^{t}Bu$_3$)$_2$ to form palladacycle (**2.4**, Scheme 2.9) for rapid subsequent cyclocarbonylation to form Münchnone (Scheme 2.10b). The latter is established to react with protonated imine to generate the observed imidazolinium salt products.[7]

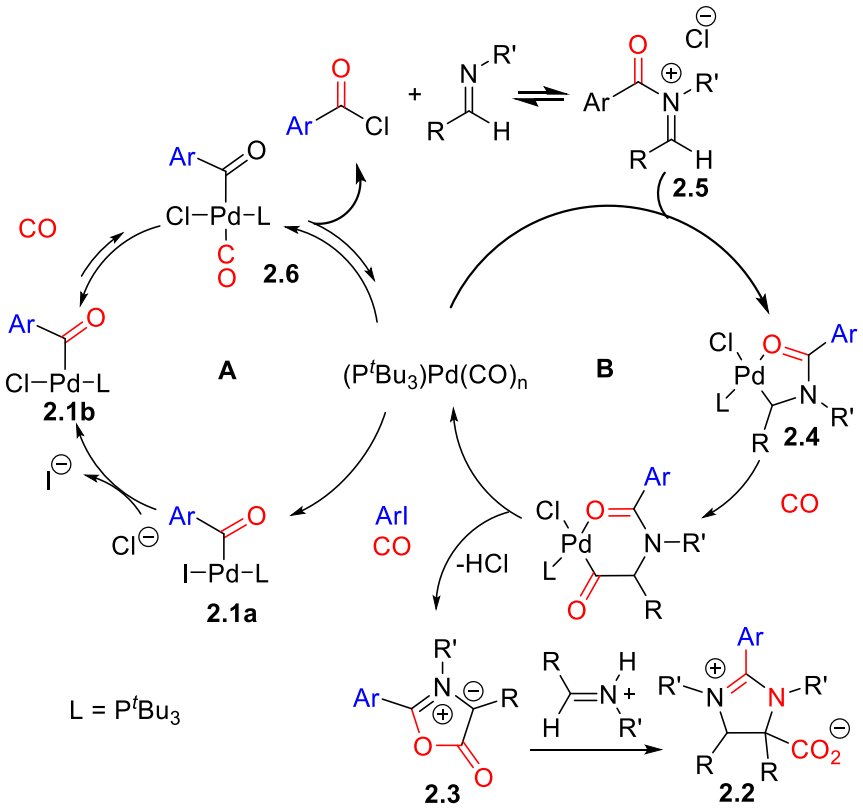

Scheme 2.11. Overall Mechanism of Imidazolium Carboxylate Formation

These data show that catalysis that proceeds via two separate carbonylation cycles (A and B), both of which are mediated by the same palladium catalyst. Monitoring the catalytic reaction by NMR provides some insight into the relative rates of these two cycles. *In situ* ^{31}P NMR analysis (Figure 2.1) shows the generation palladium-aroyl complex **2.1b** as the only observable intermediate at short reaction times. However, as catalysis proceeds, the build-up of protic acid leads to the equilibrium protonation of the phosphine, and this complex can no longer be observed. The observation of complex **2.1b** suggests that its subsequent reaction (i.e. with imine) is at least partially rate determining in the overall cycle. ^{1}H NMR analysis shows no evidence for any organic (e.g. *N*-acyl iminium salt) intermediate during the course of the reaction, and also implies that the consumption of acid chloride and iminium salt (cycle B) is more rapid than their formation (cycle A).

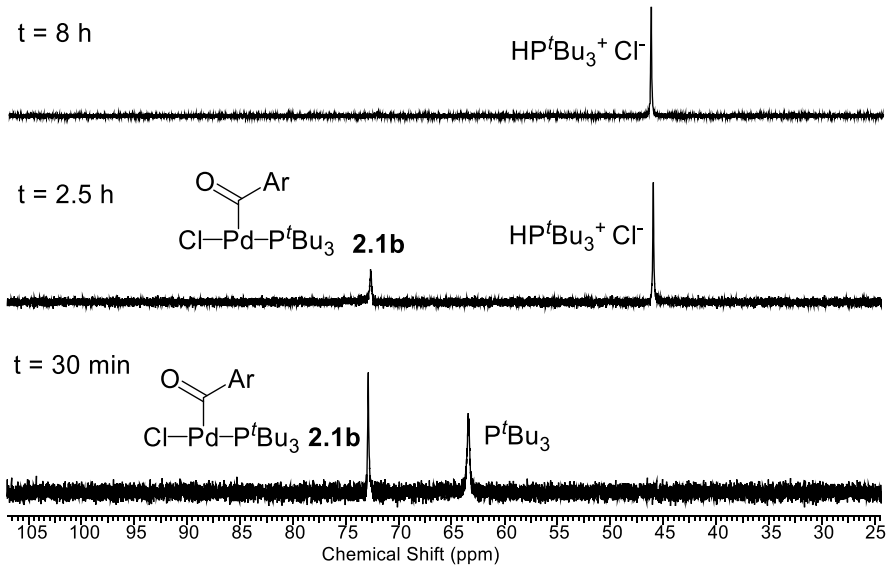

Figure 2.1. *In situ* ^{31}P NMR Analysis of the Catalytic Formation of Imidazolinium Carboxylate in Scheme 2.4.

Kinetic analysis of the catalytic reaction provides further insight into the rate determining step(s) in this system. As illustrated in Figure 2.2, the catalytic formation of imidazolinium carboxylate proceeds with the first order dependence on imine concentration, aryl iodide concentration, and carbon monoxide pressure. In considering the mechanism in Scheme 2.11, and the catalyst resting state at **2.1b**, these results are consistent with *N*-acyl iminium salt **2.5** formation from **2.1b** (cycle A) as rate determining in catalysis. While acid chloride reductive elimination is rapid, this reaction is in dynamic equilibrium due to the rapid re-addition of acid chloride to Pd(0). In this scenario, both imine and aryl iodide concentration can favor *N*-acyl iminium salt generation by trapping the acid chloride and Pd(0), respectively, and carbon monoxide pressure is established to favor this equilibrium by generating a more stable Pd(0)-carbonyl intermediate (Scheme 2.7).

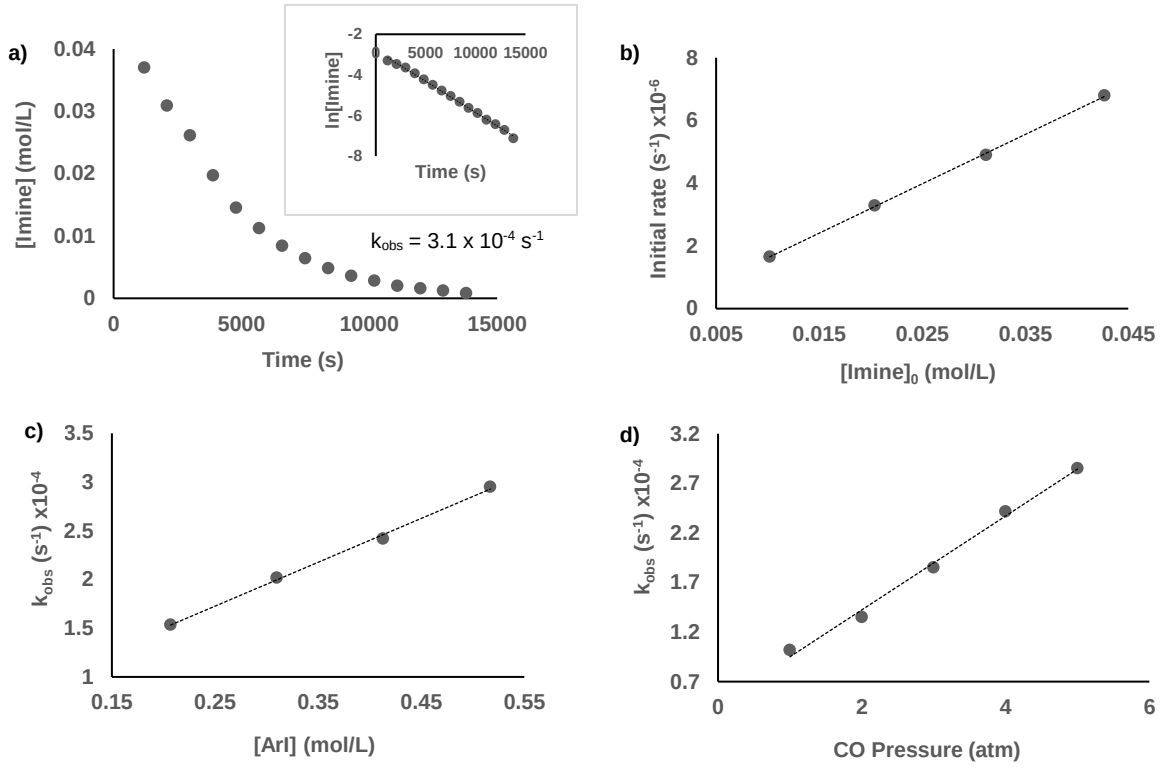

Figure 2.2. Kinetic Analysis of Catalytic Formation of Imidazolinium Carboxylate. (a) Typical plot of imine concentration vs. time for the reaction in Scheme 2.3 with 10 mol% $Pd(P^tBu_3)_2$ and 1 eq. Bu_4NCl at 40 °C. Inset: ln plot of data; (b) Initial rate dependence on imine

concentration; (c) Rate dependence on *p*-tolyl iodide concentration; (d) Rate dependence on CO pressure.

2.3.3. Catalytic Münchnone Synthesis

We next turned our attention to the potential use of this chemistry as a general route to prepare Münchnones. The data in Scheme 2.10 shows that amine base can inhibit imidazolinium carboxylate formation and allow the build-up of Münchnone. Similarly, the use of catalytic $Pd(P^tBu_3)_2$ in the reaction of aryl iodide, imine and CO in the presence of NEt^iPr_2 leads to the catalytic formation of Münchnone **2.3a** (Table 2.1, entry 1), but in low yield (20%). Instead, we note the build-up of a second product: β-lactam **2.7a** (32%). The generation of β-lactam presumably arises from the slow [2+2] cycloaddition of the ketene tautomer of Münchnone **2.3a** with imine.[22] As in the stoichiometric experiments, the omission of chloride completely shuts down catalysis (entry 2).

The formation of β-lactam was an anticipated challenge in this catalytic reaction, where, much like the catalytic formation of imidazolinium carboxylates, the imine reacts more rapidly with the Münchnone product as it builds up in the catalytic reaction. One approach to avoid this product would be to accelerate the catalytic formation of Münchnone, and therefore imine consumption. The mechanistic results proved useful in this regard. For example, increasing the concentration of aryl iodide favors the formation and yield of Münchnone (entries 3, 4). The latter is presumably related to the equilibrium formation of acid chloride, where a higher concentration of aryl iodide can better trap Pd(0) and favor catalysis. Similarly, increasing CO pressure leads to the faster generation of Münchnone and significantly limits the formation of β-lactam (entries 5, 6).

Table 2.1. Catalytic Formation of Münchnones

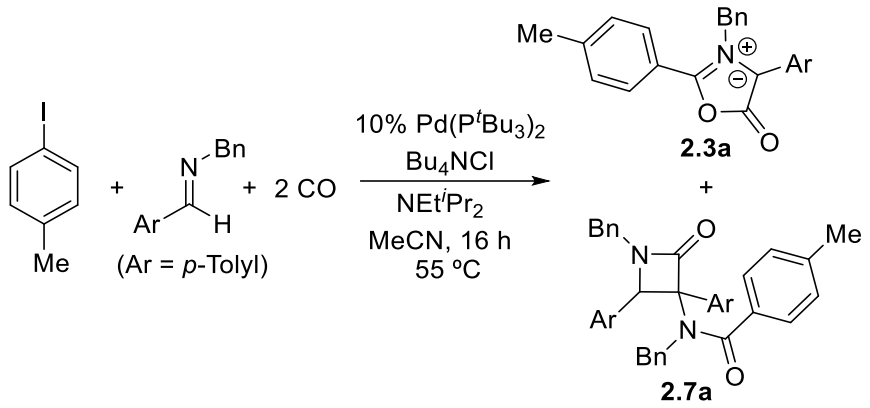

Entry	CO (atm)	Ar-I (equiv)	% 2.3a	% 2.7a
1	1	1	20	32
2[a]	1	1	0	0
3	1	3	44	50
4	1	5	50	13
5	4	1	58	19
6	10	1	65	8

4-iodotoluene (55 mg, 0.25 mmol), imine (52 mg, 0.25 mmol), Bu_4NCl (69 mg, 0.25 mmol), NEt^iPr_2 (49 mg, 0.375 mmol), $Pd(P^tBu_3)_2$ (13 mg, 25 µmol) and CO in MeCN (1.7 mL), yields of **2.3a** and **2.7a** determined by ^1H NMR analysis. [a]Bu_4NCl not added to the reaction.

The influence of ligands on this transformation was also probed. In order to screen ligands uncomplicated by catalyst activation steps, palladacycle **2.4** was used as the catalyst precursor, as it also represents an intermediate in the catalytic cycle. The use of common triaryl- or trialkylphosphines completely inhibits catalysis (Table 2.2, entries 2, 3). This may arise from the strong binding of these ligands to palladacycle **2.4**, which could inhibit carbonylation. Moving to more sterically encumbered ligands leads to low yield of Münchnones (ca. 20%, entries 7-10), or approximately one to two catalytic turnovers of the palladacycle precatalyst (i.e. cycle B, Scheme 2.10). In contrast, large bite angle phosphines can lead to double-carbonylative catalysis (entries 11-13), with P^tBu_3 the most active. This ligand is also noted to be key in catalytic acid chloride

formation, where its cone angle can create sufficient steric encumbrance on palladium to allow rapid acid chloride formation.[19] Under these combined conditions with excess aryl iodide, the formation of Münchnone is sufficiently rapid to allow us to lower the reaction temperature (entry 14). The latter further suppresses β-lactam formation, and allows the synthesis of Münchnone in high yield.

Table 2.2. Ligand Screening for Münchnone Formation

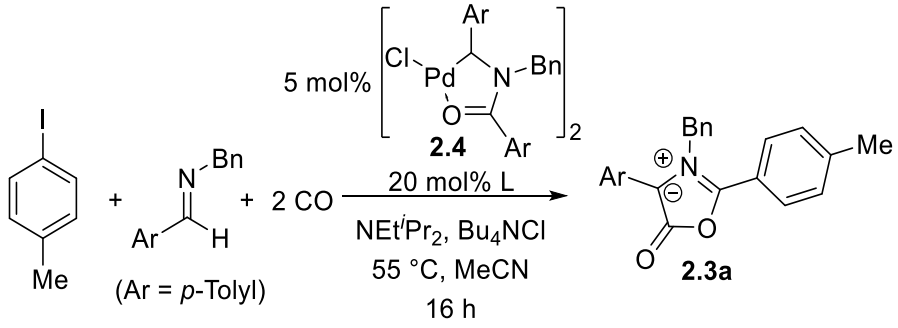

#	Ligand	% 2.3a (% 2.7a)	#	Ligand	% 2.3a (% 2.7a)
1	-	20 (2)			
2	PPh_3	0 (0)	9	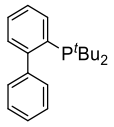	23 (4)
3	PCy_3	0 (0)			
4		0 (14)			
5	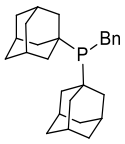	3 (2)	10	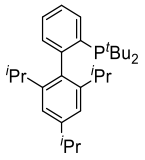	27 (6)
6	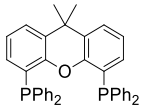	0 (0)	11	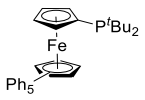	57 (14)
7	P(*o*-Tol)$_3$	18 (2)	12	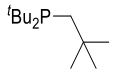	55 (19)
8	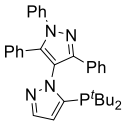	24 (6)	13	P^{t}Bu$_3$	62 (20)
			14[a]	P^{t}Bu$_3$	80 (4)

4-iodotoluene (33 mg, 0.15 mmol), imine (31 mg, 0.15 mmol) Pd catalyst **2.4** (6.8 mg, 7.5 µmol), Ligand (30 µmol), NEt^{i}Pr$_2$ (29 mg, 0.23 mmol), Bu$_4$NCl (42 mg, 0.15 mmol), and CO (4 atm), in MeCN (1 mL), yield

determined by ^{1}H NMR analysis. [a]reaction performed at 40 °C, with 4-iodotoluene (164 mg, 0.75 mmol) and CO (10 atm).

2.3.4. Catalytic Synthesis of Pyrroles

The reaction in Table 2.2 provides a new route to form a 1,3-dipole via the carbonylation of aryl iodides with imines. As discussed previously, a feature of Münchnones is their ability to participate in cycloaddition reactions to assemble heterocycles. Coupling the catalytic formation of **2.3** with cycloaddition can therefore provide an alternative to more classical multistep routes to assemble the aryl-heteroaryl motif. As an example, the catalytic generation of Münchnone **2.3a** followed by the addition of the electron deficient alkyne dimethylacetylenedicarboxylate leads to the generation of 2-aryl substituted pyrrole **2.8a** in 84% yield (Eq. 2.1), where in one pot four bonds are generated from five separate reagents (aryl iodide, imine, alkyne, and two equivalents of carbon monoxide).

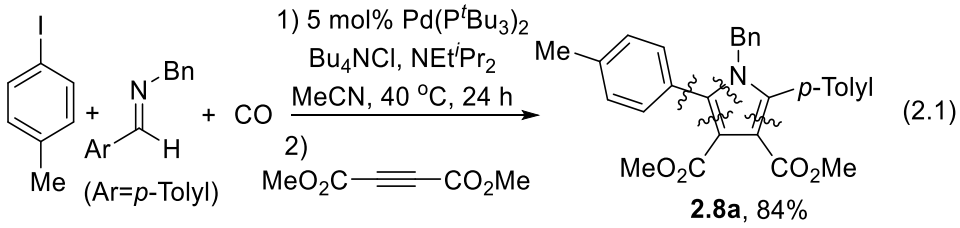

The pyrrole core, and in particular aryl-substituted pyrroles, represent a useful general class of pharmaceutically relevant heterocycle,[23] and have also found significant utility in materials chemistry.[24] In this regard, an aspect of this transformation the ability to access these heterocycles from combinations of available and easily diversified building blocks. This is highlighted in Tables 2.3 and 2.4. For example, a number of aryl iodides can be incorporated into this transformation. This includes simple aryl iodides (**2.8a**), as well as those with electron rich (**2.8b-d**) and electron

poor (**2.8g**,**h**,**k**) substituents. Each of these leads to pyrroles in high overall yield. Potentially palladium reactive aryl bromide functionalities can also be incorporated (**2.8e**). Interestingly, the reaction can move beyond simple aryl groups and incorporate heteroaryl iodides (**2.8i**,**j**). Similar modulation of the imine can be performed. *N*-alkyl and -benzyl protected imines are viable substrates in this chemistry, as are electron rich *N*-aryl imines (**2.8l**,**m**,**q**). On the imine carbon, an array of electron rich (**2.8l**,**q**) or electron poor (**2.8m**,**n**) aryl-substituents can be employed, as can heteroaryl imines (**2.8p**,**s**) and *t*-butyl substituted reagents (**2.8r**,**t**). Conversely, enolizable imines lead to enamides under the reaction conditions.[25]

The dipolarophile can also be tuned in this chemistry (Table 2.4). Examples of these include a number of substituted electron poor alkynes incorporating ketone (**2.8v**), ester (**2.8w,y,z**) or electron deficient arene (**2.8x**) functionalities. In the case of less electron deficient alkynes (e.g. **2.8w,aa**), the dipolarophile can be used in the presence of the catalytic synthesis of Münchnone, allowing the one step synthesis of substituted pyrroles. As previously noted, phenyl methylpropiolate and electron poor aryl acetylenes undergo regioselective cycloaddition to unsymmetrical Münchnones.[26] Electron poor alkenes can be similarly used in this platform, and undergo facile acid loss upon cycloaddition to generate tetra- or trisubstituted pyrroles.[27] This can be used to generate 3-substituted pyrroles from vinyl halide derivatives (**2.8ab,ac**) and nitroalkenes (**2.8af**). While acetylene does not react with **2.3**, the electron deficient triphenylvinylphosphonium salt can act as an acetylene equivalent upon acid loss to form 3,4-unsubstituted pyrroles (**8ad,ae**). Overall, this provides a method to assemble families of aryl- and heteroaryl-substituted pyrroles with independent control of all five substituents. Within the brief diversity probed in Tables 2.3 and 2.4, the combination of substrates provides the ability to generate almost 10^3 structurally different pyrroles in one pot reactions. Considering the broad availability of aryl iodides, imines,

and alkynes/alkenes, many more structural combinations are also possible. We are unaware of any other method to construct pyrroles with such broad diversity from aryl halides in combination with other fundamental and stable building blocks.

Table 2.3. Multicomponent Synthesis of Pyrroles: Aryl Iodide and Imine Diversity

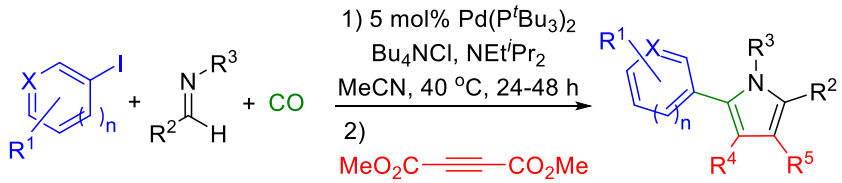

Aryl halide diversity

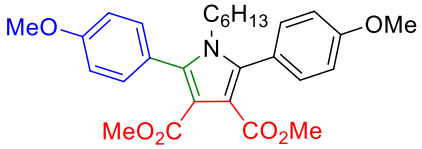

2.8b, 87%

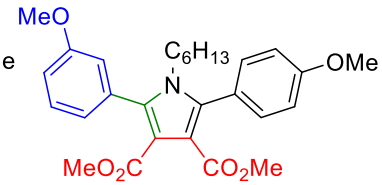

2.8c, 81%

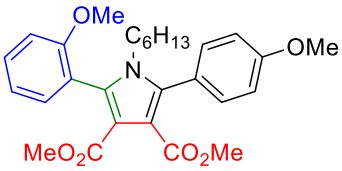

2.8d, 83%

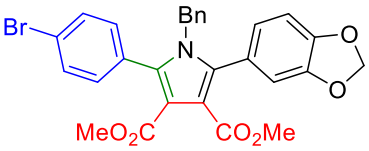

2.8e, 82%

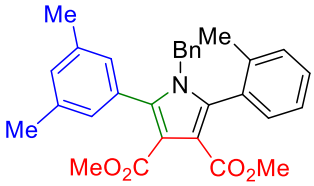

2.8f, 81%

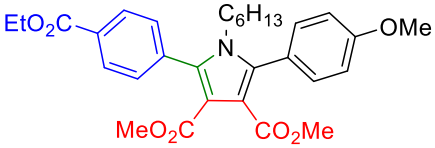

2.8g, 83%

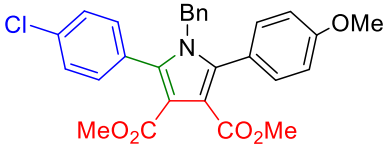

2.8h, 65%

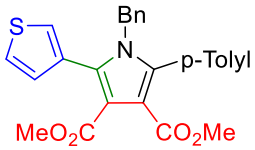

2.8i, 72%

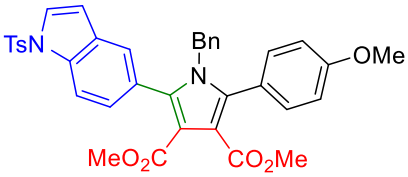

2.8j, 85%

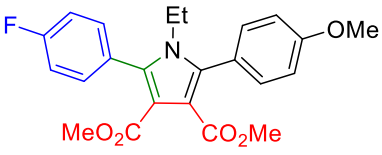

2.8k, 62%

Imine (0.50 mmol), aryl iodide (2.50 mmol), Pd(P^{t}Bu$_3$)$_2$ (12.8 mg, 0.025 mmol), Bu$_4$NCl (139.0 mg, 0.5 mmol), NEt^{i}Pr$_2$ (97.0 mg, 0.75 mmol), MeCN (3.3 mL), CO (10 atm), 40 °C. Quench with DMAD (85.3 mg, 0.60 mmol) at ambient temperature for 15 minutes.

Table 2.3. Multicomponent Synthesis of Pyrroles: Aryl Iodide and Imine Diversity (Cont.)

Imine diversity

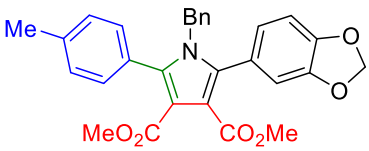

2.8l, 83%

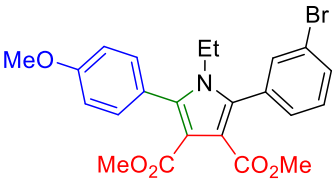

2.8m, 85%

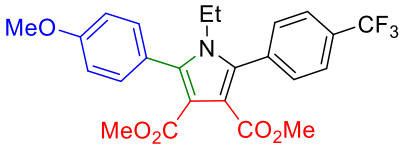

2.8n, 71%

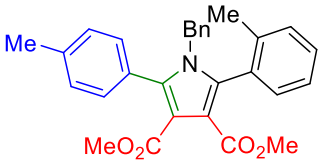

2.8o, 87%

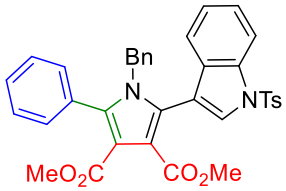

2.8p, 69%

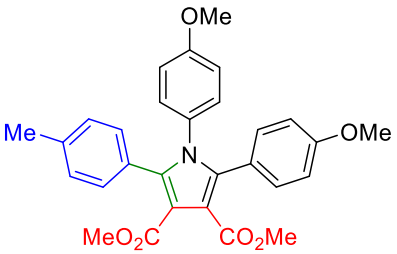

2.8q, 66%

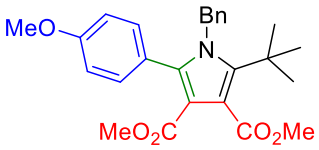

2.8r, 44%

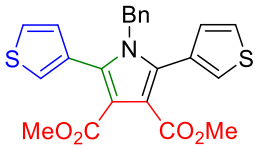

2.8s, 58%

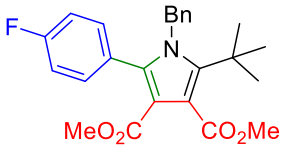

2.8t, 40%

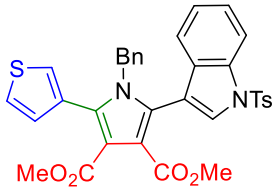

2.8u, 51%

Imine (0.50 mmol), aryl iodide (2.50 mmol), $Pd(P^tBu_3)_2$ (12.8 mg, 0.025 mmol), Bu_4NCl (139.0 mg, 0.5 mmol), NEt^iPr_2 (97.0 mg, 0.75 mmol), MeCN (3.3 mL), CO (10 atm), 40 °C. Quench with DMAD (85.3 mg, 0.60 mmol) at ambient temperature for 15 minutes.

Table 2.4. Multicomponent Synthesis of Pyrroles: Alkyne and Alkene Diversity[a]

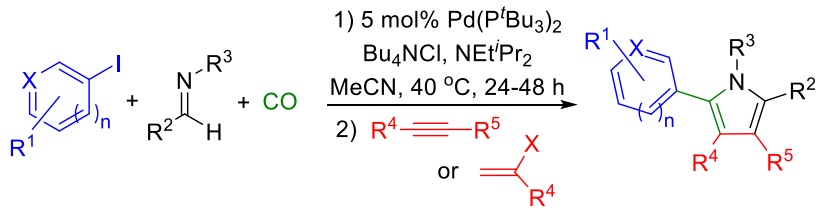

Alkyne dipolarophiles

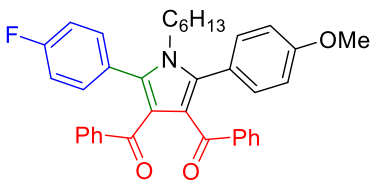

2.8v, 70%

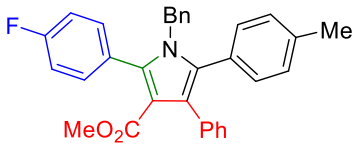

2.8w, 70%

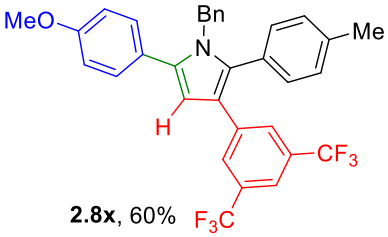

2.8x, 60%

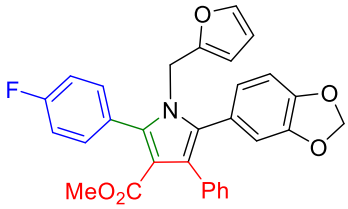

2.8y, 64%

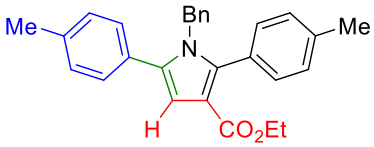

2.8z, 68%

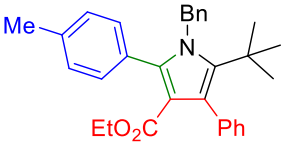

2.8aa, 60%

Alkene dipolarophiles

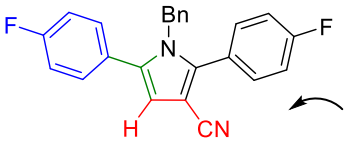

2.8ab, 60%

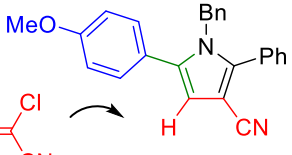

2.8ac, 77%

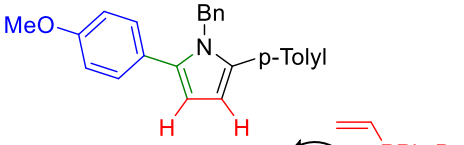

2.8ad, 77%

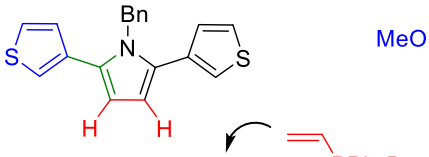

2.8ae, 56%

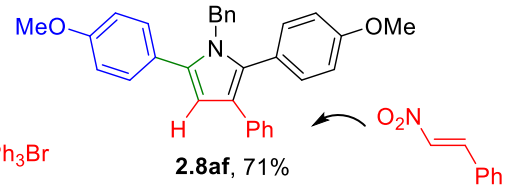

2.8af, 71%

[a] Imine (0.50 mmol), aryl iodide (2.50 mmol), Pd(P^{t}Bu$_3$)$_2$ (12.8 mg, 0.025 mmol), Bu$_4$NCl (139.0 mg, 0.5 mmol), NEt^{i}Pr$_2$ (97.0 mg, 0.75 mmol), MeCN (3.3 mL), CO (10 atm), 40 °C. For specific conditions for each dipolarophile, see Supplementary Information.

2.4. Conclusions

In conclusion, we have developed a multicomponent approach for the synthesis of Münchnones from simple aryl iodides, imines, and CO. Mechanistic studies suggest that this reaction proceeds via a tandem catalytic pathway, with the *in situ* generation of acid chlorides and *N*-acyl iminium salts. The P^tBu_3 ligand in concert with chloride is found to be unique in allowing both of these cycles to proceed under mild conditions. This presumably due to the unusual ability of this large ligand to facilitate the reductive elimination of acid chloride from palladium, as well as the lability of this large phosphine, which can allow the carbonylation of palladacyclic intermediates (**2.4**). Coupling the formation of Münchnones with alkyne/alkene cycloaddition can provide a multicomponent method to generate polysubstituted pyrroles. Notably, this synthesis employs available, inexpensive and stable reagents (aryl iodides, carbon monoxide imines, alkynes), proceeds with high efficiency, is modular, and generates pyrroles in high overall yield. Studies towards the use of this reaction to access other classes of products are currently underway.

2.5. Supporting Information

2.5.1. General Considerations

All manipulations were conducted in a glovebox under a nitrogen atmosphere. Unless otherwise noted, all reagents were purchased from commercial sources and used without purification. Research grade carbon monoxide (99.99%) was used as received. Solvents were dried by using a solvent purifier system. Solvents were stored over activated 3Å molecular sieves inside the glovebox. Deuterated acetonitrile and benzene were stirred over calcium hydride, vacuum transferred, degassed, and stored over 4Å molecular sieves. Imines were prepared using standard literature procedures.[28] Tetrabutylammonium chloride was dried in the glovebox by dissolving in

dichloromethane, allowing to stand overnight over activated molecular sieves, filtering and removing the solvent *in vacuo*. Pd(P^tBu_3)$_2$ was prepared as previously described.[29] All imidazolinium carboxylate products were characterized by comparison to previously prepared compounds.[30]

For NMR spectra of the products, see Supporting Information of publication (*J. Am. Chem. Soc.* **2016**, 138, 7315). Nuclear magnetic resonance (NMR) characterization was performed on 500 MHz spectrometers for proton, 126 MHz for carbon, and 162 MHz for phosphorus. ^{1}H and ^{13}C NMR chemical shifts were referenced to residual solvent. Mass spectra were recorded on a high-resolution electrospray ionization quadrupole mass spectrometer.

2.5.2. Experimental Procedures

Synthesis of *p*-TolylCOPd(P^tBu_3)I (2.1a)

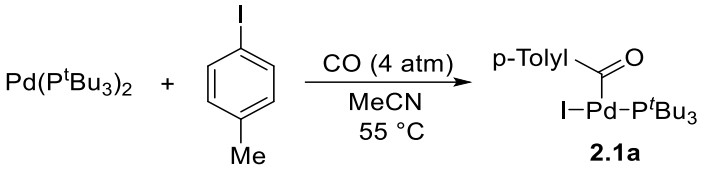

2.1a

In a glovebox, 4-iodotoluene (6.4 mg, 0.0293 mmol), Pd(P^tBu_3)$_2$ (10 mg, 0.0196 mmol), and benzyl benzoate (4.2 mg, 0.0196 mmol) were weighed. The palladium complex was dry transferred into a J-Young NMR tube, while the other two components were dissolved in CD_3CN (0.75 mL) and transferred into the tube. The NMR tube was then sealed with a screw-cap, taken out of the glovebox, 4 atm of CO added, and then it was warmed to 55ºC. ^{1}H NMR analysis after 20 minutes shows the formation of complex **2.1a** (84%) relative to the internal standard.

To obtain an analytically pure sample of **2.1a**, 4-iodotoluene (65 mg, 0.30 mmol) and Pd(P^tBu_3)$_2$ (103 mg, 0.20 mmol) were combined in a 25 mL Teflon-sealed glass vessel equipped with a magnetic stir bar in a glovebox. 8 mL acetonitrile was added (note: Pd(P^tBu_3)$_2$ is only

slightly soluble in MeCN). The vessel sealed, removed from the glovebox, and 4 atm of CO was added. Upon the addition of CO, the mixture becomes yellow and $Pd(P^tBu_3)_2$ dissolves. The vessel was placed inside an oil bath at 55ºC for 16 hours, then brought back into the glovebox and the solvent was removed *in vacuo*. The resulting dark yellow paste was washed multiple times with small portions (ca. 2 mL) of pentanes to give **2.1a** as a yellow solid (102 mg, 92% yield).[29]

^{1}H NMR (500 MHz, $CDCl_3$): δ 8.11 (d, *J* = 8.2 Hz, 2H), 7.18 (d, *J* = 8.2 Hz, 2H), 2.38 (s, 3H), 1.43 (d, *J* = 12.8 Hz, 27H). ^{13}C NMR (126 MHz, $CDCl_3$): 195.6 (d, *J* = 4.6 Hz), 144.1, 132.6 (d, *J* = 13.7 Hz), 131.6, 128.9, 39.9 (d, *J* = 7.3 Hz), 32.2 (*J* = 4.6 Hz), 21.7. ^{31}P NMR (162 MHz, $CDCl_3$): δ 71.2. Analysis for $C_{20}H_{34}IOPPd$, Theory: 43.30 %C, 6.18 %H, Found: 43.49 %C, 6.26 %H.

Reactivity of *p*-TolylCOPd(P^tBu_3)I (2.1a) with Imine and CO (Scheme 2.3)

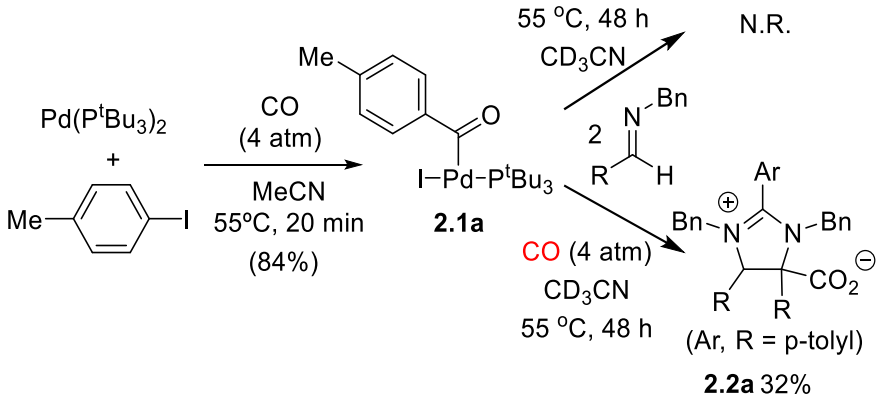

In a glove box, *p*-TolylCOPd(P^tBu_3)I **2.1a** (4.0 mg, 0.0072 mmol), (*p*-Tolyl)CH=NBn (3.0 mg, 0.0144 mmol), and benzyl benzoate standard (1.0 mg, 0.0045mmol) were dissolved in 0.75 mL CD_3CN and transferred into a J-Young NMR tube. The tube was sealed, taken out of the glovebox, and warmed to 55 ºC for 48 h. ^{1}H NMR analysis shows no change in the integrations

for any of the components in the mixture and no new signals appear. The above procedure was repeated with the addition of 4 atm CO prior to warming to 55 °C for 48 h. ^{1}H NMR analysis shows the formation of **2.2a** in 32% yield.

Influence of Chloride in Catalysis (Scheme 2.4)

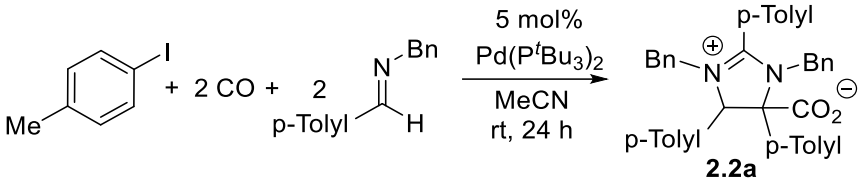

No additive: 0%
Bu_4NCl (5%): 41%
Bu_4NCl (1 eq.): 80%
$[Pd(allyl)Cl]_2$ / P^{t}Bu$_3$: 32%

In a glovebox, 4-iodotoluene (136 mg, 0.625 mmol), (*p*-Tolyl)CH=NBn (26 mg, 0.125 mmol), $[Pd(allyl)Cl]_2$ (1.1 mg, 0.0031 mmol), P^{t}Bu$_3$ (1.6 mg, 0.0081 mmol), benzyl benzoate (13 mg, 0.0625 mmol) were dissolved in 0.75 mL CD_3CN and transferred into a J-Young NMR tube. The tube was then sealed with a screwcap, taken out of the glovebox,charged with 4 atm of CO, and then allowed to react at ambient temperature for 24 h with occasional mixing. ^{1}H NMR analysis shows that **2.2a** is formed in 32% yield relative to the benzyl benzoate standard.

In a glovebox, 4-iodotoluene (136 mg, 0.625 mmol), (*p*-Tolyl)CH=NBn (26 mg, 0.125 mmol), Pd(P^{t}Bu$_3$)$_2$ (3.2 mg, 0.0063 mmol), and benzyl benzoate (13 mg, 0.0625 mmol) were dissolved in CD_3CN and transferred into a J-Young NMR tube. This procedure was repeated in two other NMR tubes with in this case the addition of Bu_4NCl (1.7 mg, 0.0063 mmol) and Bu_4NCl (35 mg, 0.125 mmol). The tubes were then sealed with a screwcap, taken out of the glovebox, charged with 4 atm of CO, and allowed to react at ambient temperature for 24 h with occasional mixing. ^{1}H NMR analysis shows 0% of **2.2a** was formed in the tube with no additive; while 41%

was formed in the tube with catalytic amount of Bu_4NCl, and 80% was produced in the tube with one full equivalent of the Bu_4NCl.

Synthesis of *p*-TolylCOPd(P^tBu_3)Cl (2.1b)

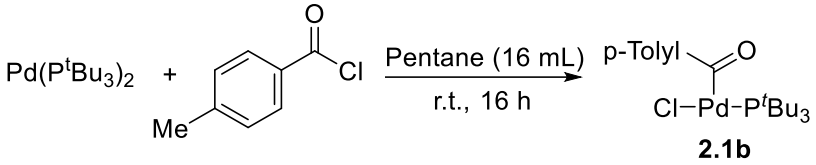

2.1b

In a glove box, a 20 mL round bottom flask was charged with Pd(P^tBu_3)$_2$ (439 mg, 0.859 mmol), and *p*-toluoyl chloride (266 mg, 1.719 mmol) in 16 mL pentanes. The yellow homogeneous mixture was allowed to stand, and the product **2.1b** began precipitating as a dark red solid after 30 minutes. After 16 h, the solid was collected by filtration, and washed with pentane (3 × 2 mL) to afford the analytically pure complex **2.1b** (369 mg, 93% yield).[4]

Orange solid. ^{1}H NMR (500 MHz, $CDCl_3$): δ 8.15 (d, *J* = 7.9 Hz, 2H), 7.20 (d, *J* = 7.9 Hz, 2H), 2.37 (s, 3H), 1.43 (d, *J* = 12.8 Hz, 27H). ^{13}C NMR (126 MHz, $CDCl_3$): δ 198.2 (d, *J* = 5.5 Hz), 144.0, 133.4 (d, *J* = 14.6 Hz), 131.3, 129.1, 39.6 (d, *J* = 9.2 Hz), 32.1 (d, *J* = 4.6 Hz), 21.7. ^{31}P NMR (162 MHz, $CDCl_3$): δ 73.0. Analysis for $C_{20}H_{34}ClOPPd$, Theory: 51.85 %C, 7.40 %H, Found: 51.69 %C, 7.39 %H.

Reactivity of p-TolylCOPd(P^{t}Bu$_3$)Cl (2.1b) with Imine and CO (Scheme 2.5)

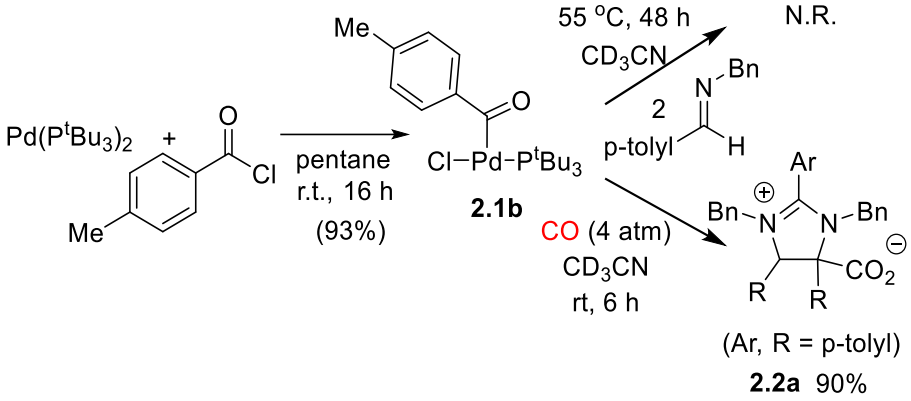

In a glove box, **2.1b** (23 mg, 0.050 mmol), (*p*-Tolyl)CH=NBn (21 mg, 0.100 mmol), and benzyl benzoate standard (10.6 mg, 0.0500 mmol) were dissolved in 0.75 mL CD_3CN and transferred into a J-Young NMR tube. The tube was then sealed with a screwcap and taken out of the glovebox. This procedure was duplicated. One of the NMR tubes was warmed to 55 ºC for 48 h, while the other was charged with 4 atm of CO and then allowed to react at ambient temperature, swirling occasionally. Both reactions were monitored via ^{1}H NMR analysis showed no formation of **2.2a** in the tube without CO; however, in the tube with CO, **2.2a** had formed in 90% after 6 hours.

Generation of Acid Chloride from 2.1b (Scheme 2.7)

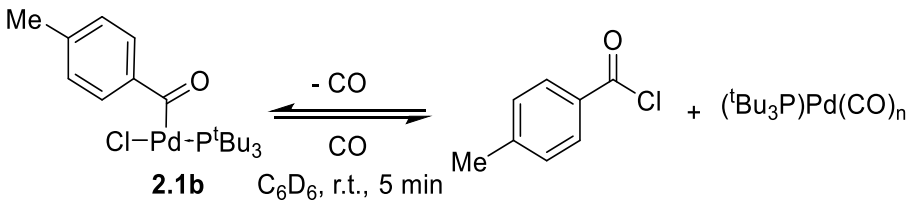

In a glove box, **2.1b** (50 mg, 0.108 mmol) and benzyl benzoate standard (24 mg, 0.115 mmol) were dissolved in 3.75 mL C_6D_6. Five J-Young NMR tubes were then charged each with

0.75 mL of the solution. The tubes were then sealed with a screwcap, taken out of the glovebox, and charged with different amounts of CO (0, 1, 2, 3, and 4 atm). After ca. 5 minutes, the mixtures were analyzed via ^{1}H NMR, and the yield of *p*-toluoyl chloride and **2.1b** was determined by integration vs. the internal standard.

CO pressure (atm)	**%2.1b**
0	0
1	18
2	30
3	42
4	52

In situ ^{1}H NMR analysis of the reaction with 4 atm CO, only aromatic and tolyl signals are listed (C_6D_6, 400 MHz): δ 8.42 (d, *J* = 8.1 Hz), 7.79 (d, *J* = 8.3 Hz), 6.83 (d, *J* = 7.8 Hz), 6.65 (d, *J* = 8.1 Hz), 1.89 (s), 1.82 (s). ^{1}H NMR data for pure p-toluoyl chloride (C_6D_6, 400 MHz): δ 7.77 (d, *J* = 8.3 Hz, 2H), 6.68 (d, *J* = 7.8 Hz, 2H), 1.86 (s, 3H). ^{1}H NMR data for pure complex **1b** (C_6D_6, 400 MHz): δ 8.43 (d, *J* = 7.9 Hz, 2H), 6.85 (d, *J* = 7.9 Hz, 2H), 1.90 (s, 3H), 1.12 (d, *J* = 12.8 Hz, 27H). *In situ* ^{13}C NMR analysis of the reaction with 4 atm CO (C_6D_6, 100 MHz): δ 187.3, 168.1, 146.7, 132.2 132.0, 131.3, 130.0, 129.5, 39.5, 37.5, 32.5, 32.3, 21.7_1, 21.7_2. ^{13}C NMR data for pure p-toluoyl chloride (C_6D_6, 100 MHz): δ 168.1, 147.1, 132.0, 131.1, 130.1, 21.8. ^{13}C NMR data for pure complex **2.1b** (C_6D_6, 100 MHz): δ 201.0 (d, *J* = 5.5 Hz), 143.8, 135.4 (d, *J* = 13.7 Hz), 132.2, 129.5, 39.6 (d, *J* = 8.2 Hz), 32.4 (d, *J* = 4.6 Hz), 21.7.

Intermediacy of N-Acyl Iminium Salt (Scheme 2.8)

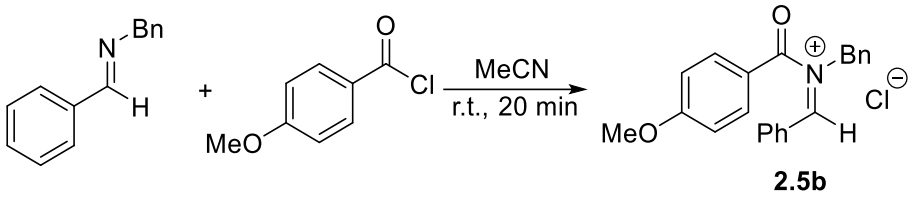

2.5b

In a glovebox, PhCH=NBn (100 mg, 0.512 mmol) and 4-$MeOC_6H_4COCl$ (114 mg, 0.666 mmol) were dissolved in 2 mL MeCN. The solution was allowed to stir for 20 minutes at room temperature. The solvent was then removed *in vacuo* and the resulting oil was washed 7 times with 1 mL portions of pentanes. The yellow oil was then cooled to -33ºC for 30 minutes with a layer of pentanes on top, and a slightly yellow precipitate formed. The supernatant was decanted and the solid was dried *in vacuo* for several hours affording pale yellow iminium salt **2.5b** (113 mg, 0.308 mmol, 60% yield).

^{1}H NMR of **2.5b** (400 MHz, CD_3CN): δ 7.60 (d, *J* = 8.8 Hz, 2H), 7.57-7.55 (m, 2H), 7.43 (s, 1H), 7.39-7.33 (m, 3H), 7.16 (d, *J* = 7.1 Hz, 2H), 7.08-7.05 (m, 2H), 7.01 (d, *J* = 9.0 Hz, 2H), 4.54 (s, 2H), 3.83 (s, 3H). ^{13}C NMR of **2.5b** (100 MHz, CD_3CN): 173.7, 162.9, 139.0, 138.2, 135.4, 130.4, 130.3, 129.9, 129.4, 128.9, 128.0, 115.5, 56.7, 47.9.

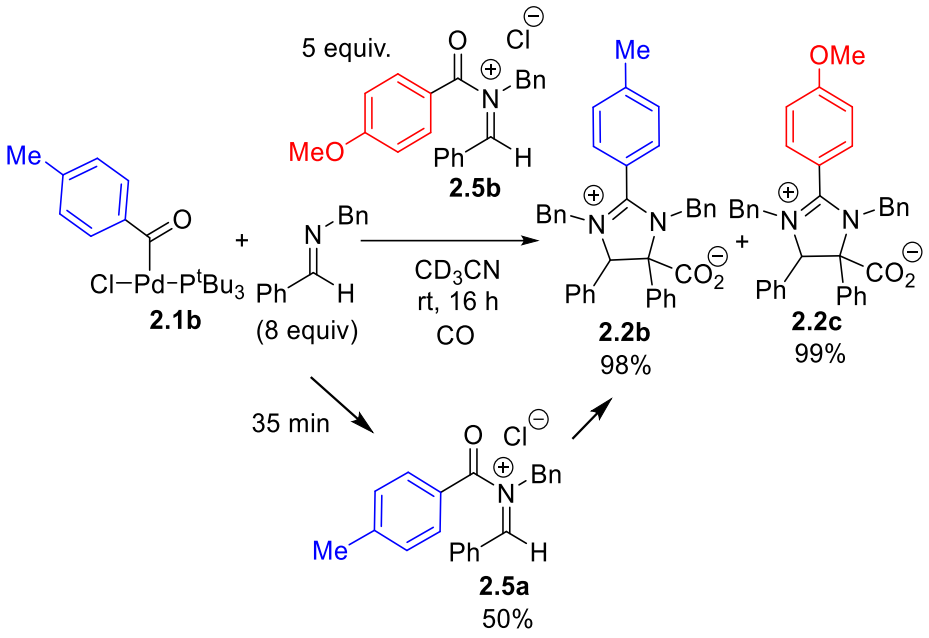

In a glove box, **2.1b** (6.6 mg, 0.0143 mmol), PhCH=NBn (39 mg, 0.200 mmol), iminium salt **2.5b** (26 mg, 0.0716 mmol), and benzyl benzoate standard (11 mg, 0.0500 mmol) were dissolved in 0.75 mL CD_3CN and transferred into a J-Young NMR tube. The tube was then sealed with a screw cap, taken out of the glove box, charged with 4 atm of CO, and allowed to stand at ambient temperature. The mixture was analyzed by ^1H and ^{31}P NMR every 10 minutes over 2 hours. ^1H NMR analysis showed that iminium salt **2.5a** was formed in 50% yield at 35 minutes, but then it was quickly consumed over the next 30 minutes. After 16 hours, upon imidazolinium carboxylates **2.2b** (98%) and **2.2c** (99%) were observed.[30]

Synthesis of Palladacycle 2.4 (Scheme 2.9)

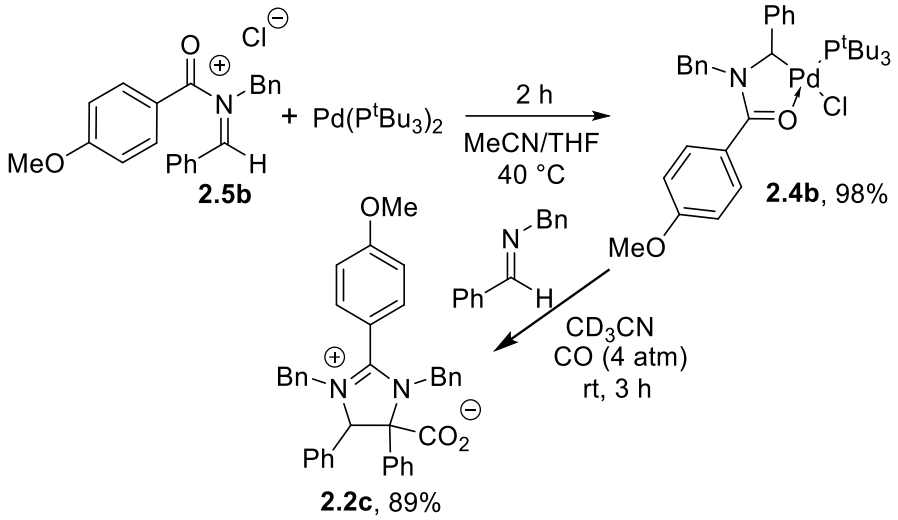

In a glove box, $Pd(P^tBu_3)_2$ (25 mg, 0.049 mmol), iminium salt **2.5b** (36 mg, 0.098 mmol), and benzyl benzoate standard (5.2 mg, 0.0245 mmol) were dissolved in 0.75 mL THF/CD_3CN (2:1) and transferred into a J-Young NMR tube. The tube was then sealed, taken out of the glove box, and heated at 40ºC. The reaction was monitored periodically via ^1H NMR analysis using double solvent suppression to eliminate the signals of THF. The yield of **2.5b** after 2 h was determined by ^1H NMR integration vs internal standard (98%). The NMR tube was brought back into the glove box and PhHC=NBn (9.3 mg, 0.049 mmol) was added. The NMR tube was sealed with a screw-cap, taken out of the glovebox, charged with 4 atm of CO and allowed to react at ambient temperature. The yield of **2c** (89%) was calculated using ^1H NMR integrations.

Due to difficulties in the isolation of an analytically pure sample of complex **2.4b**, an analogue, **2.4a**, was prepared. [Pd(*p*-tolyl)HCNBnCO(*p*-tolyl)]$_2$ was prepared as previously described.[32] To this complex (50 mg, 0.055 mmol), tri-*tert*-butylphosphine (44 mg, 0.219 mmol) was added in 5 mL toluene. The solution was allowed to stir at room temperature for 30 minutes. The solvent was removed *in vacuo*, affording an orange oil. The product was washed with 6 x 1

mL portions of pentanes. Solvent traces were then removed *in vacuo* to afford palladacycle **2.4a** as a yellow solid in 77% isolated yield (57 mg, 0.085 mmol).

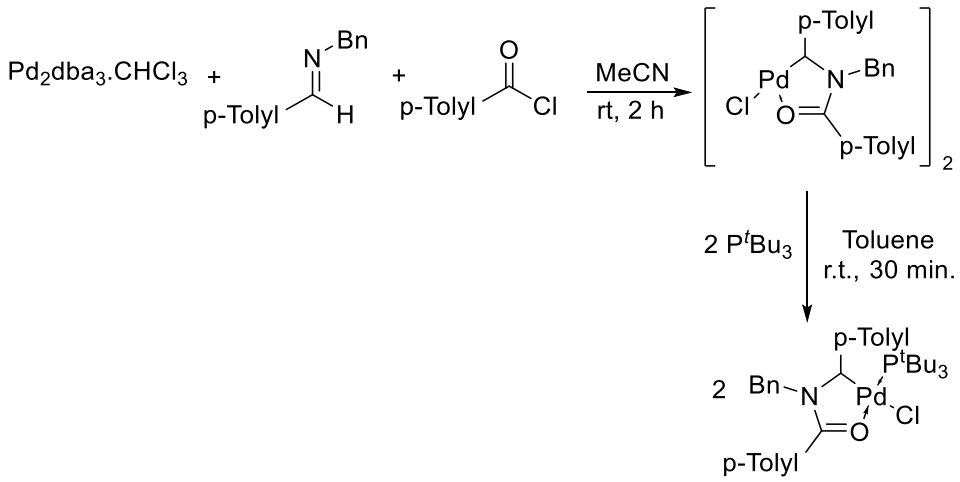

Yellow solid. ^{1}H NMR (400 MHz, C_6D_6): δ 7.61 (d, *J* = 7.1 Hz, 2H), 7.36 (d, *J* = 7.8 Hz, 2H), 7.07 (d, *J* = 7.8 Hz, 2H), 6.99-6.91 (m, 5H), 6.75 (d, *J* = 8.1 Hz, 2H), 5.94 (d, *J* = 9.3 Hz, 1H), 4.38 (dd, *J* = 15.9, 2.9 Hz, 1H) 4.01 (d, *J* = 15.9 Hz, 1H), 2.05 (s, 3H), 1.93 (s, 3H), 1.52 (d, *J* = 11.0 Hz, 27H). ^{31}P NMR (162 MHz, C_6D_6 = δ 66.4 ^{13}C NMR (100 MHz, $CDCl_3$): δ 179.7 (d, *J* = 7.3 Hz), 141.6, 139.7 (d, *J* = 5.9 Hz), 135.0, 134.7 (d, *J* = 2.9 Hz), 129.8, 129.5, 129.3 (d, *J* = 1.5 Hz), 128.9, 127.9, 127.6, 127.5, 125.6 (d, *J* = 2.9 Hz), 69.5 (d, *J* = 97.6 Hz), 52.5 (d, *J* = 4.4 Hz), 37.9, 32.7 (d, *J* = 5.9 Hz), 21.5, 21.4. HRMS (ESI$^+$) for $C_{35}H_{48}NClO_6PPd^+$; calculated 670.21914, found 670.22021 (error m/z = 1.6 ppm)

Stoichiometric Münchnone Generation (Scheme 2.10)

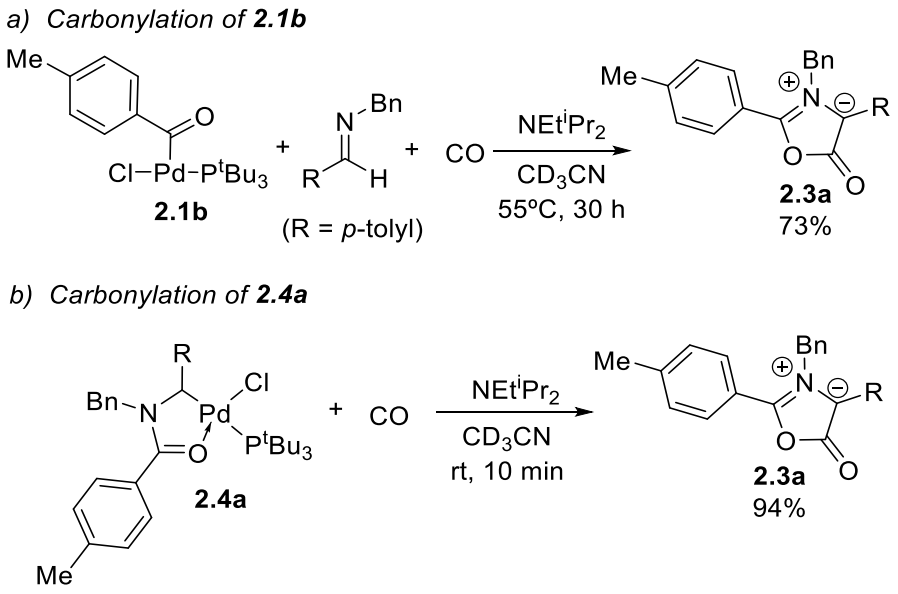

In a glove box, **2.1b** (26 mg, 0.0562 mmol), (*p*-Tolyl)CH=NBn (12 mg, 0.0562 mmol), NEt^iPr_2 (11 mg, 0.0843 mmol), and benzyl benzoate standard (12 mg, 0.0562 mmol) were dissolved in 0.75 mL CD_3CN and transferred into a J-Young NMR tube. The NMR tube was then sealed with a screw cap, taken out of the glove box, charged with 4 atm of CO and allowed to react at 55 ºC. ^1H NMR analysis showed the formation of **2.3a** in 73% yield after 30 hours.

In a glove box, **2.4a** (5.0 mg, 0.0074 mmol), NEt^iPr_2 (1.0 mg, 0.0080 mmol), and benzyl benzoate standard (0.8 mg, 0.0037 mmol) were dissolved in 0.75 mL CD_3CN and transferred into a J-Young NMR tube. The NMR tube was then sealed with a screw cap, taken out of the glove box, charged with 4 atm of CO, and allowed to react at ambient temperature. ^1H NMR analysis after 10 min showed the formation of **2.3a** in 94% yield.

***In situ* ^{31}P NMR Analysis of the Catalytic Formation of Imidazolinium Carboxylate (Figure 2.1)**

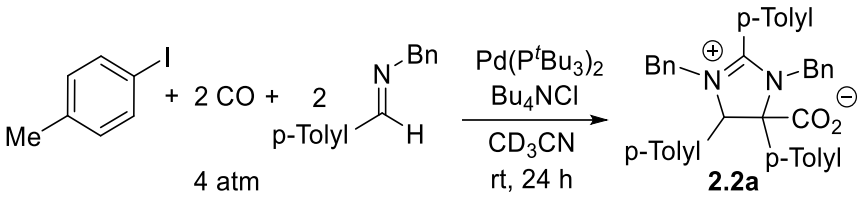

In a glove box, Pd(P^{t}Bu$_3$)$_2$ (6.4 mg, 0.0126 mmol) and Bu$_4$NCl (18 mg, 0.063 mmol) were dry-transferred into a J-Young NMR tube. (*p*-tolyl)CH=NBn (13 mg, 0.063 mmol) and 4-iodotoluene (69 mg, 0.315 mmol) were dissolved in 0.75 mL CD$_3$CN and added to the NMR tube. The NMR tube was then sealed with a screw cap, taken out of the glove box, charged with 4 atm of CO and allowed to react at ambient temperature. ^{31}P NMR (162 MHz) data was collected periodically. The only observable species at early reaction times were complex **2.1b** (72.8 ppm) and free phophine (63.4 ppm). After 8 h, protonated phosphine was observed (46.1 ppm) as the only phosphorus containing compound.

Typical Procedure for Kinetic Analysis (Figure 2.2)

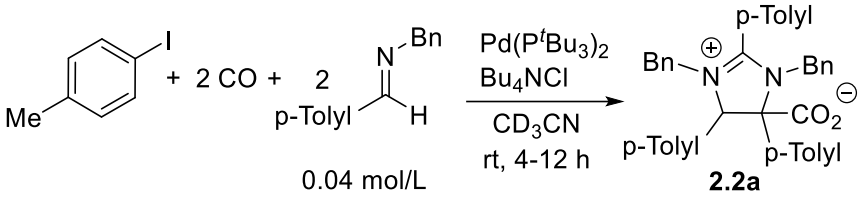

In a glove box, Pd(P^{t}Bu$_3$)$_2$ (1.6 mg, 0.0031 mmol) and Bu$_4$NCl (8.7 mg, 0.031 mmol) were transferred into a J-Young NMR tube. (p-tolyl)CH=NBn (6.6 mg, 0.031 mmol), 4-iodotoluene (68 mg, 0.310 mmol), and benzyl benzoate standard (3.3 mg, 0.0156 mmol) were dissolved in 0.75 mL CD$_3$CN and transferred into the NMR tube. The NMR tube was then sealed with a screw cap, taken out of the glove box, and charged with 4 atm of CO. The contents of the tube were kept frozen until loading into the NMR spectrometer. An array experiment was programmed to collect

^{1}H NMR spectra starting at t = 5 minutes at 40°C, with subsequent points collected every 15 minutes. The consumption of imine was monitored via ^{1}H NMR integration vs. the internal standard. This procedure was repeated in duplicate at different CO pressure, aryl iodide concentration and initial imine concentration.

A. Effect of CO Pressure on rate

CO pressure = 1 atm [ArI] = 0.40 mol/L

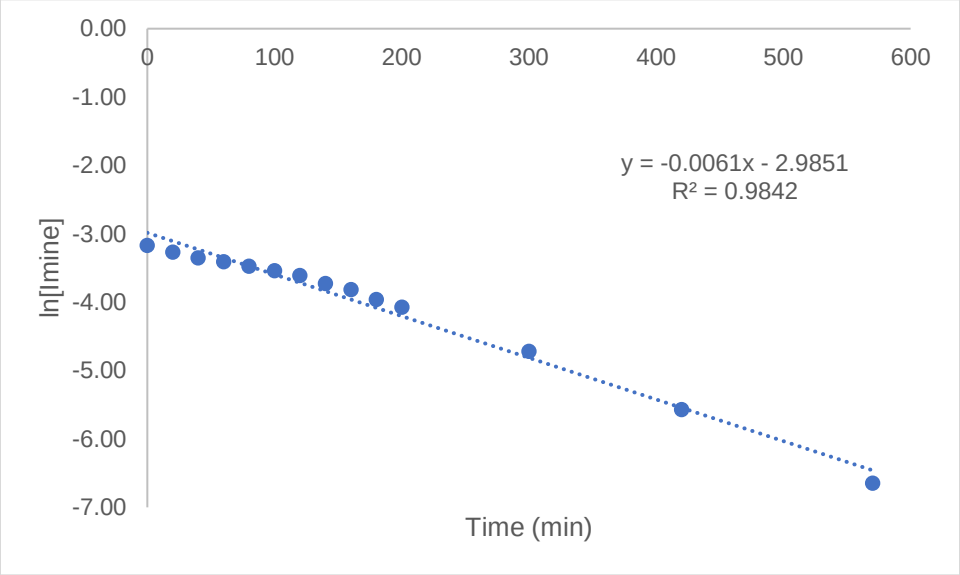

CO pressure = 2 atm [ArI] = 0.40 mol/L

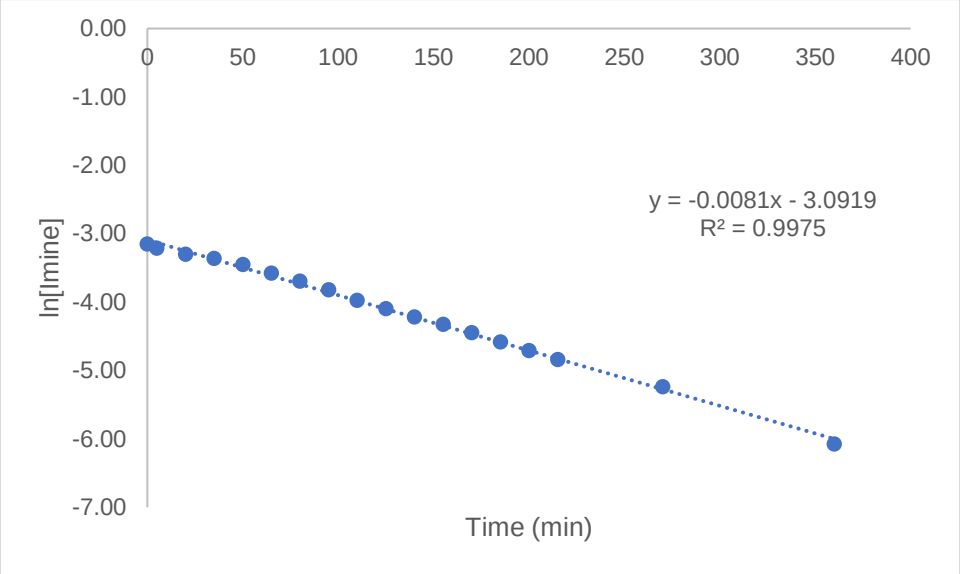

CO pressure = 3 atm [ArI] = 0.40 mol/L

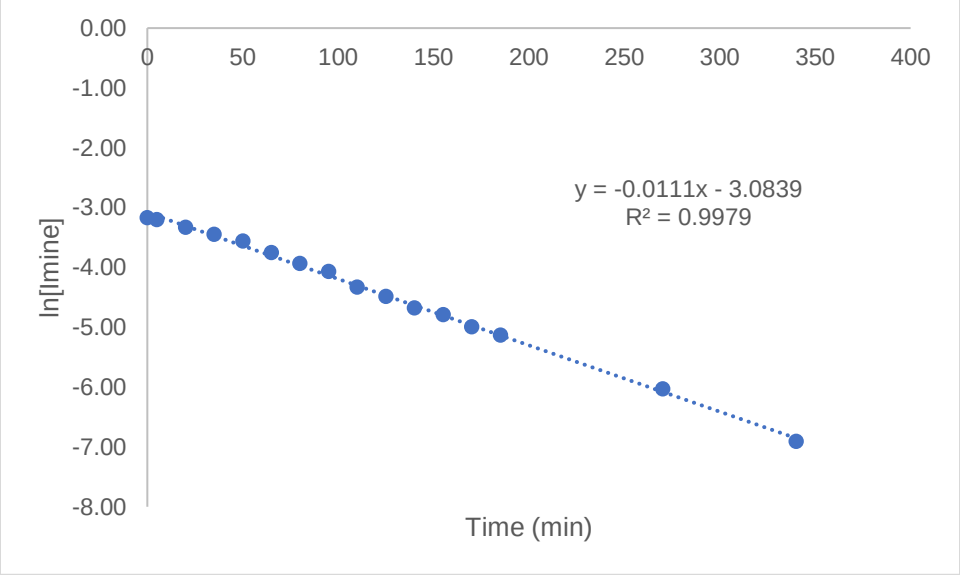

CO pressure = 4 atm [ArI] = 0.40 mol/L

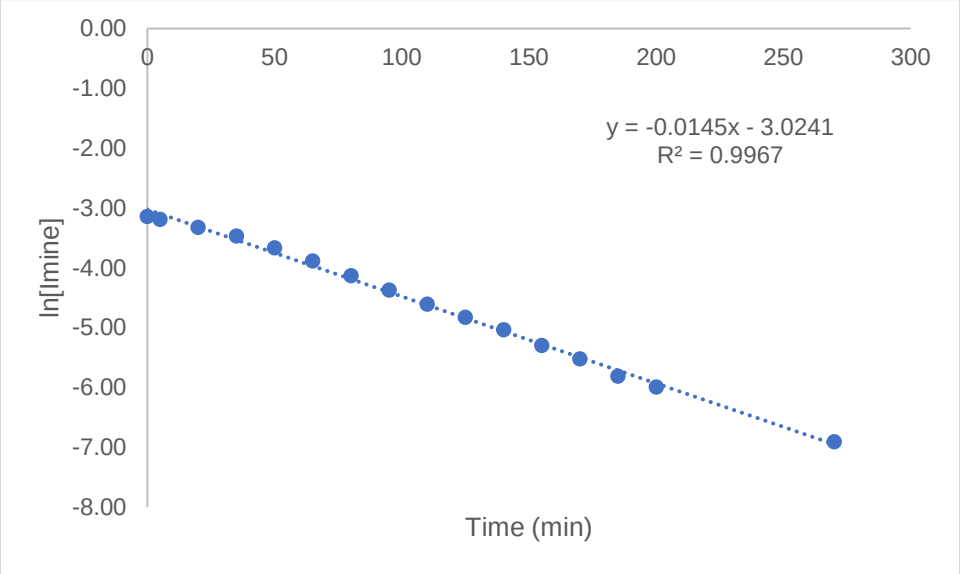

CO pressure = 5 atm [ArI] = 0.40 mol/L

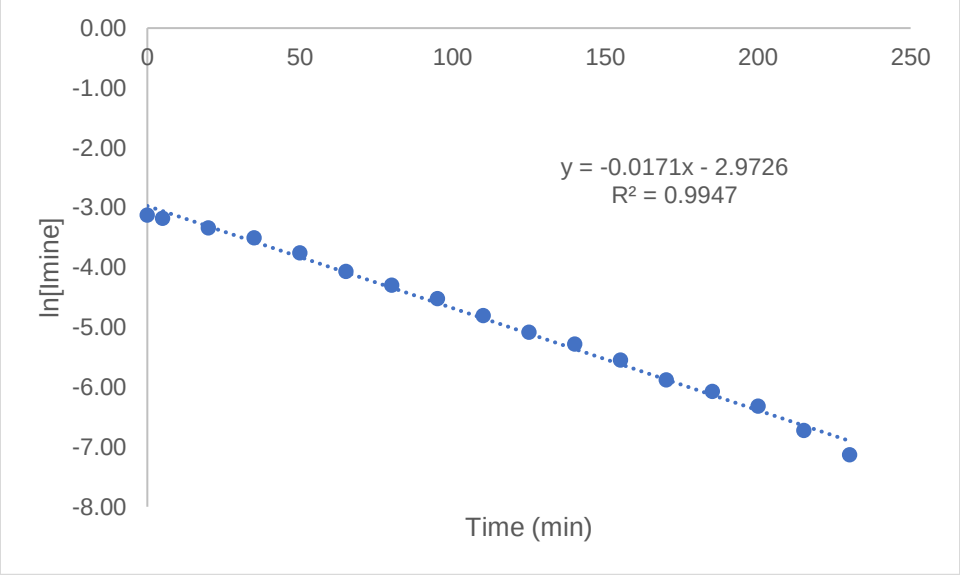

Effect of CO pressure on initial rate:

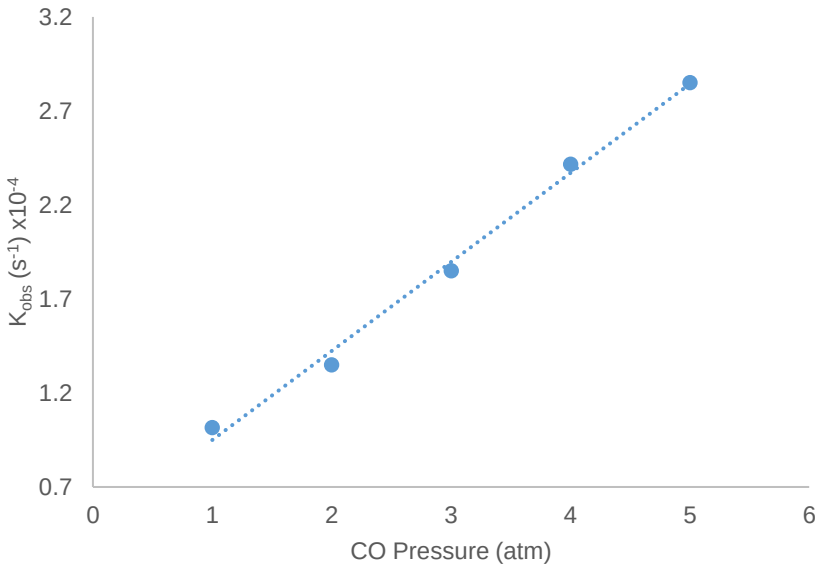

B. Effect of [aryl iodide] on rate

CO pressure = 4 atm [ArI] = 0.21 mol/L

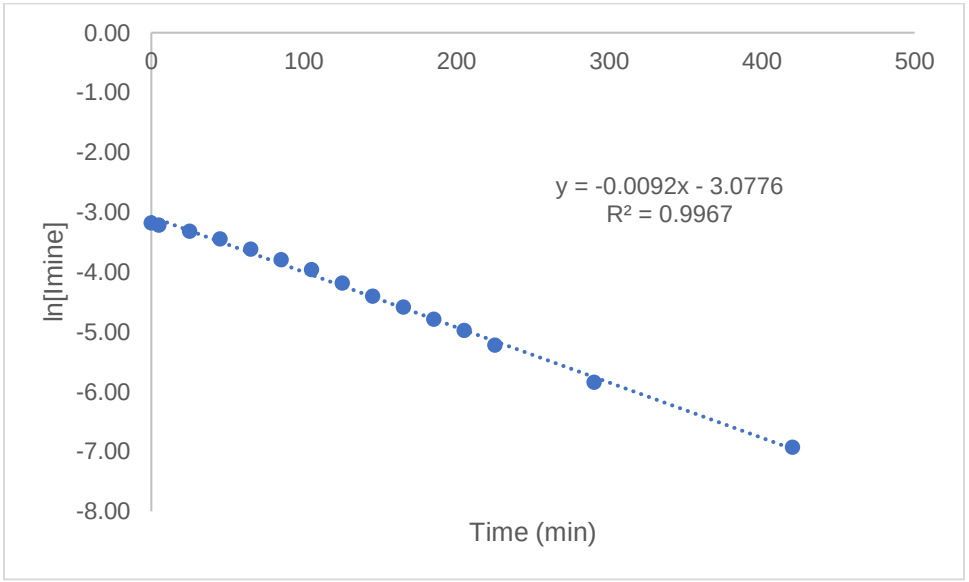

CO pressure = 4 atm [ArI] = 0.31 mol/L

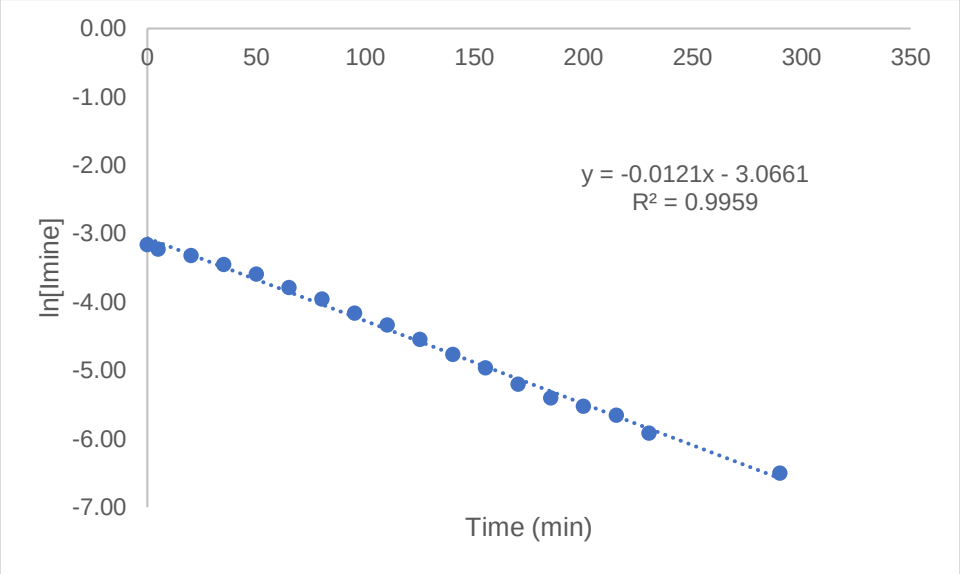

CO pressure = 4 atm [ArI] = 0.40 mol/L

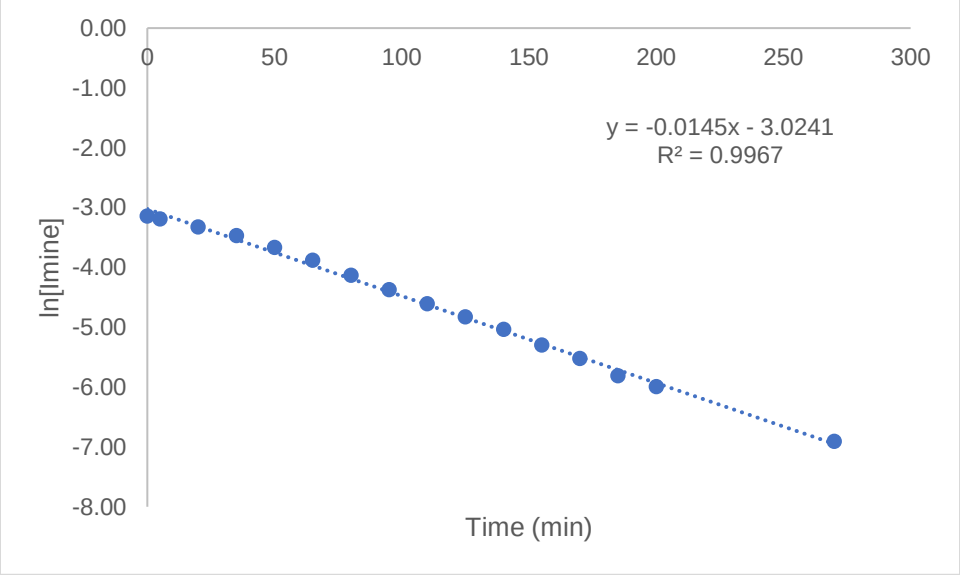

CO pressure = 4 atm [ArI] = 0.51 mol/L

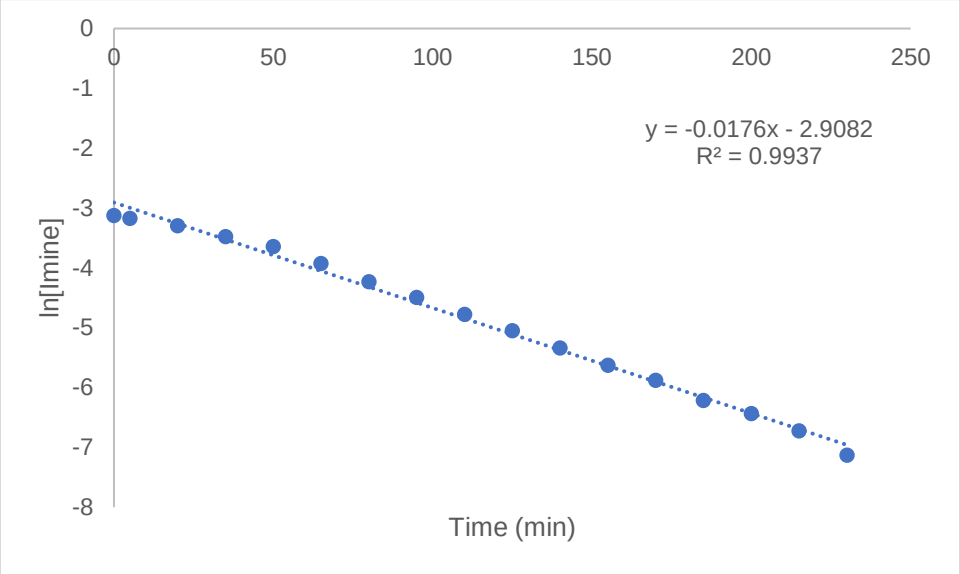

Effect of aryl iodide concentration on initial rate:

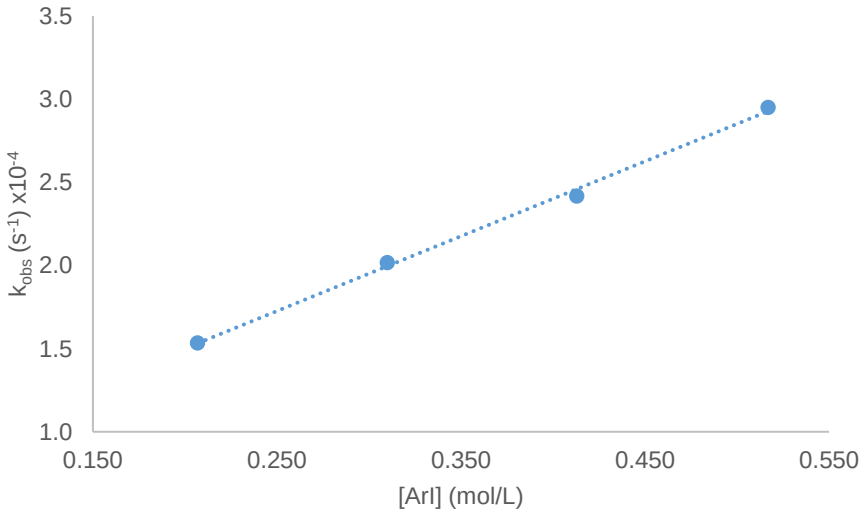

C. Influence of Imine Concentration on Initial Rate

Since imine is the limiting reagent in the reaction, its effect on the reaction rate was determined by examining initial rates at different imine concentrations.

$[Imine]_0$ = 0.01 mol/L

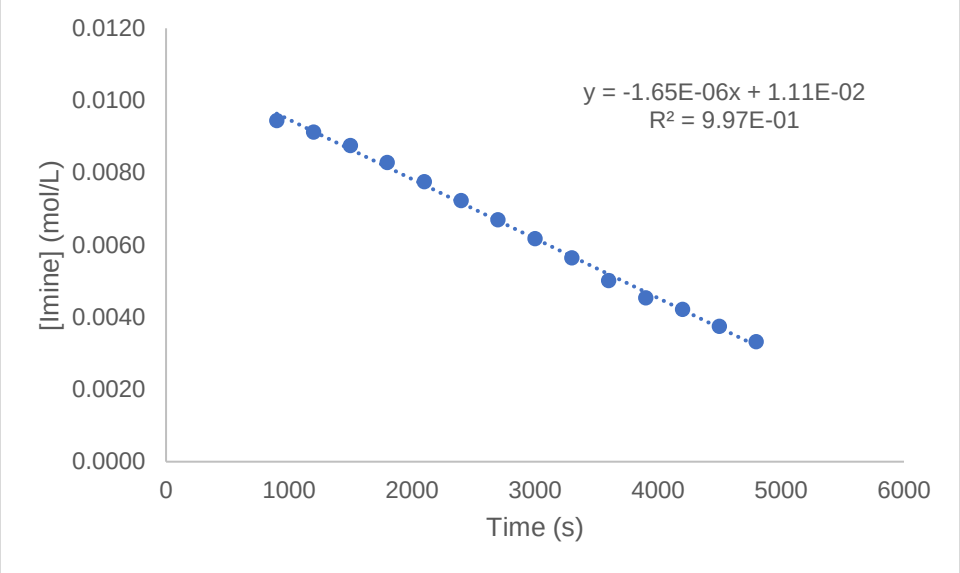

$[Imine]_0$ = 0.02 mol/L

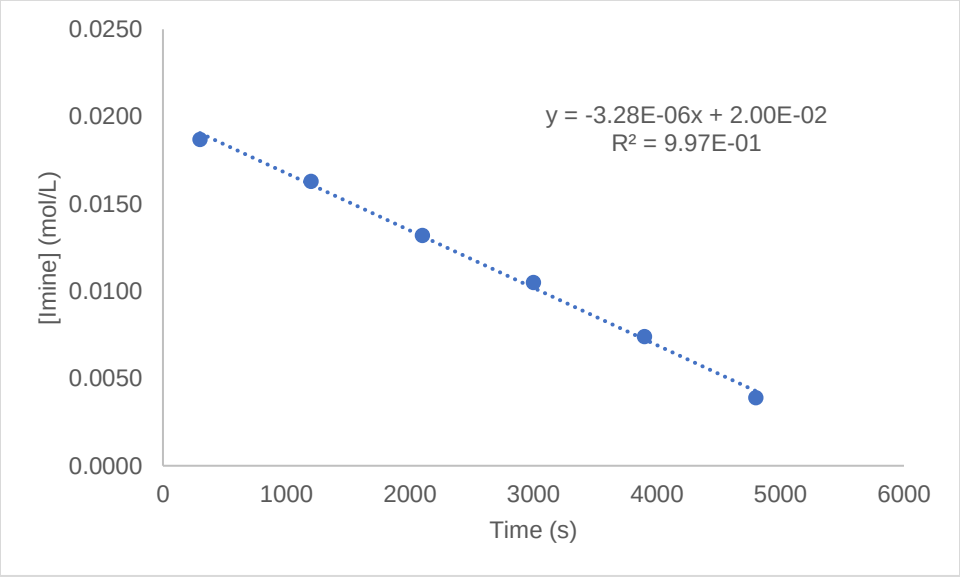

$[Imine]_0$ = 0.03 mol/L

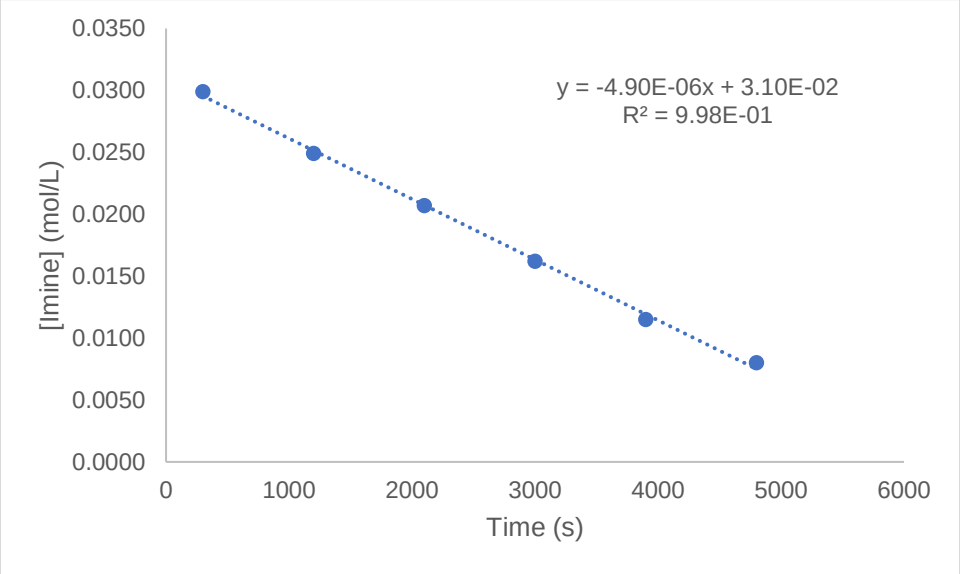

$[Imine]_0$ = 0.04 mol/L

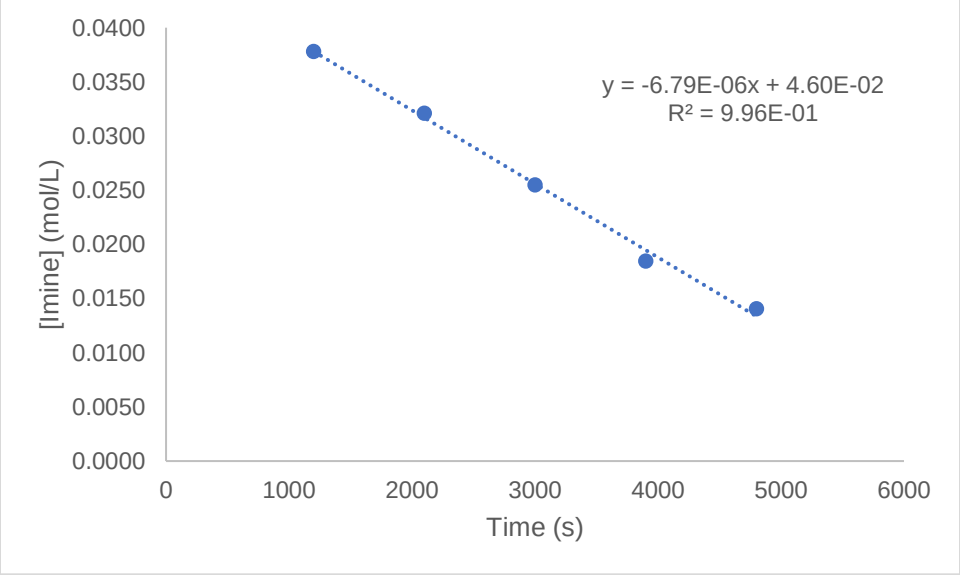

Effect of imine concentration on initial rate:

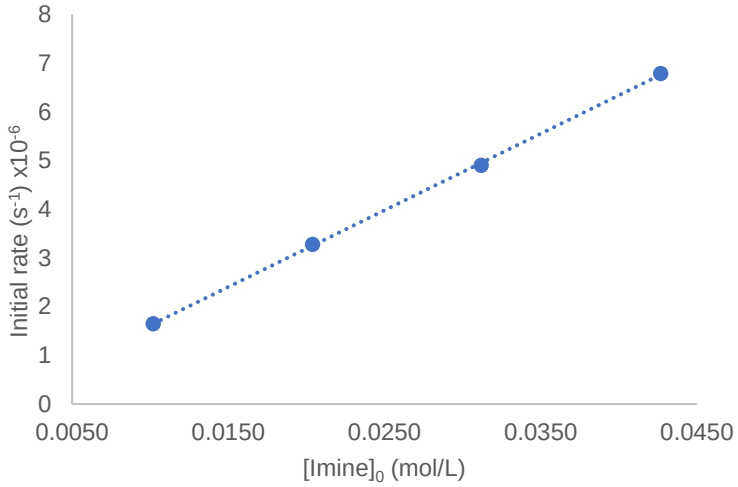

Typical Procedure for the Catalytic Münchnone Formation

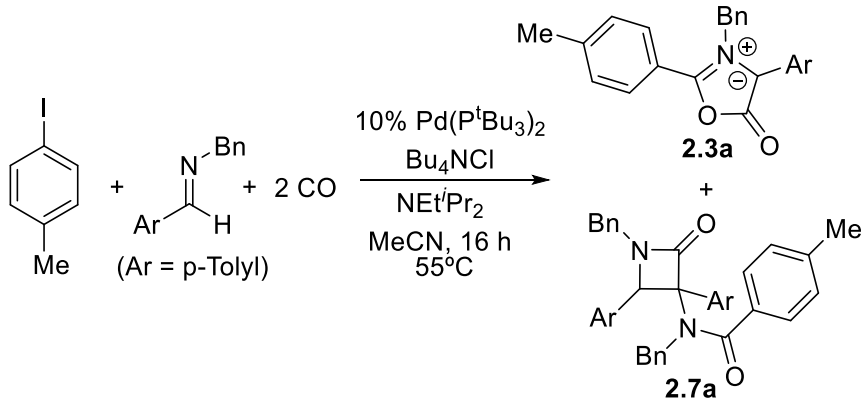

In a glovebox, $Pd(P^tBu_3)_2$ (13 mg, 0.025 mmol) and Bu_4NCl (69 mg, 0.25 mmol) were dry-transferred into a 25 mL Teflon-sealed glass Schlenk bomb vessel equipped with a magnetic stir bar. NEt^iPr_2 (49 mg, 0.375 mmol), 4-iodotoluene (55 mg, 0.25 mmol), (*p*-Tolyl)CH=NBn (52 mg, 0.25 mmol), and benzyl benzoate standard (26 mg, 0.125 mmol) were dissolved in 1.7 mL MeCN and transferred into the vessel. The vessel was taken out of the glovebox, frozen, and evacuated

before adding 1 atm of CO. The vessel was warmed to 55 ºC with stirring for 16 hours. At the end of the reaction, CO was removed and the vessel was brought back into the glovebox. The solvent was evaporated *in vacuo*; the remaining oil was dissolved in CD_3CN and the yields of Münchnone **2.3a** (20%)[32] and β-lactam **2.7a** (32%)[33] were calculated by ^1H NMR integration vs. the internal standard.

For experiments with 10 atm CO, the above procedure was repeated in a 2 mL glass vial with a pierced cap. The vial was placed inside a 40 mL Parr steel autoclave, which was sealed, taken out of the glovebox, and charged with 10 atm CO using a Parr Multiwell Reactor 5000. The reactor was then submerged in a constant temperature bath at 55 ºC and stirred magnetically.

Typical Procedure for Phosphine Ligand Screening

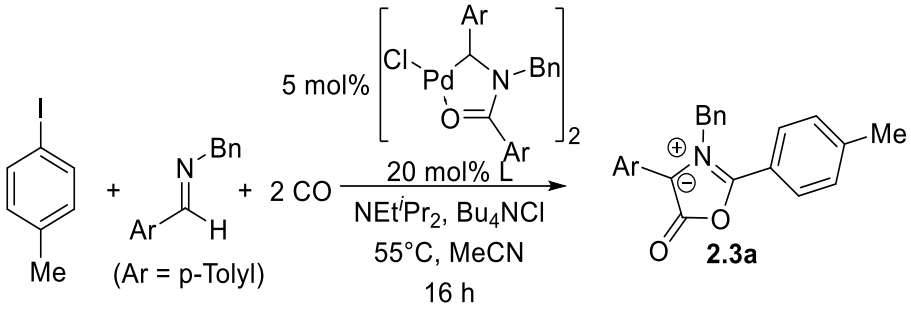

In a glovebox, **2.4a** (6.8 mg, 0.0075 mmol) and Bu_4NCl (42 mg, 0.15 mmol), NEt^iPr_2 (29 mg, 0.225 mmol), 4-iodotoluene (33 mg, 0.15 mmol), (*p*-Tolyl)CH=NBn (31 mg, 0.15 mmol), P^tBu_3 (6.1 mg. 0.03 mmol), and benzyl benzoate standard (16 mg, 0.075 mmol) were dissolved in 1 mL CD_3CN and transferred into a 25 mL Teflon-sealed glass Schlenk bomb vessel equipped with a magnetic stir bar. The vessel was taken out of the glovebox, charged with 4 atm of CO, then heated to 55 ºC with magnetic stirring for 16 hours. The CO was then removed, and the vessel was brought back into the glovebox. The mixture was transferred into an NMR tube and the yield of

Münchnone **2.3a** (62%) and β-lactam **2.7a** (20%) were calculated via ^{1}H NMR integrations vs the internal standard.

Typical Procedure for Pyrrole Synthesis

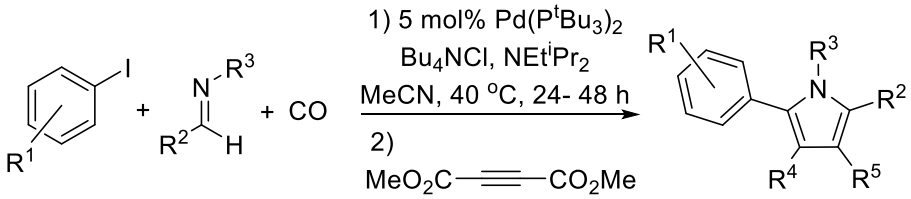

In a glovebox, Pd(P^{t}Bu$_3$)$_2$ (13 mg, 0.025 mmol), and Bu$_4$NCl (139 mg, 0.5 mmol) were placed in a 4 mL vial equipped with a magnetic stir bar. (p-Tolyl)HC=NBn (105 mg, 0.5 mmol), 4-iodotoluene (545 mg, 2.5 mmol), and NEt^{i}Pr$_2$ (97 mg, 0.75 mmol) were dissolved in 3.3 mL of MeCN and transferred into the 4 mL glass vial. (For the synthesis of pyrrole **2.8e**, a mixture of MeCN/THF (2:1) was used as the solvent due to the limited solubility of the aryl iodide in pure MeCN.) The vial was closed with a pierced plastic cap, placed inside a Parr steel autoclave, sealed, and taken out of the glovebox. The reactor was charged with 10 atm CO using a Parr Multiwell Reactor 5000. The autoclave was then submerged in a constant temperature bath at 40ºC and magnetically stirred. After 16 h, CO was removed, and the vessel back into the glovebox. The reactor was opened and dimethylacetelynedicarboxylate (DMAD) (107 mg, 0.75 mmol) was added. The mixture was allowed to stir for 15 minutes and then the vessel was taken out of the glovebox. The pyrrole product was isolated by flash chromatography on silica gel (230-400 mesh) with hexanes-ethyl acetate 4:1 (**2.8a-v,y,z,aa**) or hexanes-ethyl acetate 9:1 (**2.8w,x,ab,af**). The fractions containing pyrrole were evaporated under reduced pressure and solvent traces were removed *in vacuo*. Pyrrole **2.8a** was obtained in 84% (191 mg, 0.42 mmol) as a pale yellow solid.

For the synthesis of **2.8j**, the reaction was carried out in 12 mL MeCN, due to the insolubility of the heteroaryl iodide. The mixture of reagents was placed inside a 20 mL glass vessel equipped with a stir bar. The vessel was placed inside a Parr steel autoclave and the rest of the procedure was followed as described above. For pyrrole **2.8r,t,y** the reaction was carried out at 60°C, for 48 h, with 10 mol% catalyst (26 mg, 0.05 mmol). The Münchnone for **2.8s,af** was synthesized at room temperature for 5h. After the synthesis of Münchnone, the vessel was opened and the dipolarophiles were added in the following manner:

Alkyne dipolarophiles were added directly into the reaction mixture (0.75 mmol) and the solution was allowed to stir at room temperature for different times: 15 minutes for DMAD (**2.8a-u)** and dibenzoylacetylene (**2.8v**) derived pyrroles, 24 hours for **2.8w**, 5 hours for **2.8x**. For pyrroles derived from methyl or ethyl phenylpropiolate (**2.8y,z,aa**), the alkyne was added *in situ* at the beginning of the reaction (0.75 mmol).

For alkene dipolarophiles, additional NEt^iPr_2 (97 mg, 0.75 mmol) was first added followed by the dipolarophile (1.0 mmol). The reaction mixture was stirred for 3 hours affording pyrroles (**2.8ab,ac,ae,af)**. Pyrrole **2.8ad** was obtained by first evaporating the crude Münchnone mixture *in vacuo*. The resulting oil was redissolved in THF and diisopropylcarbodiimide (DIPC) (189 mg, 1.5 mmol) was added to the mixture followed by trans-β-nitrostyrene (112 mg, 0.75 mmol). The reaction vessel was placed back in the Parr steel autoclave and brought out of the glove box. The reactor was heated at 55 ºC for 24 hours.[34]

2.5.3. Characterization Data

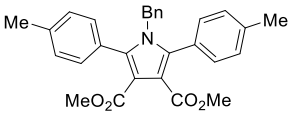

Dimethyl 1-benzyl-2,5-di-p-tolyl-1H-pyrrole-3,4-dicarboxylate (2.8a) Isolated yield 84%. Pale yellow solid. ^{1}H NMR (500 MHz, $CDCl_3$): δ 7.18-7.11 (m, 11H), 6.59-6.57 (m, 2H), 4.91 (s, 2H), 3.68 (s, 6H), 2.33 (s, 6H). ^{13}C NMR (126 MHz, $CDCl_3$): δ 165.5, 138.5, 137.4, 137.2, 130.4, 128.8, 128.3, 127.6, 127.1, 126.1, 114.6, 51.6, 48.4, 21.4. HRMS (ESI^+) for $C_{29}H_{28}O_4N^+$; calculated 454.20128, found 454.20120 (error m/z = 1.79 ppm)

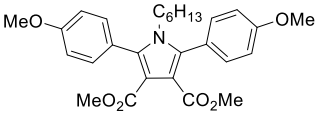

Dimethyl 1-hexyl-2,5-bis(4-methoxyphenyl)-1H-pyrrole-3,4-dicarboxylate (2.8b) Isolated yield 87%. Yellow oil. ^{1}H NMR (500 MHz, $CDCl_3$): δ 7.33 (d, *J* = 8.8 Hz, 4H), 6.97 (d, *J* = 8.8 Hz, 4H), 3.86 (s, 6H), 3.66 (s, 6H), 3.68-3.65 (m, 2H), 1.20-1.15 (m, 2H), 1.06-0.98 (m, 2H), 0.90-0.80 (m, 4H), 0.72 (t, *J* = 7.3 Hz, 3H). ^{13}C NMR (126 MHz, $CDCl_3$): δ 165.6, 159.8, 136.3, 131.8, 123.2, 114.1, 113.7, 55.2, 51.5, 44.8, 30.7, 30.1, 25.8, 22.1, 13.8. HRMS (ESI^+) for $C_{28}H_{34}O_6N^+$; calculated 480.23806, found 480.23775 (error m/z = -0.65 ppm)

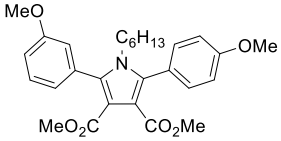

Dimethyl 1-hexyl-2-(3-methoxyphenyl)-5-(4-methoxyphenyl)-1H-pyrrole-3,4-dicarboxylate (2.8c)
Isolated yield 81%. Yellow oil. ^{1}H NMR (500 MHz, $CDCl_3$): δ 7.37-7.32 (m, 3H), 7.00-6.95 (m, 5H), 3.86 (s, 3H), 3.84 (s, 3H), 3.70-3.66 (m, 2H), 3.67 (s, 3H), 3.67 (s, 3H) 1.22-1.16 (m, 2H), 1.06-0.98 (m, 2H), 0.90-0.80 (m, 4H), 0.73-0.70 (t, *J* = 7.2 Hz, 3H). ^{13}C NMR (126 MHz, $CDCl_3$): δ 165.6, 165.4, 159.8, 159.3, 136.6, 135.9, 132.3, 131.8, 129.2, 123.1, 122.9, 116.0, 114.5, 114.4,

114.0, 113.7, 55.3, 55.2, 51.6, 51.5, 44.9, 30.7, 30.2, 25.8, 22.1, 13.8. HRMS (ESI^+) for $C_{28}H_{33}NNaO_6^+$; calculated 502.2200, found 502.2208 (error m/z = 1.6 ppm)

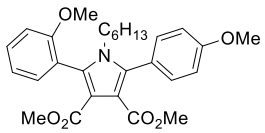

Dimethyl 1-hexyl-2-(2-methoxyphenyl)-5-(4-methoxyphenyl)-1H-pyrrole-3,4-dicarboxylate (2.8d)

Isolated yield 83%. Yellow oil. ^1H NMR (500 MHz, $CDCl_3$): δ 7.43-7.39 (m, 1H), 7.37-7.35 (d, *J* = 8.8 Hz, 2H), 7.31-7.29 (dd, *J* = 7.6, 1.8 Hz, 1H), 7.04-7.01 (td, *J* = 7.6, 0.9 Hz, 1H), 6.98-6.95 (m, 3H), 3.86 (s, 3H), 3.80 (s, 3H), 3.66-3.51 (m, 2H), 3.66 (s, 3H), 3.63 (s, 3H) 1.21-1.11 (m, 2H), 1.05-0.97 (m, 2H), 0.89-0.78 (m, 4H), 0.72-0.70 (t, *J* = 7.3 Hz, 3H). ^{13}C NMR (126 MHz, $CDCl_3$): δ 165.7, 165.4, 159.7, 157.6, 136.4, 133.5, 132.8, 131.9, 130.5, 123.4, 120.4, 120.1, 114.3, 114.2, 113.6, 110.9, 55.5, 55.2, 51.5, 51.3, 45.0, 30.8, 30.0, 25.8, 22.1, 13.8. HRMS (ESI^+) for $C_{28}H_{33}NNaO_6^+$; calculated 502.2200, found 502.2204 (error m/z = -0.9 ppm)

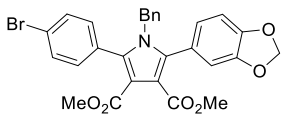

Dimethyl 2-(benzo[d][1,3]dioxol-5-yl)-1-benzyl-5-(4-bromophenyl)-1H-pyrrole-3,4-dicarboxylate (2.8e)

Isolated yield 82%. Pale yellow solid. ^1H NMR (500 MHz, $CDCl_3$): δ 7.45 (d, *J* = 8.5 Hz, 2H), 7.16-7.10 (m, 5H), 6.77 (d, *J* = 1.2 Hz, 2H), 6.75 (dd, *J* = 1.2, 0.9, 1H), 6.60-6.58 (m, 2H), 5.98 (s, 2H), 4.89 (s, 2H), 3.72 (s, 3H), 3.67 (s, 3H). ^{13}C NMR (126 MHz, $CDCl_3$): δ 165.3, 165.0, 148.2, 147.4, 136.9$_4$, 136.8$_6$, 135.7, 132.1, 131.3, 129.5, 128.5, 127.4, 125.9, 124.6, 123.6, 123.2, 115.1, 114.8, 110.9, 108.2, 101.3, 51.8, 51.7, 48.5. HRMS (ESI^+) for $C_{28}H_{23}NO_6Br^+$; calculated 548.07033, found 548.06982 (error m/z = -0.93 ppm)

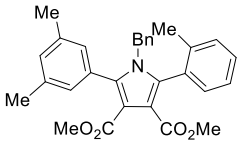

Dimethyl 1-benzyl-2-(3,5-dimethylphenyl)-5-(o-tolyl)-1H-pyrrole-3,4-dicarboxylate (2.8f)

Isolated yield 81%. Pale yellow solid. ^{1}H NMR (500 MHz, $CDCl_3$): δ 7.29-7.25 (m, 1H), 7.18-7.05 (m, 6H), 6.99 (s, 1H), 6.94 (m, 2H), 6.52 (d, *J* = 6.7 Hz, 2H), 4.80 (d, *J* = 15.6 Hz, 1H), 4.73 (d, *J* = 15.6 Hz, 1H), 3.70 (s, 3H), 3.62 (s, 3H), 2.29 (s, 6H), 1.97 (s, 3H). ^{13}C NMR (126 MHz, $CDCl_3$): δ 165.9, 164.8, 138.8, 137.6, 137.0, 136.9$_7$, 136.9$_5$, 131.0, 130.6, 130.4$_1$, 130.3$_9$, 129.8, 129.0, 128.4, 128.1, 127.2, 126.7, 125.3, 114.9, 114.0, 51.7, 51.3, 48.5, 21.3, 19.5. HRMS (ESI$^+$) for $C_{30}H_{30}NO_4^+$; calculated 468.21693, found 468.21793 (error m/z = 2.13 ppm)

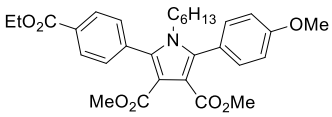

Dimethyl 2-(4-(ethoxycarbonyl)phenyl)-1-hexyl-5-(4-methoxyphenyl)-1H-pyrrole-3,4-dicarboxylate (2.8g)

Isolated yield 83%. Pale yellow oil. ^{1}H NMR (500 MHz, $CDCl_3$): δ 8.13 (d, *J* = 8.5 Hz, 2H), 7.49 (d, *J* = 8.5 Hz, 2H), 7.33 (d, *J* = 8.8 Hz, 2H), 6.98 (d, *J* = 8.8 Hz, 2H), 4.41 (q, *J* = 7.0 Hz, 2H), 3.86 (s, 3H), 3.67 (m, 2H), 3.67 (s, 3H), 3.64 (s, 3H), 1.42 (t, *J* = 7.0 Hz, 3H), 1.18-1.12 (m, 2H), 1.04-0.96 (m, 2H), 0.88-077 (m, 4H), 0.70 (t, *J* = 7.3 Hz, 3H). ^{13}C NMR (126 MHz, $CDCl_3$): δ 166.2, 165.4, 165.2, 159.9, 137.1, 135.8, 135.1, 131.8, 130.5$_5$, 130.4$_9$, 129.4, 122.7, 114.8, 114.6, 113.8, 61.2, 55.3, 51.6, 45.0, 30.7, 30.2, 25.7, 22.1, 14.3, 13.8. HRMS (ESI$^+$) for $C_{30}H_{36}NO_7^+$; calculated 522.24863, found 522.24853 (error m/z = -0.18 ppm)

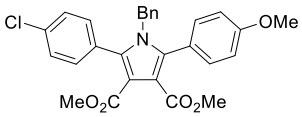

Dimethyl 1-benzyl-2-(4-chlorophenyl)-5-(4-methoxyphenyl)-1H-pyrrole-3,4-dicarboxylate (2.8h)

Isolated yield 65%. White solid. ^{1}H NMR (500 MHz, $CDCl_3$): δ 7.29 (d, *J* = 8.5 Hz, 2H), 7.22 (d, *J* = 8.8 Hz, 2H), 7.19 (d, *J* = 8.5 Hz, 2H), 7.15-7.11 (m, 3H), 6.86 (d, *J* = 8.5Hz, 2H), 6.60-6.58

(m, 2H), 4.88 (s, 2H), 3.81 (s, 3H), 3.69 (s, 3H), 3.68 (s, 3H). ^{13}C NMR (126 MHz, $CDCl_3$): δ 165.4, 165.1, 159.9, 137.3, 137.1, 135.6, 134.9, 131.9, 131.8, 129.2, 128.4$_4$, 128.3$_9$, 127.4, 126.0, 122.4, 115.0, 114.9, 113.7, 55.2, 51.7, 51.6, 48.4. HRMS (ESI^+) for $C_{28}H_{25}NO_5Cl^+$; calculated 490.14158, found 490.14122 (error m/z = -0.73 ppm)

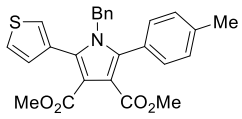

Dimethyl 1-benzyl-2-(thiophen-3-yl)-5-(p-tolyl)-1H-pyrrole-3,4-dicarboxylate (2.8i)

Isolated yield 70%. Light red solid. ^{1}H NMR (500 MHz, $CDCl_3$): δ 7.28-7.26 (m, 1H), 7.22 (dd, *J* = 2.8, 1.2 Hz, 1H), 7.19-7.16 (m, 5H), 7.13 (d, *J* = 7.9 Hz, 2H), 6.99 (dd, *J* = 4.9, 1.2 Hz, 1H), 6.68 (m, 2H), 4.93 (s, 2H), 3.72 (s, 3H), 3.68 (s, 3H), 2.35 (s, 3H). ^{13}C NMR (126 MHz, $CDCl_3$): δ 165.6, 165.2, 138.7, 137.7, 137.5, 131.4, 130.4, 130.2, 129.2, 128.9, 128.5, 127.5, 127.3, 126.5, 125.9, 125.1, 115.5, 114.5, 51.7, 51.6, 48.5, 21.4. HRMS (ESI^+) for $C_{26}H_{23}NNaO_4S^+$; calculated 468.1240, found 468.1232 (error m/z = 1.7 ppm)

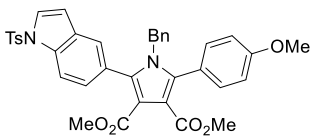

Dimethyl 1-benzyl-2-(4-methoxyphenyl)-5-(1-tosyl-1H-indol-5-yl)-1H-pyrrole-3,4-dicarboxylate (2.8j)

Isolated yield 90%. Pale yellow solid. ^{1}H NMR (500 MHz, $CDCl_3$) δ 7.91 (d, *J* = 8.6 Hz, 1H), 7.78 (d, *J* = 8.3 Hz, 2H), 7.56 (d, *J* = 3.6 Hz, 1H), 7.42 (s, 1H), 7.25 (d, *J* = 10.1 Hz, 2H), 7.20 (dd, *J* = 8.8, 2.5 Hz, 3H), 7.08 (t, *J* = 7.3 Hz, 1H), 7.01 (t, *J* = 7.5 Hz, 2H), 6.85 (d, *J* = 8.6 Hz, 2H), 6.58 (d, *J* = 3.6 Hz, 1H), 6.48 (d, *J* = 7.5 Hz, 2H), 4.85 (s, 2H), 3.80 (s, 3H), 3.67 (s, 3H), 3.60 (s, 3H), 2.36 (s, 3H). ^{13}C NMR (126 MHz, $CDCl_3$) δ 165.6, 165.5$_7$, 160.0, 145.2, 137.3, 137.2, 136.9, 135.4, 134.8, 132.0, 130.5, 130.1, 128.3, 127.3, 127.1, 127.0, 127.0,

126.2, 125.8, 123.9, 122.8, 114.9, 114.7, 113.7, 113.2, 109.1, 55.3, 51.7, 51.6$_8$, 48.6, 21.7. HRMS (ESI$^+$) for $C_{37}H_{33}N_2O_7S^+$; calculated 649.20030, found 649.19998 (error m/z = -0.49) ppm).

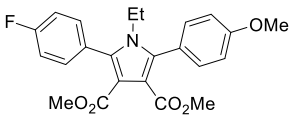

Dimethyl 1-ethyl-2-(4-fluorophenyl)-5-(4-methoxyphenyl)-1H-pyrrole-3,4-dicarboxylate (2.8k)

Isolated yield 62%. White solid. ^{1}H NMR (500 MHz, $CDCl_3$): δ 7.4 (dd, *J* = 8.8, 5.5 Hz, 2H), 7.34 (d, *J* = 8.5 Hz, 2H), 7.15 (t, *J* = 8.5 Hz, 2H), 6.98 (d, *J* = 8.8 Hz, 2H), 3.87 (s, 3H), 3.70 (q, *J* = 7.0, 2H), 3.67 (s, 3H), 3.66 (s, 3H), 0.84 (t, *J* = 7.0 Hz, 3H). ^{13}C NMR (126 MHz, $CDCl_3$): δ 165.5, 165.3, 163.9 (d, *J* = 248.1 Hz), 159.9, 136.2, 135.0, 132.4 (d, *J* = 8.2 Hz), 131.8, 127.0 (d, *J* = 3.7 Hz), 122.8, 115.5, 115.3, 114.5$_4$, 114.4$_7$, 113.8, 55.3, 51.6, 51.5, 39.8, 16.1. HRMS (ESI$^+$) for $C_{23}H_{23}NO_5F^+$; calculated 412.15548, found 412.15598 (error m/z = 1.23 ppm)

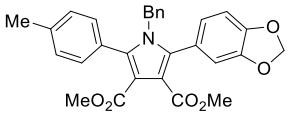

Dimethyl 2-(benzo[d][1,3]dioxol-5-yl)-1-benzyl-5-(p-tolyl)-1H-pyrrole-3,4-dicarboxylate (2.8l)

Isolated yield 83%. White solid. ^{1}H NMR (500 MHz, $CDCl_3$): δ 7.17 (d, *J* = 8.2 Hz, 2H), 7.14-7.12 (m, 5H), 6.77-6.72 (m, 3H), 6.61-6.59 (m, 2H), 5.97 (s, 2H), 4.91 (s, 2H), 3.71 (s, 3H), 3.68 (s, 3H), 2.35 (s, 3H). ^{13}C NMR (126 MHz, $CDCl_3$): δ 165.4$_3$, 165.4$_1$, 148.0, 147.3, 138.6, 137.3, 137.2, 136.5, 130.4, 128.9, 128.3, 127.5, 127.2, 126.1, 124.6, 124.0, 114.8, 114.5, 111.0, 108.1, 101.2, 51.7, 51.6, 48.4, 21.4. HRMS (ESI$^+$) for $C_{29}H_{25}NNaO_6^+$; calculated 506.1574, found 506.1587 (error m/z = 2.5 ppm)

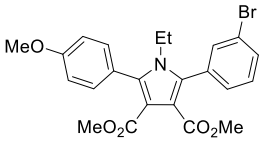

Dimethyl 2-(3-bromophenyl)-1-ethyl-5-(4-methoxyphenyl)-1H-pyrrole-3,4-dicarboxylate (2.8m)

Isolated yield 85%. Pale yellow solid. ^{1}H NMR (500 MHz, $CDCl_3$): δ 7.57 (d, *J* = 7.6 Hz, 2H), 7.39-7.32 (m, 4H), 6.98 (d, *J* = 8.5 Hz, 2H), 3.86 (s, 3H), 3.72 (q, *J* = 7.0 Hz, 2H), 3.67 (s, 6H), 0.85 (t, *J* = 7.0 Hz, 3H). ^{13}C NMR (126 MHz, $CDCl_3$): δ 165.4, 165.1, 159.9, 136.5, 134.3, 133.3, 133.1, 131.8$_3$, 131.7$_6$, 129.8, 129.3, 122.7, 122.2, 114.8, 114.6, 113.8, 113.5, 55.3, 51.6, 39.9, 16.1. HRMS (ESI$^+$) for $C_{23}H_{23}NO_5Br^+$; calculated 472.07541, found 472.07502 (error m/z = -0.84 ppm)

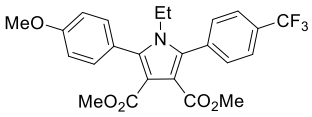

Dimethyl 1-ethyl-2-(4-methoxyphenyl)-5-(4-(trifluoromethyl) phenyl)-1H-pyrrole-3,4-dicarboxylate (2.8n)

Isolated yield 71%. White solid. ^{1}H NMR (500 MHz, $CDCl_3$): δ 7.72 (d, *J* = 8.2 Hz, 2H), 7.57 (d, *J* = 7.9 Hz, 2H), 7.35 (d, *J* = 8.8 Hz, 2H), 6.99 (d, *J* = 8.8 Hz, 2H), 3.87 (s, 3H), 3.72 (q, *J* = 7.3 Hz, 2H), 3.68 (s, 3H), 3.66 (s, 3H), 0.84 (t, *J* = 7.3 Hz, 3H). ^{13}C NMR (126 MHz, $CDCl_3$): δ 165.4, 165.0, 160.0, 136.5, 134.9 (d, *J* = 2.7 Hz), 134.4, 131.7, 130.6, 127.2, 125.3 (q, *J* = 3.7 Hz), 125.1, 122.9, 122.6, 114.9 (d, *J* = 17.4 Hz), 113.9, 55.3, 51.7, 51.6, 39.9, 16.1. HRMS (ESI$^+$) for $C_{24}H_{23}NO_5F_3^+$; calculated 462.15228, found 462.15156 (error m/z = -1.56 ppm)

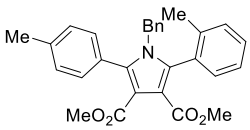

Dimethyl 1-benzyl-2-(o-tolyl)-5-(p-tolyl)-1H-pyrrole-3,4-dicarboxylate (2.8o)

Isolated yield 87%. Pale yellow solid. ^{1}H NMR (500 MHz, $CDCl_3$): δ 7.26 (m, 3H), 7.18 (m, 3H), 7.10 (m, 5H), 6.52 (d, *J* = 7.0 Hz, 2H), 4.83 (d, *J* = 15.6 Hz, 1H), 3.73 (d, *J* = 15.8 Hz, 1H), 3.70 (s, 3H), 3.62 (s, 3H), 2.37 (s, 3H), 1.97 (s, 3H). ^{13}C NMR (126 MHz, $CDCl_3$): δ 165.8, 164.9, 138.7, 138.6, 136.9, 136.8, 136.8, 131.0, 130.5$_4$, 130.4$_7$, 129.8, 129.1, 129.0, 128.2, 127.6, 127.3, 126.6, 125.3, 114.9, 114.2, 51.7, 51.4, 48.3, 21.4, 19.6. HRMS (ESI$^+$) for $C_{29}H_{28}NO_4^+$; calculated 454.20128, found 454.20040 (error m/z = -1.94 ppm)

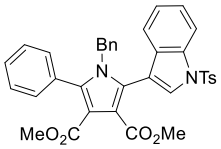

Dimethyl 1-benzyl-2-phenyl-5-(1-tosyl-1H-indol-3-yl)-1H-pyrrole-3,4-dicarboxylate (2.8p)

Isolated yield 69%. Pale yellow solid. ^{1}H NMR (500 MHz, $CDCl_3$): δ 7.96 (d, *J* = 7.6 Hz, 1H), 7.66 (d, *J* = 8.5 Hz, 2H), 7.52 (s, 1H), 7.38-7.29 (m, 7H), 7.21 (td, *J* = 7.9, 0.9 Hz, 1H), 7.17 (d, *J* = 7.9 Hz, 2H), 7.13-7.06 (m, 3H), 6.49 (d, *J* = 6.7 Hz, 2H), 4.85 (s, 2H), 3.69 (s, 3H), 3.50 (s, 3H), 2.33 (s, 3H). ^{13}C NMR (126 MHz, $CDCl_3$): δ 164.8, 145.0, 138.2, 137.0, 135.0, 134.4, 130.4$_3$, 130.4$_2$, 129.9, 128.9, 128.4, 128.2, 127.8, 127.5, 127.4, 126.8, 125.8, 125.0, 123.7, 120.2, 116.8, 115.5, 113.7, 112.4, 51.7, 51.5, 48.9, 21.6. HRMS (ESI$^+$) for $C_{36}H_{31}N_2O_6S^+$; calculated 619.18973, found 619.19161 (error m/z = 3.03 ppm)

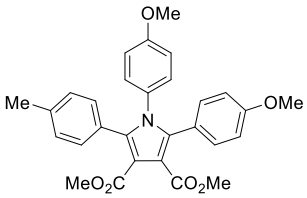

Dimethyl 1,2-bis(4-methoxyphenyl)-5-(p-tolyl)-1H-pyrrole-3,4-dicarboxylate (2.8q)

Isolated yield 66%. Pale yellow solid. ^{1}H NMR (500 MHz, $CDCl_3$): δ 7.11 (d, *J* = 8.8 Hz, 2H), 7.07 (d, *J* = 7.9 Hz, 2H), 7.01 (d, *J* = 7.9 Hz, 2H), 6.77-6.73 (m, 4H), 6.61 (d, *J* = 8.8 Hz, 2H), 3.77 (s, 3H), 3.74 (s, 6H), 3.71 (s, 3H), 2.29 (s, 3H). ^{13}C NMR (126 MHz, $CDCl_3$): δ 165.8, 165.7, 159.2, 158.6, 137.7, 136.9, 136.8, 132.1, 130.6, 129.9, 129.8, 128.4, 128.2, 127.4, 114.4, 114.2, 113.7, 113.1, 55.2, 55.1, 51.8, 51.7, 21.3. HRMS (ESI$^+$) for $C_{29}H_{28}NO_6^+$; calculated 486.19111, found 486.19046 (error m/z = -1.34 ppm)

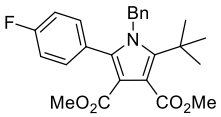

Dimethyl 1-benzyl-2-(tert-butyl)-5-(4-fluorophenyl)-1H-pyrrole-3,4-dicarboxylate (2.8r)

Isolated yield: 40%. White solid. ^{1}H NMR (500 MHz, $CDCl_3$) δ 7.22 – 7.13 (m, 3H), 6.95 (dd, *J* = 8.4, 5.5 Hz, 2H), 6.85 (t, *J* = 8.7 Hz, 2H), 6.66 – 6.60 (m, 2H), 5.17 (s, 2H), 3.91 (s, 3H), 3.52 (s, 3H), 1.39 (s, 9H). ^{13}C NMR (126 MHz, $CDCl_3$) δ 170.0, 164.0, 162.7 (d, *J* = 248.0 Hz), 139.0, 138.1, 132.4 (d, *J* = 8.3 Hz), 128.5, 127.6 (d, *J* = 3.5 Hz), 127.3, 125.6, 115.7, 114.9 (d, *J* = 21.6 Hz), 112.3, 52.6, 51.2, 50.1, 33.9, 30.9. HRMS (ESI^+) for $C_{25}H_{27}NO_4F^+$; calculated 424.19186, found 424.19178 (error m/z = -0.20 ppm).

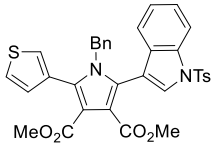

Dimethyl 1-benzyl-2-(thiophen-3-yl)-5-(1-tosyl-1H-indol-3-yl)-1H-pyrrole-3,4-dicarboxylate (2.8s)

Isolated yield: 51%. Pale yellow solid. ^{1}H NMR (500 MHz, $CDCl_3$) δ 7.95 (d, *J* = 8.3 Hz, 1H), 7.62 (d, *J* = 8.4 Hz, 2H), 7.47 (s, 1H), 7.33 – 7.26 (m, 4H), 7.22 – 7.18 (m, 1H), 7.18 – 7.13 (m, 5H), 7.02 (dd, *J* = 4.9, 1.2 Hz, 1H), 6.60 (dd, *J* = 7.2, 2.0 Hz, 2H), 4.87 (s, 2H), 3.73 (s, 3H), 3.47 (s, 3H), 2.32 (s, 3H). ^{13}C NMR (126 MHz, $CDCl_3$) δ 165.5, 164.7, 145.2, 137.4, 135.1, 134.5, 132.7, 130.6, 130.0, 129.2, 128.8, 128.2, 127.7, 127.5, 126.9, 126.8, 125.7, 125.5, 125.2, 123.8, 120.4, 116.8, 116.2, 113.8, 112.4, 52.0, 51.6, 49.1, 21.7. HRMS (ESI^+) for $C_{34}H_{29}N_2O_6S_2^+$; calculated 625.14615, found 625.14657 (error m/z = 0.67 ppm).

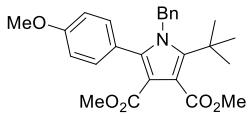

Dimethyl 1-benzyl-2-(tert-butyl)-5-(4-methoxyphenyl)-1H-pyrrole-3,4-dicarboxylate (2.8t)

Isolated yield 44%. White solid. ^{1}H NMR (500 MHz, $CDCl_3$): δ 7.21-7.16 (m, 3H), 6.93 (d, *J* = 8.5 Hz, 2H), 6.71 (d, *J* = 8.8 Hz, 2H), 6.65 (d, J = 8.2 Hz, 2H), 5.19 (s, 2H), 3.91 (s, 3H), 3.76 (s, 3H), 3.55 (s, 3H), 1.38 (s, 9H). ^{13}C NMR (126 MHz, $CDCl_3$): δ 170.0, 164.0, 159.4, 140.1, 138.4,

137.6, 131.6, 128.3, 127.0, 125.5, 123.6, 115.5, 113.1, 111.9, 55.1, 52.4, 51.0, 49.8, 33.8, 30.8. HRMS (ESI^+) for $C_{26}H_{30}NO_5^+$; calculated 436.21185, found 436.21175 (error m/z = -0.23 ppm).

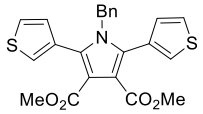

Dimethyl 1-benzyl-2,5-di(thiophen-3-yl)-1H-pyrrole-3,4-dicarbo-xylate (2.8u)

Isolated yield 58%. Pale yellow solid. ^1H NMR (500 MHz, $CDCl_3$) δ 7.27 (dd, *J* = 4.9, 3.1 Hz, 2H), 7.22 (d, *J* = 3.1 Hz, 5H), 6.98 (d, *J* = 4.9 Hz, 2H), 6.80 – 6.71 (m, 2H), 4.95 (s, 2H), 3.71 (s, 6H). ^{13}C NMR (126 MHz, $CDCl_3$) δ 165.4, 137.8, 132.0, 130.1, 129.3, 128.8, 127.5, 126.7, 125.9, 125.3, 115.5, 51.9, 48.8. HRMS (ESI^+) for $C_{23}H_{19}NO_4S_2Na^+$; calculated 460.06477, found 460.06404 (error m/z = -1.58 ppm).

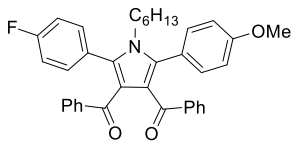

(2-(4-fluorophenyl)-1-hexyl-5-(4-methoxyphenyl)-1H-pyrrole-3,4-diyl)bis(phenylmethanone) (2.8v)

Isolated yield 70%. Pale yellow solid. ^1H NMR (500 MHz, $CDCl_3$): δ 7.45-7.40 (m, 6H), 7.36 (d, *J* = 8.5 Hz, 2H), 7.29-7.25 (m, 2H), 7.10 (td, *J* = 7.9, 2.3 Hz, 4H), 7.06 (t, *J* = 8.8 Hz, 2H), 6.88 (d, *J* = 8.8 Hz, 2H), 3.84-3.79 (m, 2H), 3.81 (s, 3H), 1.30-1027 (m, 2H), 1.09-1.05 (m, 2H), 0.95-0.90 (m, 4H), 0.75 (t, *J* = 7.3 Hz, 3H). ^{13}C NMR (126 MHz, $CDCl_3$): δ 192.3, 163.8 (d, *J* = 249.0 Hz), 159.8, 139.6$_2$, 139.5$_9$, 137.1, 135.7, 132.9, 132.8, 132.2, 131.7, 131.6, 128.8 (d, *J* = 4.6 Hz), 127.7$_5$, 127.7$_0$, 127.0$_0$, 126.9$_7$, 123.8, 123.6, 122.8, 115.4 (d, *J* = 21.9 Hz), 113.7, 55.3, 44.9, 30.7, 30.2, 25.9, 22.2, 13.8. HRMS (ESI^+) for $C_{37}H_{34}NNaO_3F^+$; calculated 582.2415, found 582.2415 (error m/z = 0.1 ppm).

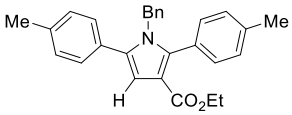

Ethyl 1-benzyl-2,5-di-p-tolyl-1H-pyrrole-3-carboxylate (2.8w)

Isolated yield 68%. White solid. ^{1}H NMR (500 MHz, $CDCl_3$): δ 7.25 (d, *J* = 7.9 Hz, 2H), 7.19-7.13 (m, 9H), 6.80 (s, 1H), 6.71 (d, *J* = 8.2 Hz, 1H), 6.68-6.66 (m, 2H), 5.06 (s, 2H), 4.17 (q, *J* = 7.0 Hz, 2H), 2.37 (s, 3H), 2.36 (s, 3H), 1.19 (t, *J* = 7.0 Hz, 3H). ^{13}C NMR (126 MHz, $CDCl_3$): δ 164.8, 140.0, 138.4, 138.0, 137.5, 135.0, 130.6, 129.8, 129.2, 129.1, 129.0, 128.6, 128.3, 127.0, 125.9, 114.0, 110.5, 59.4, 48.4, 21.4, 21.2, 14.3. HRMS (ESI^+) for $C_{28}H_{28}NO_2^+$; calculated 410.21146, found 410.21046 (error m/z = -2.42 ppm).

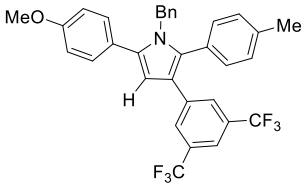

1-benzyl-3-(3,5-bis(trifluoromethyl)phenyl)-5-(4-methoxy phenyl)-2-(p-tolyl)-1H-pyrrole (2.8x)

Isolated yield 60%. Red/orange solid. ^{1}H NMR (500 MHz, $CDCl_3$): δ 7.60 (s, 2H), 7.54 (s, 1H), 7.32 (d, *J* = 8.8 Hz, 2H), 7.19-7.15 (m, 3H), 7.13 (d, *J* = 7.9 Hz, 2H) 7.08 (d, *J* = 7.9, 2H), 6.98 (d, *J* = 8.8 Hz, 2H), 6.72 (dd, *J* = 7.8, 1.7 Hz, 2H), 6.57 (s, 1H), 5.10 (s, 2H), 3.83 (s, 3H), 2.36 (s, 3H). ^{13}C NMR (126 MHz, $CDCl_3$): δ 159.1, 138.8, 138.5, 138.4, 135.7, 133.1, 132.3, 131.4, 131.1, 130.9, 130.8, 130.6, 130.5, 129.5, 129.2, 129.0, 128.9, 128.3, 127.0, 126.9_5, 126.9_2, 126.7, 125.9, 125.3, 124.6, 122.4, 120.2, 120.1, 118.1_4, 118.1_1, 118.0_8, 118.0_5, 114.3, 113.9, 108.1, 55.3, 48.4, 21.2. HRMS (ESI^+) for $C_{33}H_{25}NOF_6^+$; calculated 565.18349, found 565.18434 (error m/z = 1.5 ppm).

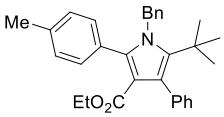

Ethyl 1-benzyl-5-(tert-butyl)-4-phenyl-2-(p-tolyl)-1H-pyrrole-3-carboxylate (2.8y)

Isolated yield 60%. White solid. ^{1}H NMR (500 MHz, Chloroform-*d*) δ 7.35 (d, *J* = 6.9 Hz, 2H), 7.29 (q, *J* = 8.5, 7.4 Hz, 3H), 7.21 (t, *J* = 7.3 Hz, 2H), 7.18 – 7.13 (m, 1H), 7.01 (s, 4H), 6.68 (d, *J*

= 7.4 Hz, 2H), 5.29 (s, 2H), 3.73 (q, *J* = 7.1 Hz, 2H), 2.29 (s, 3H), 1.15 (s, 9H), 0.63 (t, *J* = 7.1 Hz, 3H). ^{13}C NMR (126 MHz, $CDCl_3$) δ 165.3, 139.7, 139.7, 137.6, 137.0, 131.5, 130.5, 129.8, 128.5, 128.3, 127.0, 126.8, 126.2, 125.6, 123.5, 115.2, 59.1, 50.2, 34.4, 32.9, 21.4, 13.5. HRMS (ESI^+) for $C_{31}H_{34}NO_2^+$; calculated 452.25841, found 452.25838 (error m/z = -0.06 ppm).

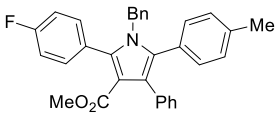

Methyl 1-benzyl-2-(4-fluorophenyl)-4-phenyl-5-(p-tolyl)-1H-pyrrole-3-carboxylate (2.8z)

Isolated yield 70%. Pale yellow solid. ^{1}H NMR (500 MHz, $CDCl_3$): δ 7.30-7.27 (m, 2H), 7.24-7.19 (m, 4H), 7.18-7.14 (m, 4H), 7.04-6.99 (m, 6H), 6.66-6.64 (m, 2H), 4.94 (s, 2H), 3.45 (s, 3H), 2.28 (s, 3H). ^{13}C NMR (126 MHz, $CDCl_3$): δ 165.6, 163.7 (d, *J* = 248.1 Hz), 138.1, 137.6, 137.5, 135.2, 133.2, 132.6 (d, *J* = 8.2 Hz), 131.2, 130.6, 128.9, 128.4, 128.3, 128.2, 127.2, 127.1, 126.0, 125.9, 124.3, 115.0 (d, *J* = 22.0 Hz), 113.4, 50.6, 48.5, 21.2. HRMS (ESI^+) for $C_{32}H_{27}NO_2F^+$; calculated 476.20203, found 476.20121 (error m/z = -1.73 ppm).

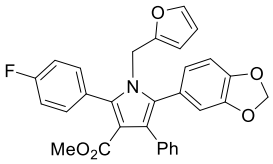

Methyl 5-(benzo[d][1,3]dioxol-5-yl)-2-(4-fluorophenyl)-1-(furan-2-ylmethyl)-4-phenyl-1H-pyrrole-3-carboxylate (2.8aa)

Isolated yield 64%. White solid. ^{1}H NMR (500 MHz, $CDCl_3$): δ 7.38 (dd, *J* = 8.5, 5.2 Hz, 2H), 7.24-7.15 (m, 6H), 7.11 (t, *J* = 8.8 Hz, 2H), 6.71 (d, *J* = 8.2 Hz, 1H), 6.67 (dd, *J* = 5.2, 1.5 Hz, 2H) 6.16 (dd, *J* = 3.2, 1.9 Hz, 1H), 6.95 (s, 2H), 5.57 (dd, *J* = 3.1, 0.7 Hz, 1H), 4.83 (s, 2H), 3.43 (s, 3H). ^{13}C NMR (126 MHz, $CDCl_3$): δ 165.5, 163.8 (d, *J* = 248.1 Hz), 150.1, 147.4, 147.3, 142.0, 137.2, 135.0, 132.7 (d, *J* = 8.2 Hz), 132.3, 130.5, 128.1 (d, *J* = 3.7 Hz), 127.3, 126.0, 125.5, 124.9, 124.3, 115.1 (d, J = 21.1 Hz), 113.3, 111.7, 110.3, 108.1, 107.6, 101.1,

50.6, 42.1. HRMS (ESI$^+$) for $C_{30}H_{23}NO_5F^+$; calculated 496.15548, found 496.15479 (error m/z = -1.39 ppm).

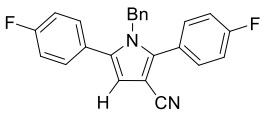

1-benzyl-2,5-bis(4-fluorophenyl)-1H-pyrrole-3-carbonitrile (2.8ab)

Isolated yield 60%. Red-orange solid. ^{1}H NMR (500 MHz, $CDCl_3$): δ 7.36 (dd, *J* = 8.8, 5.2 Hz, 2H), 7.25 (ddd, *J* = 8.8, 5.4, 2.4, 2H), 7.20-7.18 (m, 3H), 7.10 (t, *J* = 5.5 Hz, 2H), 7.03 (t, *J* = 8.8 Hz, 2H), 6.64-6.62 (m, 2H), 6.56 (s, 1H), 5.09 (s, 2H). ^{13}C NMR (126 MHz, $CDCl_3$): δ 164.2 (d, *J* = 299.4 Hz), 163.8 (d, *J* = 199.6 Hz), 141.6, 137.2, 135.5, 131.7 (d, *J* = 9.2 Hz), 131.4 (d, *J* = 8.2 Hz), 128.7, 127.6, 127.5, 125.7, 125.6 (d, *J* = 3.7 Hz), 116.8, 116.1 (d, *J* = 21.1 Hz), 115.8 (d, *J* = 22.0 Hz), 112.1, 93.6, 49.0. HRMS (ESI$^+$) for $C_{24}H_{17}N_2F_2^+$; calculated 371.13543, found 371.13520 (error m/z = -0.62 ppm).

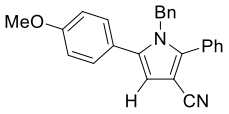

1-benzyl-5-(4-methoxyphenyl)-2-phenyl-1H-pyrrole-3-carbonitrile (2.8ac)

Isolated yield 77%. White solid. ^{1}H NMR (500 MHz, $CDCl_3$): δ 7.41-7.39 (m, 5H), 7.23 (d, *J* = 7.9, 2H), 7.18-7.17 (m, 3H), 6.88 (d, *J* = 8.2 Hz, 2H), 6.65-6.64 (m, 2H), 6.55 (s, 1H), 5.15 (s, 2H), 3.82 (s, 3H). ^{13}C NMR (126 MHz, $CDCl_3$): δ 159.7, 142.4, 137.6, 136.4, 130.8, 129.8, 129.7, 129.1, 128.8, 128.6, 127.4, 125.9, 123.9, 117.3, 114.0, 111.7, 93.1, 55.3, 49.0. HRMS (ESI$^+$) for $C_{25}H_{19}N_2O^+$; calculated 363.15029, found 363.15024 (error m/z = -0.14 ppm).

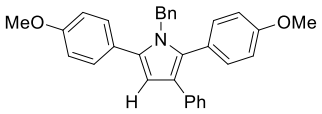

1-benzyl-2,5-bis(4-methoxyphenyl)-3-phenyl-1H-pyrrole (2.8ad)

Isolated yield 71%. Pale yellow solid. ^{1}H NMR (500 MHz, $CDCl_3$): δ 7.33 (d, *J* = 8.8 Hz, 2H), 7.26 (dd, *J* = 8.5, 1.1 Hz, 2H), 7.20-7.11 (m, 7H), 7.08 (tt, *J* = 7.3, 1.2

Hz, 1H), 6.88 (d, *J* = 8.8 Hz, 2H), 6.80 (d, *J* = 8.8 Hz, 2H), 6.73 (d, *J* = 7.9 Hz, 2H), 6.54 (s, 1H), 5.06 (s, 2H), 3.82 (s, 3H), 3.80 (s, 3H). ^{13}C NMR (126 MHz, $CDCl_3$): δ 159.1, 158.9, 139.4, 136.4, 134.9, 132.5, 131.4, 130.4, 128.2, 128.0, 127.4, 126.7, 126.0, 125.9, 125.5, 125.0, 122.8, 113.8_4, 113.8_2, 108.7, 55.3, 55.2. HRMS (ESI^+) for $C_{31}H_{27}NO_2^+$; calculated 445.20363, found 445.20341 (error m/z = -0.49 ppm).

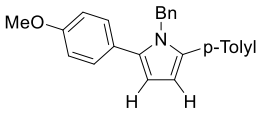

1-benzyl-2-(4-methoxyphenyl)-5-(p-tolyl)-1H-pyrrole (2.8ae)

Isolated yield 77%. White solid. ^{1}H NMR (500 MHz, $CDCl_3$): δ 7.29-7.27 (m, 4H), 7.20-7.14 (m, 5H), 6.86 (d, *J* = 8.8 Hz, 2H), 6.73 (d, *J* = 8.2 Hz, 2H), 6.35 (d, *J* = 3.7 Hz, 1H), 6.32 (d, *J* = 3.7 Hz, 1H), 5.22 (s, 2H), 3.82 (s, 3H), 2.37 (s, 3H). ^{13}C NMR (126 MHz, $CDCl_3$): δ 158.8, 139.6, 136.6, 136.2, 136.1, 130.9, 130.4, 129.0, 128.9, 128.3, 126.7, 126.4, 125.9, 113.7, 109.2, 109.1, 55.3, 48.5, 21.2. HRMS (ESI^+) for $C_{25}H_{23}NO^+$; calculated 353.17742, found 353.17824 (error m/z = 2.34 ppm).

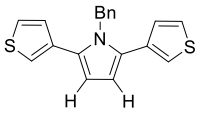

1-benzyl-2,5-di(thiophen-3-yl)-1H-pyrrole (2.8af)

Isolated yield 56%. White solid. ^{1}H NMR (500 MHz, $CDCl_3$) δ 7.34 (t, *J* = 7.5 Hz, 2H), 7.28 (d, *J* = 7.4 Hz, 1H), 7.27 – 7.23 (m, 2H), 7.07 (dd, *J* = 5.0, 1.1 Hz, 2H), 7.02 (d, *J* = 7.4 Hz, 2H), 6.99 (dd, *J* = 2.8, 1.1 Hz, 2H), 6.43 (s, 2H), 5.31 (s, 2H). ^{13}C NMR (126 MHz, $CDCl_3$) δ 139.7, 133.8, 131.2, 129.1, 128.5, 127.3, 125.7, 125.4, 121.1, 109.2, 49.0. HRMS (ESI^+) for $C_{19}H_{15}NS_2^+$; calculated 321.0640, found 321.0641 (error m/z = -0.3 ppm).

2.5.4. NMR Spectra of Products

See Supporting Information of publication (*J. Am. Chem. Soc.* **2016**, 138, 7315)

2.6. References

1. (a) Schoenberg, A.; Bartoletti, I.; Heck, R. F. *J. Org. Chem.* **1974**, *39*, 3318. (b) Schoenberg, A.; Heck, R. F. *J. Org. Chem.* **1974**, *39*, 3327.

2. For reviews: (a) Brennführer, A.; Neumann, H.; Beller, M. *Angew. Chem. Int. Ed.* **2009**, *48*, 4114. (b) Wu, X.; Neumann, H.; Beller, M. *Chem. Soc. Rev.* **2011**, *40*, 4986. (c) Barnard, C. F. J. *Organometallics* **2008**, *27*, 5402. (d) Sumino, S.; Fusano, A.; Fukuyama, T.; Ryu, I. *Acc. Chem. Res.* **2014**, *47*, 1563. (e) Fang, W.; Zhu, H.; Deng, Q.; Liu, S.; Liu, X.; Shen, Y.; Tu, T. *Synthesis* **2014**, *46*, 1689. (f) Mutton, S. P.; Grigg, R. *Tetrahedron* **2010**, 66, 5515. (g) Wu, X. –F.; Barnard, C. F. J. Palladium-catalyzed carbonylative coupling and C-H activation. In *New Trends in Cross-Coupling: Theory and Applications*, Colacot, T. J. The Royal Society of Chemistry: 2015; p. 479. (h) Morimoto, T.; Kakiuchi, K. *Angew. Chem. Int. Ed.* **2004**, *43*, 5580. (i) Liu, Q.; Zhang, H.; Lei, A. *Angew. Chem. Int. Ed.* **2011***, 50*, 10788.

3. For representative recent examples: (a) Xu, T.; Alper, H. *J. Am. Chem. Soc.* **2014**, *136*, 16970. (b) Liu, Q.; Wu, L.; Jiao, H.; Fang, X.; Jackstell, R.; Beller, M. *Angew. Chem. Int. Ed.* **2013**, *52*, 8064. (c) Fang, X.; Li, H.; Jackstell, R.; Beller, M. *J. Am. Chem. Soc.* **2014**, *136*, 16039. (d) Wu, X.; Zhao, Y.; Ge, H. *J. Am. Chem. Soc.* **2015**, *137*, 4924. (e) Xie, P.; Xie, Y.; Qian, B.; Zhou, H.; Xia, C.; Huang, H. *J. Am. Chem. Soc.* **2012**, *134*, 9902. (f) Andersen, T. L.; Friis, S. D.; Audrain, H.; Nordeman, P.; Antoni, G.; Skrydstrup, T. *J. Am. Chem. Soc.* **2015**, *137*, 1548. (g) Makarov, I. S.; Kuwahara, T.; Jusseau, X.; Ryu, I.; Lindhardt, A. T.; Skrydstrup. T. *J. Am. Chem. Soc.* **2015**, *137*, 14043. (h) Li, H.; Neumann, H.; Beller, M.; Wu, X. –F. *Angew. Chem. Int. Ed.* **2014**, *53*, 3183.

4. Wu, X.-F.; Beller, M., *Transition Metal Catalyzed Carbonylative Synthesis of Heterocycles*. Springer International Publishing: 2016; Vol. 42.

5. For reviews: (a) Church, T. L.; Getzler, Y.; Byrne, C. M.; Coates, G. W. *Chem. Commun.* **2007**, 657. (b) Khumtaveeporn, K.; Alper, H., *Acc. Chem. Res.* **1995**, *28*, 414. Recent examples: (c) Mulzer, M.; Whiting, B. T.; Coates, G. W. *J. Am. Chem. Soc.* **2013**, *135*, 10930. (d) Mulzer, M.; Tiegs, B. J.; Wang, Y.; Coates, G. W.; O'Doherty, G. A. *J. Am. Chem. Soc.* **2014**, *136*, 10814.

6. Reviews on intramolecular carbonylations: (a) Ojima, I.; Commandeur, C.; Chiou, W. H., Amidocarbonylation, Cyclohydrocarbonylation, and Related Reactions. In *Comprehensive Organometallic Chemistry III*, Mingos, D. M. P.; Crabtree, R.H., Ed. Elsevier: 2007; p 511. (b) Omae, I., *Coord. Chem. Rev.* **2011**, *255*, 139. (c) Vasapollo, G.; Mele, G., *Curr. Org. Chem.* **2006**, *10*, 1397. (d) Wu, X. –F.; Neumann, H.; Beller, M. *Chem. Rev.* **2013**, *113*, 1. (e) Gabriele, B.; Mancuso, R.; Salerno, G. *Eur. J. Org. Chem.* **2012**, *77*, 6825. (f) Mihovilovic, M. D.; Stanetty, P. *Angew. Chem. Int. Ed.* **2007**, *46*, 3612. Recent examples: (g) Hasegawa, N.; Charra, V.; Inoue, S.; Fukumoto, Y.; Chatani, N. *J. Am. Chem. Soc.* **2011**, *133*, 8070. (h) Gabriele, B.; Mancuso, R.; Salerno, G. *Eur. J. Org. Chem.* **2012**, 6825. (i) Li, X.; Li, X.; Jiao, N. *J. Am. Chem. Soc.* **2015**, *137*, 9246. (j) Li, W.; Liu, C.; Zhang, H.; Ye, K.; Zhang, G.; Zhang, W.; Duan, Z.; You, S.; Lei, A. *Angew. Chem. Int. Ed.* **2014**, *53*, 2443. (k) Chen, M.; Ren, Z. –H.; Guan, Z. –H. *J. Am. Chem. Soc.* **2012**, *134*, 17490. (l) Li, S.; Chen, G.; Feng, C. –G.; Gong, W.; Yu, J. –Q. *J. Am. Chem. Soc.* **2014**, *136*, 5267.

7. Recent examples: (a) Zhu, C.; Yang, B.; Backvall, J.-E. *J. Am. Chem. Soc.* **2015**, *137*, 11868. (b) Frutos-Pedreño, R.; González-Herrero, P.; Vicente, J. *Organometallics* **2012**, *31*, 3361. (c) Volla, C. M.R.; Mazuela, J.; Bäckvall, J. -E. *Chem. Eur. J.* **2014**, *20*, 7608.

8. (a) Willy, B.; Müller, T. J. J. *Curr. Org. Chem.* **2009**, *13*, 1777. (b) Arndtsen, B. A. *Chem. Eur. J.* **2009**, *15*, 302. (c) Blaquiere, N.; Staben, S. T. *Angew. Chem. Int. Ed.* **2010**, *49*, 325.

9. Bontemps, S.; Quesnel, J. S.; Worrall, K.; Arndtsen, B. A. *Angew. Chem. Int. Ed.* **2011**, *50*, 8948.

10. For reviews: (a) Alberico, D.; Scott, M. E.; Lautens, M. *Chem. Rev.* **2007**, *107*, 174. (b) Torborg, C.; Beller, M. *Adv. Synth. Catal*. **2009**, *351*, 3027. (c) Magano, J.; Dunetz, J. R. *Chem. Rev*. **2011**, *111*, 2177. (d) Bateman, L. M.; McGlacken, G. P. *Chem. Soc. Rev.* **2009**, *38*, 2447. (e) Jordan, A. M.; Roughley, S. D. *J. Med. Chem*. **2011**, *54*, 3451. (f) Baumann, M.; Baxendale, I. R.; Ley, S. V.; Nikbin, N. *Beilstein J. Org. Chem.* **2011,** *7*, 442. (g) Wu, X. –F.; Beller, M. Five-Membered Heterocycle Synthesis. In *Heterocycles from Double-Functionalized Arenes: Transition Metal Catalyzed Coupling Reactions*, The Royal Society of Chemistry: 2015; p 4. (h) Bur, S. K.; Padwa, A. The Synthesis of Heterocycles Using Cascade Chemistry. In *Advances in Heterocyclic Chemistry*, Katritzky, A. R. Ed Elsevier Inc.: 2007; Vol. 94, p 1. (i) D'hooge, M.; Ha, H. –J. Synthesis of 4- to 7-membered Heterocycles by Ring Expansion. In *Topics in Heterocyclic Chemistry*, Maes, B. U. W.; Cossy, J.; Polanc, S. Ed. Springer: 2016, Vol. 41. (j) Zirak, M.; Eftekhari-Sis, B. *Chem. Rev.* **2015**, *115*, 151.

11. (a) Gingrich, H. L.; Baum, J. S., Mesoionic Oxazoles. In *Chemistry of Heterocyclic Compounds: Oxazoles*, Turchi, I. J., Ed. John Wiley & Sons, Inc.: 1986; Vol. 45, pp 731. (b) Gribble, G. W., Mesoionic Oxazoles. In *The Chemistry of Heterocyclic Compounds, Volume 60: Oxazoles: Synthesis, Reactions, and Spectroscopy, Part A*, Palmer, D. C., Ed. John Wiley & Sons, Inc.: 2003; Vol. 60, pp 473. (c) Reissig, H. U.; Zimmer, R., *Angew. Chem. Int. Ed.* **2014**, *53*, 9708.

12. (a) Dhawan, R.; Dghaym, R. D.; Arndtsen, B. A. *J. Am. Chem. Soc.* **2003**, *125*, 1474. (b) Dhawan, R.; Arndtsen, B. A. *J. Am. Chem. Soc.* **2004**, *126*, 468. (c) Worrall, K.; Xu, B.; Bontemps, S.; Arndtsen, B. A. *J. Org. Chem.* **2011**, *76*, 170. (d) Leitch, D. C.; Kayser, L. V.; Han, Z. –Y.; Siamaki, A. R.; Keyzer, E. N.; Gefen, A.; Arndtsen, B. A. *Nat. Commun.* **2015**, *6*, 7411.

13. (a) Merlic, C. A.; Baur, A.; Aldrich, C. C. *J. Am. Chem. Soc.* **2000**, *122*, 7398. (b) Alper, H.; Tanaka, M. *J. Am. Chem. Soc.* **1979**, *101*, 4245.

14. Dghaym, R. D.; Dhawan, R.; Arndtsen, B. A. *Angew. Chem. Int. Ed.* **2001**, *40*, 3228.

15. For examples see: (a) Korsager, S.; Taaning, R. H.; Skrydstrup, T. *J. Am. Chem. Soc*. **2013**, *135*, 2891. (b) Sergeev, A. G.; Spannenberg, A.; Beller, M. *J. Am. Chem. Soc*. **2008**, *130*, 15549. (c) Sergeev, A. G.; Spannenberg, A.; Beller, M. *J. Am. Chem. Soc.* **2008**, *130*, 15549.

16. (a) Littke, A.F.; Schwarz, L.; Fu, G. C. *J. Am. Chem. Soc.* **2002**, *124*, 6343. (b) Fu, G. C. *Acc. Chem. Res.* **2008**, *41*, 1555.

17. (a) Cantat, T.; Génin, E.; Giroud, C.; Meyer, G.; Jutand, A. *J. Organomet. Chem.* **2003**, 365. (b) Jeffery, T., *J. Chem. Soc. Chem. Commun.* **1984**, 1987. (c) Reetz, M. T.; Westerman, E., *Angew. Chem. Int. Ed.* **2000**, *39*, 165. (d) Carrow, B. P.; Hartwig, J. F. *J. Am. Chem. Soc.* **2010**, *132*, 79. (e) Jutand, A. *Eur. J. Inorg. Chem.* **2003**, 2017.

18. (a) Dghaym, R. D.; Yaccato, K. J.; Arndtsen, B. A. *Organometallics* **1998,** *17*, 4. (b) Kacker, S.; Kim, J. S.; Sen, A. *Angew. Chem. Int. Ed.* **1998,** *37*, 1251. (c) Davis, J. L.; Arndtsen, B. A. *Organometallics* **2000**, *19*, 4657. (d) Lafrance, D.; Davis, J. L.; Dhawan, R.; Arndtsen, B. A. *Organometallics* **2001**, *20*, 1128.

19. (a) Quesnel, J. S.; Arndtsen, B. A., *J. Am. Chem. Soc.* **2013,** *135*, 16841. (b) Quesnel, J. S.; Kayser, L. V.; Fabrikant, A.; Arndtsen, B. A. *Chem. Eur. J.* **2015,** *21*, 9550. (c) Quesnel, J. S.; Fabrikant, A.; Arndtsen, B. A. *Chem. Sci.* **2016**, *7*, 295.

20. Control experiments show that the reaction of imine PhCH=NBn with anisoyl chloride in CD_3CN leads leads to the formation of iminium salt **5b** in 82% yield in 5 minutes.

21. For mechanistic insights on palladium-catalyzed carbonylations see: (a) Hu, Y.; Liu, J.; Lü, Z.; Luo, X.; Zhang, H.; Lan, Y.; Lei, A. *J. Am. Chem. Soc.* **2010**, *132*, 3153. (b) Lin, Y. S.;

Yamamoto, A. *Organometallics* **1998**, *17*, 3466. (c) Martinelli, J. R.; Clark, T. P.; Watson, D. A.; Munday, R .H.; Buchwald, S. L. *Angew. Chem. Int. Ed.* **2007**, *46*, 8460. (d) Fernández-Álvarez, V. M.; de la Fuente, V.; Godard, C.; Castillón, S.; Claver, C.; Maseras, F.; Carbó, J. J. *Chem. Eur. J.* **2014**, *20*, 10982. (e) Nielsen, D. U.; Lescott, C.; Gogsig, T. M.; Lindhardt, A. T.; Skrydstrup, T. *Chem. Eur. J.* **2013**, *19*, 17926. (f) Ziolkowski, J.; Trzeciak, A. M. *Coord. Chem. Rev.* **2005**, *249*, 2308. For ligand effects on reductive elimination, see: (g) Roy, A. H.; Hartwig, J. F. *J. Am. Chem. Soc.* **2003**, *125*, 13944. (h) Roy, A. H.; Hartwig, J. F. *Organometallics* **2004**, *23*, 1533.

22. (a) Bayer, H. O.; Knorr, R.; Schaefer, F. C.; Huisgen, R. *Chem. Ber.* **1970**, *103*, 2581. (b) Dhawan, R.; Dghaym, R. D.; St. Cyr, D. J.; Arndtsen, B. A. *Org. Lett.* **2006**, *8*, 3927.

23. For reviews on the synthesis of pyrroles see: (a) Leeper, F. J.; Kelly, J. M. *Organic Preparations and Procedures International* **2013**, *45*, 171. (b) Toube, T. P.; Trofimov, B. A.; Cirrincione, G.; Almerico, A. M.; Aiello, E.; Datollo, G.; McNab, H.; Monahan, L. C. *Chemistry of Heterocyclic Compounds: Pyrroles, Part 2: The Synthesis, Reactivity, and Physical Properties of Substituted Pyrroles*, Jones, A. R., John Wiley & Sons, Inc.: 1992; Vol. 48. (c) Gianatassio, R.; Lopchuck, J. M. In *Progress in Heterocyclic Chemistry*, Gribble, G. W.; Joule, J. A., Ed. Elsevier: 2015; Vol. 27, p 159. (d) Yoshikai, N.; Wei, Y. *Asian. J. Org. Chem.* **2013**, *2*, 466. (e) Gilchrist, T. L. *J. Chem. Soc. Perkin Trans.* **1999**, *1*, 615. (f) Estévez, V.; Villacampa, M.; Menéndez, J. C. *Chem. Soc. Rev.* **2014**, *43*, 4633. (g) Bauer, I.; Knölker, H. –J. Synthesis of Pyrrole and Carbazole Alkaloids. In *Alkaloid Synthesis*. Knölker, H. –J., Springer-Verlag Berlin Heidelberg: 2012; Vol. 302, p 213. For recent examples see: (h) Ueda, K.; Amaike, K.; Maceiczyk, R. M.; Itami, K.; Yamaguchi, J. *J. Am. Chem. Soc.* **2014**, *136*, 13226. For examples of pharmaceutically relevant pyrrole development see: (i) Muchowski, J. M. *Adv. Med. Chem.* **1992**, *1*, 109. (j) Mongelli, N.

Cozzi, P., *Curr. Pharm. Des.* **1998**, *4*, 181. (k) Fürstner, A.; Szillat, H.; Gabor, B.; Mynott, R., *J. Am. Chem. Soc.* **1998**, *120*, 8305.

24. For reviews, see: (a) Curran, D.; Perera, S. D.; Grimshaw, J. *Chem. Soc. Rev.* **1991**, 20, 391. (b) Qu, S.; Tian, H. *Chem. Commun.* **2012**, 48, 3039. (c) Maeda, H. *Bull. Chem. Soc. Jpn.* **2013**, 86, 1359. (d) Maekawa, T.; Segawa, Y.; Itami, K. *Angew. Chem. Int. Ed.* **2015**, 54, 66.

25. For example, the use of *i*PrCH=NBn leads to exclusive enamide formation.

26. In the case of other alkynes, regioisomeric mixtures often arise, thus only symmetrical Münchnones were employed. For discussions of regioselectivity: (a) Lopchuk, J. M.; Hughes, R. P.; Gribble, G. W. *Org. Lett.* **2013**, *15*, 5218. (b) Morin, M. S. T.; St. Cyr, D. J.; Arndtsen, B. A.; Krenske, E. H.; Houk, K. N. *J. Am. Chem. Soc.* **2013**, *135*, 17349.

27. (a) Li, Y.; Wang, Z.; Zhang, P.; Liu, Y.; Xiong, L.; Wang, Q. *J. Heterocyclic Chem.* **2014**, *51*, 1410. (b) Liu, Y. –X.; Zhang, P. –X.; Li, Y. –Q.; Song, H. –B.; Wang, Q. –M. *Mol. Divers.* **2014**, *18*, 593. (c) Coppola, B. P.; Noe, M. C.; Schwartz, D. J.; Abdon, R. L.; Trost, B. M. *Tetrahedron* **1994**, *50*, 93. (d) Lopchuck, J. M.; Gribble, G. W. *Heterocycles.* **2011**, *82*, 1617

28. Layer, R. W. *Chem. Ber*. **1963**, *63*, 489.

29. Quesnel, J. S.; Kayser, L. V.; Fabrikant, A.; Arndtsen, B. A. *Chem. Eur. J*. **2015**, 21, 9550.

30. Bontemps, S.; Quesnel, J. S.; Worrall, K.; Arndtsen, B. A. *Angew. Chem. Int. Ed*. **2011**, 50, 8948.

31. Quesnel, J. S.; Arndtsen, B.A. *J. Am. Chem. Soc.* **2013,** *135*, 16841.

32. Dhawan, R.; Dghaym, R. D.; Arndtsen, B. A. *J. Am. Chem. Soc.* **2003**, 125, 1474.

33. Dhawan, R.; Dhgaym, R. D.; St. Cyr, D. J.; Arndtsen, B. A. *Org. Lett.* **2006,** *8*, 3927

34. Lopchuck, J. M.; Gribble, G. W. *Heterocycles*. **2011**, 2, 1617.

Chapter 3. Development of a Palladium Catalyzed Multicomponent Synthesis of Fused-Ring Pyrroles

3.1. Preface

Chapter 2 demonstrated that the palladium catalyzed formation of Münchnones from aryl iodides, imines, and carbon monoxide can be combined with alkyne cycloaddition to allow the overall synthesis of polysubstituted pyrroles. A visiting PhD student to our group, Neda Firoozi, subsequently took up the project together with myself, and showed that by performing the reaction with alkyne-tethered imines this chemistry could also be used to assemble polycyclic pyrroles. The work was published in *The Journal of Organic Chemistry* (**2016**, 81, 11145). This chapter will describe my specific contributions to this project, which include the catalyst development for the reaction using alkyne-tethered aryl iodides or imines, and the use of Sonogashira reactions in concert with our catalytic approach to generate highly substituted polycyclic pyrroles.

3.2. Introduction

Polycyclic pyrroles and their reduced derivatives are found in array of natural products and related pharmaceutically relevant products.[1-4] Unlike the many methods available for the synthesis of simple pyrroles, the formation of polycyclic pyrroles typically requires the cyclization of elaborate and synthetic precursors. A common example is the cycloaddition reaction of Münchnones with tethered alkynes (Scheme 3.1).[5-12] For example, the Bélanger group developed a synthesis of fused-ring pyrroles via the formation of Münchnone from alkynyl-substituted amino acids (Scheme 3.1a).[13] In a related work, Martinelli showed that various tethers between the alkynyl unit and amino acid can be used to form Münchnones and undergo intramolecular 1,3-

dipolar cycloaddition.[14] Pinho e Melo developed a related synthesis of chiral, tricyclic pyrrolo-thiazoles utilizing this tethered-alkyne strategy.[15] Nevertheless, these approaches are inherently limited due to the need to synthesize the substituted amino acid derivative precursor to Münchnones with the correctly positioned alkyne unit for intramolecular cycloaddition.

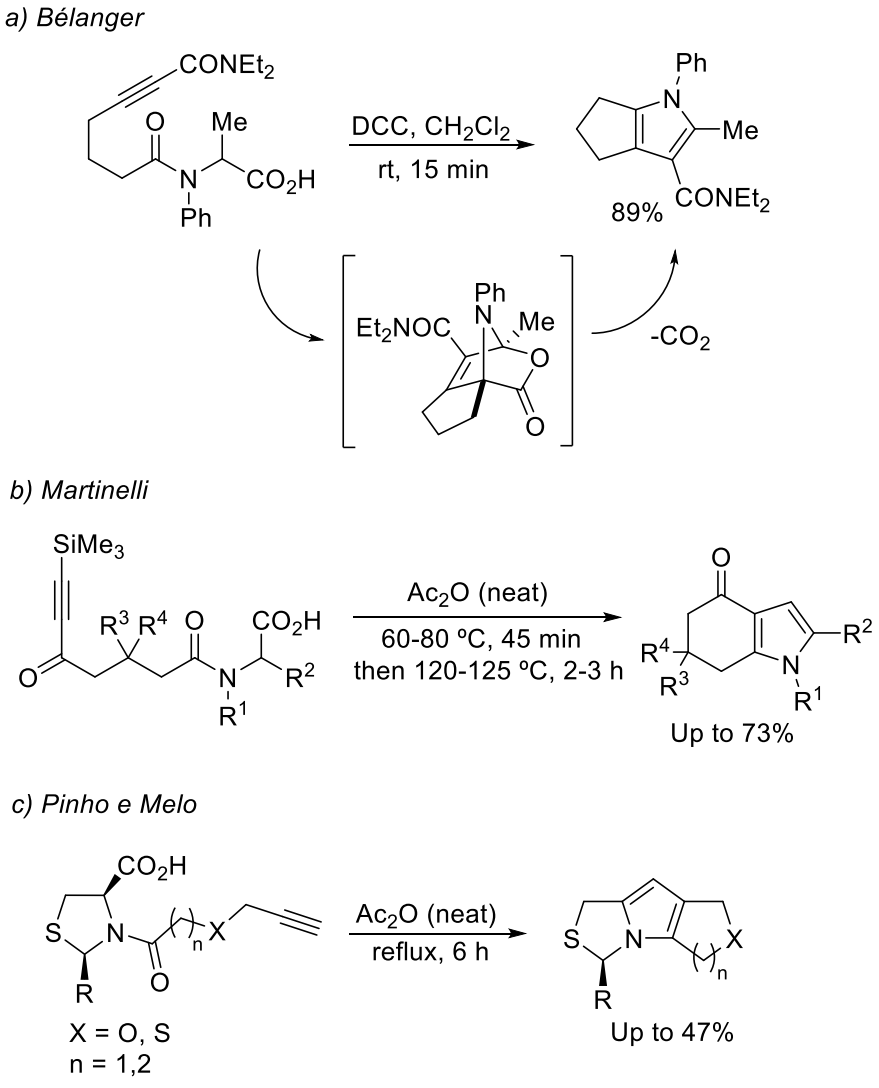

Scheme 3.1. Intramolecular Münchnone cycloadditions

As discussed in Chapter 2, the palladium catalyzed coupling of aryl iodides, imines, and carbon monoxide provides a straightforward route to generate Münchnones. The latter can be used to

generate diversely substituted pyrroles via cycloaddition with alkynes. We next questioned if this transformation might open a new approach to prepare polycyclic pyrroles via the use of alkyne-tethered substrates (Scheme 3.2).[16-20] In addition to providing a streamlined approach to generate such products, the intramolecular cycloaddition of Münchnones with a tethered alkyne should be regioselective, and could perhaps allow the use of less activated alkynes. Both of the latter are significant limitations of classic intermolecular 1,3-dipolar cycloaddition with Münchnones.[21-22] For example, Münchnones often require electron deficient dipolarophiles to react with the electron rich dipole, limiting the scope of alkynes in this chemistry to those with strong electron withdrawing units.[5, 7-8] In addition, many unsymmetrical alkynes react with Münchnones to form mixtures of products, unless, the Münchnone itself is symmetrical.[23-28]

Described below are my contributions towards the development and use of this transformation. These illustrate that alkyne-tethered imines in particular can be coupled with aryl iodides and two equivalents of carbon monoxide in a single, tandem catalytic transformation to afford an array of polycyclic pyrrole products. Moreover, the alkyne functional group is amenable to palladium catalyzed Sonogashira coupling, which offers an additional avenue for functionalization of the polycyclic core.

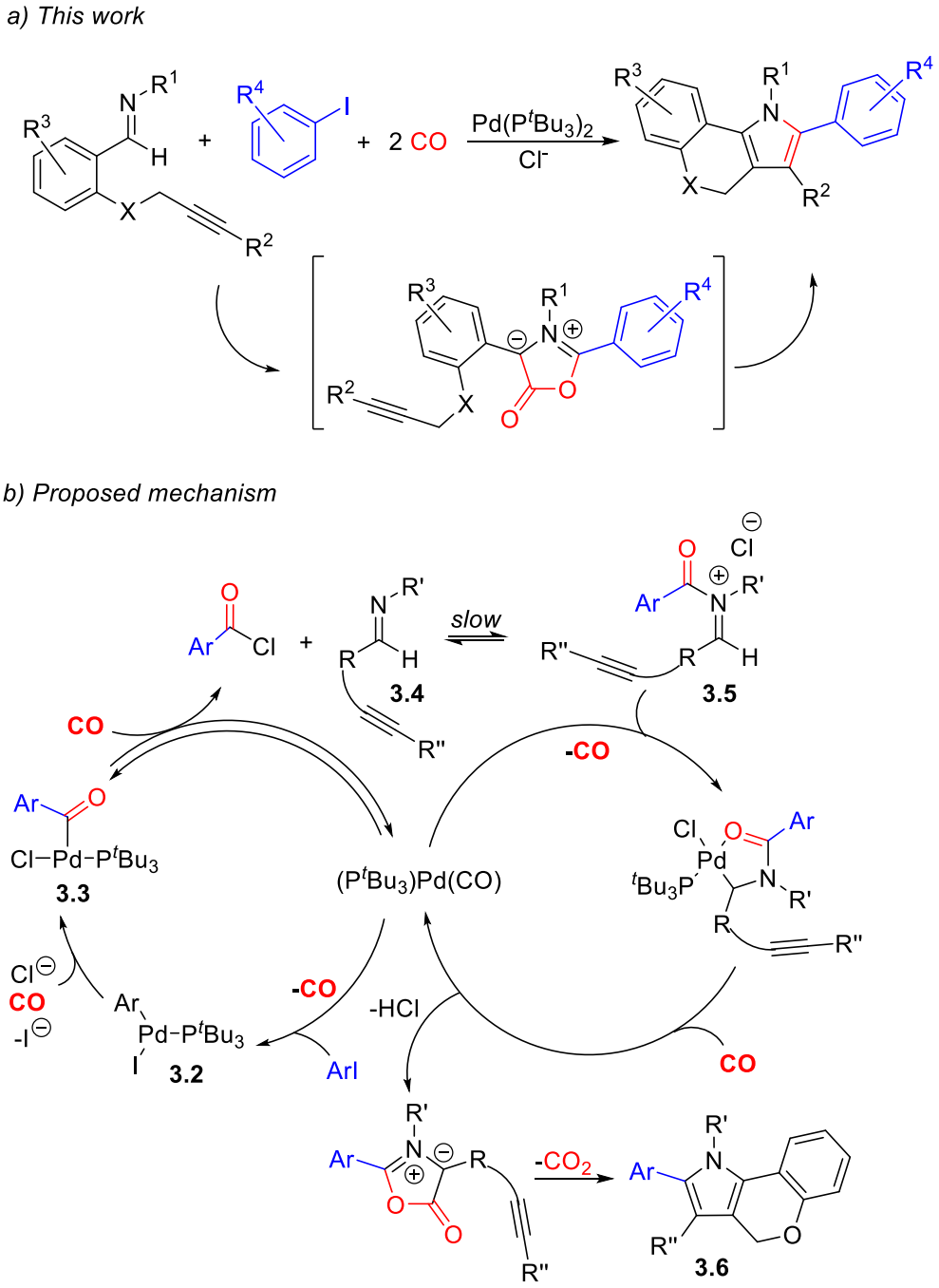

Scheme 3.2. A Palladium Catalyzed Route to Alkyne Tethered Münchnones

3.3. Results and Discussion

My first studies towards developing this reaction examined the reactivity of *o*-alkyne tethered aryl iodides with imines and carbon monoxide. The aryl iodide **3.1** can be easily prepared via nucleophilic substitution of propargyl bromide with *o*-iodophenol (Scheme 3.3).[20] This affords **3.1** in 80% yield after isolation.

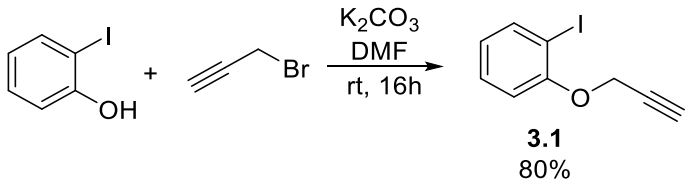

Scheme 3.3. Synthesis of *o*-Alkyne Tethered Aryl Iodide

As shown in Table 3.1, the reaction of **3.1** with the imine p-tolyl(H)C=NBn and 4 atm CO using our previously employed catalyst system for pyrrole synthesis, $[Pd(allyl)Cl]_2$ / P^tBu_3, led to consumption of the aryl iodide (entry 1). However, the imine is not consumed. Instead, a complex mixture of products is observed. We postulate that this may arise from the ability of the alkyne to undergo insertion onto the palladium-carbon bond generated upon aryl iodide oxidative addition (e.g. intermediate **3.2**, Scheme 3.2) rather than reaction with imine. Similar results were observed with a number of other catalyst systems, suggesting that this approach would not be a viable route to generate alkyne-tethered Münchnones.

Table 3.1. Reactivity of *ortho*-Alkyne Tethered Aryl iodide, Imine, and CO

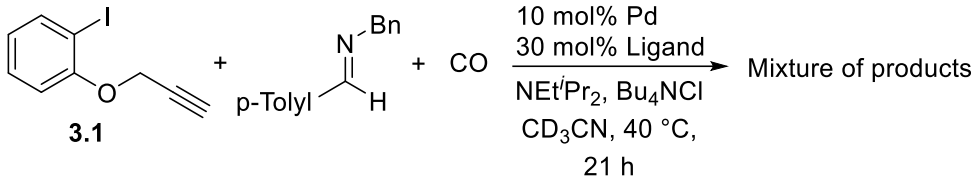

Entry	Pd Cat.	PR_3	Remaining Aryl Iodide (%)	Remaining Imine (%)	Pyrrole (%)
1	$[Pd(allyl)Cl]_2$	P^tBu_3	5	94	-
2	$[Pd(allyl)Cl]_2$	P(*o*-tolyl)$_3$	67	87	-
3	$Pd_2dba_3{\cdot}CH_3Cl$	-	38	96	-
4	$[Pd(OAc)_2$	PPh_3	34	94	-
5	$[Pd(allyl)Cl]_2$	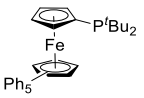	5	49	-

1-iodo-2-(prop-2-yn-1-yloxy)benzene (12 mg, 0.045 mmol), (p-tolyl)HC=NBn (6.3 mg, 0.03 mmol), NEt^{i}Pr$_2$ (7.8 mg, 0.06 mmol), Pd precursor (0.003 mmol), Bu$_4$NCl (17 mg, 0.06 mmol), ligand (0.009 mmol), benzyl benzoate internal standard (3.2 mg, 0.015 mmol), 0.75 mL CD$_3$CN, and 4 atm CO.

We next moved to examine the reactivity of alkyne-tethered imine **3.4a**. The latter can also be easily generated, in this case from salicylaldehyde.[29-30] This involves the initial coupling of the phenolic unit in salicylaldehyde with a propargyl bromide in the presence of base (Scheme 3.4). Subsequent condensation with ethylamine affords **3.4a** in 88% yield.

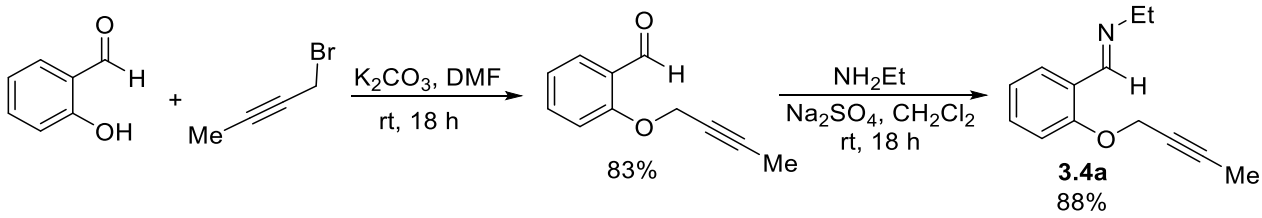

Scheme 3.4. Synthesis of *o*-Alkyne Tethered Imine

We were pleased to find that the $[Pd(allyl)Cl]_2$ / P^tBu_3 catalyzed reaction of **3.4a**, *p*-tolyl iodide and 4 atm CO in the presence of a chloride source (Bu_4NCl) allows the formation of polycyclic pyrrole **3.6a** in good yield (Table 3.2, entry 1). The use of smaller phosphine ligands affords no product (entries 2-5) or produced **3.6a** in reduced yields (entries 6-9). These results are similar to our observations in Chapter 2, and presumably arise from the lower steric profile of these latter phosphines, which cannot competently drive the reductive elimination of acid chloride (see Scheme 3.2 for postulated mechanism). Indeed, in the absence of a chloride source, no pyrrole product is observed (entry 3). Our mechanistic observations in Chapter 2 suggested that the rate limiting step in this reaction is the equilibrium formation of *N*-acyl iminium salt **3.5** from the palladium-acyl intermediate **3.3** (Scheme 3.2b). Carbon monoxide plays a role in driving forward the equilibrium by favoring the reductive elimination of acid chloride. Consistent with this rate limiting step, performing the reaction at elevated CO pressure (10 atm) to further drive acid chloride generation allows the formation of **3.6a** in 76% isolated yield with 5 mol% $Pd(P^tBu_3)_2$ catalyst (entry 10).

Table 3.2. Catalyst Design for the Carbonylative Synthesis of 3.6a.[a]

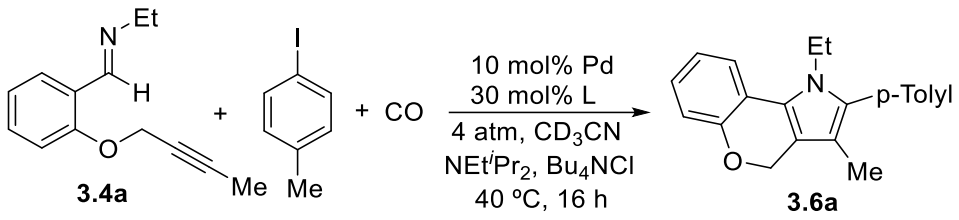

Entry	Pd cat.	Ligand	Yield (%)[b]
1	$[Pd(allyl)Cl]_2$	P^tBu_3	70
2	$[Pd(allyl)Cl]_2$	-	0
3	$Pd_2dba_3 \cdot CH_3Cl$	-	0
4	$[Pd(allyl)Cl]_2$	PCy_3	0
5	$[Pd(allyl)Cl]_2$	PPh_3	0
6	$[Pd(allyl)Cl]_2$	P(*o*-tolyl)$_3$	23
7	$[Pd(allyl)Cl]_2$	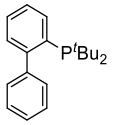	19
8	$[Pd(allyl)Cl]_2$	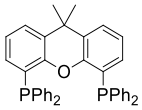	12
9	$[Pd(allyl)Cl]_2$	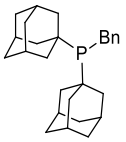	40
10	5% $Pd(P^tBu_3)_2$	-	76[c,d]

[a]Imine (6 mg, 0.03 mmol), 4-iodotoluene (33 mg, 0.15 mmol), Pd precursor (0.003 mmol), ligand (0.009 mmol) Bu_4NCl (8 mg, 0.03 mmol), NEt^iPr_2 (6 mg, 0.045 mmol), CO (4 atm), 0.75 mL CD_3CN. [b]NMR yield. [c]0.5 mmol scale with 5 mol% $Pd(P^tBu_3)_2$ (13 mg, 0.025 mmol), Bu_4NCl (139 mg, 0.5 mmol), 10 atm CO. [d]Isolated yield.

With this catalyst system developed, a diverse range of polycyclic pyrroles were prepared. This was done by Neda Firoozi, and examples are shown in Scheme 3.5. Of note, the reaction proceeds in good yield with an array of aryl or heteroaryl iodides, and alkyne cycloaddition is viable with various unactivated alkynes. The latter presumably arises from the favored intramolecular cycloaddition reaction.[12, 14, 23]

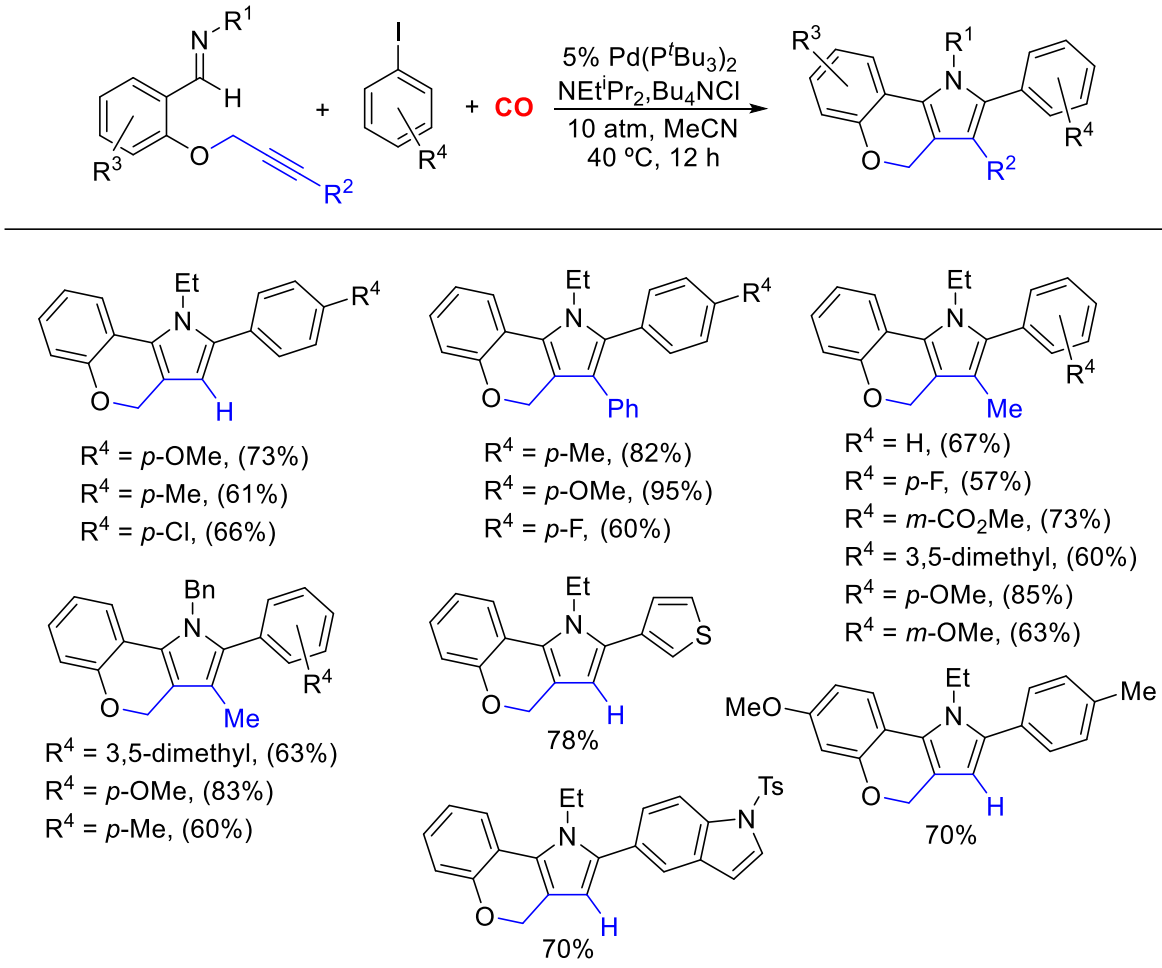

Scheme 3.5. Scope of the Palladium Catalyzed Carbonylative Synthesis of Fused-Ring Pyrroles

As highlighted in Scheme 3.5, terminal alkynes can also be used in the reaction. This is intriguing, as these can also undergo palladium catalyzed Sonogashira reactions with aryl iodides.[31] The lack of Sonogashira coupling presumably arises from the more rapid insertion of carbon monoxide into the *in situ* generated Pd-aryl bond than reaction with the terminal alkyne. This implies that CO could be used as a switch to change the reactivity of the palladium catalyst. Neda Firoozi demonstrated that this could be exploited, where performing the reaction with a CuI

cocatalyst leads to an initial Sonogashira coupling. The subsequent addition of CO to the same reaction mixture allows the formation of substituted pyrroles in a one pot reaction from now two equivalents of aryl iodide (Scheme 3.6). Additional P^tBu_3 is required in this reaction, which is postulated to stabilize the palladium catalyst from decomposition after the initial Sonogashira coupling step.

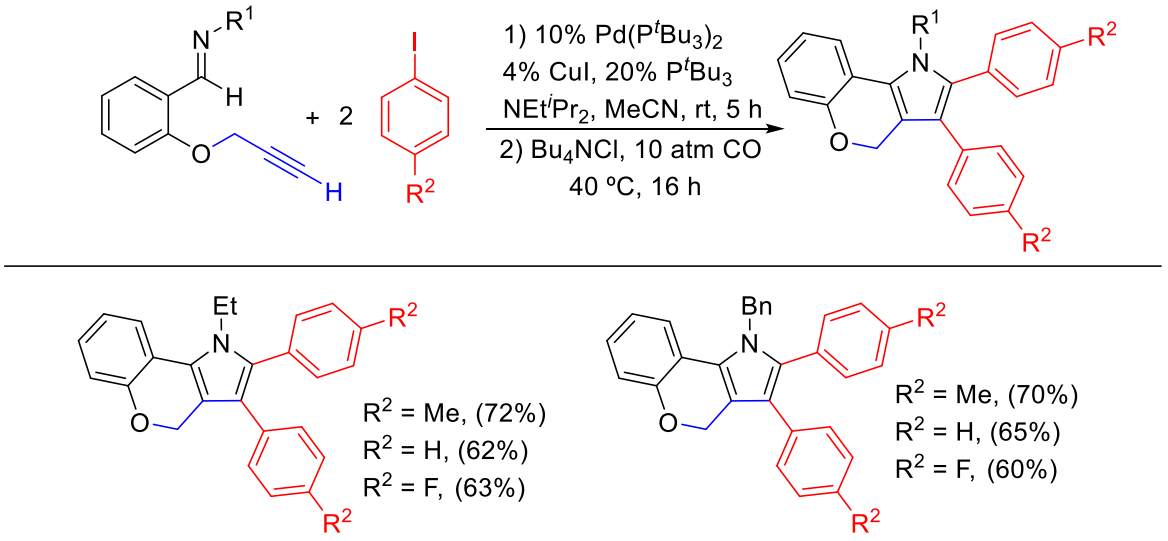

Scheme 3.6. Tandem Four-Component Synthesis of Fused-Ring Pyrroles

One limitation of the approach above is that the resulting pyrrole has two identical aryl substituents. In principle, it should be possible to address this limitation by performing the initial Sonogashira coupling with only a stoichiometric amount of aryl iodide, followed by the addition of a second aryl iodide with carbon monoxide to form pyrrole (Table 3.3). Such an approach presents several challenges. Firstly, the initial Sonogashira coupling will need to completely consume the terminal alkyne using only a stoichiometric amount of aryl iodide, as any uncoupled

alkyne with undergo cycloaddition to afford a tetrasubstituted pyrrole. Secondly, there can be no remaining aryl iodide from the initial step, as it will lead to mixtures in the subsequent formation of Münchnone and pyrrole. My initial attempts at this reaction with two different aryl iodides led to incomplete conversion to the initial Sonogashira product (Table 3.3 entries 1 and 2). While reasons for this lack of reactivity are unclear, it is possible that the steric bulk or coordinating ability of these aryl iodides may slow the reaction. Upon switching to a slightly smaller 3-iodothiophene as the first substrate, the Sonogashira product was obtained in near quantitative yield (entry 3). In this case, however, the subsequent cyclization step with 4-iodoanisole was inefficient (31% yield of pyrrole). The latter may arise from the relatively electron rich tethered-alkyne formed with thiophene, which would presumably undergo sluggish cycloaddition with a Münchnone.

There have been reports that the strong, bulky DABCO base can enhance the yields of Sonogashira reactions involving challenging substrates.[32] This proved to be effective here as well, where performing this reaction with a *para*-substituted and electron deficient aryl iodide and DABCO leads to significant rate increases relative to NEt^iPr_2 (entries 4 and 5). The subsequent addition to excess 3-iodothiophene and carbon monoxide allowed the overall formation of the pyrrole **3.7a** in 58% yield, or in 53% isolated yield when performed on a 0.5 mmol scale (Scheme 3.7). Utilizing non-heterocyclic aryl iodide substrates led to the higher yield formation of **3.7b**. Both of these latter represent a new approach to assemble polysubstituted pyrroles from four substrates that are each of which are either commercially available or easily generated.

Table 3.3. Development of the Four-Component Synthesis of Polycyclic Pyrroles[a]

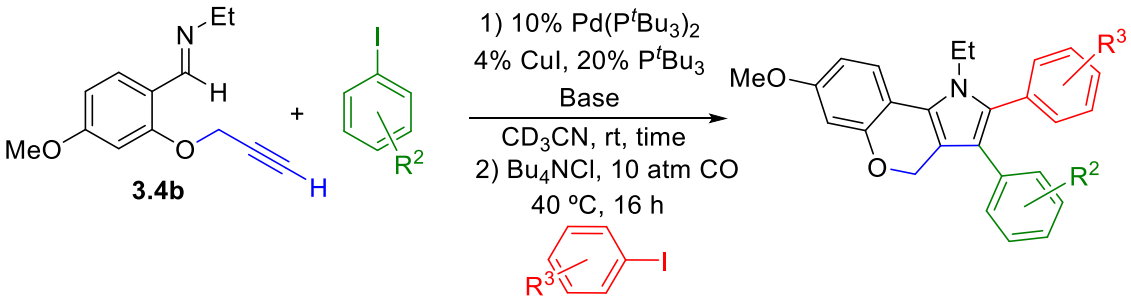

Entry	ArI[1]	ArI[2]	Base	Time (h)	%Yield Sonogashira[b]	%Yield Pyrrole[b]
1	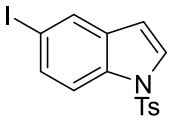	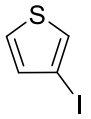	NEt^{i}Pr$_2$	24	33	-
2	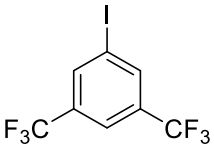	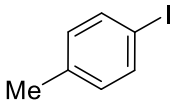	NEt^{i}Pr$_2$	24	50	-
3	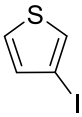	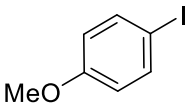	NEt^{i}Pr$_2$	4	92	31
4	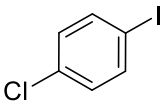	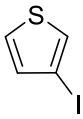	NEt^{i}Pr$_2$	48	41	-
5	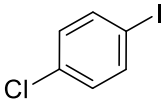	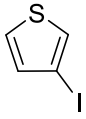	DABCO[c]	48	87	58

[a]Imine **3.4b** (11 mg, 0.05 mmol), aryl iodide 1 (0.05 mmol), Pd(P^{t}Bu$_3$)$_2$ (2.5 mg, 0.005 mmol), P^{t}Bu$_3$ (2.0 mg, 0.01 mmol), CuI (0.25 mL 5.0 mM solution in CD$_3$CN, 1.25 µmol), NEt^{i}Pr$_2$ (19 mg, 0.15 mmol), benzyl benzoate (5.3 mg, 0.025 mmol), CD$_3$CN (0.5 mL), room temperature, 4-48 hours. Then Bu$_4$NCl (28 mg, 0.10 mmol), aryl iodide 2 (0.25 mmol), CO (4 atm), 40 °C, 16 h. [b]NMR yield. [c] DABCO (17 mg, 0.15 mmol)

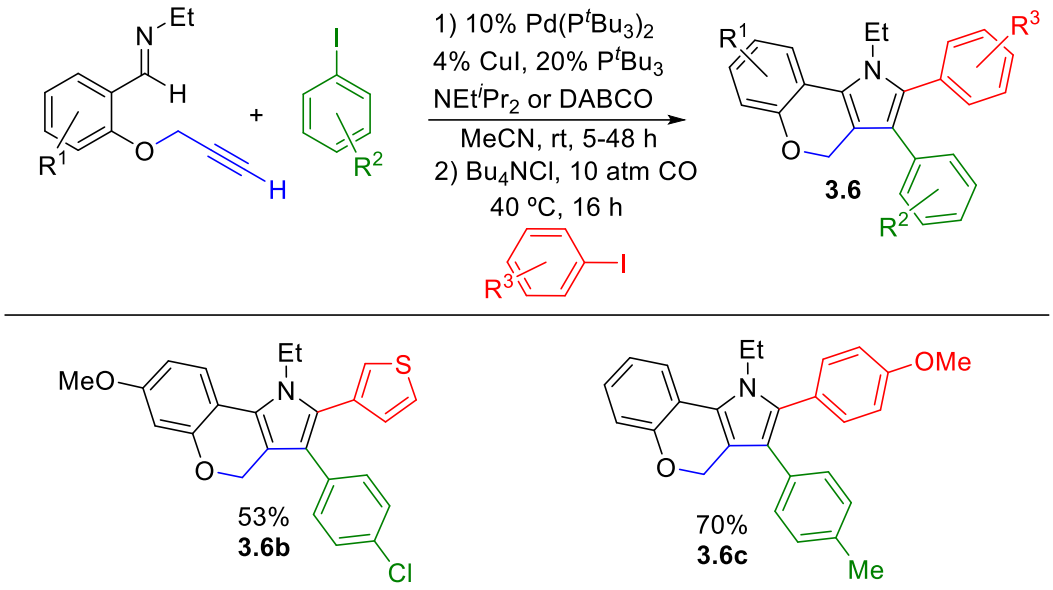

Scheme 3.7. Tandem Four-Component Synthesis of Polycyclic Pyrroles with Two Different Aryl Iodides

3.4. Conclusions

We have shown that the combination of alkyne-tethered imines, aryl iodides, and carbon monoxide provides a modular platform to generate complex polycyclic pyrroles. This reaction is mediated by a palladium catalyst incorporating the bulky P^{t}Bu$_3$ ligand, requires the presence of chloride, and is accelerated by CO pressure. Each of these are consistent with the ability of these systems to allow the *in situ* build-up of acid chlorides and then Münchnones, followed by intramolecular cycloaddition. Moreover, the reaction can be combined with Sonogashira coupling when employing terminal alkynes to create a one pot route to prepare polysubstituted pyrroles from four different reagents.

3.5. Experimental Section

3.5.1. General Procedures

All manipulations were conducted in a glovebox under a nitrogen atmosphere. Unless otherwise noted, all reagents were purchased from commercial sources and used without purification. Solvents were dried by using a solvent purifier system and stored over activated 4Å molecular sieves inside the glovebox. Deuterated acetonitrile was stirred over calcium hydride, vacuum transferred, degassed, and stored over 4Å molecular sieves. Tetrabutylammonium chloride was dried in the glovebox by dissolving in dichloromethane, allowing to stand overnight over activated molecular sieves, filtering and removing the solvent in vacuo. Research grade carbon monoxide (99.99%) was used as received. For reactions performed in a J-Young NMR tubes, carbon monoxide was added by first freezing the solution in liquid nitrogen, evacuating the headspace *in vacuo*, and then condensing in 4 atm CO. For reactions at 10 atm CO, a 4 mL glass vial containing the reaction mixture was equipped with a magnetic stir bar and a pierced plastic cap. The vial was placed inside a high pressure steel autoclave, sealed, and taken out of the glovebox. The autoclave was then connected to a Parr Multiwell Reactor 5000 system and pressurized with 10 atm CO on top of the nitrogen atmosphere inside. Nuclear magnetic resonance (NMR) characterization was performed on 500 MHz spectrometers for proton, 126 MHz for carbon, and 162 MHz for phosphorus. ^{1}H and ^{13}C NMR chemical shifts were referenced to residual solvent. Mass spectra were recorded on a high-resolution electrospray ionization quadrupole mass spectrometer.

3.5.2. Experimental Procedures

Synthesis of alkyne tethered aryl iodide

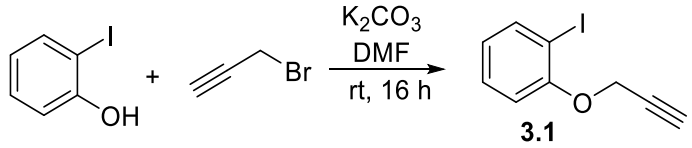

Alkyne tethered aryl iodide was synthesized using a literature procedure.[20] A solution of 2-iodophenol (858 mg, 3.9 mmol) and K_2CO_3 (815 mg, 5.9 mmol) in DMF (15 ml) was prepared in a 100 mL round bottom flask equipped with a magnetic stir bar. The solution was allowed to stir for 20 minutes at room temperature. To the solution was added a propargyl bromide solution in toluene 80% w/w (758 mg, 5.1 mmol). The reaction mixture was stirred overnight at room temperature. Water (20 mL) was then added and the resulting mixture was extracted three times with diethyl ether (15 mL portions). The ether fractions were combined and filtered through $MgSO_4$. The solvent was removed *in vacuo* and the crude residue was purified by column chromatography on silica gel (eluent: n-hexane/ethyl acetate 10:1) to afford 1-iodo-2-(prop-2-yn-1-yloxy)benzene **3.1** as a colorless liquid in 80% yield (798 mg, 3.1 mmol).

1-iodo-2-(prop-2-yn-1-yloxy)benzene (**3.1**):[20] Isolated yield 80% yield (798 mg, 3.1 mmol). Colorless liquid. ^{1}H NMR (500 MHz, $CDCl_3$) δ 7.80 (dd, *J* = 7.8, 1.6 Hz, 1H), 7.38 – 7.28 (m, 1H), 7.00 (dd, *J* = 8.2, 1.0 Hz, 1H), 6.76 (td, *J* = 7.6, 1.2 Hz, 1H), 4.76 (d, *J* = 2.4 Hz, 2H), 2.54 (t, *J* = 2.4 Hz, 1H). ^{13}C NMR (125 MHz, $CDCl_3$) ^{13}C NMR (126 MHz, $CDCl_3$) δ 156.3, 139.8, 129.4, 123.5, 113.1, 86.7, 78.1, 76.2, 57.0. HRMS: Calculated for C_9H_7OI (M^+): 257.9536, found: 257.9531.

Attempted synthesis of pyrroles from alkyne-tethered aryl iodide, imine, and CO

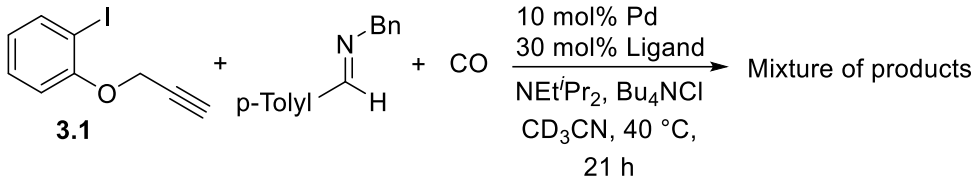

In a glovebox**, 3.1** (12 mg, 0.045 mmol), (p-tolyl)HC=NBn (6.3 mg, 0.03 mmol), NEt^{i}Pr$_2$ (7.8 mg, 0.06 mmol), Bu$_4$NCl (17 mg, 0.06 mmol), P^{t}Bu$_3$ (1.8 mg, 0.009 mmol), and BnOBz internal standard (3.2 mg, 0.015 mmol) were dissolved in 0.75 mL of a 2.0 mM solution of [Pd(allyl)Cl]$_2$ in CD$_3$CN (1.5 μmol [Pd(allyl)Cl]$_2$), prepared by dissolving 3.7 mg of [Pd(allyl)Cl]$_2$ in 5 mL CD$_3$CN, and transferred into a J-Young NMR tube. The NMR tube was then sealed with a screw-cap, taken out of the glovebox, and charged with 4 atm of CO. The tube was then heated in an oil bath at 40 ºC. The reaction was analyzed by ^{1}H NMR over the course of 21 h, and the consumption of starting material was quantified via integration against the internal standard. ^{1}H NMR analysis reveals the protonation of the base and the partial disappearance of the aryl iodide. In most cases, imine is left intact and there is no evidence of pyrrole formation.

Typical synthesis of alkyne-tethered imines

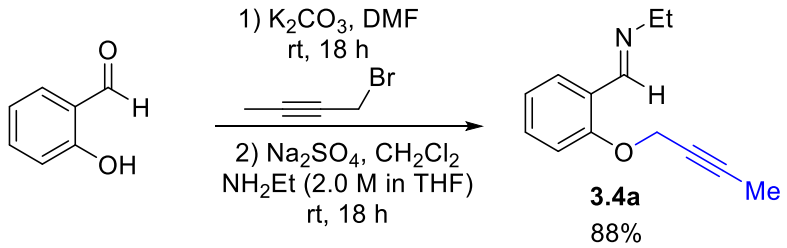

Alkyne tethered imines **3.4** were synthesized following a known literature procedure.[29-30] A solution of salicylaldehyde (366 mg, 3.0 mmol) and K$_2$CO$_3$ (1.0 g, 7.5 mmol) in DMF (15 ml) was

prepared in a 100 mL round bottom flask equipped with a magnetic stir bar. The solution was allowed to stir for 20 minutes at room temperature. To the solution was added 1-bromobut-2-yne (519 mg, 3.9 mmol). The reaction mixture was allowed to stir overnight at room temperature. Water (20 mL) was then added and the resulting mixture was extracted three times with diethyl ether (15 mL portions). The ether fractions were combined and filtered through $MgSO_4$. The solvent was removed *in vacuo* and the product was recrystallized in ethanol to afford 2-(but-2-yn-1-yloxy)benzaldehyde (435 mg, 2.5 mmol) as a yellow solid in 83% yield. To a solution of this 2-(but-2-yn-1-yloxy)benzaldehyde (435 mg, 2.5 mmol) in dichloromethane (10 mL) was added Na_2SO_4 (1.0 g, 7.0 mmol) and ethylamine (2.0 M in THF) (1.6 mL, 3.25 mmol). The heterogeneous mixture was stirred at room temperature for 18 h. The reaction mixture was filtered, and the solvent and excess amine were removed *in vacuo* to afford (*E*)-1-(2-(but-2-yn-1-yloxy)phenyl)-N-ethylmethanimine **3.4a** (453 mg, 2.2 mmol) as a yellow oil (88%).

1-(2-(but-2-yn-1-yloxy)phenyl)-*N*-ethylmethanimine (**3.4a**):[29-30] Isolated yield 88% (453 mg, 2.20 mmol). Yellow oil. ^{1}H NMR (500 MHz, $CDCl_3$) δ 8.73 (s, 1H), 7.96 (dd, J = 7.6, 1.7 Hz, 1H), 7.40 – 7.30 (m, 1H), 7.00 (m, 2H), 4.71 (q, J = 2.3 Hz, 2H), 3.65 (qd, J = 7.3, 1.3 Hz, 2H), 1.85 (t, J = 2.3 Hz, 3H), 1.29 (t, J = 7.3 Hz, 3H). ^{13}C NMR (125 MHz, $CDCl_3$) δ 156.9, 156.3, 131.4, 127.2, 125.4, 121.4, 112.7, 84.0, 73.9, 56.9, 56.0, 16.4, 3.6. HRMS: Calculated for $C_{13}H_{15}NNaO$ (MNa^+): 224.1046, found: 224.1052.

(*E*)-N-ethyl-1-(4-methoxy-2-(prop-2-yn-1-yloxy)phenyl)methanimine (**3.4b**) Isolated yield 85% (463 mg, 2.10 mmol). Yellow powder. m.p. 57-58 °C. ^{1}H NMR (500 MHz, $CDCl_3$) δ 8.61 (s, 1H), 7.93 – 7.87 (m, 1H), 6.59 – 6.52 (m, 2H), 4.72 (d, J = 2.4 Hz, 2H), 3.82 (s, 3H), 3.60 (qd, J = 7.3, 1.4 Hz, 2H), 2.54 (t, J = 2.4 Hz, 1H), 1.27 (t, J = 7.3 Hz, 3H). ^{13}C NMR (125 MHz, $CDCl_3$) δ

162.6, 157.9, 155.7, 128.6, 118.8, 106.6, 99.7, 78.3, 76.1, 56.4, 56.1, 55.5, 16.6. HRMS: Calculated for $C_{13}H_{16}NO_2$ (MH^+) 218.1176, found: 218.1178.

N-ethyl-1-(2-(prop-2-yn-1-yloxy)phenyl)methanimine (**3.4c)** Isolated yield 95% (445 mg, 2.40 mmol). Yellow oil. ^{1}H NMR (500 MHz, $CDCl_3$) δ 8.73 (s, 1H), 7.97 (dd, J = 8.1, 1.6 Hz, 1H), 7.42 – 7.33 (m, 1H), 7.03 (m, 2H), 4.76 (d, J = 2.4 Hz, 2H), 3.65 (qd, J = 7.3, 1.4 Hz, 2H), 2.53 (t, J = 2.4 Hz, 1H), 1.30 (t, J = 7.3 Hz, 3H). ^{13}C NMR (125 MHz, $CDCl_3$) δ 156.6, 156.1, 131.4, 127.4, 125.6, 121.8, 112.6, 78.3, 75.8, 56.3, 56.1, 16.3. HRMS: Calculated for $C_{12}H_{14}NO$ (MH^+) 188.1070, found: 188.1070.

Typical procedure for catalyst development for the formation of polycyclic pyrroles with alkyne-tethered imines, aryl iodides, and CO

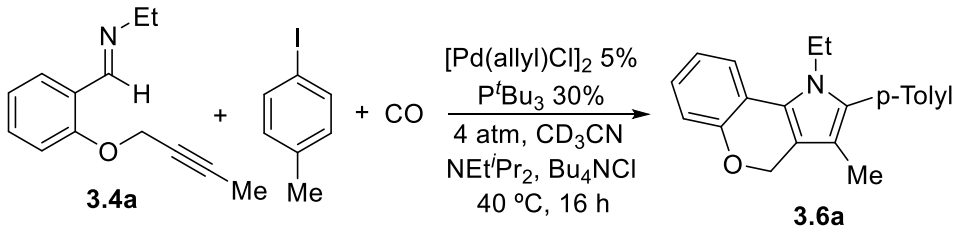

In a glovebox, *ortho*-alkyne tethered imine **3.4a** (6 mg, 0.03 mmol), 4-iodotoluene (33 mg, 0.15 mmol), NEt^iPr_2 (6 mg, 0.045 mmol), Bu_4NCl (8 mg, 0.03 mmol), P^tBu_3 (1.8 mg, 0.009 mmol), and benzyl benzoate internal standard (3.2 mg, 0.015 mmol) were dissolved in 0.75 mL of a 2.0 mM solution of $[Pd(allyl)Cl]_2$ in CD_3CN (1.5 µmol $[Pd(allyl)Cl]_2$), prepared by dissolving 3.7 mg of $[Pd(allyl)Cl]_2$ in 5 mL CD_3CN, and transferred into a J-Young NMR tube. The tube was sealed with a screw-cap, taken out of the glovebox, and charged with 4 atm of CO. The tube was then heated in an oil bath at 40 ºC. The reaction was analyzed by ^{1}H NMR over the course of 16 h, and

the yield of product was quantified via integration against the internal standard. ^{1}H NMR analysis reveals the formation of pyrrole **3.6a** in 70% yield.

Typical procedure for the formation of polycyclic pyrroles with alkyne-tethered imines, aryl iodides, and CO

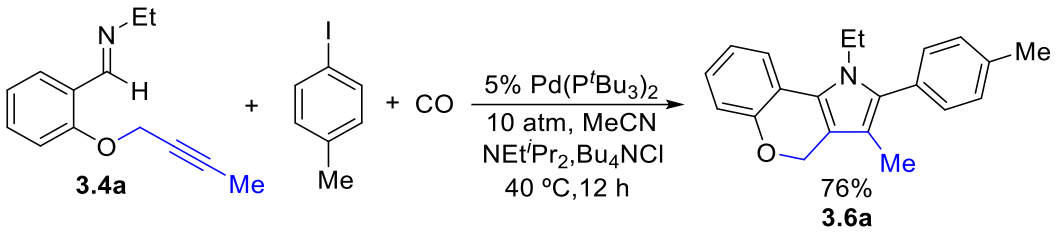

In a glovebox, imine **3.4a** (101 mg, 0.50 mmol), 4-iodotoluene (545 mg, 2.5 mmol), NEt^{i}Pr$_2$ (97 mg, 0.75 mmol) in 3.3 ml acetonitrile were added to Pd(P^{t}Bu$_3$)$_2$ (13 mg, 0.025 mmol) and Bu$_4$NCl (139 mg, 0.5 mmol) in a 4 mL glass vial equipped with a magnetic stir bar. The vial was capped with a pierced plastic cap and placed inside a 50 mL Parr steel autoclave, which was sealed and taken out of the glovebox. The reactor was charged with 10 atm CO using a Parr Multiwell Reactor 5000. The reactor was heated to 40 °C for 12 h in an oil bath. After allowing sufficient time to cool to room temperature, the CO atmosphere was evacuated inside a well-ventilated fume hood. The crude residue was purified by column chromatography on silica gel (eluent: n-hexane/ethyl acetate 10:1) to afford 1-ethyl-3-methyl-2-(p-tolyl)-1,4-dihydrochromeno[4,3-*b*]pyrrole **3.6a** as a light yellow solid in 76% (115 mg, 0.38 mmol).

Typical procedure for the development of the catalytic synthesis of polycyclic pyrroles with two aryl iodides (Table 3.3)

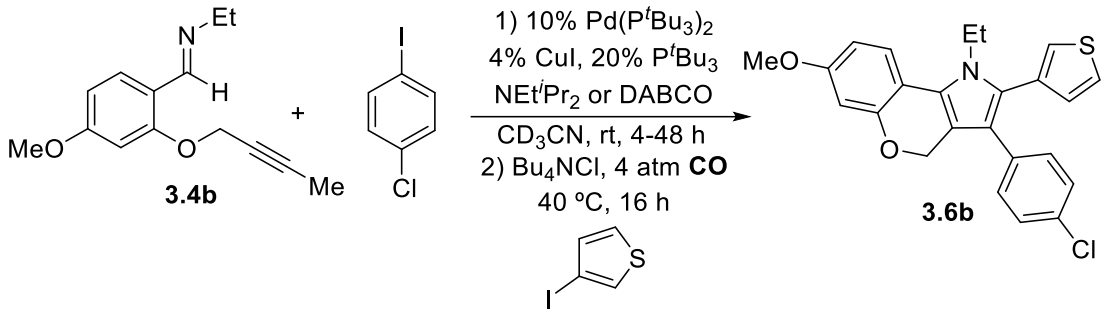

In a glovebox, *ortho*-alkyne tethered imine **3.4b** (11 mg, 0.05 mmol), 1-chloro-4-iodobenzene (12 mg, 0.05 mmol), NEt^{i}Pr$_2$ (19 mg, 0.15 mmol) or DABCO (17 mg, 0.15 mmol), Pd(P^{t}Bu$_3$)$_2$ (2.5 mg, 0.005 mmol), P^{t}Bu$_3$ (2.0 mg, 0.01 mmol), and benzyl benzoate internal standard (5.3 mg, 0.025 mmol) were dissolved in 0.5 mL CD_3CN and transferred into a J-Young NMR tube. To this solution was added 0.25 mL of a 5.0 mM solution of CuI in CD_3CN (1.25 μmol CuI), prepared by dissolving 4.8 mg of CuI in 5 mL CD_3CN. The tube was sealed with a screw-cap, taken out of the glovebox, and periodically shaken manually. The yield of the Sonogashira product was quantified via NMR integrations against the benzyl benzoate internal standard. The reaction using DABCO as a base generated the Sonogashira product in 87% yield after 48 hours. The NMR tube was brought back into the glovebox. To this tube was added Bu_4NCl (28 mg, 0.10 mmol) and 3-iodothiophene (52 mg, 0.25 mmol). The tube was capped, taken out of the glovebox, and charged with 4 atm of CO. The tube was then heated in an oil bath at 40 °C. The reaction was analyzed by ^{1}H NMR over the course of 16 h, and the yield of product was quantified via integration against the internal standard. ^{1}H NMR analysis reveals the formation of pyrrole **3.6b** in 58% yield.

Procedure for the synthesis of fused-ring pyrroles with two aryl iodides

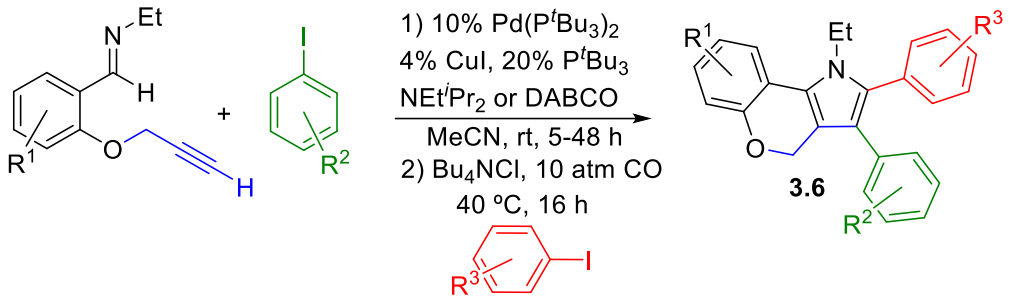

For **3.6b**, the low solubility of the complex mixture in MeCN necessitated dilute conditions. *N*-ethyl-1-(4-methoxy-2-(prop-2-yn-1-yloxy)phenyl)methanimine **3.4b** (109 mg, 0.5 mmol), 1-chloro-4-iodobenzene (119 mg, 0.5 mmol), DABCO (168 mg, 1.5 mmol), and P^tBu_3 (20 mg, 0.1 mmol) were dissolved in 9 mL of MeCN and added to a 20 mL vial containing CuI (2.4 mg, 0.0125 mmol) and $Pd(P^tBu_3)_2$ (26 mg, 0.05 mmol). The vial was equipped with a stir bar and the mixture was allowed to stir at room temperature for 48 h. Afterwards, Bu_4NCl (278 mg, 1.0 mmol) and 3-iodothiophene (525 mg, 2.5 mmol) were dissolved in 3 mL MeCN and added to the mixture. The vial was placed inside a 50 mL steel autoclave, which was sealed, and taken out of the glovebox. The reactor was charged with 10 atm CO using a Parr Multiwell Reactor 5000. The reactor was then heated to 40 °C for 16 h inside an oil bath. After allowing sufficient time to cool to room temperature, the CO atmosphere was evacuated inside a well-ventilated fume hood. The crude residue was purified by column chromatography on silica gel (eluent: n-hexane/ethyl acetate 10:1) to afford 3-(4-chlorophenyl)-1-ethyl-7-methoxy-2-(thiophen-3-yl)-1,4-dihydrochromeno[4,3-b]pyrrole **3.6b** as a light yellow solid (112 mg, 0.26 mmol) in 53% yield.

Pyrrole **3.6c** was synthesized as follows: In a glovebox, *N*-ethyl-1-(2-(prop-2-yn-1-yloxy)phenyl)methanimine **3.4c** (93 mg, 0.5 mmol), 4-iodotoluene (120 mg, 0.55 mmol), and NEt^iPr_2 (250 mg, 2 mmol) in 3.3 ml acetonitrile were added to a 4 mL vial containing $Pd(P^tBu_3)_2$

(26 mg, 0.05 mmol), CuI (4.8 mg, 0.025 mmol), P^{t}Bu$_3$ (20 mg, 0.1 mmol). The vial was equipped with a magnetic stir barr and the mixture was allowed to stir at room temperature for 4 h. Afterwards, Bu_4NCl (278 mg, 1.0 mmol) and 4-iodoanisole (585 mg, 2.5 mmol) were added to the mixture. The vial was sealed with a pierced plastic cap and placed inside a 50 mL Parr steel autoclave, which was sealed and taken out of the glovebox. The reactor was charged with 10 atm CO using a Parr Multiwell Reactor 5000. The reactor was then heated to 40 ^oC for 16 h. After allowing sufficient time to cool to room temperature, the CO atmosphere was evacuated and the crude residue was purified by column chromatography on silica gel (eluent: n-hexane/ethylacetate 10:1) to afford **3.6c** (138 mg, 0.35 mmol) as a light-yellow solid in 70% yield

3.5.3. Characterization Data

1-ethyl-3-methyl-2-(*p*-tolyl)-1,4-dihydrochromeno[4,3-*b*]pyrrole (**3.6a**) Isolated yield 76% (115 mg, 0.38 mmol). Light yellow solid, mp 113-115 ^oC. ^1H NMR (500 MHz, $CDCl_3$) δ 7.42 (dd, J = 7.7, 1.6 Hz, 1H), 7.32 – 7.27 (m, 2H), 7.25 (d, J = 8.1 Hz, 2H), 7.08 (ddd, J = 8.7, 7.3, 1.6 Hz, 1H), 7.03 – 6.95 (m, 2H), 5.24 (s, 2H), 4.11 (q, J = 7.1 Hz, 2H), 2.45 (s, 3H), 1.94 (s, 3H), 1.26 (t, J = 7.1 Hz, 3H). ^{13}C NMR (125 MHz, $CDCl_3$) δ 153.2, 137.3, 134.0, 130.7, 129.3, 129.1, 126.1, 122.1, 121.6, 120.2, 119.9, 117.2, 116.2, 112.1, 64.9, 30.3, 21.3, 16.6, 9.3. HRMS: Calculated for $C_{21}H_{21}NNaO$ (MNa^+): 326.1515, found: 326.1516.

3-(4-chlorophenyl)-1-ethyl-7-methoxy-2-(thiophen-3-yl)-1,4-dihydrochromeno[4,3-b]pyrrole (**3.6b**) Isolated yield 53% (112 mg, 0.26 mmol). Light orange solid. m.p. 132-134 °C. ^1H NMR (500 MHz, $CDCl_3$) δ 7.40 – 7.33 (m, 2H), 7.22 – 7.14 (m, 3H), 7.01 – 6.97 (m, 1H), 6.91 (d, J = 8.4 Hz, 2H), 6.64 (d, J = 2.6 Hz, 1H), 6.59 (dd, J = 8.6, 2.6 Hz, 1H), 5.23 (s, 2H), 4.16 (q, J = 7.1 Hz, 2H), 3.82 (s, 3H), 1.34 (t, J = 7.2 Hz, 3H). ^{13}C NMR (125 MHz, $CDCl_3$) δ 159.0, 155.3, 133.5,

132.0, 131.5, 130.3, 130.0, 128.5, 126.9, 126.1, 125.9, 123.8, 121.5, 118.9, 113.1, 112.8, 107.8, 103.5, 65.2, 55.5, 40.3, 16.7. HRMS: Calculated for $C_{24}H_{20}NClSO_2$ (M^+): 421.0898, found: 421.0890.

1-ethyl-2-(4-methoxyphenyl)-3-(p-tolyl)-1,4-dihydrochromeno[4,3-b]pyrrole (**3.6c**) Isolated yield 70% (138 mg, 0.35 mmol). Light yellow solid, m.p. 133-136 °C. ^{1}H NMR (500 MHz, $CDCl_3$) δ 7.45 (dd, *J* = 7.7, 1.3 Hz, 1H), 7.25 – 7.19 (m, 2H), 7.12 – 7.07 (m, 1H), 7.04 – 6.97 (m, 4H), 6.94 – 6.90 (m, 2H), 6.88 (d, *J* = 8.1 Hz, 2H), 5.28 (s, 2H), 4.15 (q, *J* = 7.1 Hz, 2H), 3.84 (s, 3H), 2.29 (s, 3H), 1.30 (t, *J* = 7.1 Hz, 3H). ^{13}C NMR (125 MHz, $CDCl_3$) δ 159.4, 153.8, 135.0, 133.1, 132.8, 131.9, 129.1, 129.0, 126.6, 124.7, 122.7, 121.8, 120.6, 120.0, 119.3, 117.5, 115.3, 114.0, 65.2, 55.4, 40.1, 21.2, 16.7. HRMS: Calculated for $C_{27}H_{26}NO_2$ (MH^+): 396.1958, found: 396.1961.

3.5.4. NMR Spectra of Products

See Supporting Information of publication (*J. Org. Chem.* **2016**, 81, 11145)

3.6. References

1. Fan, H.; Peng, J.; Hamann, M. T.; Hu, J.-F. *Chem. Rev.* **2008,** *108*, 264.
2. Bhardwaj, V.; Gumber, D.; Abbot, V.; Dhiman, S.; Sharma, P. *RSC Adv.* **2015,** *5*, 15233.
3. Domagala, A.; Jarosz, T.; Lapkowski, M. *Eur. J. Med. Chem.* **2015,** *100*, 176.
4. Gholap, S. S. *Eur. J. Med. Chem.* **2016,** *110*, 13.
5. Gribble, G. W., Mesoionic Oxazoles. In *Oxazoles: Synthesis, Reactions, and Spectroscopy*, Palmer, D. C., Ed. 2003; Vol. 60, pp 473.
6. Fisk, J. S.; Mosey, R. A.; Tepe, J. J. *Chem. Soc. Rev.* **2007,** *36*, 1432.

7. Gingrich, H. L.; Baum, J. S., Mesoionic Oxazoles. In *Chemistry of Heterocyclic Compounds*, Turchi, I. J., Ed. 2008; pp 731.

8. Lopchuk, J. M., Mesoionics. In *Metalation of Azoles and Related Five-Membered Ring Heterocycles*, Gribble, G. W., Ed. Springer Berlin Heidelberg: Berlin, Heidelberg, 2012; pp 381.

9. Reissig, H.-U.; Zimmer, R. *Angew. Chem. Int. Ed.* **2014,** *53*, 9708.

10. Sainsbury, M.; Strange, R. H.; Woodward, P. R.; Barsanti, P. A. *Tetrahedron* **1993,** *49*, 2065.

11. Coldham, I.; Hufton, R. *Chem. Rev.* **2005,** *105*, 2765.

12. Padwa, A.; Lim, R.; MacDonald, J. G.; Gingrich, H. L.; Kellar, S. M. *J. Org. Chem.* **1985,** *50*, 3816.

13. Bélanger, G.; April, M.; Dauphin, É.; Roy, S. *J. Org. Chem.* **2007,** *72*, 1104.

14. Nayyar, N. K.; Hutchison, D. R.; Martinelli, M. J. *J. Org. Chem.* **1997,** *62*, 982.

15. Pinho e Melo, T. M. V. D.; Soares, M. I. L.; Paixão, J. A.; Beja, A. M.; Silva, M. R.; Alte da Veiga, L.; Pessoa, J. C. *J. Org. Chem.* **2002,** *67*, 4045.

16. Layer, R. W. *Chem. Rev.* **1963,** *63*, 489.

17. Bera, K.; Sarkar, S.; Biswas, S.; Maiti, S.; Jana, U. *J. Org. Chem.* **2011,** *76*, 3539.

18. Guo, D.-C.; Zhang, C.; Li, F.; Zhang, F.; Yu, F.; He, Y.-P. *Synthesis* **2017,** *49*, 1356.

19. Higuchi, Y.; Mita, T.; Sato, Y. *Org. Lett.* **2017,** *19*, 2710.

20. Hadden, M.; Goodman, A.; Guo, C.; Guzzo, P. R.; Henderson, A. J.; Pattamana, K.; Ruenz, M.; Sargent, B. J.; Swenson, B.; Yet, L.; Liu, J.; He, S.; Sebhat, I. K.; Lin, L. S.; Tamvakopoulos, C.; Peng, Q.; Kan, Y.; Palyha, O.; Kelly, T. M.; Guan, X.-M.; Metzger, J. M.; Reitman, M. L.; Nargund, R. P. *Bioorg. Med. Chem. Lett.* **2010,** *20*, 2912.

21. Padwa, A.; Gingrich, H. L.; Lim, R. *Tetrahedron Lett.* **1980,** *21*, 3419.

22. Padwa, A.; Burgess, E. M.; Gingrich, H. L.; Roush, D. M. *J. Org. Chem.* **1982,** *47*, 786.

23. Croce, P. D.; Ferraccioli, R.; Rosa, C. L.; Pilati, T. *J. Chem. Soc., Perkin Trans. 2* **1993**, 1511.

24. Bonati, L.; Ferraccioli, R.; Moro, G. *J. Phys. Org. Chem.* **1995,** *8*, 452.

25. Avalos, M.; Babiano, R.; Cabanillas, A.; Cintas, P.; Jiménez, J. L.; Palacios, J. C.; Aguilar, M. A.; Corchado, J. C.; Espinosa-García, J. *J. Org. Chem.* **1996,** *61*, 7291.

26. Coppola, B. P.; Noe, M. C.; Hong, S. S.-K. *Tetrahedron Lett.* **1997,** *38*, 7159.

27. Lopchuk, J. M.; Hughes, R. P.; Gribble, G. W. *Org. Lett.* **2013,** *15*, 5218.

28. Morin, M. S. T.; St-Cyr, D. J.; Arndtsen, B. A.; Krenske, E. H.; Houk, K. N. *J. Am. Chem. Soc.* **2013,** *135*, 17349.

29. Pérez-Serrano, L.; Blanco-Urgoiti, J.; Casarrubios, L.; Domínguez, G.; Pérez-Castells, J. *J. Org. Chem.* **2000,** *65*, 3513.

30. Dhawan, R.; Arndtsen, B. A. *J. Am. Chem. Soc.* **2004,** *126*, 468.

31. Chinchilla, R.; Nájera, C. *Chem. Soc. Rev.* **2011,** *40*, 5084.

32. Li, J.-H.; Li, J.-L.; Wang, D.-P.; Pi, S.-F.; Xie, Y.-X.; Zhang, M.-B.; Hu, X.-C. *J. Org. Chem.* **2007,** *72*, 2053.

Chapter 4: A Palladium Catalyzed, Multicomponent Approach to β-Lactams via Aryl Halide Carbonylation

4.1. Preface

In Chapter 2, we observed that β-lactams were formed as a side-product in the palladium catalyzed synthesis of Münchnones. This reaction presumably arises from the ketene-like reactivity of Münchnones with imines to form amido substituted β-lactams. This chapter describes our efforts to selectively generate β-lactam products via the palladium catalyzed combination of two imines, aryl halides, and CO. This project was started by Dr. Jeffrey Quesnel during his PhD by performing preliminary reaction development. A visiting post-doctoral fellow, Dr. Veeranna Yempally, contributed to the initial catalyst and reaction development. Oliver Williams, an undergraduate honors student in our lab, helped me develop the conditions for the synthesis of β-lactams using two different imines and also synthesized some of the products in Table 4.4. Maximiliano De La Higuera Macias, a MSc student in our lab, developed the synthesis of spirocyclic β-lactams, characterized these products by X-Ray crystallography, and synthesized the products in Table 4.5. My contributions include catalyst development for the synthesis of β-lactams using both aryl iodides and aryl bromides, the diversifications in Tables 4.3 and 4.4, and writing the manuscript. This work was published in *J. Org. Chem.* **2016**, 81, 12106.

4.2. Introduction

β-lactams are an important structural core in a diverse range of products, including natural products (e.g. β-lactam based antibiotics),[1] related biologically active compounds,[2] monomers for polyamide synthesis,[3] and as synthetic precursors in organic chemistry.[4] The utility of β-lactams,

as well as the recent rise of antibiotic resistance,[5] has driven interest in the design of efficient methods to access new variants of these structures. A common approach to β-lactam synthesis is through the formal [2+2] cycloaddition of imine and ketenes, known as the Staudinger reaction.[6] This typically relies upon the initial generation of a carboxylic acid precursor to ketenes (e.g. acid chlorides, Scheme 4.1a). A number of alternative approaches to β-lactam synthesis have been devised, including many that employ transition metal catalysis or multicomponent reactions.[7-12] Examples of these include catalytic ketene cycloadditions,[7] carbonylations,[8] alkyne-nitrone cycloaddition (Kinugasa reaction),[10] imine-α-haloketone condensation (Gilman-Speeter reaction),[11] and the use of the Petasis-Ugi reaction.[12] Our own research group has developed a variant of this reaction involving the palladium-catalyzed carbonylation of α-chloroamides.[13] This reaction generates mesoionic 1,3-oxazolium-5-olates (Münchnones), which are in equilibrium with their tautomeric ketene structure.[14] Similar to early reports by Huisgen with pre-synthesized Münchnones,[15] a Staundinger reaction with this *in situ* generated ketene yields access to the amide-substituted β-lactam core. One drawback of this chemistry is its required used of acid chlorides, which is common to many approaches to β-lactams. Acid chlorides are highly electrophilic blocks, require themselves a synthesis with high energy and toxic halogenating agents (e.g. $SOCl_2$, PCl_3, oxalyl chloride), and can be challenging to handle or generate in the presence of reactive functional groups. The high reactivity of acid chlorides has also made elaborating this platform to more synthetically complex β-lactam structures problematic.

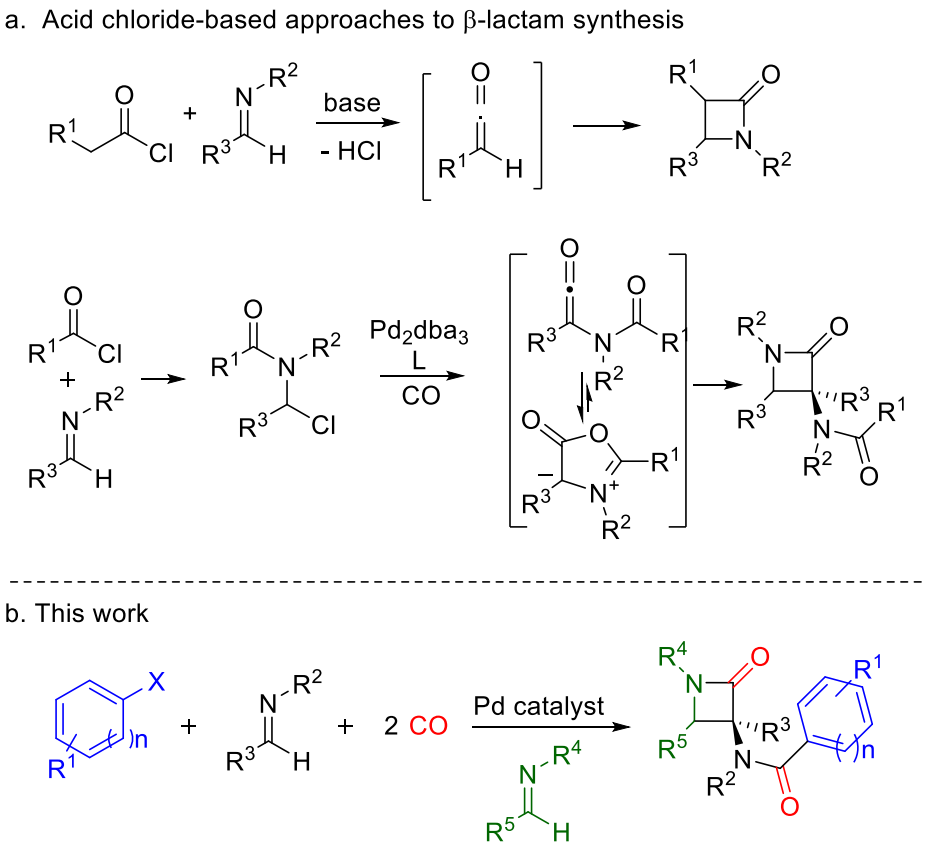

Scheme 4.1. Substituted β-Lactams and Synthetic Approaches via Münchnones

We have recently reported an alternative route to construct Münchnones via the carbonylative coupling of aryl iodides with imines.[16] A feature of this transformation is its high atom economy (HI as the sole byproduct) and the stability of the reagents, each of which is inexpensive, available in large scale, and, in the case of aryl iodides and imines, are easily generated in many different forms. We therefore questioned if this chemistry might provide a more flexible approach to construct diversely substituted lactams (Scheme 4.1b). We describe below our studies towards this goal. These demonstrate that β-lactams can be readily generated from the multicomponent coupling of stable reagents, in a modular fashion, and with broad substrate scope. In addition, the

stability of aryl halides can allow the facile incorporation of further structural complexity into these reactions. This includes multicomponent route to access families of spirocyclic β-lactams.

4.3. Results and Discussion

Catalyst Development for β-Lactam Synthesis The postulated mechanism for this catalytic β-lactam synthesis is shown in Scheme 4.2. This involves coupling two palladium catalyzed carbonylation reactions, the first to generate *in situ* acid chloride **4.1** and the second a cyclocarbonylation of an *in situ* generated *N*-acyl iminium salt to generate Münchnone **4.2**, with imine nucleophilic attack, and ultimately ketene trapping by imine to form β-lactam. We anticipated that the nature of the palladium catalyst will prove critical in balancing these operations. For example, our initial studies involving the palladium catalyzed carbonylation of *p*-iodotoluene in the presence of imine shows no β-lactam formation with simple alkyl- or aryl-phosphines, nor with bidentate ligands (Table 4.1, entries 1-4). However, with more sterically encumbered ligands we do see β-lactam formation (entries 5-8), and with P^tBu_3 there is a significant spike in catalytic activity (entry 9). Further experiments demonstrated that $Pd(P^tBu_3)_2$ can also serve as a catalyst for this reaction (entry 10), but requires the presence of a chloride source to proceed in reasonable yields (e.g. Bu_4NCl, entry 11).

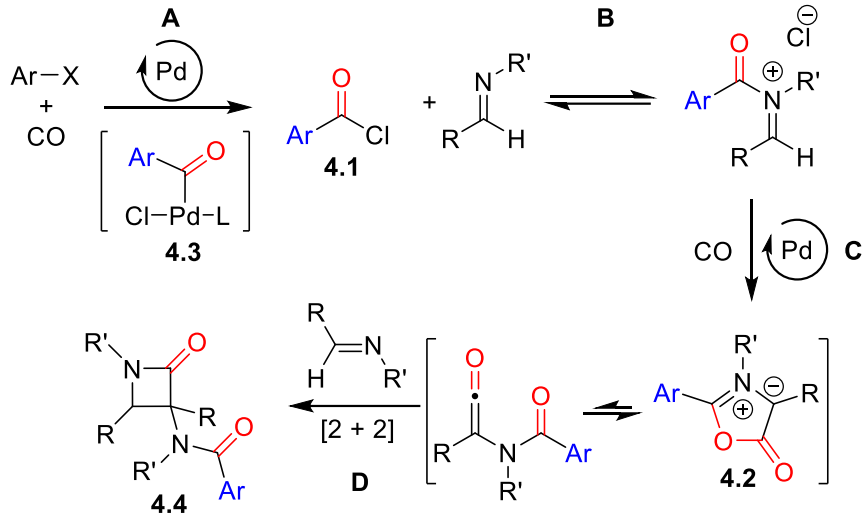

Scheme 4.2. Mechanistic Postulate for a Palladium-Catalyzed Synthesis of β-Lactams from Aryl Halides, Imines and CO

The observation of catalysis with P^{t}Bu$_3$ and a chloride source is consistent with the *in situ* generation of acid chloride (step A, Scheme 4.2), where chloride is a required reagent and the sterically encumbered P^{t}Bu$_3$ ligand can favor reductive elimination of this intermediate from **4.3** as a mechanism to relieve steric strain.[17] Increasing the temperature with this catalyst system, which can help drive imine trapping of an *in situ* generated Münchnone, can allow the formation of β-lactam in high yield (entry 12). Notably, under these conditions the catalyst loading can be lowered to 1 mol% without a significant loss in yield (entry 13).

Table 4.1. β-Lactam Synthesis via Aryl Iodide Carbonylation[a]

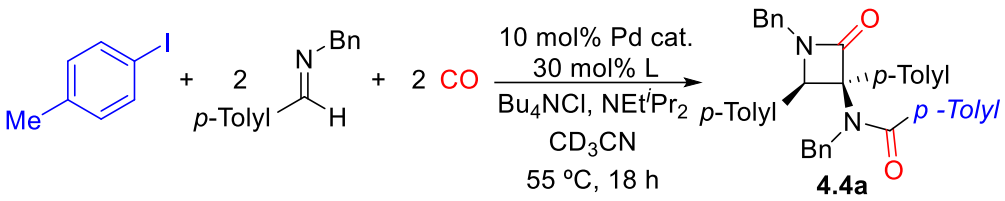

Entry	Pd cat.	Ligand	% 4.4a[b]
1	$[Pd(allyl)Cl]_2$	PPh_3	0
2	$[Pd(allyl)Cl]_2$	PCy_3	0
3	$[Pd(allyl)Cl]_2$	dppe	0
4	$[Pd(allyl)Cl]_2$	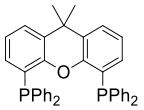	0
5	$[Pd(allyl)Cl]_2$	P(*o*-tolyl)$_3$	9
6	$[Pd(allyl)Cl]_2$	(2-biphenyl)P^{t}Bu$_2$	8
7	$[Pd(allyl)Cl]_2$	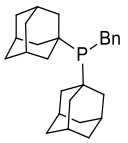	28
8	$[Pd(allyl)Cl]_2$	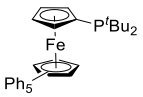	34
9	$[Pd(allyl)Cl]_2$	P^{t}Bu$_3$	69
10	$Pd(P^tBu_3)_2$	-	64
11[c]	$Pd(P^tBu_3)_2$	-	18
12[d]	$Pd(P^tBu_3)_2$	-	91
13[e]	1% $Pd(P^tBu_3)_2$	-	88

[a] 4-Iodotoluene (6.5 mg, 0.03 mmol), imine (25 mg, 0.12 mmol), NEt^iPr_2 (5.8 mg, 0.045 mmol), Bu_4NCl (8.3 mg, 0.03 mmol), Pd (1.5 µmol), L (0.009 mmol), 5 atm CO, CD_3CN (0.75 mL), 55 °C, 18h. [b]NMR yield. [c]No Bu_4NCl. [d]70 °C. [e]1% $Pd(P^tBu_3)_2$, 70 °C.

Aryl Bromide Substrates Relative to aryl iodides, aryl bromides are less expensive, and, with the advent of palladium catalyzed cross coupling reactions, much more broadly available reagents. Unfortunately, the stronger Ar-Br bond typically requires more pressing conditions to activate it towards carbonylations, and these substrates have not been previously shown to be viable building blocks for catalytic Münchnone formation.[16] The latter is potentially due to the lability of this product and the *N*-acyl iminium salt intermediate at elevated temperatures.[18] However, the rapid trapping of these intermediates in the tandem catalytic β-lactam synthesis above suggests this

platform might be expanded to use aryl bromide reagents. Indeed, as shown in Table 4.2, the carbonylative coupling of 4-bromotoluene and imine can also allow the generation of β-lactams. This reaction does not proceed to an appreciable extent at temperatures below 80 °C (entries 1,2), and in only low yields at elevated temperatures and CO pressure (entry 4,5). However, we note the formation of palladium black under each of these conditions, which presumably reflects the slow oxidative addition of aryl bromide in the presence of CO and ultimate loss of the P^{t}Bu$_3$ ligand from palladium. The addition of excess P^{t}Bu$_3$ and use of a less coordinating solvent helps minimize these effects and leads to the formation of β-lactam in yields similar to those observed with aryl iodides (entries 6, 7).

Table 4.2. Synthesis of β-Lactams via Aryl Bromide Carbonylation[a]

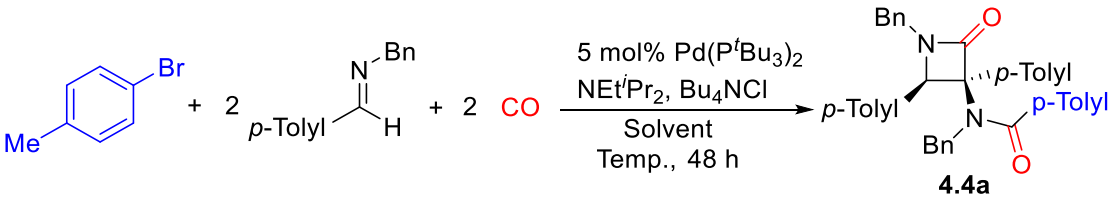

Entry	Temp. (°C)	Solvent	% 4a[b]
1	55	MeCN	0
2	70	MeCN	0
3	80	MeCN	0
4[c]	90	MeCN	10
5	80	PhH	18
6[d]	80	PhH	37
7[e]	80	PhH	73

[a]4-bromotoluene (26 mg, 0.15 mmol), imine (126 mg, 0.6 mmol), NEt^{i}Pr$_2$ (29 mg, 0.23 mmol), Bu$_4$NCl (42 mg, 0.15 mmol), Pd(P^{t}Bu$_3$)$_2$ (3.8 mg, 7.5 µmol), 5 atm CO, 1 mL solvent; [b]NMR yield. [c] 20 atm CO, [d] 0.015 mmol P^{t}Bu$_3$. [e]0.045 mmol P^{t}Bu$_3$

Scope of β-Lactam Synthesis With a method for the efficient synthesis of β-lactams in hand, we next probed the scope of this reaction (Table 4.3). A useful feature in this regard is the broad

availability of the imine and aryl halide reagents. As such, the reaction can be performed with a diverse array of aryl iodides, including those with electron-donating (**4.4b**,**c**) and electron-withdrawing (**4.4d**) groups. *Meta*-substitution on the aryl iodide is also tolerated (**4.4e**). We see similar diversity employing aryl bromide substrates, where this reagent can be modulated to incorporate alkyl (**4.4i**), ketone (**4.4f**), aryl (**4.4h**), and even indoles (**4.4g**). As noted above, these reactions require more elevated temperatures, but proceed in yields comparable to that noted with aryl iodides. The imine can also be systematically modulated to include substrates derived from various aromatic aldehydes. Of note, alkyl (**4.4a**), halide (**4.4c**), and methoxy (**4.4g**) substituents are all compatible with the transformation. Heteroaryl imines also afford β-lactams (**4.4d**). Conversely, imines derived from enolizable aldehydes are not compatible with the reaction conditions due to the formation of enamides.[19] In each of these reactions, **4.4** is generated as a single diastereomer with a *trans*-orientation of the aromatic units.[20] The latter is presumably to minimize steric interactions between these substituents on cyclization.[6e]

Table 4.3. Scope of β-Lactams Synthesis[a,b]

Aryl Iodides

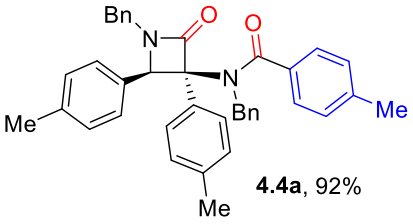

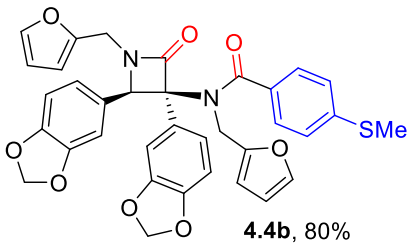

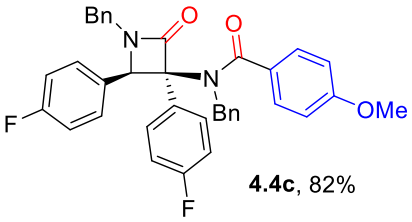

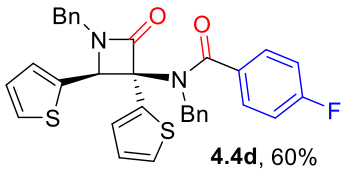

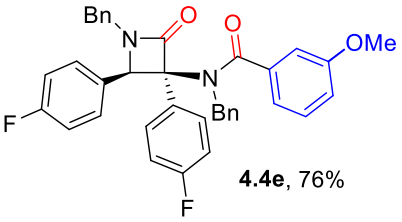

Aryl Bromides

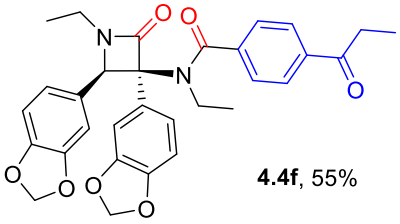

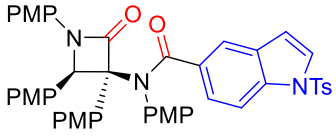

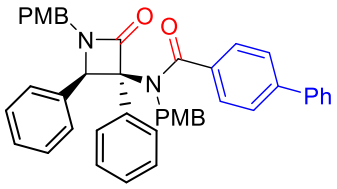

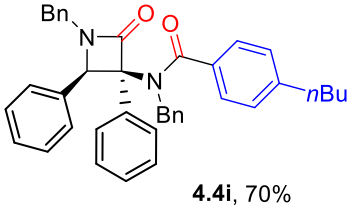

[a]Aryl halide (0.5 mmol), Imine (2.0 mmol), NEt^{i}Pr$_2$ (97 mg, 0.75 mmol), Pd(P^{t}Bu$_3$)$_2$ (2.6 mg, 5.0 μmol), Bu$_4$NCl (0.5 mmol), 5 atm CO, 3.3 mL MeCN 24-36 h, 70 °C. [b]Ar-Br: Pd(P^{t}Bu$_3$)$_2$ (0.025 mmol), P^{t}Bu$_3$ (30 mg, 0.15 mmol), 3.3 mL C$_6$H$_6$, 48-60 h, 80 °C.

One limitation of the above reactions is the incorporation of two identical imines into the β-lactam core. In principle, this can be addressed by the initial catalytic formation of Münchnone **4.3**, followed by the addition of a second imine. In contrast to many ketenes, the stability of the cyclic Münchnone can allow this latent ketene to be built up in solution. This is illustrated in Table 4.4, where the initial catalytic generation of **4.2** followed by the addition of a second imine lead to the formation of diversely substituted β-lactams. In order to enforce imine selectivity, an excess of aryl iodide is used in this transformation, which allows the high yield formation of β-lactams **4.5** with a range of imines. The functional group compatibility of this reaction is similar to that demonstrated in Table 4.2. Moreover, the second imine employed in cycloaddition one can incorporate a broad range of substituents. This includes various heterocyclic substrates (thiophene, furan, indole, **4.5a**,**b**,**i**), and even coordinating imidazyl-imines (**4.5g**). Overall, this reaction provides a straightforward method to prepare families of β-lactams from simple building blocks, where all five substituents can be individually varied.

Table 4.4. Synthesis of β-Lactams from Different Imines[a]

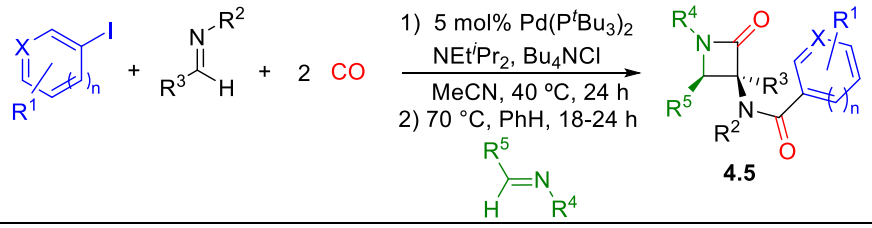

4.5

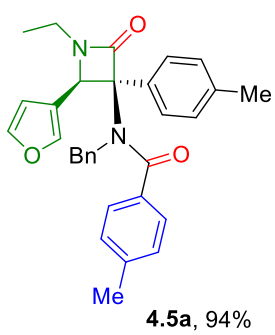

4.5a, 94%

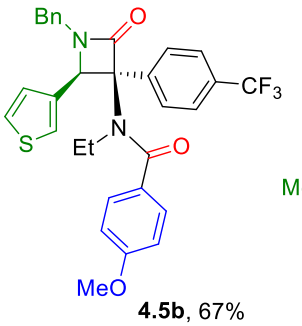

4.5b, 67%

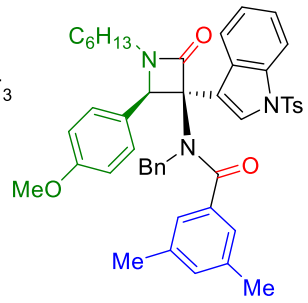

4.5c, 65%

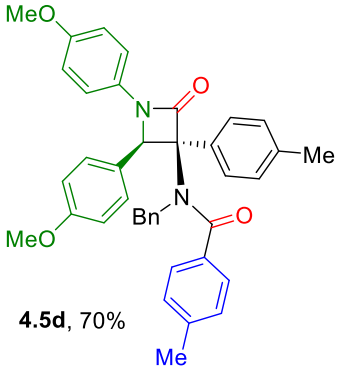

4.5d, 70%

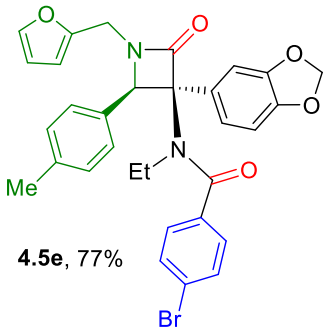

4.5e, 77%

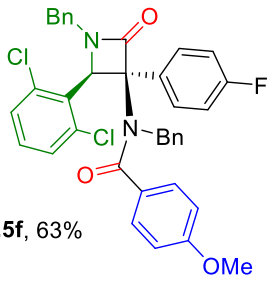

4.5f, 63%

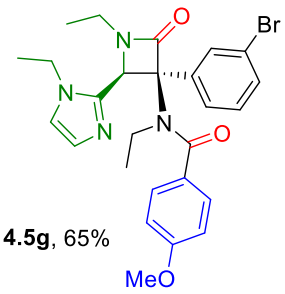

4.5g, 65%

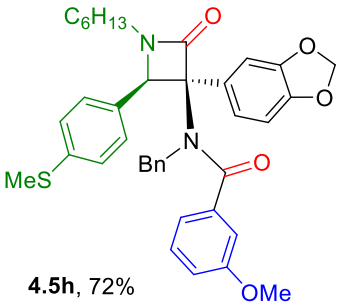

4.5h, 72%

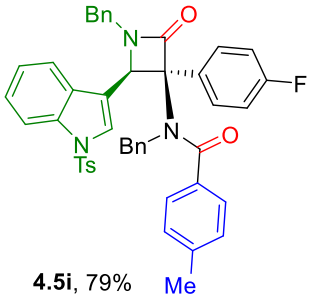

4.5i, 79%

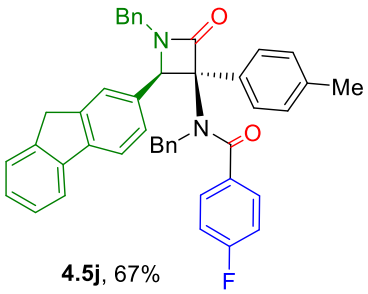

4.5j, 67%

[a] 1) Imine (0.5 mmol), aryl iodide (2.5 mmol), NEt^{i}Pr$_2$ (97 mg, 0.75 mmol), Bu$_4$NCl (139 mg, 0.5 mmol), Pd(P^{t}Bu$_3$)$_2$ (13 mg, 0.025 mmol), CO (10 atm), MeCN (3.3 mL), 40 °C, 24 h. 2) Imine (1.0 mmol), 70 °C, 18-24h.

Synthesis of Spirocyclic β-Lactams Finally, we have probed its ability to access new variants of β-lactams. A feature of this reaction is its ability to generate β-lactams from substrates that are

all by themselves relatively inert (aryl halides, imines, CO). This suggested the potential of incorporating more structural complexity into this transformation. For example, spirocyclic β-lactams have recently attracted attention as effective β-lactamase inhibitors.[21] This is believed to arise from the strain in the lactam ring, which modulates its reactivity with the enzyme.[21b] While common routes to these products involve the use of reactants with an exocyclic functionality (either exocyclic ketenes or imines), we postulated that the carbonylation of simply *ortho*-iodo substituted aryl-imines might open a more straightforward route to generate these products (Scheme 4.3a). This reaction would also create non-Münchnone stabilized ketenes **4.7**, as these cannot cyclize, and therefore should display enhanced cycloaddition reactivity. Interestingly, although the palladium-catalyzed carbonylation of *ortho*-haloimines have previously been examined as a way of preparing isoindolinone derivatives,[22] products arising from a second carbonylation event are unknown.

The feasibility of this multicomponent strategy is shown in Scheme 4.3b. Employing the conditions developed for aryl iodides with 2-iodo substituted imine **4.8a** gives the spiro product **4.9a** in a modest 40% yield. A second imine can also be used as the cycloaddition partner. As with the results using only **4.8a**, this reaction proceeds in only low yields at 40 ºC (entry 1), and even less efficiently at more elevated temperatures (entry 2). We postulated that this may arise from the lack of stabilization of the ketene intermediate **4.7** in this reaction, since it cannot cyclize to form a Münchnone. Lower reaction temperatures did lead to an increase in yield (entry 3). In addition, there is a marked influence of base on the reaction, and increase the amount of NEt^iPr_2 (entry 4), or employing an inorganic base (entry 5), allows the formation of **4.9b** in good yield (85%). This may arise from the greater difficulty associated with deprotonation to form **4.7**, as it does not lead to a stabilized ketene.

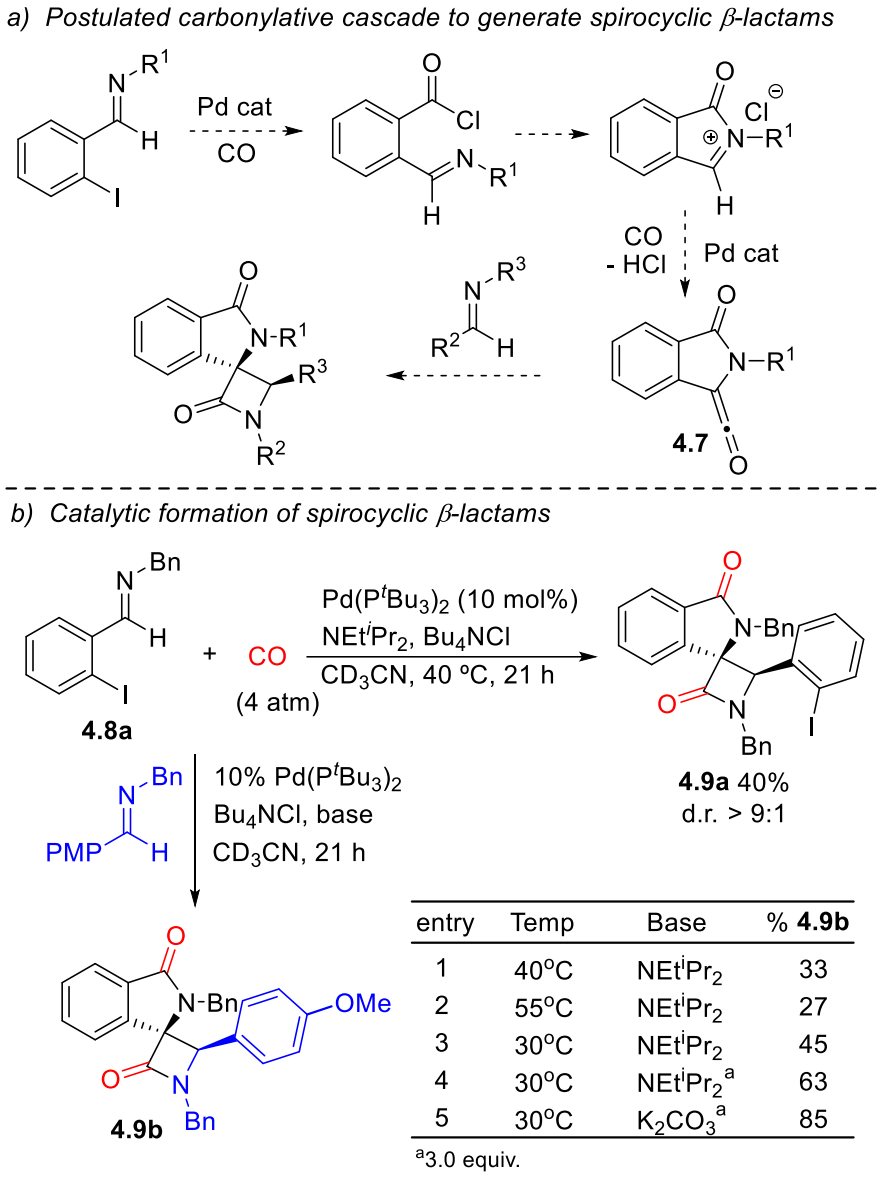

entry	Temp	Base	% **4.9b**
1	40°C	NEt^{i}Pr$_2$	33
2	55°C	NEt^{i}Pr$_2$	27
3	30°C	NEt^{i}Pr$_2$	45
4	30°C	NEt^{i}Pr$_2$[a]	63
5	30°C	K$_2$CO$_3$[a]	85

[a]3.0 equiv.

Scheme 4.3. Spirocyclic β-Lactams from Iodoaryl-Substituted Imines and CO

As with the results in Tables 4. 3 and 4.4 above, this reaction can also be diversified to form various spirocyclic β-lactams (Table 4.5). Of note, *N*-alkyl or –benzyl substituents can be incorporated only the aryl iodide reagent (**4.9c-e**). Alternatively, the imine employed in cycloaddition can include not only substituted donor or acceptor aryl-substituents (**4.9e-g**), but also heterocyclic (**4.9c**) and even vinyl-units (**4.9h**). These products are also generated with a

trans orientation of the aromatic units, as confirmed by NOE analysis and the crystal structure of **4.9g** (see Supporting Information for details). As far as we are aware, this represents the first carbonylative method to synthesize spirocyclic β-lactam products.

Table 4.5. Scope of the Synthesis of Spirocylic β-Lactams[a]

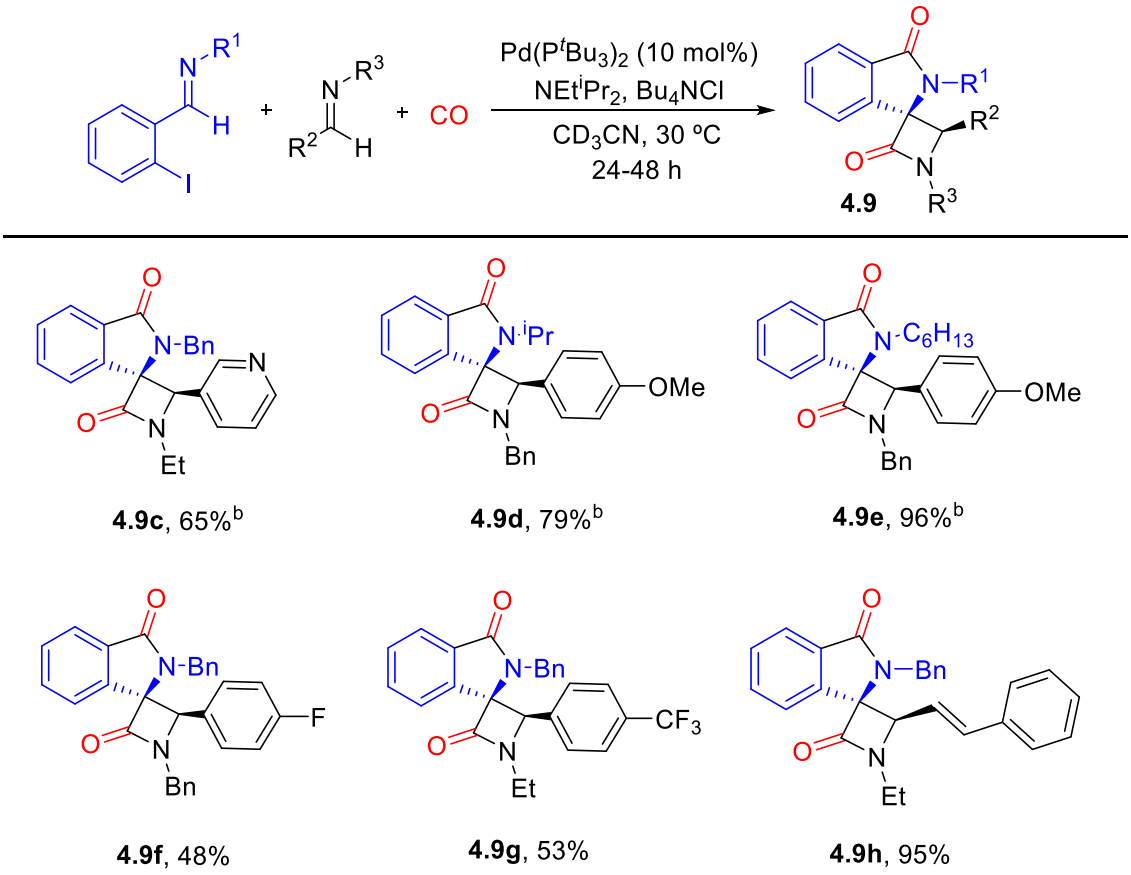

[a] Aryl iodide (0.024 mmol), imine (0.096 mmol), Bu$_4$NCl (20 mg, 0.072 mmol), NEt^{i}Pr$_2$ (9.3 mg, 0.072 mmol), Pd(P^{t}Bu$_3$)$_2$ (1.2 mg, 0.0024 mmol) and 4 atm CO, MeCN (0.75 mL). [b] NEt^{i}Pr$_2$ (4.7 mg, 0.036 mmol) and K$_2$CO$_3$ (4.9 mg, 0.036 mmol).

4.4. Conclusions

In conclusion, a versatile platform for the multicomponent synthesis of β-lactams has been developed. This reaction employs a single palladium catalyst in a tandem sequence of two separate carbonylations, and provides a route to generate amido-substituted β-lactams in a single operation

from substrates that are all available, stable and easily diversified: aryl halides, imines and carbon monoxide. The availability and stability of these reagents also make it straightforward to extend this chemistry more complex polysubstituted and spirocyclic β-lactam products. Importantly, systematic variation of each the building blocks can allow the generation of families of β-lactams, and with minimal synthetic effort relative to classical protocols.

4.5. Experimental Section

4.5.1. General Procedures

All manipulations were conducted in a glovebox under a nitrogen atmosphere. Unless otherwise noted, all reagents were purchased from commercial sources and used without purification. Research grade carbon monoxide (99.99%) was used as received. Solvents were dried by using a solvent purifier system and stored over activated 3Å molecular sieves inside the glovebox. Deuterated acetonitrile and benzene were stirred over calcium hydride, vacuum transferred, degassed, and stored over 4Å molecular sieves. Imines were prepared using standard literature procedures.[23] Tetrabutylammonium chloride was dried in the glovebox by dissolving in dichloromethane, allowing to stand overnight over activated molecular sieves, filtering and removing the solvent *in vacuo*. $Pd(P^tBu_3)_2$ was prepared as previously described.[24] Nuclear magnetic resonance (NMR) characterization was performed on 500 MHz spectrometers for proton and 126 MHz for carbon. ^1H and ^{13}C NMR chemical shifts were referenced to residual solvent. Mass spectra were recorded on a high-resolution electrospray ionization quadrupole mass spectrometer. IR spectra were recorded on a Bruker Alpha FT-IR with a single reflection Platinum ATR module. X-ray data was obtained with a Bruker Venture Metaljet diffractometer. Note: safety precautions should always be exercised when performing pressurized reactions, and when using

toxic CO gas. For NMR spectra of the products, see Supporting Information of publication (*J. Org. Chem.* **2016**, 81, 12106)

4.5.2. Experimental Procedures

Catalyst Development for β-Lactam Synthesis via Aryl Iodide Carbonylation

In a glovebox, 4-iodotoluene (6.5 mg, 0.03 mmol), *(p*-tolyl)HC=NBn (25 mg, 0.12 mmol), NEt^iPr_2 (5.8 mg, 0.045 mmol), Bu_4NCl (8.3 mg, 0.03 mmol), $[Pd(allyl)Cl]_2$ (0.5 mg, 1.5 µmol), P^tBu_3 (1.8 mg, 9.0 µmol), and benzyl benzoate standard (3.2 mg, 0.015 mmol) were weighed, dissolved in CD_3CN (0.75 mL) and transferred into a Norell J-Young NMR tube capable of withstanding up to 5 bar pressure. The NMR tube was then sealed with a screw-cap, taken out of the glovebox, 5 atm of CO was added, and the tube was warmed to 55 ºC. The yield of β-lactam was determined by ^1H NMR analysis relative to against the benzyl benzoate internal standard after 18 hours.

Catalyst Development for β-Lactam Synthesis via Aryl Bromide Carbonylation

In a glovebox, $Pd(P^tBu_3)_2$ (3.8 mg, 7.5 µmol), P^tBu_3 (9.1 mg, 0.045 mmol), and Bu_4NCl (42 mg, 0.15 mmol) were weighed and dry-transferred into a thick-walled 50 mL Chemglass Schlenk bomb equipped with a magnetic stir bar. 4-bromotoluene (26 mg, 0.15 mmol), (*p*-tolyl)HC=NBn (126 mg, 0.60 mmol), NEt^iPr_2 (29 mg, 0.23 mmol), and benzyl benzoate standard (16 mg, 0.075 mmol) in 1 mL benzene was added. The vessel was sealed with a Teflon cap, taken out of the glove box, charged with 5 atm of CO warmed to 80 °C for 48 h. The CO was then removed, and the yield of β-lactam was determined by ^1H NMR analysis.

Typical Synthesis of β-Lactams with Aryl Iodides

In a glovebox, $Pd(P^tBu_3)_2$ (2.6 mg, 5.0 μmol) and Bu_4NCl (139 mg, 0.5 mmol) were dry-transferred into a thick-walled 25 mL Chemglass Schlenk bomb equipped with a magnetic stir bar. 4-iodotoluene (109 mg, 0.5 mmol), (*p*-tolyl)CH=NBn (419 mg, 2.0 mmol), and NEt^iPr_2 (97 mg, 0.75 mmol) were dissolved in 3.3 mL MeCN and added to the Schlenk bomb. The vessel was sealed with a Teflon cap, taken out of the glove box, charged with 5 atm of CO, and warmed to 70 °C for 24 h. The CO was removed on a Schlenk line, the solvent removed in vacuo, and the product was purified by flash chromatography on silica gel using hexanes-ethyl acetate (4:1) to afford **4.4a** in 92% yield (260 mg, 0.46 mmol) as a white solid.

Typical Synthesis of β-Lactams with Aryl Bromides

In a glovebox, $Pd(P^tBu_3)_2$ (12.8 mg, 0.025 mmol), P^tBu_3 (30 mg, 0.15 mmol), and Bu_4NCl (139 mg, 0.5 mmol) were dry-transferred into a thick-walled Chemglass 50 mL Schlenk bomb equipped with a magnetic stir bar. *p*-BrC_6H_4COEt (107 mg, 0.5 mmol), 1-(benzo[*d*][1,3]dioxol-5-yl)HC=NEt (354 mg, 2.0 mmol), and NEt^iPr_2 (97 mg, 0.75 mmol) were dissolved in 3.3 mL benzene and transferred into the Schlenk bomb. The vessel was sealed with a Teflon cap, charged with 5 atm of CO, and warmed to 80 °C for 62 h with stirring. The CO was then removed on a Schlenk line, the solvent removed *in vacuo*, and the product was purified by flash chromatography on silica gel using hexanes-ethyl acetate (3:2) to afford **4.4f** in 55% yield (149.2 mg, 0.27 mmol) as a white solid.

Typical Synthesis of Cross-Coupled β-Lactams

In a glovebox, $Pd(P^tBu_3)_2$ (13 mg, 0.025 mmol), and Bu_4NCl (139 mg, 0.5 mmol) were added to a 4 mL vial equipped with a magnetic stir bar. (*p*-tolyl)HC=NBn (105 mg, 0.5 mmol), 4-iodotoluene (545 mg, 2.5 mmol), and NEt^iPr_2 (97 mg, 0.75 mmol) were dissolved in 3.3 mL of MeCN and transferred into the vial. The vial was closed with a pierced plastic cap, placed inside a Parr steel autoclave, sealed, and charged with 10 atm CO. The autoclave was stirred at 40 ºC for 24 h. The CO was then removed, and the vessel was brought back into the glovebox. The crude solution was transferred into a thick-walled 25 mL Chemglass Schlenk bomb, the solvent was evaporated *in vacuo*, the remaining oil was dissolved in 3.5 mL benzene, and (3-furanyl)HC=NEt (123 mg, 1.0 mmol) was added. The reactor was sealed with a Teflon cap, and heated at 70°C with stirring for 18 hours. The β-lactam product was isolated by flash chromatography on silica gel with hexanes-ethyl acetate 4:1, to afford β-lactam **4.5a** in 94% yield (224 mg, 0.47 mmol) as a pale yellow solid.

Typical Synthesis of Spirocyclic β-Lactams

In a glovebox, $Pd(P^tBu_3)_2$ (25 mg, 0.05 mmol) and Bu_4NCl (417 mg, 1.5 mmol) were dry-transferred into a thick-walled Chemglass 50 mL Schlenk bomb. (*o*-IC_6H_4)CH=NBn (161 mg, 0.50 mmol), (*p*-$MeOC_6H_4$)CH=NBn (451 mg, 2.0 mmol) and NEt^iPr_2 (194 mg, 1.5 mmol) were dissolved in 16 mL MeCN and added. The vessel was sealed with a Teflon cap, taken out of the glove box, charged with 4 atm of CO, and stirred at 30 ºC for 48 h. The CO was then removed, and the product purified by flash chromatography on silica gel using hexanes-ethyl acetate (3:1) to afford **4.9b** in 79% yield (187 mg, 0.40 mmol) as a white solid.

4.5.3. Characterization Data of Products

N-benzyl-*N*-(1-benzyl-2-oxo-3,4-di-*p*-tolylazetidin-3-yl)-4-methylbenzamide (**4.4a**) Isolated yield 92% (260 mg, 0.46 mmol). White solid. m.p. 48-53 °C. ^{1}H NMR (500 MHz, $CDCl_3$) δ 7.41 – 7.31 (m, 5H), 7.16 (dd, *J* = 7.6, 1.7 Hz, 2H), 7.10 – 6.95 (m, 11H), 6.87 (d, *J* = 8.0 Hz, 2H), 6.68 (d, *J* = 7.3 Hz, 2H), 5.43 (s, 1H), 4.93 – 4.83 (m, 2H), 4.75 (d, *J* = 17.0 Hz, 1H), 3.79 (d, *J* = 14.6 Hz, 1H), 2.27 (s, 3H), 2.26 (s, 3H), 2.22 (s, 3H). ^{13}C NMR (126MHz, CD_3Cl) δ 173.9, 165.7, 139.8, 138.6, 137.8, 137.7, 135.2, 134.1, 132.5, 131.2, 129.8, 129.4, 129.1, 128.9, 128.8, 128.7, 128.6, 128.1, 128.0, 126.7, 126.6, 126.5, 80.7, 66.2, 52.0, 44.1, 21.45, 21.36, 21.27. HRMS: Calculated for $C_{39}H_{36}O_2N_2Na$ (MNa^+): 587.2669, found: 587.2677. FT-IR ATR: υ_{CO} = 1749 and 1637 cm^{-1}.

N-(2,3-bis(benzo[d][1,3]dioxol-5-yl)-1-(furan-2-ylmethyl)-4-oxoazetidin-3-yl)-*N*-(furan-2-ylmethyl)-4-(methylthio)benzamide (**4.4b**) Isolated yield 80% (253 mg, 0.40 mmol). Light yellow solid. m.p. 76-79 °C. ^{1}H NMR (500 MHz, $CDCl_3$) δ 7.38 (dd, *J* = 1.9, 0.8 Hz, 1H), 7.34 – 7.29 (m, 2H), 7.22 – 7.17 (m, 2H), 7.02 – 6.96 (m, 2H), 6.88 (d, *J* = 1.8 Hz, 1H), 6.69 (d, *J* = 7.4 Hz, 2H), 6.63 – 6.58 (m, 1H), 6.51 (d, *J* = 8.1 Hz, 1H), 6.30 (dd, *J* = 3.2, 1.9 Hz, 1H), 6.16 (dd, *J* = 3.2, 0.8 Hz, 1H), 5.99 (dd, *J* = 3.3, 1.8 Hz, 1H), 5.89 – 5.84 (m, 2H), 5.82 – 5.77 (m, 2H), 5.64 (dd, *J* = 3.2, 0.9 Hz, 1H), 5.25 (s, 1H), 4.90 – 4.85 (m, 1H), 4.83 (d, *J* = 15.6 Hz, 1H), 4.77 (dd, *J* = 16.9, 0.9 Hz, 1H), 3.98 (d, *J* = 15.6 Hz, 1H), 2.47 (s, 3H). ^{13}C NMR (126MHz, CD_3Cl) δ 173.6, 166.0, 150.8, 148.4, 147.40, 147.38, 147.2, 142.8, 141.7, 141.4, 132.9, 128.7, 127.9, 127.7, 125.7, 123.4, 122.8, 110.7, 110.2, 110.1, 109.4, 109.2, 107.9, 107.8, 107.3, 101.0, 100.9, 81.0, 66.8, 45.7, 37.1, 15.4. HRMS: Calculated for $C_{35}H_{29}O_8N_2S$ (M^+ by APCI): 637.1639, found: 637.1635. FT-IR ATR: υ_{CO} = 1751 and 1637 cm^{-1}.

N-benzyl-*N*-(1-benzyl-2,3-bis(4-fluorophenyl)-4-oxoazetidin-3-yl)-4-methoxybenzamide (**4.4c**) Isolated yield 82% (241 mg, 0.41 mmol). White solid. m.p. 134-137 °C. ^{1}H NMR (500 MHz, $CDCl_3$) δ 7.48 – 7.42 (m, 2H), 7.39 – 7.31 (m, 3H), 7.20 – 7.09 (m, 6H), 7.07 – 6.96 (m, 3H), 6.89 – 6.82 (m, 2H), 6.77 – 6.66 (m, 6H), 5.34 (s, 1H), 4.95 – 4.87 (m, 3H), 3.80 (d, *J* = 14.6 Hz, 1H), 3.76 (s, 3H). ^{13}C NMR (126MHz, CD_3Cl) δ 173.8, 165.4, 162.6 (d, *J* = 247.3 Hz), 162.4 (d, *J* = 248.2 Hz), 161.1, 138.0, 134.7, 132.0 (d, *J* = 8.1 Hz), 131.3 (d, *J* = 3.3 Hz), 131.1 (d, *J* = 8.3 Hz), 129.9 (d, *J* = 3.1 Hz), 129.0, 128.97, 128.8, 128.77, 128.3, 128.2, 126.8, 126.79, 115.1 (d, *J* = 21.5 Hz), 114.8 (d, *J* = 21.2 Hz), 113.8, 80.5, 65.7, 55.4, 52.4, 44.3. HRMS: Calculated for $C_{37}H_{30}O_3N_2F_2Na$ (MNa^+): 611.2117, found: 611.2111. FT-IR ATR: υ_{CO} = 1748 and 1638 cm^{-1}.

N-benzyl-*N*-(1-benzyl-2-oxo-3,4-di(thiophen-3-yl)azetidin-3-yl)-4-fluorobenzamide (**4.4d**) Isolated yield 60% (167 mg, 0.30 mmol). Yellow solid. m.p. 48-50 °C. ^{1}H NMR (500 MHz, $CDCl_3$) δ 7.54 (dd, *J* = 3.0, 1.3 Hz, 1H), 7.36 (td, *J* = 5.0, 2.3 Hz, 3H), 7.18 – 7.07 (m, 9H), 7.02 (dd, *J* = 5.1, 3.0 Hz, 1H), 6.93 (dd, *J* = 5.1, 1.3 Hz, 1H), 6.90 – 6.85 (m, 2H), 6.80 (dd, *J* = 4.8, 1.5 Hz, 1H), 6.76 – 6.70 (m, 2H), 5.39 (s, 1H), 4.91 – 4.80 (m, 2H), 4.71 (d, *J* = 17.0 Hz, 1H), 3.88 (d, *J* = 14.6 Hz, 1H). ^{13}C NMR (126MHz, CD_3Cl) δ 172.7, 164.8, 163.5 (d, *J* = 250.4 Hz), 138.3, 136.0, 135.6, 134.9, 132.5 (d, *J* = 3.3 Hz), 129.1 (d, *J* = 9.1 Hz), 129.0, 128.97, 128.7, 128.5, 128.2, 127.7, 127.0, 126.3, 126.1, 125.3, 125.27, 125.18, 115.4 (d, *J* = 21.9 Hz), 62.8, 51.8, 44.4. HRMS: Calculated for $C_{32}H_{25}O_2N_2FS_2Na$ (MNa^+): 575.1234, found: 575.1235. FT-IR ATR: υ_{CO} = 1752 and 1637 cm^{-1}.

N-benzyl-*N*-(1-benzyl-2,3-bis(4-fluorophenyl)-4-oxoazetidin-3-yl)-3-methoxybenzamide (**4.4e**) Isolated yield 76% (224 mg, 0.38 mmol). White solid. m.p. 114-116 °C. ^{1}H NMR (500 MHz, $CDCl_3$) δ 7.50 – 7.42 (m, 2H), 7.41 – 7.32 (m, 3H), 7.20 – 7.10 (m, 5H), 7.09 – 6.97 (m, 3H), 6.90 – 6.81 (m, 3H), 6.79 – 6.72 (m, 3H), 6.71 – 6.66 (m, 2H), 6.59 (dd, *J* = 2.6, 1.5 Hz, 1H),

5.40 (s, 1H), 4.92 (d, *J* = 14.3 Hz, 1H), 4.87 (s, 1H), 4.80 (d, *J* = 16.8 Hz, 1H), 3.81 (d, *J* = 14.6 Hz, 1H), 3.55 (s, 3H). ^{13}C NMR (126MHz, CD_3Cl) δ 173.7, 165.1, 162.7 (d, *J* = 247.3 Hz), 162.5 (d, *J* = 248.4 Hz), 159.4, 138.1, 137.7, 134.7, 131.8 (d, *J* = 8.1 Hz), 131.3 (d, *J* = 3.4 Hz), 131.1 (d, *J* = 8.2 Hz), 129.8 (d, *J* = 3.1 Hz), 129.6, 129.10, 129.06, 128.3, 128.2, 126.8, 126.7, 115.1 (d, *J* = 20.9 Hz), 114.9, 80.3, 65.7, 55.3, 52.1, 44.4. HRMS: Calculated for $C_{37}H_{30}O_3N_2F_2Na$ (MNa^+): 611.2117, found: 611.2118. FT-IR ATR: υ_{CO} = 1753 and 1635 cm^{-1}.

N-(2,3-bis(benzo[d][1,3]dioxol-5-yl)-1-ethyl-4-oxoazetidin-3-yl)-*N*-ethyl-4-propionylbenzamide (**4.4f**) Isolated yield 55% (149.2 mg, 0.27 mmol). White solid. m.p. 145-149 °C. ^{1}H NMR (500 MHz, $CDCl_3$) δ 8.05 – 7.97 (m, 2H), 7.57 – 7.49 (m, 2H), 7.09 (dd, *J* = 8.1, 1.8 Hz, 1H), 6.98 (d, *J* = 1.8 Hz, 1H), 6.74 (dd, *J* = 8.1, 1.7 Hz, 1H), 6.71 (d, *J* = 1.7 Hz, 1H), 6.62 (dd, *J* = 10.2, 8.1 Hz, 2H), 5.90 – 5.83 (m, 4H), 5.43 (s, 1H), 3.78 – 3.70 (m, 1H), 3.65 (dq, *J* = 14.7, 7.4 Hz, 1H), 3.61 – 3.52 (m, 1H), 3.00 (dq, *J* = 21.0, 7.2 Hz, 3H), 1.23 (t, *J* = 7.2 Hz, 3H), 1.18 (t, *J* = 7.3 Hz, 3H), 0.71 (t, *J* = 7.0 Hz, 3H). ^{13}C NMR (126MHz, CD_3Cl) δ 200.1, 172.5, 165.8, 147.56, 147.50, 147.47, 147.44, 141.4, 137.7, 130.0, 128.3, 128.2, 127.0, 123.1, 123.0, 109.9, 109.4, 107.9, 107.7, 101.08, 101.06, 80.1, 66.0, 43.3, 35.2, 32.1, 16.0, 12.7, 8.2. HRMS: Calculated for $C_{31}H_{30}O_7N_2Na$ (MNa^+): 565.1945, found: 565.1965. FT-IR ATR: υ_{CO} = 1748, 1687, and 1635 cm^{-1}.

N-(4-methoxyphenyl)-1-tosyl-*N*-(1,2,3-tris(4-methoxyphenyl)-4-oxoazetidin-3-yl)-1*H*-indole-5-carboxamide (**4.4g**) Isolated yield 84% (338.5 mg, 0.42 mmol). Yellow solid. m.p. 133-137 °C. ^{1}H NMR (500 MHz, $CDCl_3$) δ 7.75 – 7.70 (m, 1H), 7.65 – 7.60 (m, 2H), 7.53 (dd, *J* = 1.7, 0.6 Hz, 1H), 7.46 (d, *J* = 3.7 Hz, 1H), 7.36 – 7.28 (m, 4H), 7.26 (dd, *J* = 8.8, 1.7 Hz, 2H), 7.23 (d, *J* = 7.9 Hz, 2H), 7.18 – 7.12 (m, 2H), 6.81 – 6.76 (m, 2H), 6.72 – 6.66 (m, 2H), 6.60 – 6.56 (m, 3H), 6.50 (dd, *J* = 3.7, 0.8 Hz, 3H), 6.08 (s, 1H), 3.73 (s, 3H), 3.72 (s, 3H), 3.70 (s, 3H), 3.65 (s, 3H), 2.32

(s, 3H). ^{13}C NMR (126MHz, CD_3Cl) δ 172.6, 162.7, 159.4, 159.1, 158.8, 156.3, 145.2, 135.1, 135.0, 132.9, 132.3, 132.2, 131.6, 130.8, 130.3, 130.1, 129.9, 127.3, 126.91, 126.87, 126.76, 125.1, 122.2, 119.4, 114.3, 113.5, 113.4, 113.0, 112.9, 109.4, 81.2, 67.1, 55.5, 55.24, 55.20, 55.1, 21.6. HRMS: Calculated for $C_{47}H_{41}O_8N_3SNa$ (MNa^+): 830.2507, found: 830.2525. FT-IR ATR: υ_{CO} = 1742 and 1642 cm^{-1}.

N-(4-methoxybenzyl)-*N*-(1-(4-methoxybenzyl)-2-oxo-3,4-diphenylazetidin-3-yl)-[1,1'-biphenyl]-4-carboxamide (**4.4h**) Isolated yield 82% (271 mg, 0.41 mmol). White solid. m.p. 79-83 °C. ^{1}H NMR (500 MHz, $CDCl_3$) δ 7.55 – 7.51 (m, 2H), 7.51 – 7.47 (m, 2H), 7.47 – 7.39 (m, 4H), 7.39 – 7.33 (m, 1H), 7.24 – 7.15 (m, 7H), 7.13 – 7.02 (m, 5H), 6.91 – 6.86 (m, 2H), 6.53 (q, *J* = 8.9 Hz, 4H), 5.44 (s, 1H), 4.91 (d, *J* = 14.6 Hz, 1H), 4.88 – 4.78 (m, 2H), 3.83 (s, 3H), 3.78 (d, *J* = 14.6 Hz, 1H), 3.71 (s, 3H). ^{13}C NMR (126MHz, CD_3Cl) δ 173.7, 165.5, 159.5, 158.4, 142.6, 140.3, 135.9, 135.6, 134.3, 130.4, 130.3, 129.9, 129.4, 129.0, 128.2, 128.15, 128.11, 127.96, 127.95, 127.90, 127.3, 127.2, 127.1, 127.0, 114.3, 113.5, 81.1, 66.1, 55.4, 55.3, 51.7, 43.7. HRMS: Calculated for $C_{44}H_{38}O_4N_2Na$ (MNa^+): 681.2724, found: 681.2721. FT-IR ATR: υ_{CO} = 1749 and 1636 cm^{-1}.

N-benzyl-*N*-(1-benzyl-2-oxo-3,4-diphenylazetidin-3-yl)-4-butylbenzamide (**4.4i**) Isolated yield 70% (202 mg, 0.35 mmol). Clear oil. ^{1}H NMR (500 MHz, $CDCl_3$) δ 7.52 – 7.47 (m, 2H), 7.39 – 7.32 (m, 3H), 7.21 – 7.14 (m, 7H), 7.11 – 6.94 (m, 10H), 6.63 (d, *J* = 7.3 Hz, 2H), 5.47 (s, 1H), 4.96 (d, *J* = 14.7 Hz, 1H), 4.88 (s, 2H), 3.83 (d, *J* = 14.7 Hz, 1H), 2.53 (t, *J* = 7.7 Hz, 2H), 1.56 – 1.46 (m, 2H), 1.29 (dq, *J* = 14.6, 7.3 Hz, 2H), 0.90 (t, *J* = 7.3 Hz, 3H). ^{13}C NMR (126MHz, CD_3Cl) δ 174.0, 165.7, 145.0, 138.3, 135.5, 135.0, 134.3, 134.2, 129.9, 129.4, 129.01, 128.99, 128.3, 128.2, 128.12, 128.11, 128.0, 127.94, 127.91, 126.85, 126.76, 126.6, 81.2, 66.2, 52.3, 44.3,

35.5, 33.5, 22.2, 14.0. HRMS: Calculated for $C_{40}H_{38}O_2N_2Na$ (MNa^+): 601.2826, found: 601.2821. FT-IR ATR: υ_{CO} = 1751 and 1637 cm^{-1}.

N-benzyl-*N*-(1-ethyl-2-(furan-3-yl)-4-oxo-3-(p-tolyl)azetidin-3-yl)-4-methylbenzamide (**4.5a**) Isolated yield 94% (224 mg, 0.47 mmol). Light yellow solid. m.p. 152-154 °C. ^{1}H NMR (500 MHz, $CDCl_3$) δ 7.47 – 7.39 (m, 3H), 7.25 – 7.20 (m, 2H), 7.16 (t, *J* = 1.8 Hz, 1H), 7.14 – 7.08 (m, 3H), 7.05 (d, *J* = 7.8 Hz, 2H), 6.97 (d, *J* = 8.1 Hz, 2H), 6.88 (dd, *J* = 7.4, 2.2 Hz, 2H), 6.08 (d, *J* = 1.7 Hz, 1H), 5.62 (s, 1H), 4.87 (d, *J* = 16.9 Hz, 1H), 4.79 (d, *J* = 16.9 Hz, 1H), 3.58 (dq, *J* = 14.6, 7.4 Hz, 1H), 2.99 (dq, *J* = 14.2, 7.2 Hz, 1H), 2.29 (s, 3H), 2.25 (s, 3H), 1.15 (t, *J* = 7.3 Hz, 3H). ^{13}C NMR (126MHz, CD_3Cl) δ 174.0, 165.3, 142.6, 142.2, 139.9, 138.5, 137.9, 133.8, 132.1, 129.2, 128.9, 128.6, 128.0, 126.7, 126.6, 126.5, 120.6, 110.3, 79.8, 59.6, 51.9, 35.0, 21.3, 21.1, 12.5. HRMS: Calculated for $C_{31}H_{30}O_3N_2Na$ (MNa^+): 501.2149, found: 501.2150. FT-IR ATR: υ_{CO} = 1750 and 1634 cm^{-1}.

N-(1-benzyl-2-oxo-4-(thiophen-3-yl)-3-(4-(trifluoromethyl)phenyl)azetidin-3-yl)-*N*-ethyl-4-methoxybenzamide (**4.5b**) Isolated yield 67% (189 mg, 0.33 mmol). Light brown solid. m.p. 118-121 °C. ^{1}H NMR (500 MHz, $CDCl_3$) δ 7.67 (d, *J* = 8.2 Hz, 2H), 7.39 (d, *J* = 8.2 Hz, 2H), 7.37 – 7.30 (m, 5H), 7.25 – 7.20 (m, 2H), 7.10 (dd, *J* = 3.1, 1.2 Hz, 1H), 7.04 (dd, *J* = 5.0, 3.0 Hz, 1H), 6.95 – 6.88 (m, 2H), 6.78 (dd, *J* = 5.0, 1.3 Hz, 1H), 5.35 (s, 1H), 4.99 (d, *J* = 14.8 Hz, 1H), 3.97 (d, *J* = 14.8 Hz, 1H), 3.84 (s, 4H), 3.68 (dq, *J* = 14.5, 7.1 Hz, 1H), 0.67 (t, *J* = 7.1 Hz, 3H). ^{13}C NMR (126MHz, CD_3Cl) δ 173.8, 165.6, 161.1, 140.5, 135.7, 135.0, 130.3 (q, *J* = 32.2 Hz), 129.7, 129.1, 129.0, 128.8, 128.6, 128.2, 127.6, 125.5, 125.1, 124.9 (q, *J* = 3.6 Hz), 123.0, 114.0, 80.5, 62.8, 55.5, 44.6, 44.0, 15.9. HRMS: Calculated for $C_{31}H_{27}O_3N_2F_3SNa$ (MNa^+): 587.1587, found: 587.1589. FT-IR ATR: υ_{CO} = 1749 and 1636 cm^{-1}.

N-benzyl-*N*-(1-hexyl-2-(4-methoxyphenyl)-4-oxo-3-(1-tosyl-1H-indol-3-yl)azetidin-3-yl)-3,5-dimethylbenzamide (**4.5c**) Isolated yield 65% (250 mg, 0.32 mmol). Light yellow solid. m.p. 58-61 °C. ^{1}H NMR (500 MHz, $CDCl_3$) δ 7.87 (d, *J* = 8.1 Hz, 1H), 7.79 (dt, *J* = 8.4, 0.9 Hz, 1H), 7.61 – 7.54 (m, 2H), 7.38 (s, 1H), 7.17 – 7.10 (m, 3H), 7.04 – 6.96 (m, 4H), 6.95 – 6.87 (m, 3H), 6.82 (d, *J* = 1.7 Hz, 2H), 6.66 (dd, *J* = 8.2, 1.2 Hz, 2H), 6.52 – 6.44 (m, 2H), 5.55 (s, 1H), 4.85 (d, *J* = 16.6 Hz, 1H), 4.69 – 4.60 (m, 1H), 3.66 (s, 3H), 3.50 (dt, *J* = 13.9, 7.8 Hz, 1H), 2.81 (dt, *J* = 14.0, 7.0 Hz, 1H), 2.30 (s, 3H), 2.18 (s, 6H), 1.49 (q, *J* = 7.3 Hz, 2H), 1.36 – 1.22 (m, 7H), 0.89 (t, *J* = 6.9 Hz, 3H). ^{13}C NMR (126MHz, CD_3Cl) δ 174.0, 165.6, 159.7, 144.8, 138.3, 138.1, 136.8, 135.3, 134.6, 131.5, 130.2, 129.8, 129.0, 128.5, 128.0, 127.0, 126.9, 126.7, 126.4, 124.8, 124.7, 124.5, 123.2, 116.8, 113.4, 112.9, 76.4, 65.6, 55.3, 52.2, 40.6, 31.5, 27.2, 26.9, 22.7, 21.7, 21.2, 14.2. HRMS: Calculated for $C_{47}H_{49}O_5N_3SNa$ (MNa^+): 790.3285, found: 790.3290. FT-IR ATR: υ_{CO} = 1751 and 1639 cm^{-1}.

N-benzyl-*N*-(1,2-bis(4-methoxyphenyl)-4-oxo-3-(p-tolyl)azetidin-3-yl)-4-methylbenzamide (**4.5d**) Isolated yield 70% (220 mg, 0.37 mmol). Yellow solid. m.p. 102-106 °C. ^{1}H NMR (500 MHz, $CDCl_3$) δ 7.37 (d, *J* = 8.3 Hz, 2H), 7.26 – 7.20 (m, 6H), 7.04 (d, *J* = 7.9 Hz, 2H), 7.02 – 6.95 (m, 3H), 6.87 (d, *J* = 8.1 Hz, 2H), 6.81 – 6.72 (m, 4H), 6.69 – 6.63 (m, 2H), 6.00 (s, 1H), 4.91 (d, *J* = 16.8 Hz, 1H), 4.86 (d, *J* = 16.9 Hz, 1H), 3.74 (s, 3H), 3.72 (s, 3H), 2.29 (s, 3H), 2.21 (s, 3H). ^{13}C NMR (126MHz, CD_3Cl) δ 174.0, 163.0, 159.3, 156.4, 140.1, 138.4, 137.84, 134.0, 131.8, 130.8, 130.3, 129.8, 129.0, 128.6, 128.1, 126.9, 126.7, 126.6, 126.6, 119.3, 114.3, 113.5, 80.3, 67.1, 55.5, 55.2, 52.4, 21.5, 21.2. HRMS: Calculated for $C_{39}H_{36}O_4N_2Na$ (MNa^+): 619.2567, found: 619.2576. FT-IR ATR: υ_{CO} = 1736 and 1633 cm^{-1}.

N-(3-(benzo[d][1,3]dioxol-5-yl)-1-(furan-2-ylmethyl)-2-oxo-4-(p-tolyl)azetidin-3-yl)-4-bromo-*N*-ethylbenzamide (**4.5e**) Isolated yield 77% (227 mg, 0.39 mmol). Light yellow solid. m.p.

130-134 °C. ^{1}H NMR (500 MHz, $CDCl_3$) δ 7.58 – 7.51 (m, 2H), 7.36 (dd, *J* = 1.9, 0.8 Hz, 1H), 7.31 – 7.27 (m, 2H), 7.10 – 7.03 (m, 3H), 7.01 – 6.93 (m, 3H), 6.58 (d, *J* = 8.2 Hz, 1H), 6.29 (dd, *J* = 3.2, 1.9 Hz, 1H), 6.13 (dd, *J* = 3.2, 0.7 Hz, 1H), 5.84 (dd, *J* = 10.0, 1.5 Hz, 2H), 5.28 (s, 1H), 4.88 (d, *J* = 15.7 Hz, 1H), 3.94 (d, *J* = 15.6 Hz, 1H), 3.80 – 3.71 (m, 1H), 3.63 – 3.52 (m, 1H), 2.26 (s, 3H), 0.70 (t, *J* = 7.1 Hz, 3H). ^{13}C NMR (126MHz, CD_3Cl) δ 172.4, 166.0, 148.5, 147.4, 147.4, 142.8, 137.9, 136.2, 131.9, 130.9, 129.9, 129.0, 128.7, 128.5, 124.2, 123.2, 110.6, 110.1, 109.1, 107.6, 101.0, 80.8, 66.8, 43.5, 37.0, 21.3, 15.9. HRMS: Calculated for $C_{31}H_{27}O_5N_2BrNa$ (MNa^+): 609.0996, found: 609.1000. FT-IR ATR: υ_{CO} = 1748 and 1631 cm^{-1}.

N-benzyl-*N*-(1-benzyl-2-(2,6-dichlorophenyl)-3-(4-fluorophenyl)-4-oxoazetidin-3-yl)-4-methoxybenzamide (**4.5f**) Isolated yield 63% (201 mg, 0.31 mmol). White solid. m.p. 112-116 °C. ^{1}H NMR (500 MHz, $CDCl_3$) δ 7.49 – 7.40 (m, 2H), 7.37 (dd, *J* = 8.1, 1.3 Hz, 1H), 7.26 – 7.25 (m, 3H), 7.23 – 7.19 (m, 2H), 7.17 – 7.10 (m, 4H), 7.07 – 7.02 (m, 2H), 6.99 (dd, *J* = 8.1, 1.4 Hz, 1H), 6.96 – 6.89 (m, 2H), 6.76 – 6.68 (m, 4H), 5.99 (s, 1H), 4.84 (d, *J* = 17.3 Hz, 1H), 4.77 (d, *J* = 17.2 Hz, 1H), 4.72 (d, *J* = 14.3 Hz, 1H), 3.79 (d, *J* = 14.4 Hz, 1H), 3.73 (s, 3H). ^{13}C NMR (126MHz, CD_3Cl) δ 172.9, 165.3, 162.5 (d, *J* = 247.9 Hz), 160.9, 138.6, 138.1, 136.7, 133.6, 131.6 (d, *J* = 8.0 Hz), 130.5 (d, *J* = 3.4 Hz), 130.3, 129.5, 129.4, 129.3, 128.8, 128.7, 128.4, 128.0, 127.0, 126.2, 114.4 (d, *J* = 21.1 Hz), 113.6, 78.5, 63.7, 55.4, 52.1, 46.2. HRMS: Calculated for $C_{37}H_{29}Cl_2FN_2NaO_3$ (MNa^+): 661.1431, found: 661.1430. FT-IR ATR: υ_{CO} = 1754 and 1637 cm^{-1}.

N-(3-(3-bromophenyl)-1-ethyl-2-(1-ethyl-1*H*-imidazol-2-yl)-4-oxoazetidin-3-yl)-*N*-ethyl-4-methoxybenzamide (**4.5g**) Isolated yield 65% (170 mg, 0.32 mmol). Yellow oil. ^{1}H NMR (500 MHz, $CDCl_3$) δ 7.67 (s, 1H), 7.50 (d, *J* = 7.9 Hz, 1H), 7.44 (d, *J* = 8.3 Hz, 2H), 7.30 (d, *J* = 8.0 Hz, 1H), 7.03 (t, *J* = 7.9 Hz, 1H), 6.94 (d, *J* = 8.3 Hz, 2H), 6.82 (d, *J* = 9.6 Hz, 2H), 5.57 (s, 1H),

4.55 – 4.33 (m, 1H), 4.22 (h, *J* = 7.0 Hz, 1H), 3.84 (s, 3H), 3.79 – 3.72 (m, 2H), 3.65 (dq, *J* = 13.5, 6.7, 6.1 Hz, 1H), 3.09 (dq, *J* = 14.4, 7.3 Hz, 1H), 1.39 (t, *J* = 7.3 Hz, 3H), 1.14 (t, *J* = 7.3 Hz, 3H), 0.77 (t, *J* = 7.0 Hz, 3H). ^{13}C NMR (126MHz, CD_3Cl) δ 173.5, 164.8, 161.0, 140.5, 138.1, 132.0, 131.3, 129.4, 129.2, 128.7, 127.8, 122.0, 119.9, 114.0, 80.0, 58.3, 55.5, 44.0, 40.8, 35.3, 16.9, 16.0, 12.4. HRMS: Calculated for $C_{26}H_{30}O_3N_4Br$ (MH^+): 525.1496, found: 525.1496. FT-IR ATR: υ_{CO} = 1752 and 1628 cm^{-1}.

N-(3-(benzo[d][1,3]dioxol-5-yl)-1-hexyl-2-(4-(methylthio)phenyl)-4-oxoazetidin-3-yl)-*N*-benzyl-3-methoxybenzamide (**4.5h**) Isolated yield 72% (229 mg, 0.36 mmol). Yellow solid. m.p. 36-38 °C. ^{1}H NMR (500 MHz, $CDCl_3$) δ 7.20 – 7.14 (m, 3H), 7.09 – 7.03 (m, 6H), 6.97 (d, *J* = 1.7 Hz, 1H), 6.89 (dt, *J* = 7.5, 1.1 Hz, 1H), 6.85 (ddd, *J* = 8.3, 2.6, 0.8 Hz, 1H), 6.78 (dd, *J* = 6.5, 2.9 Hz, 2H), 6.69 (dd, *J* = 2.4, 1.5 Hz, 1H), 6.52 (d, *J* = 8.2 Hz, 1H), 5.83 (dd, *J* = 14.1, 1.5 Hz, 2H), 5.57 (s, 1H), 4.87 (d, *J* = 16.8 Hz, 1H), 4.82 (d, *J* = 16.8 Hz, 1H), 3.58 (s, 3H), 3.57 – 3.52 (m, 1H), 2.84 – 2.76 (m, 1H), 2.43 (s, 3H), 1.51 (q, *J* = 8.0 Hz, 2H), 1.35 – 1.26 (m, 6H), 0.89 (t, *J* = 6.9 Hz, 3H). ^{13}C NMR (126MHz, CD_3Cl) δ 173.6, 165.7, 159.5, 147.35, 147.32, 138.55, 138.49, 138.1, 131.3, 129.7, 129.5, 129.1, 128.1, 126.8, 126.7, 125.9, 123.8, 118.9, 116.5, 111.5, 110.5, 107.5, 101.0, 80.3, 66.6, 55.3, 52.2, 40.2, 31.5, 27.4, 26.9, 22.7, 15.7, 14.2. HRMS: Calculated for $C_{38}H_{41}O_5N_2S$ (M^+ by APCI): 637.2731, found: 637.2738. FT-IR ATR: υ_{CO} = 1748 and 1637 cm^{-1}.

N-benzyl-*N*-(1-benzyl-3-(4-fluorophenyl)-2-oxo-4-(1-tosyl-1H-indol-3-yl)azetidin-3-yl)-4-methylbenzamide (**4.5i**) Isolated yield 79% (295 mg, 0.39 mmol). White solid. m.p. 79-83 °C. ^{1}H NMR (500 MHz, $CDCl_3$) δ 7.88 (d, *J* = 8.4 Hz, 1H), 7.57 (d, *J* = 8.3 Hz, 2H), 7.52 – 7.45 (m, 3H), 7.35 – 7.29 (m, 4H), 7.23 (dt, *J* = 7.2, 3.0 Hz, 3H), 7.13 – 6.95 (m, 11H), 6.70 (d, *J* = 7.2 Hz, 2H), 6.46 (t, *J* = 8.7 Hz, 2H), 5.59 (s, 1H), 4.93 – 4.87 (m, 2H), 4.84 (d, *J* = 16.8 Hz, 1H), 3.77 (d, *J* =

14.7 Hz, 1H), 2.40 (s, 3H), 2.29 (s, 3H). ^{13}C NMR (126MHz, CD_3Cl) δ 173.9, 165.0, 162.3 (d, *J* = 247.8 Hz), 145.2, 140.3, 138.0, 135.2, 134.9, 134.7, 133.7, 131.9 (d, *J* = 3.2 Hz), 131.5 (d, *J* = 8.2 Hz), 130.0, 129.5, 129.1, 129.0, 128.9, 128.3, 128.2, 126.9, 126.82, 126.80, 126.7, 124.8, 123.5, 121.0, 116.6, 114.7 (d, *J* = 21.1 Hz), 113.4, 79.9, 59.9, 52.1, 44.5, 21.7, 21.5.. HRMS: Calculated for $C_{46}H_{38}O_4N_3FNaS$ (MNa^+): 770.2459, found: 770.2478. FT-IR ATR: υ_{CO} = 1752 and 1636 cm^{-1}.

N-benzyl-*N*-(1-benzyl-2-(9H-fluoren-2-yl)-4-oxo-3-(p-tolyl)azetidin-3-yl)-4-fluoro benzamide (**4.5j**) Isolated yield 67% (216 mg, 0.34 mmol). White solid. m.p. 85-90 °C. ^{1}H NMR (500 MHz, $CDCl_3$) δ 7.74 (d, *J* = 7.5 Hz, 1H), 7.58 (d, *J* = 7.9 Hz, 1H), 7.52 (d, *J* = 7.4 Hz, 1H), 7.44 – 7.40 (m, 3H), 7.36 (q, *J* = 6.1, 4.8 Hz, 4H), 7.30 (t, *J* = 7.7 Hz, 1H), 7.19 (dd, *J* = 7.2, 1.7 Hz, 2H), 7.14 (d, *J* = 7.8 Hz, 1H), 7.10 – 7.05 (m, 3H), 7.02 (t, *J* = 7.4 Hz, 2H), 6.90 – 6.82 (m, 4H), 6.63 (d, *J* = 7.4 Hz, 2H), 5.53 (s, 1H), 4.94 (d, *J* = 14.7 Hz, 1H), 4.88 (d, *J* = 17.0 Hz, 1H), 4.75 (d, *J* = 17.0 Hz, 1H), 3.88 (d, *J* = 14.7 Hz, 1H), 3.83 (d, *J* = 22.2 Hz, 1H), 3.70 (d, *J* = 21.8 Hz, 1H). ^{13}C NMR (126 MHz, CD_3Cl) δ 173.0, 165.6, 163.3 (d, *J* = 249.9 Hz), 143.7, 143.0, 141.7, 141.6, 138.4, 138.1, 135.1, 133.2 (d, *J* = 3.4 Hz), 132.9, 132.2, 129.7, 129.2, 129.0, 128.8, 128.7 (d, *J* = 8.6 Hz), 128.3, 128.1, 127.9, 126.90, 126.86, 126.77, 126.5, 126.4, 125.2, 120.1, 119.4, 115.3 (d, *J* = 21.8 Hz), 80.9, 66.5, 52.1, 44.4, 36.9, 21.2. HRMS: Calculated for $C_{44}H_{35}O_2N_2FNa$ (MNa^+): 665.2575, found: 665.2592. FT-IR ATR: υ_{CO} = 1749 and 1638 cm^{-1}.

(*E*)-*N*-benzyl-1-(2-iodophenyl)methanimine (**4.8a**). Isolated yield 71% (5.80 g, 18 mmol). Clear liquid. ^{1}H NMR (500 MHz, $CDCl_3$) δ 8.59 (s, 1H), 8.04 (dd, *J* = 7.8, 1.8 Hz, 1H), 7.87 (dd, *J* = 7.9, 1.2 Hz, 1H), 7.41 – 7.33 (m, 5H), 7.33 – 7.26 (m, 1H), 7.11 (td, *J* = 7.6, 1.8 Hz, 1H), 4.89 (d, *J* = 1.6 Hz, 2H). ^{13}C NMR (101 MHz, $CDCl_3$) δ 165.3, 139.7, 139.1, 137.1, 132.2, 129.1, 128.7,

128.5, 128.2, 127.2, 100.3, 65.1. HRMS: Calculated for $C_{14}H_{13}IN$ (MH^+): 322.0087, found: 322.0084.

(*E*)-1-(2-iodophenyl)-*N*-isopropylmethanimine (**4.8b**). Isolated yield 36% (850 mg, 3.1 mmol). Clear liquid. ^{1}H NMR (500 MHz, $CDCl_3$) δ 8.45 (s, 1H), 7.95 (dd, *J* = 7.8, 1.8 Hz, 1H), 7.83 (dd, *J* = 7.9, 1.2 Hz, 1H), 7.34 (td, *J* = 7.5, 7.0, 0.9 Hz, 1H), 7.06 (td, *J* = 7.6, 1.8 Hz, 1H), 3.63 (hept, *J* = 6.3 Hz, 1H), 1.28 (d, *J* = 6.4 Hz, 6H). ^{13}C NMR (126 MHz, $CDCl_3$) δ 161.6, 139.5, 137.3, 131.8, 128.9, 128.4, 100.0, 61.4, 24.2. HRMS: Calculated for $C_{10}H_{13}IN$ (MH^+): 274.0087, found: 274.0080.

(*E*)-*N*-hexyl-1-(2-iodophenyl)methanimine (**4.8c**). Isolated yield 53% (1.41 g, 5.5 mmol). Clear liquid. ^{1}H NMR (500 MHz, $CDCl_3$) δ 8.42 (s, 1H), 7.93 (dd, *J* = 7.8, 1.8 Hz, 1H), 7.84 (dd, *J* = 8.0, 1.2 Hz, 1H), 7.36 (tt, *J* = 8.0, 1.0 Hz, 1H), 7.13 – 7.04 (m, 1H), 3.66 (td, *J* = 7.0, 1.4 Hz, 2H), 1.71 (p, *J* = 7.0 Hz, 2H), 1.41 – 1.30 (m, 6H), 0.95 – 0.83 (m, 3H). ^{13}C NMR (126 MHz, $CDCl_3$) δ 164.1, 139.7, 137.3, 131.9, 128.9, 128.5, 100.0, 61.7, 31.8, 30.9, 27.1, 22.8, 14.2. HRMS: Calculated for $C_{13}H_{19}IN$ (MH^+): 316.0557, found: 316.0552.

1,2'-dibenzyl-2-(2-iodophenyl)spiro[azetidine-3,1'-isoindoline]-3',4-dione (**4.9a**). Isolated yield 40% (114 mg, 0.20 mmol). White solid. m.p. 165-166 ºC. ^{1}H NMR (500 MHz, $CDCl_3$) δ 7.85 – 7.78 (m, 1H), 7.68 (dd, *J* = 7.9, 1.2 Hz, 1H), 7.48 – 7.42 (m, 5H), 7.41 – 7.36 (m, 3H), 7.32 (td, *J* = 7.6, 1.2 Hz, 1H), 7.18 – 7.10 (m, 3H), 7.01 (dd, *J* = 7.8, 1.8 Hz, 2H), 6.92 (td, *J* = 7.7, 1.7 Hz, 1H), 6.82 – 6.76 (m, 1H), 5.19 (d, *J* = 14.4 Hz, 1H), 5.08 (s, 1H), 4.40 (d, *J* = 16.0 Hz, 1H), 4.18 (d, *J* = 14.5 Hz, 1H), 3.96 (d, *J* = 16.0 Hz, 1H). ^{13}C NMR (126 MHz, $CDCl_3$) δ 169.6, 166.9, 143.4, 140.5, 137.2, 136.3, 135.3, 132.6, 131.3, 130.4, 129.5, 129.4, 128.9, 128.3, 128.1, 127.4, 127.2, 126.9, 124.1, 120.6, 98.0, 81.6, 70.1, 46.5, 46.0. HRMS: Calculated for $C_{30}H_{23}IN_2NaO_2$ (MNa^+): 593.0696, found: 593.0692. FT-IR ATR: υ_{CO} = 1760 and 1704 $cm^{-1.}$

1,2'-dibenzyl-2-(4-methoxyphenyl)spiro[azetidine-3,1'-isoindoline]-3',4-dione (**4.9b**). Isolated yield 79% (187 mg, 0.40 mmol). White solid. m.p. 146-147 °C. ^{1}H NMR (500 MHz, $CDCl_3$) δ 7.84 – 7.79 (m, 1H), 7.49 – 7.41 (m, 5H), 7.40 – 7.35 (m, 2H), 7.20 – 7.12 (m, 3H), 7.03 (ddd, *J* = 7.5, 4.1, 1.2 Hz, 4H), 6.86 – 6.78 (m, 3H), 5.18 (d, *J* = 14.4 Hz, 1H), 4.93 (s, 1H), 4.44 (d, *J* = 16.0 Hz, 1H), 4.22 (d, *J* = 14.4 Hz, 1H), 3.92 (d, *J* = 16.0 Hz, 1H), 3.78 (s, 3H). ^{13}C NMR (126 MHz, $CDCl_3$) δ 169.1, 166.4, 160.0, 142.7, 136.4, 135.5, 132.7, 130.8, 129.4, 129.3, 128.7, 128.0, 127.6, 127.4, 126.9, 125.6, 124.1, 120.7, 114.7, 81.3, 66.5, 55.3, 46.2, 45.9. HRMS: Calculated for $C_{31}H_{26}O_3N_2Na$ (MNa^+): 497.1836, found: 497.1849. FT-IR ATR: υ_{CO} = 1756 and 1703 $cm^{-1.}$

2'-benzyl-1-ethyl-4-(pyridin-3-yl)spiro[azetidine-3,1'-isoindoline]-2,3'-dione (**4.9c**). Isolated yield 65% (125 mg, 0.33 mmol). White solid. m.p. 169-171 °C. ^{1}H NMR (500 MHz, $CDCl_3$) δ 8.45 (d, *J* = 2.4 Hz, 1H), 8.41 (dd, *J* = 4.9, 1.6 Hz, 1H), 7.89 (d, *J* = 7.5 Hz, 1H), 7.69 (td, *J* = 7.5, 1.2 Hz, 1H), 7.61 – 7.51 (m, 2H), 7.35 (dt, *J* = 8.0, 2.0 Hz, 1H), 7.11 (dd, *J* = 5.2, 2.0 Hz, 3H), 7.07 (dd, *J* = 7.9, 4.8 Hz, 1H), 6.93 (dd, *J* = 7.2, 2.5 Hz, 2H), 5.21 (s, 1H), 4.30 (d, *J* = 16.1 Hz, 1H), 4.07 (d, *J* = 16.1 Hz, 1H), 3.99 (dq, *J* = 14.7, 7.4 Hz, 1H), 3.35 (dq, *J* = 14.2, 7.1 Hz, 1H), 1.42 (t, *J* = 7.3 Hz, 3H). ^{13}C NMR (126 MHz, $CDCl_3$) δ 169.3, 165.8, 150.3, 147.6, 142.2, 136.0, 134.0, 133.1, 130.8, 130.0, 129.9, 128.2, 127.0, 126.9, 124.5, 123.8, 120.5, 82.0, 65.5, 46.5, 37.1, 13.4. HRMS: Calculated for $C_{24}H_{22}O_2N_3$ (MH^+): 384.1707, found: 384.1696. FT-IR ATR: υ_{CO} = 1755 and 1708 $cm^{-1.}$

1-benzyl-2'-isopropyl-2-(4-methoxyphenyl)spiro[azetidine-3,1'-isoindoline]-3',4-dione (**4.9d**). Isolated yield 79% (169 mg, 0.40 mmol). White solid. m.p. 59-61 °C. ^{1}H NMR (500 MHz, $CDCl_3$) δ 7.75 – 7.70 (m, 1H), 7.45 – 7.37 (m, 7H), 7.06 (d, *J* = 8.5 Hz, 2H), 6.92 (d, *J* = 8.8 Hz, 2H), 6.85 – 6.81 (m, 1H), 5.26 (d, *J* = 14.3 Hz, 1H), 4.86 (s, 1H), 4.23 (d, *J* = 14.3 Hz, 1H), 3.81 (s, 3H), 3.29 (hept, *J* = 6.9 Hz, 1H), 1.38 (d, *J* = 6.7 Hz, 3H), 0.58 (d, *J* = 6.8 Hz, 3H). ^{13}C NMR (126

MHz, $CDCl_3$) δ 169.0, 166.9, 160.0, 142.1, 135.4, 132.5, 132.2, 129.4, 129.33, 129.27, 128.7, 127.9, 125.9, 123.5, 120.5, 114.6, 82.6, 66.7, 55.5, 49.7, 46.2, 19.4, 19.2. HRMS: Calculated for $C_{27}H_{26}O_3N_2Na$ (MNa^+): 449.1836, found: 449.1848. FT-IR ATR: υ_{CO} = 1759 and 1693 $cm^{-1.}$

1-benzyl-2'-hexyl-2-(4-methoxyphenyl)spiro[azetidine-3,1'-isoindoline]-3',4-dione (**4.9e**). Isolated yield 96% (225 mg, 0.48 mmol). White solid. m.p. 58-60 ºC. ^{1}H NMR (500 MHz, $CDCl_3$) δ 7.79 – 7.73 (m, 1H), 7.47 – 7.37 (m, 7H), 7.06 (d, *J* = 8.4 Hz, 2H), 6.94 – 6.88 (m, 2H), 6.85 – 6.80 (m, 1H), 5.26 (d, *J* = 14.3 Hz, 1H), 4.89 (s, 1H), 4.25 (d, *J* = 14.3 Hz, 1H), 3.82 (s, 3H), 3.00 (ddd, *J* = 13.8, 11.3, 5.4 Hz, 1H), 2.81 (ddd, *J* = 13.9, 11.1, 5.0 Hz, 1H), 1.54 (dddd, *J* = 11.4, 10.1, 8.9, 5.1 Hz, 1H), 1.26 – 1.15 (m, 2H), 1.15 – 1.03 (m, 3H), 1.03 – 0.93 (m, 1H), 0.84 (t, *J* = 7.3 Hz, 3H), 0.67 – 0.57 (m, 1H). ^{13}C NMR (126 MHz, $CDCl_3$) δ 169.1, 167.2, 160.1, 142.4, 135.4, 132.3, 131.3, 129.4, 129.4, 129.3, 128.8, 127.6, 126.0, 123.8, 120.5, 114.7, 81.3, 66.5, 55.5, 46.2, 43.5, 31.5, 27.4, 26.9, 22.7, 14.2. HRMS: Calculated for $C_{30}H_{32}N_2NaO_3$ (MNa^+): 491.2305, found: 491.2296. FT-IR ATR: υ_{CO} = 1761 and 1703 $cm^{-1.}$

1,2'-dibenzyl-2-(4-fluorophenyl)spiro[azetidine-3,1'-isoindoline]-3',4-dione (**4.9f**). Isolated yield 48% (110 mg, 0.24 mmol). White solid. m.p. 195-197 °C. ^{1}H NMR (500 MHz, $CDCl_3$) δ 7.85 – 7.80 (m, 1H), 7.51 – 7.42 (m, 5H), 7.40 – 7.35 (m, 2H), 7.18 – 7.13 (m, 3H), 7.09 – 7.04 (m, 2H), 7.02 – 6.93 (m, 4H), 6.86 – 6.81 (m, 1H), 5.18 (d, *J* = 14.4 Hz, 1H), 4.94 (s, 1H), 4.40 (d, *J* = 16.0 Hz, 1H), 4.21 (d, *J* = 14.5 Hz, 1H), 3.94 (d, *J* = 15.9 Hz, 1H). ^{13}C NMR (126 MHz, $CDCl_3$) δ 169.2, 166.4, 162.9 (d, *J* = 248.7 Hz), 142.5, 136.2, 135.2, 132.8, 130.7, 129.62, 129.60, 129.44, 129.36, 128.9, 128.14, 128.12 (d, *J* = 7.6 Hz), 127.3, 127.0, 124.2, 120.7, 116.4 (d, *J* = 21.8 Hz), 81.5, 66.3, 46.4, 46.1. HRMS: Calculated for $C_{30}H_{23}O_2N_2FNa$ (MNa^+): 485.1636, found: 485.1646. FT-IR ATR: υ_{CO} = 1765 and 1704 $cm^{-1.}$

2'-benzyl-1-ethyl-4-(4-(trifluoromethyl)phenyl)spiro[azetidine-3,1'-isoindoline]-2,3'-dione (**4.9g**). Isolated yield 53% (120 mg, 0.27 mmol). White solid. m.p. 108-109 °C. ^{1}H NMR (500 MHz, $CDCl_3$) δ 7.90 (dt, *J* = 7.5, 0.9 Hz, 1H), 7.69 (td, *J* = 7.6, 1.2 Hz, 1H), 7.62 – 7.53 (m, 2H), 7.45 (d, *J* = 8.1 Hz, 2H), 7.22 (d, *J* = 8.0 Hz, 2H), 7.11 – 7.04 (m, 3H), 6.94 – 6.85 (m, 2H), 5.25 (s, 1H), 4.26 (d, *J* = 16.1 Hz, 1H), 4.11 (d, *J* = 16.2 Hz, 1H), 4.01 (dq, *J* = 14.7, 7.4 Hz, 1H), 3.35 (dq, *J* = 14.2, 7.1 Hz, 1H), 1.43 (t, *J* = 7.3 Hz, 3H). ^{13}C NMR (126 MHz, $CDCl_3$) δ 169.4, 165.9, 142.4, 138.1, 136.1, 133.1, 131.1 (q, *J* = 32.7 Hz), 130.8, 130.0, 129.1, 128.1, 127.0, 126.8, 126.1 (q, *J* = 3.7 Hz), 124.5, 123.7 (q, *J* = 272.3 Hz), 120.6, 82.2, 67.0, 46.6, 37.1, 13.4. HRMS: Calculated for $C_{26}H_{21}O_2N_2F_3Na$ (MNa^+): 473.1447, found: 473.1463. FT-IR ATR: υ_{CO} = 1750 and 1701 $cm^{-1.}$

(*E*)-2'-benzyl-1-ethyl-4-styrylspiro[azetidine-3,1'-isoindoline]-2,3'-dione (**4.9h**). Isolated yield 95% (194 mg, 0.48 mmol). Light yellow solid. m.p. 141-144 °C. ^{1}H NMR (500 MHz, $CDCl_3$) δ 7.90 (dt, *J* = 7.5, 1.0 Hz, 1H), 7.66 (td, *J* = 7.6, 1.2 Hz, 1H), 7.58 – 7.49 (m, 2H), 7.34 – 7.29 (m, 2H), 7.24 – 7.14 (m, 6H), 6.80 – 6.73 (m, 2H), 6.50 (d, *J* = 15.7 Hz, 1H), 5.85 (dd, *J* = 15.7, 8.9 Hz, 1H), 5.15 (d, *J* = 16.3 Hz, 1H), 4.69 (dd, *J* = 8.9, 0.8 Hz, 1H), 4.59 (d, *J* = 16.4 Hz, 1H), 3.67 (dq, *J* = 14.5, 7.3 Hz, 1H), 3.32 (dq, *J* = 14.3, 7.2 Hz, 1H), 1.35 (t, *J* = 7.3 Hz, 3H). ^{13}C NMR (126 MHz, $CDCl_3$) δ 170.1, 165.3, 142.1, 137.5, 137.2, 134.9, 132.8, 131.0, 129.7, 128.7, 128.6, 128.5, 127.3, 127.1, 126.8, 124.3, 122.9, 120.8, 82.1, 68.3, 47.4, 36.1, 13.7. HRMS: Calculated for $C_{27}H_{25}O_2N_2$ (MH^+): 409.1911, found: 409.1922. FT-IR ATR: υ_{CO} = 1758 and 1698 $cm^{-1.}$

4.5.4. NMR Data of Products

See Supporting Information of publication (*J. Org. Chem.* **2016**, 81, 12106)

4.5.5. Crystallographic Data

Crystal structure of 4.9g:

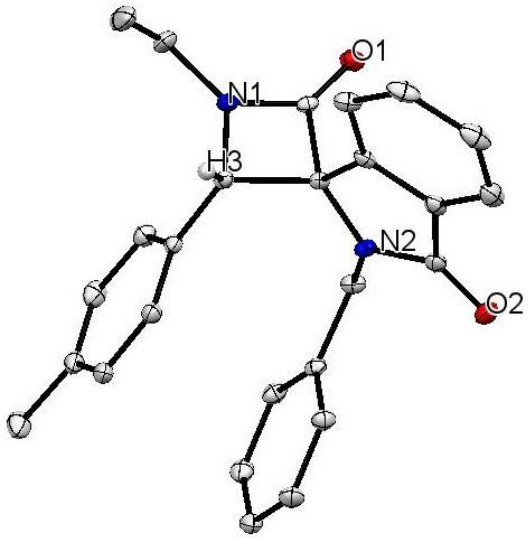

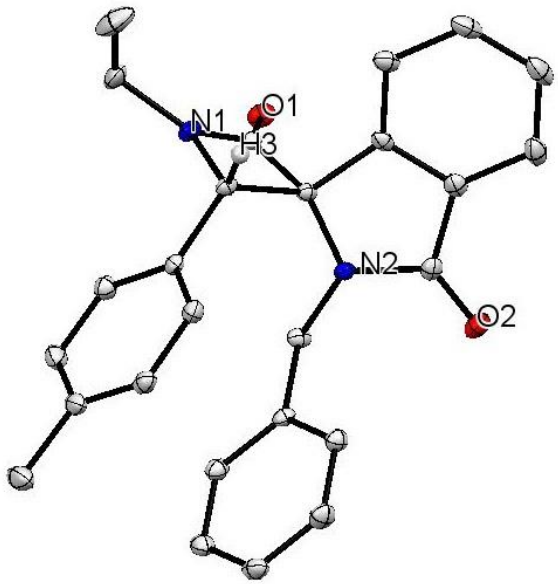

[a] Structure solved and refined in the laboratory of X-ray diffraction Université de Montréal by Thierry Maris. b Ellipsoids displayed at 50% probability. c Hydrogen and fluorine atoms removed for clarity.

Molecular structure of 4.9g:

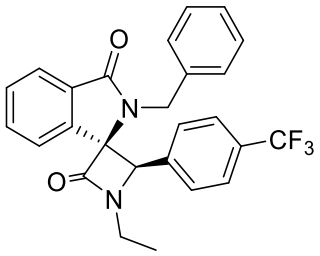

Crystals for spirocyclic product **4.9g** were grown by vapor diffusion from a toluene solution using pentane. A suitable crystal was selected and mounted on a Cryolop on a Bruker Venture Metaljet diffractometer. The crystal was kept at 100 K during data collection. Using Olex2, the structure was solved with the XT structure solution program using Intrinsic Phasing and refined with the XL refinement package using Least Squares minimization. Crystal structure available at the Cambridge Crystallographic Data Centre (CCDC) under the deposition number 1512437.

Table S4.1 Crystal Data and Structure Refinement for 4.9g

Identification code	ARST402
Empirical formula	$C_{26}H_{21}F_3N_2O_2$
Formula weight	450.45
Temperature/K	100
Crystal system	monoclinic
Space group	C2/c
a/Å	24.1714(6)
b/Å	15.5157(4)
c/Å	12.1639(3)
α/°	90
β/°	106.879(1)
γ/°	90
Volume/Å^3	4365.38(19)
Z	8
ρ_{calc}g/cm^3	1.371
μ/mm^{-1}	0.564
F(000)	1872.0
Crystal size/mm^3	0.28 × 0.27 × 0.27
Radiation	GaKα (λ = 1.34139)
2Θ range for data collection/°	5.968 to 121.41
Index ranges	$-31 \leq h \leq 31$, $-20 \leq k \leq 20$, $-15 \leq l \leq 15$
Reflections collected	45256
Independent reflections	5028 [R_{int} = 0.0287, R_{sigma} = 0.0140]

Data/restraints/parameters	5028/42/310
Goodness-of-fit on F^2	1.098
Final R indexes [I>=2σ (I)]	R_1 = 0.0529, wR_2 = 0.1289
Final R indexes [all data]	R_1 = 0.0536, wR_2 = 0.1298
Largest diff. peak/hole / e Å^{-3}	0.45/-0.53

Table S4.2 Fractional Atomic Coordinates (×10^4) and Equivalent Isotropic Displacement Parameters (Å^2×10^3) for 4.9g.
U_{eq} is defined as 1/3 of of the trace of the orthogonalised U_{IJ} tensor.

Atom	*x*	*y*	*z*	U_{eq}
O1	6277.1(4)	5342.2(5)	7484.4(7)	15.7(2)
N1	6621.8(4)	5666.7(6)	5905.9(8)	12.9(2)
C1	6562.1(5)	4331.1(7)	6076.4(9)	10.1(2)
O2	6727.4(4)	2249.5(5)	7290.0(8)	18.2(2)
N2	6885.9(4)	3635.6(6)	6759.6(8)	11.2(2)
C2	6459.7(5)	5179.7(7)	6680.8(9)	11.1(2)
C3	6814.7(5)	4952.8(7)	5301.4(9)	10.7(2)
C4	6575.0(6)	6588.7(8)	5655.0(11)	19.2(3)
C5	6249.9(7)	6755.7(10)	4401.2(13)	29.5(3)
C6	7455.3(5)	4961.3(7)	5415.8(9)	11.3(2)
C7	7838.8(5)	5508.4(8)	6185.4(10)	14.9(2)
C8	8419.9(5)	5533.4(8)	6224.1(11)	17.7(3)
C9	8622.5(5)	5001.3(8)	5505.3(11)	17.1(3)
C10	8248.1(5)	4441.7(7)	4745.8(10)	15.4(2)
C11	7664.9(5)	4434.1(7)	4692.9(10)	13.2(2)
C12	9250.6(6)	5044.2(9)	5540.0(13)	25.2(3)
C13	5991.5(5)	3907.2(7)	5475.5(9)	11.8(2)
C14	5513.4(5)	4233.8(8)	4646.2(10)	15.9(3)
C15	5025.9(5)	3705.4(9)	4284.6(11)	20.6(3)
C16	5019.0(5)	2883.0(9)	4744.6(12)	22.0(3)
C17	5501.5(5)	2553.3(8)	5560.5(11)	18.8(3)
C18	5986.0(5)	3079.6(7)	5906.3(10)	13.5(2)
C19	6558.9(5)	2901.9(7)	6730.4(10)	12.8(2)
C20	7438.1(5)	3743.7(7)	7637.1(9)	12.5(2)
C21	7954.4(5)	3375.1(7)	7328.0(9)	11.7(2)
C22	7902.9(5)	2692.8(7)	6560.4(10)	14.0(2)
C23	8395.2(5)	2347.4(8)	6355.1(10)	16.8(3)

C24	8939.5(5)	2677.9(8)	6903.1(11)	16.9(3)
C25	8991.9(5)	3365.3(8)	7657.4(10)	16.8(3)
C26	8499.2(5)	3708.1(7)	7869(1)	14.5(2)
F1	9530(4)	5688(6)	5991(9)	37.1(4)
F2	9438(3)	4502(5)	5130(7)	32.5(3)
F3	9583(3)	5061(8)	6786(10)	63.8(6)
F1A	9432.3(6)	5864.4(9)	5561.8(14)	37.1(4)
F2A	9333.1(4)	4756.6(8)	4530.8(12)	32.5(3)
F3A	9589.6(5)	4551.7(15)	6329.2(16)	63.8(6)

Table S4.3 Anisotropic Displacement Parameters ($Å^2×10^3$) for 4.9g

The Anisotropic displacement factor exponent takes the form: $-2\pi^2[h^2a^{*2}U_{11}+2hka^*b^*U_{12}+\ldots]$

Atom	U_{11}	U_{22}	U_{33}	U_{23}	U_{13}	U_{12}
O1	19.2(4)	16.3(4)	13.0(4)	-1.0(3)	6.6(3)	3.4(3)
N1	15.5(5)	10.1(5)	14.5(4)	-0.1(3)	6.4(4)	2.7(3)
C1	9.7(5)	9.8(5)	10.5(5)	-0.7(4)	2.6(4)	1.5(4)
O2	23.1(5)	12.2(4)	20.6(4)	3.1(3)	8.5(3)	2.9(3)
N2	10.9(4)	9.6(4)	12.3(4)	0.1(3)	1.9(3)	2.1(3)
C2	9.8(5)	10.6(5)	11.5(5)	-0.8(4)	1.0(4)	1.5(4)
C3	12.1(5)	9.5(5)	10.5(5)	-0.5(4)	3.4(4)	1.6(4)
C4	21.8(6)	9.7(5)	28.7(6)	3.3(4)	11.5(5)	2.8(4)
C5	43.6(8)	23.3(7)	28.6(7)	13.7(5)	21.6(6)	15.7(6)
C6	12.2(5)	9.9(5)	11.5(5)	2.3(4)	3.2(4)	0.5(4)
C7	15.6(5)	13.7(5)	14.7(5)	-0.7(4)	3.5(4)	-0.3(4)
C8	14.3(5)	16.3(6)	19.5(6)	1.4(4)	0.4(4)	-3.3(4)
C9	12.4(5)	16.4(6)	22.5(6)	7.8(4)	5.3(4)	1.0(4)
C10	16.6(6)	13.2(5)	19.1(6)	4.2(4)	9.4(4)	2.6(4)
C11	15.4(5)	11.1(5)	14.0(5)	0.3(4)	5.6(4)	-0.5(4)
C12	13.9(6)	26.6(7)	35.1(7)	12.3(6)	7.1(5)	1.1(5)
C13	9.3(5)	13.7(5)	13.2(5)	-4.4(4)	4.6(4)	-0.1(4)
C14	12.4(5)	17.3(5)	16.8(5)	-3.4(4)	2.5(4)	3.1(4)
C15	10.3(5)	27.9(7)	21.7(6)	-9.0(5)	1.4(4)	2.3(5)
C16	12.8(5)	25.7(6)	28.3(7)	-13.1(5)	7.1(5)	-5.6(5)
C17	17.4(6)	15.9(6)	25.5(6)	-6.8(5)	9.9(5)	-4.4(4)
C18	13.2(5)	14.0(5)	14.8(5)	-3.9(4)	6.6(4)	-0.4(4)
C19	15.0(5)	11.4(5)	13.9(5)	-1.8(4)	7.4(4)	0.2(4)
C20	12.3(5)	13.4(5)	10.3(5)	-2.3(4)	0.8(4)	2.3(4)
C21	12.7(5)	11.1(5)	10.1(5)	1.6(4)	1.8(4)	2.8(4)
C22	14.2(5)	13.1(5)	14.2(5)	-1.8(4)	3.4(4)	0.5(4)
C23	19.5(6)	14.1(5)	18.4(6)	-2.4(4)	8.2(5)	2.0(4)
C24	14.9(5)	17.3(6)	20.5(6)	4.8(4)	8.1(4)	4.8(4)
C25	12.4(5)	17.9(6)	18.1(5)	4.6(4)	1.5(4)	0.8(4)
C26	15.0(5)	12.6(5)	13.6(5)	-0.4(4)	0.7(4)	1.2(4)

F1	21.1(6)	31.3(7)	62.7(10)	-1.5(6)	18.1(6)	-10.8(5)
F2	18.1(5)	43.1(7)	41.9(8)	-3.7(5)	17.3(5)	1.5(4)
F3	13.9(5)	106.4(14)	69.8(11)	65.7(10)	10.0(6)	14.7(7)
F1A	21.1(6)	31.3(7)	62.7(10)	-1.5(6)	18.1(6)	-10.8(5)
F2A	18.1(5)	43.1(7)	41.9(8)	-3.7(5)	17.3(5)	1.5(4)
F3A	13.9(5)	106.4(14)	69.8(11)	65.7(10)	10.0(6)	14.7(7)

Table S4.4 Bond Lengths for 4.9g.

Atom	Atom	Length/Å	Atom	Atom	Length/Å
O1	C2	1.2102(14)	C12	F2	1.136(7)
N1	C2	1.3519(15)	C12	F3	1.495(11)
N1	C3	1.4778(14)	C12	F1A	1.3439(19)
N1	C4	1.4602(15)	C12	F2A	1.374(2)
C1	N2	1.4457(13)	C12	F3A	1.3116(18)
C1	C2	1.5623(15)	C13	C14	1.3903(16)
C1	C3	1.5894(15)	C13	C18	1.3885(16)
C1	C13	1.5112(14)	C14	C15	1.3975(17)
O2	C19	1.2219(14)	C15	C16	1.395(2)
N2	C19	1.3803(14)	C16	C17	1.3909(19)
N2	C20	1.4565(14)	C17	C18	1.3889(16)
C3	C6	1.5140(15)	C18	C19	1.4807(16)
C4	C5	1.5214(19)	C20	C21	1.5160(15)
C6	C7	1.3972(16)	C21	C22	1.3931(15)
C6	C11	1.3991(15)	C21	C26	1.3896(16)
C7	C8	1.3923(17)	C22	C23	1.3922(16)
C8	C9	1.3909(18)	C23	C24	1.3889(17)
C9	C10	1.3931(17)	C24	C25	1.3886(18)
C9	C12	1.5079(17)	C25	C26	1.3948(17)
C10	C11	1.3925(16)	F1	F3	1.351(13)
C12	F1	1.241(9)			

Table S4.5 Bond Angles for 4.9g

Atom	Atom	Atom	Angle/º	Atom	Atom	Atom	Angle/º
C2	N1	C3	97.19(9)	F2	C12	F3	107.0(6)
C2	N1	C4	132.27(10)	F3	C12	C9	105.6(3)
C4	N1	C3	130.30(10)	F1A	C12	C9	111.28(12)
N2	C1	C2	119.47(9)	F1A	C12	F2A	101.18(13)
N2	C1	C3	123.84(9)	F2A	C12	C9	111.51(12)
N2	C1	C13	102.64(9)	F3A	C12	C9	113.88(12)
C2	C1	C3	84.74(8)	F3A	C12	F1A	113.96(17)
C13	C1	C2	110.32(9)	F3A	C12	F2A	104.05(15)
C13	C1	C3	115.53(9)	C14	C13	C1	129.94(11)

C1	N2	C20	124.27(9)	C18	C13	C1	109.12(9)
C19	N2	C1	112.98(9)	C18	C13	C14	120.91(11)
C19	N2	C20	120.65(9)	C13	C14	C15	117.51(12)
O1	C2	N1	133.97(11)	C16	C15	C14	121.16(12)
O1	C2	C1	134.47(10)	C17	C16	C15	121.16(11)
N1	C2	C1	91.45(8)	C18	C17	C16	117.28(12)
N1	C3	C1	85.91(8)	C13	C18	C17	121.95(11)
N1	C3	C6	114.18(9)	C13	C18	C19	108.54(10)
C6	C3	C1	120.63(9)	C17	C18	C19	129.50(11)
N1	C4	C5	111.25(11)	O2	C19	N2	124.97(11)
C7	C6	C3	121.92(10)	O2	C19	C18	128.78(11)
C7	C6	C11	119.05(11)	N2	C19	C18	106.25(9)
C11	C6	C3	118.97(10)	N2	C20	C21	114.84(9)
C8	C7	C6	120.40(11)	C22	C21	C20	122.21(10)
C9	C8	C7	119.88(11)	C26	C21	C20	118.53(10)
C8	C9	C10	120.48(11)	C26	C21	C22	119.20(10)
C8	C9	C12	119.44(12)	C23	C22	C21	119.88(11)
C10	C9	C12	120.07(12)	C24	C23	C22	120.78(11)
C11	C10	C9	119.34(11)	C25	C24	C23	119.52(11)
C10	C11	C6	120.82(11)	C24	C25	C26	119.72(11)
F1	C12	C9	117.5(4)	C21	C26	C25	120.90(11)
F1	C12	F3	58.3(7)	C12	F1	F3	70.3(8)
F2	C12	C9	118.7(3)	F1	F3	C12	51.4(5)
F2	C12	F1	123.7(5)				

Table S4.6 Torsion Angles for 4.9g

A	B	C	D	Angle/º	A	B	C	D	Angle/º
N1	C3	C6	C7	10.38(15)	C8	C9	C12	F2	164.7(5)
N1	C3	C6	C11	-166.66(10)	C8	C9	C12	F3	44.7(5)
C1	N2	C19	O2	-175.55(10)	C8	C9	C12	F1A	-44.36(18)
C1	N2	C19	C18	4.45(12)	C8	C9	C12	F2A	-156.51(12)
C1	N2	C20	C21	-109.45(12)	C8	C9	C12	F3A	86.1(2)
C1	C3	C6	C7	-89.70(13)	C9	C10	C11	C6	-1.95(17)
C1	C3	C6	C11	93.26(13)	C9	C12	F1	F3	92.0(6)
C1	C13	C14	C15	-176.47(11)	C9	C12	F3	F1	-113.1(6)
C1	C13	C18	C17	176.16(10)	C10	C9	C12	F1	161.8(5)
C1	C13	C18	C19	-4.19(12)	C10	C9	C12	F2	-16.3(5)
N2	C1	C2	O1	-51.16(17)	C10	C9	C12	F3	-136.3(5)
N2	C1	C2	N1	132.45(10)	C10	C9	C12	F1A	134.68(14)
N2	C1	C3	N1	-127.96(10)	C10	C9	C12	F2A	22.52(17)
N2	C1	C3	C6	-12.17(15)	C10	C9	C12	F3A	-94.9(2)
N2	C1	C13	C14	-175.50(11)	C11	C6	C7	C8	0.57(17)
N2	C1	C13	C18	6.49(11)	C12	C9	C10	C11	-177.52(11)

N2	C20	C21	C22	-26.50(15)	C13	C1	N2	C19	-6.71(12)
N2	C20	C21	C26	156.29(10)	C13	C1	N2	C20	-170.29(9)
C2	N1	C3	C1	6.67(8)	C13	C1	C2	O1	67.35(15)
C2	N1	C3	C6	-115.19(10)	C13	C1	C2	N1	-109.04(10)
C2	N1	C4	C5	-123.47(13)	C13	C1	C3	N1	104.29(9)
C2	C1	N2	C19	115.67(11)	C13	C1	C3	C6	-139.92(10)
C2	C1	N2	C20	-47.91(15)	C13	C14	C15	C16	0.36(18)
C2	C1	C3	N1	-5.74(7)	C13	C18	C19	O2	-179.98(11)
C2	C1	C3	C6	110.04(10)	C13	C18	C19	N2	0.03(12)
C2	C1	C13	C14	56.14(15)	C14	C13	C18	C17	-2.06(17)
C2	C1	C13	C18	-121.87(10)	C14	C13	C18	C19	177.58(10)
C3	N1	C2	O1	176.81(13)	C14	C15	C16	C17	-1.43(19)
C3	N1	C2	C1	-6.77(8)	C15	C16	C17	C18	0.75(18)
C3	N1	C4	C5	49.69(16)	C16	C17	C18	C13	0.97(17)
C3	C1	N2	C19	-139.73(10)	C16	C17	C18	C19	-178.59(11)
C3	C1	N2	C20	56.69(14)	C17	C18	C19	O2	-0.4(2)
C3	C1	C2	O1	-177.34(13)	C17	C18	C19	N2	179.64(11)
C3	C1	C2	N1	6.27(8)	C18	C13	C14	C15	1.34(17)
C3	C1	C13	C14	-37.79(16)	C19	N2	C20	C21	88.16(12)
C3	C1	C13	C18	144.19(9)	C20	N2	C19	O2	-11.30(17)
C3	C6	C7	C8	-176.47(10)	C20	N2	C19	C18	168.69(9)
C3	C6	C11	C10	178.04(10)	C20	C21	C22	C23	-176.44(11)
C4	N1	C2	O1	-8.4(2)	C20	C21	C26	C25	176.94(10)
C4	N1	C2	C1	167.99(12)	C21	C22	C23	C24	-0.33(18)
C4	N1	C3	C1	-168.24(12)	C22	C21	C26	C25	-0.36(17)
C4	N1	C3	C6	69.89(15)	C22	C23	C24	C25	-0.51(18)
C6	C7	C8	C9	-1.00(18)	C23	C24	C25	C26	0.91(18)
C7	C6	C11	C10	0.92(16)	C24	C25	C26	C21	-0.48(18)
C7	C8	C9	C10	-0.05(18)	C26	C21	C22	C23	0.76(17)
C7	C8	C9	C12	178.98(11)	F2	C12	F1	F3	-90.1(8)
C8	C9	C10	C11	1.51(17)	F2	C12	F3	F1	119.5(7)
C8	C9	C12	F1	-17.3(5)					

Table S4.7 Hydrogen Atom Coordinates (Å×10^4) and Isotropic Displacement Parameters (Å^2×10^3) for 4.9g

Atom	x	y	z	Ueq
H3	6579	4924	4477	13
H4A	6967	6841	5830	23
H4B	6370	6874	6152	23
H5A	6447	6463	3908	44
H5B	6238	7377	4251	44
H5C	5854	6535	4238	44
H7	7702	5865	6685	18
H8	8678	5913	6740	21

H10	8389	4069	4269	18
H11	7406	4066	4159	16
H14	5518	4795	4337	19
H15	4693	3910	3716	25
H16	4679	2542	4496	26
H17	5500	1991	5869	23
H20A	7413	3465	8354	15
H20B	7505	4367	7797	15
H22	7533	2464	6178	17
H23	8358	1880	5834	20
H24	9273	2435	6763	20
H25	9362	3601	8028	20
H26	8537	4176	8390	17

Table S4.8 Atomic Occupancy for 4.9g

Atom	Occupancy	Atom	Occupancy	Atom	Occupancy
F1	0.152(2)	F2	0.152(2)	F3	0.152(2)
F1A	0.848(2)	F2A	0.848(2)	F3A	0.848(2)

Crystal structure determination of 4.9g

Crystal Data for $C_{26}H_{21}F_3N_2O_2$ (*M* =450.45 g/mol): monoclinic, space group C2/c (no. 15), *a* = 24.1714(6) Å, *b* = 15.5157(4) Å, *c* = 12.1639(3) Å, *β* = 106.8790(10), *V* = 4365.38(19) $Å^3$, *Z* = 8, *T* = 100 K, μ(GaKα) = 0.564 mm^{-1}, *Dcalc* = 1.371 g/cm^3, 45256 reflections measured (5.968° ≤ 2Θ ≤ 121.41°), 5028 unique (R_{int}= 0.0287, R_{sigma}= 0.0140) which were used in all calculations. The final R_1 was 0.0529 (I > 2σ(I)) and wR_2 was 0.1298 (all data).

Refinement model description

Number of restraints - 42, number of constraints - unknown.

Details:

1. Fixed Uiso

At 1.2 times of:

All C(H) groups, All C(H,H) groups

At 1.5 times of:

All C(H,H,H) groups

2. Uiso/Uaniso restraints and constraints

F1 ≈ F2 ≈ F3 ≈ F1A ≈ F2A ≈ F3A: within 2A with sigma of

0.005 and sigma for terminal atoms of 0.02

Uanis(F1) = Uanis(F1A)

Uanis(F2) = Uanis(F2A)

Uanis(F3) = Uanis(F3A)

3. Others

Sof(F1A)=Sof(F2A)=Sof(F3A)=1-FVAR(1)

Sof(F1)=Sof(F2)=Sof(F3)=FVAR(1)

4.a Ternary CH refined with riding coordinates:

C3(H3)

4.b Secondary CH2 refined with riding coordinates:

C4(H4A,H4B), C20(H20A,H20B)

4.c Aromatic/amide H refined with riding coordinates:

C7(H7), C8(H8), C10(H10), C11(H11), C14(H14), C15(H15), C16(H16), C17(H17),

C22(H22), C23(H23), C24(H24), C25(H25), C26(H26)

4.d Idealised Me refined as rotating group:

C5(H5A,H5B,H5C)

4.6. References

1. (a) Southgate, R.; Branch, C.; Coulton, S.; Hunt, E. in *Recent Progress in the Chemical Synthesis of Antibiotics and Related Microbial Products* Lukacs, G. Ed.; Springer, Berlin, **1993**, p. 621 (b) Testero, S. A.; Fisher. J. F.; Mobashery, S. β-Lactam Antibiotics, in *Burger's Medicinal Chemistry, Drug Discovery and Development*, Abraham, D. J., Rotella, D. P., Eds.; Wiley: Hoboken, NJ, **2010**; pp 259-404. (c) Von. Nussbaum, F.; Brands, M.; Hinzen, B.; Weigand, S.; Habich, D., *Angew. Chem. Int. Ed.* **2006**, *45*, 5072. (d) *The Organic Chemistry of β-Lactams*; Georg, G. I., Ed.; VCH Publications: New York, **1993**.

2. (a) Rothstein, J. D.; Patel, S.; regan, M. R.; Haenggeli, C.; Huang, Y. H.; Bergles, D. E.; Jin, L.; Hoberg, M. D.; Vidensky, S.; Chung, D. S.; Toan, S. V.; Bruihn, L. I.; Su, Z.-Z.; Gupta, P.; Fisher, P. B. *Nature* **2005**, *433*, 73; (b) Miller, T. M.; Cleveland, D. W. *Science*, **2005**, *307*, 361; (c) Xing, B.; Rao, J.; Liu, R., *Mini Rev. Med. Chem.* **2008**, *8*, 455. (d) Palomo, C.; Aizpurua, J. M.; Benito, A.; Miranda, J. I.; Fratila, R. M.; Matute, C.; Domercq, M.; Gago, F.; Martin-Santamaria, S.; Linden, A. *J. Am. Chem. Soc.* **2003**, *125*, 16243. (e) Feledziak, M.; Michaux, C.; urbach, A.; Labar, G.; Muccioli, G. G.; Lambert, D. M.; Marchand-Brynaert, J. *J. Med. Chem.* **2009**, *52*, 7054; (f) Bonneau, P. R.; Hasani, F.; Plouffe, C.; Malenfant, E.; LaPlante, S. R.; Guse, I.; Ogilvie, W. W.; Plante, R.; Davidson, W. C.; Hopkins, J. L.; Morelock, M. M.; Cordingley, M. G.; Déziel, R. *J. Am. Chem. Soc.* **1999**, *121*, 2965. (g) Jamieson, A. G.; Boutard, N.; Beauregard, K.; Bodas, M. S.; Ong, H.; Quiniou, C.; Chemtob, S.; Lubell, W. D. *J. Am. Chem. Soc.* **2009**, *131*, 7917

3. (a) Hashimoto, K. *Prog. Polym, Sci.* **2000**, *25*, 1411; (b) Gangloff, N.; Ulbricht, J.; Lorson, T.; Schlaad, H.; Luxenhofer, R., *Chem. Rev.* **2016**, *116*, 1753. (c) Deming, T. J., *Adv. Drug Deliv. Rev.* **2002**, *54*, 1145. (d) Dane, E. L.; Grinstaff, M. W. *J. Am. Chem. Soc.* **2012**, *134*, 16255-16264;

(e) Zhang, J.; Kissounko, D. A.; Lee, S. E.; Gellman, S. H.; Stahl, S. S. *J. Am. Chem. Soc.* **2009**, *131*, 1589. (f) Deming, T. J.; Cheng, J., *J. Am. Chem. Soc.* **2001**, *123*, 9457. (g) Mowery, B. P.; Lee, S. E.; Kissounko, D. A.; Epand, R. F.; Epand, R. M.; Weisblum, B.; Stahl, S. S.; Gellman, S. H. *J. Am. Chem. Soc.* **2007**, *129*, 15474. (h) Macías, A.; Ramallal, A. M.; Alonso, E.; del Pozo, C.; González, J. *J. Org. Chem.* **2006**, *71*, 7721.

4. For recent review: Alcaide, B.; Almendros, P.; Aragoncillo, C. *Chem. Rev.* **2007**, *107*, 4437.

5. (a) Fisher, J. F.; Meroueh, S. O.; Mobashery, S., *Chem. Rev.* **2005,** *105*, 395. (b) Dale-Skinner, J. W.; Bonev, B. B.In *New Strategies Combating Bacterial Infection*, Ahmad, I.; Aqil, F., Eds. WILEY-VCH Verlag 2009; pp 1-46. (c) Lewis, K., *Nat. Rev. Drug Discov.* **2013,** *12*, 371. (d) Walsh, C. T.; Wencewicz, T. A. *J. Antibiot.* **2013**, *67*, 7

6. (a) Fu, N.; Tidwell, T. T., *Tetrahedron* **2008,** *64*, 10465. (b) Paull, D. H.; Weatherwax, A.; Lectka, T., *Tetrahedron* **2009,** *65*, 6771. (c) Konaklieva, M. I.; Plotkin, B. J., Asymmetric Synthesis of β-Lactams via the Staudinger Reaction. In *Amino Acids, Peptides and Proteins in Organic Chemistry: Protection Reactions, Medicinal Chemistry, Combinatorial Synthesis*, Hughes, A. B., Ed. Wiley-VCH Verlag & Co. KGaA: **2011**; Vol. 4, p 293. (d) Wright, S. W., Staudinger Ketene-Imine Cycloaddition. In *Name Reactions for Carbocyclic Ring Formations*, Li, J. J., Ed. John Wiley & Sons, Inc.: **2010**; Vol. 1, p 45. (e) Jiao, L.; Liang, Y.; Xu, J. *J. Am. Chem. Soc.* **2006**, 128, 6060.

7. For reviews: (a) France, S.; Weatherwax, A.; Taggi, A. E.; Lectka, T., *Acc. Chem. Res.* **2004,** *37*, 592. (b) Alcaide, B.; Almendros, P.; Luna, A., The Chemistry of 2-Azetidinones (β-Lactams). In *Modern Heterocyclic Chemistry*, Alvarez-Builla, J.; Vaquero, J. J.; Barluenga, J.,

Eds. Wiley-VCH Verlag & Co. KGaA: **2011**; Vol. 4, p 2117. (c) Tuba, R., *Org. Biomol. Chem.* **2013,** *11*, 5976.

8. Carbonylative approaches: (a) Zhou, Z.; Alper, H., *J. Org. Chem.* **1996,** *61*, 1256. (b) Davoli, P.; Moretti, I.; Prati, F.; Alper, H., *J. Org. Chem.* **1999,** *64*, 518. (c) Lu, S.-M.; Alper, H., *J. Org. Chem.* **2004,** *69*, 3558. (d) Fontana, F.; Tron, G. C.; Barbero, N.; Ferrini, S.; Thomas, S. P.; Aggarwal, V. K., *Chem. Commun.* **2010,** *46*, 267. (e) Li, W.; Liu, C.; Zhang, H.; Ye, K.; Zhang, G.; Zhang, W.; Duan, Z.; You, S.; Lei, A., *Angew. Chem. Int. Ed.* **2014,** *53*, 2443. (f) Paul, N. D.; Chirila, A.; Lu, H.; Zhang, X. P.; de Bruin, B., *Chem. Eur. J.* **2013,** *19*, 12953. (g) Xie, P.; Qian, B.; Huang, H.; Xia, C., *Tetrahedron Lett.* **2012,** *53*, 1613. (h) Tanaka, H.; Hai, A. K. M. A.; Sadakane, M.; Okumoto, H.; Torii, S., *J. Org. Chem.* **1994,** *59*, 3040.

9. Other recent metal catalyzed methods: (a) Alcaide, B.; Almendros, P.; Carrascosa, R.; Casarrubios, L.; Soriano, E. *Chem. Eur. J.* **2015**, *21*, 2200; (b) Zhao, Q.; Li, C. *Org. Lett.* **2008**, *10*, 4037; (c) France, S.; Shah, M. H.; Weatherwax, A.; Wack, H.; Roth, J. P.; Lectka, T., *J. Am. Chem. Soc.* **2005,** *127*, 1206. (d) Jiao, L.; Zhang, Q.; Liang, Y.; Zhang, S.; Xu, J., *J. Org. Chem.* **2006,** *71*, 815. (e) Lawlor, M. D.; Lee, T. W.; Danheiser, R. L., *J. Org. Chem.* **2000,** *65*, 4375.

10. For review: a) Marco-Contelles, J., *Angew. Chem. Int. Ed.* **2004,** *43*, 2198. Recent examples: (b) Wolosewicz, K.; Michalak, M.; Adamek, J.; Furman, B., *Eur. J. Org. Chem.* **2016**, 2212. (c) Kabala, K.; Grzeszczyk, B.; Stecko, S.; Furman, B.; Chmielewski, M., *J. Org. Chem.* **2015,** *80*, 12038. (d) Zhang, X.; Hsung, R. P.; Li, H.; Zhang, Y.; Johnson, W. L.; Figueroa, R., *Org. Lett.* **2008,** *10*, 3477.

11. For review: (a) Mandal, B.; Basu, B., *Top. Heterocycl. Chem*. **2013,** *30*, 85. Recent examples: (b) Isoda, M.; Sato, K.; Funakoshi, M.; Omura, K.; Tarui, A.; Omote, M.; Ando, A., *J. Org. Chem.* **2015,** *80*, 8398. (c) Smith, S. R.; Douglas, J.; Prevet, H.; Shapland, P.; Slawin, A. M.

Z.; Smith, A. D., *J. Org. Chem.* **2014,** *79*, 1626. (d) Yoshimura, T.; Takuwa, M.; Tomohara, K.; Uyama, M.; Hayashi, K.; Yang, P.; Hyakutake, R.; Sasamori, T.; Tokitoh, N.; Kawabata, T., *Chem. Eur. J.* **2012,** *18*, 15330. (e) Evans, C. D.; Mahon, M. F.; Andrews, P. C.; Muir, J.; Bull, S. D., *Org. Lett.* **2011,** *13*, 6276.

12. (a) Li, Z.; Sharma, U. K.; Liu, Z.; Sharma, N.; Harvey, J. N.; Van der Eycken, E. V. *Eur. J. Org. Chem.* **2015**, 3957. (b) Cornier, P. G.; Delpiccolo, C. M. L.; Boggián, D. B.; Mata, E. G. *Tetrahedron Lett.* **2013**, *54*, 4742. (c) Vishwanatha, T. M.; Narendra, N.; Sureshbabu, V. V. *Tetrahedron Lett.* **2011**, *52*, 5620. (d) Cariou, C. C. A.; Clarkson, G. J.; Shipman, M. *J. Org. Chem.* **2008**, *73*, 9762. (e) Kolb, J.; Beck, B.; Dömling, A. *Tetrahedron Lett.* **2002**, *43*, 6897.

13. Dhawan, R.; Dghaym, R. D.; St. Cyr, D. J.; Arndtsen, B. A., *Org. Lett.* **2006,** *8*, 3927.

14. For reviews on Münchnones: (a) Gingrich, H. L.; Baum, J. S., Mesoionic Oxazoles. In *Chemistry of Heterocyclic Compounds: Oxazoles*, Turchi, I. J., Ed. John Wiley & Sons, Inc.: 1986; pp 731. (b) Gribble, G. W., Mesoionic Oxazoles. In *The Chemistry of Heterocyclic Compounds, Volume 60: Oxazoles: Synthesis, Reactions, and Spectroscopy, Part A*, Palmer, D. C., Ed. John Wiley & Sons, Inc.: 2003; pp 473. (c) Fisk, J. S.; Mosey, R. A.; Tepe, J. J. *Chem. Soc. Rev.* **2007**, 36, 1432. (d) Reissig, H. U.; Zimmer, R., *Angew. Chem. Int. Ed.* **2014**, *53*, 9708.

15. Huisgen, R.; Funke, E.; Schaefer, F. C.; Knorr, R., *Angew. Chem. Int. Ed.* **1967,** *6*, 367.

16. (a) Torres, G. M.; Quesnel, J. S.; Bijou, D.; Arndtsen, B. A., *J. Am. Chem. Soc.* **2016,** *138*, 7315; (b) Bontemps, S.; Quesnel, J. S.; Worrall, K.; Arndtsen, B. A. *Angew. Chem. Int. Ed.* **2011**, *50*, 8948.

17. (a) Quesnel, J. S.; Arndtsen, B. A. *J. Am. Chem. Soc.* **2013**, *135*, 16841. (b) Quesnel, J. S.; Kayser, L. V.; Fabrikant, A.; Arndtsen, B. A. *Chem. Eur. J.* **2015**, *21*, 9550.

18. *N*-acyl iminium salts generated from imines and acid chlorides undergo decomposition in the pressence of amine base at temperatures above 65 ^{o}C (unpublished results).

19. For example, the use of ^{i}PrCH=NBn leads to exclusive enamide formation.

20. The stereochemistry of all β-lactam products was determined by NOE analysis. See Supporting Information for details.

21. For reviews: (a) Bari, S.; Bhalla, A., *Top. Heterocycl. Chem* **2010,** *22*, 49. (b) Zheng, Y.; Tice, C. M.; Singh, S. B., *Bioorg. Med. Chem. Lett.* **2014,** *24*, 3673. (c) Singh, G. S.; D'hooghe, M.; De Kimpe, N., *Tetrahedron* **2011**, *67*, 1989. (d) Benfatti, F.; Cardillo, G.; Gentilucci, L.; Tolomelli, A., *Bioorg. Med. Chem. Lett.* **2007**, *17*, 1946. (e) Sandanayaka, V. P.; Prashad, A. S.; Yang, Y.; Williamson, R. T.; Ling, Y. I.; Mansour, T. S., *J. Med. Chem.* **2003**, *46*, 2569. For representative examples: (f) Bhalla, A.; Bari, S. S.; Bhalla, J.; Khullar, S.; Mandal, S. *Tetrahedron Lett.* **2016**, *57*, 2822. (g) Bittermann, H.; Gmeiner, P. *J. Org. Chem.* **2006**, *71*, 97. (h) Clayden, J.; Hamilton, S. D.; Mohammed, R. T. *Org. Lett.* **2005**, *7*, 3673.

22. Cho, C. S.; Chu, D. Y.; Lee, D. Y.; Shim, S. C.; Kim, T. J.; Lim, W. T.; Heo, N. H., *Synth. Commun.* **1997,** *27*, 4141.

23. Layer, R. W. *Chem. Rev.* **1963**, *63*, 489.

24. Quesnel, J. S.; Kayser, L. V.; Fabrikant, A.; Arndtsen, B. A. *Chem. Eur. J*. **2015**, 21, 9550.

Chapter 5: A Dual Light Driven Approach to Palladium Catalysis and Carbonylation Reactions

5.1. Preface

In Chapters 2-4, we utilized the palladium catalyzed carbonylation of aryl halides to acid chlorides as a key step in tandem catalytic approaches to various heterocycles. Though efficient, the features that enable the palladium catalyst to undergo the challenging reductive elimination of acid chloride also hinder its reactivity towards oxidative addition. In consequence, the scope of aryl halides compatible with this transformation is limited to relatively activated aryl iodides and bromides. Recent advances in the field of photoredox catalysis led us to question if we could approach this palladium catalyzed carbonylation from a different perspective and use visible light, rather than ligand effects, to drive this chemistry. The following chapter is the manuscript we have prepared on this topic and is currently in submission. This shows, in particular, that the palladium catalyst can drive the full oxidative addition/reductive elimination cycle, and thereby access the most broadly applicable catalyst for carbonylations of which we are aware. This work was done with Yi Liu, a PhD student in our lab. She developed the photochemical carbonylation of aryl bromides, performed some mechanistic control experiments, synthesized a number of the compounds in Figure 5.11, and performed the multistep synthesis of Fenofibrate. My personal contributions include reaction discovery, catalyst development, reaction development for aryl iodides and alkyl halides, performed mechanistic experiments, and synthesized some of the compounds in Figures 5.11 and 5.14.

5.2. Introduction

The ability of transition metals to break and form covalent bonds *via* the fundamental operations of oxidative addition and reductive elimination is central to the field of catalysis and its use in molecular synthesis. Examples with palladium or nickel alone include such prominent systems as cross coupling reactions,[1,2] C-H bond functionalization,[3,4] hydrogenations,[5] oxidations,[6,7] or reductions,[8] and are exploited across the spectrum of pharmaceutical synthesis and fine chemical production. While there has been significant progress in these areas, there are also well-documented and intrinsic limitations to the use of oxidative addition/reductive elimination chemistry. These arise from the reverse nature of these operations on the metal center, wherein the steric or electronic features of the catalyst that favor one direction often has an inhibitory influence on the opposite (Figure 5.1A).[9] Balancing these steps is often a critical feature of reaction design and can often be the source of substrate specific catalysts. In addition, despite extensive efforts, it remains difficult or not viable to perform catalysis involving both difficult oxidative addition and reductive elimination steps, limiting the ability to assemble many important classes of products.[10]

One area where features have proven particularly problematic is in palladium catalyzed carbonylative coupling reactions. Carbonylations offer in principle one of the most efficient routes available to convert feedstock chemicals into carbonyl-containing products, which are the most common functionalities found in pharmaceutically relevant compounds.[11-13] However, the inhibitory influence of CO coordination to palladium on oxidative addition often requires the use of pressing conditions relative to analogous coupling chemistry (e.g. cross coupling reactions), and limits the use of difficult yet useful reagents such as simple alkyl halides.[14] Efforts to address the use of alkyl halides have been described by Alexanian and Ryu using electron rich catalysts or UV light, respectively, but by strongly favoring oxidative addition, are often limited to the use of

simple nucleophilic partners (Figure 5.1B).[15,16] Carbonylations also often require nucleophiles that can readily associate to palladium for reductive elimination. Research here has also been reported using sterically hindered ligands to favor the elimination of electrophilic acyl halides/triflates that react with an array of nucleophiles or even arenes (Figure 5.1C).[17,18] In this case, the catalysts required to favor reductive elimination of these reactive products now restricts this chemistry to substrates that can undergo facile oxidative addition.[19]

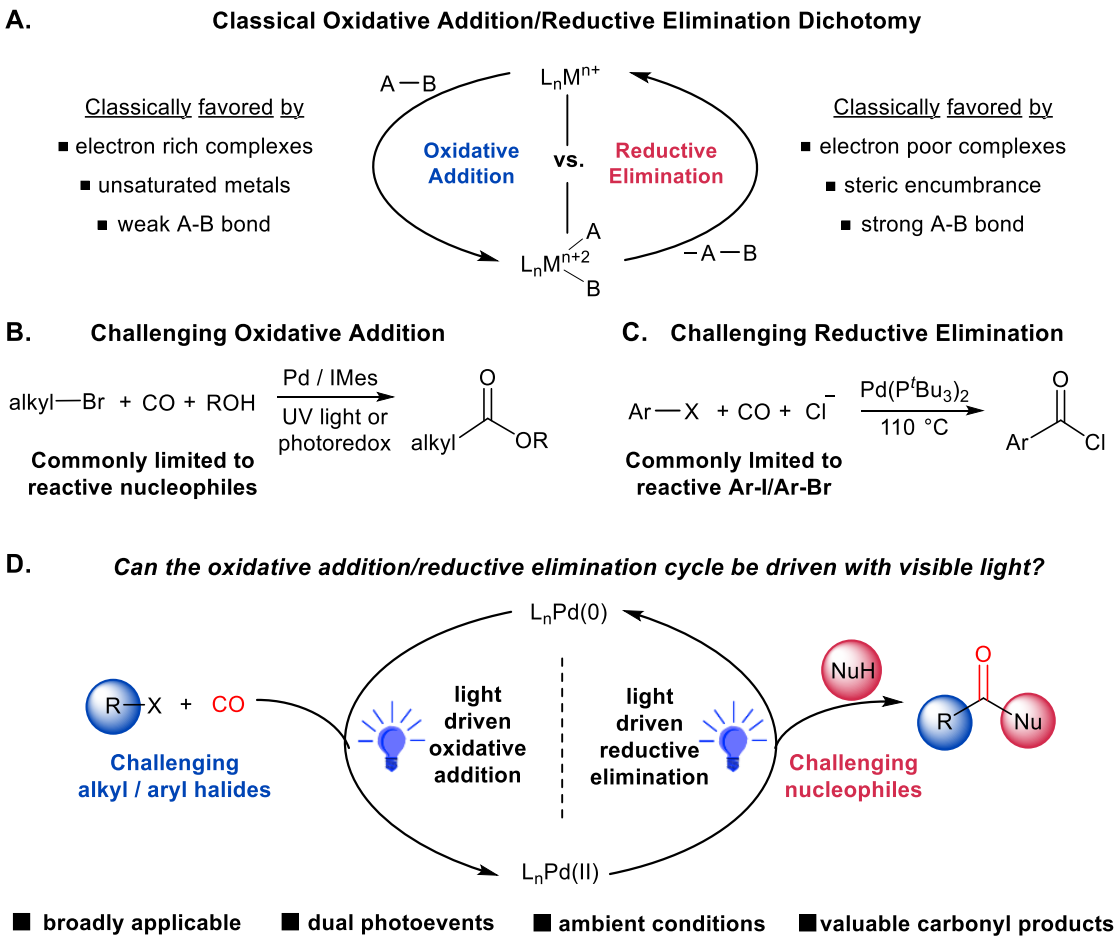

Figure 5.1. A Light-Based Strategy for the Oxidative Addition/Reductive Elimination Cycle. Opposing influences on these operations, their limiting affects in carbonylation chemistry, and concept: exploiting multiple photoevents to access potent, broadly applicable palladium catalysts.

An attractive alternative approach to metal catalyzed coupling chemistry that is of growing utility is to use external factors to drive these reactions. For example, seminal reports by Sanford, Osawa, Molander, MacMillan, and Doyle have shown that the use of visible light photocatalysts with group 10 metals can accelerate challenging steps in coupling reactions.[20-28] These can even be performed without exogenous photocatalysts, as recently demonstrated by Gervorgyan and others,[29-33] and have been applied by Odell to carbonylative Suzuki coupling with alkyl halides.[34] Nevertheless, the other steps in the catalytic cycle rely upon the classic steric and electronic factors of the metal, and are limited in catalyst activity and scope by the thermal barriers inherent to these operations.

In considering these features, we questioned if light might do more than this in catalysis. For example, could visible light excitation offer a pathway to completely eliminate the need to balance oxidative addition and reductive elimination steps and drive both in the same transformation? Since light driven reactions can proceed with low barriers, such a system would offer, at least in principle, a method to perform reactions without having to compromise with ligand effects each step in the cycle, and thus access exceptionally potent and versatile catalysts. The use of two different photoredox events to simultaneously accelerate opposing operations such as oxidative addition and reductive elimination has not been reported, and would pose a significant design challenge of balancing two reverse redox events, as well as the highly plausible self-quenching.[35] Nevertheless, light has been shown to have multiple different influences on catalysis beyond photoredox chemistry, which could offer a pathway towards such a reaction. We describe herein our studies towards this goal. This has led to the discovery of the most broadly applicable carbonylation catalyst of which we are aware, where light driven chemistry directly on palladium can activate an unprecedented range of organic halides towards carbonylation, and at the same

time build-up *via* light driven elimination high energy acid chloride electrophiles that can react with an array of challenging nucleophiles (Figure 5.1D). Mechanistic studies illustrate the novel role of visible light in driving both oxidative addition and reductive elimination *via* excitation of both Pd(0) and Pd(II) complexes, which together offer an alternative to classical metal/ligand effects to access a general palladium catalyst.

5.3. Results and Discussion

5.3.1. Reaction Development

Our initial efforts to develop this catalyst system focused on the use of light to favor the palladium-based build-up of acid chlorides. As noted above, the catalytic formation of acid chlorides offers a route to apply carbonylations to a diverse array of nucleophiles, but the ligands needed to favor this challenging elimination (P^tBu_3/CO) limit oxidative addition to activated substrates at high temperatures.[19] We postulated that this might be addressed by exploiting instead photoredox chemistry to oxidize *in situ* generated palladium-acyl complexes to a transient Pd(III) intermediate to induce the reductive elimination of acid chlorides, in analogy to recent reports in nickel catalysis.[25,36] Nevertheless, it was unclear if photoredox chemistry could drive reductive elimination from a stable palladium(II) center, nor if such a catalyst might also better facilitate oxidative addition.

In order to trap and identify *in situ* generated acid chloride, the carbonylation of aryl iodide was examined in the presence of Bu_4NCl and the bulky amine 2,6-diisopropylaniline (Figure 5.2). As shown in Figure 5.2A, this amine does not have the ability to participate in classical palladium catalyzed carbonylation to form amides at ambient temperature. We postulate this arises from its steric bulk, which makes it unable to coordinate to palladium for reductive elimination.[18] However,

it does rapidly react with acid chloride to form amide **5.1a** in near quantitative yield (Figure 5.2B). As such, it can serve as a useful acid chloride trap during catalysis.

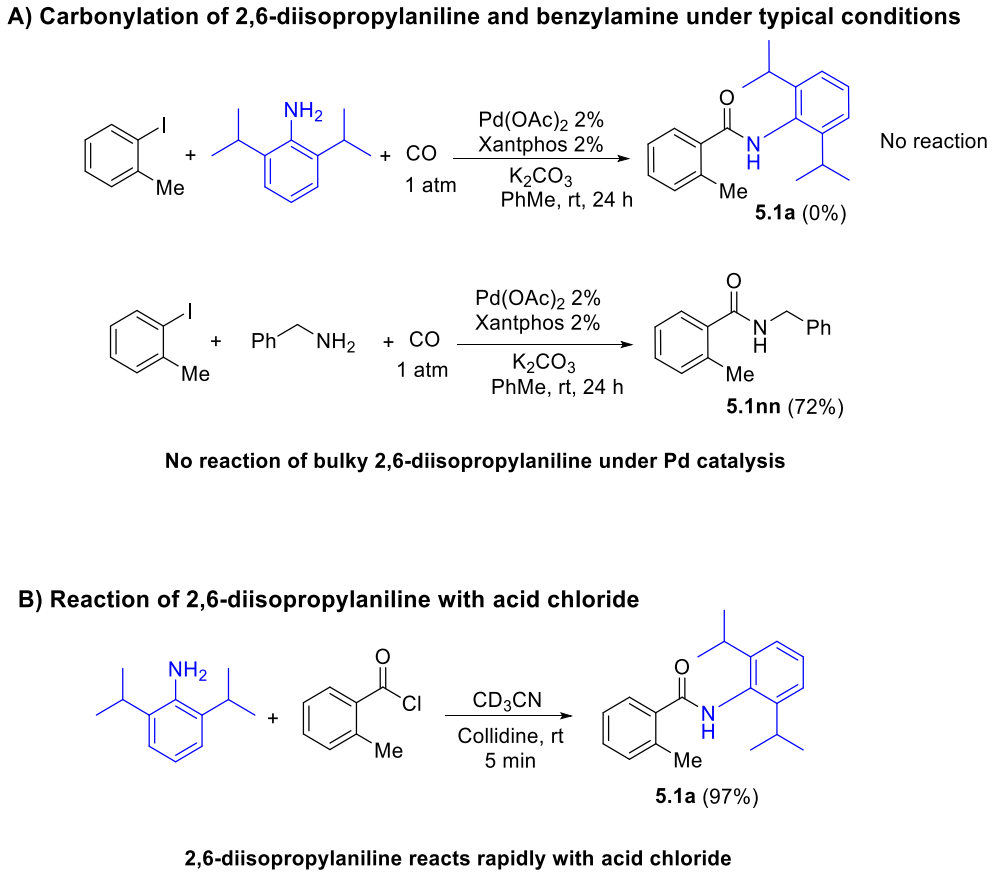

Figure 5.2. Use of 2,6-Diisopropylaniline as a Test for *in situ* Acid Chloride Formation.

After probing different ligand systems and iridium photocatalysts, we were pleased to find that the combination of Xantphos/$[Pd(allyl)Cl]_2$ and in the presence of blue LED light and the photocatalyst $[Ir(dF(CF_3)ppy)_2(dtbpy)]PF_6$[37] leads to the ambient temperature formation of amide **5.1a** in 34% yield (Figure 5.3). No reaction is observed in the absence of light, under green or red LED irradiation, or without the palladium catalyst, suggesting this is a light driven palladium catalyzed carbonylation. To our surprise, however, when the reaction was performed in the absence of the iridium photocatalyst, amide was generated in similar yield (30%).

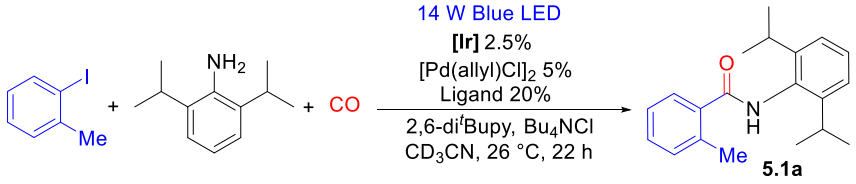

variation in conditions	PPh_3	Ligand: P^tBu_2	PPh_2 PPh_2
No Light	--	12%	3%
Blue LED / [Ir]	2%	10%	34%
Blue LED / fac-Ir(ppy)$_3$ replaces [Ir]			36%
Blue LED, no [Ir]			**30%**

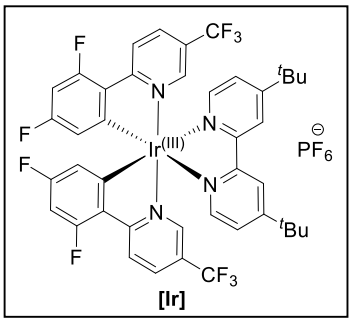

[Ir]

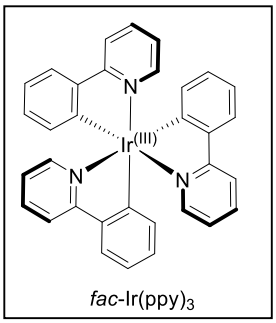

fac-Ir(ppy)$_3$

Figure 5.3. Catalyst Development in the Presence of an Ir Photocatalyst. 2-iodotoluene (13 mg, 0.06 mmol), 2,6-diisopropylaniline (7.1 mg, 0.04 mmol), 2,6-di-*tert*-butylpyridine (11 mg, 0.06 mmol), Bu_4NCl (11 mg, 0.04 mmol), Xantphos (4.6 mg, 8 µmol), [Ir] (1.1 mg, 1 µmol), 4 atm CO, $[Pd(allyl)Cl]_2$ (2 µmol) in 0.75 mL CD_3CN. ^1H NMR yield.

A number of ligands were examined in the reaction without a photocatalyst. In general, monodentate ligands show little to no enhanced reactivity under blue LED irradiation compared to the background thermal reaction (Figures 5.4 and 5.5B). Similarly, there is minimal reaction with a diverse array bidentate ligands. In contrast, the DPE-Phos ligand, which has a similar diphenylether backbone as Xantphos, shows enhanced activity, and forms **5.1a** in 66% yield. Increasing the steric bulk around phosphorus in this phosphine (e.g. with ^{t}Bu or *o*-Tol groups on phosphorus) inhibits catalysis leads to palladium black formation.

The yield of this reaction can be further enhanced by modulation of the base and the solvent (Figure 5.4). For example, the relatively weak base 2,6-di-*tert*-butylpyridine employed above leads to a build-up of protonated 2,6-diisopropylaniline which slows the reaction. We probed a series of stronger bases and found that 2,4,6-collidine can increase the yield of amide without itself reacting with the acid chloride produced during the reaction. The reaction is also more efficient in benzene solvent, presumably due to higher solubility of CO, and under these combined conditions with the 2,6-diisopropylaniline as the limiting reagent, forms amide **5.1a** in near quantitative yield (Figure 5.5B). The generation of acid chloride (**5.2a**) in this transformation can clearly be seen by performing the same reaction in the absence of amine (Figure 5.5C).

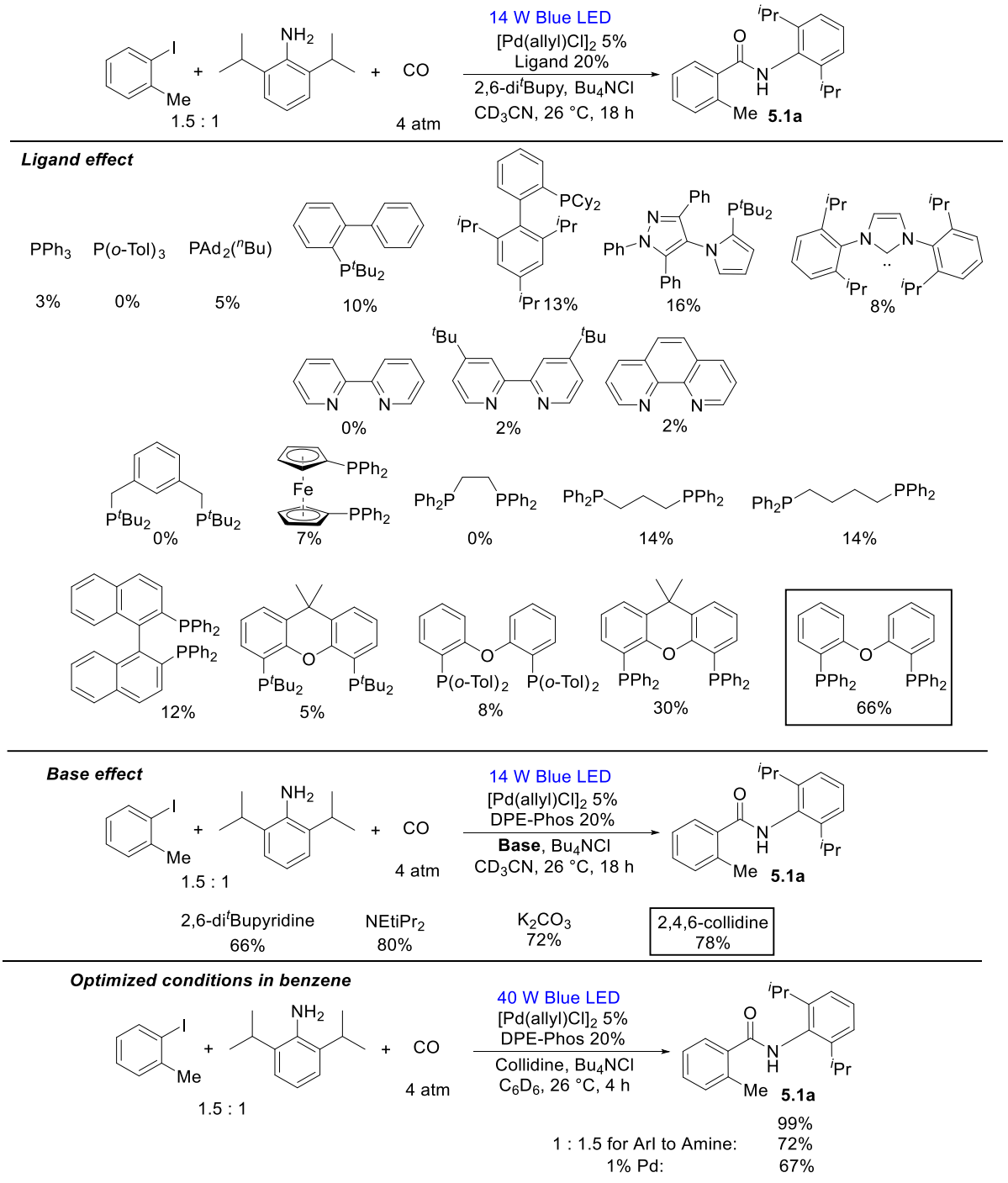

Figure 5.4. Catalyst Development in the Absence of Ir Photocatalyst. Conditions as in Figure 5.3.

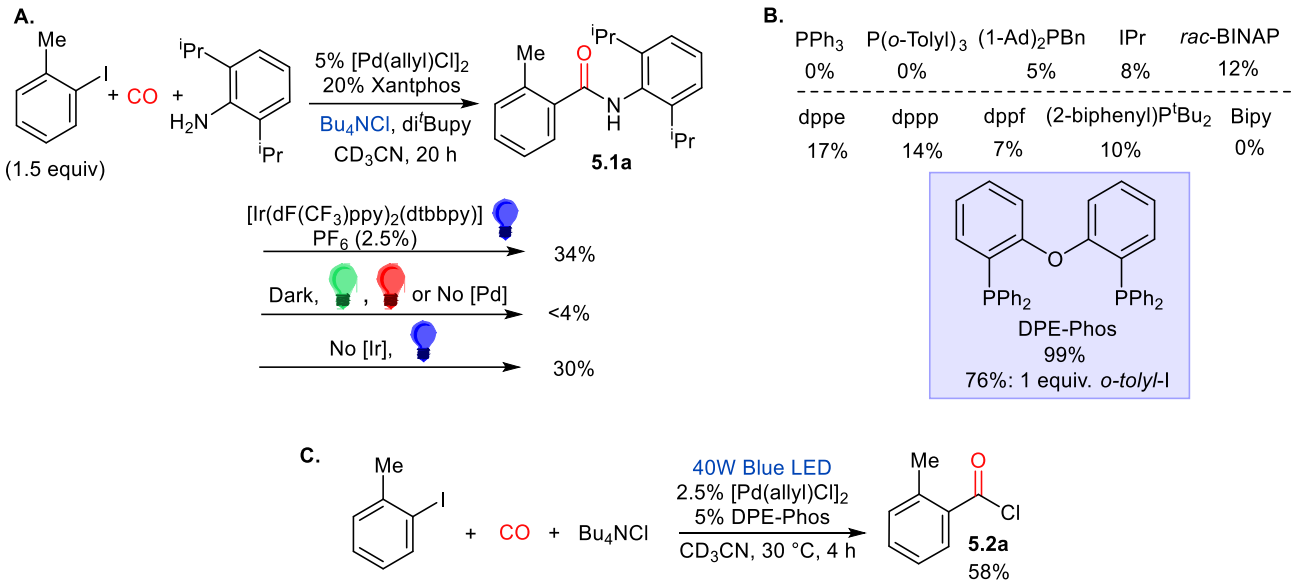

Figure 5.5. Light and Ligand Effects on the Palladium Catalyzed Carbonylation of Aryl Iodides to Acid Chlorides. A. Unusual effect of light on in situ acid chloride generation (di^{t}Bupy = 2,6-di-*t*-butylpyridine); B. Accelerated coupling with the DPE-Phos (using collidine base in benzene); C. Catalytic synthesis of acid chloride with light.

5.3.2. Mechanistic Analysis

Visible light excitation on Pd(0) is known to accelerate oxidative addition *via* light induced electron transfer from palladium to the organic halide.[31,32] However, the ability to induce the room temperature build-up of a reactive acid chloride, and do so without an added photocatalyst, is unexpected, since this elimination typically requires pressing conditions (>100 °C, high CO pressure). This raises the question of what precisely is the influence of light in the reaction. In order to study more closely the product forming step, we generated the Pd(II)-acyl complex **5.3b** (see experimental section for synthesis). Complex **5.3b** undergoes slow reductive elimination in the presence of CO (Figure 5.6A), but it also absorbs blue light (λ_{abs} = 330 to 460 nm, Figure 5.6C). In addition, the irradiation of **5.3b** even at low temperatures leads to the rapid, near quantitative light induced reductive elimination of acid chloride **5.2b** within 5 minutes (Figure 5.6A). This reverts to an equilibrium mixture with **5.3b** in the absence of light.

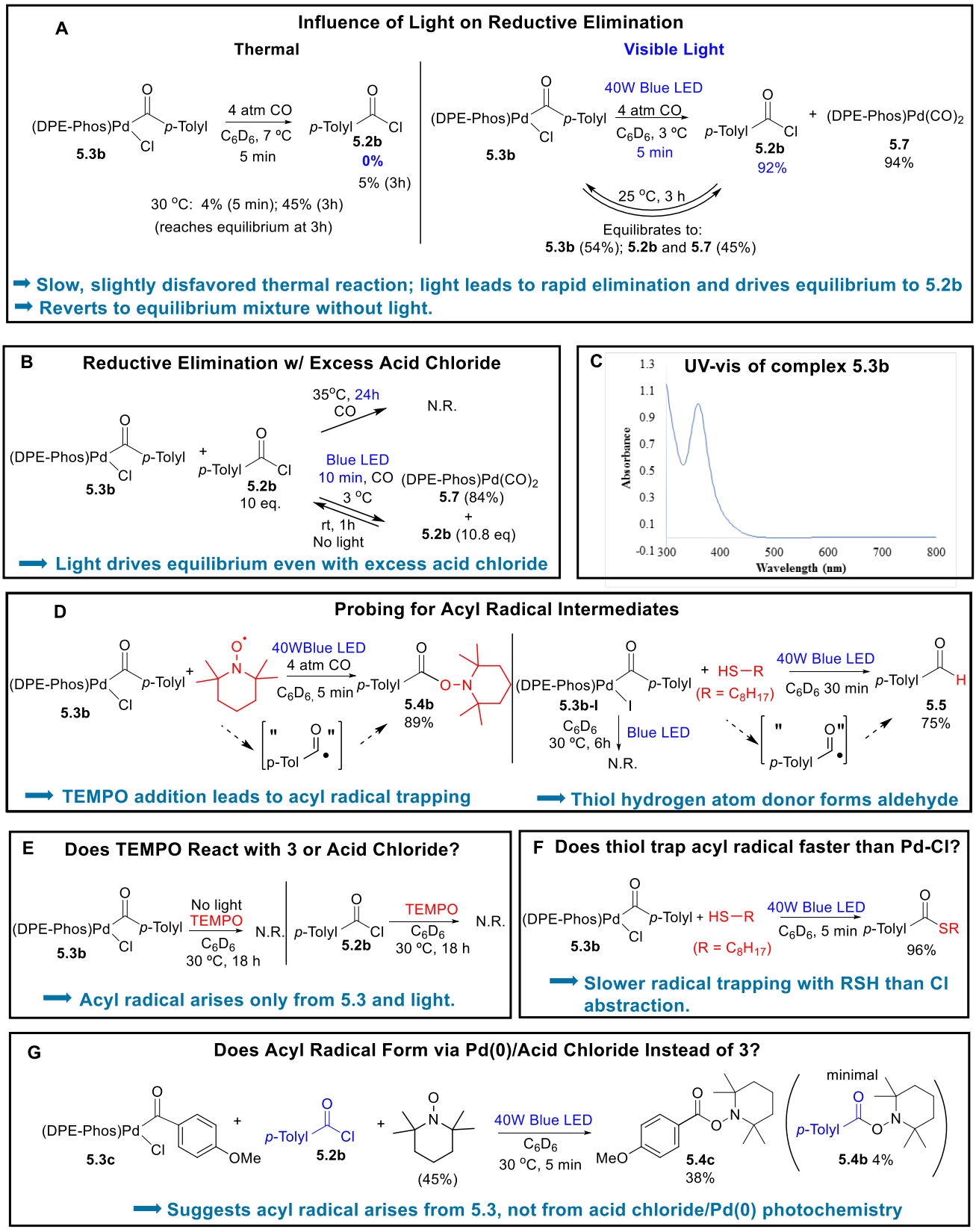

Figure 5.6 Mechanistic Experiments on Light Induced Reductive Elimination from 5.3.

The ability of visible light to drive reductive elimination in palladium catalysis has not been previously reported. There are various plausible pathways by which this step might occur, some of which are shown in Figure 5.7. These include isomerization of the square planar palladium complex to a tetrahedral geometry, and thus increasing the steric strain in the complex.[51] Alternatively there could be a photolytic cleavage of either the Pd-acyl bond or the Pd-Cl bond, followed by attack of these radicals on the resulting Pd(I) complex.[52-53] Finally, the complex could undergo MLCT, generating a transient Pd(III) that undergoes facile reductive elimination.[54]

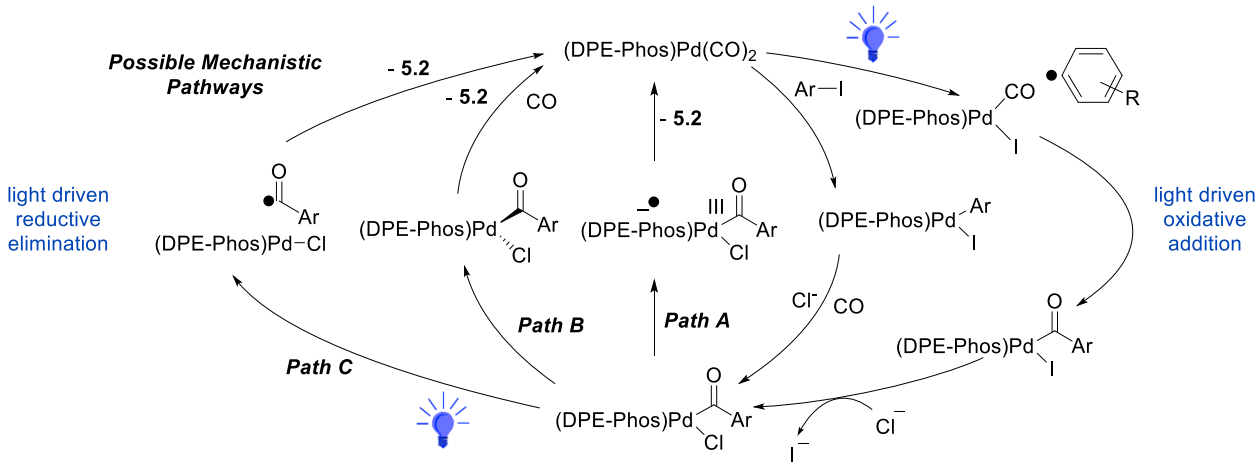

Figure 5.7. Viable Mechanisms for Catalysis.

As one experiment to attempt to distinguish between these possibilities, complex **5.3b** was irradiated in the presence of the radical TEMPO, which leads to the rapid formation of the acyl-radical trapping product **5.4** (Figure 5.6D). A similar reaction with a thiol leads to radical hydrogen atom abstraction and aldehyde **5.5** generation even faster than the known thioester formation from reaction at palladium (Figure 5.6D).[38] Control experiments show that neither TEMPO nor the thiol react with either the palladium complex or acid chloride to form these products (Figure 5.6E,F). Both of these reactions are suggestive of the formation of acyl radicals upon excitation of **5.3** (path

C, Figure 5.7), which could drive the formation of acid chloride by subsequent chloride abstraction from palladium. Metal-acyl bonds have been shown in stoichiometric chemistry to undergo UV light driven homolysis, although not in catalysis.[39,40] Consistent with acyl radical formation upon excitation of the palladium-acyl complex, the irradiation of **5.3b** in the presence of TEMPO and a second acid chloride leads to exclusive radical trapping of the Pd-acyl ligand, rather than fragmentation of the unbound acid chloride (Figure 5.6G). The accelerating influence of light on this reductive elimination is sufficient to drive acid chloride formation even in the presence of a large excess of product **5.2b** (Figure 5.6B), which quantitatively regenerates palladium complex **5.3b** when light is removed.

While these data show the role of light in reductive elimination, we were intrigued to find that light is indeed also involved in Pd(0) oxidative addition chemistry. Initial evidence in this case came from closer analysis of the catalytic reaction mixture, where we observe the low yield formation of a second product in addition to amide **5.2a**, the biaryl *o*-$CH_3C_6H_4$-C_6H_5 (**5.6a**, 8%, Figure 5.8A). Compound **5.6a** would arise from aryl radical addition to the C_6H_6 solvent, and implies the photoreduction of aryl iodide has occurred.[41]

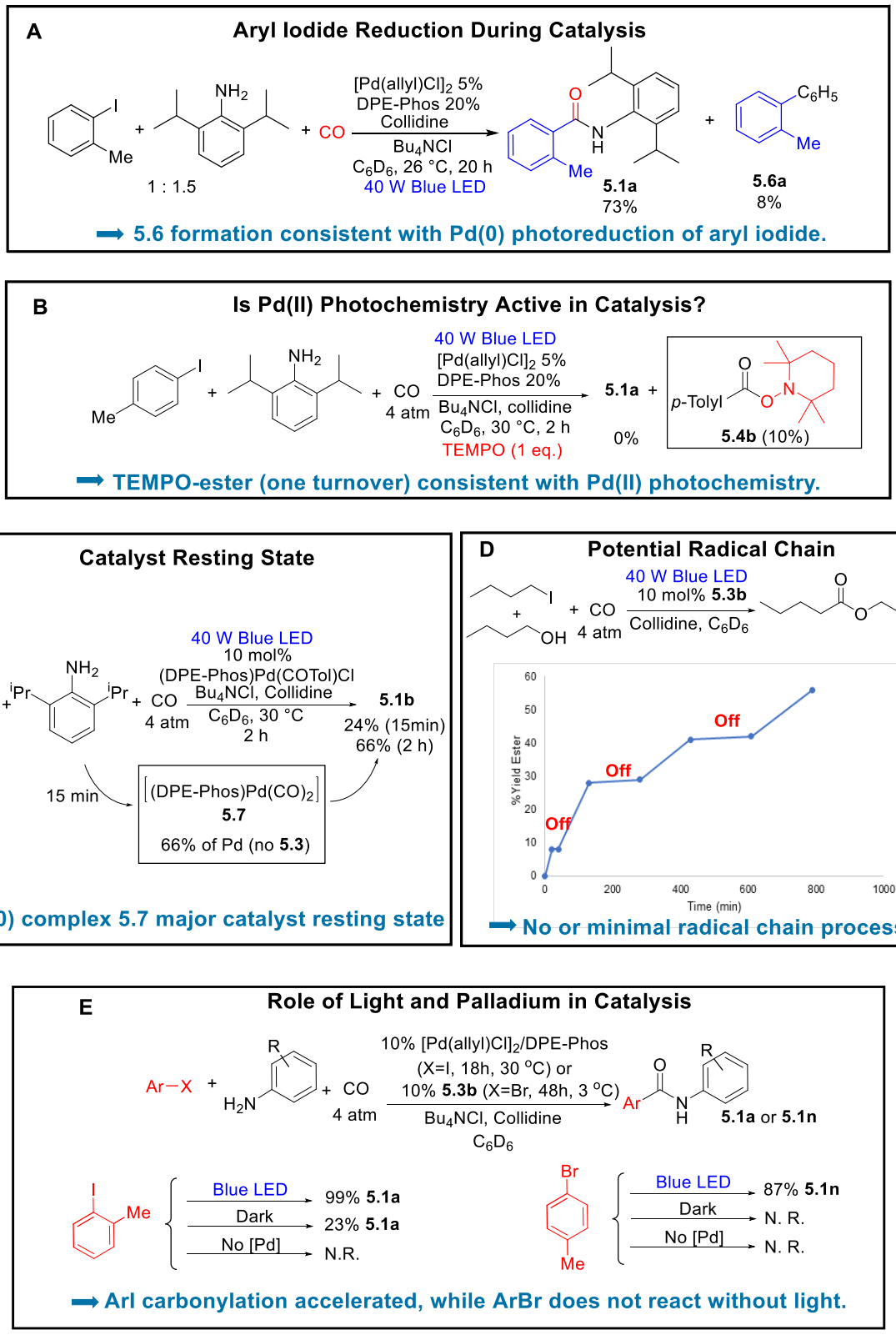

Figure 5.8. Mechanistic Studies on the Catalytic Reaction.

Control experiments show that biaryl generation does not involve the Pd(II)-acyl complex **5.3** (Figure 5.9A), but instead arises from the photochemistry between aryl iodide and a second palladium complex: (DPE-Phos)Pd$(CO)_2$ (**5.7**). The Pd(0) complex **5.7** is generated upon acid chloride reductive elimination above, and offers in this case a novel system with which to directly probe Pd(0) stoichiometric reactivity (see experimental section for independent synthesis).[33] UV/Vis analysis of **5.7** shows it also absorbs blue light (λ_{abs} = 300 to 420 nm, Figure 5.9E), and its irradiation in the presence of aryl iodide leads to rapid oxidative addition to form **5.3** (Figure 5.9B). While aryl iodides can undergo slow thermal oxidative addition, similar light induced reactivity is observed between **5.7** and unreactive aryl bromides (Figure 5.9C) and even alkyl halides (Figure 5.9D). Performing these reactions in the presence of a thiol as hydrogen atom donor inhibits oxidative addition and leads to radical trapping product anisole (Figure 5.9G), and radical clock substrates result in rapid ring opening (Figure 5.9H), supporting the previously postulated role of single electron transfer (SET) in the visible light induced oxidative addition to palladium(0).[30,31]

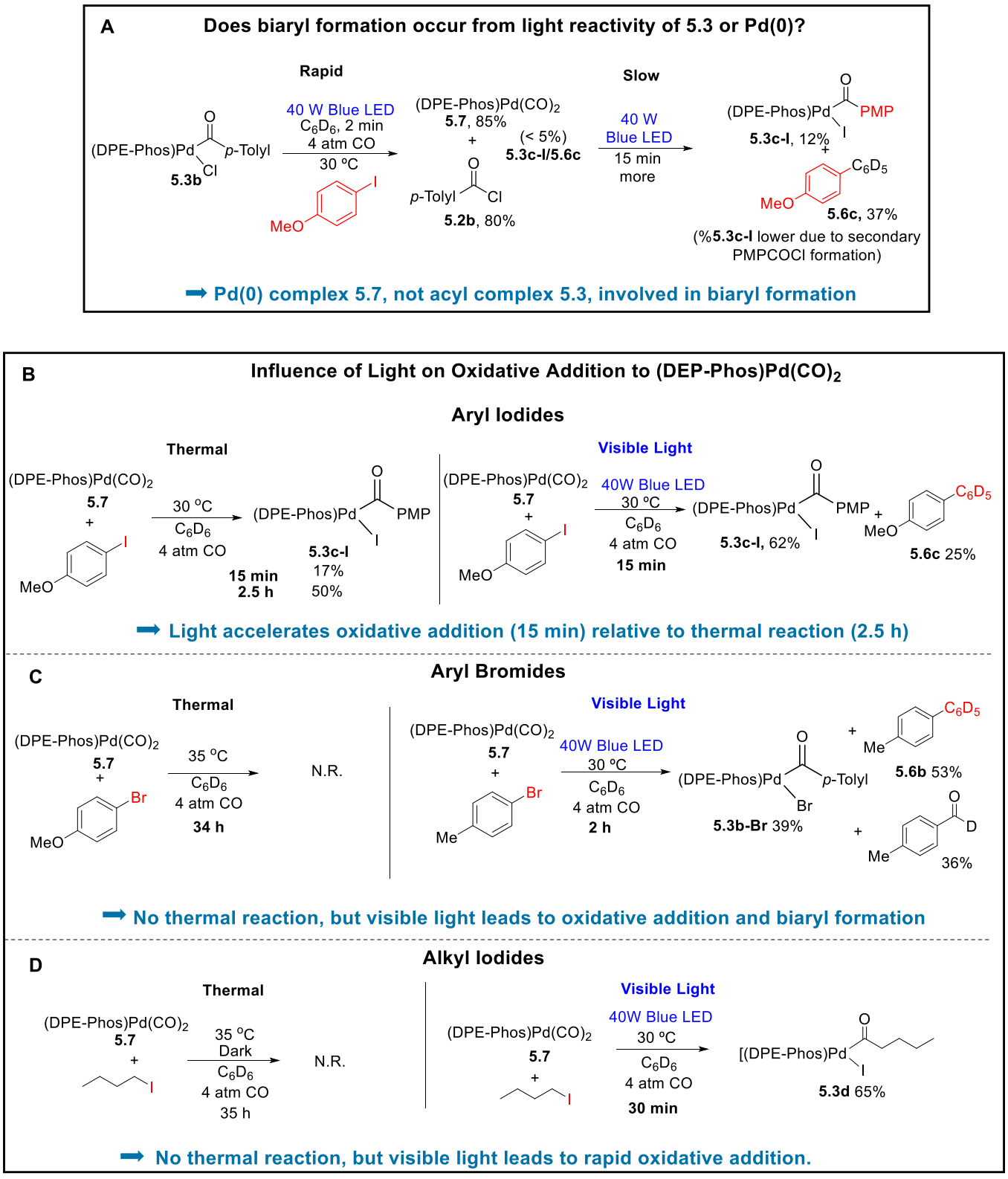

Figure 5.9. Mechanistic Experiments on Visible Light Induced Oxidative Addition.

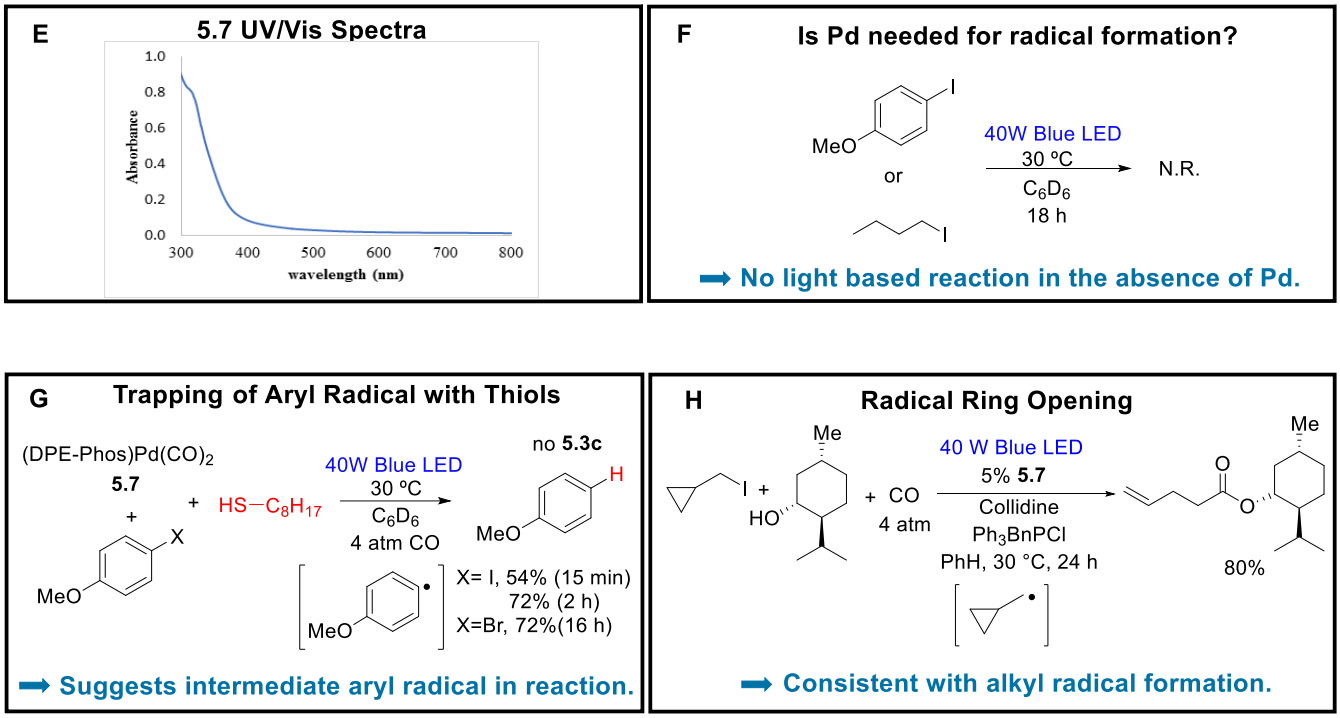

Figure 5.9. Mechanistic Experiments on Visible Light Induced Oxidative Addition (continued).

Together, this stoichiometric data suggests that this reaction proceeds *via* a combination of two different photoevents, where direct excitation on Pd(II) drives the equilibrium reductive elimination of acid chlorides, and excitation of Pd(0) facilitates rapid oxidative addition. Importantly, evidence for the role of both these steps in catalysis is also seen: as noted above, biaryl **5.6a** is generated in addition to amide **5.1a** in the catalytic mixture (Figure 5.8A), suggesting the role of light favored aryl iodide oxidative addition in the reaction, and performing catalysis in the presence of TEMPO leads to a single turnover to form the acyl radical trapping product **5.4** (Figure 5.8B). Catalysis is not observed when light is removed, arguing against a long-lived radical chain driving this chemistry (Figure 5.8C). *In situ* NMR analysis of the catalytic reaction shows that complex **5.7** is the catalyst resting state (Figure 5.8D), which is consistent with the

rates of the two individual photolytic steps. The accelerating effect of light in catalysis under these conditions with both aryl iodides and aryl bromides (Figure 5.8E).

5.3.3. Synthetic Applications

In addition to a fundamental finding, the ability to accelerate oxidative addition and reductive elimination with visible light suggests the ability to perform carbonylations in a now general fashion, where light can drive the reaction with *both* challenging R-X electrophiles and nucleophiles. For example, catalysis proceeds with an array of aryl iodides, including those with electron withdrawing or donating substituents in the para-, meta-, and ortho-positions (**5.1a-i**, Figure 5.10). The reaction is compatible with potentially coordinating groups such as aldehydes (**5.1i**), protected amines (**5.1h**), esters (**5.1c, 5.1d**), nitriles (**5.1f**), thioethers (**5.1e**) or even heterocyclic substrates (**5.1j**). Aryl bromides, which have to date have required high temperatures for carbonylation to acid chlorides (100-120 °C), can also undergo carbonylations to generate *in situ* acid chlorides. In this case, the reaction is performed at -3 ºC in semi-frozen benzene, which inhibits aryl radical addition to the benzene solvent (Figure 5.11). We postulate this increased selectivity in semi-frozen benzene may arise from the slowed diffusion of the aryl radical away from a Pd(I) intermediate, which may favor radical recombination for catalysis. As with aryl iodides, a variety of functionalized aryl bromides can undergo carbonylation to generate *in situ* acid chlorides under these conditions, including those with methoxy (**5.1p**), nitrile (**5.1q**), trifluoromethyl (**5.1s**), ketone (**5.1r**) substituents, as well as heterocycles (**5.1t**).

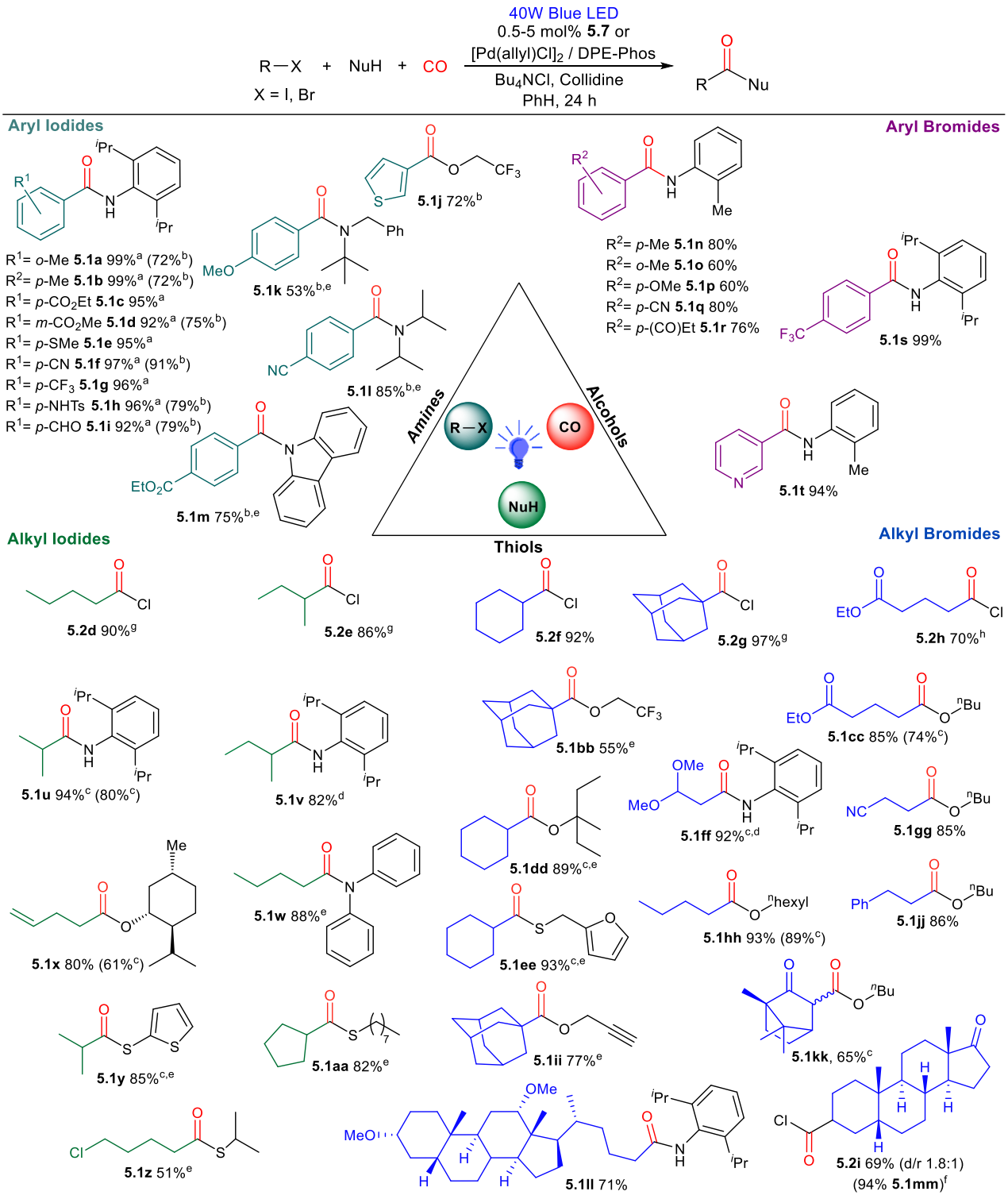

Figure 5.10. A Broadly Applicable, Light Driven Approach to Carbonyl-Containing Products. Reactions performed with 1.5 equiv. aryl iodide, 2 equiv. aryl bromide, or 1 equiv. alkyl halide and 40W Blue LED lamp, unless noted. [a]14W light. [b]Aryl iodide as limiting reagent. [c][Pd(allyl)Cl]$_2$/DPE-Phos as catalyst. [d]1% **5.7**. [e]Nucleophile added in a second step. [f]Yield of amide with 2,6-diisopropylaniline. [g] Bu_4NCl/Ph_3BnPCl (1:1) as chloride sources. [h]At 0 °C.

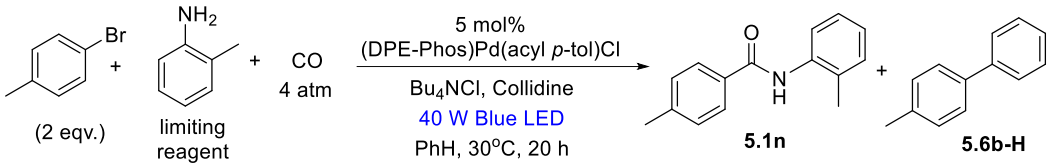

Entry	Deviation from standard condition	5.1n %	5.6b %	Entry	Deviation from standard condition	5.1n %	5.6b %
1	none	19	24	11	NaOTf instead of Bu_4NCl	20	21
2[a]	in NMR tube instead of 25mL vessel	36	28	12	20% $CuCl_2$	18	20
3	anisole solvent	16	20	13	20% CuI or Ag_2CO_3	0	0
4	PhCl solvent	20	40	14[a,b]	10% $Ir(ppy)_3$	17	8
5	THF solvent	8	-	15[a,b]	10% $IrdfCF_3$	9	6
6	MeCN solvent	9	-	16[a,b]	50 °C	30	28
7	cyclohexane solvent	10	-	17[a,b]	- 3 °C	21	11
8	C_6F_6 solvent	0	0	18[c]	- 3 °C	28	15
9	$(Octyl)_4NCl$ instead of Bu_4NCl	23	26	19[c]	10 % Pd, -3 °C, 48 h	50	17
10	NaI instead of Bu_4NCl	23	24	20[d]	10 % Pd, -3 °C, 48 h	87	34

Figure 5.11. Catalyst Development for Visible Light Induced Carbonylation of Aryl Bromides. Conditions: 4-bromotoluene (0.08 mmol), *o*-toluidine (0.04 mmol), **5.3b** (4.2 mg, 2 μmol) collidine (0.04 mmol), Bu_4NCl (0.04 mmol), benzene (0.8 mL), 4 atm CO, 25 mL teflon cap sealable Schlenk bomb, 40 W Blue LED lamp. [a]Performed in J-Young NMR tube. [b]with 0.04 mmol ArBr, 0.08 mmol aniline. [c]with 0.25 mmol ArBr, 0.50 mmol aniline. [d]with 0.50 mmol ArBr, 0.25 mmol aniline.

The visible light driven system can also offer what is to our knowledge a unique route to carbonylate alkyl halides and generate from these useful acid chloride products (**5.2d-h**). In this case, the choice of chloride is important to inhibit alkyl chloride formation (Figure 5.12). For example, the phosphonium salt Ph_3PBnCl is sparingly soluble in benzene solvent, which helps maintain the chloride concentration low and inhibit the competing nucleophilic substitution reaction during acid chloride formation with activated substrates such as primary alkyl iodides

and bromides (Figure 5.12A). Conversely, the sterically encumbered secondary and tertiary alkyl halides undergo substitution more slowly, thus more soluble chloride sources such as Bu_4NCl allow the formation of acid chloride in high yield. When amine or alcohol nucleophiles are present in the mixture, the acid chloride is trapped rapidly, therefore only a catalytic amount of chloride is necessary to form esters and amides in high yields (Figure 5.12B). Under the optimized conditions, the reaction proceeds efficiently with both alkyl iodide and bromide reagents, where catalyst loads can be dropped to as low as 1 mol% palladium. These features are presumably the result of the low reduction potential of alkyl halides, coupled with the rapid light driven reductive elimination.[42] A diverse array of primary (**5.1w, ff-hh**), secondary (**5.1u, v, aa, dd**), and even tertiary (**5.1bb, ii**) alkyl iodides or bromides can be incorporated into this reaction, as well as those with various ester (**5.1cc**), ketone (**5.1kk**), nitrile (**5.1gg**), or alkyl chloride (**5.1z**) substituents. The reaction of cyclopropylmethyl iodide affords the ring-opened alkene product **5.1x**, further supporting the role of single electron transfer in oxidative addition (Figure 5.10).

Importantly, since each of these transformations leads to the formation of acid chlorides, a broad array of nucleophiles can at the same time be incorporated into this chemistry. Examples include substituted anilines (**5.1n-r**), sterically hindered secondary amines (**5.1k-l**), tertiary alcohols (**5.1dd**), or even weakly nucleophilic *N*-heterocycles (**5.1m**). In reactions where the nucleophile is not compatible with the reaction conditions, it can be added after the catalytic build-up of acid chlorides. For example, thiols were incompatible due to the competing donation of a hydrogen atom to the alkyl or aryl radical generated in the reaction forming the reduced arene or alkane products. However, adding the thiol after the initial build-up of acid chloride allowed the formation of a wide range of thioesters (**5.1y, z, aa, ee**). This strategy has also allowed the unprecedented build-up of challenging substrate combinations (**5.1x-bb, ee, ii**), and the generation

of structurally more elaborate products (terpenes, **5.1kk**; β-acetals, **5.1ff**; steroidal acid chlorides, **5.2i**), none of which are viable *via* classical carbonylation chemistry. Overall, this represents the most versatile platform of which we are aware to perform carbonylations with a broad array of challenging electrophilic and nucleophilic components at room temperature.

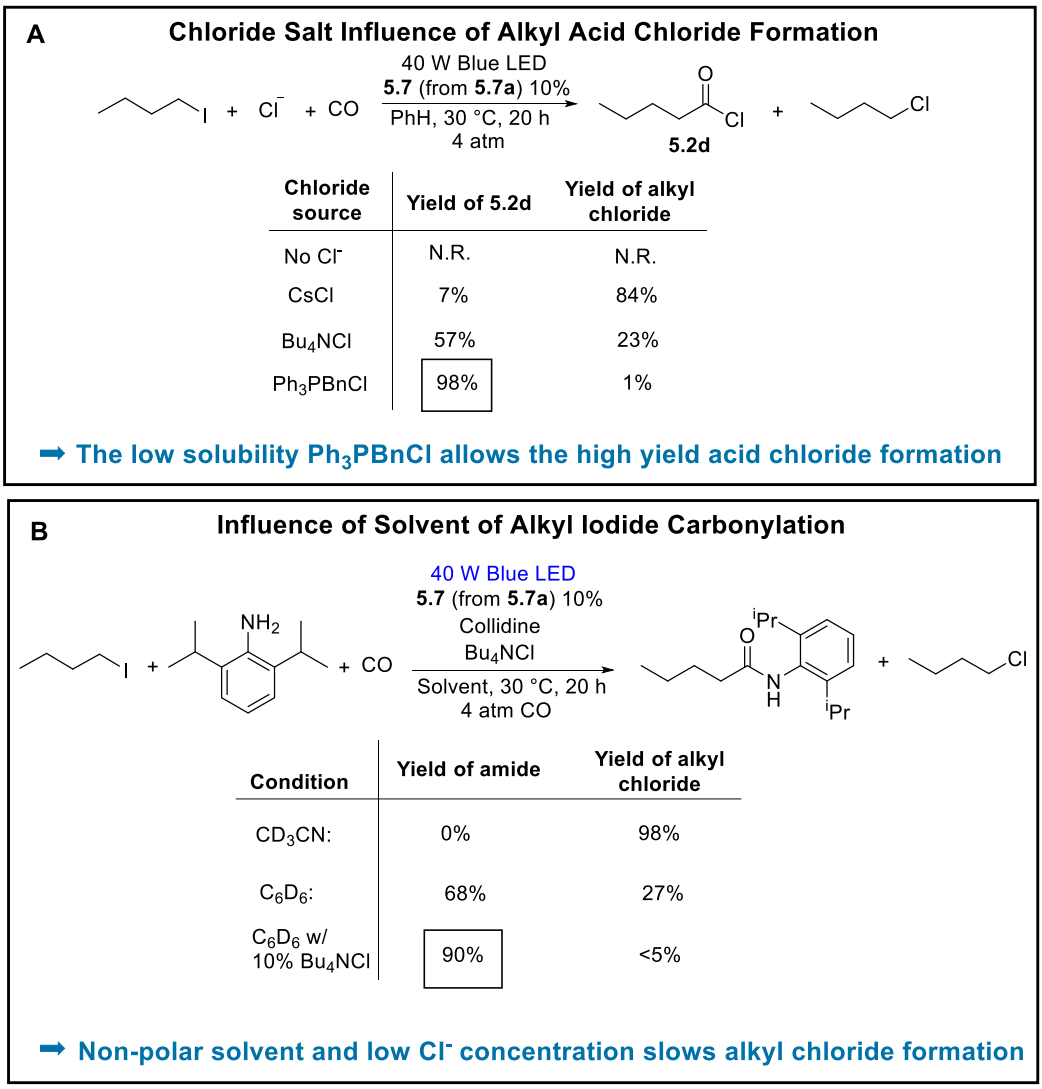

Figure 5.12. Reaction Development with Alkyl Iodides. A: 1-iodobutane (7.4 mg, 0.04 mmol), 2,6-diisopropylaniline (11 mg, 0.06 mmol), Bu_4NCl (11 mg, 0.04 mmol), collidine (7.3 mg, 0.06 mmol), **5.7a** (2.6 mg, 0.002 mmol), 4 atm CO, 40W Blue LED lamp, in 0.75 mL C_6D_6. B: 1-iodobutane (46 mg, 0.25 mmol), Ph_3PBnCl (107 mg, 0.275 mmol), **5.7a** (16 mg, 0.0125 mmol), 4 atm CO, 40W Blue LED lamp, in 3.5 mL benzene. ^1H NMR yields.

We have preliminarily examined the use of this chemistry to access even more challenging classes of carbonyl-containing products. For example, the generation of acid chlorides from alkyl halides offers access to useful biologically relevant structures. One such system are β-amino acid derivatives, which are important reagents in the preparation of peptoids. As shown in Figure 5.13A, the light driven activation of alkyl bromides followed by acid chloride elimination can be used to generate the first carbonylative method to synthesize β-peptide derivatives, in contrast to their common synthesis by multistep protocols.[43,44] Alternatively, the high reactivity of acid chlorides can be applied to other reactions, such Friedel-Crafts acylations. This can be used to design a new carbonylative route to alkyl-substituted ketones directly from (hetero)arenes (Figure 5.13B).[45] The versatility of this approach can as well open new routes to targeted synthesis, such as the cholesterol lowering drug Fenofibrate (Figure 5.13C).[46] The power to do both alkyl and aryl carbonylations to acid chlorides is on display in this synthesis, where the initial functionalization of the 2-iodopropane to form an acid chloride for coupling with isopropanol, followed by an aryl halide carbonylative Friedel-Crafts reaction, affords **5.10** from two equivalents of carbon monoxide. Together, this suggests the ability to access many of the important classes of carbonyl-containing products in an atom economical fashion using visible light driven palladium catalysis.

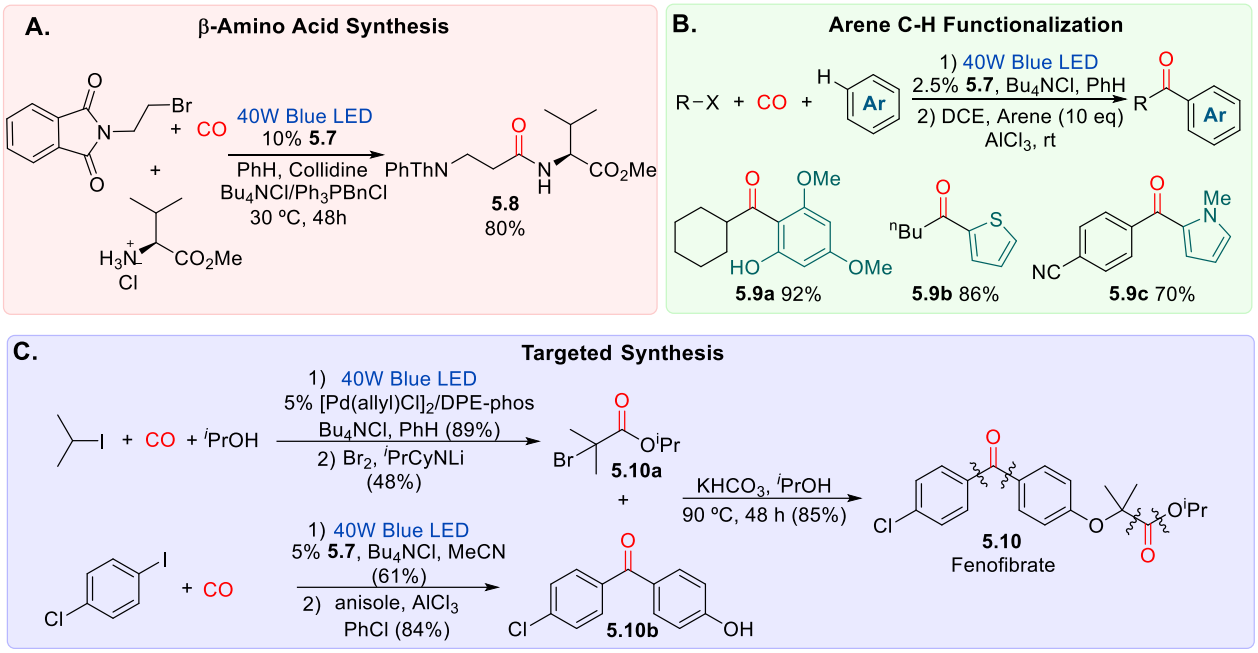

Figure 5.13. Application to Arene β-Amino Acids, C-H Bond Functionalization, and Targeted Synthesis via Sequential Carbonylation. See experimental section for reaction details.

5.4. Conclusions

In summary, we have found that simple visible light can offer a powerful approach to favor oxidative addition and reductive elimination chemistry, wherein both of these operations can be driven by excitation directly on a palladium catalyst and in the same reaction. This has opened a general platform to perform carbonylations at ambient conditions, and with scope and activity rivaling or in some areas exceeding that of non-carbonylative coupling chemistry. Considering the diversity of carbonylation and related transformations where oxidative addition/reductive elimination play a central role, we anticipate that this visible light chemistry could offer a general pathway to access potent and versatile catalyst systems for coupling reactions.

5.5. Experimental Data

5.5.1. General Considerations

All manipulations were conducted in a glovebox under a nitrogen atmosphere. Unless otherwise noted, all reagents were purchased from commercial sources and used without purification. Solvents were dried by using a solvent purifier system and stored over activated 4Å molecular sieves inside the glovebox. Deuterated acetonitrile and benzene were stirred over calcium hydride, vacuum transferred, degassed, and stored over 4Å molecular sieves. Tetrabutylammonium chloride was dried in the glovebox by dissolving in dichloromethane, allowing to stand overnight over activated molecular sieves, filtering and then removing the solvent *in vacuo*. Benzyltriphenyl phosphonium chloride was prepared by literature procedures[47] and was dried in vacuo (ca. 50 mtorr) while heating (ca. 200 °C) for 48 hours. $[Ir(dF(CF_3)ppy)_2(dtbbpy)]PF_6$, *fac*-$Ir(ppy)_3$, and $Pd(P^tBu_3)_2$ were prepared according to literature procedures.[48-50] Research grade carbon monoxide (99.99%) was used as received. For reactions performed in a J-Young NMR tube, carbon monoxide was added by first freezing the solution in liquid nitrogen, evacuating the headspace *in vacuo*, and then condensing in 4 atm CO. For reaction in Schlenk bombs at 1 atm CO, the solution was frozen in liquid nitrogen, evacuated, and the tube was pressurized to 1 atm CO. For reaction in Schlenk bombs at 4 atm CO, 4 atm CO was simply added to the existing atmosphere of nitrogen.

Blue, red, and green LED strips were purchased from NeoMagnetic LED Montreal, and Kessil 40 W A160WE Tuna Blue LED lamps were purchased from Reef Supplies. Nuclear magnetic resonance (NMR) characterization was performed on 500 MHz spectrometers for proton, 126 MHz for carbon, and 162 MHz for phosphorus. ^1H and ^{13}C NMR chemical shifts were referenced to residual solvent. For NMR data of the products, see Appendix 3. Mass spectra were recorded on a high-resolution electrospray ionization quadrupole mass spectrometer. IR spectra were recorded

on a Bruker Alpha FT-IR with a single reflection Platinum ATR module. UV-Vis was recorded on a Jasco V-670 spectrophotometer. Fluorescence spectra were recorded on a Cary Eclipse fluorescence spectrophotometer.

5.5.2. Supplementary Figures

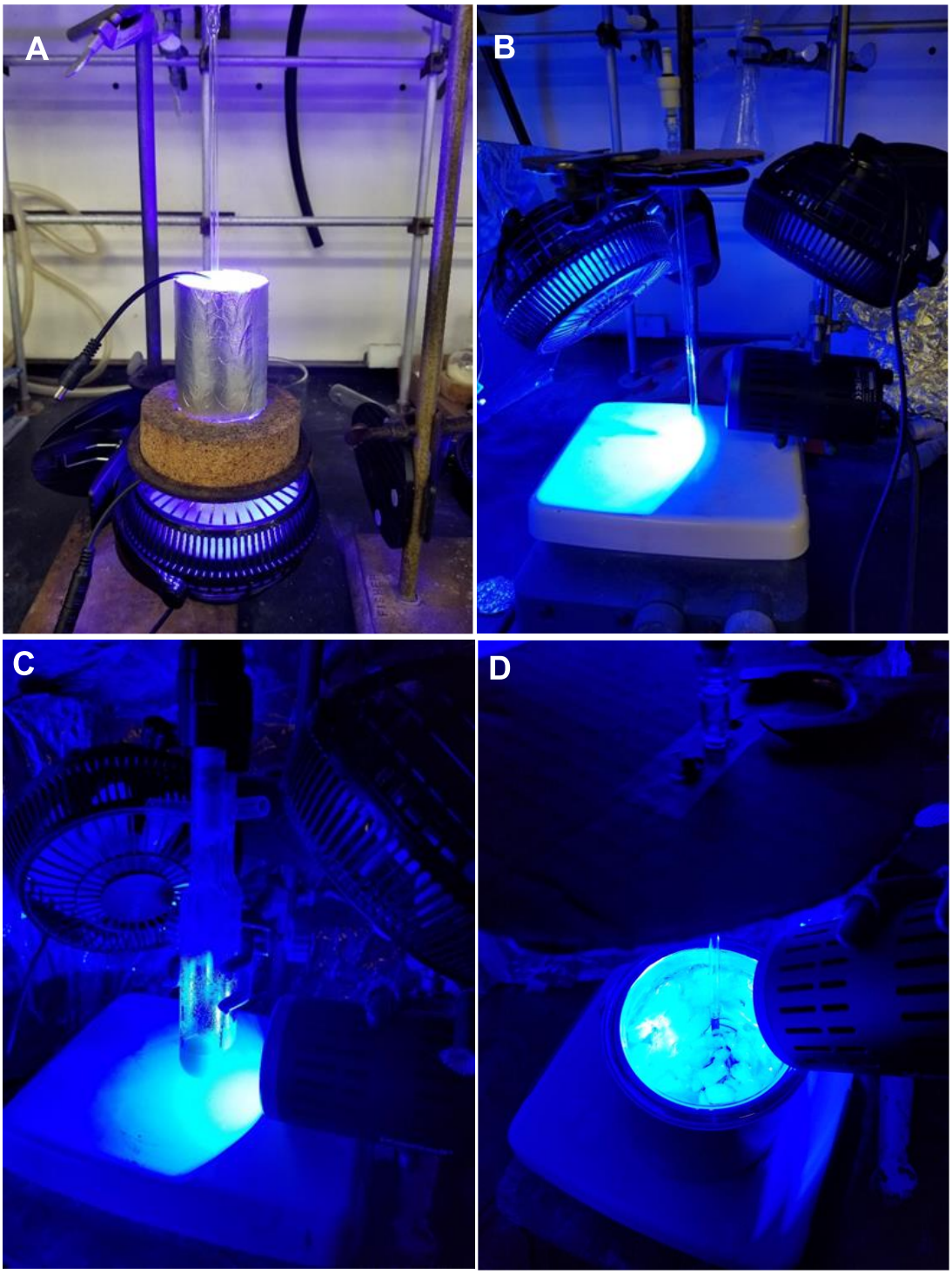

Figure 5.14. Blue Light Irradiation. A: Setup for NMR tube and Schlenk bomb experiments using 14 W LED strips. B: NMR tube experiments using 40 W LED lamp. C: Schlenk bomb experiments using 40 W LED lamp. D. NMR tube experiments in ice/water bath with 40 W Blue LED lamp.

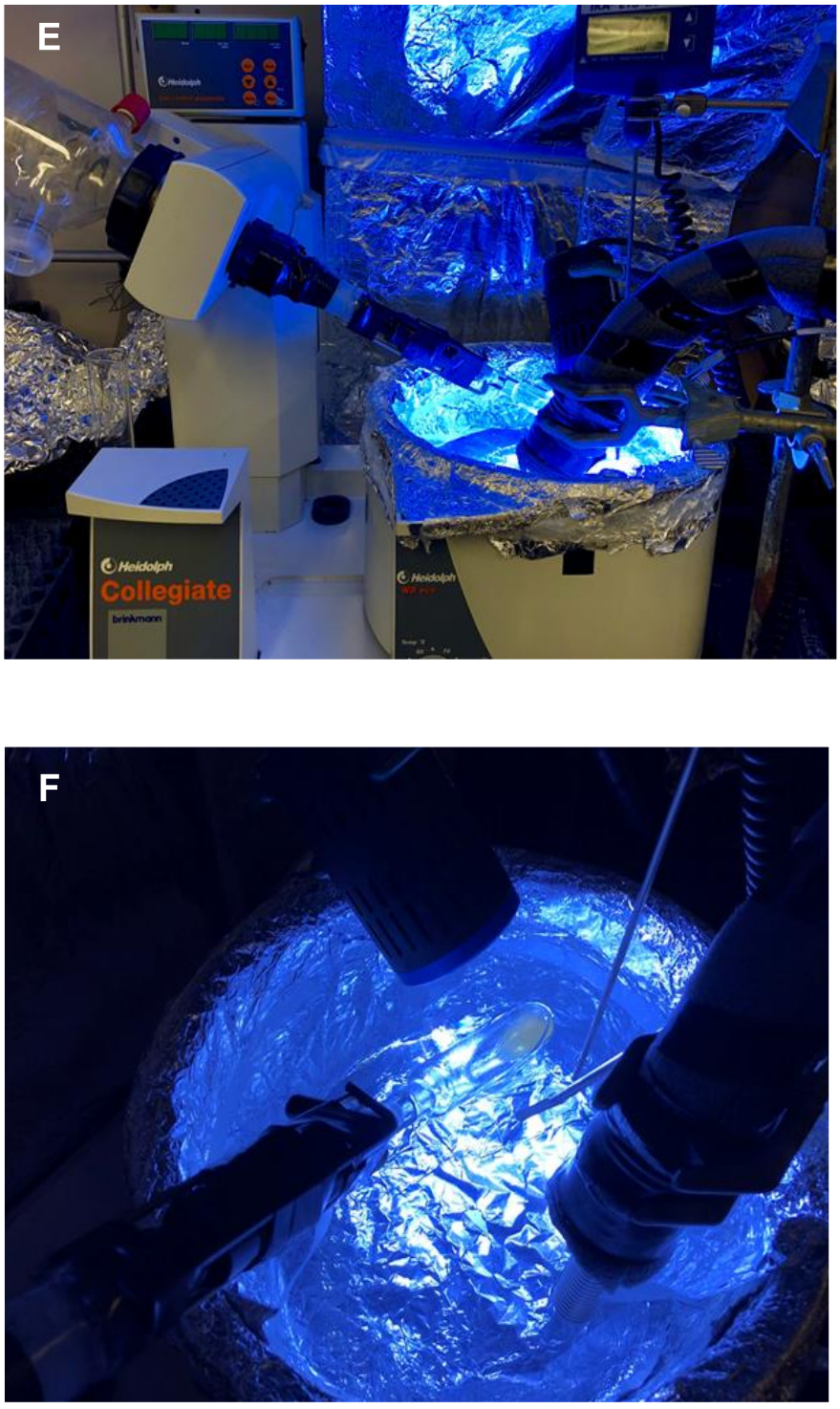

Figure 5.14. Blue Light Irradiation (cont). E: System for low temperature experiments. F: Different view of the system used for low temperature experiments.

5.5.3. Experimental Procedures

Reaction Development

Typical Procedure for Reaction Development with Aryl Iodides (Figure 5.3)

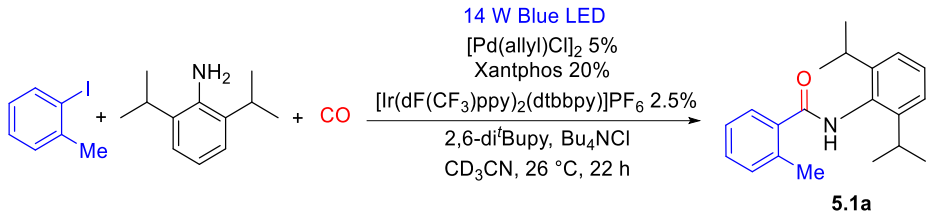

In a glovebox, 2-iodotoluene (13 mg, 0.06 mmol), 2,6-diisopropylaniline (7.1 mg, 0.04 mmol), 2,6-di-*tert*-butylpyridine (11 mg, 0.06 mmol), Bu_4NCl (11 mg, 0.04 mmol), Xantphos (4.6 mg, 8 µmol), $[Ir(dF(CF_3)ppy)_2(dtbbpy)]PF_6$ (1.1 mg, 1 µmol) and benzyl benzoate standard (4.2 mg, 0.02 mmol) were dissolved in were dissolved in 0.75 mL of a 2.7 mM solution of $[Pd(allyl)Cl]_2$ in CD_3CN. The latter was prepared by dissolving 7.3 mg of $[Pd(allyl)Cl]_2$ in 7.5 mL CD_3CN (total $[Pd(allyl)Cl]_2$ in the reaction = 2 µmol). This solution was transferred into a J-Young NMR tube. The tube was taken out of the glovebox, frozen under liquid nitrogen, evacuated and then 4 atm CO were condensed into the tube. A 14W Blue LED strip was coiled inside a plastic cylinder lined up with aluminum foil. The NMR tube was suspended inside the cylinder using a clamp, and a fan was placed under the source of light to cool the system during irradiation, keeping the temperature at 26 °C (Figure 5.14A). After 22 hours, irradiation was stopped and the yield of amide **5.1a** (34%, relative to limiting amine) was calculated via ^1H NMR analysis relative to the benzyl benzoate internal standard. Similar procedures were followed to screen ligands without the photocatalyst (Figures 5.4 and 5.5.) and the effect of base (Figure 5.4). For the latter, NEt^iPr_2 and collidine showed similar results, but collidine was subsequently used as it is less redox active.

Final Reaction Conditions with Aryl Iodides (Figures 5.4 and 5.5)

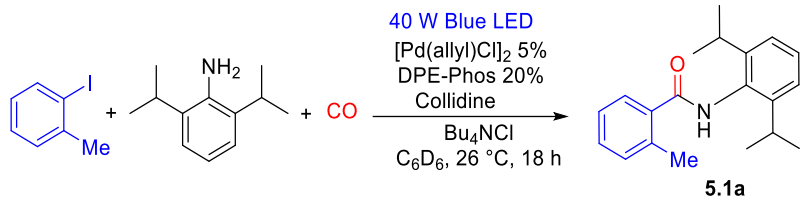

5.1a

An analogous procedure to that described above was performed using collidine (7.3 mg, 0.06 mmol) as base and in 0.75 mL $[Pd(allyl)Cl]_2$ 2.7 mM in C_6D_6 (prepared by dissolving 7.3 mg of $[Pd(allyl)Cl]_2$ in 7.5 mL C_6D_6; total $[Pd(allyl)Cl]_2$ in the reaction = 2 µmol). The reaction mixture was irradiated with a 40W Blue LED lamp as seen in Figure 5.14B and the reaction temperature was kept under 30 °C with a fan. After 20 hours, the yield of amide **5.1a** (99% relative to limiting amine) was calculated via ^{1}H NMR integrations relative to the benzyl benzoate internal standard (amine limiting reagent).

Reaction with Aryl Iodide as Limiting Reagent (Figures 5.4 and 5.5)

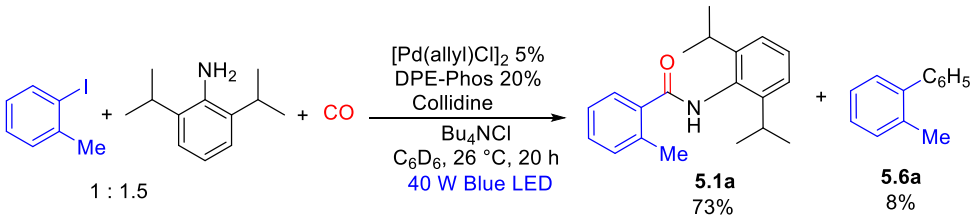

5.1a 73%

5.6a 8%

An analogous reaction to that above was performed with 2-iodotoluene (8.7 mg, 0.04 mmol) and 2,6-diisopropylaniline (11 mg, 0.06 mmol). After 20 hours, the yields of amide **5.1a** (73%) and biaryl **5.6a** (8%) were calculated via ^{1}H NMR integrations relative to the benzyl benzoate internal standard.

Catalytic Formation of Acid Chloride from Aryl Iodide (Figure 5.5C)

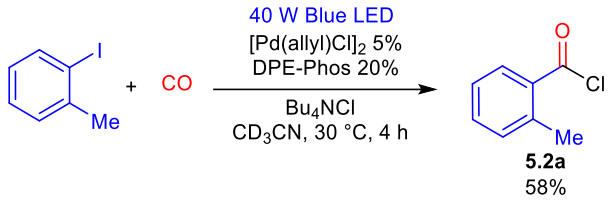

In a glovebox, 2-iodotoluene (8.7 mg, 0.04 mmol), Bu_4NCl (16 mg, 0.06 mmol), DPE-Phos (2.1 mg, 4 µmol), and benzyl benzoate internal standard (4.2 mg, 0.02 mmol) were combined with 0.25 mL of 8 mM $[Pd(allyl)Cl]_2$. The latter was prepared by dissolving 5.8 mg of $[Pd(allyl)Cl]_2$ in 2 mL CD_3CN (total $[Pd(allyl)Cl]_2$ in the reaction = 2 µmol). This mixture was transferred to a J-Young NMR tube and the vial was washed with 2 x 0.25 mL portions of CD_3CN and combined with the solution in the tube. The tube was sealed with a screw-cap, taken out of the glovebox, frozen under liquid nitrogen, evacuated and then 4 atm CO were condensed into the tube. The reaction mixture was irradiated with a 40W Blue LED lamp (Figure 5.14B) and the reaction temperature was kept under 30 ºC with two fans. After 4 hours, the yield of acid chloride **5.2a** was 58%. The identity of *o*-toluoyl chloride was confirmed by *in situ* ^1H and ^{13}C NMR and comparison to the known compound and subsequent derivatization.

In situ ^1H NMR of **5.2a** (500 MHz, CD_3CN) δ 8.22 (dd, J = 8.0, 1.4 Hz, 1H), 2.53 (s, 3H). I*n situ* ^{13}C NMR (126 MHz, CD_3CN) δ 168.2, 142.3, 135.6, 134.7, 133.1, 133.0, 127.6, 22.0.

Pure *o*-$CH_3C_6H_4COCl$; ^1H NMR (500 MHz, CD_3CN) δ 8.21 (dd, J = 8.1, 1.4 Hz, 1H), 7.58 (td, J = 7.6, 1.4 Hz, 1H), 7.44 – 7.38 (m, 1H), 7.38 – 7.33 (m, 1H), 2.52 (s, 3H): ^{13}C NMR (126 MHz, CD_3CN) δ 168.2, 142.3, 135.6, 134.7, 133.1, 133.0, 127.6, 22.0.

The formation of acid chloride was further confirmed by its derivatization to a known N-benzyl amide. In a glovebox, 2-iodotoluene (54 mg, 0.25 mmol), Bu_4NCl (104 mg, 0.37 mmol), DPE-Phos (26.9 mg, 0.05 mmol), and $[Pd(allyl)Cl]_2$ (4.6 mg, 0.012 mmol) were dissolved in 3.5 mL

MeCN and transferred into a thick-walled 25 mL teflon cap sealable Schlenk bomb and equipped with a magnetic stir bar. The bomb was sealed, taken out of the glovebox, 4 atm CO was added on top of the nitrogen atmosphere, and then clamped on top of a stirring plate and irradiated using an LED lamp as seen in Figure 5.14C. After 24 hours, the bomb was taken out of the irradiation system, the excess CO was removed on a Schlenk line, and the bomb was brought into the glovebox. Benzylamine (32 mg, 0.30 mmol) and *N*,*N*-diisopropylethylamine (49 mg, 0.37 mmol) in 0.5 mL MeCN was added to the reaction and stirred for 30 minutes at room temperature outside the glovebox. The solvent was removed *in vacuo*, and product was isolated by flash chromatography on silica gel (230-400 mesh) with hexanes-ethyl acetate (3:1), leading to the isolation of amide **5.1ll** in 66% yield (37 mg, 0.17 mmol) as a white solid.

***N*-benzyl-2-methylbenzamide (5.1ll)**. Isolated yield 66% (37 mg, 0.17 mmol). White solid. ^{1}H NMR (500 MHz, $CDCl_3$) δ 7.36 (d, J = 4.4 Hz, 5H), 7.33 – 7.28 (m, 2H), 7.22 (d, J = 7.6 Hz, 1H), 7.18 (td, J = 7.5, 1.3 Hz, 1H), 6.07 (s, 1H), 4.62 (d, J = 5.7 Hz, 2H), 2.47 (s, 3H). ^{13}C NMR (126MHz, $CDCl_3$) δ 170.0, 138.3, 136.4, 136.3, 131.2, 130.1, 128.9, 128.0, 127.7, 126.8, 125.9, 44.0, 20.0. HRMS: Calculated for $C_{15}H_{16}ON$ (MH^+): 226.12264, found: 226.12282.

Typical Procedure for Reaction Development with Aryl Bromides (Figure 5.11)

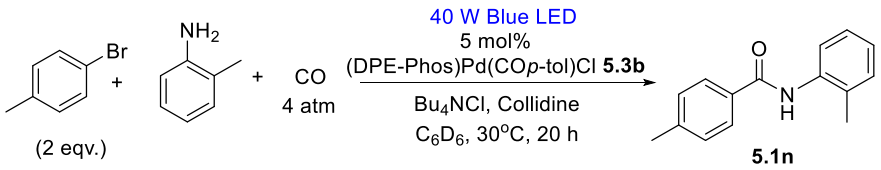

In a glovebox, 4-bromotoluene (14 mg, 0.08 mmol), *o*-toluidine (4.3 mg, 0.04 mmol), collidine (9.7 mg, 0.08 mmol), Bu_4NCl (1.7 mg, 0.04 mmol), complex **5.3b** (4.2 mg, 2 μmol) and benzyl benzoate (4.2 mg, 0.02 mmol) were dissolved in 0.8 mL of C_6D_6 and transferred into a 25 mL teflon cap sealable thick-walled Schlenk bomb equipped with a magnetic stir bar. An aliquot was

taken out for initial ^{1}H NMR analysis. The bomb was sealed with a Teflon cap, taken out of the glovebox, 4 atm CO was added on top of the N_2 atmosphere, and irradiated with a 40W blue LED as above (see Figure 5.14B). The reaction temperature was kept under 30 °C with a fan. After 20 h, the yield of amide **5.1n** (19% amine limiting reagent) the biaryl 4-$CH_3C_6H_4$-C_6D_5 (24%) were calculated via ^{1}H NMR analysis relative to the benzyl benzoate internal standard.

Typical Procedure for Aryl Bromide Carbonylation at Low Temperature (Figure 5.11)

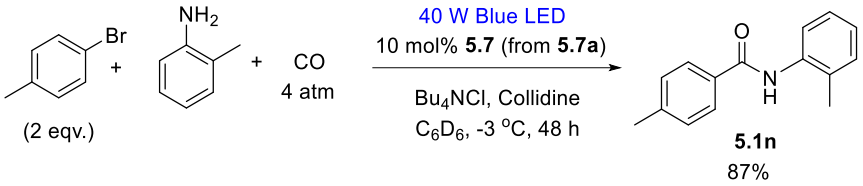

In a glovebox, 4-bromotoluene (85.6 mg, 0.50 mmol), *o*-toluidine (26.8 mg, 0.25 mmol), collidine (61 mg, 0.50 mmol), Bu_4NCl (69 mg, 0.25 mmol), **5.7** (16.5 mg, 13 μmol), and benzyl benzoate (25.4 mg, 0.12 mmol) were dissolved in 6 mL benzene and transferred into a thick-walled 25 mL Schlenk bomb, and sealed with a Teflon cap. The bomb was taken out of the glovebox and 4 atm CO was added on top of the N_2 atmosphere. The bomb was attached to a rotary evaporator with electrical tape. The solution was rotated at 100 rpm and cooled down to - 3 ºC by a cooling bath equipped with a chiller. The solution was irradiated using a 40W Blue LED lamp. (Figure 5.14E and F) After 48 hours, the bomb was taken out of the irradiation system and the excess CO was removed by opening the bomb inside a well-ventilated fume hood. The yield of amide **5.1n** (87%, amine limiting reagent) and the biaryl 4-$CH_3C_6H_4$-C_6D_5 (**5.6b,** 34%) were calculated via ^{1}H NMR analysis relative to the benzyl benzoate internal standard.

Typical Procedure for Reaction Development for Alkyl Acid Chloride Synthesis (Figure 5.12A)

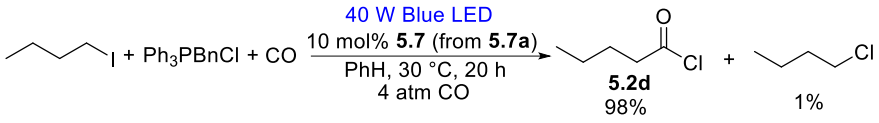

Catalyst **7** was generated in situ as follows. In a glovebox, 1-iodobutane (46 mg, 0.25 mmol), Ph_3PBnCl (107 mg, 0.275 mmol), $[(DPE\text{-}Phos)Pd]_2(\mu\text{-}CO)$ **5.7a** (16 mg, 0.0125 mmol), and benzyl benzoate standard (26 mg, 0.125 mmol) were dissolved in 3.5 mL benzene and transferred into a thick-walled 25 mL teflon cap sealable Schlenk bomb and equipped with a magnetic stir bar. The bomb was taken out of the glovebox, and 4 atm CO was added on top of the nitrogen atmosphere, leading to the rapid in situ generation of catalyst **5.7**. The reaction mixture was irradiated with a 40W Blue LED lamp as seen in Figure 5.14C and the reaction temperature was kept under 30 °C with fans. After 20 hours, excess CO was removed on a Schlenk line, and the bomb was brought back into the glovebox. A 0.1 mL aliquot was taken, the solvent removed in vacuo, and the material dissolved in C_6D_6. ^1H NMR shows the formation of acid chloride **5.2d** in 98% NMR yield relative to the internal standard and only traces of alkyl chloride.

Typical Procedure for Reaction Development with Alkyl Halides (Figure 5.12B)

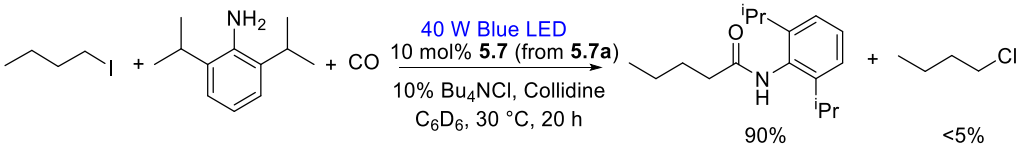

Catalyst **5.7** was generated in situ as follows. In a glovebox, 1-iodobutane (7.4 mg, 0.04 mmol), 2,6-diisopropylaniline (11 mg, 0.06 mmol), Bu_4NCl (1.1 mg, 0.004 mmol), collidine (7.3 mg, 0.06 mmol), $[(DPE\text{-}Phos)Pd]_2(\mu\text{-}CO)$ **5.7a** (2.6 mg, 0.002 mmol), and benzyl benzoate standard (4.2 mg, 0.02 mmol) were dissolved in 0.75 mL C_6D_6 and transferred into a J-Young NMR tube. The

tube was taken out of the glovebox, frozen under liquid nitrogen, evacuated and then 4 atm CO were condensed into the tube, leading to the rapid in situ generation of catalyst **5.7**. The reaction mixture was irradiated with a 40W Blue LED lamp as seen in Figure 5.14B and the temperature was kept under 30 °C with a fan. Yields were calculated via ^{1}H NMR integrations relative to the internal standard and show the formation of amide in 90% yield with <5% alkyl chloride side-product.

Synthesis of Palladium Complexes

Synthesis of [(DPE-Phos)Pd]$_2$(μ-CO) (5.7a)

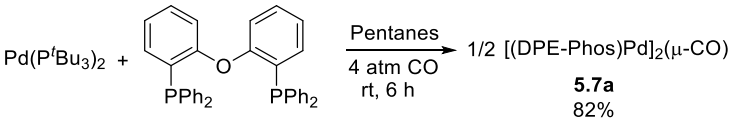

In a glovebox, a 20 mL vial was charged with Pd(P^{t}Bu$_3$)$_2$ (77 mg, 0.15 mmol) and DPE-Phos (89 mg, 0.17 mmol). The mixture was dissolved in pentanes (5 mL) and transferred into a thick-walled teflon cap sealable 50 mL Schlenk bomb equipped with a magnetic stir bar. Any remaining solids in the vial were transferred using additional pentanes (5 mL). The bomb was sealed with a Teflon cap and taken out of the glovebox. 4 atm CO was added to top of the nitrogen atmosphere, and the solution stirred for 6 h at room temperature. The resulting solution was frozen under liquid nitrogen, the CO headspace was removed under vacuum on a Schlenk line, and the vessel was refilled with N_2. The frozen solution was then thawed and brought back into the glovebox. The resulting suspension was poured into a 20 mL vial and the pentanes were decanted. The remaining solid was washed with 3 X 3 mL pentanes. Residual solvent was removed *in vacuo* for 10 minutes,

affording [(DPE-Phos)Pd]$_2$(μ-CO) **5.7a** (82 mg, 0.06 mmol) as an orange solid. Due to poor solubility, a satisfactory ^{13}C NMR spectra of **5.7a** could not be obtained.

^{1}H NMR (500 MHz, C_6D_6): δ 7.71 (d, *J* = 6.8 Hz, 16H), 6.93 – 6.84 (m, 24H), 6.72 (t, *J* = 7.1 Hz, 8H), 6.61 (d, *J* = 8.2 Hz, 4H), 6.50 (td, *J* = 7.4, 1.2 Hz, 4H). ^{31}P NMR (203 MHz, C_6D_6) δ 6.11 (s). IR υ_{CO} = 1809 cm^{-1}. HRMS was acquired by ESI from a MeCN solution of **5.7a** with dry ^{i}PrOH as an additive. Analysis for $C_{73}H_{57}O_3P_4Pd_2$, Theory: 1317.13223, Found: 1317.13487.

In Situ Generation of (DPE-Phos)Pd(CO)$_2$ (5.7)

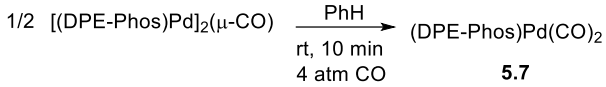

In a glovebox, [(DPE-Phos)Pd]$_2$(μ-CO) **5.7a** (5 mg, 4 μmol) was suspended in 0.75 mL CD_2Cl_2 and transferred into a J-Young NMR tube. The tube was sealed with a screw-cap and taken out of the glovebox. The tube was frozen, evacuated, and then charged with 1 atm of CO. NMR analysis shows the quantitative, *in situ* formation of **5.7**. This complex reverts to **5.7a** immediately upon removal of the carbon monoxide atmosphere, precluding its isolation. ^{1}H, ^{13}C, and ^{31}P NMR spectra were acquired at room temperature and at -75 ºC, and are analogous to that reported for related complexes.[56] IR and UV/Vis analyses were performed by generating **5.7** in an analogous procedure either in a sealed cuvette (Figure S5.2A), or in a vial and quickly transferring by syringe into a CO purged IR cell (Figure S5.2B). Of note, the IR analysis shows υ_{CO} at 1994 and 1846 cm^{-1}, suggesting this complex may instead contain one terminal and one bridging CO ligand (e.g. [(DPE-Phos)Pd(CO)]$_2$(μ-CO)).

^{1}H NMR (500 MHz, CD_2Cl_2): δ 7.42 – 7.33 (m, 9H), 7.33 – 7.25 (m, 11H), 7.08 (td, *J* = 7.7, 1.7 Hz, 2H), 6.81 (t, *J* = 7.4 Hz, 2H), 6.77 (dd, *J* = 8.2, 4.2 Hz, 2H), 6.59 (td, *J* = 7.3, 1.7 Hz, 2H). ^{31}P NMR (162 MHz, CD_2Cl_2) δ 6.62 (s). ^{13}C NMR (101 MHz, CD_2Cl_2, -75 ºC, formed with ^{13}C labeled

CO) δ 193.7 (t, *J* = 5.2 Hz), 157.3 (d, *J* = 13.0 Hz), 135.1 (d, *J* = 23.5 Hz), 133.2 (d, *J* = 15.2 Hz), 130.3, 129.0, 128.1, 128.0, 127.1 (d, *J* = 19.9 Hz), 123.5, 120.4. IR υ_{CO} = 1994 and 1846 cm^{-1}.

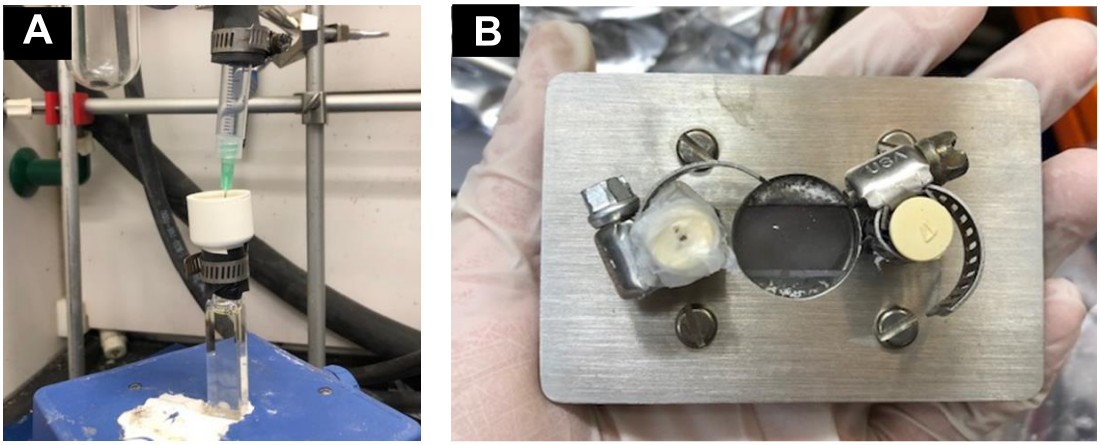

Figure 5.15. Sample Preparation for UV-vis (A) and IR (B).

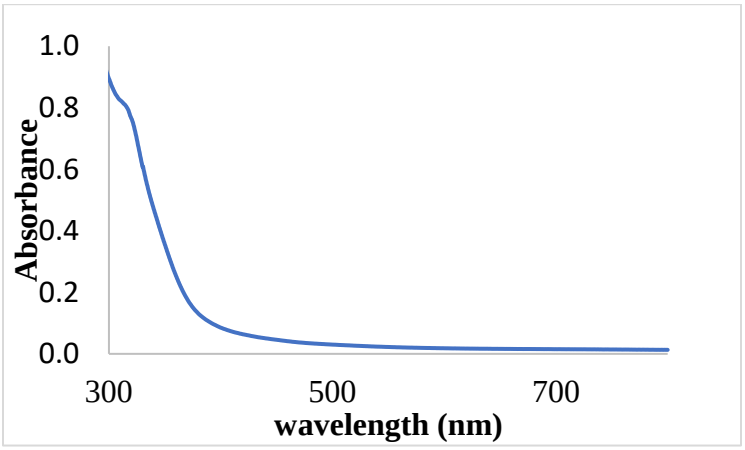

Figure 5.16. UV-Vis Spectrum of 5.7 in Benzene

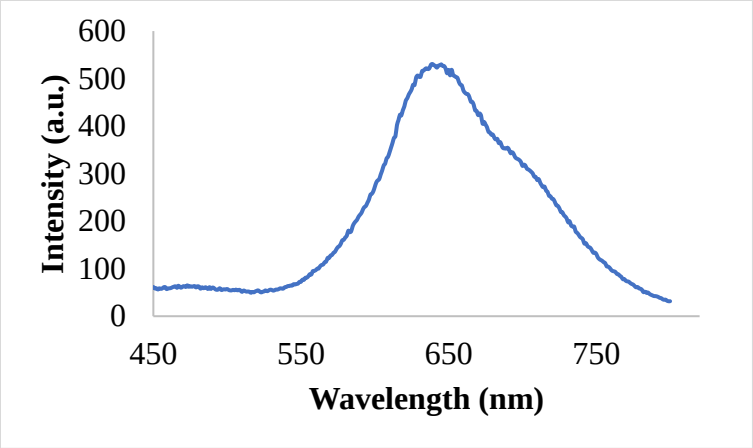

Figure 5.17. Emission Spectrum of 5.7 in Benzene (Excitation at 320 nm)

Synthesis of (DPE-Phos)Pd(CO(*p*-Tolyl))Cl (5.3b)

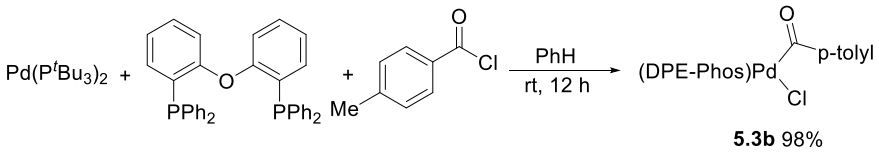

5.3b 98%

A modified literature procedure was employed.[55] In a glovebox, a 20 mL vial was charged with $Pd(P^tBu_3)_2$ (100 mg, 0.196 mmol) and DPE-Phos (116 mg, 0.215 mmol). Benzene (2 mL) was added to the vial and it was swirled for 5 minutes, affording a bright yellow solution. *p*-Toluoyl chloride (45 mg, 0.29 mmol) in 2 mL benzene was added, and the vial was swirled for 2 minutes. The mixture was allowed to stand for 12 h, after which a yellow solid had precipitated. The excess benzene was decanted, and the resulting solid was washed with 2 mL benzene, followed by 3 X 2mL pentanes. The residual solvent was removed *in vacuo,* affording **5.3b** (153 mg, 0.191 mmol) as a bright yellow solid.

^{1}H NMR (800 MHz, Methylene Chloride-d_2, -10 ºC) δ 7.65 (s, 5H), 7.50 (t, J = 7.4 Hz, 1H), 7.48 – 7.42 (m, 3H), 7.42 – 7.40 (m, 1H), 7.38 (s, 2H), 7.27 – 7.20 (m, 2H), 7.20 – 7.12 (m, 2H), 7.08 (s, 3H), 7.05 – 7.00 (m, 2H), 6.97 (s, 4H), 6.68 (t, J = 7.4 Hz, 1H), 6.61 (dd, J = 7.4, 4.4 Hz, 1H),

6.37 (s, 1H), 2.27 (s, 3H). ^{13}C NMR (201 MHz, CD_2Cl_2, 20 ºC) δ 226.0 (d), 158.7 (bs), 142.5, 136.9, 136.7, 136.6, 135.8 (bs), 135.3 (bs), 134.1 (bs), 132.9 (bs), 132.0, 131.8 (bs), 131.1, 130.5 (bs), 128.7, 128.6 (bs), 125.8 (bs), 124.6 (bs), 123.3 (bs), 116.9 (bs), 21.8.^{31}P NMR (162 MHz, Methylene Chloride-d_2 25 ºC) δ 10.90 (bs), 2.28 (bs). IR υ_{CO} = 1665 cm^{-1}. Analysis for $C_{44}H_{35}O_2ClP_2PdNa$, Theory: 821.07279, Found: 821.06759.

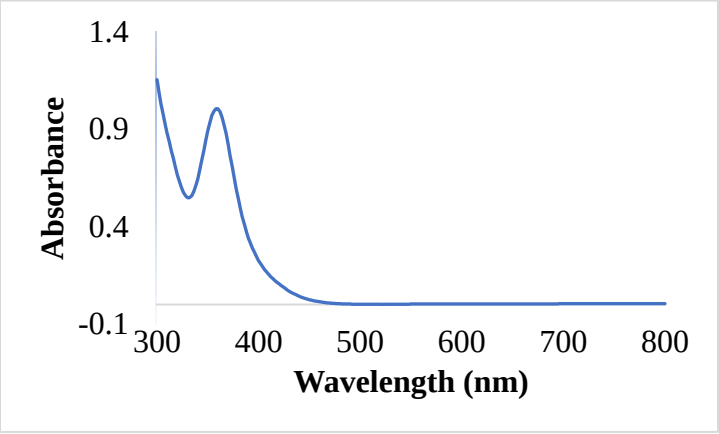

Figure 5.18. UV-Vis Spectrum of 5.3b in Benzene.

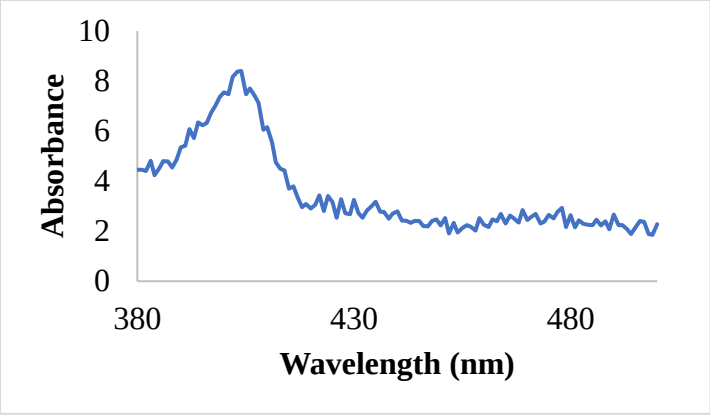

Figure 5.19. Emission Spectrum of 5.3b in Benzene (Excitation at 360 nm).

Synthesis of (DPE-Phos)Pd(CO(*p*-C$_6$H$_4$OCH$_3$))Cl (5.3c)

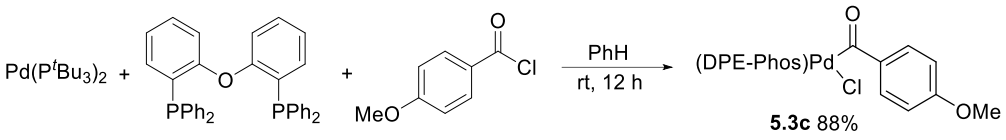

The *p*-methoxyphenyl (PMP) acyl complex **5.3c** was prepared using the same method as **5.3b** above. **5.3c** (141 mg, 0.172 mmol) was isolated as a yellow solid in 88% yield.

^{1}H NMR (800 MHz, Methylene Chloride-d_2, -10 °C) δ 7.70 (d, J = 50.6 Hz, 6H), 7.53 – 7.47 (m, 1H), 7.47 – 7.42 (m, 3H), 7.40 (d, J = 5.8 Hz, 1H), 7.37 (s, 2H), 7.25 – 7.19 (m, 2H), 7.19 – 7.13 (m, 2H), 7.11 – 7.05 (m, 3H), 7.05 – 7.01 (m, 2H), 6.98 (s, 2H), 6.71 – 6.63 (m, 3H), 6.63 – 6.58 (m, 1H), 3.75 (s, 3H). ^{13}C NMR (201 MHz, CD_2Cl_2, 20 ºC) δ 224.7 (d), 162.5, 158.8 (bs), 158.6 (bs), 135.8 (bs), 135.3(bs), 134.2 (bs), 133.0, 132.4, 132.2, 132.1, 131.7 (bs), 130.8 (bs), 130.5 (bs), 128.6 (bs), 125.8 (bs), 124.6 (bs), 124.4 (bs), 123.3 (bs), 116.9, 113.2, 55.9. ^{31}P NMR (162 MHz, CD_2Cl_2, 25 ºC) δ 10.9, 2.2. Analysis for $C_{44}H_{35}O_3P_2Pd$ (M-Cl), Theory: 779.10908, Found: 779.11267.

Synthesis of (DPE-Phos)Pd(CO(*p*-C$_6$H$_4$OCH$_3$))I (5.3c-I)

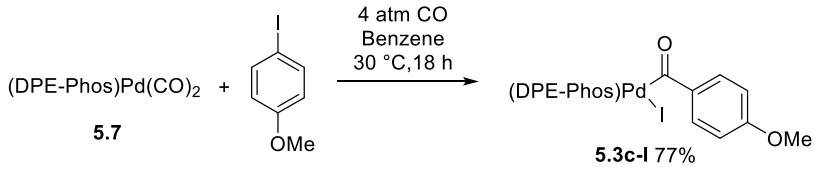

Complex **5.7** was generated in situ as follows: in a glovebox, [(DPE-Phos)Pd](μ-CO) **5.7a** (30 mg, 0.020 mmol) was suspended in 4 mL benzene and transferred into a 25 mL teflon cap sealable thick-walled Schlenk bomb equipped with a magnetic stir bar. The bomb was sealed with a Teflon cap and taken out of the glovebox. 4 atm of CO were added, affording a pale-yellow solution of

5.7. The contents of the bomb were frozen under liquid nitrogen and the headspace was evacuated on a Schlenk time. The frozen bomb was brought into the glovebox. A solution of 4-iodoanisole (14 mg, 0.06 mmol) in 1 mL benzene was added on top of the frozen solution in the bomb. The vessel was quickly taken out of the glovebox and refilled with 4 atm CO. The bomb was placed inside an oil bath at 30 ºC and stirred for 18 h. The excess CO was then removed on a Schlenk line and the bomb was brought back into the glovebox. The solvent was reduced to 1 mL under vacuum, pentanes (2 mL) was added, and yellow solid precipitated. The solid was collected and washed/triturated with 3x3 mL portions of pentanes. Residual solvent was removed *in vacuo*, affording **5.3c-I** (32 mg, 0.040 mmol) as a yellow solid in 77% yield.

^{1}H NMR (400 MHz, CD_2Cl_2, -20 ºC): δ 7.84 (bs, 3H), 7.69 – 7.50 (m, 5H), 7.48 (bs, 3H), 7.41 (t, *J* = 7.3 Hz, 4H), 7.28 – 7.22 (m, 1H), 7.22 – 6.67 (m, 11H), 6.60 (q, *J* = 8.1, 7.5 Hz, 3H), 6.52 – 6.41 (m, 2H), 3.74 (s, 3H). ^{13}C NMR (201 MHz, CD_2Cl_2) δ 224.6 (d), 162.2, 158.6 (bs), 138.3, 136.9, 136.5 (d), 135.9 (bs), 135.4 (bs), 134.7 (bs), 134.3 (d), 133.2, 132.5 (d), 131.4, 131.4, 131.3, 131.2, 130.5 (bs), 128.5, 128.5, 128.4, 127.7, 127.2 (d), 126.1 (bs), 125.0 (bs), 124.2 (bs), 120.7 (d), 116.4, 114.1, 112.9, 55.9. ^{31}P NMR (162 MHz, Methylene Chloride-d_2, 25 ºC) δ 4.92, 1.21. IR υ_{CO} = 1637 cm^{-1}. Analysis for $C_{44}H_{35}O_3P_2Pd$ (M-I), Theory: 779.10908, Found: 779.11048.

Synthesis of (DPE-Phos)Pd(CO(*p*-C$_6$H$_4$CH$_3$))I (5.3b-I)

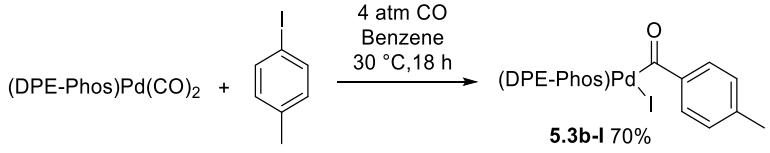

5.3b-I was synthesized using the same method as 5.**3c-I**. The product was isolated as a yellow solid in 70% (29 mg, 0.030 mmol) yield.

^{1}H NMR (400 MHz, $CDCl_3$, -20 ºC): δ 7.66 – 7.52 (m, 4H), 7.44 (d, *J* = 6.1 Hz, 5H), 7.35 (d, *J* = 8.0 Hz, 5H), 7.20 – 7.13 (m, 3H), 7.11 – 7.04 (m, 4H), 6.98 (p, *J* = 8.4, 7.8 Hz, 6H), 6.85 (d, *J* = 7.5 Hz, 2H), 6.62 (t, *J* = 7.5 Hz, 1H), 6.54 – 6.45 (m, 2H), 2.19 (s, 3H). ^{13}C NMR (201 MHz, CD_2Cl_2) δ 226.0 (d), 158.6 (bs), 142.1, 141.3, 141.2, 141.1, 138.3, 136.5 (d), 135.8 (bs), 134.7 (bs), 134.3 (d), 132.5 (d), 131.4, 131.3, 131.3, 131.2, 130.5 (bs), 128.5, 128.4, 128.4, 127.7, 127.2, 127.2, 125.0, 120.7 (d), 116.4 (bs), 21.7. ^{31}P NMR (162 MHz, CD_2Cl_2, 25 ºC) δ 4.5 (bs), 1.4 (bs). IR υ_{CO} = 1657 cm^{-1}. Analysis for $C_{44}H_{35}O_2IP_2PdNa$, Theory: 913.00840, Found: 913.01001.

Synthesis of (DPE-PhosPd(CO(*p*-Tolyl))Br (5.3b-Br)

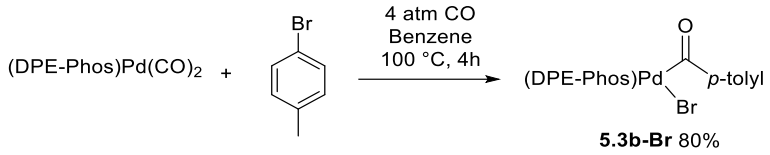

5.3b-Br 80%

(DPE-Phos)Pd(CO(*p*-Tolyl))Br **5.3b-Br** was synthesized using similar method as **5.3c-I** but at 100 ºC for 4 h. The product was isolated as a yellow solid in 80% (27.0 mg, 0.032 mmol) yield as a yellow solid.

^{1}H NMR (400 MHz, Benzene-d_6, 25 ºC) δ 8.11 (d, *J* = 8.0 Hz, 2H), 7.72 – 7.61 (m, 4H), 6.96 (s, 16H), 6.78 (t, *J* = 8.3 Hz, 1H), 6.68 (t, *J* = 7.0 Hz, 3H), 6.40 (dd, *J* = 8.0, 4.1 Hz, 5H), 6.30 (t, *J* = 7.6 Hz, 1H), 1.93 (s, 3H). ^{1}H NMR (800 MHz, Methylene Chloride-d_2, -10 ºC) δ 7.84 – 7.57 (m, 8H), 7.57 – 7.50 (m, 2H), 7.40 (d, *J* = 28.6 Hz, 4H), 7.23 (s, 2H), 7.19 – 7.12 (m, 3H), 7.10 (s, 2H), 7.05 (s, 3H), 7.02 – 6.86 (m, 6H), 6.70 – 6.61 (m, 1H), 6.61 – 6.52 (m, 1H), 6.40 (s, 1H), 2.25 (s, 3H). ^{13}C NMR (201 MHz, CD_2Cl_2) δ 225.9, 158.6 (bs), 142.4, 138.3, 138.3, 138.2, 136.5 (d), 135.5 (bs), 135.1 (bs), 134.3, 134.3, 132.9 (bs), 132.5 (d), 131.6 (d), 131.4, 131.3, 131.2, 131.1, 130.5 (bs), 128.6, 128.5, 127.9, 127.2 (d), 125.9 (bs), 124.8 (bs), 120.7 (d), 119.6, 119.1, 116.6 (bs), 21.7. ^{31}P NMR (162 MHz, Methylene Chloride-d_2, 25 ºC) δ 9.46 (bs), 1.61(bs). Analysis for

$C_{43}{}^{13}CH_{36}O_2BrP_2Pd$ ($[M+H]^+$), Theory: 844.04368, Found: 844.04532. Analysis for $C_{44}H_{35}O_2P_2Pd$ ($[M-Br]^+$), Theory: 763.11416, Found: 763.11525. A

Synthesis of (DPE-Phos)Pd(COC_4H_7)I (5.3d)

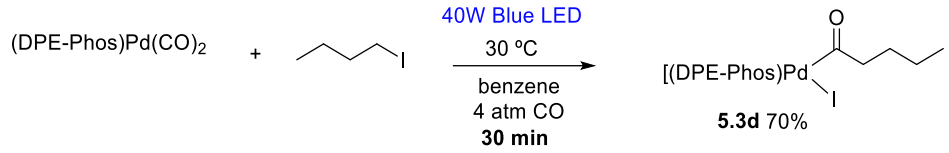

Complex **5.7** was generated as follows: in a glovebox, [(DPE-Phos)Pd](μ-CO) **5.7a** (32.9 mg, 0.025 mmol) was dissolved in 1.5 mL benzene and transferred into a thick-walled 25 mL teflon cap sealable Schlenk bomb equipped with a magnetic stir bar. The suspension was frozen in a-33 °C freezer. A solution of *n*butyl iodide (11.5 mg, 0.063 mmol) in 0.5 mL benzene was added on top of the frozen solution. The bomb was capped, quickly taken out of the glovebox, frozen in liquid nitrogen and 4 atm of CO was added on top of the nitrogen atmosphere, leading to the *in situ* formation of **5.7**. The solution was thawed and then quickly mixed and irradiated using the set-up described in Figure 5.14C for 1 h. The resulting solution was frozen under liquid nitrogen, the CO headspace was removed under vacuum on a Schlenk line and brought back into the glovebox. The resulting suspension was poured into a 20 mL vial, 5 mL pentane slowly added on top of the benzene solution, the vial was placed in a -33 °C freezer for 5 min, and purple precipitate formed. The solvent was decanted and the solid was washed with 2 mL X 3 mL of pentane. The solid was then dissolved in 0.5 mL of benzene and slowly added to another vial that has 5 mL of pentane. Pink solid formed and the solvent was decanted and the solid was then washed with 3 X 3 mL pentane. Residual solvent was removed *in vacuo* for 20 minutes, affording **5.3d** in 70% (15.0 mg, 0.018 mmol) yield as a pink solid.

^{1}H NMR (800 MHz, Benzene-d_6) δ 7.72 (s, 8H), 7.00 (s, 12H), 6.86 (t, J = 4.1 Hz, 2H), 6.66 (t, J = 7.7 Hz, 2H), 6.43 (t, J = 7.6 Hz, 2H), 6.34 (d, J = 7.6 Hz, 2H), 3.01 (s, 2H), 1.44 (p, J = 7.3 Hz, 2H), 1.04 (h, J = 7.4 Hz, 2H), 0.67 (t, J = 7.3 Hz, 3H). ^{13}C NMR (201 MHz, C_6D_6) δ 228.3 (t), 158.6 (m), 135.3 (t), 134.6, 132.3 (m), 131.3, 130.1, 128.4, 125.4 (m), 124.4, 120.3, 59.8 (t), 28.4, 22.4, 14.0. Analysis for $C_{41}H_{36}O_2IP_2Pd$ ($[M+H]^+$), Theory: 855.02646, Found: 855.02729.

Mechanistic Experiments

Irradiation of Complex 5.3b (Figure 5.6A)

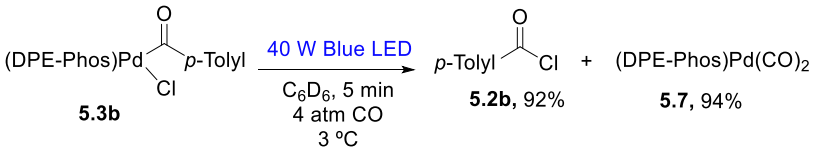

Complex **5.3b** was generated *in situ* to ensure its full dissolution in benzene. In a glovebox, [(DPE-Phos)Pd](μ-CO) **5.7a** (1.3 mg, 1 μmol) was combined with 4-toluoyl chloride (1 μmol) and benzyl benzoate standard (1 μmol) in 0.2 mL C_6D_6.. The latter was prepared by taking 200 μL of a 0.01 mM solution of 4-toluoyl chloride and benzyl benzoate (1:1) in C_6D_6. The mixture was transferred into a J-Young NMR tube and diluted to a final volume of 0.75 mL with C_6D_6. The mixture was swirled at room temperature, affording a bright-yellow homogeneous solution. ^{1}H NMR analysis shows the quantitative formation of complex **5.3b**. The NMR tube was then frozen under liquid nitrogen, evacuated, and then 4 atm CO was condensed into the tube. The NMR tube was quickly placed in an ice/water bath at 3 °C, and then irradiated at 3 °C for 5 minutes with a 40W Blue LED lamp (Figure 5.14D). The cooled tube was placed inside an NMR pre-cooled at 7 °C. ^{1}H NMR analysis showed a mixture of 4-toluoyl chloride **5.2b** (92%), complex **5.7** (94%), and acyl-palladium complex **5.3b** (4%).

In situ data on **5.2b:** ^{1}H NMR (800 MHz, C_6D_6, 7 ºC) δ 7.79 (d, *J* = 8.3 Hz, 2H), 6.60 (d, J = 8.0 Hz, 2H), 1.77 (s, 3H). ^{13}C NMR (201 MHz, C_6D_6, 7 ºC) δ 167.9, 146.4, 131.7, 130.8, 129.7, 21.3. Pure *p*-toluoyl chloride: ^{1}H NMR (500 MHz, C_6D_6) δ 7.77 (d, *J* = 8.4 Hz, 2H), 6.69 (d, *J* = 7.8 Hz, 2H), 1.87 (s, 3H). ^{13}C NMR (126 MHz, C_6D_6) δ 167.8, 146.6, 131.7, 130.9, 129.7, 21.4.

In order to confirm the formation of acid chloride above, it was converted to an *N*-benzyl amide. In a glovebox, [(DPE-Phos)Pd](μ-CO) **5.7a** (33 mg, 0.025 mmol) and 4-toluoyl chloride **5.2b** (8 mg, 0.05 mmol) were dissolved in 8 mL benzene and transferred into thick-walled teflon cap sealable 25 mL Schlenk bomb equipped with a magnetic stir bar. The mixture was stirred for 15 minutes at room temperature to afford a homogeneous solution of **5.3b**. The bomb was taken out of the glovebox, 4 atm CO was added on top of the nitrogen atmosphere, then clamped on top of an ice/water bath at 3 ºC and the solution was irradiated using an LED lamp as seen in Figure 5.14C. After 30 minutes, the bomb was taken out of the irradiation system, frozen under liquid nitrogen, the excess CO was removed on a Schlenk line, and finally the bomb was brought into the glovebox with the contents still frozen. Benzylamine (8 mg, 0.070 mmol) and $NEt^{i}Pr_2$ (9 mg, 0.070 mmol) were dissolved in 0.5 mL benzene and added on top of the frozen solution. The mixture was stirred and allowed to warm up to room temperature for 30 minutes. The solvent was the removed in vacuo, and product isolated by flash chromatography on silica gel (230-400 mesh) with hexanes-ethyl acetate (3:1) to afford *N*-benzyl-4-methylbenzamide in 93% yield (11 mg, 0.046 mmol) as a white solid.

***N*-benzyl-4-methylbenzamide (5.1oo).** Isolated yield 93% (11 mg, 0.046 mmol). White solid. ^{1}H NMR (500 MHz, $CDCl_3$) δ 7.69 (d, *J* = 8.2 Hz, 2H), 7.35 (d, *J* = 4.4 Hz, 4H), 7.30 (ddt, *J* = 7.6, 4.8, 3.7 Hz, 1H), 7.22 (d, *J* = 7.9 Hz, 2H), 6.41 (s, 1H), 4.64 (d, *J* = 5.7 Hz, 2H), 2.39 (s, 3H). ^{13}C

NMR (126MHz, $CDCl_3$) δ 167.4, 142.1, 138.4, 131.7, 129.4, 128.9, 128.1, 127.7, 127.1, 44.2, 21.6. Calculated for $C_{15}H_{16}ON$ (MH^+): 226.12264, found: 226.12236.

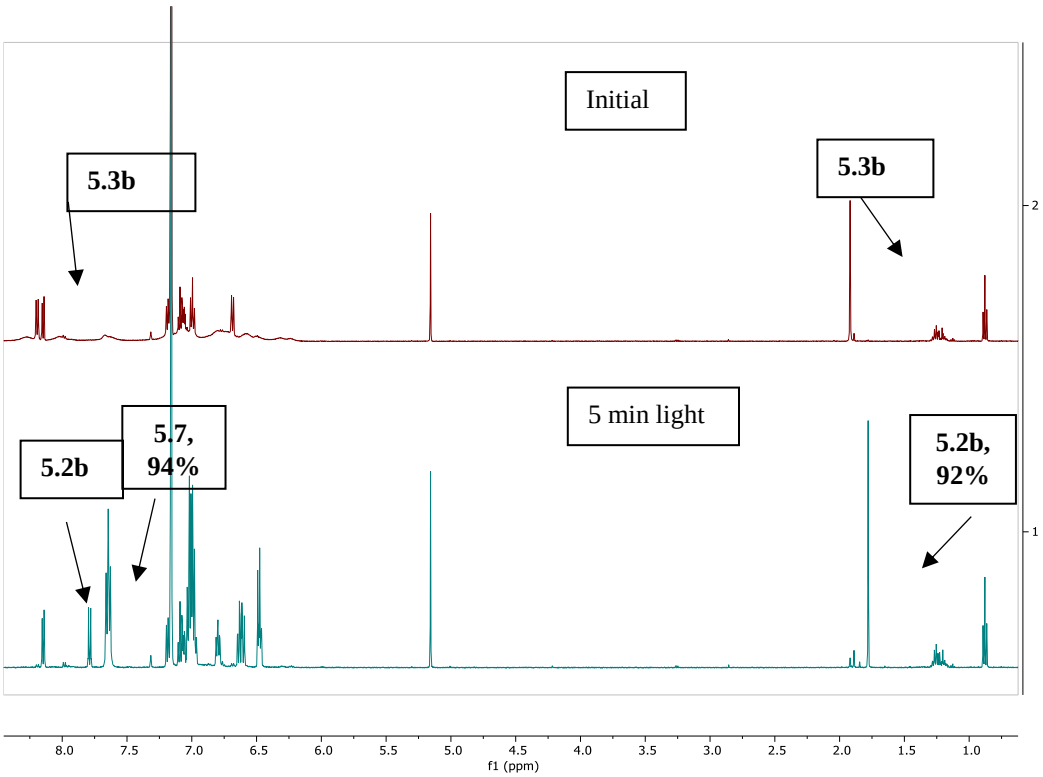

Figure 5.20. ^{1}H NMR Spectra of Irradiation of 5.3b at 3 ºC.

At near room temperature

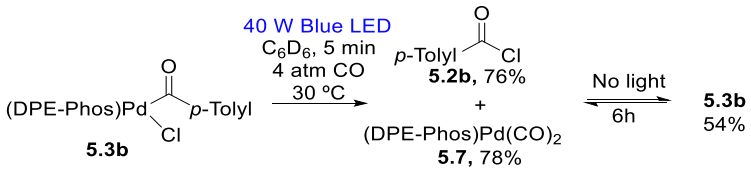

A similar procedure performed at 30 °C led to a mixture of 4-toluoyl chloride **5.2b** (76%), complex **7** (78%), and acyl-palladium complex **5.3b** (18%) after 5 min irradiation. The mixture was then kept in the dark and analyzed by ^{1}H NMR. After 6 hours of no irradiation, it reverted to the thermal equilibrium: **5.3b** (54%), **5.2b** (45%), **5.7** (48%).

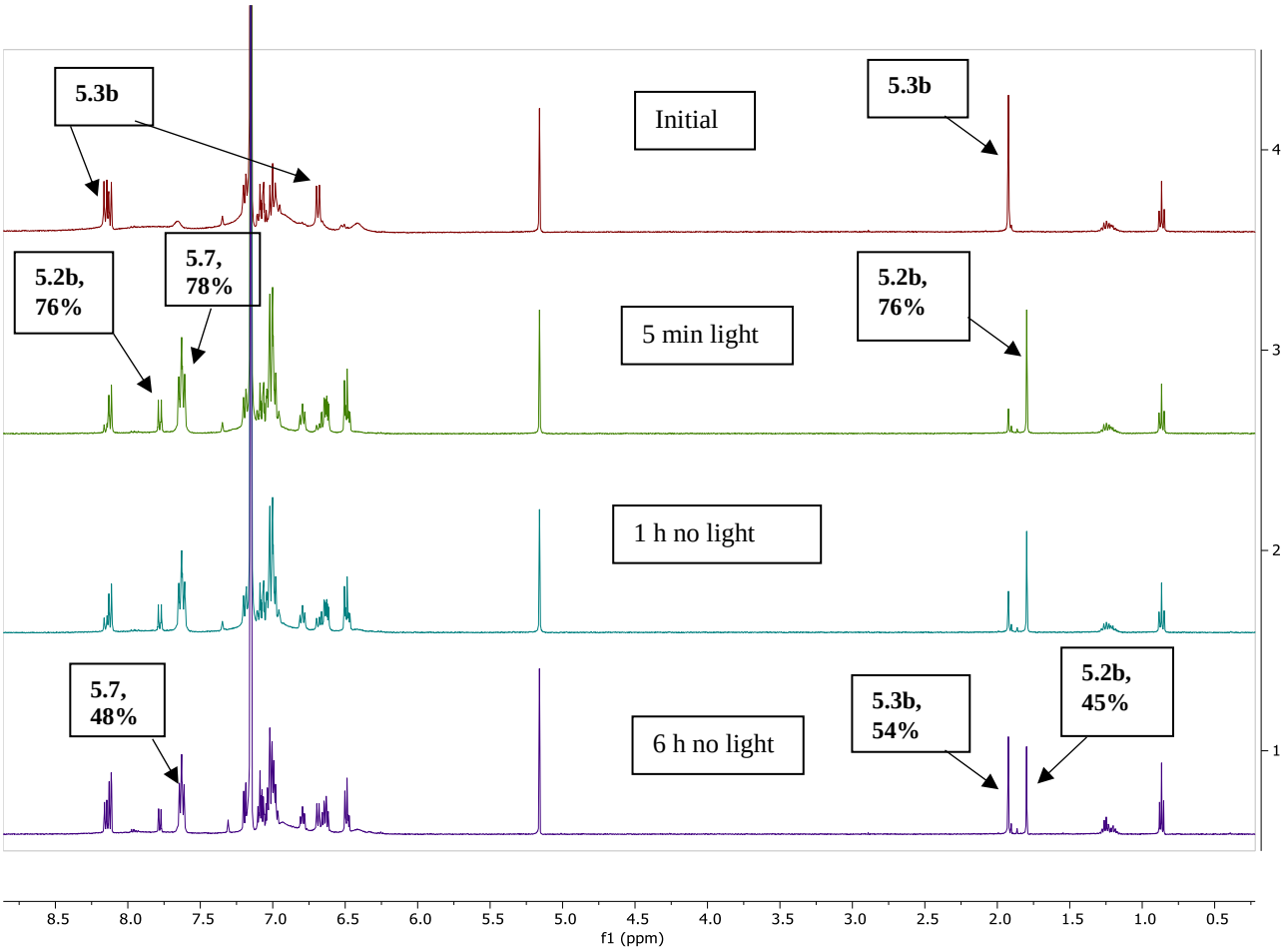

Figure 5.21. ^{1}H NMR Spectra of Irradiation of 5.3b at 30 ºC.

Thermal reductive elimination of acid chloride from 5.3b (Figure 5.6A)

At 7 °C:

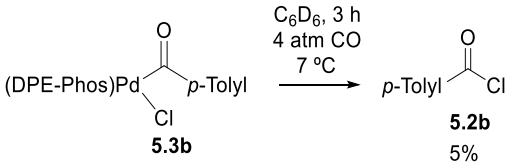

Complex **5.3b** was generated *in situ* as described in experiment 5.3A above and in a J-Young NMR tube. The tube was frozen under liquid nitrogen, evacuated, and 4 atm CO was condensed into the tube. The tube was thawed and immediately placed inside a 500 MHz NMR pre-cooled at 7 ºC

without allowing it to warm further. The mixture was monitored over time with ^{1}H NMR analysis, and the yields were determined by integration using benzyl benzoate as internal standard. For the first 60 minutes, ^{1}H NMR analysis showed no sign of acid chloride **5.2b**. After 3 hours, the yield of **5.2b** was 5%.

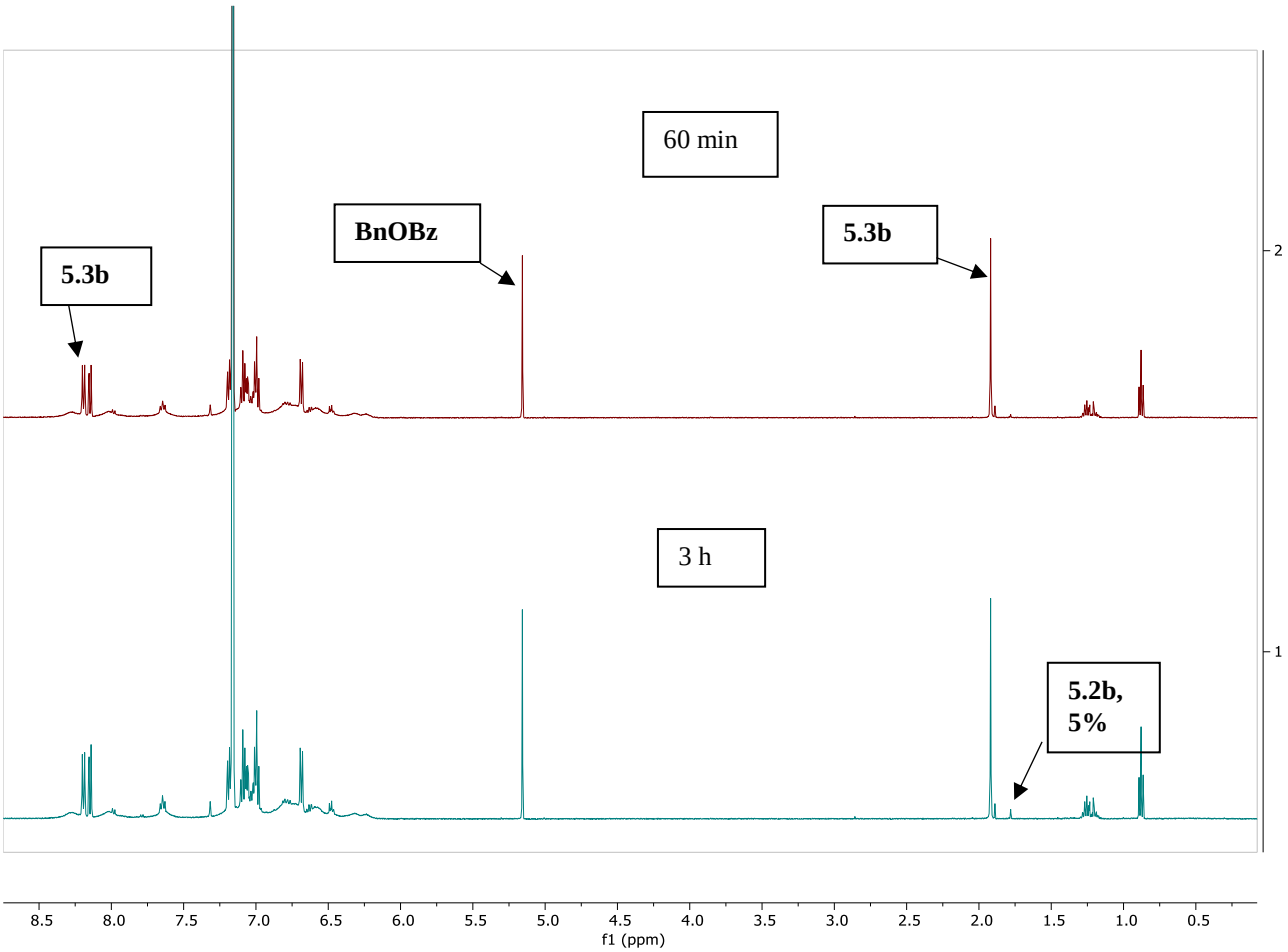

Figure 5.22. ^{1}H NMR Spectra of Thermal Reductive Elimination of Acid Chloride from 5.3b at 7 ºC.

At 30 °C:

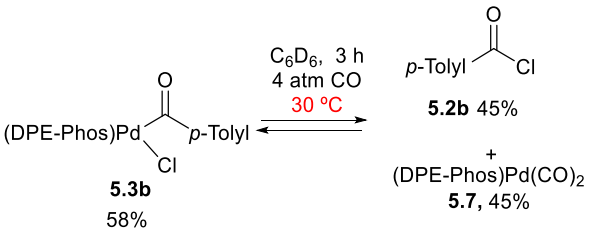

A similar procedure to the above was performed at 30 °C in a 500 MHz NMR. ^{1}H NMR analysis shows the formation of 4% acid chloride **5.2b** and 4% **5.7** after 15 min. After 3 h, the reaction formed an equilibrium mixture of 58% **5.3b**, 45% **5.2b**, and 45% **5.7**. No further change was observed after 3 h.

Thermal and photochemical reactivity of 5.3b in the presence of excess acid chloride 5.2b (Figure 5.6B)

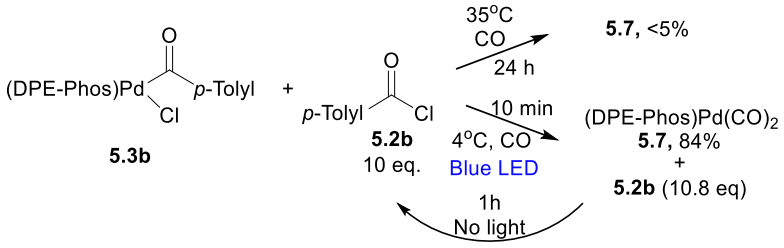

Complex **5.3b** was generated *in situ* to ensure its full dissolution in benzene. In a glovebox, [(DPE-Phos)Pd](μ-CO) **5.7a** (1.3 mg, 1 μmol) was combined with 4-toluoyl chloride (3.0 mg, 0.02 mmol) and benzyl benzoate standard (1 mg, 4 μmol) in 0.75 mL C_6D_6. The mixture was transferred into a J-Young NMR tube and swirled at room temperature, affording a bright-yellow homogeneous solution. The NMR tube was capped and taken out of the glovebox. Then the tube was frozen under liquid nitrogen, evacuated, and 4 atm CO was condensed into the tube. The NMR tube was thawed and placed inside an oil bath at 35 °C. The reaction was monitored via ^{1}H NMR analysis. After 24 hours, less than 5% **5.7** was observed, thus the thermal equilibrium was heavily

suppressed. Afterwards, the tube was frozen under liquid nitrogen, CO was evacuated, and the tube was sealed and brought back into the glovebox. The headspace was refilled with N_2 from the box and the mixture was swirled at room temperature for 15 minutes to fully generate any trace **5.3b** that was lost in the experiment above. The tube was brought out of the glovebox, frozen under liquid nitrogen, evacuated, and 4 atm CO was again condensed into the tube. The NMR tube was thawed and placed inside an ice-water bath at 3 ºC. The tube was irradiated with a 40W Blue LED lamp for 10 minutes (Figure 5.14D). The tube was kept inside an ice-water bath and immediately placed inside a 500 MHz NMR pre-cooled to 7 ºC. ^{1}H NMR analysis showed the formation of **5.7** in 84%, **5.3b** 16% remaining, and an increase in the amount of **5.2b** (10.8 eqs.). ^{31}P NMR analysis showed only a singlet at 7.14 ppm, which correlates with complex **5.7**. The tube was then allowed to stand at room temperature in the dark. After 1 hour, ^{1}H NMR analysis showed that the mixture had reverted to the thermal equilibrium mixture: 95% **5.3b** and 5% **5.7.** ^{31}P NMR analysis showed a small signal at 7.14 (complex **5.7**) and two broad signals at 1.75 and 11.40 ppm (**5.3b**).

Reactivity of Palladium Complex 5.3c-I (Figure 5.6D)

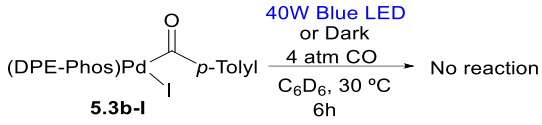

In a glovebox, complex **5.3b-I** (3.6 mg, 0.004 mmol) and benzyl benzoate standard (1 mg, 0.004 mmol) were dissolved in 0.75 mL C_6D_6 and transferred into a J-Young NMR tube. The NMR tube was sealed with a screw-cap, taken out of the glovebox, frozen under liquid nitrogen, evacuated, and 4 atm CO was condensed into the tube. The NMR tube was irradiated using the system shown in Figure 5.14B. After 6 hours of irradiation, ^{1}H NMR analysis shows the amount of **5.3b-I** left in solution was 98%.

A similar procedure was repeated, but instead the tube was placed inside an oil bath at 35 ºC. After 18 hours of irradiation, ^{1}H NMR analysis showed amount of **5.3b-I** left in solution was 96%.

Irradiation of 5.3b in the presence of TEMPO (Figure 5.6D)

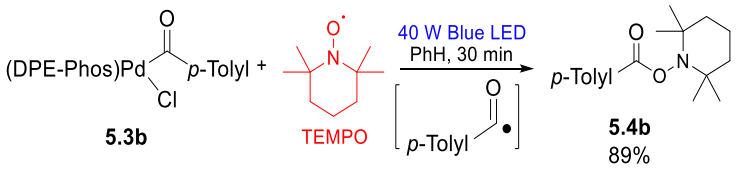

In a glovebox, complex **5.3b** (45 mg, 0.06 mmol) and TEMPO (22 mg, 0.14 mmol) were dissolved in 8 mL benzene and transferred into a thick-walled 25 mL Schlenk bomb, equipped with a magnetic stir bar, and covered with a Teflon cap. The vessel was irradiated for 30 min with a 40W Blue LED lamp (Figure 5.14C). ^{1}H NMR analysis showed the full consumption of **5.3b** and the formation of 2,2,6,6-tetramethylpiperidin-1-yl 4-methylbenzoate **5.4b**. **5.4b** was isolated by flash chromatography on silica gel using hexanes/ethyl acetate (4:1), affording ester **5.4b** as a white solid in 89% yield (14 mg, 0.05 mmol).

2,2,6,6-tetramethylpiperidin-1-yl 4-methylbenzoate (5.4b) ^{1}H NMR (500 MHz, $CDCl_3$) δ 8.04 (d, *J* = 7.9 Hz, 2H), 7.32 (d, *J* = 7.8 Hz, 2H), 2.49 (s, 3H), 1.90 – 1.71 (m, 3H), 1.70 – 1.61 (m, 2H), 1.53 (dt, *J* = 13.7, 3.5 Hz, 1H), 1.34 (s, 6H), 1.18 (s, 6H). ^{13}C NMR (126 MHz, $CDCl_3$) δ 165.3, 142.4, 128.5, 128.1, 125.8, 59.2, 38.0, 30.9, 20.6, 19.8, 15.9. Analysis for $C_{17}H_{26}NO_2$, Theory: 276.19581, Found: 276.19647.

A similar procedure was repeated to prepare the p-methoxyphenyl (PMP) analogue from the PMP acyl complex **5.3c.** Ester **5.4c** was isolated as white solid in 85% yield (15 mg, 0.05 mmol).

2,2,6,6-tetramethylpiperidin-1-yl 4-methoxybenzoate (5.4c)[57] ^{1}H NMR (500 MHz, $CDCl_3$) δ 8.06 – 7.99 (m, 2H), 6.98 – 6.89 (m, 2H), 3.87 (s, 3H), 1.83 – 1.62 (m, 4H), 1.58 (dt, *J* = 12.3, 2.7

Hz, 2H), 1.50 – 1.41 (m, 1H), 1.26 (s, 6H), 1.11 (s, 6H). ^{13}C NMR (126 MHz, $CDCl_3$) δ 166.3, 163.4, 131.7, 122.2, 113.8, 60.5, 55.6, 39.2, 32.1, 21.0, 17.2.

Thermal Reaction of 5.3b with TEMPO (Figure 5.6E)

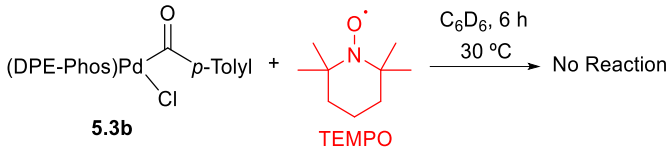

Complex **5.3b** was generated *in situ* in a J-Young NMR tube to ensure its full dissolution in benzene as noted in procedure 3A above. To this was added TEMPO (1.3 mg, 8 µmol) in 0.25 mL C_6D_6. The NMR tube was capped, taken out of the glovebox, and placed inside an oil bath at 30 ºC for 6 h. ^{1}H NMR analysis showed no change over time.

Thermal and Photochemical Reactivity of Acid Chloride 5.2b with TEMPO (Figure 5.6E)

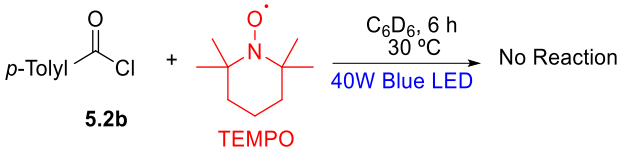

In a glovebox, p-toluoyl chloride (1.5 mg, 0.01 mmol) and TEMPO (3.1 mg, 0.02 mmol) were dissolved in 0.75 mL C_6D_6 in a J-Young NMR tube. The NMR tube was capped, taken out of the glovebox, and irradiated for 6 h using an blue LED lamp as seen in Figure 5.14B. ^{1}H NMR analysis showed no change over 6 h.

A similar procedure was repeated, but instead the NMR tube was placed inside an oil bath at 30 ºC for 6 h. ^{1}H NMR analysis showed no change over 6 h.

Irradiation of 5.3b-I in the Presence of 1-Octanethiol (Figure 5.6D)

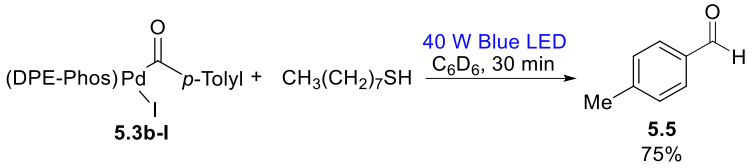

In a glovebox, complex **5.3b-I** (3.6 mg, 0.004 mmol) and benzyl benzoate (1 mg, 0.004 mmol) were dissolved in 0.6 mL C_6D_6 and transferred into a J-Young NMR tube. The solution was frozen in a -33 ºC freezer. On top of the frozen solution was added 1-octanethiol (12 mg, 0.08 mmol) in 0.2 mL C_6D_6. The NMR tube was sealed with a screw-cap, taken out of the glovebox, thawed and then quickly irradiated using the setup described in Figure 5.14B. After 30 minutes, ^{1}H NMR analysis shows the formation of *p*-tolualdehyde **5.5** in 75% yield.

In situ data on **5.5:** ^{1}H NMR (500 MHz, C_6D_6) δ 9.70 (s, 1H), 7.50 (d, *J* = 8.1 Hz, 2H), 1.92 (s, 3H) (overlap with another signal). ^{13}C NMR (126 MHz, C_6D_6) δ 190.9, 144.8, 135.0, 129.8, 129.7, 21.5. GC-MS = 135.1 (M-1)

Pure *p*-tolualdehyde: ^{1}H NMR (500 MHz, C_6D_6) δ 9.71 (s, 1H), 7.50 (d, *J* = 8.1 Hz, 2H), 6.82 (d, *J* = 8.1 Hz, 2H), 1.93 (s, 3H).^{13}C NMR (126 MHz, C_6D_6) δ 191.0, 144.9, 135.0, 129.8, 129.7, 21.5.

Irradiation of 5.3b in the Presence of 1-Octanethiol (Figure 5.6F)

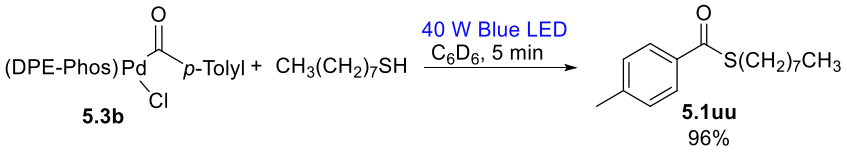

In a glovebox, complex **5.3b** (3.2mg, 0.004 mmol) and benzyl benzoate standard (1 mg, 0.004 mmol) were dissolved in 0.6 mL C_6D_6 and transferred into a J-Young NMR tube. The solution was frozen in a -33 ºC freezer. On top of the frozen solution was added 1-octanethiol (12 mg, 0.08 mmol) in 0.2 mL C_6D_6. The NMR tube was sealed with a screw-cap and taken out of the glovebox.

The mixture was thawed and quickly irradiated using the setup described in Figure 5.14B. After 5 minutes, ^{1}H NMR analysis shows full consumption of **5.3b** and near quantitative formation of thioester *p*-$CH_3C_6H_4C(O)SC_8H_{17}$ **5.1uu** (96%). The product was characterized *in situ* by comparison with a pure sample:

In situ data on p-$CH_3C_6H_4CO(SC_8H_{17})$: ^{1}H NMR (500 MHz, Benzene-d_6) δ 8.04 (d, *J* = 8.1 Hz, 2H), 6.83 (d, *J* = 7.9 Hz, 2H), 3.03 (t, *J* = 7.3 Hz, 2H), 1.92 (s, 3H), 1.57 (p, *J* = 7.4 Hz, 2H), 1.27 (overlaps with the excess thiol), 1.17 (overlaps with the excess thiol), 0.89 (overlaps with the excess thiol). ^{13}C NMR (126 MHz, C_6D_6) δ 190.5, 143.5, 135.1, 129.1, 127.3, 31.8 (overlaps with the excess thiol), 29.8, 29.2, 29.1, 28.9, 28.8, 22.7(overlaps with the excess thiol), 21.0, 14.0 (overlaps with the excess thiol).

Pure thioester (see below for synthesis): ***S*-octyl 4-methylbenzothioate (5.1uu).** Pale yellow liquid. ^{1}H NMR (400 MHz, Benzene-d_6) δ 8.05 (d, *J* = 8.2 Hz, 2H), 6.82 (d, *J* = 8.1 Hz, 2H), 3.03 (t, *J* = 7.3 Hz, 2H), 1.91 (s, 3H), 1.57 (s, 2H), 1.27 (dt, *J* = 14.5, 7.3 Hz, 4H), 1.17 (d, *J* = 4.0 Hz, 6H), 0.89 (s, 3H). ^{13}C NMR (101 MHz, C_6D_6) δ 190.5, 143.5, 135.1, 129.1, 127.3, 31.8, 29.8, 29.2, 29.1, 28.9, 28.8, 22.7, 21.0, 14.0. HRMS: Calculated for $C_{16}H_{24}OSNa^+$ (MNa^+): 287.1447, found: 287.1440.

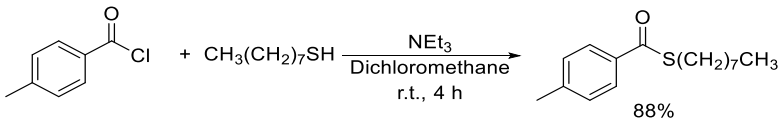

p-toluoyl chloride (39 mg, 0.25 mmol) and 1-octanethiol (37 mg, 0.25 mmol) were mixed in dichloromethane (0.5 mL) in a 25 mL vial. 5 drops of NEt_3 was added to the mixture to form a white slurry. The mixture was stirred at room temperature for 4 h. The mixture was extracted with 2 X 10 mL DCM and washed with 2 X 5 mL H_2O. The organic solution was dried over $NaSO_4$

and filtered. Residual solvent was removed *in vacuo*, affording *S*-octyl 4-methylbenzothioate **5.1uu** (55 mg, 0.22 mmol) as a pale yellow liquid in 88% yield.

Probing for Acyl Radical Generation from Acid Chloride with TEMPO (Figure 5.6G)

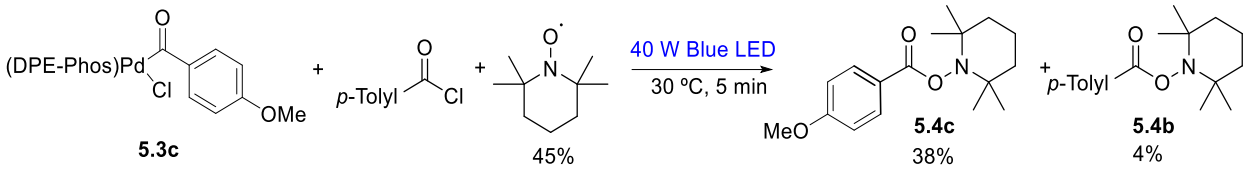

Complex **5.3c** was generated *in situ* to ensure its full dissolution in benzene. In a glovebox, [(DPE-Phos)Pd](μ-CO) **5.7a** (2.6 mg, 0.002 mmol) was chloride and TEMPO in C_6D_6 was added (prepared by dissolving 1.6 mg TEMPO and 6.2 mg p-toluoyl chloride in 2 mL C_6D_6). The NMR tube was capped, taken out of the glovebox, and immediately irradiated with a blue LED lamp for 5 minutes. ^{1}H NMR analysis using benzyl benzoate as internal standard showed the formation of TEMPO ester **5.4c** in 38% yield as the major TEMPO containing product. 2,2,6,6-tetramethylpiperidin-1-yl 4-methylbenzoate **5.4b** was observed in very low yield (4%).

*In situ data on **5.4c**:* ^{1}H NMR (500 MHz, C_6D_6) δ 8.16 (d, *J* = 8.0 Hz, 2H), 6.70 (d, *J* = 7.9 Hz, 2H), 3.17 (s, 3H), 1.68 (t, *J* = 12.9 Hz, 2H), 1.50 – 1.42 (m, 1H), 1.37 – 1.32 (m, 3H), 1.26 (s, 6H), 1.19 (s, 6H). ^{13}C NMR (126 MHz, C_6D_6) δ 165.7, 163.6, 131.9, 123.0, 114.1, 60.2, 54.9, 39.6, 32.3, 20.9, 17.4.

Pure **5.4c**: ^{1}H NMR (500 MHz, C_6D_6) δ 8.18 (d, *J* = 8.9 Hz, 2H), 6.66 (d, *J* = 8.8 Hz, 2H), 3.17 (s, 3H), 1.68 (ddd, *J* = 15.5, 8.4, 3.6 Hz, 2H), 1.45 (dt, *J* = 13.7, 3.6 Hz, 1H), 1.34 (dt, *J* = 13.5, 3.1 Hz, 3H), 1.26 (s, 6H), 1.18 (s, 6H).^{13}C NMR (126 MHz, C_6D_6) δ 165.7, 163.6, 131.9, 123.0, 114.1, 60.2, 54.9, 39.5, 32.2, 20.9, 17.4.

Synthesis of Biaryls 5.6a-c

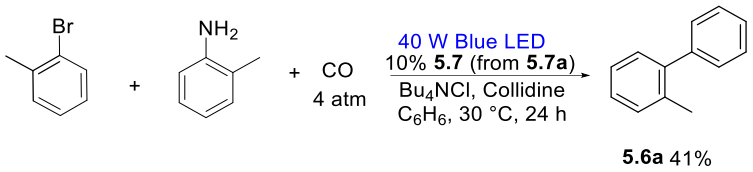

Catalyst **5.7** was generated in situ as follows: in a glovebox, 2-bromotoluene (43 mg, 0.25 mmol), 0-toluidine (54 mg, 0.50 mmol), Bu_4NCl (69 mg, 0.25 mmol), collidine (45 mg, 0.37 mmol), and [(DPE-Phos)Pd](μ-CO) **5.7a** (16.5 mg, 12 μmol) were dissolved in 3.0 mL C_6H_6 and transferred into a 25 mL sealable, thick-walled Schlenk bomb equipped with a magnetic stir bar. The vessel was sealed with a Teflon cap and taken out of the glovebox, and 4 atm of CO was added on top of the nitrogen atmosphere, leading to the *in situ* formation of **5.7**. The solution was then irradiated for 24 hours using the setup described in Figure 5.14C. The excess CO was then removed inside a well-ventilated fume hood, the solvent removed in vacuo, and biaryl **5.6a** was isolated using flash chromatography on silica gel using hexanes/ethyl acetate 5%, affording **5.6a** as a colorless liquid in 41% yield (17 mg, 0.10 mmol).

2-methyl-1,1'-biphenyl (5.6a) colorless liquid, 41% yield (17 mg, 0.10 mmol). ^{1}H NMR (400 MHz, Chloroform-*d*) δ 7.46 – 7.40 (m, 2H), 7.35 (td, *J* = 7.1, 6.5, 1.4 Hz, 3H), 7.30 – 7.21 (m, 4H), 2.29 (s, 3H). ^{13}C NMR (101 MHz, $CDCl_3$) δ 142.0, 142.0, 135.4, 130.3, 129.8, 129.2, 128.8, 128.1, 127.3, 127.2, 126.8, 125.8, 20.5. ^{1}H NMR (500 MHz, Benzene-d_6) δ 7.24 – 7.17 (m, 5H), 7.12 (tdd, *J* = 6.8, 4.3, 2.0 Hz, 4H), 2.15 (s, 3H). ^{13}C NMR (126 MHz, C_6D_6) δ 142.2, 142.1, 135.1, 130.3, 129.8, 129.2, 128.7, 128.0, 127.2, 126.7, 125.8, 20.2. HRMS Analysis of $C_{13}H_{12}$, Theory: 168.09335, Found: 168.09341.

Similar procedures were performed for the generation of **5.6b** and **5.6c**. In these cases, **5.6** was isolated as a side product upon amide formation with either 2,6-diisopropylaniline or *o*-toluidine, and 5% **7** was used.

4-methyl-1,1'-biphenyl-2',3',4',5',6'-d_5 (5.6b) white solid, 58% yield (25 mg, 0.145 mmol).^{1}H NMR (500 MHz, C_6D_6) δ 7.42 (d, *J* = 8.0 Hz, 2H), 7.05 (d, *J* = 7.9 Hz, 2H), 2.15 (s, 3H). ^{13}C NMR (126 MHz, C_6D_6) δ 141.5, 138.9, 137.0, 129.8, 127.4, 21.1. HRMS Analysis of $C_{13}H_7D_5O$, Theory: 173.12474, Found: 173.12511.

To verify the identity of 5.**6b**, it was compared to a commercial sample of 4-methylbiphenyl (**5.6b-H)**:

^{1}H NMR (500 MHz, C_6D_6) δ 7.50 (dt, *J* = 8.2, 1.7 Hz, 2H), 7.42 (d, *J* = 8.1 Hz, 2H), 7.23 (t, *J* = 7.6 Hz, 2H), 7.15 – 7.11 (m, 1H), 7.05 (d, *J* = 7.8 Hz, 2H), 2.15 (s, 3H). ^{13}C NMR (126 MHz, C_6D_6) δ 141.7, 138.9, 137.0, 129.8, 129.0, 127.4, 127.3, 127.2, 21.1.

4-methoxy-1,1'-biphenyl-2',3',4',5',6'-d_5 (5.6c) white solid, 47% yield (22 mg, 0.11 mmol) ^{1}H NMR (500 MHz, $CDCl_3$) δ 7.59 – 7.48 (m, 2H), 7.03 – 6.93 (m, 2H), 3.86 (s, 3H). ^{13}C NMR (126 MHz, $CDCl_3$) δ 159.3, 140.8, 133.9, 128.3, 114.3, 55.5. HRMS Analysis of $C_{13}H_7D_5O$, Theory: 189.11965, Found: 189.11974.

4-methoxy-1,1'-biphenyl (5.6c-H) white solid, 55% yield (25 mg, 0.14 mmol) ^{1}H NMR (500 MHz, $CDCl_3$) δ 7.55 (ddd, *J* = 10.5, 7.5, 1.7 Hz, 4H), 7.42 (t, *J* = 7.7 Hz, 2H), 7.33 – 7.28 (m, 1H), 6.98 (d, J = 8.8 Hz, 2H), 3.86 (s, 3H). ^{13}C NMR (126 MHz, $CDCl_3$) δ 159.3, 141.0, 133.9, 128.9, 128.3, 126.9, 126.8, 114.3, 55.5.

Catalytic Reaction in the Presence of TEMPO (Figure 5.8B)

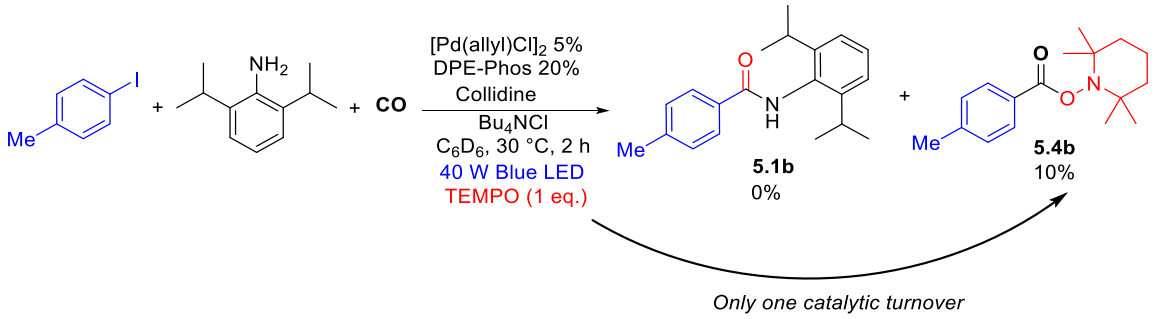

In a glovebox, 4-iodotoluene (8.7 mg, 0.04 mmol), 2,6-diisopropylaniline (11 mg, 0.06 mmol), collidine (7.3 mg, 0.06 mmol), Bu_4NCl (11 mg, 0.04 mmol), DPE-Phos (4.3 mg, 8 µmol), TEMPO (6.2 mg, 0.04 mmol), and benzyl benzoate standard (4.2 mg, 0.02 mmol) were dissolved in 0.75 mL 2.7 mM solution of $[Pd(allyl)Cl]_2$ in C_6D_6 (prepared by dissolving 7.3 mg of $[Pd(allyl)Cl]_2$ in 7.5 mL CD_3CN; total $[Pd(allyl)Cl]_2$ in the reaction = 2 µmol) and transferred into a J-Young NMR tube. The tube was taken out of the glovebox, frozen in liquid nitrogen, evacuated, and then 4 atm CO was condensed into the tube. The reaction mixture was thawed, and then irradiated with a 40W Blue LED lamp as seen in Figure 5.14B, and the reaction temperature was kept under 30 °C with a fan. ^1H NMR analysis after 15 h showed no amide product and instead the TEMPO ester **5.4b** was formed in 10% yield, which represents one catalytic turnover. The ^{31}P NMR spectra showed no phosphorus signal, and the solution in the NMR tube turned dark. The irradiation was prolonged for 2 hours, and no change was observed.

Catalyst Resting State Analysis (Figure 5.8C)

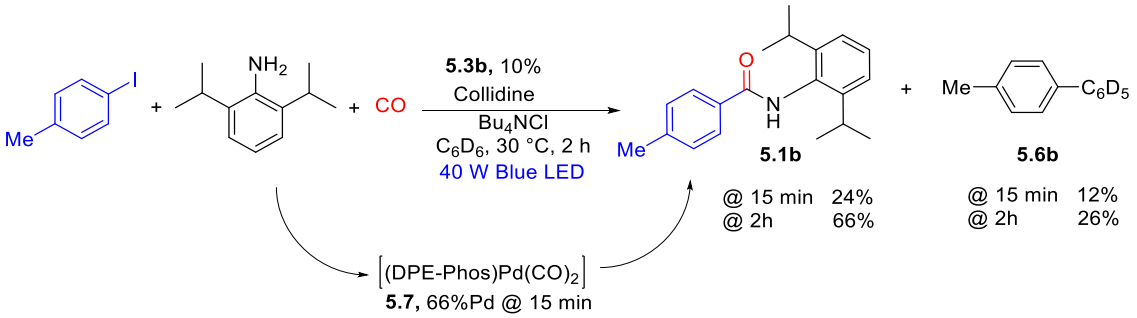

In a glovebox, 4-iodotoluene (8.7 mg, 0.04 mmol), 2,6,-diisopropylaniline (11 mg, 0.06 mmol), collidine (7.3 mg, 0.06 mmol), Bu_4NCl (11 mg, 0.04 mmol), complex **5.3b** as catalyst (3.2 mg, 4µmol), and benzyl benzoate standard (4.2 mg, 0.02 mmol) were dissolved in C_6D_6 and transferred into a J-Young NMR tube. The tube was taken out of the glovebox, frozen in liquid nitrogen, evacuated, and then 4 atm CO was condensed into the tube. The reaction mixture was thawed, and then irradiated with a 40W Blue LED lamp (Figure 5.14B) and the reaction temperature was kept under 30 °C with a fan. After 15 minutes, a new ^{31}P signal appeared at 7.15 ppm along with new, partially overlapped, aromatic signals in the ^{1}H NMR. These shifts match with those of complex **7** in (6% yield, or 60% of all palladium). A second small signal can be observed at 17.44 ppm (ca. 30% of phosphine) and no complex **5.3b** is observed. At this time, the yield of amide **5.1b** was 24% and 12% biaryl **5.6b.** After 2 hours, the same signals persisted in the ^{1}H and ^{31}P NMR spectra, and the yield of amide **5.1b** was 66% and biaryl was produced in 26% yield. The ^{31}P NMR spectra showed the slow loss of **5.7** and growth of the signal at 17.44 ppm (1.6:1 ratio), suggesting that the catalyst decomposes over time, potentially due to unproductive biaryl formation.

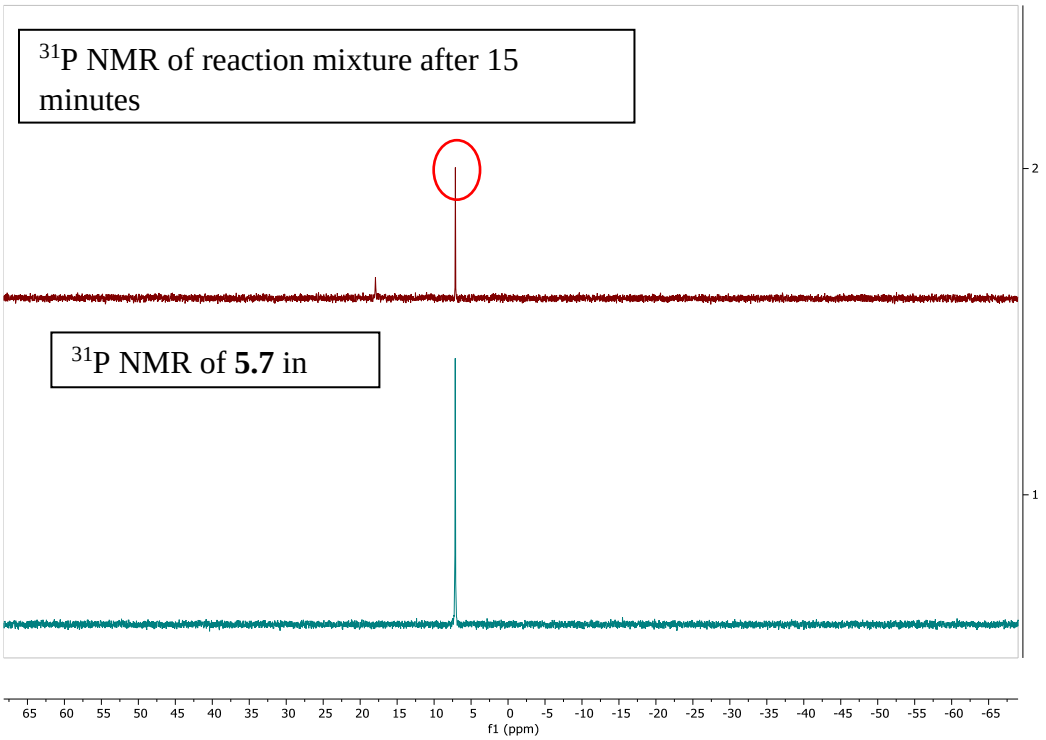

Figure 5.23. ^{31}P NMR of the Reaction Mixture and Complex 5.7

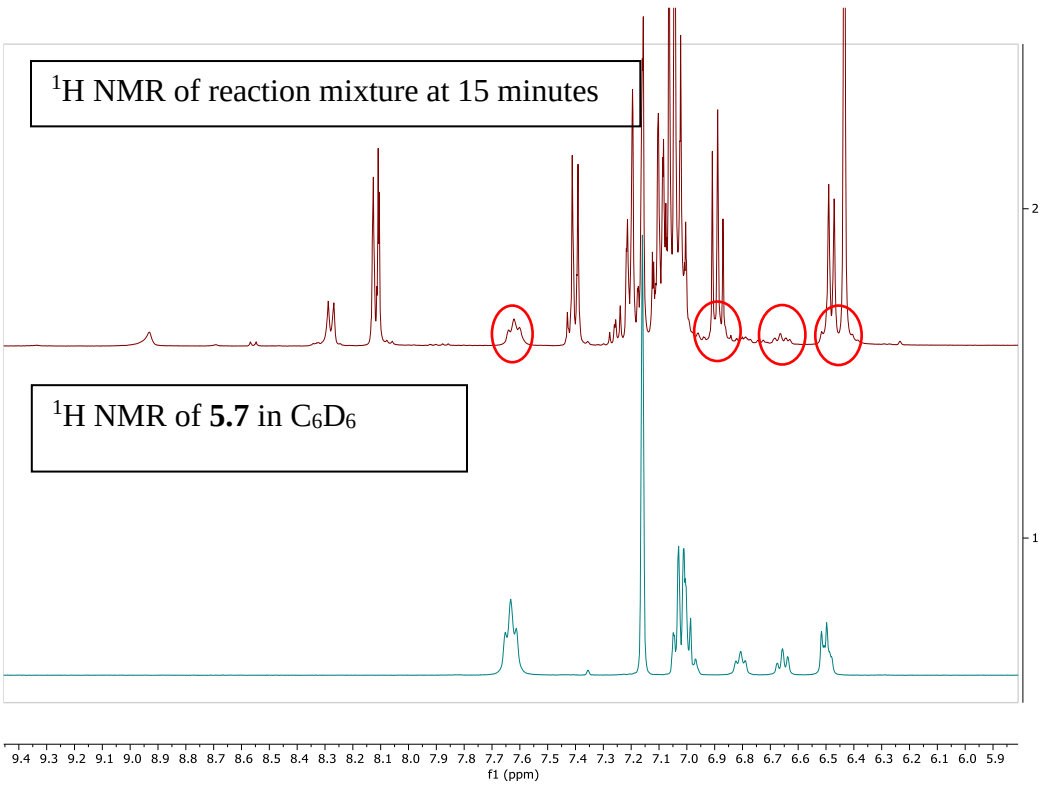

Figure 5.24. ^{1}H NMR of the Reaction Mixture and Complex 5.7

Light On/Off Experiment (Figure 5.8D)

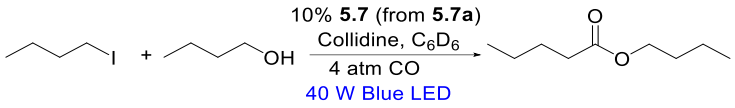

Catalyst **5.7** was generated in situ as follows. In a glovebox, 1-iodobutane (7.4 mg, 0.04 mmol), 1-butanol (4.4 mg, 0.06 mmol), Bu_4NCl (1.1 mg, 0.004 mmol), collidine (7.3 mg, 0.06 mmol), [(DPE-Phos)Pd](μ-CO) **5.7a** (2.6 mg, 0.002 mmol), and benzyl benzoate standard (4.2 mg, 0.02 mmol) were dissolved in 0.75 mL C_6D_6 and transferred into a J-Young NMR tube. The tube was taken out of the glovebox, frozen in liquid nitrogen, evacuated, and then 4 atm CO was condensed into the tube, leading to the rapid formation of catalyst **5.7**. The reaction mixture was irradiated with a 40W Blue LED lamp as seen in Figure 5.14B and the reaction temperature was kept under 30 °C with a fan. NMR yields were calculated via ^{1}H NMR integrations using benzyl benzoate as internal standard. The reaction was subjected to varying periods of irradiation and darkness. ^{1}H NMR analysis showed that during periods of irradiation, the yield of ester increased. However, when the reaction was left in the dark, no change was observed. (See graph below)

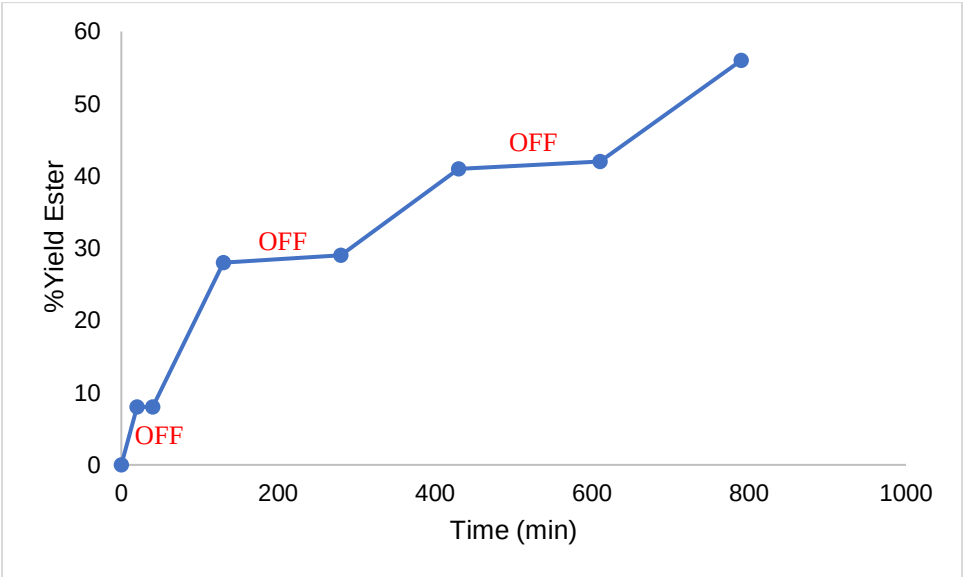

Figure 5.25. Light On/Off Experiment.

Thermal Catalytic Reaction with Aryl Iodide (Figure 5.8E)

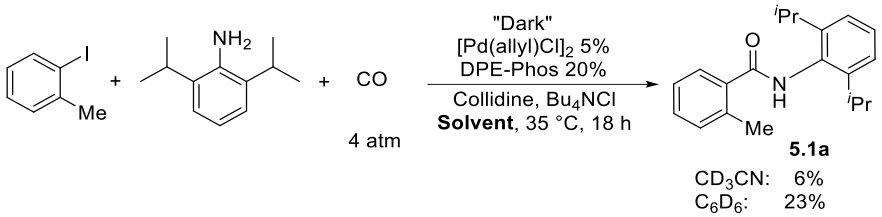

In a glovebox, 2-iodotoluene (13 mg, 0.06 mmol), 2,6-diisopropylaniline (7.1 mg, 0.04 mmol), collidine (7.3 mg, 0.06 mmol), Bu_4NCl (11 mg, 0.04 mmol), DPE-Phos (4.3 mg, 8 μmol), and benzyl benzoate standard (4.2 mg, 0.02 mmol) were dissolved in 0.75 mL of a 2.7 mM solution of $[Pd(allyl)Cl]_2$ in CD_3CN (prepared by dissolving 7.3 mg of $[Pd(allyl)Cl]_2$ in 7.5 mL CD_3CN; total $[Pd(allyl)Cl]_2$ in the reaction = 2 μmol) and transferred into a J-Young NMR tube. The tube was taken out of the glovebox, frozen in liquid nitrogen, evacuated, and then 4 atm CO was condensed into the tube. The reaction mixture was thawed, placed inside an oil bath at 35 ºC, and completely covered with aluminum foil to keep it in the dark. After 18 h, ^1H NMR analysis shows the yield of amide **5.1a** is 6%.

This procedure was repeated in C_6D_6 (total volume 0.75 mL). In this case, the yield of **5.1a** was 23% after 18 h.

Thermal Catalytic Reaction with Aryl Bromide (Figure 5.8E)

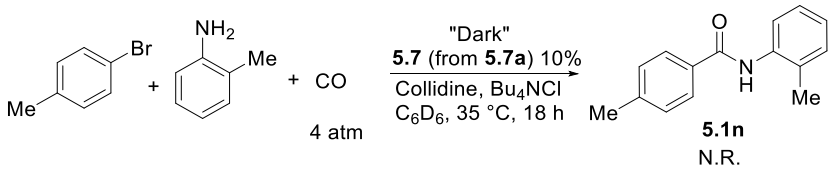

In a glovebox, 4-bromotoluene (14 mg, 0.08 mmol), *o*-toluidine (4.3 mg, 0.04 mmol), collidine (7.3 mg, 0.06 mmol), Bu_4NCl (11 mg, 0.04 mmol), [(DPE-Phos)Pd](μ-CO) **5.7a** (2.6 mg, 2 μmol), and benzyl benzoate standard (4.2 mg, 0.02 mmol) were dissolved in 0.75 mL C_6D_6 and transferred

into a J-Young NMR tube. The tube was taken out of the glovebox, frozen in liquid nitrogen, evacuated, and then 4 atm CO was condensed into the tube, leading to the rapid formation of catalyst **7**. The reaction mixture was placed inside an oil bath at 35 ºC. The reaction system was completely covered with aluminum foil to keep it in the dark. ^{1}H NMR analysis after 18 h shows no amide product.

Irradiation of 3b in the Presence of Aryl Iodide (Figure 5.9A)

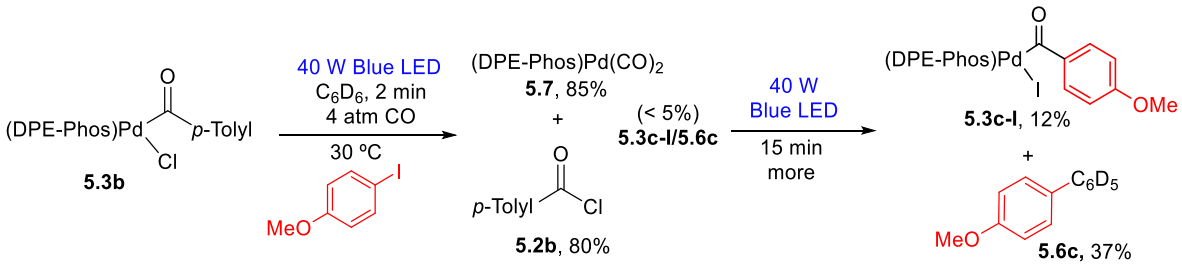

Complex **5.3b** (1 µmol) in 0.5 mL C_6D_6 was generated *in situ* in a J-Young NMR tube to ensure its full dissolution in benzene by the procedure 3A above. To this solution in a glove box was added a solution of 4-iodoanisole (1.4 mg, 6 µmol) in 0.25 mL C_6D_6. The NMR tube was capped with a screw-cap, taken out of the glovebox, frozen under liquid nitrogen, evacuated, and 4 atm CO was condensed into the tube. The tube was thawed and irradiated for 2 minutes with a 40W Blue LED lamp using the set-up in Figure 5.14B. ^{1}H NMR analysis showed the formation of acid chloride **5.2b** in 80% yield, carbonyl complex **5.7** in 85% yield, and <5% of other products. Irradiation was prolonged for 15 minutes. Over time, **5.7** was consumed producing a mixture of the iodide complex **5.3c-I** (12%) and biaryl **5.6c** (37%). Note: the ratio of **5.3c-I** to **5.6c** is different under these conditions due to chloride exchange leading to complex **5.3c**, which produces anisoyl chloride (23% after 15 minutes) and regenerates carbonyl complex **5.7**.

Irradiation of Complex 5.7 in the Presence of Aryl Iodide (Figure 5.9B)

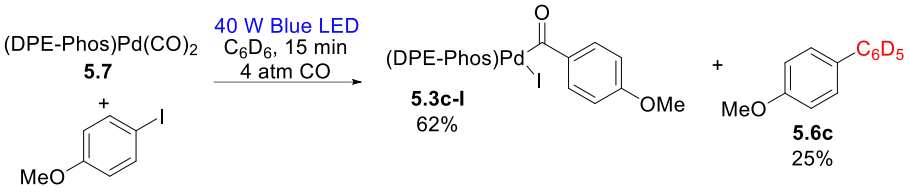

Complex **5.7** was generated *in situ* and quickly irradiated with aryl iodide to ensure minimal thermal reaction via the following procedure. In a glovebox, [(DPE-Phos)Pd](μ-CO) **5.7a** (2.6 mg, 2μmol) and benzyl benzoate standard (1 mg, 4 μmol) were dissolved in 0.5 mL C_6D_6 and transferred into a J-Young NNR tube. The tube was sealed with a screw-cap, taken out of the glovebox, frozen under liquid nitrogen, evacuated, then 4 atm CO was condensed in the NMR tube, and it was thawed and mixed for 2 minutes affording a homogeneous solution of **5.7**. The tube was frozen again, and the headspace of CO was removed on a Schlenk line. The tube was kept frozen brought into the glovebox, and a solution of 4-iodoanisole (12 mg, 0.08 mmol) in 0.25 mL C_6D_6 was added on top of the frozen solution. The tube was capped, taken out of the glovebox, frozen under liquid nitrogen, evacuated, and 4 atm of CO were condensed in the tube. Immediately after thawing the tube, the solution was mixed and quickly irradiated using the set-up described in Figure 5.14B. After 15 minutes of irradiation, ^{1}H NMR analysis showed that a mixture of **5.3c-I** (62%) and **5.6c** (25%) was produced.

Thermal reaction of complex 5.7 with Aryl Iodide (Figure 5.9B)

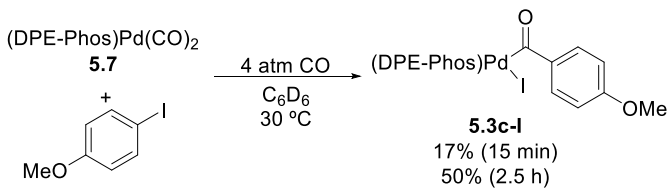

The reaction was setup using a same procedure to the one described above. However, instead of irradiation, the NMR tube was placed inside an oil bath at 30 ºC. The reaction was monitored by

^{1}H NMR, and after 15 minutes 17% complex **5.3c-I** had formed. After 2.5 hours, the amount of **5.3c-I** in solution had increased to 50% and no biaryl **5.6c** was observed.

Irradiation of Complex 5.7 in the Presence of Aryl Bromide (Figure 5.9C)

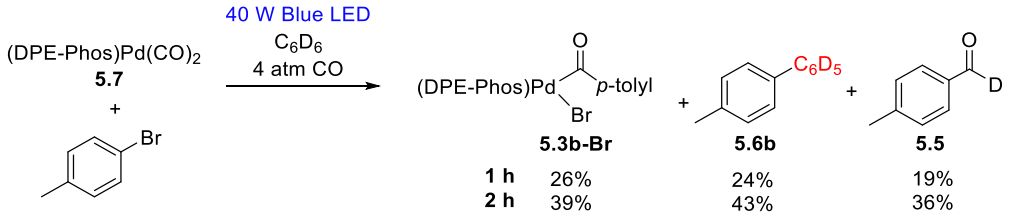

Complex **5.7** was generated *in situ* and quickly irradiated with aryl bromide to ensure minimal thermal reaction via the following procedure. In a glovebox, [(DPE-Phos)Pd](μ-CO) **5.7a** (10.5 mg, 8μmol) was dissolved in 0.6 mL C_6D_6 and transferred into a J-Young NNR tube. The tube was sealed with a screw-cap and taken out of the glovebox, frozen under liquid nitrogen, evacuated, then 4 atm CO was condensed in the NMR tube, finally it was thawed and mixed for 2 minutes affording a homogeneous solution of **5.7**. The tube was frozen again, and the headspace of CO was removed in a Schlenk line. The tube was kept frozen, brought into the glovebox, and a solution of 4-bromoanisole (34.2 mg, 0.20 mmol) in 0.20 mL C_6D_6 was added on top of the frozen solution. The tube was capped, taken out of the glovebox quickly, frozen in liquid nitrogen, evacuated, and 4 atm of CO were condensed. Immediately after thawing the tube, the solution was mixed and irradiated using the set-up described in Figure 5.14B. ^{1}H NMR analysis shows the formation of **5.3b-Br** (39%), **5.6b** (43%), and aldehyde **5.5** (36%) over 2 h.

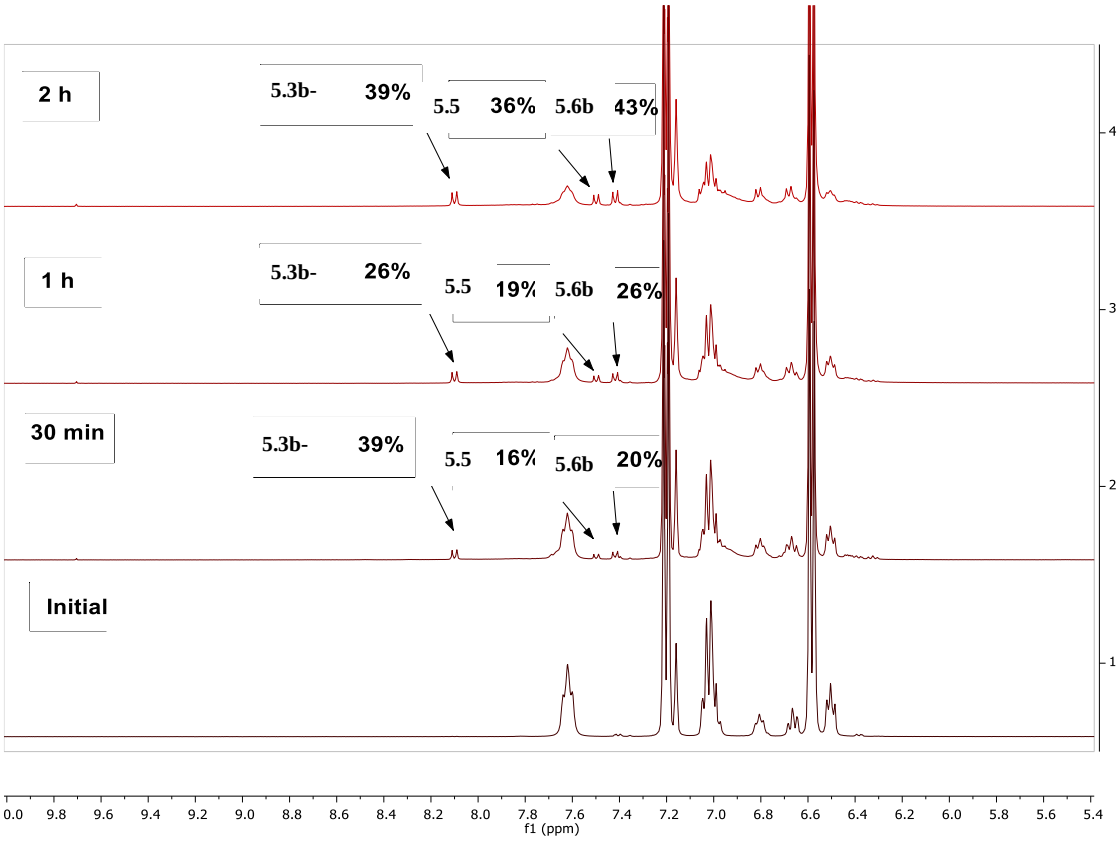

Figure 5.26. ^{1}H NMR Spectra of Irradiation of Carbonyl Complex 5.7 in the Presence of Aryl Bromide.

Thermal Reaction of 5.7 and Aryl Bromide (Figure 5.9C)

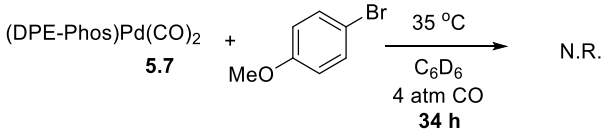

Complex **5.7** was generated in situ as follows. In a glovebox, [(DPE-Phos)Pd](μ-CO) **5.7a** (5.3 mg, 0.004 mmol) and benzyl benzoate standard (1.3 mg, 0.006 mmol) were dissolved in 0.6 mL C_6D_6 and transferred into a J-Young NMR tube. The tube was sealed with a screw-cap and taken out of the glovebox, frozen under liquid nitrogen, evacuated, and 4 atm CO was condensed in the NMR tube. Then it was thawed and mixed for 2 minutes affording a homogeneous solution of **5.7**. The tube was frozen again, and the headspace of CO was removed in a Schlenk line. The tube was

kept frozen and brought into the glovebox. Then, a solution of 4-bromoanisole (1.9 mg, 0.010 mmol) in 0.20 mL C_6D_6 was added on top of the frozen solution. The tube was capped, taken out of the glovebox quickly, frozen in liquid nitrogen, evacuated, and loaded with 4 atm of CO. The tube was thawed and placed in an oil bath at ºC. ^{1}H NMR analysis shows no reaction over 34 h.

Irradiation of Complex 5.7 in the Presence of n-butyliodide (Figure 5.9D)

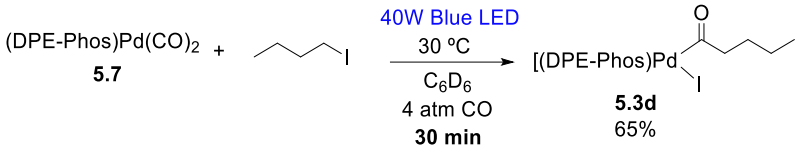

Complex **5.7** was generated in situ as follows. In a glovebox, [(DPE-Phos)Pd](μ-CO) **5.7a** (5.3 mg, 0.004 mmol) and benzyl benzoate standard (0.8 mg, 0.004 mmol) were dissolved in 0.7 mL C_6D_6 and transferred into a J-Young NMR tube. The tube was sealed with a screw-cap, taken out of the glovebox, frozen under liquid nitrogen, evacuated, then 4 atm CO was condensed in the NMR tube. The tube was thawed and mixed for 2 minutes affording a homogeneous solution of **5.7**. The tube was frozen again, and the headspace of CO was removed on a Schlenk line. The tube was kept frozen and brought into the glovebox. A solution of ^{n}butyl iodide (1.8 mg, 0.010 mmol) in 0.10 mL C_6D_6 was added on top of the frozen solution. The tube was capped, taken out of the glovebox quickly, frozen in liquid nitrogen, evacuated, and 4 atm of CO was condensed in the tube, then thawed and immediately irradiated using the set-up described in Figure 5.14B. ^{1}H NMR analysis reveals the formation of complex **5.3d** (65%) after 30 min.

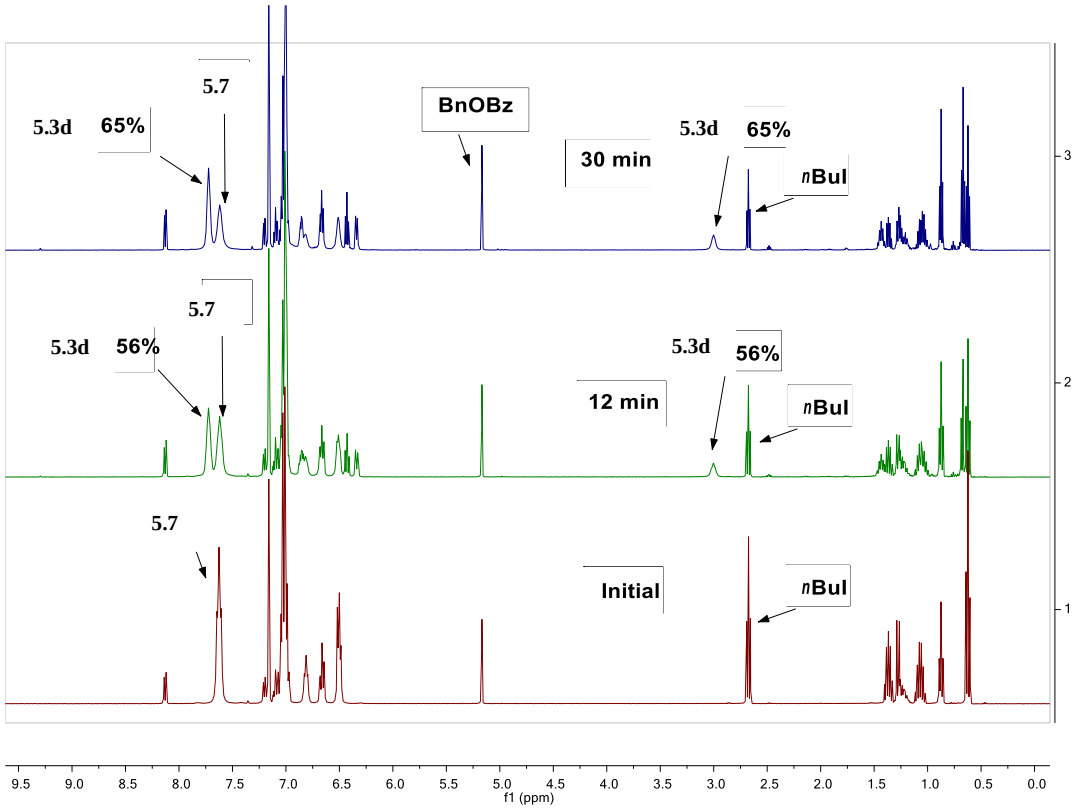

Figure 5.27. ^{1}H NMR Spectra of Irradiation of Complex 5.7 in the Presence of ^{n}BuI.

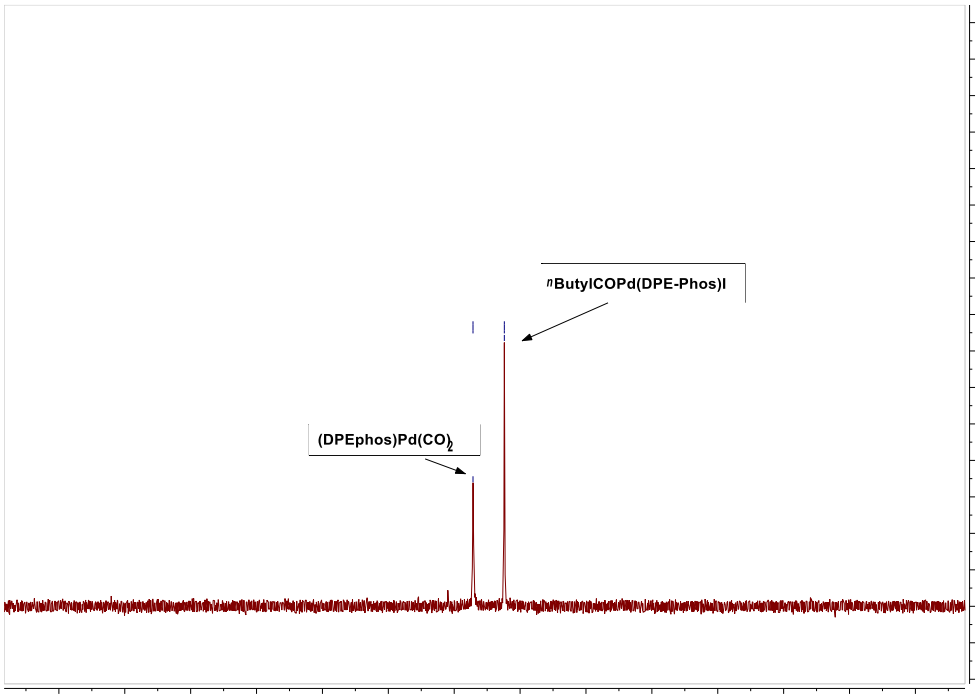

Figure 5.28. ^{31}P NMR Spectra of Irradiation of Complex 5.7 in the Presence of ^{n}BuI.

Thermal Reaction of 5.7 and *n*-Butyliodide (Figure 5.9D)

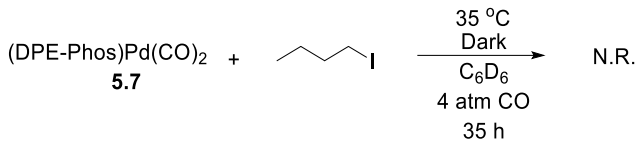

An analogous reaction to that above was employed, except the reaction was performed at 35 ºC in the dark. ^{1}H NMR analysis shows no reaction after 35 h.

Irradiation of Aryl Iodide and Alkyl Iodide (Figure 5.9F)

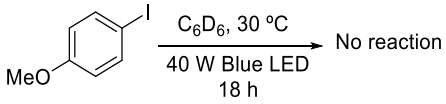

In a glovebox, 1-iodo-4-methoxybenzene (9.4 mg, 0.04 mmol) and benzyl benzoate internal standard (4.2 mg, 0.02 mmol) were dissolved in 0.75 mL C_6D_6. The mixture was transferred to a J-Young NMR, the tube was sealed with a screw-cap, and taken out of the glovebox. The mixture was irradiated with a 40W Blue LED lamp as seen in Figure 5.14B, and the reaction temperature was kept under 30 ºC with two fans. ^{1}H NMR analysis after 18 h shows no reaction.

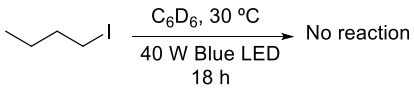

In a glovebox, 1-iodobutane (7.4 mg, 0.04 mmol) and benzyl benzoate internal standard (4.2 mg, 0.02 mmol) were dissolved in 0.75 mL C_6D_6. The mixture was transferred to a J-Young NMR, the tube was sealed with a screw-cap, and taken out of the glovebox. The mixture was irradiated with a 40W Blue LED lamp as seen in Figure 5.14B, and the reaction temperature was kept under 30 ºC with two fans. ^{1}H NMR analysis after 18 h shows no reaction.

Irradiation of Complex 5.7 in the Presence of Aryl Iodide and 1-Octanethiol (Figure 5.9G)

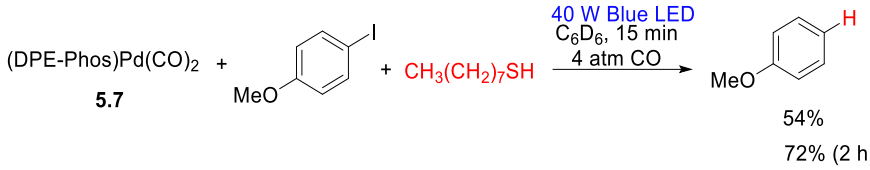

Complex **5.7** was generated *in situ* and quickly irradiated with aryl iodide to ensure minimal thermal reaction via the following procedure. In a glovebox, [(DPE-Phos)Pd](μ-CO) **5.7a** (2.6 mg, 2μmol) and benzyl benzoate (1 mg, 4 μmol) were dissolved in 0.6 mL C_6D_6 and transferred into a J-Young NMR tube. The tube was sealed with a screw-cap and taken out of the glovebox, frozen under liquid nitrogen, evacuated, then 4 atm CO was condensed in the NMR tube, finally it was thawed and mixed for 2 minutes affording a homogeneous solution of **5.7**. The tube was frozen again, and the headspace of CO was removed on a Schlenk line. The tube was kept frozen and brought into the glovebox. Then, a solution of 4-iodoanisole (2.8 mg, 0.012 mmol) and 1-octanethiol (12 mg, 0.08 mmol) in 0.2 mL C_6D_6 was added on top of the frozen solution. The tube was capped, taken out of the glovebox, frozen under liquid nitrogen, and 4 atm of CO was condensed in the tube. Immediately after thawing the tube, the solution was mixed and quickly irradiated using the set-up described in Figure 5.14B. ^{1}H NMR analysis after 15 min shows the formation of anisole in 54% yield. After 2 h, the yield of anisole was 72%. The product was characterized *in situ*:

In situ ^{1}H NMR (400 MHz, C_6D_6) δ 7.12 (m, 2H, partial overlap), 6.84 (m, 1H, partial overlap), 6.79 (m, 2H, partial overlap), 3.30 (s, 3H). ^{13}C NMR (126 MHz, C_6D_6) δ 160.2, 129.7, 120.8, 114.3, 54.6. *Pure compound*: ^{1}H NMR (500 MHz, C_6D_6) δ 7.12 (dd, J = 8.7, 7.4 Hz, 1H), 6.84 (tt, J = 7.5, 1.1 Hz, 1H), 6.80 (dt, J = 7.9, 1.0 Hz, 2H), 3.30 (s, 2H). *In situ* ^{13}C NMR (126 MHz, C_6D_6)

δ 160.2, 129.7, 120.8, 114.3, 54.6. *Pure compound*: ^{13}C NMR (126 MHz, C_6D_6) δ 160.2, 129.7, 120.8, 114.3, 54.6. GC-MS = 108.1. GC-MS = 108.1

Irradiation of Complex 5.7 in the Presence of Aryl Bromide and 1-Octanethiol (Figure 5.9G)

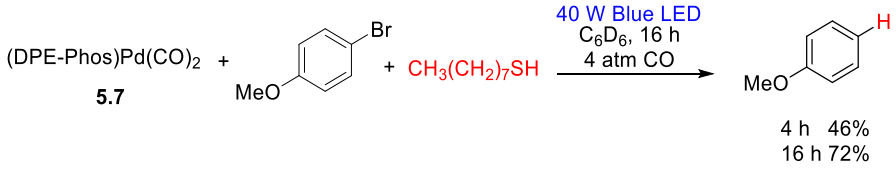

Complex **5.7** was generated *in situ* and quickly irradiated with aryl bromide to ensure minimal thermal reaction via the following procedure. In a glovebox, [(DPE-Phos)Pd](μ-CO) **5.7a** (5.3 mg, 4μmol) and benzyl benzoate standard (1 mg, 4 μmol) were dissolved in 0.6 mL C_6D_6 and transferred into a J-Young NNR tube. The tube was sealed with a screw-cap and taken out of the glovebox, frozen under liquid nitrogen, evacuated, then 4 atm CO was condensed in the NMR tube, finally it was thawed and mixed for 2 minutes affording a homogeneous solution of **5.7**. The tube was frozen again, and the headspace of CO was removed in a Schlenk line. The tube was kept frozen, brought into the glovebox, and a solution of 4-bromoanisole (4.5 mg, 0.024 mmol) and 1-octanethiol (23.4 mg, 0.16 mmol) in 0.2 mL C_6D_6 was added on top of the frozen solution. The tube was capped, taken out of the glovebox, frozen under liquid nitrogen, evacuated, and 4 atm of CO was condensed in the tube. Immediately after thawing the tube, the solution was mixed and irradiated using the set-up described in Figure 5.14B. ^{1}H NMR analysis after 16 h shows the formation of anisole in 72% yield. The product was characterized *in situ*:

In situ ^{1}H NMR (400 MHz, Benzene-d_6) δ 7.15 – 7.08 (m, 2H), 6.84 (tt, J = 7.1, 0.9 Hz, 1H), 6.82 – 6.77 (m, 2H), 3.30 (s, 3H). ^{13}C NMR (126 MHz, C_6D_6) δ 160.2, 129.7, 120.8, 114.3, 54.6.

Radical Clock Experiment (Figure 5.9H)

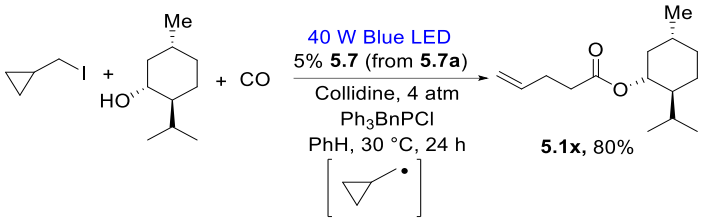

Catalyst **5.7** was generated in situ as follows. In a glovebox, (iodomethyl)cyclopropane (46 mg, 0.25 mmol), (±)-menthol (57 mg, 0.37 mmol), collidine (45 mg, 0.37 mmol), Ph_3PBnCl (97 mg, 0.25 mmol), and [(DPE-Phos)Pd](μ-CO) **5.7a** (precursor to **7**, 8.2 mg, 6.2 μmol) were dissolved in 3.5 mL benzene and transferred into thick-walled 25 mL Schlenk bomb, equipped with a magnetic stir bar, and covered with a Teflon cap. The bomb was taken out of the glovebox and charged with 4 atm CO on top of the nitrogen atmosphere, leading to the rapid generation of catalyst **5.7**. The bomb was clamped on top of a stirring plate and the solution was irradiated using an LED lamp as seen in Figure 5.14C. After 24 hours, the bomb was taken out of the irradiation system and the excess CO was removed by opening the bomb inside a well-ventilated fume hood. The product was isolated by flash chromatography on silica gel (230-400 mesh) with hexanes-ethyl acetate (4:1). Fractions were spotted on silica gel TLC plates and stained using a mixture of $KMnO_4$ and K_2CO_3 in water. The fractions that contained ester were combined and then evaporated under reduced pressure and solvent traces were removed *in vacuo*. Ester **5.1x** was obtained as the sole product in 80% (48 mg, 0.20 mmol) as a pale-yellow solid.

Catalytic Carbonylative Coupling Reactions

Typical Procedure for Carbonylative Coupling with Aryl Iodides (Figure 5.10)

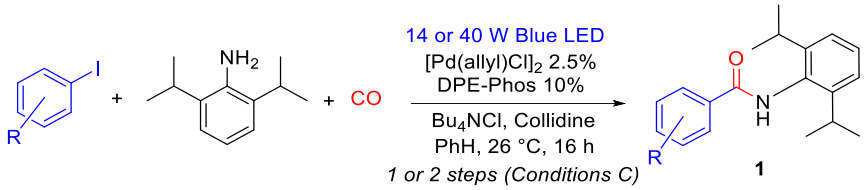

Conditions A, Amine as limiting reagent: In a glovebox, 4-iodotoluene (82 mg, 0.37 mmol), 2,6-diisopropylaniline (44 mg, 0.25 mmol), collidine (45 mg, 0.37 mmol), Bu_4NCl (69 mg, 0.25 mmol), $[Pd(allyl)Cl]_2$ (2.3 mg, 6.2 µmol), and DPE-Phos (14 mg, 0.025 mmol) were dissolved in 3.5 mL benzene and transferred into a thick-walled 25 mL Schlenk bomb, equipped with a magnetic stir bar, and sealable with a Teflon cap. The bomb was taken out of the glovebox and the solution was frozen under liquid nitrogen. The nitrogen atmosphere was evacuated from the bomb in a Schlenk line and then the vessel was pressurized with 1 atm CO. The bomb was then clamped on top of a stirring plate, and the solution was irradiated using a coiled 14W Blue LED strip (Figure 5.14A). Fans were used to keep the temperature below 30 ºC. After 16 hours, the bomb was taken out of the irradiation system and the excess CO was removed by opening the bomb inside a well-ventilated fume hood. The solvent was removed *in vacuo*, and product isolated by flash chromatography on silica gel (230-400 mesh) with hexanes-ethyl acetate (4:1), or hexanes-acetone (4:1) to afford amide **5.1b** in 99% yield (73 mg, 0.24 mmol, relative to amine limiting reagent) as a white solid.

Conditions B. Aryl iodide as the limiting reagent: In a glovebox, 4-iodotoluene (55 mg, 0.25 mmol), 2,6-diisopropylaniline (66 mg, 0.37 mmol), collidine (45 mg, 0.37 mmol), Bu_4NCl (69 mg, 0.25 mmol), $[Pd(allyl)Cl]_2$ (2.3 mg, 6.2 µmol), and DPE-Phos (14 mg, 0.025 mmol) were dissolved

in 3.5 mL benzene and transferred into thick-walled 25 mL Schlenk bomb, equipped with a magnetic stir bar, and sealed with a Teflon cap. The bomb was taken out of the glovebox and the solution was frozen under liquid nitrogen. The nitrogen atmosphere was evacuated from the bomb in a Schlenk line and then the vessel was pressurized with 1 atm CO. The bomb was then clamped on top of a stirring plate and the solution was irradiated using a 40W Blue LED lamp. Fans were used to keep the temperature below 30 ºC (Figure 5.14C). After 24 hours, the bomb was taken out of the irradiation system and the excess CO was removed by opening the bomb inside a well-ventilated fume hood. The solvent was removed *in vacuo*, and product was isolated by flash chromatography on silica gel (230-400 mesh) with hexanes-ethyl acetate (4:1) [hexanes-acetone (4:1) for amide **5.1f**] to afford amide **5.1b** in 72% yield (53 mg, 0.18 mmol) as a white solid.

Conditions C. Acid chloride build-up and subsequent trapping: In a glovebox, 4-iodobenzonitrile (57 mg, 0.25 mmol), Bu_4NCl (104 mg, 0.37 mmol), $[Pd(allyl)Cl]_2$ (2.3 mg, 6.2 µmol), and DPE-Phos (14 mg, 0.025 mmol) were dissolved in 3.5 mL acetonitrile and transferred into thick-walled 25 mL Schlenk bomb, equipped with a magnetic stir bar, and sealed with a Teflon cap. The bomb was taken out of the glovebox and the solution was frozen under liquid nitrogen. The nitrogen atmosphere was evacuated from the bomb in a Schlenk line and then the vessel was pressurized with 1 atm CO. The bomb was then clamped on top of a stirring plate and the solution was irradiated using a 40W Blue LED lamp as seen in Figure 5.14C. After 24 hours, the bomb was taken out of the irradiation system and the excess CO was removed on a Schlenk line and the bomb was brought into the glovebox. Diisopropylamine (38 mg, 0.37 mmol) and NEt^iPr_2 (49 mg, 0.37 mmol) in 0.5 mL acetonitrile was added, the bomb capped, and the mixture stirred for 3 hours at room temperature outside the glovebox. The solvent was removed *in vacuo*, and product isolated

by flash chromatography on silica gel (230-400 mesh) with hexanes-ethyl acetate (3:1), affording amide **5.1l** in 85% yield (49 mg, 0.21 mmol) as a white solid.

Typical Procedure for Carbonylative Coupling with Aryl Bromides (Figure 5.10)

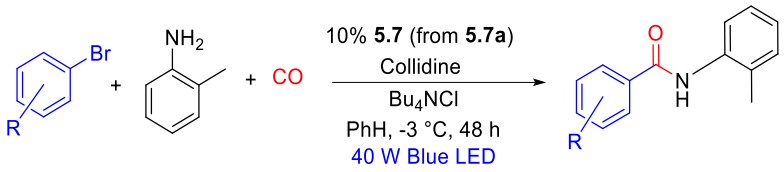

Catalyst **5.7** was generated in situ as follows. In a glovebox, 4-bromotoluene (86 mg, 0.50 mmol), o-toluidine (27 mg, 0.37 mmol), collidine (61 mg, 0.50 mmol), Bu_4NCl (69 mg, 0.25 mmol), [(DPE-Phos)Pd](μ-CO) **5.7a** (16.5 mg, 13 μmol), were dissolved in 6 mL benzene and transferred into a thick-walled 25 mL Schlenk bomb, and covered with a Teflon cap. The bomb was taken out of the glovebox and charged with 4 atm CO on top of the nitrogen atmosphere, leading to the rapid formation of catalyst **5.7**. The bomb was attached to a rotary evaporator with electrical tape. The solution was rotated at 100 rpm and cooled down to –3 ºC with a cooling bath equipped with a chiller. The solution was irradiated using a 40W Blue LED lamp (Figure 5.14E and 5.14F). After 48 hours, the bomb was taken out of the irradiation system and the excess CO was removed by opening the bomb inside a well-ventilated fume hood. The solvent was removed *in vacuo*, and the product was isolated by flash chromatography on silica gel (230-400 mesh) with hexanes-ethyl acetate (4:1), affording amide **5.1n** in 80% yield (45 mg, 0.20 mmol) as a white solid.

Typical Procedures for Carbonylative Coupling with Alkyl Halides (Figure 5.10)

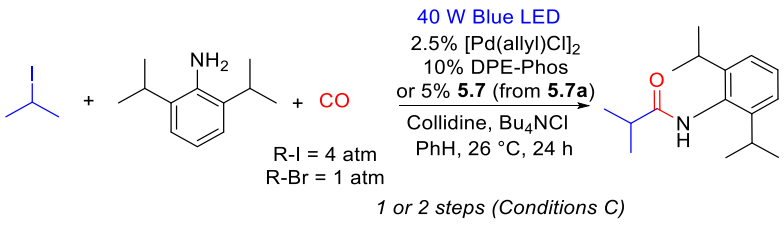

Conditions A (**5.7** as catalyst): Catalyst **5.7** was generated in situ as follows. In a glovebox, 2-iodopropane (43 mg, 0.25 mmol), 2,6-diisopropylaniline (67 mg, 0.37 mmol), collidine (45 mg, 0.37 mmol), Bu_4NCl (6.9 mg, 0.025 mmol), and [(DPE-Phos)Pd](μ-CO) **5.7a** (1.3 mg, 1 μmol) were dissolved in 3.5 mL benzene and transferred into thick-walled 25 mL Schlenk bomb, equipped with a magnetic stir bar, and covered with a Teflon cap. The bomb was taken out of the glovebox and 4 atm CO was added on top of the nitrogen atmosphere, leading to the rapid formation of catalyst **5.7**. The bomb was clamped on top of a stirring plate and the solution was irradiated using a 40W Blue LED lamp as seen in Figure 5.14C. After 24 hours, the bomb was taken out of the irradiation system and the excess CO was removed by opening the bomb inside a well-ventilated fume hood. The product was isolated by flash chromatography on silica gel (230-400 mesh) with hexanes-ethyl acetate (4:1) (1% NEt_3 additive). The fractions containing amide were evaporated under reduced pressure and solvent traces were removed *in vacuo*. Amide **5.1u** was obtained in 94% (58 mg, 0.24 mmol) as a white solid.

Conditions B ($[Pd(allyl)Cl]_2$ / DPE-Phos as catalyst): In a glovebox, 2-iodopropane (43 mg, 0.25 mmol), 2,6-diisopropylaniline (67 mg, 0.37 mmol), collidine (45 mg, 0.37 mmol), Bu_4NCl (6.9 mg, 0.025 mmol), $[Pd(allyl)Cl]_2$ (2.3 mg, 6.2 μmol), and DPE-Phos (14 mg, 0.025 mmol) were dissolved in 3.5 mL benzene and transferred into thick-walled 25 mL Schlenk bomb, equipped with a magnetic stir bar, and sealed with a Teflon cap. The bomb was taken out of the glovebox, 4 atm CO was added on top of the nitrogen atmosphere, clamped on top of a stirring plate, and the solution was irradiated using a 40W Blue LED lamp as seen in Figure 5.14C. After 24 hours, the bomb was taken out of the irradiation system and the excess CO was removed by opening the bomb inside a well-ventilated fume hood. The solvent was removed *in vacuo*, and the product

isolated by flash chromatography on silica gel (230-400 mesh) with hexanes-ethyl acetate (4:1) (1% NEt_3 additive), affording Amide **5.1u** in 80% yield (49 mg, 0.20 mmol) as a white solid.

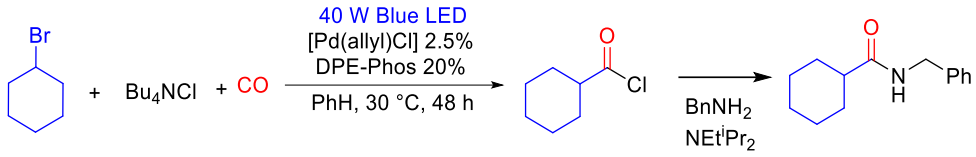

Conditions C. Acid chloride formation: In a glovebox, bromocyclohexane (41 mg, 0.25 mmol), Bu_4NCl (104 mg, 0.37 mmol), $[Pd(allyl)Cl]_2$ (2.3 mg, 6.2 µmol), and DPE-Phos (27 mg, 0.05 mmol) were dissolved in 3.5 mL benzene and transferred into a thick-walled 25 mL Schlenk bomb, equipped with a magnetic stir bar, and sealed with a Teflon cap. The bomb was taken out of the glovebox, 4 atm CO was added on top of the nitrogen atmosphere, clamped on top of a stirring plate, and the solution was irradiated using a 40W Blue LED lamp as seen in Figure 5.14C. After 48 hours, the bomb was taken out of the irradiation system and the excess CO was removed on a Schlenk line and the bomb was brought into the glovebox. An aliquot was taken and dissolved in C_6D_6. The acid chloride **5.2f** was characterized *in situ* by ^1H and ^{13}C NMR analysis.

In order to confirm the identity and yield of acid chloride, the aliquot was returned to the full reaction mixture, and to this mixture was added benzylamine (32 mg, 0.3 mmol) and NEt^iPr_2 (39 mg, 0.3 mmol) in 0.5 mL benzene. The capped mixture was stirred for 30 minutes at room temperature outside the glovebox. The solvent was removed in vacuo, and the product isolated by flash chromatography on silica gel (230-400 mesh) with hexanes-ethyl acetate (4:1) (1% NEt_3 additive), affording amide **5.1rr** in 80% yield (43 mg, 0.20 mmol) as a white solid.

Acid chlorides **5.2g**, **5.2h** and **5.2i** were generated using **5.7** (generated in situ from **5.7a**) as the catalyst. A mixture of Bu_4NCl/Ph_3BnPCl (1:1) was used for the synthesis of acid chlorides **5.2d**,

5.2e, and **5.2g**. Acid chloride **5.2h** was generated at 0 °C. Acid chloride **5.2i** was trapped with 2,6-diisopropylaniline and stirred for overnight at 50 °C.

Synthesis of Alkyl Bromides

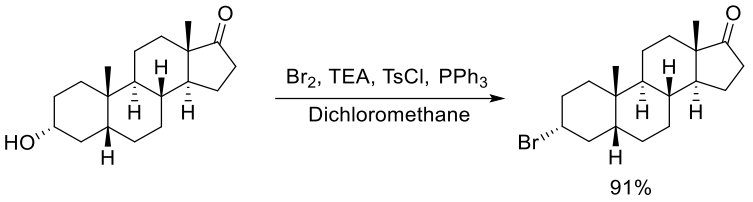

The following procedure was adapted from the literature.[74] Triphenylphosphine (0.66 g, 2.5 mmol) and dry dichloromethane (25 mL) were added to a 100 mL round-bottom flask. The solution was cooled down to 0 °C and bromine (75 μL, 1.5 mmol) was added dropwise to the solution. Triethyl amine (0.21 mL, 1.5 mmol) and *p*-toluenesulfonyl chloride (42 mg, 0.2 mmol) were added and the reaction was stirred for 10 minutes at 0 °C. A solution of 330 mg (1.1 mmol) of *trans*-androsterone in dichloromethane (5 mL) was added dropwise to the mixture. The reaction mixture was allowed to warm up to room temperature and stirred overnight. The reaction was quenched with water, and the aqueous layer was extracted with ethyl acetate (30 mL × 3). The combined organic layers were washed with water (30 mL) and brine (30 mL × 2), and then was dried over Na_2SO_4 followed by filtration. The solvent was removed in *vacuo* to give the crude product. The residue was further purified by flash chromatography on silica gel (230-400 mesh) with ethyl acetate/hexanes (5-10% gradient), affording the bromide, **5.11**, in 91% yield (0.35 g, 1.0 mmol) as a white solid.

(3R,5S,8R,9S,10S,13S,14S)-3-bromo-10,13-dimethylhexadecahydro-17H cyclopenta[a]phenanthren-17-one (5.11) ^{1}H NMR (400 MHz, Chloroform-*d*) δ 4.72 (t, *J* = 2.8 Hz, 1H), 2.43 (ddd, *J* = 19.1, 8.9, 1.1 Hz, 1H), 2.07 (dt, *J* = 19.2, 9.0 Hz, 1H), 1.94 (qt, *J* = 8.3, 3.8 Hz, 3H), 1.85 – 1.65 (m, 6H), 1.61 – 1.40 (m, 4H), 1.35 – 1.18 (m, 5H), 1.13 – 0.98 (m, 1H), 0.94

– 0.87 (m, 1H), 0.85 (s, 3H), 0.81 (s, 3H). ^{13}C NMR (101 MHz, $CDCl_3$) δ 221.3, 55.6, 54.0, 51.4, 47.8, 40.2, 37.2, 36.4, 35.8, 35.0, 32.9, 31.5, 30.9, 30.6, 27.6, 21.7, 20.1, 13.8, 12.3.

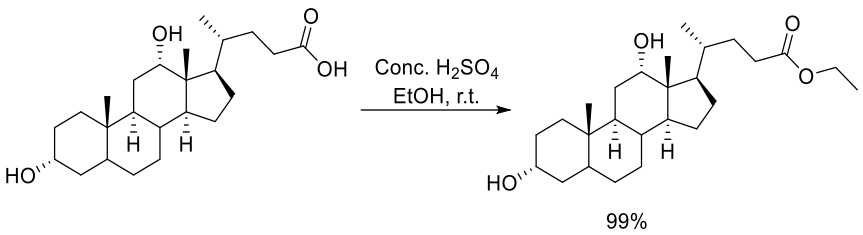

99%

To a 100 mL round bottom flask was added deoxycholic acid（1.96 g, 5 mmol） and ethanol (20 mL). Concentrated H_2SO_4 (2 mL) was added to the solution dropwise. The mixture was stirred at room temperature for overnight. The reaction was quenched with H_2O (~ 80 mL), and the aqueous layer was extracted with ethyl acetate (50 mL × 3). The combined organic layers were washed with saturated $NaHCO_3$ (50mL) and brine (30 mL × 2), and then was dried over Na_2SO_4, followed by filtration. The solvent was removed in *vacuo* to give ethyl deoxycholate, **5.12**, in 99% yield (2.08 g, 4.95 mmol) as a white solid.

Ethyl (4R)-4-((3R,9S,10S,12S,13R,14S,17R)-3,12-dihydroxy-10,13-dimethylhexadecahydro-1H-cyclopenta[a]phenanthren-17-yl)pentanoate (5.12) ^{1}H NMR (400 MHz, Chloroform-*d*) δ 4.10 (q, *J* = 7.1 Hz, 2H), 3.96 (t, *J* = 3.0 Hz, 1H), 3.59 (tt, *J* = 11.1, 4.6 Hz, 1H), 2.34 (ddd, *J* = 14.8, 9.8, 4.8 Hz, 1H), 2.20 (ddd, *J* = 15.5, 9.2, 6.7 Hz, 1H), 1.99 – 1.60 (m, 10H), 1.60 – 1.46 (m, 5H), 1.45 – 1.29 (m, 8H), 1.24 (t, *J* = 7.1 Hz, 3H), 1.10 (dtd, *J* = 25.8, 12.6, 11.6, 4.9 Hz, 3H), 0.96 (d, *J* = 6.2 Hz, 3H), 0.89 (s, 3H), 0.66 (s, 3H). ^{13}C NMR (101 MHz, $CDCl_3$) δ 174.3, 73.1, 71.8, 60.2, 48.3, 47.3, 46.5, 42.1, 36.4, 36.0, 35.2, 35.1, 34.1, 33.6, 31.4, 30.9, 30.5, 28.6, 27.5, 27.1, 26.1, 23.7, 23.2, 17.3, 14.3, 12.7. HRMS: Calculated for $C_{26}H_{44}O_4Na$ (MNa^+): 443.3137, found: 443.3132.

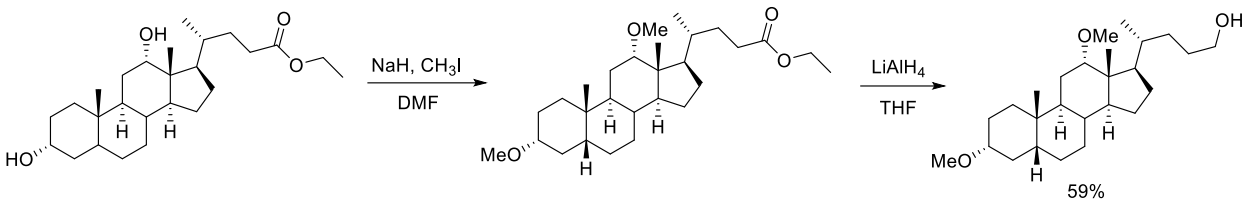

The following procedure was adapted from the literature.[75] To a 250 mL of round bottom flask was added NaH (0.28 g of a 60 % suspension in mineral oil, 7.1 mmol, 3 equiv.) and 40 mL of dry DMF. The mixture was cooled to 0 °C, and was added ethyl deoxycholate, **5.12**, (1.0 g, 2.4 mmol) in portions. The reaction mixture was stirred at 0 °C for 10 min, and then was added methyl iodide (0.70 mL, 11.9 mmol, 5 equiv.). The reaction mixture was stirred for 24 h at room temperature and then was added a second portion of NaH (0.19 g, 4.8 mmol, 2.0 equiv), followed by more methyl iodide (0.70 mL, 11.9 mmol, 5 equiv.). The reaction was stirred for an additional 24 h at room temperature. The reaction was quenched with slow addition of H_2O at 0 °C, and the aqueous layer was extracted with ethyl acetate (50 mL × 3). The combined organic layers were washed with saturated water (30mL× 2) and brine (30 mL × 2), and then was dried over Na_2SO_4, followed by filtration. The solvent was removed in *vacuo* and afford the crude product, di-methoxy ethyl deoxycholate that was taken on to the next step without further purification.

To a 100 mL flask was added crude di-methoxy ethyl deoxycholate with THF (7.0 mL). The mixture was cooled at 0 ^{o}C and purged with argon for 5 minutes. $LiAlH_4$ (0.27 g, 7.1 mmol, 3.00 equiv.) was added in three portions with vigorous stirring under argon. The reaction mixture was then stirred and heated to reflux for 24 h. The reaction was cooled down and quenched with 1 M H_2SO_4 solution at 0 ^{o}C. The aqueous layer was extracted with ethyl acetate (50 mL × 3). The combined organic layers were washed with saturated water (30mL× 2) and brine (30 mL × 2), and

then was dried over Na_2SO_4, followed by filtration. The solvent was removed in *vacuo* and afford the crude product. The residue was further purified by flash chromatography on silica gel (230-400 mesh) with ethyl acetate/hexanes (10-20% gradient), affording the alcohol, **5.13**, in 59 % yield (0.58 g, 1.4 mmol) as an oil and slowly solidified as white solid.

(4R)-4-((3R,5R,9S,10S,12S,13R,14S,17R)-3,12-dimethoxy-10,13-dimethylhexadecahydro-1H-cyclopenta[a]phenanthren-17-yl)pentan-1-ol (5.13) ^{1}H NMR (500 MHz, Chloroform-*d*) δ 3.61 (t, *J* = 6.4 Hz, 2H), 3.39 (t, *J* = 2.4 Hz, 1H), 3.34 (s, 3H), 3.25 (s, 3H), 3.19 – 3.10 (m, 1H), 1.91 – 1.67 (m, 8H), 1.61 – 1.50 (m, 4H), 1.47 – 0.95 (m, 14H), 0.92 (d, *J* = 5.9 Hz, 6H), 0.66 (s, 3H). ^{13}C NMR (126 MHz, $CDCl_3$) δ 82.3, 80.5, 63.7, 55.7, 55.5, 48.9, 46.7, 46.3, 42.1, 36.0, 35.4, 35.3, 34.5, 33.6, 32.6, 31.8, 29.5, 27.6, 27.4, 26.8, 26.1, 23.7, 23.3, 22.0, 17.7, 12.7.

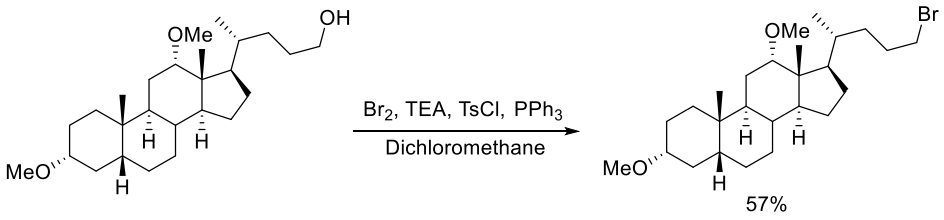

Triphenylphosphine (0.20 g, 0.75 mmol, 2 equiv.) and dry dichloromethane (7 mL) were added to a 50 mL round-bottom flask. The solution was cooled down to 0 °C and bromine (38 μL, 2.0 mmol) was added to the solution. Triethyl amine (0.10 mL, 0.75 mmol, 2.0 equiv.) and *p*-toluenesulfonyl chloride (14 mg, 0.075 mmol, 0.2 equiv.) were added and the reaction was stirred for 10 minutes at 0 °C. A solution of 0.15 g (0.38 mmol) of alcohol **5.13** in dichloromethane (3 mL) was added dropwise to the mixture. The reaction mixture was allowed to warm up to room temperature and stirred overnight.

The reaction was quenched with water, and the aqueous layer was extracted with ethyl acetate (15 mL × 3). The combined organic layers were washed with water (15 mL) and brine (15 mL × 2),

and then was dried over Na_2SO_4 followed by filtration. The solvent was removed in *vacuo* to give the crude product. The residue was further purified by flash chromatography on silica gel (230-400 mesh) with ethyl acetate/hexanes (5-10% gradient), affording the bromide, **5.14**, in 57% yield (0.10 g, 0.21 mmol) as a pale-yellow oil.

(3R,5R,9S,10S,12S,13R,14S,17R)-17-((R)-5-bromopentan-2-yl)-3,12-dimethoxy-10,13-dimethylhexadecahydro-1H-cyclopenta[a]phenanthrene (5.14) ^{1}H NMR (400 MHz, Chloroform-*d*) δ 3.44 – 3.34 (m, 3H), 3.33 (s, 3H), 3.24 (s, 3H), 3.14 (tt, *J* = 10.8, 4.4 Hz, 1H), 1.99 – 1.64 (m, 10H), 1.64 – 1.44 (m, 4H), 1.36 (t, *J* = 11.7 Hz, 4H), 1.29 – 0.93 (m, 8H), 0.91 (t, *J* = 3.3 Hz, 6H), 0.66 (s, 3H). ^{13}C NMR (101 MHz, $CDCl_3$) δ 82.2, 80.5, 55.6, 55.5, 48.8, 46.6, 46.33, 42.1, 36.0, 35.3, 35.0, 34.6, 34.5, 34.44, 33.5, 32.6, 29.7, 27.5, 27.4, 26.8, 26.1, 23.7, 23.3, 21.9, 17.7, 12.7. HRMS: Calculated for $C_{26}H_{44}BrO_2$: 467.2514, found: 467.2519.

β-Peptide Synthesis (Figure 5.13A)

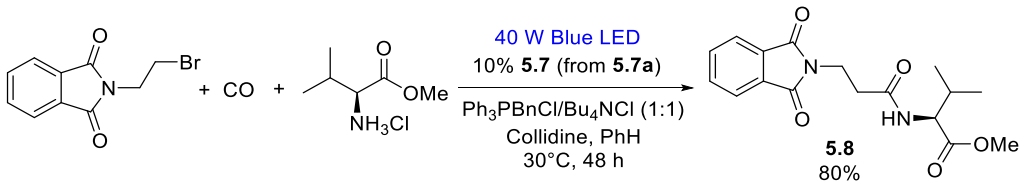

Catalyst **5.7** was generated *in situ* as follows. In a glovebox, 2-(2-bromoethyl)isoindoline-1,3-dione (64 mg, 0.25 mmol), *L*-valine methyl ester hydrochloride (63 mg, 0.37 mmol), collidine (109 mg, 0.90 mmol), and [(DPE-Phos)Pd](μ-CO) **5.7a** (16 mg, 0.010 mmol) were dissolved in 3.5 mL benzene and transferred into thick-walled 25 mL Schlenk bomb. Bu_4NCl (52 mg, 0.18 mmol) and Ph_3PBnCl (73 mg, 0.18 mmol) were dry transferred into the bomb, which was then equipped with a magnetic stir bar, and sealed with a Teflon cap. The bomb was taken out of the glovebox, 4 atm CO was added on top of the nitrogen atmosphere, leading to the rapid formation of catalyst **5.7**. Then the bomb was clamped on top of a stirring plate, and the solution was irradiated using a 40W

Blue LED lamp as seen in Figure 5.14C. After 48 hours, the bomb was taken out of the irradiation system and the excess CO was removed by opening the bomb inside a well-ventilated fume hood. The solvent was removed *in vacuo*, and product was isolated by flash chromatography on silica gel (230-400 mesh) with hexanes-ethyl acetate (1:1) (1% NEt_3 additive), affording **5.8** in 80% yield (66 mg, 0.20 mmol) as a pale-yellow solid.

Methyl (3-(1,3-dioxoisoindolin-2-yl)propanoyl)-L-valinate (5.8). Isolated yield 80% (66 mg, 0.20 mmol). Pale yellow solid. ^{1}H NMR (500 MHz, $CDCl_3$) δ 7.83 (dd, *J* = 5.4, 3.0 Hz, 2H), 7.70 (dd, *J* = 5.4, 3.0 Hz, 2H), 6.12 (d, *J* = 8.4 Hz, 1H), 4.53 (dd, *J* = 8.7, 5.0 Hz, 1H), 4.01 (t, *J* = 7.3 Hz, 2H), 3.69 (s, 3H), 2.69 (td, *J* = 7.1, 1.2 Hz, 2H), 2.11 (dtd, *J* = 13.7, 6.9, 5.2 Hz, 1H), 0.94 – 0.78 (m, 6H).^{13}C NMR (126MHz, $CDCl_3$) δ 172.5, 169.7, 168.2, 134.1, 132.2, 123.4, 57.2, 52.3, 34.8, 34.4, 31.3, 18.9, 18.0. HRMS: Calculated for $C_{17}H_{21}O_5N_2$ (MH^+): 333.14450, found: 333.14399.

Friedel-Crafts Carbonylation (Figure 5.13B)

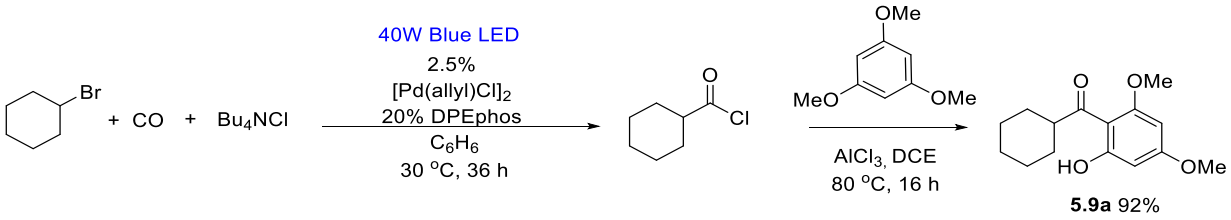

In a glovebox, bromocyclohexane (41 mg, 0.25 mmol), Bu_4NCl (104 mg, 0.38 mmol), $[Pd(allyl)Cl]_2$ (2.2 mg, 6 μmol) and DPE-Phos (27 mg, 0.05 mmol) were dissolved in 3.5 mL benzene and transferred into thick-walled 25 mL Schlenk bomb, equipped with a magnetic stir bar, and sealed with a Teflon cap. The bomb was taken out of the glovebox, 4 atm CO was added on

top of the nitrogen atmosphere, clamped on top of a stir plate, and the solution was irradiated using a 40W Blue LED lamp as seen in Figure 5.14C. Fans were used to keep the temperature below 30 ºC. After 36 hours, the bomb was taken out of the irradiation system and was frozen. The headspace of CO was removed on a Schlenk line and the bomb brought into the glovebox. Then, a solution of trimethoxybenzene (210 mg, 1.25 mmol) in 1 mL dichloroethane and a solution of $AlCl_3$ (100 mg, 0.75 mmol) in 1 mL dichloroethane was added. The bomb was capped, taken out of the glovebox, and heated at 80 °C in an oil bath for 16 h. The solvent was removed *in vacuo*, and the product was isolated by flash chromatography on silica gel (230-400 mesh) with hexanes-ethyl acetate (5:1). The ketone product eluted together with the excess of trimethoxybenzene. The trimethoxybenzene was then removed by sublimation under vacuum. Ketone **5.9a** was obtained in an overall yield of 92% (61 mg, 0.23 mmol) as a yellow liquid.

Cyclohexyl(2-hydroxy-4,6-dimethoxyphenyl)methanone (5.9a). Isolated yield 92% (61 mg, 0.23 mmol). Yellow liquid. ^{1}H NMR (500 MHz, Chloroform-*d*) δ 14.14 (s, 1H), 6.07 (d, *J* = 2.4 Hz, 1H), 5.92 (d, *J* = 2.4 Hz, 1H), 3.86 (s, 3H), 3.81 (s, 3H), 3.44 (tt, *J* = 11.3, 3.0 Hz, 1H), 1.93 – 1.78 (m, 4H), 1.77 – 1.66 (m, 1H), 1.49 – 1.13 (m, 6H). ^{13}C NMR (126 MHz, $CDCl_3$) δ 209.3, 168.0, 165.6, 162.4, 105.2, 93.8, 90.9, 77.3, 77.0, 76.8, 55.7, 55.5, 50.1, 29.5, 26.3, 26.2. HRMS: Calculated for $C_{15}H_{20}O_4Na^+$ (MNa^+): 287.1254, found: 287.1248.

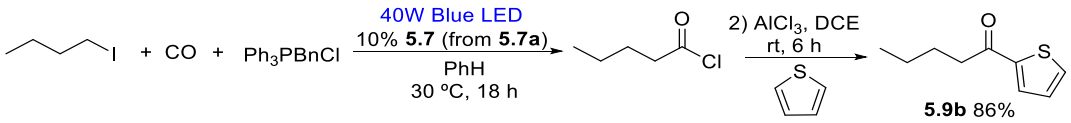

Catalyst **5.7** was generated in situ as follows. In a glovebox, 1-iodobutane (46 mg, 0.25 mmol), Ph_3PBnCl (107 mg, 0.275 mmol), and [(DPE-Phos)Pd](μ-CO) **5.7a** (16 mg, 0.0125 mmol) were dissolved in 3.5 mL benzene and transferred into a thick-walled 25 mL teflon cap sealable Schlenk

bomb and equipped with a magnetic stir bar. The bomb was taken out of the glovebox, 4 atm CO was added on top of the nitrogen atmosphere, leading to the rapid formation of catalyst **5.7**. Then the bomb was irradiated with a 40W Blue LED lamp as seen in Figure 5.14C, and the reaction temperature was kept under 30 °C with fans. After 18 hours, excess CO was removed on a Schlenk line, and the bomb was brought back into the glovebox. The mixture was passed through a 1 cm plug of celite to remove the solids. The remaining homogeneous solution was placed in a 20 mL glass vial with a cap. This mixture was diluted with 1,2-dichloroethane (DCE, 3.5 mL). To this solution was added $AlCl_3$ (33 mg, 0.25 mmol) and thiophene (210 mg, 2.5 mmol). The mixture was stirred at ambient temperature with a magnetic stir bar for 6 hours. The solvent was removed *in vacuo*, and the product was isolated via flash chromatography on silica gel (230-400 mesh) with hexanes-ethyl acetate (4:1), affording ketone **5.9b** in 86% yield (36 mg, 0.21 mmol) as a white solid.

1-(thiophen-2-yl)pentan-1-one (5.9b). Isolated yield 86% (36 mg, 0.21 mmol). Clear oil. ^{1}H NMR (500 MHz, $CDCl_3$) δ 7.70 (dd, *J* = 3.8, 1.2 Hz, 1H), 7.61 (dd, *J* = 4.9, 1.2 Hz, 1H), 7.12 (dd, *J* = 5.0, 3.7 Hz, 1H), 2.89 (t, *J* = 7.5 Hz, 2H), 1.73 (p, *J* = 7.5 Hz, 2H), 1.46 – 1.36 (m, 2H), 0.95 (t, *J* = 7.4 Hz, 3H). ^{13}C NMR (126MHz, $CDCl_3$) δ 193.7, 144.7, 133.4, 131.8, 128.1, 39.3, 27.0, 22.6, 14.0. HRMS: Calculated for $C_9H_{13}OS$ (MH^+): 169.06816, found: 169.06836.

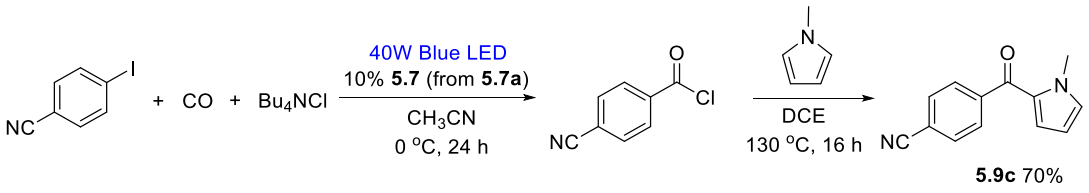

Catalyst **5.7** was generated in situ as follows. In a glovebox, 4-iodobenzonitrile (57 mg, 0.25 mmol), Bu_4NCl (104 mg, 0.38 mmol), [(DPE-Phos)Pd](μ-CO) **5.7a** (8.2 mg, 6 μmol) were dissolved in 3.5 mL acetonitrile and transferred into thick-walled 25 mL Schlenk bomb, equipped

with a magnetic stir bar, and sealed with a Teflon cap. The bomb was taken out of the glovebox, 4 atm CO was added on top of the nitrogen atmosphere, leading to the rapid formation of catalyst **5.7**. Then the bomb was clamped on top of a stir plate, and the solution was irradiated using using a 40W Blue LED lamp as seen in Figure 5.14C, with fans to keep the temperature below 30 ºC. After 24 hours, the bomb was taken out of the irradiation system and was frozen. The headspace of CO was removed on a Schlenk line and the bomb brought into the glovebox. The solvent was removed *in vacuo*. A solution of *N*-methyl pyrrole (101 mg, 1.25 mmol) in 2 mL dichloroethane was added. The bomb was capped, taken out of the glovebox, and heated at 130 °C in an oil bath for 16 h. The solvent was removed *in vacuo*, and the product isolated by flash chromatography on silica gel (230-400 mesh) with hexanes-ethyl acetate (4:1), affording ketone **5.9c** in an overall yield of 70% (37 mg, 0.18 mmol) as a brown solid.

4-(1-methyl-1*H*-pyrrole-2-carbonyl)benzonitrile (5.9c). Isolated yield 70% (37 mg, 0.18 mmol). Light brown solid. ^{1}H NMR (500 MHz, Chloroform-*d*) δ 7.91 – 7.82 (m, 2H), 7.79 – 7.70 (m, 2H), 6.97 (t, *J* = 2.1 Hz, 1H), 6.67 (dd, *J* = 4.1, 1.7 Hz, 1H), 6.18 (dd, *J* = 4.1, 2.4 Hz, 1H), 4.04 (s, 3H). ^{13}C NMR (126 MHz, $CDCl_3$) δ 184.0, 143.7, 132.6, 132.0, 129.8, 129.5, 123.5, 118.3, 114.7, 108.8, 37.5. HRMS: Calculated for $C_{13}H_{11}ON^{+}$ (MH^{+}): 211.08659, found: 211.08682.

Synthesis of Fenofibrate (Figure 5.13C)

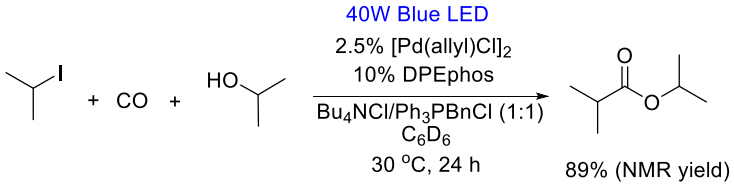

In a glovebox, 2-iodopropane (42 mg, 0.25 mmol), 2-propanol (23 mg, 0.37 mmol), collidine (45 mg, 0.37 mmol), Bu_4NCl (35 mg, 0.12 mmol), Ph_3PBnCl (49 mg, 0.12 mmol), $[Pd(allyl)Cl]_2$ (2.3

mg, 2.5 μmol), DPEphos (13 mg, 0.025 mmol), and benzyl benzoate (26 mg, 0.12 mmol) were dissolved in 3.5 mL C_6D_6 and transferred into thick-walled 25 mL Schlenk bomb, equipped with a magnetic stir bar, and covered with a Teflon cap. The bomb was taken out of the glovebox, 4 atm CO was added on top of the nitrogen atmosphere, clamped on top of a stirring plate and the solution was irradiated using a 40W Blue LED lamp as seen in Figure 5.14C. After 24 hours, the bomb was taken out of the irradiation system and the excess CO was removed by opening the bomb inside a well-ventilated fume hood. A 0.8 mL aliquot was taken and the yield of ester (89%) was determined by ^{1}H NMR analysis relative to the benzyl benzoate internal standard. Due to issues with purification, the ester was characterized *in situ*:

In situ: ^{1}H NMR (500 MHz, C_6D_6) δ 5.00 (hept, *J* = 6.3 Hz, 1H), 2.35 (hept, *J* = 6.9 Hz, 1H), 1.06 (d, *J* = 7.0 Hz, 6H), 1.03 (d, *J* = 6.3 Hz, 6H). ^{13}C NMR (126 MHz, C_6D_6) δ 175.9, 67.0, 34.4, 21.8, 19.1. *Pure compound*: ^{1}H NMR (500 MHz, C_6D_6) δ 5.00 (hept, *J* = 6.3 Hz, 1H), 2.36 (hept, *J* = 7.0 Hz, 1H), 1.06 (d, *J* = 7.0 Hz, 6H), 1.03 (d, *J* = 6.3 Hz, 6H). ^{13}C NMR (126 MHz, C_6D_6) δ 176.0, 67.1, 34.4, 21.8, 19.1.

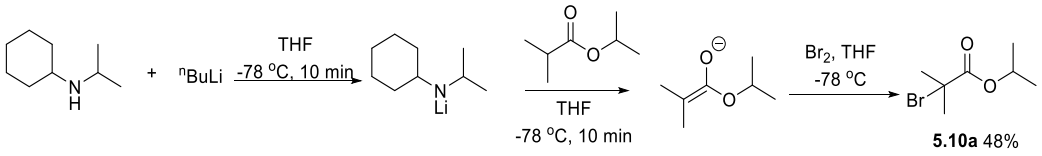

The following procedure was adapted from the literature.[60,61] To a 10 mL round bottom flask was added *N*-cyclohexyl,isopropylamine (1.554 g, 11 mmol) and dry THF (10 mL). The flask was purged with argon and cooled to -78 ºC. ^{n}BuLi solution (2.5 M in hexanes, 4.4 ml, 11 mmol) was added dropwise *via* syringe. The mixture was stirred at -78 ºC for 10 min, and then an isopropyl isobutyrate (1.302 g, 10 mmol)/THF solution (5 mL) was added dropwise over the course of 10 min. The mixture was stirred for 10 min at -78 ºC.

To a 50 ml round bottom flask was added dry THF (5 ml), purged with argon and cooled to -78 ºC. Br_2 (0.67 ml, 13 mmol) was added to the flask *via* syringe to give an orange solution. Note: the solubility of Br_2 in THF can vary by the scale of the reaction: lower the temperature until Br_2 starts to precipitate. The enolate solution above was added to the Br_2/THF solution dropwise over 30 min *via* cannula, maintaining the temperature at -78 ºC. The mixture was quenched with conc. HCl (5 mL) right after the addition of the enolate at -78 ºC. The reaction mixture was stirred for 5 min followed by addition of sat. sodium thiosulfate solution (5 mL). The flask was then allowed to warm to room temperature. The mixture was extracted with 3 x 20 mL pentane, washed with brine (20 mL), dried over $MgSO_4$, and filtered. The pentane was removed carefully *via* low vacuum. Isopropyl 2-bromo-2-methylpropanoate, **5.10a**, was isolated by distillation under reduced pressure (60 ºC, 50 Torr): 48% yield (0.995 g, 4.76 mmol).

Isopropyl 2-bromo-2-methylpropanoate (5.10a).[72] ^{1}H NMR (500 MHz, Chloroform-*d*) δ 5.05 (hept, *J* = 6.2 Hz, 1H), 1.92 (s, 6H), 1.28 (d, *J* = 6.3 Hz, 6H). ^{13}C NMR (126 MHz, $CDCl_3$) δ 171.1, 69.6, 56.4, 30.7, 21.4.

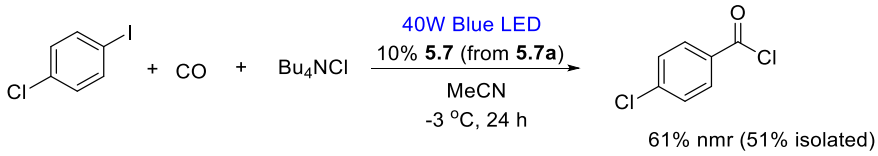

Catalyst **5.7** was generated in situ as follows. In a glovebox, 1-chloro-4-iodobenzene (60 mg, 0.25 mmol), Bu_4NCl (104 mg, 0.38 mmol), and [(DPE-Phos)Pd](μ-CO) **5.7a** (32.9 mg, 0.025 mmol) were dissolved in 3.5 mL acetonitrile and transferred into thick-walled 25 mL Schlenk bomb, equipped with a magnetic stir bar, and sealed with a Teflon cap. The bomb was taken out of the glovebox, and 4 atm CO was added on top of the nitrogen atmosphere. The bomb was attached to a rotary evaporator with electrical tape, then rotated at 100 rpm and cooled down to – 3 ºC by a

cooling bath equipped with a chiller. The solution was irradiated using a 40W Blue LED lamp (Figure 5.14C). After 24 hours, the bomb was taken out of the irradiation system, CO was removed on a Schlenk line, and the bomb brought into the glovebox. The reaction mixture was filtered and extracted with 4 x 10 mL pentane. The solvent was removed *in vacuo* to afford 4-chlorobenzoyl chloride, **5.10c** in yield of 51% (22 mg, 0.13 mmol) as a viscous cloudy oil (low melting point solid).

4-chlorobenzoyl chloride (5.10c). ^{1}H NMR (500 MHz, Chloroform-*d*) δ 8.09 – 8.03 (m, 2H), 7.52 – 7.48 (m, 2H). ^{13}C NMR (126 MHz, $CDCl_3$) δ 167.4, 142.3, 132.6, 131.7, 129.4, 77.3, 77.0, 76.8.

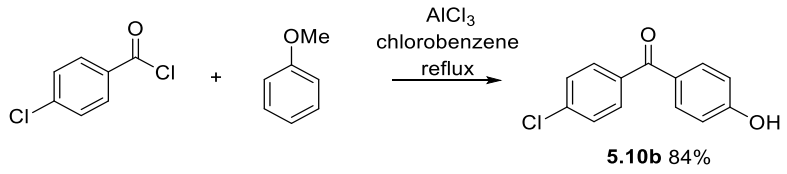

5.10b 84%

The following procedure was adapted from the literature.[59] In a glovebox, anisole (357 mg, 3.3 mmol) and $AlCl_3$ (600 mg, 4.5 mmol) were transferred into a thick-walled 25 mL Schlenk bomb, equipped with a magnetic stir bar. 4-chlorobenzoyl chloride **5.10c** (525 mg, 3.0 mmol) in a chlorobenzene (1 mL) solution was added to the mixture dropwise. After the addition, the bomb was sealed with a Teflon cap, taken out of the glovebox to place into an oil bath at 140 ºC. The reaction mixture was stirred for 2 h. The mixture was then cooled to room temperature, placed into an ice bath and quenched with water (2 mL). Additional water (3 mL) was added until the precipitate was fully dissolved. Upon further addition of water (ca. 5 mL), a new orange precipitate was formed. The pH of the aqueous phase was 4~5. The orange solid was collected by vacuum filtration to obtain the crude product. The product was further purified by flash chromatography

on silica gel (230-400 mesh) with hexanes-ethyl acetate (4:1, 100 mL), then ethyl acetate-2-propanol (1:1, 50 mL), affording phenol **5.10b** in 84% yield (588 mg, 2.5 mmol) as an orange solid.

(4-chlorophenyl)(4-hydroxyphenyl)methanone (5.10b).[71] ^{1}H NMR (500 MHz, Chloroform-*d*) δ 7.79 – 7.74 (m, 2H), 7.73 – 7.68 (m, 2H), 7.48 – 7.44 (m, 2H), 6.94 – 6.89 (m, 2H), 5.46 (s, 1H). ^{13}C NMR (126 MHz, $CDCl_3$) δ 194.4, 159.8, 138.4, 136.4, 132.8, 131.2, 130.1, 128.6, 115.3.

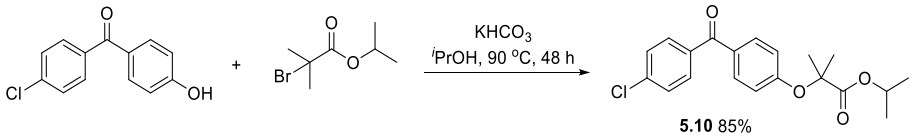

5.10 85%

The following procedure was adapted from the literature.[62] To a 25 mL round bottom flask equipped with a magnetic stir bar, (4-chlorophenyl)(4-hydroxyphenyl)methanone **5.10a** (116.3 mg, 0.50 mmol) was added followed by 3 mL isopropanol. Potassium bicarbonate (90.1 mg, 0.90 mmol) was added to the solution and the mixture was stirred at room temperature for 10 min. An isopropyl 2-bromo-2-methypropanoate **5.10b** (208.6 mg, 1.0 mmol) solution in isopropanol (0.5 mL) was added dropwise to the mixture. The flask was heated to 90 ºC to reflux with vigorous stirring for 48 h. The reaction mixture was then allowed to cool to room temperature, then filtered through celite with excess ethyl acetate. The solvent was removed *in vacuo* to give the crude product. The residue was further purified by flash chromatography on silica gel (230-400 mesh) with hexanes-ethyl acetate (from 9:1 to 4:1), affording fenofibrate **5.10** in 85% yield (153.0 mg, 0.42 mmol) as a colorless solid.

Fenofibrate (5.10). ^{1}H NMR (500 MHz, Chloroform-*d*) δ 7.75 (d, *J* = 8.8 Hz, 2H), 7.72 (d, *J* = 8.5 Hz, 2H), 7.47 (d, *J* = 8.5 Hz, 2H), 6.89 (d, *J* = 8.8 Hz, 2H), 5.11 (hept, *J* = 6.3 Hz, 1H), 1.69 (s, 6H), 1.23 (d, *J* = 6.3 Hz, 5H). ^{13}C NMR (126 MHz, $CDCl_3$) δ 194.27, 173.11, 159.75, 138.37,

136.45, 131.96, 131.17, 130.24, 128.55, 117.26, 79.44, 77.28, 77.23, 77.02, 76.77, 69.36, 25.38, 21.54.

5.5.4. Characterization Data of Amides, Esters, Thioesters, Ketones, and Acid Chlorides

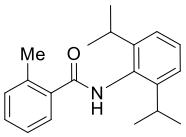

***N*-(2,6-diisopropylphenyl)-2-methylbenzamide (5.1a)**. Isolated yield 99% (73 mg, 0.24 mmol). White solid. ^{1}H NMR (500 MHz, $CDCl_3$) δ 7.60 (d, *J* = 7.7 Hz, 1H), 7.43 – 7.38 (m, 1H), 7.38 – 7.34 (m, 1H), 7.31 (t, *J* = 8.1 Hz, 2H), 7.26 (d, *J* = 13.8 Hz, 1H), 7.02 (s, 1H), 3.26 (hept, *J* = 6.9 Hz, 2H), 2.57 (s, 3H), 1.28 (d, *J* = 6.9 Hz, 12H). ^{13}C NMR (126MHz, $CDCl_3$) δ 169.6, 146.5, 137.0, 136.4, 131.6, 130.9, 130.4, 128.7, 126.7, 126.0, 123.7, 29.1, 23.8, 20.0. HRMS: Calculated for $C_{20}H_{26}ON$ (MH^+): 296.2009, found: 296.2015.

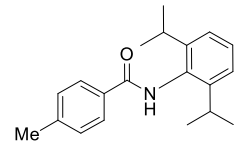

***N*-(2,6-diisopropylphenyl)-4-methylbenzamide (5.1b)**. Isolated yield 99% (73 mg, 0.24 mmol). White solid. ^{1}H NMR (500 MHz, $CDCl_3$) δ 7.83 (d, *J* = 8.1 Hz, 2H), 7.32 (m, 4H), 7.22 (d, *J* = 7.7 Hz, 2H), 3.14 (hept, *J* = 6.9 Hz, 2H), 2.45 (s, 3H), 1.22 (d, *J* = 6.9 Hz, 12H). ^{13}C NMR (126MHz, $CDCl_3$) δ 166.9, 146.5, 142.4, 131.9, 131.4, 129.6, 128.5, 127.3, 123.7, 29.0, 23.8, 21.6. HRMS: Calculated for $C_{20}H_{26}ON$ (MH^+): 296.2009, found: 296.2014.

Ethyl 4-((2,6-diisopropylphenyl)carbamoyl)benzoate (5.1c). Isolated yield 95% (84 mg, 0.23 mmol). Yellow solid. ^{1}H NMR (500 MHz, $CDCl_3$) δ 8.13 (d, *J* = 8.4 Hz, 2H), 7.95 (d, *J* = 8.4 Hz, 2H), 7.48 (s, 1H), 7.36 (t, *J* = 7.7 Hz, 1H), 7.23 (d, *J* = 7.8 Hz, 2H), 4.43 (q, *J* = 7.1 Hz, 2H), 3.12 (hept, *J* = 6.8 Hz, 2H), 1.43 (t, *J* = 7.1 Hz, 3H), 1.22 (d, *J* = 6.9 Hz, 12H). ^{13}C NMR (126MHz,

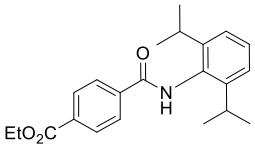

$CDCl_3$) δ 166.3, 165.9, 146.4, 138.4, 133.5, 131.0, 130.1, 128.8, 127.3, 123.8, 61.6, 29.1, 23.8, 14.4. HRMS: Calculated for $C_{20}H_{27}O_3NNa$ (MNa^+): 376.1883, found: 376.1874.

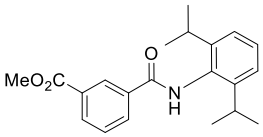

Methyl 3-((2,6-diisopropylphenyl)carbamoyl)benzoate (5.1d). Isolated yield 92% (78 mg, 0.23 mmol). White solid. ^1H NMR (500 MHz, $CDCl_3$) δ 8.56 (t, *J* = 1.6 Hz, 1H), 8.24 (dt, *J* = 7.8, 1.4 Hz, 1H), 8.17 (dt, *J* = 7.7, 1.3 Hz, 1H), 7.59 (t, *J* = 7.8 Hz, 1H), 7.45 (s, 1H), 7.38 – 7.32 (m, 1H), 7.23 (d, *J* = 7.7 Hz, 2H), 3.97 (s, 3H), 3.13 (hept, *J* = 6.8 Hz, 2H), 1.22 (d, *J* = 6.9 Hz, 12H). ^{13}C NMR (126MHz, $CDCl_3$) δ 166.5, 166.0, 146.5, 135.0, 132.8, 132.2, 131.0, 130.9, 129.3, 128.8, 127.9, 123.8, 52.6, 29.1, 23.8. HRMS: Calculated for $C_{21}H_{25}O_3NNa$ (MNa^+): 362.1727, found: 362.1739.

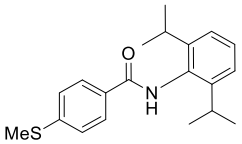

N-(2,6-diisopropylphenyl)-4-(methylthio)benzamide (5.1e). Isolated yield 95% (78 mg, 0.24 mmol). White solid. ^1H NMR (500 MHz, $CDCl_3$) δ 7.83 (d, *J* = 8.4 Hz, 2H), 7.32 (t, *J* = 8.4 Hz, 4H), 7.22 (d, *J* = 7.7 Hz, 2H), 3.12 (hept, *J* = 6.8 Hz, 2H), 2.54 (s, 3H), 1.21 (d, *J* = 6.9 Hz, 12H). ^{13}C NMR (126MHz, $CDCl_3$) δ 166.5, 146.5, 144.0, 131.3, 130.7, 128.6, 127.7, 125.8, 123.7, 29.1, 23.8, 15.3. HRMS: Calculated for $C_{20}H_{25}ONSNa$ (MNa^+): 350.1549, found: 350.1553.

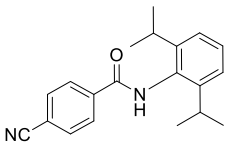

4-cyano-*N*-(2,6-diisopropylphenyl)benzamide (5.1f). Isolated yield 97% (75 mg, 0.24 mmol). Yellow solid. ^1H NMR (500 MHz, $CDCl_3$) δ 7.96 (d, *J* = 8.4 Hz, 2H), 7.71 (d, *J* = 8.4 Hz, 2H), 7.57 (s, 1H), 7.39 (t, *J* = 7.8 Hz, 1H), 7.24 (d, *J* = 7.8 Hz, 2H), 3.07 (hept, *J* = 6.8 Hz, 2H), 1.20 (d, *J* = 6.9 Hz, 12H). ^{13}C NMR (126MHz,

$CDCl_3$) δ 165.4, 146.4, 138.4, 132.8, 130.7, 129.1, 128.0, 123.9, 118.1, 115.5, 29.1, 23.8. HRMS: Calculated for $C_{20}H_{23}ON_2$ (MH^+): 307.1805, found: 307.1802.

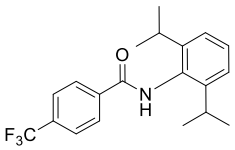

N-(2,6-diisopropylphenyl)-4-(trifluoromethyl)benzamide (5.1g). Isolated yield 96% (84 mg, 0.24 mmol). White solid. ^{1}H NMR (500 MHz, $CDCl_3$) δ 8.00 (d, *J* = 8.1 Hz, 2H), 7.72 (d, *J* = 8.2 Hz, 2H), 7.50 (s, 1H), 7.37 (t, *J* = 7.8 Hz, 1H), 7.24 (d, *J* = 7.8 Hz, 2H), 3.10 (hept, *J* = 6.8 Hz, 2H), 1.21 (d, *J* = 6.9 Hz, 12H). ^{13}C NMR (126MHz, $CDCl_3$) δ 165.8, 146.4, 137.8, 133.6 (q, *J* = 32.8 Hz), 130.9, 128.9, 127.8, 126.0 (q, *J* = 3.6 Hz), 123.8, 123.8 (q, *J* = 272.7 Hz), 29.1, 23.8. HRMS: Calculated for $C_{20}H_{23}ONF_3$ (MH^+): 350.1726, found: 350.1730.

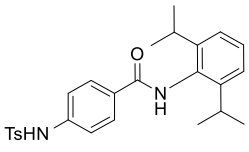

***N*-(2,6-diisopropylphenyl)-4-((4-methylphenyl)sulfonamido)benzamide (5.1h)**. Isolated yield 96% (108 mg, 0.24 mmol). White solid. ^{1}H NMR (500 MHz, DMSO-d_6) δ 10.67 (s, 1H), 9.57 (s, 1H), 7.86 (d, *J* = 8.7 Hz, 2H), 7.74 (d, *J* = 8.3 Hz, 2H), 7.38 (d, *J* = 8.1 Hz, 2H), 7.30 – 7.25 (m, 1H), 7.22 (d, *J* = 8.7 Hz, 2H), 7.17 (d, *J* = 7.7 Hz, 2H), 3.01 (hept, *J* = 6.8 Hz, 2H), 2.35 (s, 3H), 1.09 (dd, *J* = 32.9, 6.6 Hz, 12H). ^{13}C NMR (126 MHz, DMSO-d_6) δ 165.4, 146.1, 143.6, 140.8, 136.5, 132.7, 129.9, 129.2, 128.8, 127.6, 126.7, 122.9, 118.2, 28.1, 23.5, 23.3, 21.0. HRMS: Calculated for $C_{26}H_{30}O_3N_2SNa$ (MNa^+): 473.1869, found: 473.1878.

***N*-(2,6-diisopropylphenyl)-4-formylbenzamide (5.1i)**. Isolated yield 92% (71 mg, 0.23 mmol). White solid. ^{1}H NMR (500 MHz, $CDCl_3$) δ 10.11 (s, 1H), 8.03 (d, *J* = 8.2 Hz, 2H), 7.96 (d, *J* = 8.1 Hz, 2H), 7.57 (s, 1H), 7.37 (t, *J* = 7.8 Hz, 1H), 7.24 (d, *J* = 7.8 Hz, 2H), 3.11 (hept, *J* = 6.9 Hz,

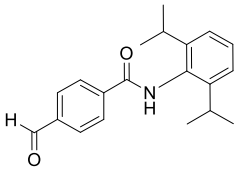

2H), 1.21 (d, *J* = 6.9 Hz, 12H). ^{13}C NMR (126MHz, $CDCl_3$) δ 191.6, 166.1, 146.4, 139.7, 138.5, 130.9, 130.2, 128.9, 128.0, 123.8, 29.1, 23.8. HRMS: Calculated for $C_{20}H_{22}O_2N$ ($M\text{-}1^+$): 308.1656, found: 308.1655.

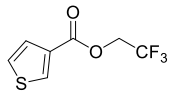

2,2,2-Trifluoroethyl thiophene-3-carboxylate (5.1j). Isolated yield 72% (38 mg, 0.18 mmol). Pale yellow liquid. ^{1}H NMR (500 MHz, Chloroform-*d*) δ 8.22 (dd, *J* = 3.1, 1.2 Hz, 1H), 7.57 (dd, *J* = 5.1, 1.2 Hz, 1H), 7.35 (dd, *J* = 5.1, 3.0 Hz, 1H), 4.66 (q, *J* = 8.4 Hz, 2H). ^{13}C NMR (126 MHz, $CDCl_3$) δ 160.8, 134.3, 131.6, 127.9, 126.6, 126.4 –119.8 (q), 60.9 – 60.0 (q). HRMS: Calculated for $C_7H_5F_3O_2SNa^+$ (MNa^+): 232.9855, found: 232.9848.

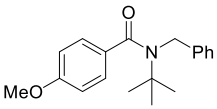

***N*-benzyl-*N*-(*tert*-butyl)-4-methoxybenzamide (5.1k).** Isolated yield 53% (39 mg, 0.13 mmol). Yellow liquid. ^{1}H NMR (500 MHz, Chloroform-*d*) δ 7.39 (d, *J* = 8.8 Hz, 2H), 7.31 (t, *J* = 7.5 Hz, 2H), 7.22 (t, *J* = 8.0 Hz, 3H), 6.79 (d, *J* = 8.7 Hz, 2H), 4.64 (s, 2H), 3.76 (s, 3H), 1.48 (s, 9H). ^{13}C NMR (126 MHz, $CDCl_3$) δ 173.9, 160.2, 140.3, 131.6, 128.5, 128.2, 126.9, 126.4, 113.6, 57.9, 55.3, 51.8, 28.8. HRMS: Calculated for $C_{19}H_{24}O_2N^+$ (MH^+): 298.18016, found: 298.18004.

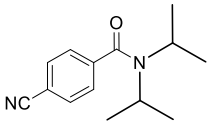

4-cyano-*N*,*N*-diisopropylbenzamide (5.1l). Isolated yield 85% (49 mg, 0.21 mmol). White solid. ^{1}H NMR (500 MHz, $CDCl_3$) δ 7.72 – 7.64 (m, 2H), 7.43 – 7.36 (m, 2H), 3.60 (bs, 2H), 1.34 (bs, 12H). ^{13}C NMR (126MHz, $CDCl_3$) δ 168.9, 143.2, 132.6, 126.4, 118.4, 112.7, 51.2, 46.2, 20.7. HRMS: Calculated for $C_{14}H_{19}ON_2$ (MH^+): 231.14919, found: 231.14963.

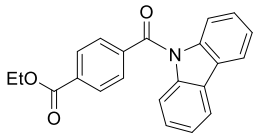

Ethyl 4-(9*H*-carbazole-9-carbonyl)benzoate (5.1m). Isolated yield 75% (64 mg, 0.19 mmol). Pale yellow solid. ^{1}H NMR (500 MHz, Chloroform-*d*) δ 8.24 – 8.18 (m, 2H), 8.05 – 7.98 (m, 2H), 7.82 – 7.74 (m, 2H), 7.49 (d, *J* = 8.2 Hz, 2H), 7.41 – 7.29 (m, 4H), 4.45 (q, *J* = 7.1 Hz, 2H), 1.45 (t, *J* = 7.1 Hz, 3H). ^{13}C NMR (126 MHz, $CDCl_3$) δ 168.7, 165.7, 139.6, 138.9, 133.7, 130.1, 128.8, 126.9, 126.2, 123.8, 119.9, 115.9, 61.6, 14.3. HRMS: Calculated for $C_{22}H_{17}O_3NNa^+$ (MNa^+): 366.1101, found: 366.1100.

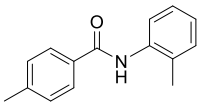

4-Methyl-*N*-(*o*-tolyl)benzamide (5.1n).[63] Isolated yield 80% (45 mg, 0.21 mmol). Colorless solid. ^{1}H NMR (500 MHz, Chloroform-*d*) δ 7.96 (d, *J* = 8.0 Hz, 1H), 7.79 (d, *J* = 8.2 Hz, 2H), 7.66 (s, 1H), 7.30 (d, *J* = 7.9 Hz, 2H), 7.25 – 7.20 (m, 1H), 7.11 (t, *J* = 8.0 Hz, 1H), 2.44 (s, 3H), 2.33 (s, 3H). ^{13}C NMR (126 MHz, $CDCl_3$) δ 165.6, 142.4, 135.9, 132.2, 130.5, 129.5, 129.1, 127.1, 126.9, 125.2, 123.0, 21.5, 17.8.

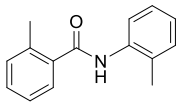

2-Methyl-N-(o-tolyl)benzamide (5.1o). Isolated yield 60% (34 mg, 0.15 mmol). Colorless solid. ^{1}H NMR (500 MHz, Chloroform-*d*) δ 7.97 (d, *J* = 6.9 Hz, 1H), 7.52 (d, *J* = 6.9 Hz, 1H), 7.38 (t, *J* = 7.4 Hz, 1H), 7.31 (d, *J* = 14.1 Hz, 3H), 7.23 (s, 1H), 7.13 (t, *J* = 7.4 Hz, 1H), 2.54 (s, 3H), 2.31 (s, 3H). ^{13}C NMR (126 MHz, $CDCl_3$) δ 168.1, 136.5, 135.8, 131.3, 130.6, 130.3, 129.1, 126.9, 126.7, 126.0, 125.4, 123.1, 19.9, 18.0. HRMS: Calculated for $C_{15}H_{16}ON^+$ (MH^+): 226.12264, found:226.12285.

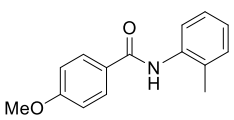

4-Methoxy-N-(o-tolyl)benzamide (5.1p).[64] Isolated yield 60% (36 mg, 0.15 mmol). Colorless solid. ^{1}H NMR (500 MHz, Chloroform-d) δ 7.95 (d, J = 8.0 Hz, 1H), 7.86 (d, J = 8.8 Hz, 2H), 7.60 (s, 1H), 7.23 (d, J = 7.5 Hz, 1H), 7.11 (t, J = 6.9 Hz, 1H),

6.99 (d, J = 8.8 Hz, 2H), 3.88 (s, 3H), 2.34 (s, 3H). ^{13}C NMR (126 MHz, $CDCl_3$) δ 165.1, 162.5, 136.0, 130.5, 129.0, 128.9, 127.2, 126.9, 125.1, 123.0, 114.0, 55.5, 17.9.

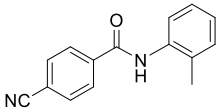

4-cyano-N-(o-tolyl)benzamide (5.1q). Isolated yield 80% (47 mg, 0.20 mmol). Pale yellow solid. ^{1}H NMR (500 MHz, Chloroform-d) δ 7.98 (d, J = 7.8 Hz, 2H), 7.87 (s, 1H), 7.79 (d, J = 8.2 Hz, 2H), 7.68 (s, 1H), 7.27 (q, J = 6.7, 5.7 Hz, 2H), 7.17 (t, J = 7.5 Hz, 1H), 2.34 (s, 3H). ^{13}C NMR (126 MHz, $CDCl_3$) δ 164.0, 138.8, 135.08, 132.7, 130.8, 129.9, 127.8, 127.0, 126.2, 123.6, 117.9, 115.4, 17.8. HRMS: Calculated for $C_{15}H_{12}N_2NaO^+$ (MNa^+): 259.0842, found: 259.0853.

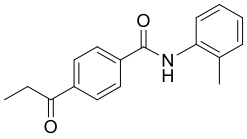

4-Propionyl-N-(o-tolyl)benzamide (5.1r). Isolated yield 80% (47 mg, 0.20 mmol). Pale yellow solid. ^{1}H NMR (500 MHz, Chloroform-d) δ 8.04 (d, J = 8.3 Hz, 2H), 7.94 (d, J = 8.1 Hz, 2H), 7.85 (d, J = 22.8 Hz, 2H), 7.26 – 7.21 (m, 2H), 7.13 (d, J = 8.3 Hz, 1H), 3.18 – 2.93 (m, 2H), 2.33 (s, 3H), 1.25 (t, J = 7.2 Hz, 3H). ^{13}C NMR (126 MHz, $CDCl_3$) δ 200.1, 164.8, 139.3, 138.6, 135.4, 130.7, 129.8, 128.4, 127.4, 126.9, 125.8, 123.5, 32.2, 17.9, 8.1. HRMS: Calculated for $C_{17}H_{17}NO_2Na^+$ (MNa^+): 290.1151, found: 290.1162.

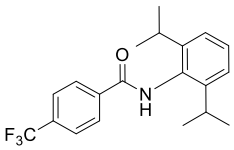

N-(2,6-diisopropylphenyl)-4-(trifluoromethyl)benzamide (5.1s). Isolated yield 96% (84 mg, 0.24 mmol). White solid. ^{1}H NMR (500 MHz, $CDCl_3$) δ 8.00 (d, *J* = 8.1 Hz, 2H), 7.72 (d, *J* = 8.2 Hz, 2H), 7.50 (s, 1H), 7.37 (t, *J* = 7.8 Hz, 1H), 7.24 (d, *J* = 7.8 Hz, 2H), 3.10 (hept, *J* = 6.8 Hz, 2H), 1.21 (d, *J* = 6.9 Hz, 12H). ^{13}C NMR (126MHz, $CDCl_3$) δ 165.8, 146.4, 137.8, 133.6 (q, *J* = 32.8 Hz), 130.9, 128.9, 127.8, 126.0 (q, *J*

= 3.6 Hz), 123.8, 123.8 (q, *J* = 272.7 Hz), 29.1, 23.8. HRMS: Calculated for $C_{20}H_{23}ONF_3$ (MH^+): 350.1726, found: 350.1730.

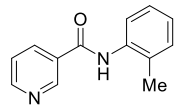

N-(o-tolyl)nicotinamide (5.1t). Isolated yield 94% (53 mg, 0.23 mmol). Pale yellow solid. ^{1}H NMR (500 MHz, Chloroform-*d*) δ 9.10 (s, 1H), 8.77 (s, 1H), 8.21 (d, *J* = 7.6 Hz, 1H), 7.91 – 7.76 (m, 2H), 7.50 – 7.40 (m, 1H), 7.29 – 7.21 (m, 2H), 7.20 – 7.11 (m, 1H), 2.33 (s, 3H). ^{13}C NMR (126 MHz, $CDCl_3$) δ 163.9, 152.6, 147.9, 135.4, 135.2, 130.7, 129.9, 127.0, 126.0, 123.8, 123.6, 17.9. HRMS: Calculated for $C_{13}H_{13}ON_2^+$ (MH^+): 213.10224, found: 213.10225.

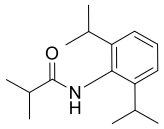

***N*-(2,6-diisopropylphenyl)isobutyramide (5.1u).** Isolated yield 94% (58 mg, 0.24 mmol). White solid. ^{1}H NMR (500 MHz, $CDCl_3$, Major rotamer, 24 ºC) δ 7.31 – 7.26 (m, 1H), 7.17 (d, J = 7.7 Hz, 2H), 6.64 (s, 1H), 3.05 (hept, J = 6.9 Hz, 2H), 2.63 (hept, J = 6.9 Hz, 1H), 1.31 (d, J = 6.9 Hz, 6H), 1.20 (d, J = 6.9 Hz, 12H). ^{13}C NMR (126MHz, $CDCl_3$, Major rotamer, 24 ºC) δ 176.1, 146.4, 131.2, 128.4, 123.5, 36.2, 28.8, 23.7, 20.0. HRMS: Calculated for $C_{16}H_{25}ONNa$ (MNa^+): 270.1828, found: 270.1829.

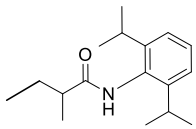

***N*-(2,6-diisopropylphenyl)-2-methylbutanamide (5.1v).** Isolated yield 82% (54 mg, 0.21 mmol). White solid. ^{1}H NMR (500 MHz, $CDCl_3$, Major rotamer, 24 ºC) δ 7.31 – 7.26 (m, 1H), 7.17 (d, J = 7.7 Hz, 2H), 6.63 (s, 1H), 3.08 (hept, J = 6.9 Hz, 2H), 2.39 (h, J = 6.9 Hz, 1H), 1.89 – 1.79 (m, 1H), 1.54 (ddd, J = 13.7, 7.4, 6.3 Hz, 1H), 1.29 (d, J = 6.9 Hz, 3H), 1.20 (dd, J = 6.9, 2.9 Hz, 12H), 1.03 (t, J = 7.4 Hz, 3H). ^{13}C NMR (126MHz, $CDCl_3$,

Major rotamer, 24 ºC) δ 175.7, 146.4, 131.3, 128.4, 123.5, 43.8, 28.8, 27.5, 23.7, 18.1, 12.2. HRMS: Calculated for $C_{17}H_{27}ONNa$ (MNa^+): 284.1985, found: 284.1985.

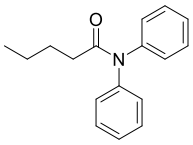

N,N-diphenylpentanamide (5.1w).[65] Isolated yield 88% (56 mg, 0.22 mmol). Colorless solid. ^{1}H NMR (500 MHz, Chloroform-*d*) δ 7.59 – 6.99 (m, 10H), 2.30 – 2.17 (m, 2H), 1.65 (p, *J* = 7.5 Hz, 2H), 1.29 (h, *J* = 7.3 Hz, 2H), 0.85 (t, *J* = 7.4 Hz, 3H). ^{13}C NMR (126 MHz, $CDCl_3$) δ 173.3, 143.0, 129.2 (broad), 126.6 (broad), 35.0, 27.7, 22.4, 13.8.

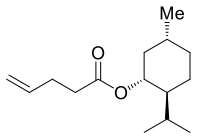

(1R,2S,5R)-2-isopropyl-5-methylcyclohexyl pent-4-enoate (5.1x).[66] Isolated yield 80% (48 mg, 0.20 mmol). Pale yellow solid. ^{1}H NMR (500 MHz, Chloroform-*d*) δ 5.90 – 5.74 (m, 1H), 5.11 – 4.92 (m, 2H), 4.68 (td, *J* = 10.9, 4.4 Hz, 1H), 2.37 (s, 4H), 1.97 (d, *J* = 11.8 Hz, 1H), 1.86 (dtd, *J* = 13.8, 7.0, 2.5 Hz, 1H), 1.71 – 1.62 (m, 2H), 1.48 (dd, *J* = 6.5, 3.4 Hz, 1H), 1.40 – 1.31 (m, 1H), 1.04 (qd, *J* = 13.6, 13.0, 3.7 Hz, 1H), 0.95 (q, *J* = 11.7 Hz, 2H), 0.90 – 0.81 (m, 7H), 0.74 (d, *J* = 7.0 Hz, 3H). ^{13}C NMR (126 MHz, $CDCl_3$) δ 172.6, 136.8, 115.4, 74.1, 47.0, 41.0, 34.3, 33.9, 31.4, 29.0, 26.2, 23.4, 22.0, 20.8, 16.3.

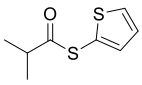

***S*-(thiophen-2-yl) 2-methylpropanethioate (5.1y).** Isolated yield 85% (40 mg, 0.21 mmol). Pale yellow oil. ^{1}H NMR (500 MHz, $CDCl_3$) δ 7.54 (dd, J = 5.3, 1.3 Hz, 1H), 7.15 (dd, J = 3.6, 1.3 Hz, 1H), 7.10 (dd, J = 5.3, 3.6 Hz, 1H), 2.87 (hept, J = 6.9 Hz, 1H), 1.27 (d, J = 6.9 Hz, 6H). ^{13}C NMR (126MHz, $CDCl_3$) δ 201.7, 135.7, 131.7, 127.9, 125.1, 42.7, 19.4. HRMS: Calculated for $C_8H_{11}OS_2$ (MH^+): 187.02458, found: 187.02528.

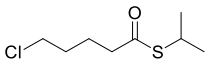

S-isopropyl 5-chloropentanethioate (5.1z). Isolated yield 51% (25 mg, 0.13 mmol). Yellow liquid. ^{1}H NMR (500 MHz, Chloroform-*d*) δ 3.71 – 3.59 (m,

1H), 3.58 – 3.48 (m, 2H), 2.60 – 2.48 (m, 2H), 1.87 – 1.75 (m, 4H), 1.29 (d, *J* = 6.9 Hz, 6H). ^{13}C NMR (126 MHz, $CDCl_3$) δ 199.1, 44.4, 43.0, 34.6, 31.6, 23.0, 22.9. HRMS: Calculated for $C_8H_{15}ClOSNa^+$ (MNa^+): 217.0424, found: 217.0426

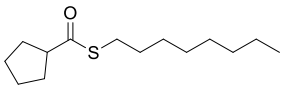

S-octyl cyclopentanecarbothioate (5.1aa). Isolated yield 82% (49 mg, 0.20 mmol). Yellow liquid. ^{1}H NMR (500 MHz, Chloroform-*d*) δ 2.96 (p, *J* = 7.9 Hz, 1H), 2.85 (t, *J* = 7.4 Hz, 2H), 1.85 (dddd, *J* = 29.9, 14.8, 12.8, 7.8 Hz, 4H), 1.77 – 1.66 (m, 2H), 1.63 – 1.51 (m, 4H), 1.41 – 1.32 (m, 2H), 1.31 – 1.21 (m, 8H), 0.88 (t, *J* = 6.8 Hz, 3H). ^{13}C NMR (126 MHz, $CDCl_3$) δ 203.3, 53.3, 31.8, 30.6, 29.7, 29.2, 29.1, 28.9, 28.8, 25.9, 22.6, 14.1. HRMS: Calculated for $C_{14}H_{27}OS^+$ (MH^+): 243.1771, found: 243.17792.

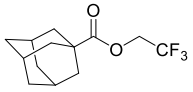

2,2,2-Trifluoroethyl adamantane-1-carboxylate (5.1bb). Isolated yield 83% (54 mg, 0.21 mmol). Colorless liquid. ^{1}H NMR (500 MHz, Chloroform-*d*) δ 4.49 – 4.37 (m, 2H), 2.04 (s, 3H), 1.93 (dd, *J* = 7.3, 2.8 Hz, 6H), 1.73 (q, *J* = 12.3 Hz, 6H). ^{13}C NMR (126 MHz, $CDCl_3$) δ 175.9, 126.4 - 119.8 (q), 60.5 - 59.6 (q), 40.8, 38.5, 36.3, 27.8. ^{19}F NMR (471 MHz, $CDCl_3$) δ -73.95. HRMS: Calculated for $C_{13}H_{18}O_2F_3^+$ (MH^+):263.12534, found: 263.12404.

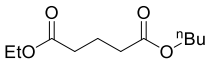

Butyl ethyl glutarate (5.1cc). Isolated yield 85% (46 mg, 0.21 mmol). Colorless solid. ^{1}H NMR (500 MHz, Chloroform-*d*) δ 4.11 (q, *J* = 7.1 Hz, 2H), 4.06 (t, *J* = 6.7 Hz, 2H), 2.34 (td, *J* = 7.4, 2.7 Hz, 4H), 1.93 (p, *J* = 7.4 Hz, 2H), 1.65 – 1.52 (m, 2H), 1.36 (dt, *J* = 15.0, 7.4 Hz, 2H), 1.23 (t, *J* = 7.1 Hz, 3H), 0.91 (t, *J* = 7.4 Hz, 3H). ^{13}C NMR (126 MHz, $CDCl_3$) δ 173.0, 173.0, 64.3, 60.4, 33.3, 30.6, 20.2, 19.1, 14.2, 13.7.

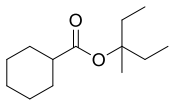

3-Methylpentan-3-yl cyclohexanecarboxylate (5.1dd). Isolated yield 89% (47 mg, 0.19 mmol). Colorless oil. ^{1}H NMR (500 MHz, $CDCl_3$) δ 2.20 (tt, J = 11.4, 3.6 Hz, 1H), 1.87 (ddd, J = 14.8, 8.8, 6.9 Hz, 4H), 1.71 (dq, J = 13.9, 7.5 Hz, 4H), 1.44 – 1.36 (m, 2H), 1.35 (s, 3H), 1.30 – 1.20 (m, 4H), 0.84 (t, J = 7.5 Hz, 6H). ^{13}C NMR (126 MHz, $CDCl_3$) δ 175.6, 84.7, 44.5, 30.6, 29.4, 26.0, 25.7, 23.0, 8.1. HRMS: Calculated for $C_{13}H_{24}O_2Na^+$ (MNa^+): 235.16685, found: 235.16671.

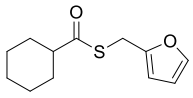

***S*-(furan-2-ylmethyl) cyclohexanecarbothioate (5.1ee).** Isolated yield 93% (52 mg, 0.23 mmol). Pale yellow oil. ^{1}H NMR (500 MHz, $CDCl_3$) δ 7.34 – 7.29 (m, 1H), 6.28 (dd, J = 3.2, 1.8 Hz, 1H), 6.20 (dd, J = 3.2, 0.9 Hz, 1H), 2.49 (tt, J = 11.5, 3.5 Hz, 1H), 1.98 – 1.87 (m, 2H), 1.78 (dt, J = 11.8, 3.1 Hz, 2H), 1.66 (dtd, J = 10.8, 3.3, 1.5 Hz, 1H), 1.47 (qd, J = 12.1, 3.1 Hz, 2H), 1.33 – 1.19 (m, 3H). ^{13}C NMR (126MHz, $CDCl_3$) δ 201.9, 150.9, 142.2, 110.7, 107.8, 52.6, 29.6, 25.7, 25.6, 25.4. HRMS: Calculated for $C_{12}H_{17}O_2S$ (MH^+): 225.09438, found: 225.09528.

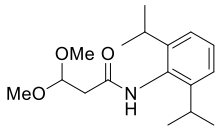

N-(2,6-diisopropylphenyl)-3,3-dimethoxypropanamide (5.1ff). Isolated yield 92% (67 mg, 0.23 mmol). Pale yellow solid. ^{1}H NMR (500 MHz, $CDCl_3$) δ 7.47 (s, 1H), 7.31 – 7.27 (m, 1H), 7.17 (d, J = 7.7 Hz, 2H), 4.80 (t, J = 5.1 Hz, 1H), 3.46 (s, 6H), 3.11 (hept, J = 6.9 Hz, 2H), 2.78 (d, J = 5.1 Hz, 2H), 1.20 (d, J = 6.9 Hz, 12H). ^{13}C NMR (126MHz, $CDCl_3$) δ 168.5, 146.3, 131.3, 128.4, 123.5, 102.5, 54.4, 41.3, 28.8, 23.7. HRMS: Calculated for $C_{17}H_{27}NO_3Na$ (MNa^+): 316.1883, found: 316.1883.

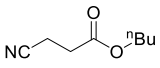

Butyl 3-cyanopropanoate (5.1gg). Isolated yield 85% (33 mg, 0.21 mmol). Pale yellow liquid. ^{1}H NMR (500 MHz, Chloroform-d) δ 4.13 (t, J = 6.7 Hz, 2H), 2.72 – 2.59 (m, 4H), 1.68 – 1.55 (m, 2H), 1.37 (h, J = 7.4 Hz, 2H), 0.93 (t, J = 7.4 Hz, 3H). ^{13}C NMR (126 MHz, $CDCl_3$) δ 170.1, 118.5, 65.3, 30.5, 30.0, 19.1, 13.6, 13.0.

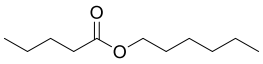

Hexyl pentanoate (5.1hh). Isolated yield 86% (40 mg, 0.21 mmol). Colorless liquid. ^{1}H NMR (500 MHz, Chloroform-*d*) δ 4.05 (t, *J* = 6.8 Hz, 2H), 2.29 (t, *J* = 7.6 Hz, 2H), 1.66 – 1.55 (m, 4H), 1.40 – 1.22 (m, 8H), 0.95 – 0.83 (m, 6H). ^{13}C NMR (126 MHz, $CDCl_3$) δ 174.0, 64.4, 34.1, 31.4, 28.6, 27.1, 25.6, 22.5, 22.3, 14.0, 13.7.

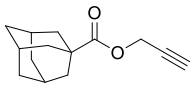

Prop-2-yn-1-yl adamantane-1-carboxylate (5.1ii). Isolated yield 77% (42 mg, 0.19 mmol). Colorless liquid. ^{1}H NMR (500 MHz, Chloroform-*d*) δ 4.65 (s, 2H), 3.71 (dt, *J* = 72.0, 5.7 Hz, 1H), 2.44 (t, *J* = 2.5 Hz, 1H), 2.02 (m, 3H), 1.92 (dd, *J* = 12.5, 2.7 Hz, 6H), 1.78 – 1.65 (m, 6H). ^{13}C NMR (126 MHz, $CDCl_3$) δ 176.8, 173.4, 78.1, 74.5, 71.4, 51.7, 42.6, 42.2, 40.7, 38.7, 38.3, 37.8, 36.6, 36.4, 36.4, 36.3, 35.9, 27.9, 27.7, 27.7, 27.4. HRMS: Calculated for $C_{14}H_{19}O_2^+$ (MH^+):219.13796, found: 219.13796.

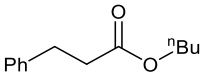

Butyl 3-phenylpropanoate (5.1jj).[66] Isolated yield 86% (44 mg, 0.22 mmol), colorless liquid. ^{1}H NMR (500 MHz, Chloroform-*d*) δ 7.38 – 7.26 (m, 5H), 4.09 (t, *J* = 6.7 Hz, 2H), 3.62 (s, 2H), 1.60 (dt, *J* = 14.5, 6.8 Hz, 2H), 1.35 (dq, *J* = 14.7, 7.4 Hz, 2H), 0.91 (t, *J* = 7.4 Hz, 3H). ^{13}C NMR (126 MHz, $CDCl_3$) δ 171.7, 134.2, 129.3, 128.5, 127.0, 64.8, 41.5, 30.6, 19.1, 13.7.

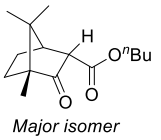

Major isomer

butyl(1R,2S,4R)-4,7,7-trimethyl-3-oxobicyclo[2.2.1]heptane-2-carboxylate (5.1kk). Isolated yield 74% (46 mg, 0.18 mmol), mixture of isomers, dr = 1:4.5.

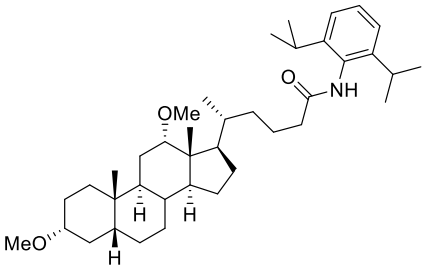

Colorless oil. ^{1}H NMR (500 MHz, $CDCl_3$, Major isomer) δ 4.10 (m, 2H, overlaps with minor isomer), 3.30 (dd, J = 4.9, 2.1 Hz, 1H), 2.40 (t, J = 4.5 Hz, 1H), 1.84 (dddd, J = 16.4, 6.4, 4.1, 2.0 Hz, 1H), 1.71 – 1.64 (m, 1H), 1.60 (q, J = 7.1 Hz, 2H), 1.57 – 1.46 (m, 2H), 1.41 – 1.31 (m, 3H), 0.99 (s, 3H), 0.92 (t, J = 3.7 Hz, 6H, overlaps with minor isomer), 0.85 (s, 3H).^{13}C NMR (126MHz, $CDCl_3$, Major isomer) δ 211.6, 169.9, 65.0, 58.6, 55.8, 47.2, 45.8, 30.7, 29.5, 22.6, 19.6, 19.2, 18.9, 13.8, 9.6. ^{13}C NMR (126MHz, $CDCl_3$, Minor isomer) δ 211.1, 168.0, 65.2, 58.7, 57.7, 46.9, 46.1, 30.2, 27.5, 20.9, 19.6, 19.2, 13.8, 9.6. HRMS: Calculated for $C_{15}H_{25}O_3$ (MH^+): 253.17982, found: 253.17947.

(5R)-N-(2,6-diisopropylphenyl)-5-((3R,5R,9S,10S,12S,13R,14S,17R)-3,12-dimethoxy-10,13 dimethylhexadecahydro-1H-cyclopenta[a]phenanthren-17-yl)hexanamide (5.1ll). Isolated yield 71% (68 mg, 0.11 mmol/0.16 mmol scale). Pale yellow liquid slowly solidify as yellow solid. ^{1}H NMR (500 MHz, $CDCl_3$, 298 K) δ 7.36 – 7.27 (m, 1H), 7.17 (dd, *J* = 14.7, 7.8 Hz, 2H), 6.69 (d, *J* = 6.3 Hz, 1H), 3.40 (s, 1H), 3.33 (d, *J* = 3.2 Hz, 4H), 3.25 (s, 3H), 3.22 (s, 1H), 3.15 (ddt, *J* = 15.6, 11.1, 5.7 Hz, 2H), 3.06 (h, *J* = 6.9 Hz, 2H), 2.38 (h, *J* = 7.4 Hz, 2H), 1.92 – 1.61 (m, 13H), 1.55 (d, *J* = 8.0 Hz, 5H), 1.38 (d, *J* = 11.9 Hz, 5H), 1.19 (d, *J* = 6.9 Hz, 12H), 0.95 – 0.90 (m, 6H), 0.67 (s, 3H). ^{13}C NMR (101 MHz, $CDCl_3$, 338 K) δ 172.1, 146.4, 131.4, 128.1, 123.3, 82.4, 80.6, 55.5, 55.3, 48.9, 46.9, 46.5, 42.3, 37.3, 36.2, 35.8, 35.5, 35.5, 34.5, 33.7, 32.8, 28.8, 27.6, 27.4,

26.9, 26.1, 23.7, 23.5, 23.2, 22.8, 22.2, 17.7, 12.6. HRMS: Calculated for $C_{39}H_{64}NO_3$ (MH^+): 594.4869, found: 594.4881.

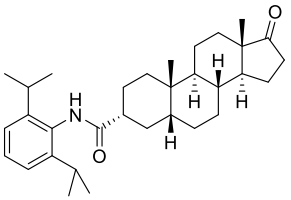

(3R,5S,8R,9S,10S,13S,14S)-N-(2,6-diisopropylphenyl)-10,13-dimethyl-17-oxohexadecahydro-1H-cyclopenta[a]phenanthrene-3-carboxamide (5.1mm-a). Isolated yield 61% (73 mg, 0.15 mmol). White solid. ^{1}H NMR (500 MHz, Chloroform-*d*) δ 7.27 (d, *J* = 8.6 Hz, 1H), 7.16 (d, *J* = 7.7 Hz, 2H), 6.78 (s, 1H), 3.06 (hept, *J* = 6.8 Hz, 2H), 2.77 (tt, *J* = 4.8, 2.0 Hz, 1H, smaller coupling constant comparing to the other diastereomer indicates the H is at equatorial position), 2.51 – 2.36 (m, 1H), 2.07 (dt, *J* = 19.1, 9.1 Hz, 2H), 1.93 (ddd, *J* = 14.1, 8.4, 6.0 Hz, 1H), 1.84-1.23 (m, 16 H), 1.20 (dd, *J* = 6.9, 2.1 Hz, 12H), 0.97 (qd, *J* = 12.8, 4.7 Hz, 1H), 0.88 (s, 3H), 0.86 (s, 3H), 0.74 (td, *J* = 10.8, 3.2 Hz, 1H). ^{13}C NMR (126 MHz, $CDCl_3$) δ 221.3, 174.1, 146.2, 131.4, 128.2, 123.4, 55.0, 51.6, 47.8, 42.6, 40.0, 36.2, 35.8, 35.1, 35.0, 31.6, 31.2, 30.9, 28.8, 28.6, 23.5, 21.8, 20.0, 13.9, 11.8. HRMS: Calculated for $C_{32}H_{48}NO_2$ (MH^+): 478.36796, found: 478.37005.

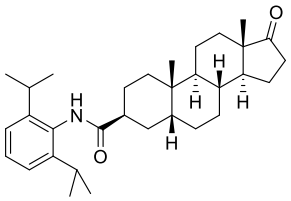

(3S,5S,8R,9S,10S,13S,14S)-N-(2,6-diisopropylphenyl)-10,13-dimethyl-17-oxohexadecahydro-1H-cyclopenta[a]phenanthrene-3-carboxamide (5.1mm-b). Isolated yield 33% (39 mg, 0.082 mmol). White solid. ^{1}H NMR (500 MHz, Chloroform-*d*) δ 7.29 (d, *J* = 7.8 Hz, 1H), 7.16 (d, *J* = 7.7 Hz, 2H), 6.64 (s, 1H), 3.04 (hept, *J* = 6.9 Hz, 2H), 2.45 (dd, *J* = 19.3, 8.5 Hz, 1H), 2.38 (dq, *J* = 11.0, 5.7, 4.1 Hz, 1H, larger coupling constant comparing to the other diastereomer indicates the H is at axial position), 2.17 – 2.02 (m, 1H), 1.98 – 1.92 (m, 1H), 1.91 –

1.75 (m, 5H), 1.71 – 1.66 (m, 1H), 1.65 – 1.61 (m, 2H), 1.52 (dtd, *J* = 21.6, 12.3, 10.8, 6.1 Hz, 1H), 1.44 – 1.22 (m, 7H), 1.19 (d, *J* = 6.7 Hz, 12H), 1.03 (dtd, *J* = 24.8, 12.7, 4.3 Hz, 2H), 0.89 (s, 3H), 0.87 (s, 3H), 0.77 (td, *J* = 12.1, 11.6, 3.9 Hz, 1H). ^{13}C NMR (126 MHz, $CDCl_3$) δ 221.4, 174.9, 146.2, 131.1, 128.3, 123.4, 54.59, 51.5, 47.8, 46.3, 38.0, 36.1, 35.9, 35.1, 31.9, 31.6, 30.9, 28.7, 28.4, 25.6, 21.8, 20.3, 13.8, 12.4. HRMS: Calculated for $C_{32}H_{48}NO_2$ (MH^+): 478.36796, found: 478.37005.

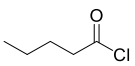

Pentanoyl chloride (5.2d). NMR yield 90%. ^{1}H NMR (500 MHz, Benzene-d_6) δ 2.14 (t, *J* = 7.4 Hz, 2H), 1.14 (dt, *J* = 15.0, 7.4 Hz, 2H), 0.86 (dq, *J* = 14.7, 7.4 Hz, 2H), 0.57 (t, *J* = 7.4 Hz, 3H). ^{13}C NMR (126 MHz, C_6D_6) δ 172.9, 46.3, 26.6, 21.2, 13.1.

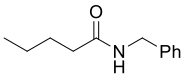

***N*-benzylpentanamide (5.1pp).**[67] Isolated yield 88% (42 mg, 0.22 mmol). Colorless solid. ^{1}H NMR (500 MHz, Chloroform-*d*) δ 7.37 – 7.31 (m, 2H), 7.31 – 7.26 (m, 3H), 5.70 (s, 1H), 4.44 (d, *J* = 5.7 Hz, 2H), 2.27 – 2.15 (m, 2H), 1.70 – 1.57 (m, 3H), 1.36 (dq, *J* = 14.7, 7.4 Hz, 2H), 0.92 (t, *J* = 7.3 Hz, 3H). ^{13}C NMR (126 MHz, $CDCl_3$) δ 172.9, 138.4, 128.7, 127.8, 127.5, 43.6, 36.6, 27.8, 22.4, 13.8.

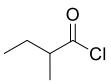

2-Methylbutanoyl chloride (5.2e). NMR yield 86%. NMR data is consistent with previous reported. ^{1}H NMR (500 MHz, Benzene-d_6) ^{1}H NMR (500 MHz, Benzene-d_6) δ 2.24 (dt, *J* = 13.5, 6.8 Hz, 1H), 1.44 – 1.35 (m, 1H), 1.13 – 1.04 (m, 1H), 0.77 (d, *J* = 6.9 Hz, 3H), 0.57 (t, *J* = 7.4 Hz, 3H). ^{13}C NMR (126 MHz, C_6D_6) δ 176.7, 52.5, 26.1, 15.8, 10.5.

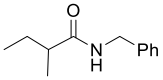

***N*-benzyl-2-methylbutanamide (5.1qq).**[68] Isolated yield 81% (39 mg, 0.20 mmol). Colorless solid. ^{1}H NMR (500 MHz, Chloroform-*d*) δ 7.38 – 7.31 (m, 2H), 7.30 – 7.26 (m, 3H), 5.74 (s, 1H), 4.52 – 4.39 (m, 2H), 2.13 (dp, *J* = 8.0, 6.8 Hz, 1H), 1.76 – 1.64 (m, 1H), 1.45 (dqd, *J* = 13.6, 7.4, 6.2 Hz, 1H), 1.16 (d, *J* = 6.9 Hz, 3H), 0.91 (t, *J* = 7.4 Hz, 3H). ^{13}C NMR (126 MHz, $CDCl_3$) δ 176.3, 138.6, 128.7, 127.8, 127.5, 43.5, 43.3, 27.4, 17.6, 12.0.

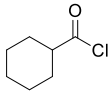

Cyclohexanecarbonyl chloride (5.2f). NMR yield 92%. NMR data is consistent with literature reported. ^{1}H NMR (800 MHz, Benzene-d_6) δ 2.18 (tt, *J* = 11.0, 3.6 Hz, 1H), 1.69 – 1.64 (m, 4H), 1.33 (dq, *J* = 8.0, 4.3 Hz, 4H), 1.22 – 1.13 (m, 6H), 0.78 (s, 5H). ^{13}C NMR (201 MHz, C_6D_6) δ 176.0, 54.5, 28.7, 25.1, 24.3.

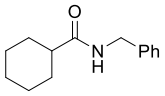

***N*-benzylcyclohexanecarboxamide (5.1rr).** Isolated yield 85% (46 mg, 0.21 mmol). Colorless solid. ^{1}H NMR (500 MHz, Chloroform-*d*) ^{1}H NMR (500 MHz, Chloroform-*d*) δ 7.37 – 7.29 (m, 2H), 7.27 (td, *J* = 7.2, 6.7, 1.7 Hz, 3H), 5.77 (s, 1H), 4.43 (d, *J* = 5.7 Hz, 2H), 2.11 (tt, *J* = 11.8, 3.5 Hz, 1H), 1.88 (dtd, *J* = 14.3, 3.6, 1.8 Hz, 2H), 1.79 (dq, *J* = 10.9, 3.8 Hz, 2H), 1.67 (m, 1H), 1.46 (qd, *J* = 12.1, 3.3 Hz, 2H), 1.35 – 1.15 (m, 3H). ^{13}C NMR (126 MHz, $CDCl_3$) δ 175.9, 138.6, 128.7, 127.7, 127.4, 45.6, 43.4, 29.7, 25.8.

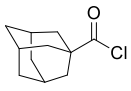

Cyclohexanecarbonyl chloride (5.2g). NMR yield 89%. ^{1}H NMR (800 MHz, Benzene-d_6) δ 1.72 (d, *J* = 2.5 Hz, 6H), 1.65 (s, 2H), 1.35 (s, 3H), 1.32 – 1.27 (m, 4H). ^{13}C NMR (201 MHz, C_6D_6) δ 178.9, 50.9, 38.6, 35.7, 27.7.

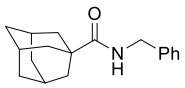

***N*-benzyladamantane-1-carboxamide (5.1ss).**[69] Isolated yield 81% (54 mg, 0.20 mmol). Colorless solid. ^{1}H NMR (500 MHz, Chloroform-*d*) δ 7.33 (dd, *J* = 8.0, 6.5 Hz, 2H), 7.29 – 7.19 (m, 3H), 5.90 (s, 1H), 4.43 (d, *J* = 5.6 Hz, 2H), 2.04 (p, *J* = 3.2 Hz, 3H), 1.88 (d, *J* = 3.0 Hz, 6H), 1.78 – 1.66 (m, 6H). ^{13}C NMR (126 MHz, $CDCl_3$) δ 177.8, 138.7, 128.7, 127.6, 127.4, 43.34, 40.7, 39.3, 36.5, 28.1.

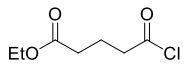

Ethyl 5-chloro-5-oxopentanoate (5.2h). NMR yield 89%. ^{1}H NMR (500 MHz, Benzene-d_6) δ 3.86 (q, *J* = 7.1 Hz, 2H), 2.24 (t, *J* = 7.2 Hz, 2H), 1.80 (t, *J* = 7.3 Hz, 2H), 1.49 (p, *J* = 7.3 Hz, 2H), 0.91 (t, *J* = 7.1 Hz, 4H). ^{1}H NMR (500 MHz, C_6D_6) δ 172.6, 171.3, 59.9, 45.5, 31.8, 24.3, 19.9.

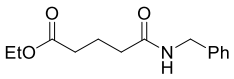

Ethyl 5-(benzylamino)-5-oxopentanoate (5.1tt).[70] Isolated yield 62% (39 mg, 0.15 mmol). Yellow liquid. ^{1}H NMR (500 MHz, Chloroform-*d*) δ 7.40 – 7.31 (m, 2H), 7.31 – 7.26 (m, 3H), 5.80 (s, 1H), 4.44 (d, *J* = 5.7 Hz, 2H), 4.12 (q, *J* = 7.1 Hz, 2H), 2.38 (t, *J* = 7.1 Hz, 2H), 2.28 (t, *J* = 7.4 Hz, 2H), 1.99 (p, *J* = 7.3 Hz, 2H), 1.24 (t, *J* = 7.1 Hz, 3H). ^{13}C NMR (126 MHz, $CDCl_3$) δ 173.2, 171.9, 138.2, 128.7, 127.8, 127.6, 60.4, 43.7, 35.5, 33.3, 20.9, 14.2.

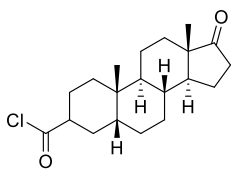

(3R,5R,8R,9S,10S,13S,14S)-10,13-dimethyl-17-oxohexadecahydro-1H-cyclopenta[a]phenanthrene-3-carbonyl chloride (5.2i-a) and **(3S,5R,8R,9S,10S,13S,14S)-10,13-dimethyl-17-oxohexadecahydro-1H-cyclopenta[a]phenanthrene-3-carbonyl chloride (5.2i-b).** NMR yield 71% (d/r = 1.35:1). ^{1}H NMR (400 MHz, Benzene-d_6) δ 2.48 (dt, *J* = 5.1, 2.4 Hz, 1H), 2.29 (tt, *J* = 12.4, 4.0 Hz, 1H).

These two peaks are corresponding to the C-H of the stereogenic carbon on the two diastereomers, respectively. Identification of other protons is difficult due to overlapping of peaks in the aliphatic region. ^{13}C NMR (101 MHz, C_6D_6) 176.3, 176.0. These two peaks are corresponding to the carbonyls of the two diastereomeric acid chlorides.

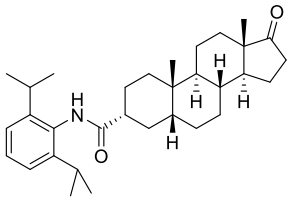

(3R,5S,8R,9S,10S,13S,14S)-N-(2,6-diisopropylphenyl)-10,13-dimethyl-17-oxohexadecahydro-1H-cyclopenta[a]phenanthrene-3-carboxamide (5.1mm-a). Isolated yield in 39% yield (38 mg, 0.079 mmol/0.2 mmol scale). Characterization data are the same as above.

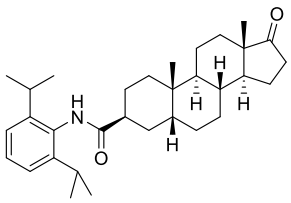

(3S,5S,8R,9S,10S,13S,14S)-N-(2,6-diisopropylphenyl)-10,13-dimethyl-17-oxohexadecahydro-1H-cyclopenta[a]phenanthrene-3-carboxamide (1mm-b). Isolated yield and in 30% yield (29 mg, 0.060 mmol/0.2 mmol scale). Characterization data are the same as above.

5.5.5. NMR Spectra of Products

See Appendix 3

5.6. References

1. A. Biffis, P. Centomo, A. Del Zotto, M. Zecca, Pd metal catalysts for cross-couplings and related reactions in the 21st century: A critical review. *Chem. Rev.* **118**, 2249-2295 (2018).

2. C. C. C. Johansson Seechurn, M. O. Kitching, T. J. Colacot, V. Snieckus, Palladium-catalyzed cross-coupling: A historical contextual perspective to the 2010 Nobel Prize. *Angew. Chem. Int. Ed.* **51**, 5062-5085 (2012).
3. J. He, M. Wasa, K. S. L. Chan, Q. Shao, J.-Q. Yu, Palladium-catalyzed transformations of alkyl C–H bonds. *Chem. Rev.* **117**, 8754-8786 (2017).
4. J. F. Hartwig, Evolution of C–H bond functionalization from methane to methodology. *J. Am. Chem. Soc.* **138**, 2-24 (2016).
5. A. O. King, R. D. Larsen, E.-I. Negishi, "Palladium-Catalyzed Hydrogenolysis" in *Handbook of Organopalladium Chemistry for Organic Synthesis,* E.-I. Negishi, Ed. (John Wiley & Sons, Inc, New York, 2002), vol. 2, pp. 2719-2752.
6. D. Wang, A. B. Weinstein, P. B. White, S. S. Stahl, Ligand-promoted palladium-catalyzed aerobic oxidation reactions. *Chem. Rev.* **118**, 2636-2679 (2018).
7. W. Shi, C. Liu, A. Lei, Transition-metal catalyzed oxidative cross-coupling reactions to form C–C bonds involving organometallic reagents as nucleophiles. *Chem. Soc. Rev.* **40**, 2761-2776 (2011).
8. M. Holmes, L. A. Schwartz, M. J. Krische, Intermolecular metal-catalyzed reductive coupling of dienes, allenes, and enynes with carbonyl compounds and imines. *Chem. Rev.* **118**, 6026-6052 (2018).
9. J. F. Hartwig Ed. *Organotransition Metal Chemistry: From Bonding to Catalysis.* (University Science Books, 2010).
10. M. R. Uehling, R. P. King, S. W. Krska, T. Cernak, S. L. Buchwald, Pharmaceutical diversification *via* palladium oxidative addition complexes. *Science* **363**, 405 (2019).

11. M. Beller, Ed. "*Catalytic Carbonylation Reactions*" in *Topics in Organometallic Chemistry* (Springer-Verlag Berlin Heidelberg, 2006), vol. 18.
12. J.-B. Peng, H.-Q. Geng, X.-F. Wu, The chemistry of CO: carbonylation. *Chem* **3**, 526-552 (2019).
13. M. Beller, B. A. Steinhoff, J. R. Zoeller, D. J. Cole-Hamilton, E. Drent, X. -F. Wu, H. Neumann, S. Ito, K. Nozaki, "Carbonylation" in *Applied Homogeneous Catalysis with Organometallic Compounds,* B. Cornils, W. A. Herrmann, M. Beller, R. Paciello, Eds. (Wiley-VCH Verlag GmbH & Co. KGaA, 2018), pp. 91-190.
14. L. Wu, X. Fang, L. Qiang, R. Jackstell, M. Beller, X.-F. Wu, Palladium-catalyzed carbonylative transformation of C(sp3)–X bonds. *ACS Catal.* **4**, 2977-2989 (2014).
15. S. Sumino, A. Fusano, T. Fukuyama, I. Ryu, Carbonylation reactions of alkyl iodides through the interplay of carbon radicals and pd catalysts. *Acc. Chem. Res.* **47**, 1563-1574 (2014).
16. M. R. Kwiatkowski, E. J. Alexanian, Transition-metal (Pd, Ni, Mn)-catalyzed C–c bond constructions involving unactivated alkyl halides and fundamental synthetic building blocks. *Acc. Chem. Res.* **52**, 1134-1144 (2019).
17. R. G. Kinney, J. Tjutrins, G. M. Torres, N. J. Liu, O. Kulkarni, B. A. Arndtsen, A general approach to intermolecular carbonylation of Arene C–H bonds to ketones through catalytic aroyl triflate formation. *Nature Chemistry* **10**, 193-199 (2018).
18. J. S. Quesnel, B. A. Arndtsen, A palladium-catalyzed carbonylation approach to acid chloride synthesis. *J. Am. Chem. Soc.* **135**, 16841-16844 (2013).
19. J. S. Quesnel, S. Moncho, K. E. O. Ylijoki, G. M. Torres, E. N. Brothers, A. A. Bengali, B. A. Arndtsen, Computational study of the palladium-catalyzed carbonylative synthesis of

aromatic acid chlorides: The synergistic effect of P^tBu_3 and CO on reductive elimination. *Chem. Eur. J.* **22**, 15107-15118 (2016).

20. M. Osawa, H. Nagai, M. Akita, Photo-activation of Pd-catalyzed Sonogashira coupling using a Ru/bipyridine complex as energy transfer agent. *Dalton Trans.*, 827-829 (2007).
21. D. Kalyani, K. B. McMurtrey, S. R. Neufeldt, M. S. Sanford, Room-temperature C–H arylation: Merger of Pd-catalyzed C–H functionalization and visible-light photocatalysis. *J. Am. Chem. Soc.* **133**, 18566-18569 (2011).
22. J. C. Tellis, D. N. Primer, G. A. Molander, Single-electron transmetalation in organoboron cross-coupling by photoredox/nickel dual catalysis. *Science* **345**, 433-436 (2014).
23. Z. Zuo, D. T. Ahneman, L. Chu, J. A. Terrett, A. G. Doyle, D. W. C. MacMillan, Merging photoredox with nickel catalysis: coupling of α-carboxyl sp3-carbons with aryl halides. *Science* **345**, 437-440 (2014).
24. S. Z. Tasker, T. F. Jamison, Highly regioselective indoline synthesis under nickel/photoredox dual catalysis. *J. Am. Chem. Soc.* **137**, 9531-9534 (2015).
25. E. B. Corcoran, M. T. Pirnot, S. Lin, S. D. Dreher, D. A. DiRocco, I. W. Davies, S. L. Buchwald, D. W. C. MacMillan, Aryl amination using ligand-free Ni(II) salts and photoredox catalysis. *Science* **353**, 279 (2016).
26. J. Twilton, C. Le, P. Zhang, M. H. Shaw, R. W. Evans, D. W. C. MacMillan, The merger of transition metal and photocatalysis. *Nature Rev. Chem.***1**, 0052 (2017).
27. M. D. Levin, S. Kim, F. D. Toste, Photoredox catalysis unlocks single-electron elementary steps in transition metal catalyzed cross-coupling. *ACS Cent. Sci.* **2**, 293-301 (2016).
28. K. L. Skubi, T. R. Blum, T. P. Yoon, Dual catalysis strategies in photochemical synthesis. *Chem. Rev.* **116**, 10035-10074 (2016).

29. M. Parasram, P. Chuentragool, D. Sarkar, V. Gevorgyan, Photoinduced formation of hybrid aryl pd-radical species capable of 1,5-HAT: Selective catalytic oxidation of silyl ethers into silyl enol ethers. *J. Am. Chem. Soc.* **138**, 6340-6343 (2016).

30. M. A. Fredricks, M. Drees, K. Köhler, Acceleration of the rate of the heck reaction through UV- and visible-light-induced palladium(II) reduction. *ChemCatChem* **2**, 1467-1476 (2010).

31. P. Chuentragool, D. Kurandina, V. Gevorgyan, Catalysis by visible light photoexcited palladium complexes. *Angew. Chem. Int. Ed.* **58**, 2-15 (2019).

32. R. Kancherla, K. Muralirajan, B. Maity, C. Zhu, P. E. Krach, L. Cavallo, M. Rueping, Oxidative addition to palladium(0) made easy through photoexcited-state metal catalysis: experiment and computation. *Angew. Chem. Int. Ed.* **58**, 3412-3416 (2019).

33. G.-Z. Wang, R. Shang, W.-M. Cheng, Y. Fu, Irradiation-induced heck reaction of unactivated alkyl halides at room temperature. *J. Am. Chem. Soc.* **139**, 18307-18312 (2017).

34. S. Roslin, L. R. Odell, Palladium and visible-light mediated carbonylative Suzuki–Miyaura coupling of unactivated alkyl halides and aryl boronic acids. *Chem. Commun.* **53**, 6895-6898 (2017).

35. For an example of a postulated two photon role in nickel catalysis: L. K. G. Ackerman, J. I. Martinez Alvarado, A. G. Doyle, Direct C–C bond formation from alkanes using Ni-photoredox catalysis. *J. Am. Chem. Soc.* **140**, 14059-14063 (2018).

36. J. A. Terrett, J. D. Cuthbertson, V. W. Shurtleff, D. W. C. MacMillan, Switching on elusive organometallic mechanisms with photoredox catalysis. *Nature* **524**, 330 (2015).

37. R. D. Costa, E. Orti, H. J. Bolink, F, Monti, G. Accorsi, N, Armaroli, Luminescent ionic transition-metal complexes for light-emitting electrochemical cells. *Angew. Chem. Int. Ed.* **51**, 8178-8211 (2012).

38. V. Hirschbeck, P. H. Gehrtz, I. Fleischer, Metal-catalyzed synthesis and use of thioesters: recent developments, *Chem. Eur. J.* **24**, 7092-7107 (2018).

39. V. F. Patel, G. Pattenden, D. M. Thompson, Cobalt-mediated reactions in synthesis. The degradation of carboxylic acids to functionalised noralkanes *via* acylcobalt salophen intermediates. *J. Chem. Soc. Perkin Trans. 1*, 2729-2734 (1990).

40. K. I. Goldberg, R. G. Bergman, Synthesis of dialkyl- and alkyl(acyl)rhenium complexes by alkylation of anionic rhenium complexes at the metal center. Mechanism of a double carbonylation reaction that proceeds *via* the formation of free methyl radicals in solution. *J. Am. Chem. Soc.* **111**, 1285-1299 (1989).

41. Ghosh, L. Marzo, A. Das, R. Shaikh, B. König, Visible light mediated photoredox catalytic arylation reactions. *Acc. Chem. Res.* **49**, 1566-1577 (2016).

42. H. G. Roth, N. A. Romero, D. A. Nicewicz, Experimental and calculated electrochemical potentials of common organic molecules for applications to single-electron redox chemistry. *Synlett* **27**, 714-723 (2016).

43. C. Cabrele, T. A. Martinek, O. Reiser, L. Berlicki, Peptides containing β-amino acid patterns: Challenges and successes in medicinal chemistry. *J. Med. Chem.* **57**, 9718−9739 (2014).

44. S. Abele, D. Seebach, Preparation of achiral and of enantiopure geminally disubstituted, β-aminoacids for, β-peptide synthesis. *Eur. J. Org. Chem.* **2000**, 1-15 (2000).

45. X.-F. Wu, H. Neumann, M. Beller, Palladium-catalyzed carbonylative coupling reactions between Ar-X and carbon nucleophiles. *Chem. Soc. Rev.* **40**, 4986-5009 (2011).

46. K. McKeage, G. M. Keating, Fenofibrate: A review of its use in dyslipidaemia. *Drugs* **71**, 1917-1946 (2011).

47. Herrero, M. A., Kremsner, J. M. & Kappe, C. O. Nonthermal Microwave Effects Revisited: On the Importance of Internal Temperature Monitoring and Agitation in Microwave Chemistry. *The Journal of Organic Chemistry* **73**, 36-47, (2008).

48. Monos, T. M., Sun, A. C., McAtee, R. C., Devery, J. J. & Stephenson, C. R. J. Microwave-Assisted Synthesis of Heteroleptic Ir(III)+ Polypyridyl Complexes. *The Journal of Organic Chemistry* **81**, 6988-6994, (2016).

49. Takayasu, S. & Shinozaki, K. Hydration of fac-tris (2-phenylpyridinato-C2,N)iridium(III) in dichloromethane solution and in solid state. *Polyhedron* **123**, 328-333, (2017).

50. Quesnel, J. S., Kayser, L. V., Fabrikant, A. & Arndtsen, B. A. Acid Chloride Synthesis by the Palladium-Catalyzed Chlorocarbonylation of Aryl Bromides. *Chemistry – A European Journal* **21**, 9550-9555, (2015).

51. Cooper, J. C., Venezky, D. L. & Lorenz, T. in Fundamental Research in Homogeneous Catalysis: Volume 3 (ed Minoru Tsutsui) 847-857 (*Springer US*, 1979).

52. Patel, V. F., Pattenden, G. & Thompson, D. M. Cobalt-mediated reactions in synthesis. The degradation of carboxylic acids to functionalised noralkanes via acylcobalt salophen intermediates. *Journal of the Chemical Society, Perkin Transactions 1*, 2729-2734, (1990).

53. Shields, B. J. & Doyle, A. G. Direct C(sp3)–H Cross Coupling Enabled by Catalytic Generation of Chlorine Radicals. *Journal of the American Chemical Society* **138**, 12719-12722, (2016).

54. Terrett, J. A., Cuthbertson, J. D., Shurtleff, V. W. & MacMillan, D. W. C. Switching on elusive organometallic mechanisms with photoredox catalysis. *Nature* **524**, 330, (2015).

55. Quesnel, J. S. & Arndtsen, B. A. A Palladium-Catalyzed Carbonylation Approach to Acid Chloride Synthesis. *Journal of the American Chemical Society* **135**, 16841-16844, (2013).

56. Miloserdov, F. M. & Grushin, V. V. Palladium-Catalyzed Aromatic Azidocarbonylation. *Angewandte Chemie International Edition* **51**, 3668-3672, (2012).

57. Guin, J., De Sarkar, S., Grimme, S. & Studer, A. Biomimetic Carbene-Catalyzed Oxidations of Aldehydes Using TEMPO. *Angewandte Chemie International Edition* **47**, 8727-8730, (2008).

58. Li, G., Wang D. Catalytic Synthesis of 4-Hydroxy-4'-chlorobenzophenon by Aluminium Trichloride. *Guangzhou Chemical Industry* **20**, 91-93 (2014).

59. Rathke, M. W. & Lindert, A. The halogenation of lithium ester enolates. A convenient method for the preparation of alpha-iodo and alpha-bromo esters. *Tetrahedron Letters* **12**, 3995-3998 (1971).

60. Rathke, M. W. & Lindert, A. Reaction of lithium N-isopropylcyclohexylamide with esters. Method for the formation and alkylation of ester enolates. *Journal of the American Chemical Society* **93**, 2318-2320 (1971).

61. Sagadevan, A., Charpe, V. P., Ragupathi, A. & Hwang, K. C. Visible Light Copper Photoredox-Catalyzed Aerobic Oxidative Coupling of Phenols and Terminal Alkynes: Regioselective Synthesis of Functionalized Ketones via C≡C Triple Bond Cleavage. *Journal of the American Chemical Society* **139**, 2896-2899, (2017).

62. Ma, Y., Song, C., Chai, Q., Ma, C. & Andrus, M. B. Palladium-imidazolium N-heterocyclic carbene-catalyzed carbonylative amidation with boronic acids, aryl diazonium ions, and ammonia. *Synthesis*, 2886-2889 (2003).

63. Correa, A., Elmore, S. & Bolm, C. Iron-Catalyzed N-Arylations of Amides. *Chemistry–A European Journal* **14**, 3527-3529 (2008).

64. Zhang, K., Peng, Q., Hou, X.-L. & Wu, Y.-D. Highly Enantioselective Palladium-Catalyzed Alkylation of Acyclic Amides. *Angewandte Chemie International Edition* **47**, 1741-1744 (2008).

65. Taber, D. F., Berry, J. F. & Martin, T. J. Convenient Synthetic Route to an Enantiomerically Pure FMOC α-Amino Acid. *The Journal of Organic Chemistry* **73**, 9334-9339 (2008).

66. Zhao, Y., Jin, L., Li, P. & Lei, A. Palladium-Catalyzed Oxidative Carbonylation of Alkyl and Aryl Indium Reagents with CO under Mild Conditions. *Journal of the American Chemical Society* **130**, 9429-9433, (2008).

67. Chiang, P.-C., Kim, Y. & Bode, J. W. Catalytic amide formation with α'-hydroxyenones as acylating reagents. *Chemical Communications*, 4566-4568, (2009).

68. Rolfe, A. et al. High-Load, Oligomeric Dichlorotriazine: A Versatile ROMP-Derived Reagent and Scavenger. *The Journal of Organic Chemistry* **73**, 8785-8790, (2008).

69. Han, C., Lee, J. P., Lobkovsky, E. & Porco, J. A. Catalytic Ester−Amide Exchange Using Group (IV) Metal Alkoxide−Activator Complexes. *Journal of the American Chemical Society* **127**, 10039-10044, (2005).

70. Bode, J. W. & Sohn, S. S. N-Heterocyclic Carbene-Catalyzed Redox Amidations of α-Functionalized Aldehydes with Amines. *Journal of the American Chemical Society* **129**, 13798-13799 (2007).

71. Prakash, G. K. S., Panja, C., Mathew, T. & Olah, G. A. BF3-H2O catalyzed Fries rearrangement of phenolic esters. *Catalysis Letters* **114**, 24-29, (2007).

72. Škoch, K., Císařová, I. & Štěpnička, P. Synthesis of a Polar Phosphinoferrocene Amidosulfonate Ligand and Its Application in Pd-Catalyzed Cross-Coupling Reactions of

Aromatic Boronic Acids and Acyl Chlorides in an Aqueous Medium. *Organometallics* **35**, 3378-3387 (2016).

73. Goldenstein, K.; Fendert, T.; Proksch, P.; Winterfeldt, E. Enantioselective preparation and enzymatic cleavage of spiroisoxazoline amides. *Tetrahedron* **56**, 4173 (2000).

74. Wang, L.; Jiang, X.; Tang, P. Silver-Mediated Fluorination of Alkyl Iodides with $TMSCF_3$ as the Fluorinating Agent. *Org. Chem. Front.* **4**, 1958-1961 (2017).

Chapter 6. Conclusions and Future Work

6.1. Conclusions and Contributions to Knowledge

As discussed in Chapter 1, palladium catalyzed carbonylations can offer efficient access to a wide variety of carbonyl-products, as well as a route to construct complex heterocyclic cores. The research in the Chapters 2-4 of this thesis has centered around the use of the latter strategy to generate reactive 1,3-dipoles (Münchnones), which can provide access to a wide variety of heterocycles via their cycloaddition with unsaturated substrates. As described in Chapter 2, all of these transformations rely on a tandem catalytic reaction in which a single palladium catalyst mediates two different carbonylations. The first catalytic process involves the carbonylation of aryl halides in the presence of chloride to form acid chlorides. This challenging transformation requires a palladium catalyst with a very bulky ligand, $Pd(P^tBu_3)_2$, to facilitate the reductive elimination of acid chloride products. The latter can then react with imine to form an *N*-acyl iminium salt that then re-adds to palladium and undergoes a second carbonylation to form the Münchnone product. Kinetic analysis of this reaction suggested that the slow step is the formation of iminium salt, which is related to the reversibility of the reductive elimination of acid chloride from the palladium-acyl intermediate in catalysis. As a result, CO pressure plays an important role in the catalytic synthesis of Münchnones. We found that the reaction is favored by high pressure and with an excess of aryl iodide to help drive this transformation.

With an understanding of the factors that contribute to the palladium catalyzed synthesis of Münchnones, we moved on to exploit the reactivity of these 1,3-dipoles in the construction of other heterocyclic products. In Chapter 2 we couple Münchnone formation with alkyne or alkene dipolarophiles to generate a wide variety of substituted pyrroles. In Chapter 3, we elaborated on this approach to generate more complex pyrrole structures. In particular, the combination of

alkyne-tethered imines, aryl iodides, and carbon monoxide was found to form Münchnones that can undergo spontaneous intramolecular 1,3-dipolar cycloaddition to generate polycyclic pyrroles. This reaction is amenable to less activated alkynes than those used in typical Münchnone cycloadditions, including terminal alkynes. Taking advantage of the latter, we incorporated Sonogashira coupling of the terminal alkyne with aryl halides into our catalytic synthesis of Münchnones to form polycyclic pyrroles with two different aryl iodides. Finally, in Chapter 4 we explored the ketene-like reactivity of Münchnones with imines to generate amido substituted β-lactams. Due to the compatibility of this reaction with high reaction temperatures, aryl bromides can now be used as substrates as well as aryl iodides. We also demonstrate that more diversely substituted β-lactams can be formed by first building up a Münchnone utilizing the conditions described in Chapter 2, and then reacting it with a different imine. In addition, the use of *o*-imine tethered aryl iodides in this chemistry leads to the formation of spirocyclic β-lactams.

Each of these reactions relies on the catalytic generation of acid chlorides from aryl halides and CO. This challenging step necessitates the use of the bulky P^tBu_3 ligand to drive the reductive elimination. Due to this, our heterocycle synthetic approaches are limited to easily activated aryl halide substrates (e.g. aryl iodides), and are incompatible with alkyl halide substrates, which limits the scope of these transformations. In Chapter 5 we address these limitations by redesigning our palladium catalyzed synthesis of acid chlorides. We show that visible light can drive this reaction via the direct photoexcitation of the palladium catalyst to unlock a single electron transfer mechanism for the oxidative addition step. This allows the activation of a wide variety of aryl and alkyl halide substrates under much milder conditions than typical carbonylation reactions. Furthermore, we demonstrate that visible light also plays a role in the reductive elimination of acid chloride via the excitation of the palladium-acyl intermediate. Both of these features work in

concert to provide a general platform to do carbonylative coupling reactions with new combinations of challenging organic halides and nucleophiles, and under exceptionally mild conditions.

6.2. Suggestions for Future work

A. Visible Light/Palladium Catalyzed Carbonylations for the Synthesis of Acid Fluorides

The use of visible light in palladium catalyzed carbonylation described in Chapter 5 to synthesize acid chlorides provides a new avenue for the synthesis of complex molecules. However, certain applications of this chemistry could necessitate the separation of the acid chloride product from the reaction mixture. Acid chlorides are highly electrophilic and thus incompatible with typical chromatographic methods.[1] In fact, this was one of the challenges we faced in the multistep synthesis of Fenofibrate (Chapter 5). Most of our attempts to isolate acid chlorides from the reaction mixture in high purity and good yield utilizing non-chromatographic methods were unsuccessful. A straightforward way to facilitate the isolation and handling of these electrophilic products would be to use the visible light/Pd chemistry to instead generate acid fluorides.

Compared to acid chlorides, acid fluorides are generally more stable and compatible with chromatographic purification methods, but still sufficiently electrophilic to react with a variety of nucleophiles.[2-3] They are also less reactive towards oxidative addition to metal catalysts,[3] which, as previously discussed, is one of the challenges in the catalytic formation of electrophiles in these reactions. Acid fluorides have found numerous applications, notably in peptide couplings, where their superior stability and functional group compatibility allows the formation of complex

peptides.[2,4] However, acid fluorides are typically generated from carboxylic acids using synthetic, high energy fluorinating agents, albeit under mild conditions.[2-3]

The addition of a fluoride source to our light driven carbonylation system should in principle offer a straightforward and new method to generate alkyl acid fluoride products. This reaction would, in theory, proceed in a similar fashion to the mechanism postulated in Chapter 5. An intermediate palladium-acyl fluoride complex could be presumably photoexcited to reductively eliminate acid fluoride (Scheme 6.1).

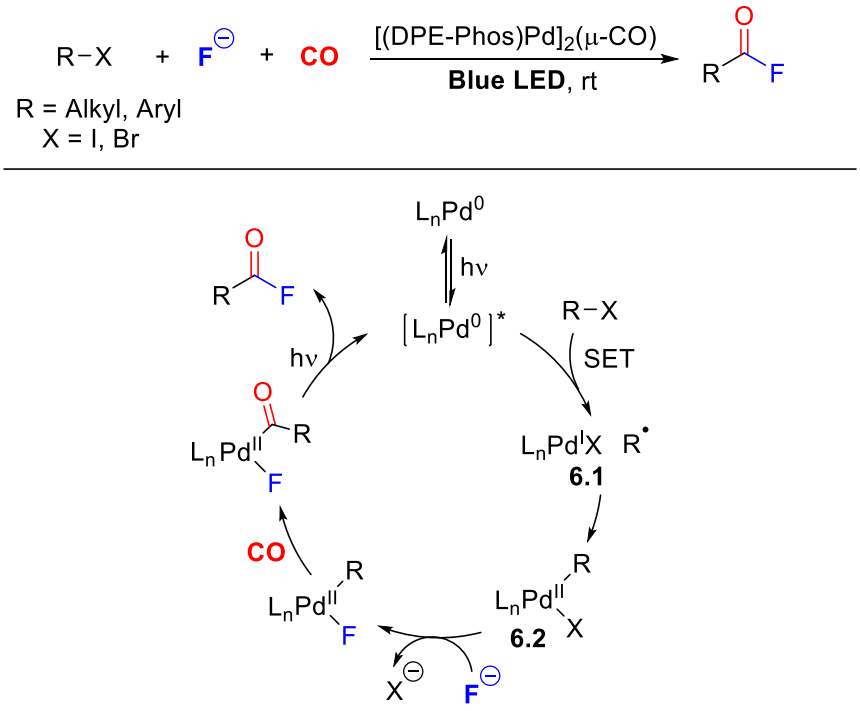

Scheme 6.1. Visible Light Driven Palladium Catalyzed Synthesis of Acid Fluorides

A potential challenging aspect of this transformation is the susceptibility of alkyl halides towards nucleophilic substitution by fluoride. An analogous reaction was observed during the development of the synthesis of acid chlorides (See Chapter 5), where primary alkyl halides would

undergo fast nucleophilic substitution with soluble chloride sources. We found that this side-reaction could be suppressed by changing the solvent polarity and/or the solubility of the chloride source. Similarly, the generation of acid fluorides with fluoride salts could be difficult, but the wide availability of covalent fluorinating reagents could be key in the success of this reaction (Scheme 6.2).

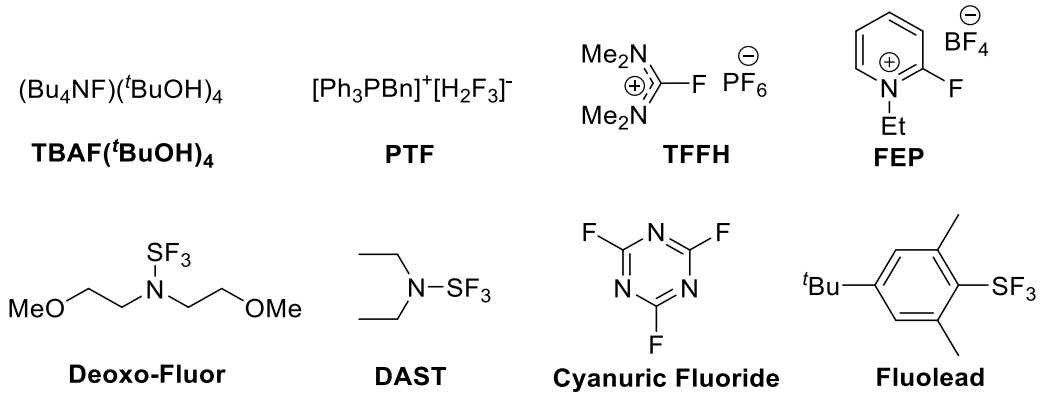

Scheme 6.2. Common Fluorinating Reagents

In Chapter 5, we showed that halophthalimides can be used to generate protected β-aminoacid chlorides and couple them to other amino acids for the synthesis of β-peptoids. The application of the chemistry described above to the carbonylation of halophthalimides could provide a new route for the synthesis of protected amino acid fluoride building blocks for peptide couplings (Scheme 6.3).

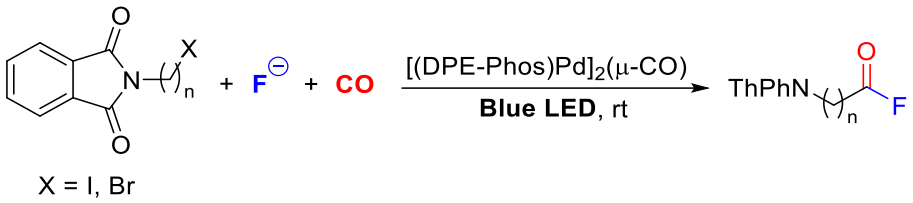

Scheme 6.3. Visible Light/Palladium Catalyzed Carbonylation of Halophthalimides for the Synthesis of Protected Amino Acid Fluorides

B. Visible Light/Palladium Catalyzed Generation of Chiral Carboxylic Acid Derivatives

In Chapter 5, we showed that the visible light driven, palladium catalyzed carbonylation of alkyl halides could be used to generate a plethora of carboxylic acid derivatives. This transformation was compatible with primary, secondary, and tertiary alkyl halides. These latter two are interesting because their carbonylation could give rise to the formation of a new stereogenic center. This was preliminarily observed in the alkoxycarbonylation of (+)3-bromocamphor which produced a mixture of two diastereomeric esters. The observed ratio of these products was not 1:1, but closer to 3:1. This selectivity could originate in the recombination step of the alkyl radical and complex **6.1** to generate the alkyl-palladium complex **6.2** (Scheme 6.1). In this case, the sterically encumbered environment around the palladium center and the stereochemistry present in the chiral starting material could act in concert to give rise to the observed diastereoselectivity.

A more general way of doing stereoselective reactions in this platform would be to employ chiral ligands to direct the radical recombination step with prochiral substrates. One of the most common phosphine ligands used in metal catalyzed asymmetric synthesis is BINAP (Scheme 6.4).[5-6] This ligand has a restricted rotation about the biaryl bond, and thus displays axial chirality. This has been exploited in many reactions, notably in asymmetric hydrogenations.[5-7] This ligand

is attractive because it can be synthesized from commercially available BINOL derivatives.[8] Over time, a number of methods have been developed to functionalize either the naphthalene core at different positions or the coordinating phosphorus atoms.[8] This provides a modular platform to tune steric effects for the stereoinduction step (Scheme 6.5).

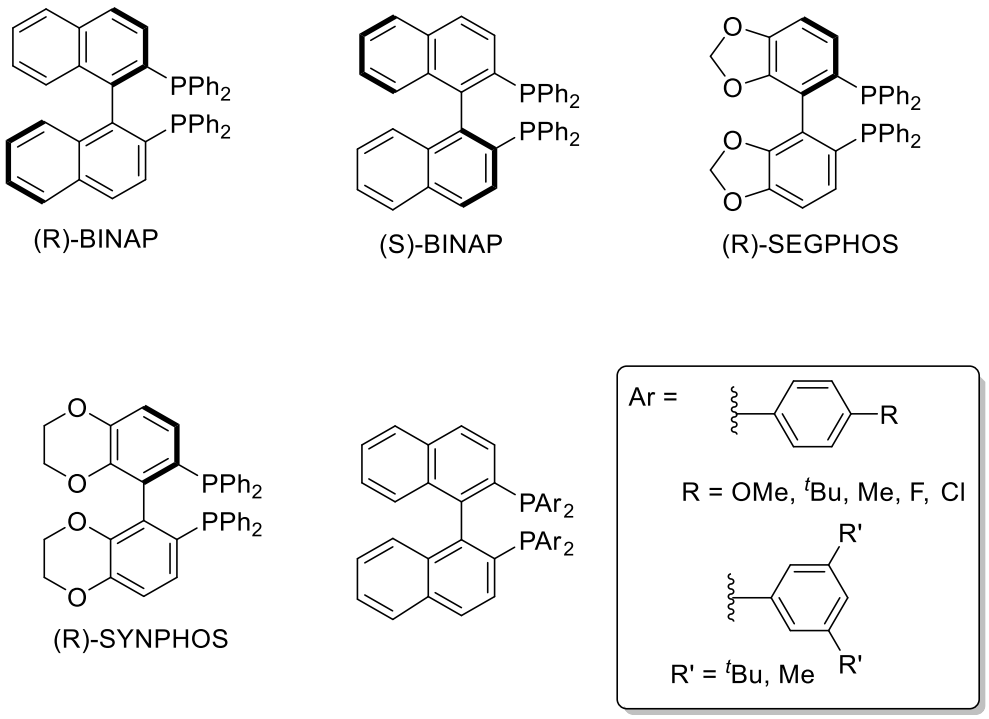

Scheme 6.4. BINAP-Type Ligands

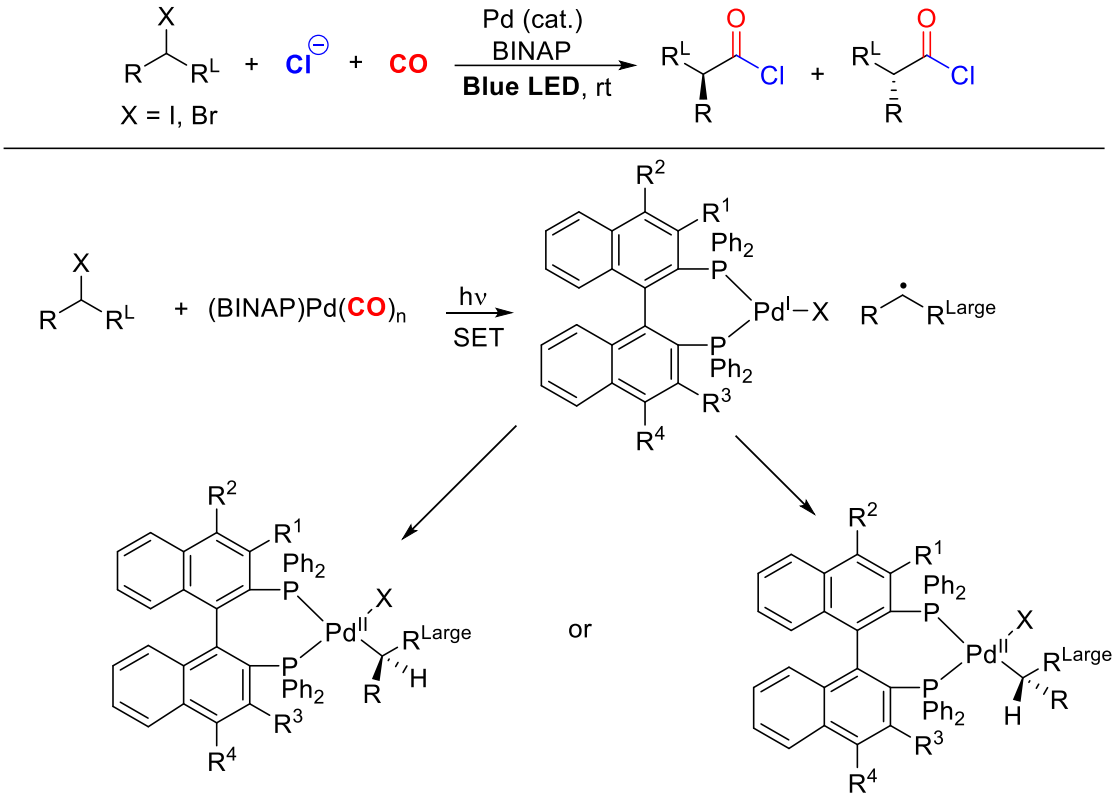

Scheme 6.5. Use of BINAP Ligands in Visible Light/Palladium Catalyzed Asymmetric Carbonylation of Alkyl Halides

The results in Chapter 5 do show that BINAP ligands have diminished reactivity (12%) relative to those with the *bis*[(2-diphenylphosphino)phenyl]ether backbone (i.e. DPE-Phos and Xantphos) in the light driven carbonylation of aryl iodides to form acid chloride derived products. However, the use of this ligand in the reaction with alkyl halides was not examined. This is important because alkyl halides are generally easier to reduce via SET than aryl halides,[9] which could allow the use of BINAP type ligands for palladium catalyzed asymmetric carbonylations. This chemistry could be coupled with the carbonylative synthesis of protected amino acid chlorides/fluorides described above as a new route to synthesize these valuable products (Scheme 6.6).

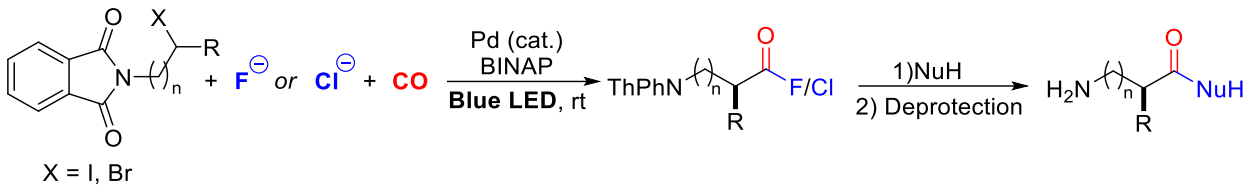

Scheme 6.6. Visible Light/Palladium Catalyzed Synthesis of Chiral Amino Acid Halide Electrophiles

6.3. References

1. Sonntag, N. O. V. *Chem. Rev.* **1953,** *52*, 237.

2. Prabhu, G.; Narendra, N.; Basavaprabhu; Panduranga, V.; Sureshbabu, V. V. *RSC Adv.* **2015,** *5*, 48331.

3. Blanchard, N.; Bizet, V. *Angew. Chem. Int. Ed.* **2019,** *58*, 6814.

4. Valeur, E.; Bradley, M. *Chem. Soc. Rev.* **2009,** *38*, 606.

5. Noyori, R.; Takaya, H. *Acc. Chem. Res.* **1990,** *23*, 345.

6. Akutagawa, S. *Applied Catalysis A: General* **1995,** *128*, 171.

7. Noyori, R.; Kitamura, M.; Ohkuma, T. *PNAS* **2004,** *101*, 5356.

8. Berthod, M.; Mignani, G.; Woodward, G.; Lemaire, M. *Chem. Rev.* **2005,** *105*, 1801.

9. Roth, H. G.; Romero, N. A.; Nicewicz, D. A. *Synlett* **2016,** *27*, 714.

Appendix 1: Mechanistic Studies on the Palladium Catalyzed Carbonylative Formation of Aroyl Triflates

A1.1. Introduction

In Chapters 2-5 of this thesis, we showed how the carbonylative generation of acid chlorides can open new routes to synthesize complex heterocycles, or, when coupled with light, expand the scope of carbonylative coupling reactions. Research in our lab has also been directed towards using this concept to build-up extremely electrophilic acylating agents capable of new types of reactivity, such as the C-H functionalization of arenes. Metal catalyzed C-H functionalization has recently emerged as an attractive approach to derivatize (hetero)arenes.[1-5] This includes numerous examples of palladium catalyzed carbonylative C-H functionalization reactions to form carboxylic acid derivatives (e.g. anhydrides, acids, esters or amides), which was popularized with the seminal work from Fujiwara.[6-11] However, the formation of ketones via this approach remains a challenge. This issue is believed to arise from the presence of carboxylate ligands commonly employed for the C-H activation step. These carboxylates can also react with the palladium-acyl intermediate leading to anhydrides (or anhydride derived products), rather than ketones (Scheme A1.1a).[12-15]

Considering the above, our group has explored the carbonylative C-H functionalization issue from a different direction. We envisioned that the palladium catalyzed generation of even more potent electrophiles, such as acid triflates, might provide a more comprehensive platform for the C-H functionalization of arenes, as these substrates are established to undergo Friedel-Crafts reactions with even unactivated arenes (Scheme A1.1b).[16-20] In contrast to the current synthesis of acid triflates from synthetic, high energy acid chlorides, this would provide a route to form these electrophiles from aryl iodide, CO and a triflate salt (Scheme A1.1c). The challenge with this

approach would be the development of a catalyst system that can reductively eliminate a potent electrophile in the presence of a less reactive aryl halide substrate.

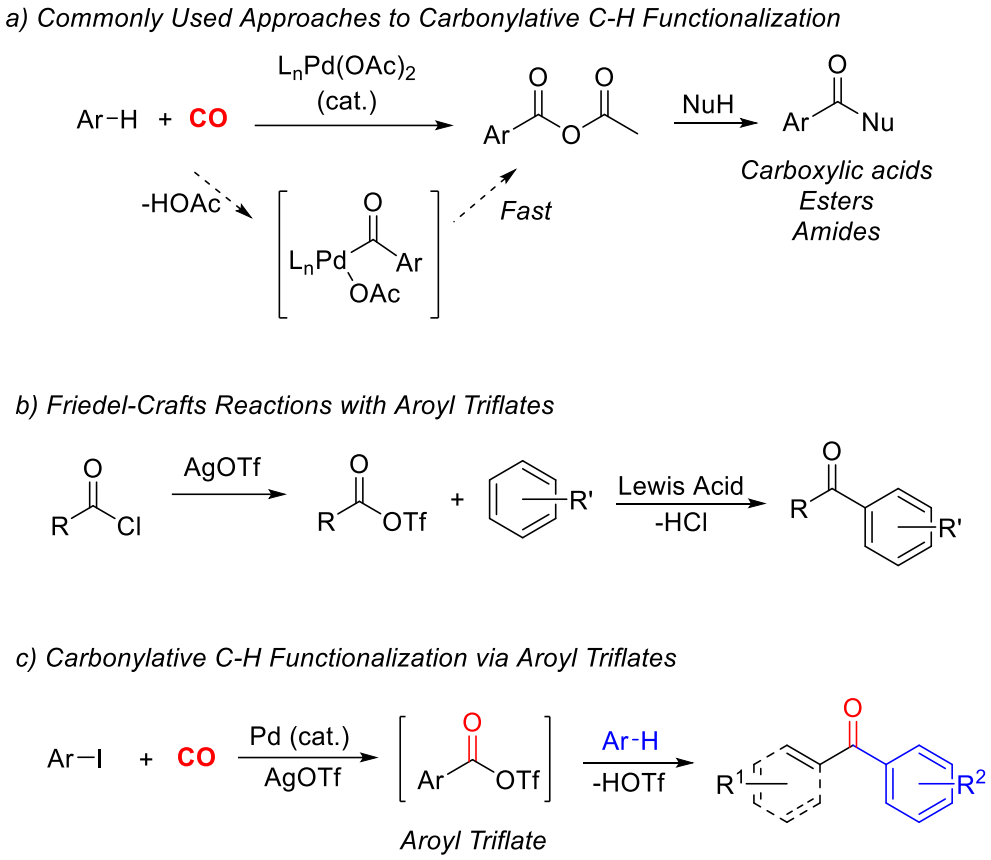

Scheme A1.1. Palladium Catalyzed Carbonylative C-H Functionalization of Arenes

Garrison Kinney, a member of our laboratory, examined the development of this chemistry. He showed that the palladium catalyzed coupling of aryl iodides, arenes, and carbon monoxide in the presence of AgOTf led to the near quantitative formation of ketone product (Scheme A1.2a). This system can be used to form ketones from a wide variety of arenes, including those that are typically challenging in Friedel-Crafts acylation reactions.[18, 20] The catalyst in this system is so potent that

the reaction can be carried out with as little as 150 ppm palladium. These studies also showed that added phosphine ligands, including the previously important P^tBu_3, slow or inhibit catalysis, and are ultimately consumed by the highly electrophilic reaction conditions (Scheme A1.2b). Instead, the most effective catalysts were simple palladium(II) sources, such as $PdCl_2$ or $[Pd(allyl)Cl]_2$. Interestingly, when the benzene trap is removed, aroyl triflate is formed in high yield. The latter was isolated, and its structure was confirmed by X-ray crystallography (Scheme A1.2c), providing definitive evidence for the catalytic generation of these species. Kinetic isotope effect studies are consistent with the intermediacy of acid triflates in the catalytic reaction, which undergo direct Friedel-Crafts acylation of arenes to afford the observed ketone products.

a) Palladium catalyzed carbonylative C-H functionalization of benzene

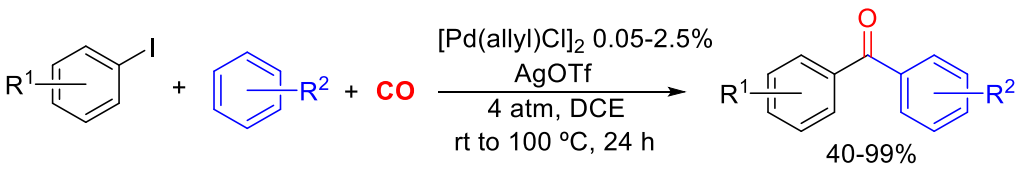

b) Ligand effects on catalysis

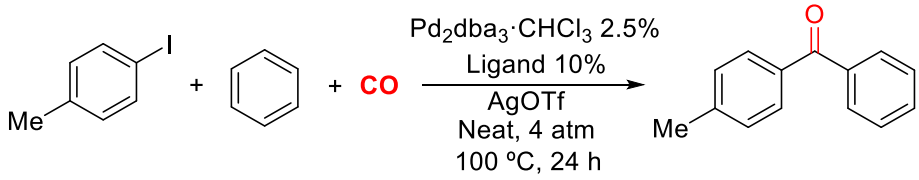

PPh_3	$P(o\text{-Tol})_3$	PCy_3	$P(C_6F_5)_3$
31%	9%	21%	29%

c) Catalytic acid triflate formation

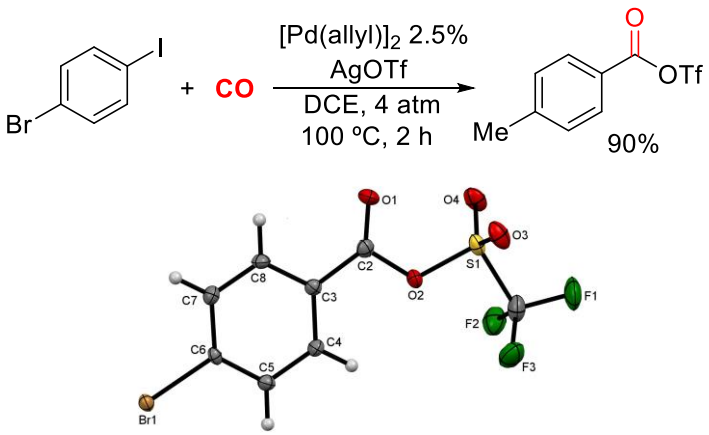

Scheme A1.2. Development of the Palladium Catalyzed Carbonylative C-H Functionalization of Benzene

The carbonylative formation of extremely reactive acylating agents such as acid triflates utilizing a simple, unligated palladium catalyst is unprecedented, since such strong electrophiles would presumably favor instead addition to Pd(0). We therefore became interested in synthesizing

the putative palladium-acyl triflate intermediate and probing its reactivity towards arenes. This Appendix will describe my personal contributions towards the synthesis, characterization, and mechanistic experiments involving this palladium complex. Additionally, it will present my efforts towards the formation of chalcone products from vinyl iodides utilizing this chemistry. This work was published in *Nature Chemistry* (**2018**, 10, 193).

A1.2. Results and Discussion

A1.2.1. Synthesis and Reactivity of Palladium-Acyl Triflate Complexes

The palladium catalyzed generation of acid triflate products described above presumably involves the initial formation of a palladium-acyl intermediate, which, in the absence of added ligands, may be stabilized by CO coordination (e.g. $(CO)_nPd(COAr)OTf$). Such electron deficient, CO-associated complexes have not been previously observed, and are presumably unstable (*vide infra*). Instead, we decided to prepare first a more stable, ligated version of the complex utilizing the P^tBu_3 ligand. The aroyl complex **A1.1** can be synthesized in high yield from the corresponding palladium-acyl chloride complex (see Chapter 2 for the synthesis of this chloride complex) by halide exchange with AgOTf (Scheme A1.3a). This complex can be crystallized by vapor diffusion of pentane into a concentrated solution of **A1.1** in 1,2-dichloroethane at -33 ºC. A crystal structure of **A1.1** was obtained (Scheme A1.3b). Consistent with previously reported P^tBu_3 coordinated Pd(II) complexes,[21] the palladium in **A1.1** adopts a 3-coordinate, T-shaped structure, where the large P^tBu_3 ligand does not allow the association of another ligand to palladium to form a square planar complex. The triflate is coordinated to palladium trans to the large phosphine (Pd-O length: 2.204(6) Å). All other bond lengths and angles are analogous to structures reported for the chloride coordinated version of this complex.[21]

a) Synthesis of Aroyl-Palladium Triflate Complex

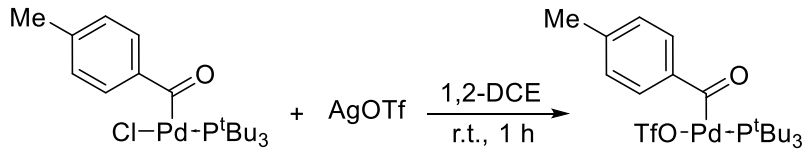

A1.1
87%

*b) X-Ray Structure of Aroyl-Palladium Triflate Complex **A1.1***

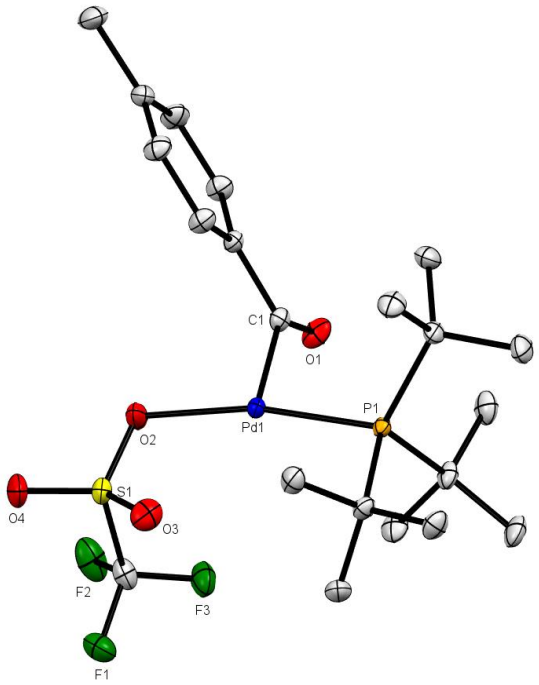

Scheme A1.3. Synthesis and Characterization of Aroyl-Palladium Triflate Complex

We next explored the reactivity of complex **A1.1**, and its potential to reductively eliminate acid triflate. This complex is stable at room temperature, and slowly decomposes at 55 ºC in C_6D_6 (30% after 2 days), but with no sign of aroyl triflate or ketone formation (Scheme A1.4a). In our studies with the analogous aroyl-palladium chloride complexes, we observed reductive elimination of acid chloride in the presence of CO (see Chapter 2). The addition of 4 atm CO to complex **A1.1**

in benzene does accelerate its decomposition (1 h at 55 ºC), but we again observed no evidence for acid triflate or ketone (Scheme A1.4a).

The stability of **A1.1** relative to the intermediates in catalysis is presumably related to the strongly coordinating P^tBu_3 ligand, and is consistent with the lack of catalysis in the presence of phosphines (Scheme A1.2b). We therefore next explored methods to remove this phosphine from palladium and generate the presumed intermediate in catalysis: $(CO)_nPd(COAr)OTf$. One possibility we considered was to protonate the phosphine with strong acids. Initial attempts at this reaction via the addition of HOTf to **A1.1** in C_6D_6 leads to the immediate decomposition of the complex before CO can be added to the mixture, and formed a complex mixture of products, including $^tBu_3PH^+OTf^-$. In order to block phosphine loss before CO is present (and thus potentially access $(CO)_nPd(COAr)OTf$), we next prepared a frozen solution of HOTf (1.2 equiv.) in C_6D_6 in an NMR tube at -35 ºC. Complex **A1.1** was layered on top of the frozen solution, and the tube immediately removed from the glovebox and 5 atm CO added. Subsequent thawing of the reaction solution and mixing in this case leads to the quantitative formation of protonated P^tBu_3 and acid triflate **A1.2** within 5 minutes (Scheme A1.4b). Heating the solution to 80 ºC leads to the eventual formation of ketone **A1.3a**.

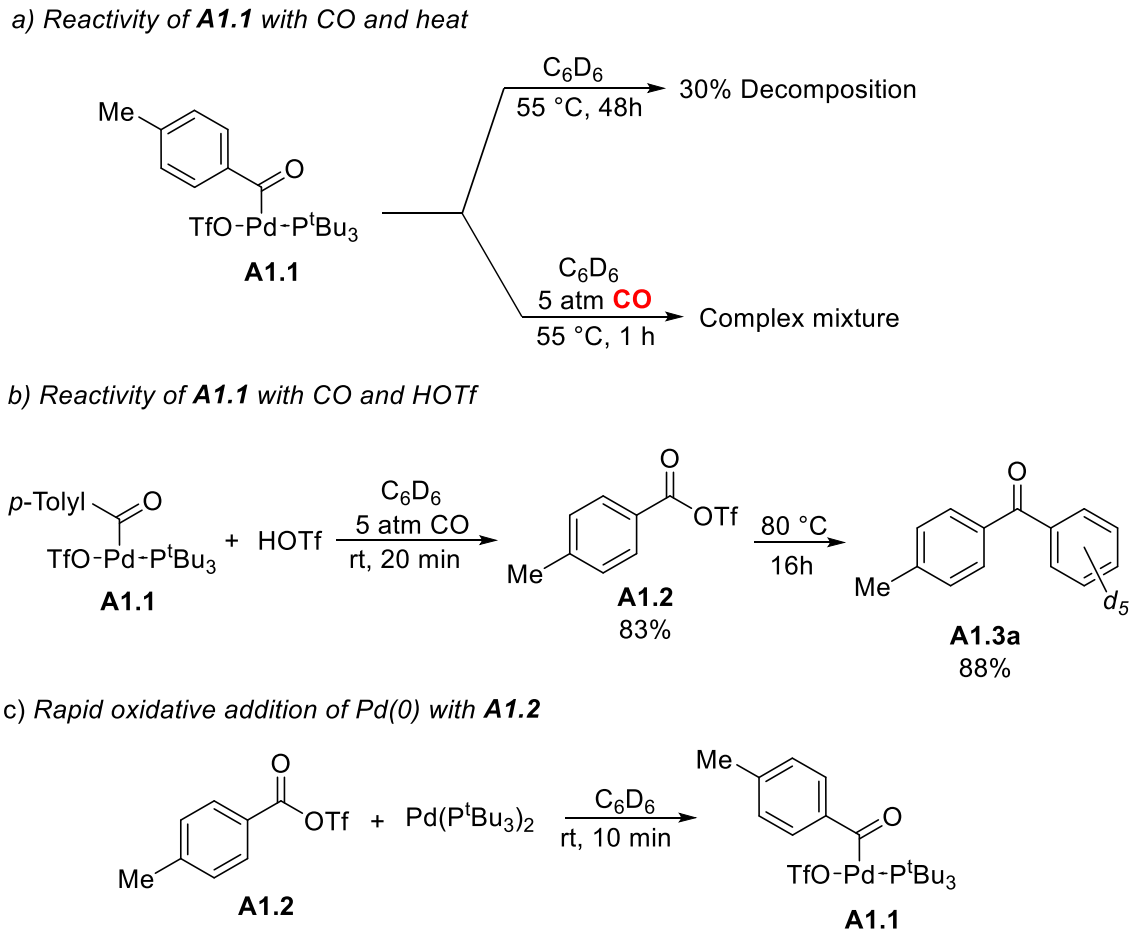

Scheme A1.4. Mechanistic Experiments with Aroyl-Palladium Triflate Complex

The above data shows that while the phosphine coordinated **A1.1** complex is relatively stable towards reductive elimination, removing the phosphine in the presence of CO results in the rapid elimination of acid triflate. These results are consistent with the enhanced ability of the CO coordinated complex, *e.g.* $(CO)_nPd(COAr)OTf$, to undergo reductive elimination during catalysis, wherein the π-acidic CO ligands presumably destabilize the Pd(II) complex and favor its conversion to Pd(0). The build-up of aroyl triflate also suggests that the CO associated Pd(0) by-product is deactivated towards oxidative addition. This also contrasts with phosphine coordinated

complexes such as $Pd(P^tBu_3)_2$, which react very quickly with aroyl triflate to generate **A1.1** within 10 minutes (Scheme A1.4c).

A1.2.2. Vinyl Iodides in Catalytic Ketone Formation

In addition to mechanistic studies, I also explored the use of vinyl iodides in catalysis. The vinyl iodide substrates were generated using several literature procedures (Scheme A1.5). For example, Z-vinyl iodides **A1.4a-c** were synthesized by the Stork-Zhao olefination of aldehydes or ketones with $Ph_3PCH_2I^+ I^-$. This reaction proceeds with high *Z*-selectivity, and was used to prepare vinyl iodides with aryl, vinyl or alkyl substituents (Scheme A1.5a).[22] To generate an *E*-vinyl iodide **A1.4d**, a selective method developed by the Charette lab was employed involving the initial deprotonation of benzyl bromide for coupling with diiodomethane, followed by the addition of DBU to drive HBr loss (Scheme A1.5b).[23] The tetra-substituted vinyl iodide **A1.4e** was formed from the commercial vinyl bromide using the copper catalyzed halide substitution reaction developed by Buchwald (Scheme A1.5c).[24]

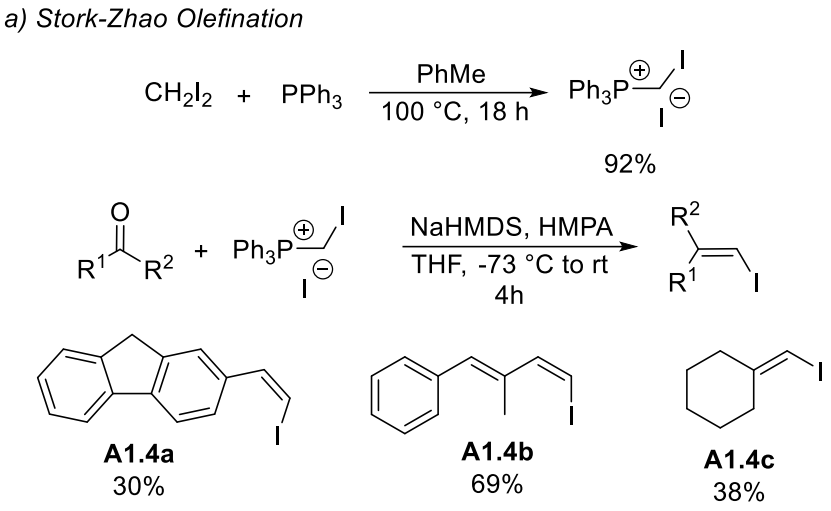

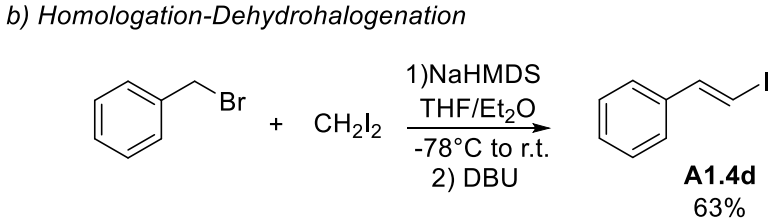

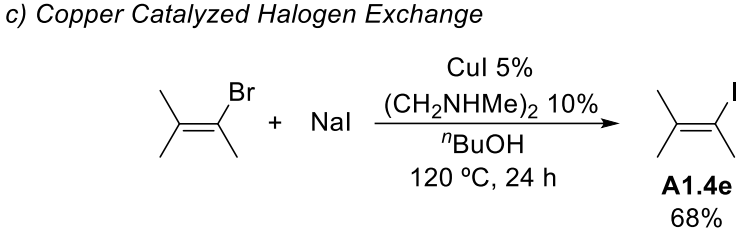

Scheme A1.5. Synthesis of Vinyl Iodide Substrates

As shown in Scheme A1.6, each of these vinyl iodides can be employed in the palladium catalyzed carbonylative C-H functionalization of thiophene to form disubstituted (**A1.3b-d**), trisubstituted (**A1.3e**), and tetrasubstituted (**A1.3f**) chalcones in very good yields. The increased reactivity of vinyl iodides towards oxidative addition allows the reaction to proceed at ambient temperature, in contrast to the 60-100 °C commonly employed with aryl iodides. The reaction is selective for acylation in the 2 position of thiophene, which is the most nucleophilic and thus the

most reactive towards the potent acid triflate intermediate generated in catalysis. Interestingly, we the *Z*-vinyl iodides all generate the *E*-isomer chalcone products **A1.3b-d**. This was attributed to the presence of acid and palladium in the reaction, which could catalyze the isomerization to the more stable *E*-products.

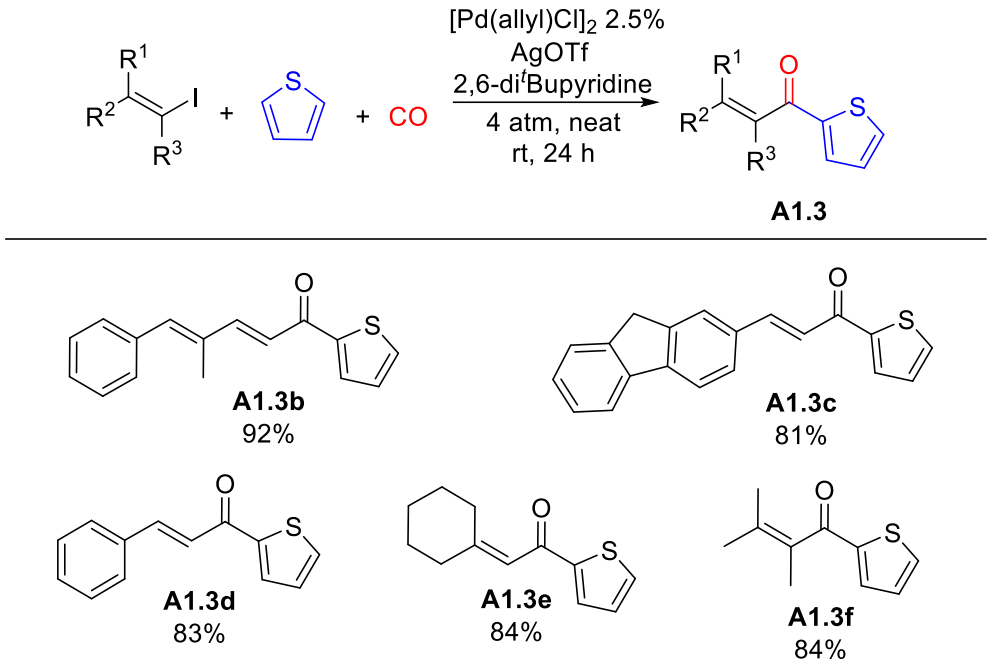

Scheme A1.6. Palladium Catalyzed Carbonylative C-H Functionalization of Arenes with Vinyl Iodides

Finally, I explored the idea of coupling palladium catalyzed hydrogenation with this chemistry, as this could offer an efficient route to access alkyl-aryl ketones. Initial attempts at this reaction using the same palladium catalyst for both the initial carbonylative C-H functionalization and hydrogenation did not lead to reduction (Scheme A1.7a). The same was true when additional 5% Pd/C was added to the mixture after the carbonylation step (Scheme A1.7b). This was attributed

to potential poisoning of the catalyst by the various components in the reaction mixture. Nevertheless, this reaction can be accomplished by first isolating the chalcone products, followed by hydrogenation with Pd/C, to generate the alkyl-aryl ketones **A1.5a,b** products in high yield (Scheme A1.7b).

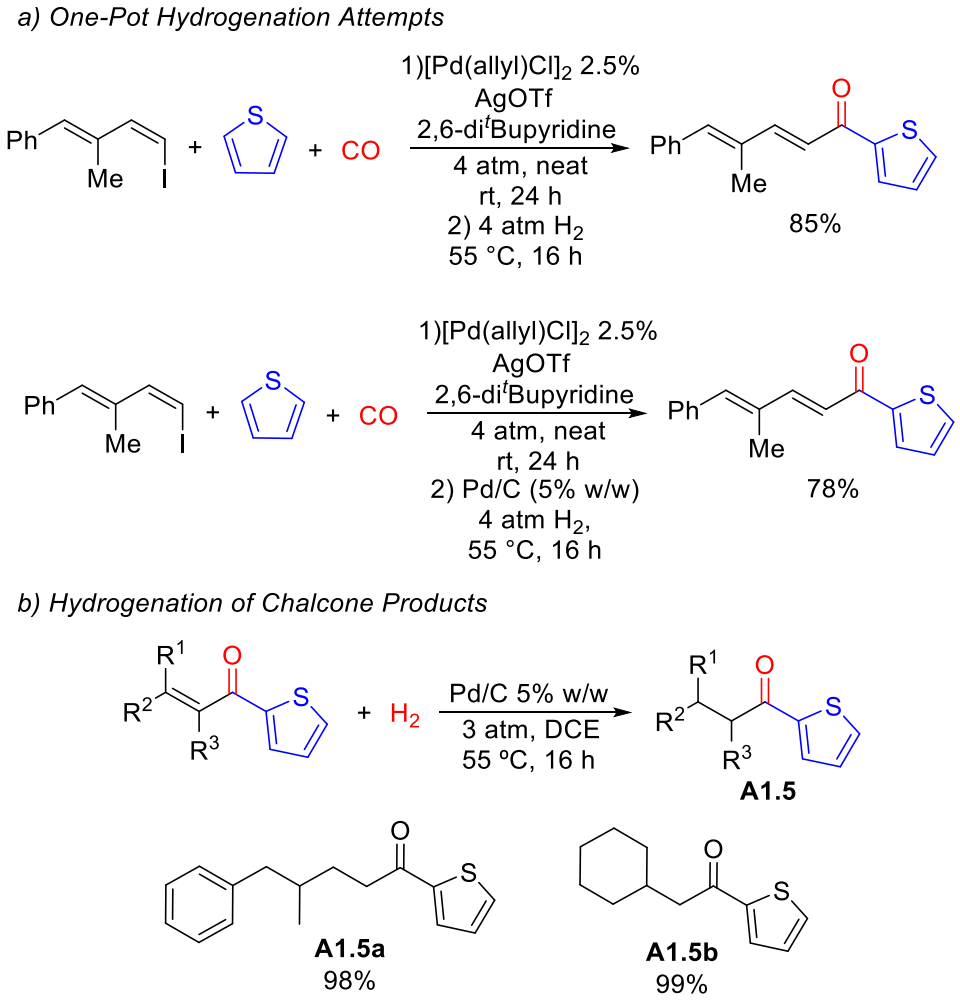

Scheme A1.7. Palladium Catalyzed Hydrogenation of Chalcone Products

A1.3. Experimental Section

A1.3.1. General Procedures

All manipulations were carried in an inert atmosphere glovebox or using standard Schlenk techniques unless stated otherwise. Research grade carbon monoxide (99.99%) was used as received. Solvents were dried over calcium hydride, distilled under argon and stored over activated 4 Å molecular sieves. Pentane was dried using a solvent purifier system and then stored over activated 4 Å molecular sieves in the glovebox. Deuterated solvents were dried over calcium hydride, vacuum transferred and stored over activated 4 Å molecular sieves. Silver triflate was dried by heating under vacuum and then stored in the glovebox. $Pd_2dba_3{\cdot}CHCl_3$ was prepared according to literature procedures and stored at -35 °C in the glovebox to avoid decomposition.[25] $Pd[(P^tBu)_3]_2$ was prepared according to a literature procedure.[21] (*E*)-(2-iodovinyl)benzene,[23] (*E*)-2-(2-iodovinyl)-9*H*-fluorene,[26] 2-iodo-3-methylbut-2-ene,[24] and (iodomethylene)cyclohexane[26] were all prepared according to literature procedures. (*p*-Tol)COOTf was prepared according to a literature procedure.[27] All other reagents were purchased from commercial suppliers and used as received. For reactions performed in a J-Young NMR tube, carbon monoxide was added by first freezing the solution in liquid nitrogen, evacuating the headspace in vacuo, and then condensing in 4 atm CO. For experiments carried out in Schlenk bombs at 4 atm, they were simply pressurized with 4 atm CO on top of the nitrogen atmosphere. All ^1H and ^{13}C NMR spectra were acquired on 400 and 500 MHz spectrometers. High-resolution mass spectra were obtained using a quadrupole-time of flight and an orbitrap detector by direct infusion in positive ESI mode or by atmospheric pressure chemical ionization.

A1.3.2. Experimental Procedures

Synthesis of *p*-TolylCOPd(P^{t}Bu$_3$)OTf (A1.1)

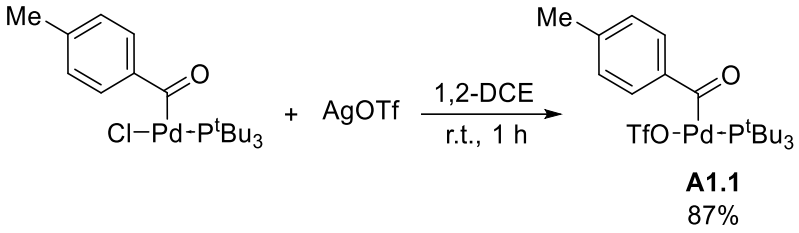

A1.1
87%

In a glovebox, *p*-TolylCOPd(P^{t}Bu$_3$)Cl (See Chaper 2) (124 mg, 0.27 mmol) was weighed in a vial equipped with a magnetic stir bar. The complex was dissolved in 2 mL 1,2-dichloroethane. To this solution, AgOTf (76 mg, 0.30 mmol) was added and the mixture was stirred for 1 hour at room temperature. The resulting suspension was filtered through a plug of celite to afford a yellow solution. The solvent was removed *in vacuo*, then the resulting oil was triturated with pentane (1 mL), and the solvent traces were removed under vacuum. The product was obtained as a dark yellow solid in 87% yield (134 mg, 0.23 mmol).

Crystals were grown by vapor diffusion of pentane into a solution of the complex in 1,2-dichloroethane (50 mg in 250 µL) at -33 ºC. The X-ray crystal structure is available at the Cambridge Crystallographic Data Centre (CCDC) under the deposition number 1554343. For additional details, see publication supporting information (*Nature Chem.* **2018**, 10, 193).

Thermal stability of complex A1.1

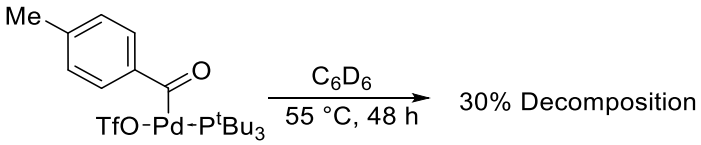

A1.1

In a glovebox, *p*-TolylCOPd(P^tBu_3)OTf (10 mg, 0.017 mmol) and dimethylsulfone (1 mg, 0.01 mmol) were dissolved in C_6D_6 (750 µL). The resulting solution was transferred into a J-Young NMR, which was capped and taken out of the glovebox. The tube was heated at 55 ºC inside an oil bath for 48 hours and the reaction was monitored by ^1H, ^{31}P, and ^{19}F NMR. The degree of decomposition was determined by ^1H NMR using dimethylsulfone as internal standard. After 48 h, a small amount of black precipitate was observed in the NMR tube and 70% of the complex remained in solution.

Reactivity of complex A1.1 with CO

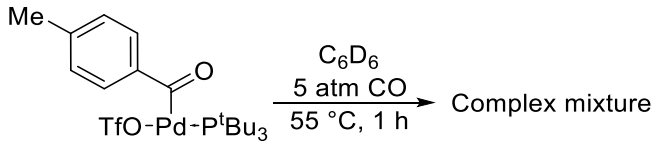

A1.1

In a glovebox, *p*-TolylCOPd(P^tBu_3)OTf (10 mg, 0.017 mmol) and dimethylsulfone (1 mg, 0.01 mmol) were dissolved in C_6D_6 (750 µL). The resulting solution was transferred into a J-Young NMR, which was capped and taken out of the glovebox. 5 atm of CO were condensed in the NMR tube and it was then heated at 55 ºC inside an oil bath. The reaction was monitored by ^1H, ^{31}P, and ^{19}F NMR. NMR yield was determined by ^1H NMR using dimethylsulfone as internal standard. Shortly after adding CO and heating a black precipitate formed inside the tube. The phosphorus NMR showed a complex mixture of products, including $HP^tBu_3^+$, and compounds preliminarily characterized as *p*-TolylCO$P^tBu_3^+$, and *p*-TolylCOP^tBu_2.

Reactivity of complex 7.1 with HOTf and CO

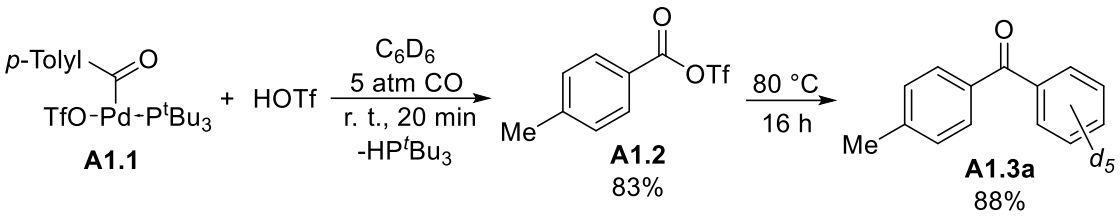

In a glovebox, triflic acid (3 mg, 0.02 mmol) and cyclohexane (1 mg, 0.02 mmol) were dissolved in C_6D_6 (750 µL) and the resulting solution was transferred into a J-Young NMR tube. The solution was frozen at -33 ºC inside the glovebox freezer. Then, *p*-TolylCOPd(P^{t}Bu$_3$)OTf (10 mg, 0.017 mmol) was added on top of the frozen solution with a spatula. The NMR tube was quickly taken out of the glovebox and placed inside liquid nitrogen. 5 atm of CO were condensed in the NMR tube and then the contents were thawed and allowed to react at room temperature. The reaction was monitored by ^{1}H, ^{31}P, and ^{19}F NMR. NMR yield was determined by ^{1}H NMR using cyclohexane as internal standard. Shortly after adding CO a black precipitate formed inside the tube. After 20 minutes, *p*-TolylCOOTf **A1.2** was formed in 83% yield and the phosphorus NMR showed a single signal at 52.6 ppm corresponding to protonated phosphine (85%). The identitty of acid triflate was corroborated by comparing the ^{1}H and ^{13}C NMR of the reaction mixture with the spectra of independently synthesized *p*-TolylCOOTf by a literature procedure.[27]

Pure acid triflate (**A1.2**): ^{1}H NMR (500 MHz, C_6D_6) δ 7.48 (d, *J* = 8.4 Hz, 2H), 6.56 (d, *J* = 7.9 Hz, 2H), 1.79 (s, 3H). ^{13}C NMR (101 MHz, C_6D_6) δ 156.3, 147.9, 131.8, 130.0, 121.7, 119.3 (q, J = 320.2 Hz), 21.5.

Reaction mixture: ^{1}H NMR (400 MHz, C_6D_6) δ 7.47 (d, J = 8.4 Hz, 2H), 6.54 (d, J = 8.0 Hz, 2H), 1.77 (s, 3H). ^{13}C NMR (101 MHz, C_6D_6) δ 156.3, 147.8, 131.8, 130.0, 121.8, 21.5. (The CF_3 quartet was not clearly visible)

The NMR tube was then heated at 80 ºC inside an oil bath for 16 hours. The ^{1}H NMR showed complete consumption of the acid triflate and the formation of phenyl(p-tolyl)methanone-d_5 **A1.3a** in 88% yield. The reaction mixture was analyzed by GC-MS and indeed the major component of the mixture was the ketone with an m/z of 201.1.

Synthesis of [HP^{t}Bu$_3$$^{+}$][OTf^{-}]

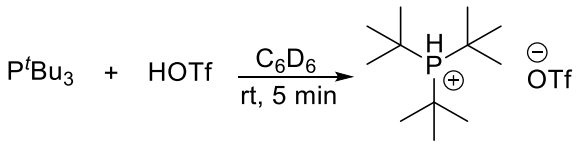

Protonated P^{t}Bu$_3$ was synthesized via a modified literature procedure.[28] In a glovebox, P^{t}Bu$_3$ (10 mg, 0.05 mmol) was dissolved in 0.5 mL C_6D_6 and transferred into a J-Young NMR tube. To this tube was added a solution of HOTf (11 mg, 0.08 mmol) in 0.25 mL C_6D_6. The NMR tube was sealed with a cap and the mixture was shaken at room temperature for 5 minutes. The NMR tube was taken out of the glovebox, and the protonated phosphine was characterized by ^{1}H and ^{31}P NMR. NMR analysis showed the full consumption of P^{t}Bu$_3$ and formation of a new phosphorus signal. ^{1}H NMR: δ 5.34 (d, J = 450.8 Hz, 1H), 1.04 (d, J = 15.4 Hz, 27H); ^{31}P NMR: δ 53.5.

Oxidative addition of phosphine ligated palladium to A1.2

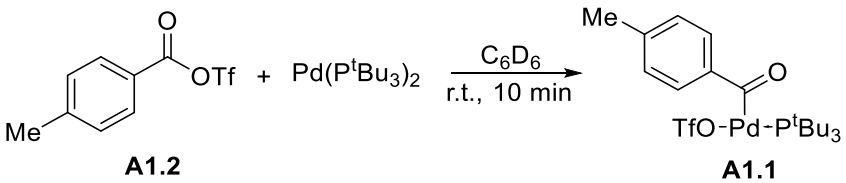

A1.2 **A1.1**

In a glovebox, *p*-TolylCOOTf (12 mg, 0.044 mmol), Pd(P^tBu_3)$_2$ (10 mg, 0.020 mmol), and cyclohexane (2 mg, 0.02 mmol) were dissolved in C_6D_6 (1 mL). The resulting solution was transferred into a J-Young NMR, which was capped and taken out of the glovebox. The mixture reacted at room temperature. The reaction was monitored by ^{1}H, ^{31}P, and ^{19}F NMR and yields were determined using cyclohexane as internal standard. After 10 minutes, *p*-TolylCOPd(P^tBu_3)OTf was formed in quantitative yield (99%).

Representative procedure for the palladium catalyzed carbonylative C-H functionalization of arenes with vinyl iodides

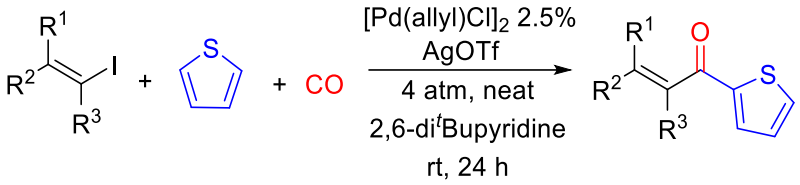

Silver triflate (96 mg, 0.37 mmol) was transferred to a Teflon sealed, thick walled 25 mL glass reaction vessel. ((1*E*,3*Z*)-4-iodo-2-methylbuta-1,3-dien-1-yl)benzene (68 mg, 0.25 mmol) and [Pd(allyl)Cl]$_2$ (2.3 mg, 6 µmol), and 2,6-di-tert-butylpyridine (57 mg, 0.30 mmol) were dissolved in thiophene (1 mL) and added. The vessel was closed, removed from the glovebox, and 4 atm of carbon monoxide were added. The reaction was stirred at room temperature for 24 h. After the reaction was done, carbon monoxide was released inside a well-ventilated fume hood. The reaction mixture was passed through a 2 cm celite/silica plug using ethyl acetate as the solvent. The crude was concentrated *in vacuo* and the residue was purified by column chromatography (silica gel, gradient hexane / ethyl acetate 0% to 20%) affording pure ketone **A1.3b** as a yellow solid in 92% yield (59 mg, 0.23 mmol).

Representative procedure for the catalytic hydrogenation of chalcones

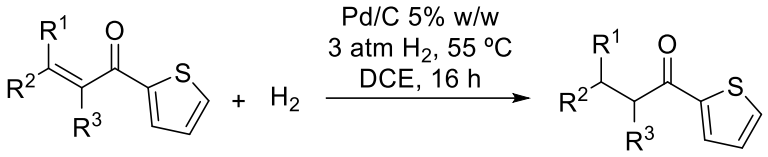

In a glovebox, (2*E*,4*E*)-4-methyl-5-phenyl-1-(thiophen-2-yl)penta-2,4-dien-1-one **A1.3b** (38 mg, 0.15 mmol) was dissolved in 2 mL 1,2-dichloroethane and transferred into a thick-walled 50 mL Schlenk bomb equipped with a magnetic stir bar. Pd/C (38 mg, 5% w/w Pd) was dry-transferred into the reaction vessel, which was then sealed with a Teflon cap, and taken out of the glovebox. The bomb was charged with 3 atm H_2, the reaction was heated at 55 ºC in an oil bath, and stirred for 16 hours. The vessel cooled down to room temperature and H_2 was released inside a fume hood. The reaction mixture was filtered through a plug of silica gel and celite, which was thoroughly washed with ethyl acetate. The reaction mixture was concentrated under vacuum and the resulting oil was triturated with pentane. The solvent was removed under reduced pressure and solvent traces were pumped off in a Schlenk line. Alkyl-aryl ketone **A1.5a** was obtained as a colorless solid in 98% yield (38 mg, 0.15 mmol).

A1.3.3. Characterization Data

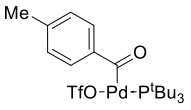

A1.1: Yellow solid, 87% yield (134 mg). ^{1}H NMR (500 MHz, $CDCl_3$): δ 8.11 (d, J = 8.3 Hz, 2H), 7.25 (d, *J* = 8.0 Hz, 2H), 2.41 (s, 3H), 1.50 (d, *J* = 13.3 Hz, 27H). ^{13}C NMR (126 MHz, $CDCl_3$): δ 198.2 (d, *J* = 7.8 Hz), 145.3, 131.1, 130.0 (d, *J* = 18.5 Hz), 129.7, 118.6, 40.1 (d, *J* = 11.1 Hz), 32.2 (d, *J* = 3.5 Hz), 22.0. ^{31}P NMR (162 MHz, $CDCl_3$): δ 80.7. Elemental analysis for $C_{21}H_{34}F_3O_4PSPd$: Theory 43.72 %C, 5.94 %H, 5.56 %S, Found 43.62 %C, 6.09 %H, 6.23 %S.

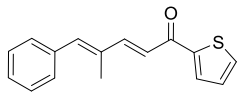

(2E,4E)-4-methyl-5-phenyl-1-(thiophen-2-yl)penta-2,4-dien-1-one (A1.3b). Yellow solid, 92% yield (59 mg). ^{1}H NMR (500 MHz, $CDCl_3$): δ 7.85 – 7.81 (m, 1H), 7.72 – 7.63 (m, 2H), 7.43 – 7.36 (m, 4H), 7.31 (ddd, *J* = 8.7, 5.7, 2.8 Hz, 1H), 7.17 (dd, *J* = 4.8, 3.9 Hz, 1H), 7.00 – 6.93 (m, 2H), 2.20 – 2.13 (m, 3H). ^{13}C NMR (126 MHz, $CDCl_3$) δ 182.4, 149.5, 145.9, 140.8, 136.8, 134.6, 133.6, 131.6, 129.7, 128.5, 128.3, 128.0, 121.1, 14.1. HRMS: Calculated for $C_{16}H_{14}OSNa$ ($M+Na^+$): 277.0658, found: 277.0659.

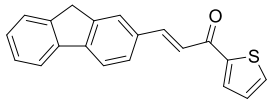

(E)-3-(9H-fluoren-2-yl)-1-(thiophen-2-yl)prop-2-en-1-one (A1.3c). Yellow solid, 81% yield (61 mg). ^{1}H NMR (500 MHz, $CDCl_3$): δ 7.95 (d, *J* = 15.5 Hz, 1H), 7.90 (dd, *J* = 3.8, 1.0 Hz, 1H), 7.86 – 7.78 (m, 3H), 7.71 – 7.65 (m, 2H), 7.58 (d, *J* = 7.4 Hz, 1H), 7.48 (d, *J* = 15.5 Hz, 1H), 7.41 (t, *J* = 7.2 Hz, 1H), 7.36 (td, *J* = 7.4, 1.1 Hz, 1H), 7.20 (dd, *J* = 4.9, 3.8 Hz, 1H), 3.96 (s, 2H). ^{13}C NMR (126 MHz, $CDCl_3$) δ 182.1, 145.9, 144.7, 144.6, 144.1, 144.0, 141.0, 133.8, 133.4, 131.8, 128.3, 128.1, 127.7, 127.2, 125.3, 125.0, 120.8, 120.6, 120.4, 37.0. HRMS: Calculated for $C_{20}H_{14}OSK$ ($M+K^+$): 341.0397, found: 341.0397.

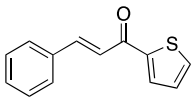

(E)-3-phenyl-1-(thiophen-2-yl)prop-2-en-1-one (A1.3d).[29] Brown oil, 83% yield (18 mg). ^{1}H NMR (500 MHz, $CDCl_3$) δ 7.92 – 7.85 (m, 2H), 7.71 (dd, *J* = 4.9, 1.1 Hz, 1H), 7.70 – 7.66 (m, 2H), 7.49 – 7.43 (m, 4H), 7.22 (dd, *J* = 4.9, 3.8 Hz, 1H). ^{13}C NMR (126 MHz, $CDCl_3$) δ 182.0, 145.5, 144.1, 134.7, 133.9, 131.8, 130.6, 129.0, 128.5, 128.3, 121.6. HRMS. Calculated for $C_{13}H_{10}SONa^+$ ($M+Na^+$): 237.0345, found 237.0347.

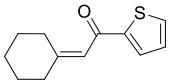

2-cyclohexylidene-1-(thiophen-2-yl)ethan-1-one (A1.3e). White solid, 84% yield (44 mg). ^{1}H NMR (500 MHz, $CDCl_3$): δ 7.70 (dd, *J* = 3.7, 1.1 Hz, 1H), 7.58 (dd, *J* = 4.9, 1.1 Hz, 1H), 7.10 (dd, *J* = 4.9, 3.8 Hz, 1H), 6.55 (s, 1H), 2.88 (t, *J* = 5.8 Hz, 2H), 2.34 – 2.23 (m, 2H), 1.72 (qd, *J* = 7.8, 7.0, 4.9 Hz, 2H), 1.68 – 1.59 (m, 4H). ^{13}C NMR (126 MHz,

$CDCl_3$) δ 184.1, 164.2, 147.1, 133.1, 131.1, 128.1, 117.9, 38.6, 30.7, 29.0, 28.1, 26.4. HRMS: Calculated for $C_{12}H_{14}OSNa$ ($M+Na^+$): 229.0658, found: 229.0657.

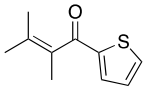

2,3-dimethyl-1-(thiophen-2-yl)but-2-en-1-one (A1.3f). Yellow oil, 84% yield (38 mg). ^1H NMR (400 MHz, $CDCl_3$) δ 7.67 (dd, *J* = 4.9, 1.1 Hz, 1H), 7.60 (dd, *J* = 3.7, 1.1 Hz, 1H), 7.13 (dd, *J* = 4.9, 3.8 Hz, 1H), 1.94 (s, 3H), 1.83 (s, 3H), 1.69 (s, 2H). ^{13}C NMR (101 MHz, $CDCl_3$) δ 193.98, 144.21, 134.22, 133.70, 133.07, 129.95, 128.13, 22.55, 20.01, 16.66. HRMS. Calculated for $C_{10}H_{12}ONaS$ ($M+Na^+$): 203.0501, found: 203.0496.

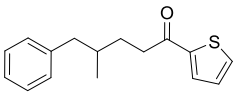

4-methyl-5-phenyl-1-(thiophen-2-yl)pentan-1-one (A1.5a). White solid, 98% yield (38 mg). ^1H NMR (500 MHz, $CDCl_3$): δ 7.66 (dd, *J* = 3.8, 1.1 Hz, 1H), 7.60 (dd, *J* = 4.9, 1.1 Hz, 1H), 7.29 – 7.23 (m, 2H), 7.20 – 7.12 (m, 3H), 7.10 (dd, *J* = 4.9, 3.8 Hz, 1H), 2.99 – 2.82 (m, 2H), 2.68 (dd, *J* = 13.5, 5.8 Hz, 1H), 2.43 (dd, *J* = 13.5, 7.8 Hz, 1H), 1.84 (tdd, *J* = 10.9, 4.7, 3.4 Hz, 2H), 1.62 (dt, *J* = 9.5, 5.7 Hz, 1H), 0.91 (d, *J* = 6.5 Hz, 3H). ^{13}C NMR (126 MHz, $CDCl_3$) δ 193.5, 144.5, 141.0, 133.5, 131.8, 129.3, 128.3, 128.2, 125.9, 43.6, 37.7, 34.9, 31.6, 19.4. HRMS: Calculated for $C_{16}H_{18}OSNa$ ($M+Na^+$): 281.0971, found: 281.0970.

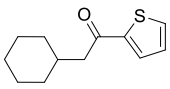

2-cyclohexyl-1-(thiophen-2-yl)ethan-1-one (A1.5b). Colourless oil, 99% yield (35 mg). ^1H NMR (500 MHz, $CDCl_3$): δ 7.69 (dd, *J* = 3.8, 1.1 Hz, 1H), 7.61 (dd, *J* = 4.9, 1.1 Hz, 1H), 7.12 (dd, *J* = 5.0, 3.8 Hz, 1H), 2.74 (d, *J* = 6.9 Hz, 2H), 2.02 – 1.93 (m, 1H), 1.80 – 1.73 (m, 2H), 1.72 – 1.62 (m, 3H), 1.27 (ddt, *J* = 12.6, 6.3, 2.6 Hz, 2H), 1.20 – 1.11 (m, 1H), 1.07 – 0.97 (m, 2H). ^{13}C NMR (126 MHz, $CDCl_3$) δ 193.3, 145.3, 133.6, 131.9, 128.2, 47.2, 35.3, 33.5, 26.3, 26.2. HRMS: Calculated for $C_{12}H_{16}OSNa$ ($M+Na^+$): 231.0814, found: 231.0819.

A1.3.4. NMR Spectra of Products

See Supporting Information of publication (*Nature Chem.* **2018**, 10, 193)

A1.4. References

1. Chen, X.; Engle, K. M.; Wang, D.-H.; Yu, J.-Q. *Angew. Chem. Int. Ed.* **2009,** *48*, 5094.
2. Colby, D. A.; Bergman, R. G.; Ellman, J. A. *Chem. Rev.* **2010,** *110*, 624.
3. Lyons, T. W.; Sanford, M. S. *Chem. Rev.* **2010,** *110*, 1147.
4. Liu, C.; Yuan, J.; Gao, M.; Tang, S.; Li, W.; Shi, R.; Lei, A. *Chem. Rev.* **2015,** *115*, 12138.
5. Hartwig, J. F. *J. Am. Chem. Soc.* **2016,** *138*, 2.
6. Jia, C.; Kitamura, T.; Fujiwara, Y. *Acc. Chem. Res.* **2001,** *34*, 633.
7. Liu, Q.; Zhang, H.; Lei, A. *Angew. Chem. Int. Ed.* **2011,** *50*, 10788.
8. Li, S.; Chen, G.; Feng, C.-G.; Gong, W.; Yu, J.-Q. *J. Am. Chem. Soc.* **2014,** *136*, 5267.
9. Yang, L.; Huang, H. *Chem. Rev.* **2015,** *115*, 3468.
10. Willcox, D.; Chappell, B. G. N.; Hogg, K. F.; Calleja, J.; Smalley, A. P.; Gaunt, M. J. *Science* **2016,** *354*, 851.
11. Bai, Y.; Davis, D. C.; Dai, M. *J. Org. Chem.* **2017,** *82*, 2319.
12. Campo, M. A.; Larock, R. C. *J. Org. Chem.* **2002,** *67*, 5616.
13. Wu, X.-F.; Anbarasan, P.; Neumann, H.; Beller, M. *Angew. Chem. Int. Ed.* **2010,** *49*, 7316.
14. Zhang, H.; Shi, R.; Gan, P.; Liu, C.; Ding, A.; Wang, Q.; Lei, A. *Angew. Chem. Int. Ed.* **2012,** *51*, 5204.
15. Lian, Z.; Friis, S. D.; Skrydstrup, T. *Chem. Commun.* **2015,** *51*, 1870.

16. Olah, G. A., FRIEDEL-CRAFTS AND RELATED REACTIONS. In *Index to Reviews, Symposia Volumes and Monographs in Organic Chemistry*, Kharasch, N.; Wolf, W., Eds. Pergamon: 1966; pp 173.

17. Effenberger, F.; Maier, A. H. *J. Am. Chem. Soc.* **2001,** *123*, 3429.

18. Sartori, G.; Maggi, R., *Advances in Friedel-Crafts Acylation Reactions: Catalytic and Green Processes*. CRC Press: 2010.

19. Sartori, G.; Maggi, R.; Santacroce, V., Catalytic Friedel–Crafts Acylation Reactions. In *Arene Chemistry*, Mortier, J., Ed. John Wiley & Sons, Inc.: 2016; pp 59.

20. Effenberger, F.; Eberhard, J. K.; Maier, A. H. *J. Am. Chem. Soc.* **1996,** *118*, 12572.

21. Quesnel, J. S.; Kayser, L. V.; Fabrikant, A.; Arndtsen, B. A. *Chem. Eur. J.* **2015,** *21*, 9550.

22. Stork, G.; Zhao, K. *Tetrahedron Lett.* **1989,** *30*, 2173.

23. Bull, J. A.; Mousseau, J. J.; Charette, A. B. *Org. Lett.* **2008,** *10*, 5485.

24. Klapars, A.; Buchwald, S. L. *J. Am. Chem. Soc.* **2002,** *124*, 14844.

25. Zalesskiy, S. S.; Ananikov, V. P. *Organometallics* **2012,** *31*, 2302.

26. Premachandra, I. D. U. A.; Nguyen, T. A.; Shen, C.; Gutman, E. S.; Van Vranken, D. L. *Org. Lett.* **2015,** *17*, 5464.

27. Effenberger, F.; Epple, G.; Eberhard, J. K.; Bühler, U.; Sohn, E. *Chem. Ber.* **1983,** *116*, 1183.

28. Netherton, M. R.; Fu, G. C. *Org. Lett.* **2001,** *3*, 4295.

29. Ried, W.; Marx, W. *Chem. Ber.* **1957,** *90*, 2683.

Appendix 2: Kinetic Studies on the Palladium Catalyzed Carbonylative Synthesis of Aromatic Acid Chlorides

A2.1. Introduction

The Pd/P^{t}Bu$_3$ catalyzed carbonylation of aryl iodides or bromides in the presence of chloride salts has been shown by our lab to generate acid chlorides as products.[1-2] This transformation is key to many of the reactions discussed in the thesis. As we have noted in other parts of the thesis, the formation of electrophilic acid chlorides is unusual in palladium catalysis, as these products typically instead undergo oxidative addition to Pd(0). Indeed, initial studies on this reaction showed that the Pd(P^{t}Bu$_3$)$_2$ catalyst is several orders of magnitude more reactive towards acid chloride than to aryl bromide.[2] Despite this, the catalytic reaction is capable of building up acid chloride, which implies that certain features of this catalyst system allow it to overcome this kinetic preference.

In an early study on this reaction, Jeffrey Quesnel, a former member of our laboratory, examined the effects of a number of ligands on the catalytic formation of acid chlorides. This showed that the most effective ligands were those with high steric bulk, particularly P^{t}Bu$_3$, while smaller ligands generated minimal product (Scheme A2.1).[1-2] The latter observation led to the postulate that the steric bulk of the phosphine is involved in driving the challenging reductive elimination. To gain more insight into this possibility, Quesnel synthesized a series of palladium-acyl complexes with different phosphine ligands. The P^{t}Bu$_3$ complex adopted a three-coordinate T-shape geometry that possessed an empty coordination site partially occupied by an agostic interaction with one of the C-H bonds in the P^{t}Bu$_3$ ligand.[2] In theory, this site could be occupied by a small molecule such as CO, which would increase the steric strain around palladium and

perhaps induce reductive elimination. Indeed, when CO is added to these complexes, we observe rapid equilibrium formation of acid chloride (see Chapter 2). These complexes do not form acid chloride upon heating in the absence of carbon monoxide, which further supports that CO has a role in inducing the reductive elimination. In contrast to P^tBu_3, smaller ligands such as PPh_3 formed stable square-planar complexes and do not generate acid chloride with or without CO.[2]

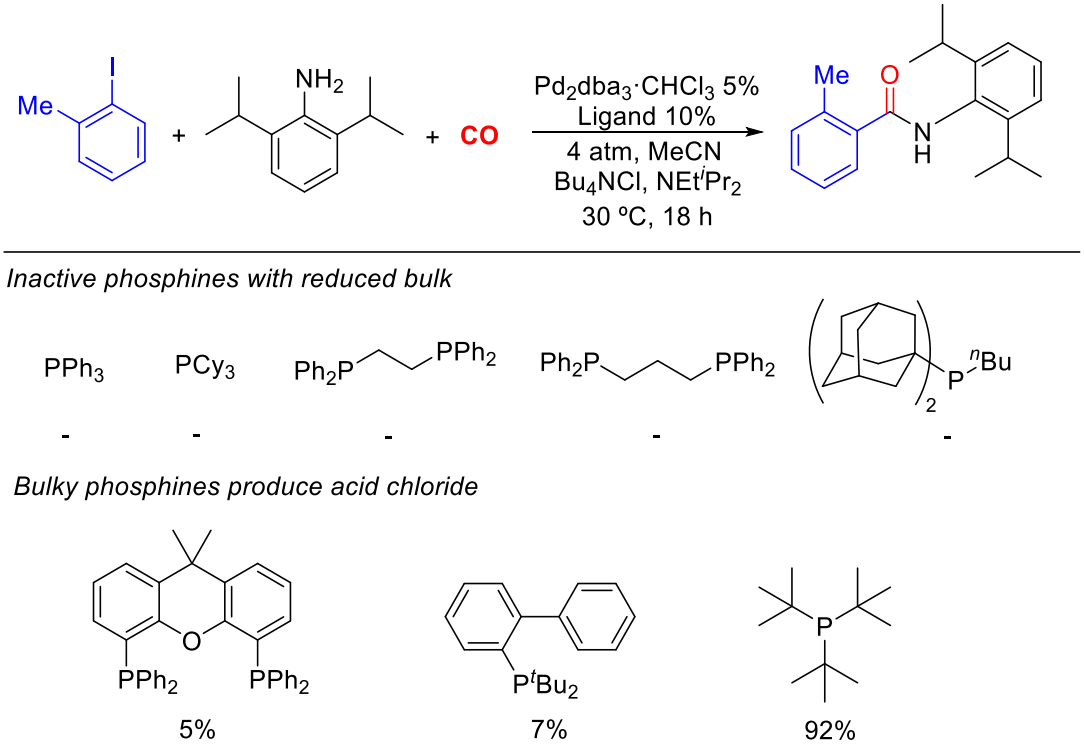

Scheme A2.1. Phosphine ligand effects in the palladium catalyzed carbonylative formation of acid chlorides

In order to better probe these mechanistic questions, we turned to computational calculations in collaboration with the Bengali group at the University of Texas A&M at Qatar and Professor Kai

Ylijoki at Saint Mary's University. The results of the DFT studies and energy profile of the reaction is summarized in Scheme A2.2. Notably, the $Pd(P^tBu_3)_2$ catalyst reacts with CO under the reaction conditions to generate a more stable tricarbonyl complex **A2.1b** (Scheme A2.2a). This complex must lose 2 CO ligands to form the active oxidative addition complex **A2.1a**. The latter reacts with phenyl iodide via oxidative addition with a calculated energy barrier of 21.7 kcal/mol. The subsequent halide exchange and CO insertion steps proceed rapidly and generate palladium-acyl complex **A2.2a**. The direct reductive elimination of acid chloride from **A2.2a** is a relatively high barrier reaction (23.6 kcal/mol). However, isomerization to **A2.2b** and CO coordination to form **A2.3** dramatically lowers the barrier to reductive elimination of acid chloride (14.2 kcal/mol). The resulting **A2.1a** complex after reductive elimination can either react with a PhI substrate or with the acid chloride product. Computation of the energetic barriers for these processes shows that oxidative addition to acid chloride is faster than to PhI (15.1 kcal/mol and 20.5 kcal/mol respectively). This latter predicts an inhibition of reductive elimination from **A2.3** as acid chloride product is built up, which is consistent with the experimental evidence.[1-2]

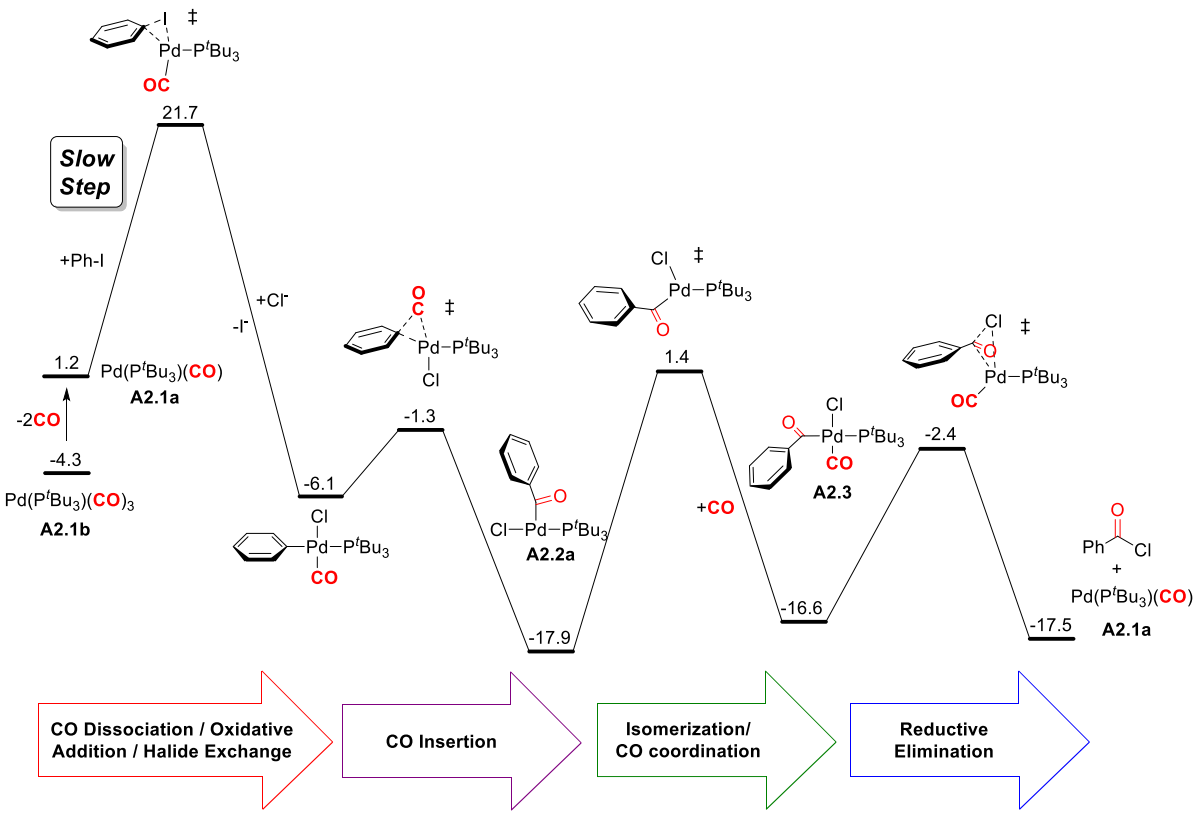

Scheme A2.2. Computed Energies for the Palladium Catalyzed Carbonylation of Phenyl Iodide to Form Benzoyl Chloride (relative energies in kcal/mol, abridged version from publication)

The role of the phosphine ligand in the reductive elimination step was further probed by DFT studies. A comparison of a series of trialkylphosphine-coordinated palladium-acyl complexes showed that a key influence of ligand sterics is in destabilizing the CO coordinated complex. In particular, less bulky phosphines show increase the stability of the complex compared to the relatively unstable **A2.3** (Scheme A2.3a). This was found to arise from strong steric interactions between the ^{t}Bu units on phosphorus and the CO ligand. These interactions elongate (and

destabilize) the Pd-P bond (Scheme A2.3b), and thus lower the barrier for acid chloride reductive elimination compared to other phosphine ligands lacking three large tertiary alkyl substituents.

a) Stabilizing effect of small phosphines in CO coordinated palladium-acyl complexes.

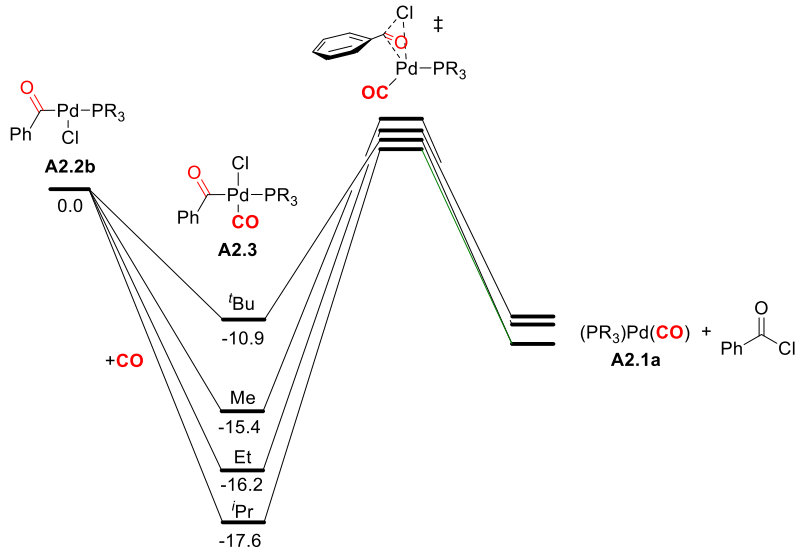

b) Calculated structures of CO coordinated tri-alkyl phosphine palladium-acyl complexes

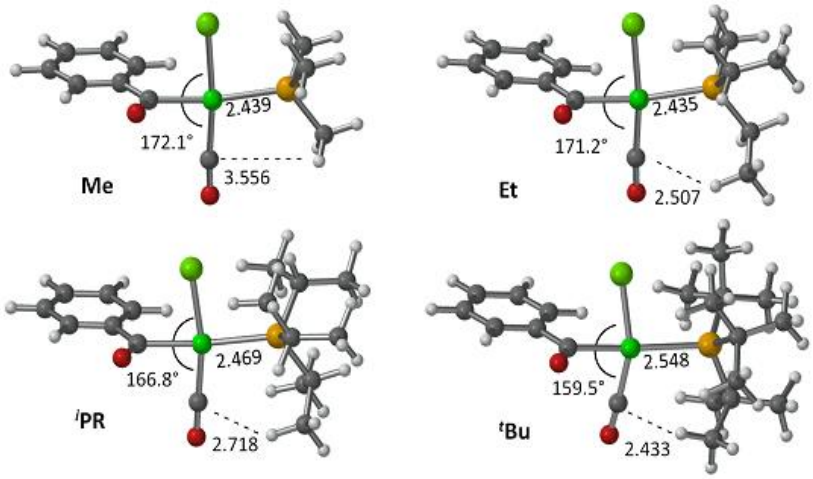

Scheme A2.3. Steric Interactions in Tri-Alkyl Coordinated Palladium-Acyl Complexes

Overall, the calculations in Scheme A2.2 suggest that the slowest formal step in catalysis is the oxidative addition of aryl iodide to the active **A2.1a** complex. However, the faster re-addition of acid chloride to Pd(0) also leads to a dynamic equilibrium under catalytic conditions, and as acid chloride builds-up, it shifts the equilibrium between the CO-coordinated **A2.1a** and the palladium-acyl complex **A2.2a** away from Pd(0), and therefore slows productive aryl iodide oxidative addition. This agrees with experimental evidence, where the Pd-acyl complex **A2.2a** is the catalyst resting state, which must then presumably undergo equilibrium acid chloride reductive elimination and aryl iodide oxidative addition as the rate determining steps in catalysis.

In light of these theoretical results, we became interested in probing the kinetic profile of this transformation as a means to consolidate our mechanistic proposal. This Appendix will describe my efforts to experimentally probe the effect of aryl iodide and carbon monoxide concentration on the rate of reaction. This work was published as part of the DFT study in *Chem. Eur. J.* **2016**, 22, 15107.

A2.2. Results and Discussion

The DFT data above suggests that the slow step in the catalytic reaction is the oxidative addition of complex **A2.1b** to aryl iodide. As such, the reaction rate should show first order dependence upon aryl iodide concentration. To experimentally probe this prediction, I examined the kinetics of the catalytic reaction under limiting aryl iodide conditions. To minimize the possibility of equilibrium acid chloride re-addition to palladium influencing the reaction rate, an *in situ* amine trap, 2,6-diisopropylaniline, was added to the reaction. Previous studies have shown that this bulky aniline has almost no reactivity towards the palladium-acyl intermediate under the catalytic reaction conditions, but it reacts rapidly with acid chloride to form an amide (see Chapter 5).

Kinetic analysis was done by monitoring the consumption of aryl iodide (and formation of amide) vs. time by ^{1}H NMR analysis. The ln plot of aryl iodide concentration vs time data (Scheme A2.4) shows that the consumption of aryl iodide follows first order kinetics. This is consistent with our calculations that suggest that the rate limiting step is oxidative addition of the aryl iodide substrate.

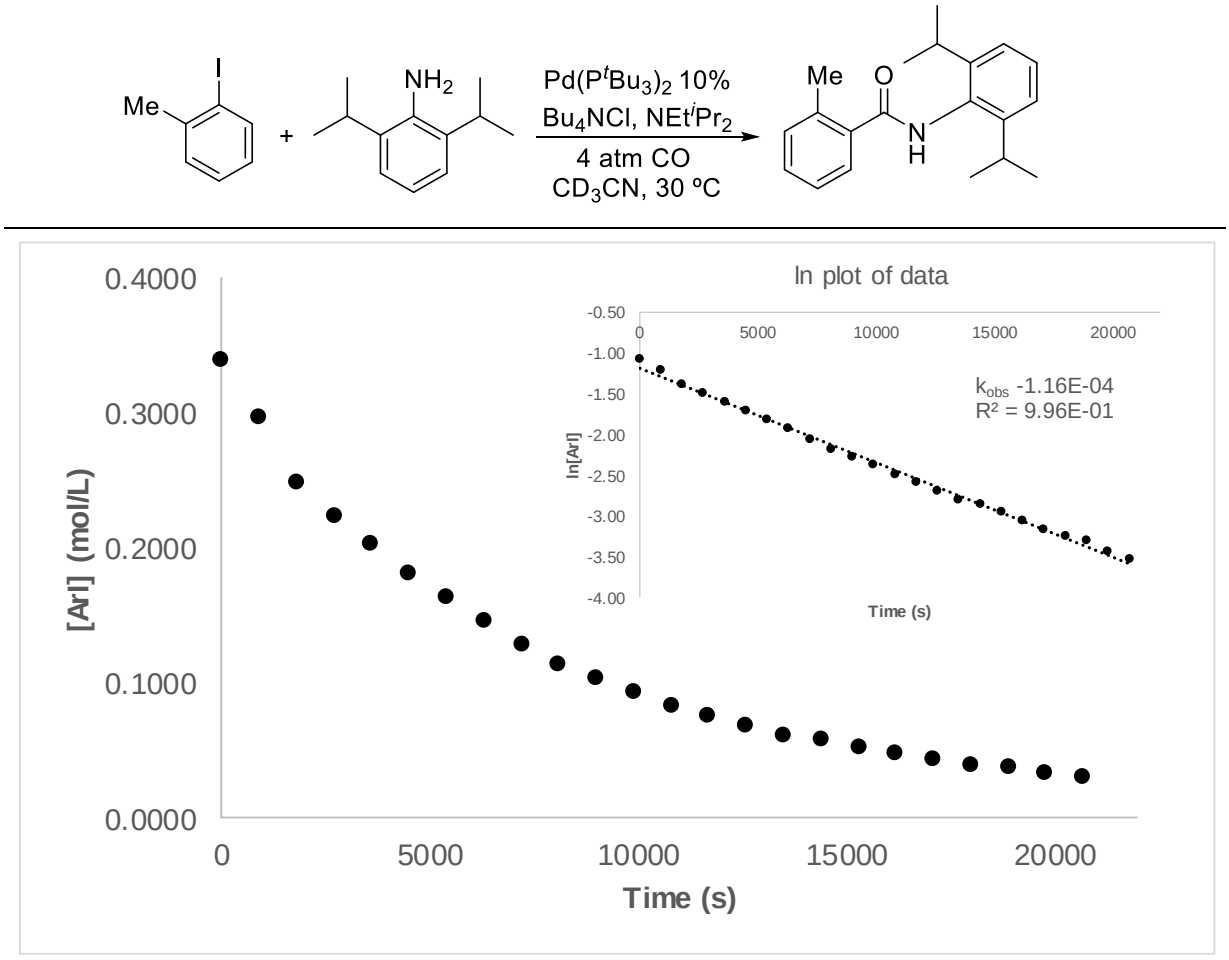

Scheme A2.4. Typical Kinetic Plot of Aryl Iodide Concentration vs Time. Inset: ln plot of data.

Our theoretical analysis suggests that CO plays multiple roles in this transformation. Firstly, the active catalyst in this reaction is complex **A2.1a**, which must form via loss of CO from

polycarbonyl complex **A2.1b** (Scheme A2.2). This should be more favorable at lower CO concentration, and CO pressure is therefore expected to have a detrimental effect on the rate. In contrast, CO can facilitate the reductive elimination of acid chloride from complex **A2.2a**. Firstly, since the CO coordinated complex **A2.3** is less stable than A**2.2a**, its formation will be favored by CO pressure. Moreover, acid chloride reductive elimination is reversible, meaning that CO pressure will help drive the formation of the Pd(0)-carbonyl complex **A2.1a** needed for aryl iodide oxidative addition. It is therefore unclear which effect of CO pressure will be more important in the catalytic reaction.

To shed some light on the overall effect of CO pressure, we examined the kinetics of the reaction at different CO pressures using the the same reaction described above, but with a large excess of aryl iodide (10 equiv.). The rate was measured by monitoring the consumption of aniline trap (Figures A2.1 to A2.4). The resulting rate constants vs CO pressure were then plotted to determine the order of CO (Figure A2.5).

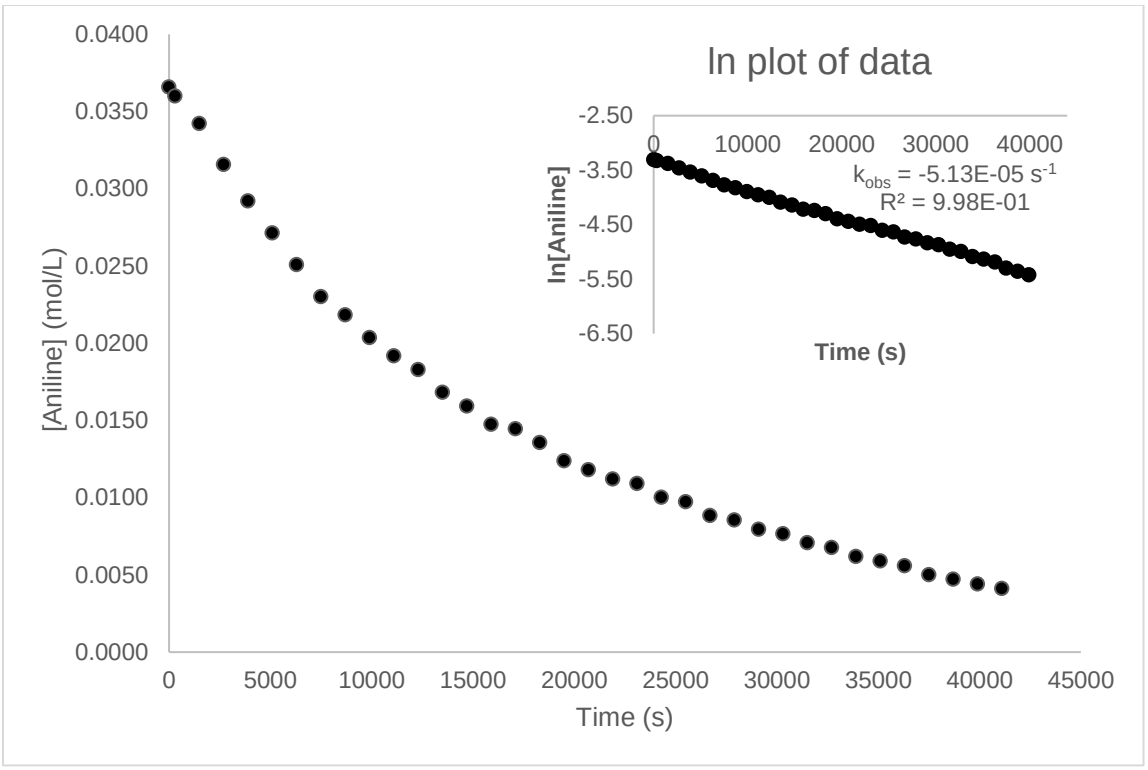

Figure A2.1. Consumption of Aniline at 1 atm CO. Inset: ln plot of data.

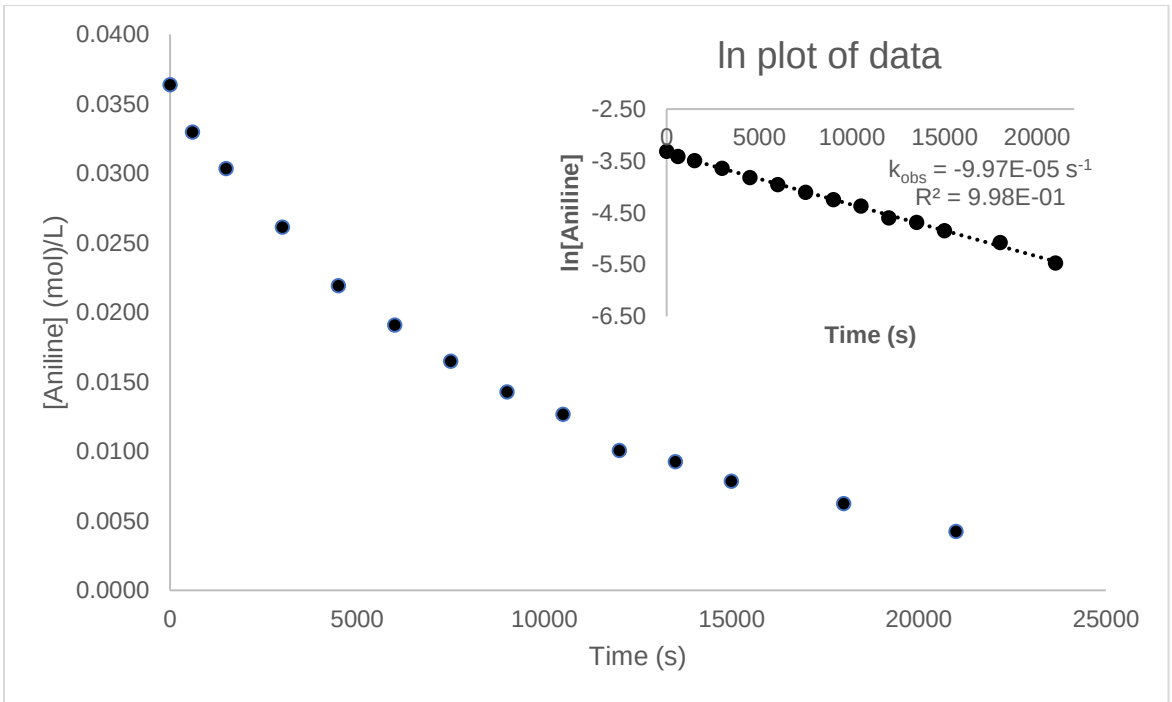

Figure A2.2. Consumption of Aniline at 2 atm CO. Inset: ln plot of data.

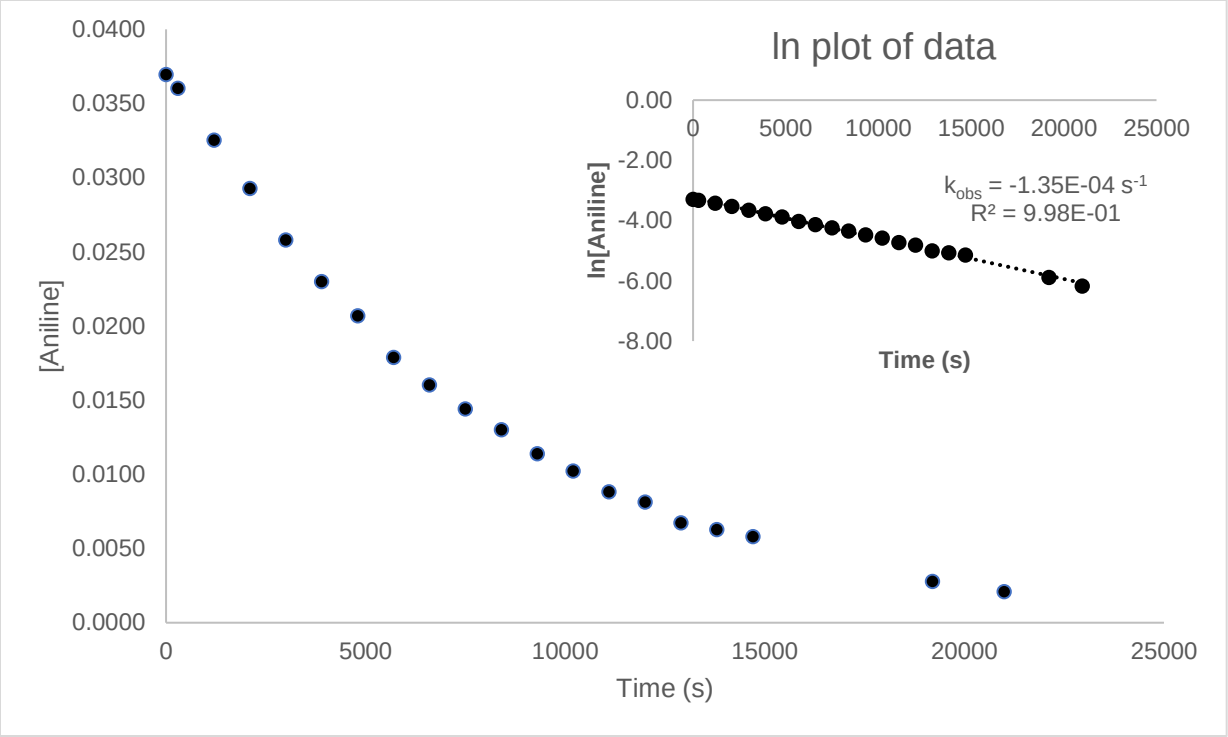

Figure A2.3. Consumption of Aniline at 3 atm CO. Inset: ln plot of data.

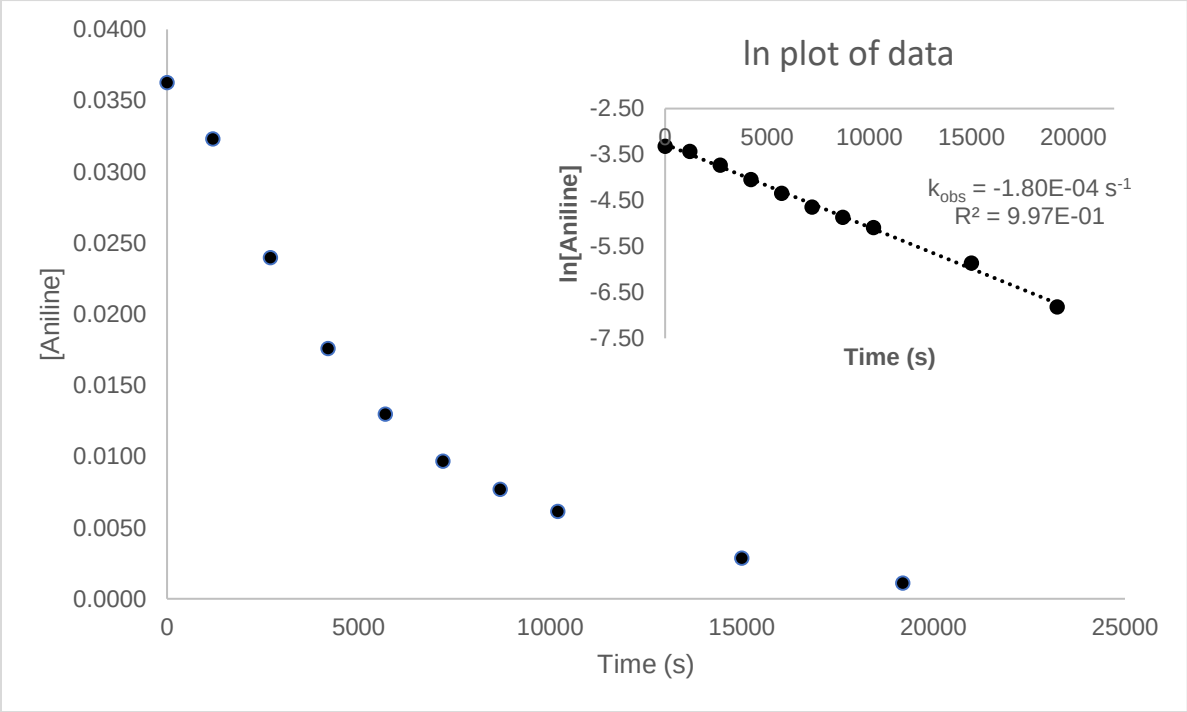

Figure A2.4. Consumption of Aniline at 4 atm CO. Inset: ln plot of data.

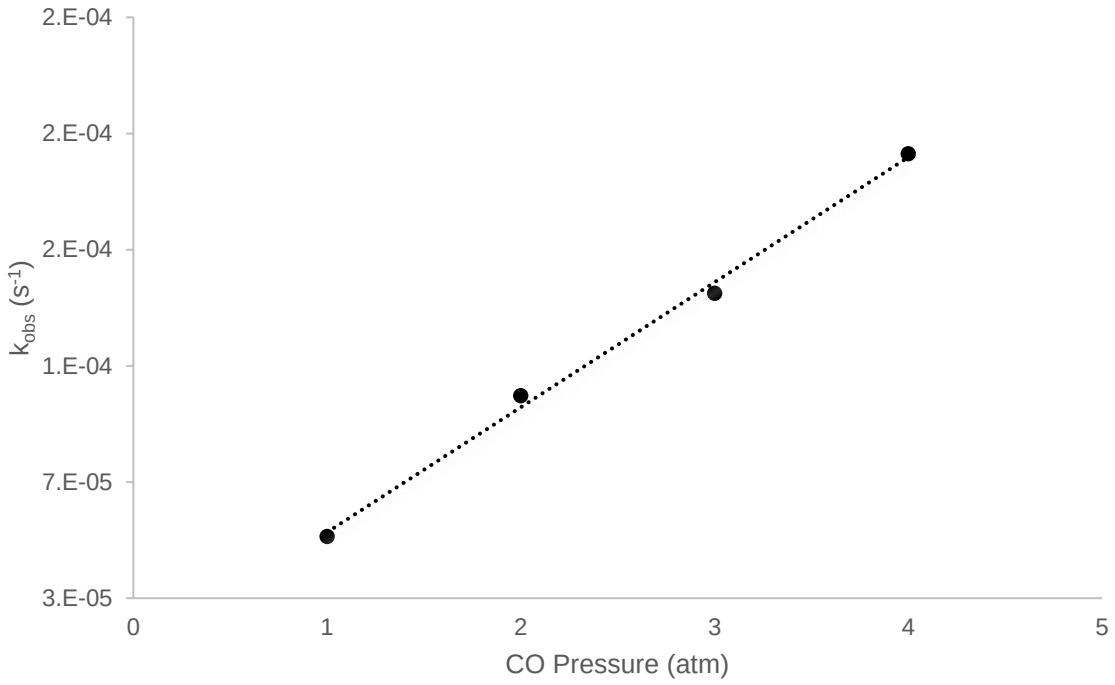

Figure A2.5. Effect of CO Pressure on the Rate of Reaction

The plot of k_{obs} vs CO pressure in Figure A2.5 shows a clear first order rate dependence on CO pressure. This observation is interesting considering that free CO is not involved directly in aryl iodide oxidative addition (the slowest step in catalysis). However, as noted above, acid chloride reductive elimination to form the Pd(0) complex **A2.1a** is rapid and reversible. This reversibility appears important even in the presence of the aniline trap. In this scenario, CO pressure would accelerate catalysis by driving this equilibrium forward to the Pd(0)-carbonyl complex **A2.1a**. Since the concentration of the latter is partially dependent on CO concentration, CO is a kinetically important ligand (as well as reagent) in this transformation.

Overall, these kinetic studies show that the catalytic formation of acid chlorides from aryl iodides, chloride, and CO has a first order dependence on the concentration of aryl iodide and

carbon monoxide. These are both consistent with the theoretical calculations, which predict that the rate determining step is the oxidative addition of complex **A2.1a** to aryl iodide. While the oxidative addition itself does not formally involve free carbon monoxide, the concentration of **A2.1a** for this step will be dependent upon CO pressure, since previous experimental studies have shown that the palladium-acyl complex **A2.3** is the catalyst resting state.[1-2] The effect of CO is therefore to increase the concentration of **A2.1a** needed for oxidative addition, as predicted by the energy profile for the reaction in Scheme A2.2.

A2.4. Experimental Section

A2.4.1. General Procedures

All manipulations were carried in an inert atmosphere glovebox or using standard Schlenk techniques unless stated otherwise. Research grade carbon monoxide (99.99%) was used as received. Solvents were dried over calcium hydride, distilled under argon and stored over activated 4 Å molecular sieves. Deuterated solvents were dried over calcium hydride, vacuum transferred and stored over activated 4 Å molecular sieves. $Pd(P^tBu_3)_2$ was prepared according to literature procedures.[2] All other reagents were purchased from commercial suppliers and used as received. For reactions performed in a J-Young NMR tube, carbon monoxide was added by first freezing the solution in liquid nitrogen, evacuating the headspace *in vacuo*, and then condensing in 4 atm CO. All ^1H spectra were acquired on 500 MHz spectrometers.

A2.4.2. Experimental Procedures

Kinetic analysis for the aryl iodide as the limiting reagent

In a glove box, $Pd(P^tBu_3)_2$ (1.5 mg, 0.003 mmol) and Bu_4NCl (8.3 mg, 0.03 mmol) were transferred into a J-Young NMR tube. 2,6-diisopropylaniline (53 mg, 0.3 mmol), 2-iodotoluene (6.5 mg, 0.03 mmol), NEt^iPr_2 (39 mg, 0.30 mmol), and hexamethylbenzene standard (1.6 mg, 0.01 mmol) were dissolved in 0.75 mL CD_3CN and transferred into the NMR tube. The NMR tube was then sealed with a screw cap, taken out of the glove box, and charged with 4 atm of CO by first freezing the solution in liquid nitrogen, evacuating the headspace *in vacuo*, and then condensing in 4 atm CO. The contents of the tube were kept frozen until loading into the NMR spectrometer. An array experiment was programmed to collect ^1H NMR (500 MHz) spectra starting at t = 5 minutes at 30 °C, with subsequent points collected every 20 minutes. The consumption of aryl iodide was monitored via ^1H NMR integration vs. the internal standard. This procedure was repeated in duplicate, and the plots in Scheme A2.4 represent an average of the two sets of data.

Typical procedure for the kinetic analysis of the effect of CO on rate

In a glove box, $Pd(P^tBu_3)_2$ (1.5 mg, 0.003 mmol) and Bu_4NCl (8.3 mg, 0.03 mmol) were transferred into a J-Young NMR tube. 2,6-diisopropylaniline (5.3 mg, 0.03 mmol), 2-iodotoluene (65 mg, 0.30 mmol), NEt^iPr_2 (39 mg, 0.30 mmol), and benzyl benzoate standard (3.2 mg, 0.015 mmol) were dissolved in 0.75 mL CD_3CN and transferred into the NMR tube. The NMR tube was then sealed with a screw cap, taken out of the glove box, and charged with 1 atm of CO by first freezing the solution in liquid nitrogen, evacuating the headspace *in vacuo*, and then condensing in 1 atm CO. The contents of the tube were kept frozen until loading into the NMR spectrometer.

An array experiment was programmed to collect ^{1}H NMR (500 MHz) spectra starting at t = 5 minutes at 22 °C, with subsequent points collected every 15 minutes. The consumption of aniline was monitored via ^{1}H NMR integration vs. the internal standard. This procedure was repeated in duplicate at 2, 3, and 4 atm of CO, and the plots in Figures A2.1-A2.4 represent an average of the two data sets.

A2.5. References

1. Quesnel, J. S.; Arndtsen, B. A. *J. Am. Chem. Soc.* **2013,** *135*, 16841.

2. Quesnel, J. S.; Kayser, L. V.; Fabrikant, A.; Arndtsen, B. A. *Chem. Eur. J.* **2015,** *21*, 9550.

Appendix 3: NMR Spectra for Chapter 5

A3.1. NMR Spectra

^{1}H and ^{13}C NMR data for 5.1a

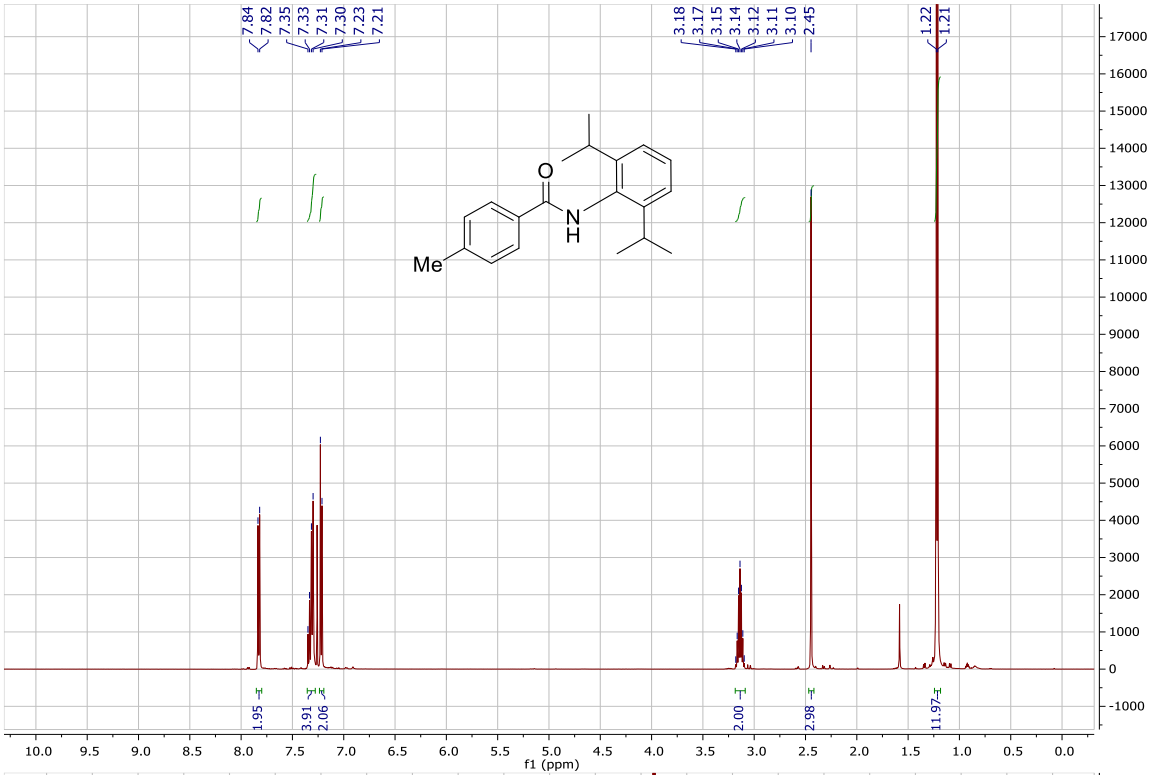

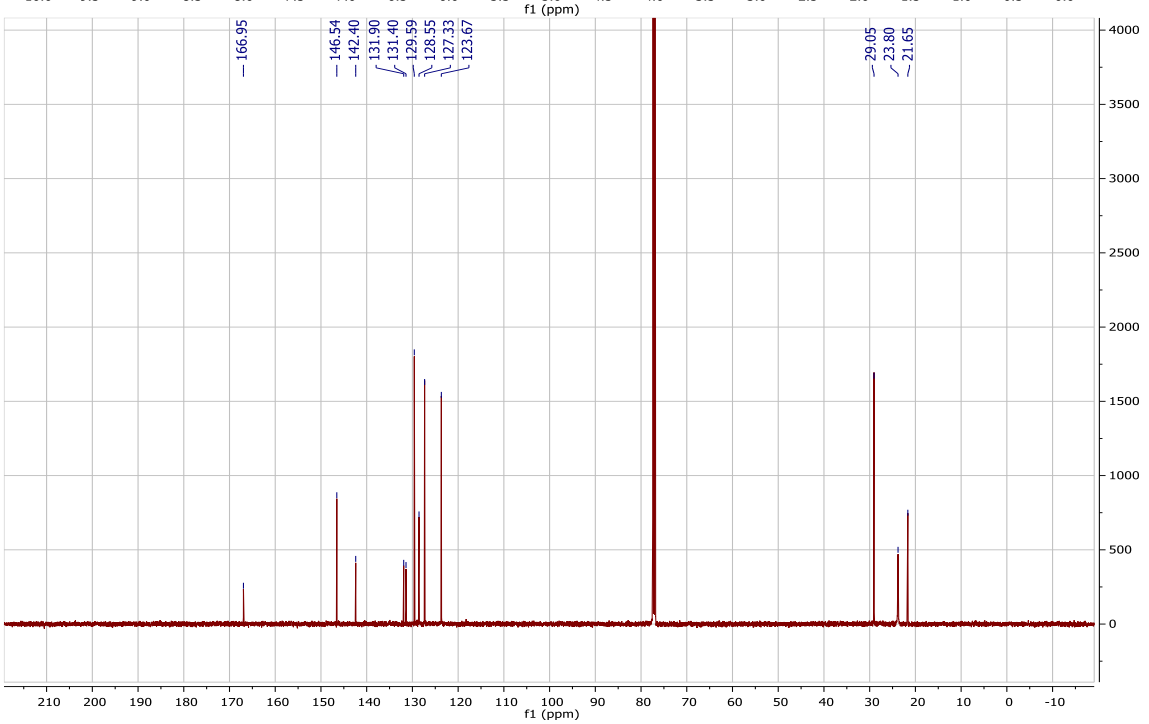

^{1}H and ^{13}C NMR data for 5.1b

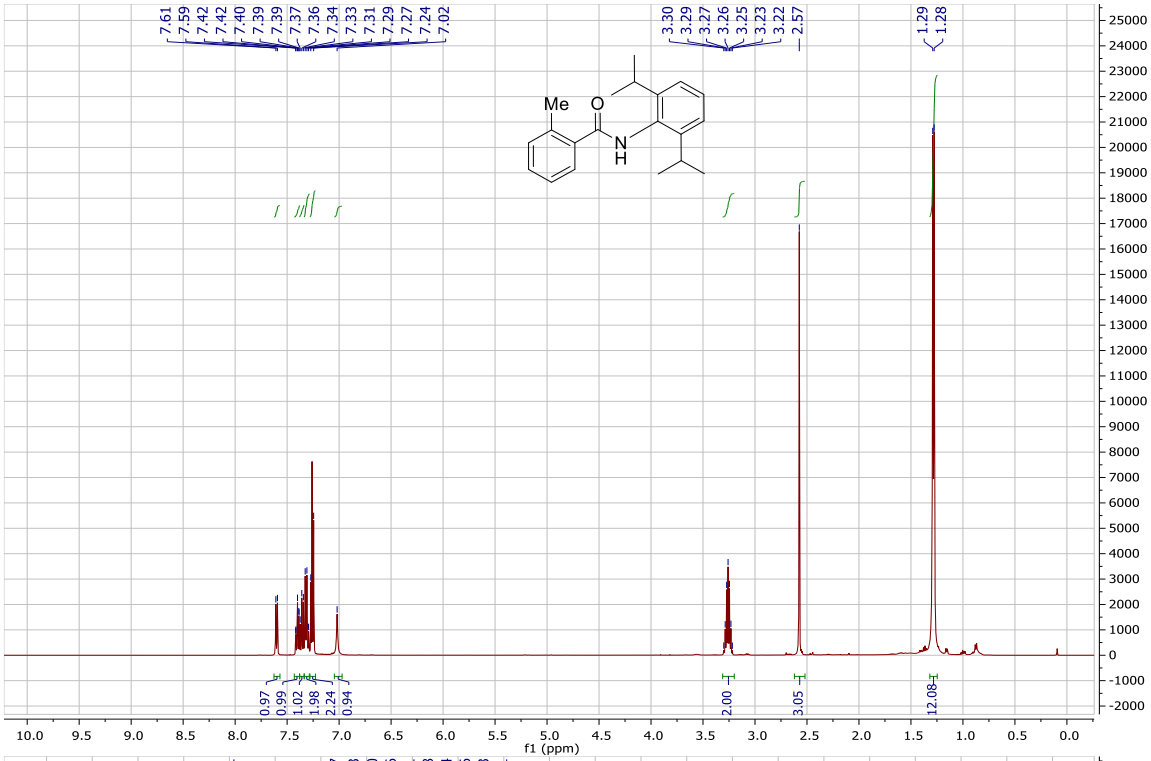

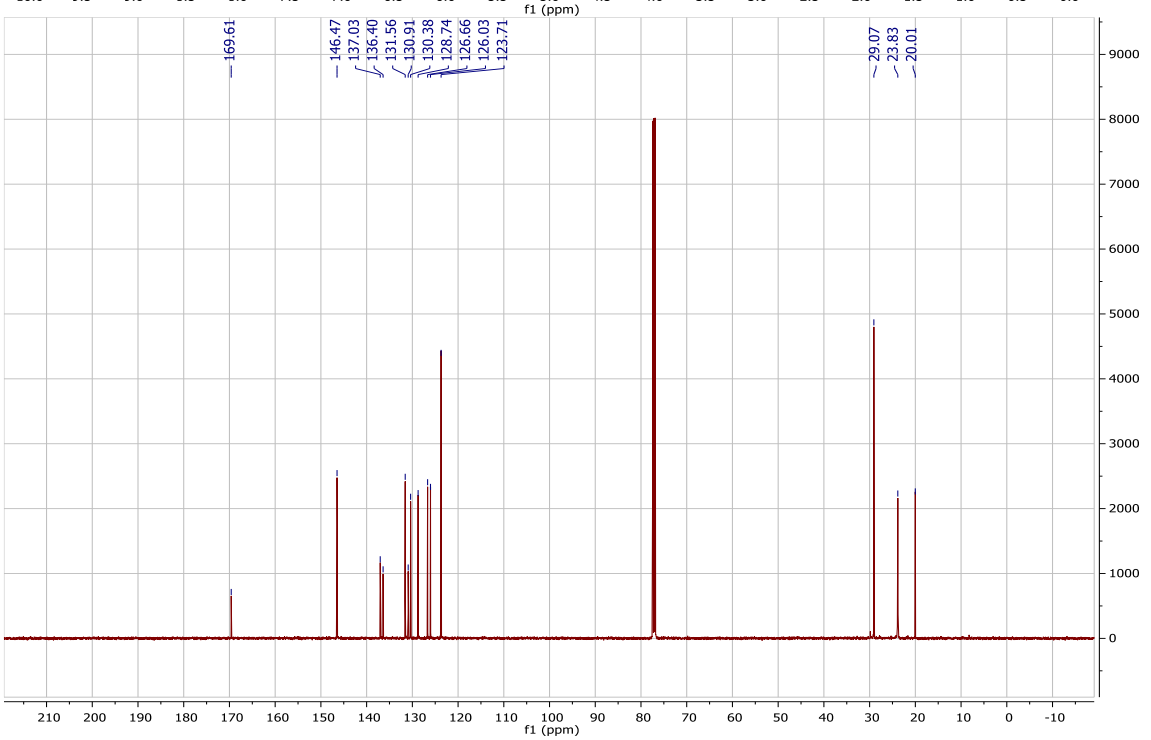

^{1}H and ^{13}C NMR data for 5.1c

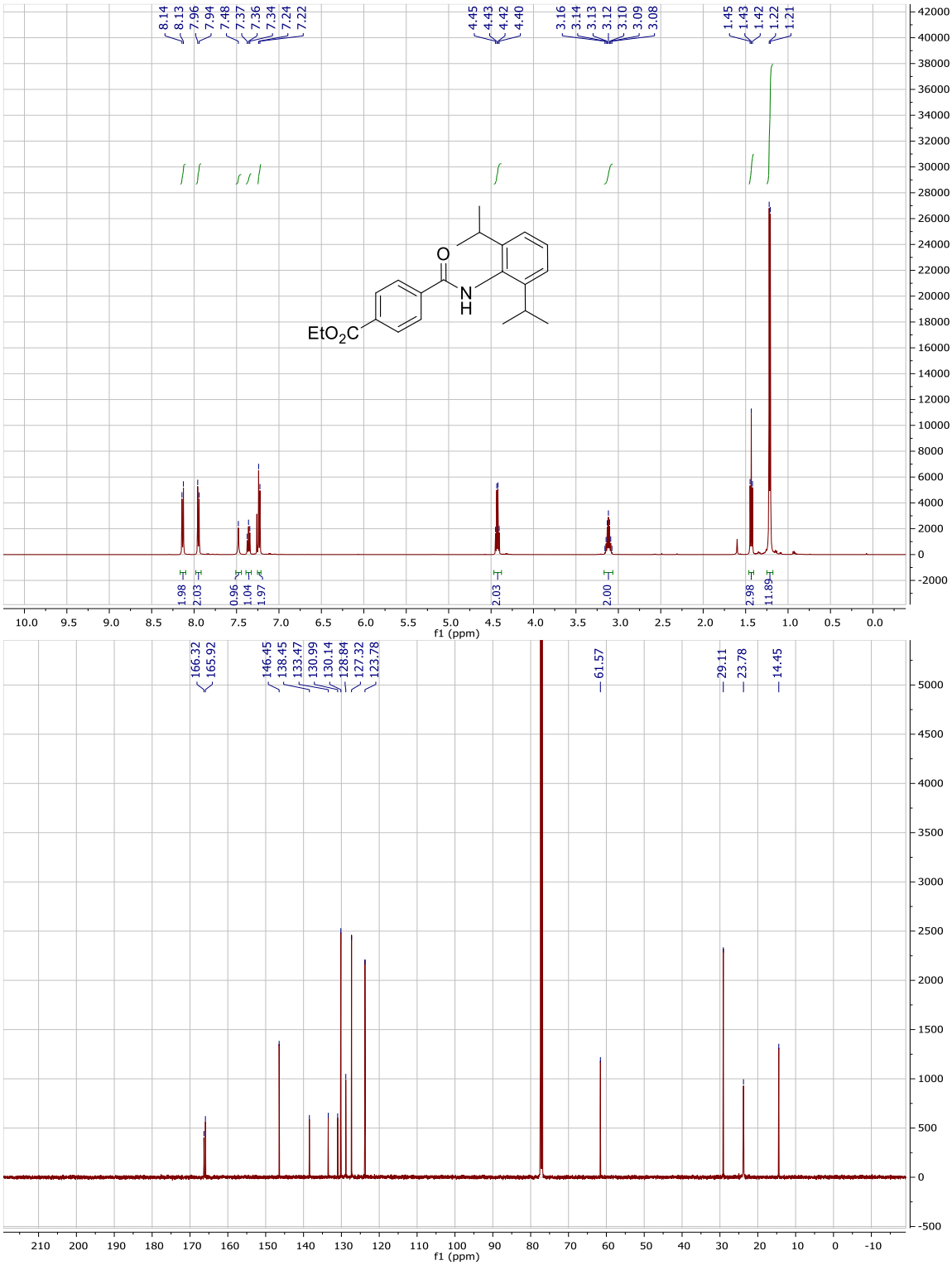

^{1}H and ^{13}C NMR data for 5.1d

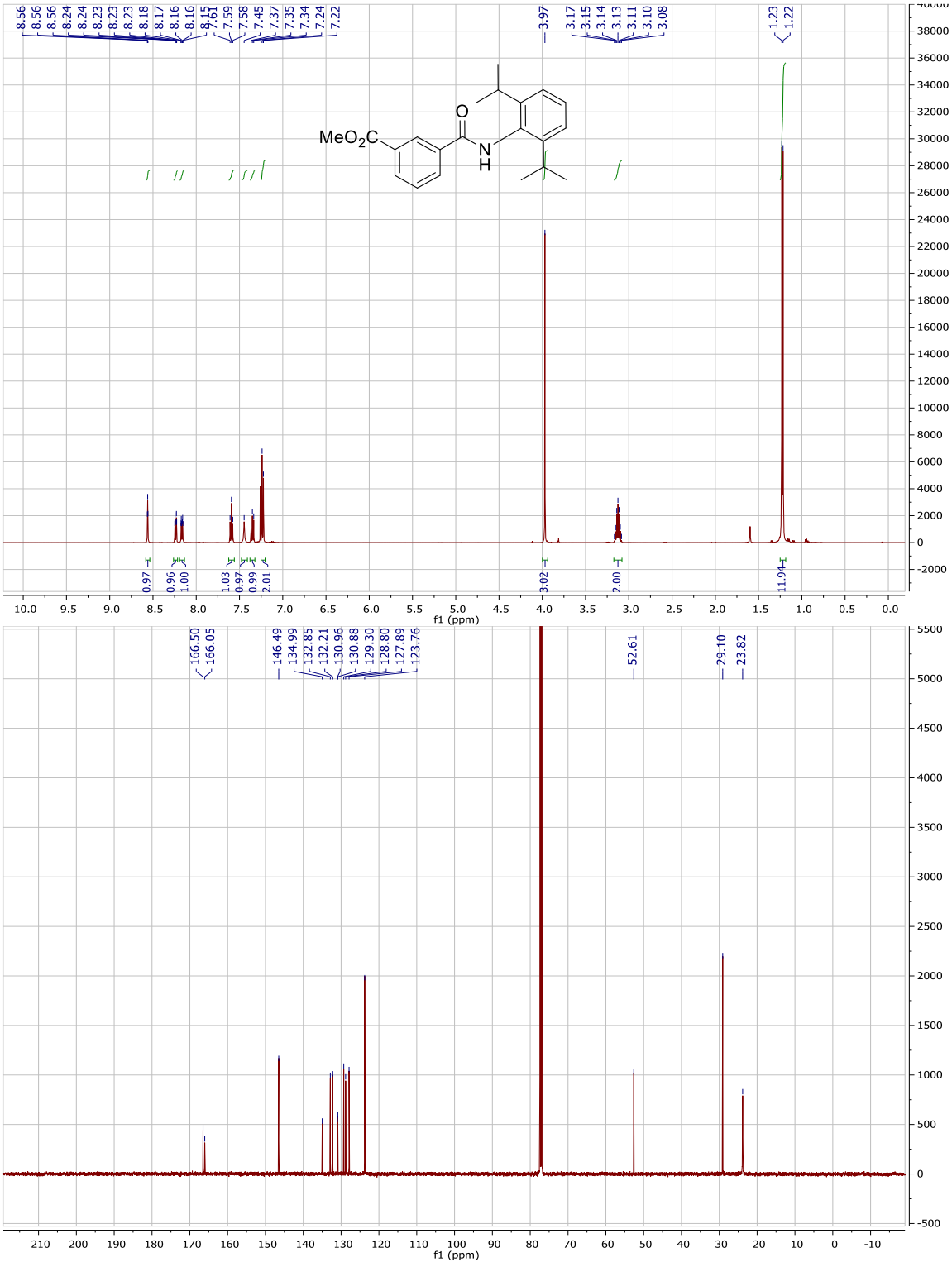

^{1}H and ^{13}C NMR data for 5.1e

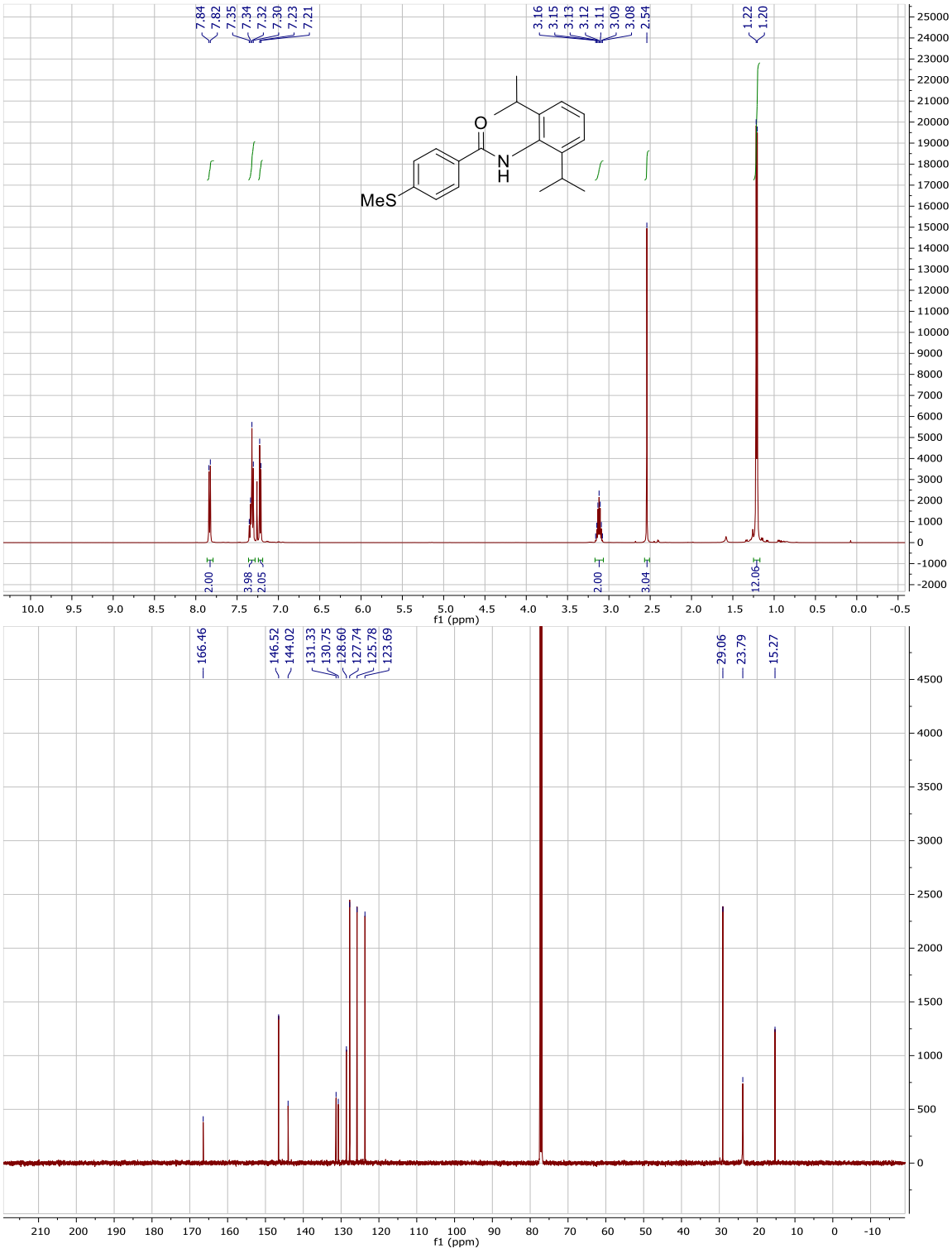

^{1}H and ^{13}C NMR data for 5.1f

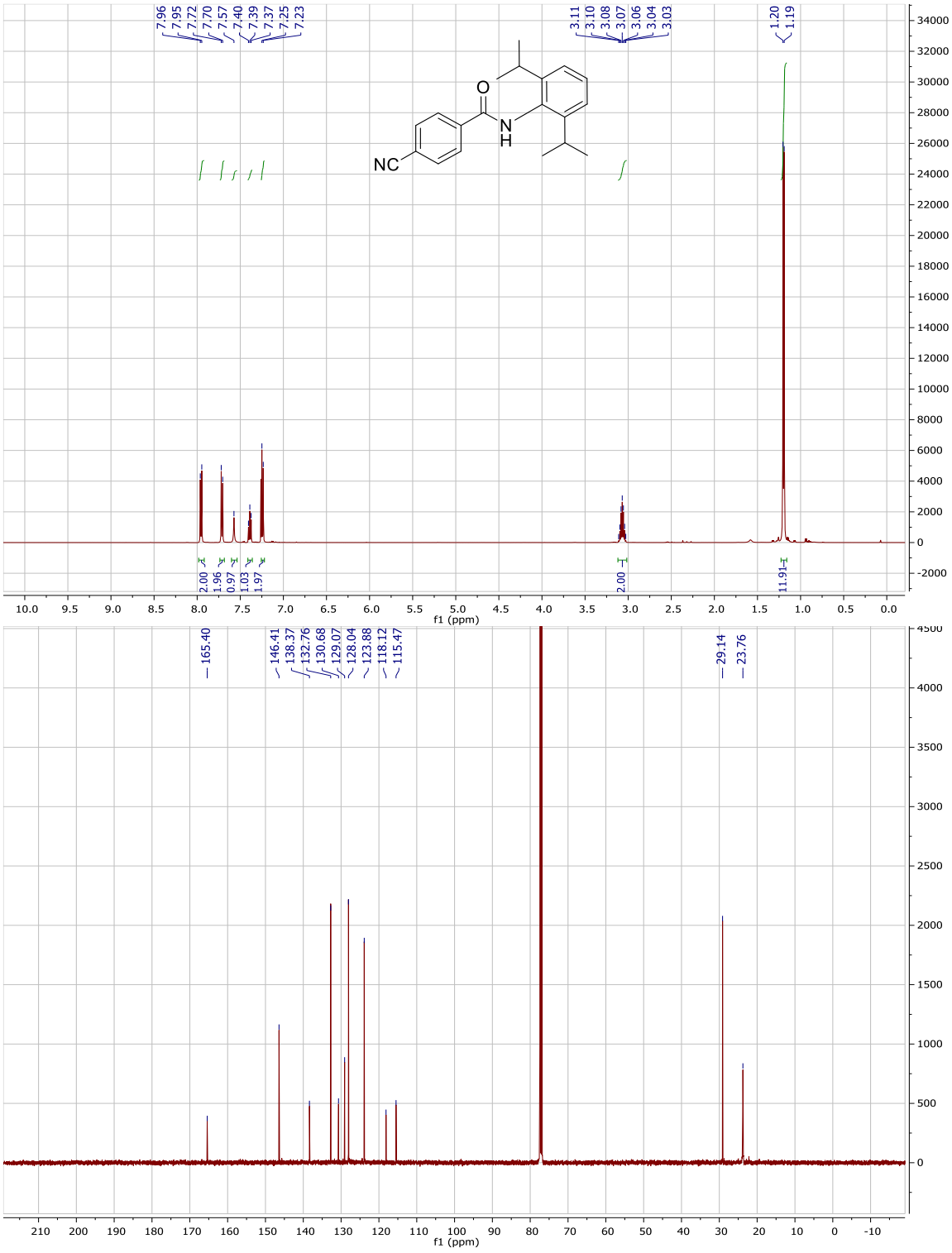

^{1}H and ^{13}C NMR data for 5.1g

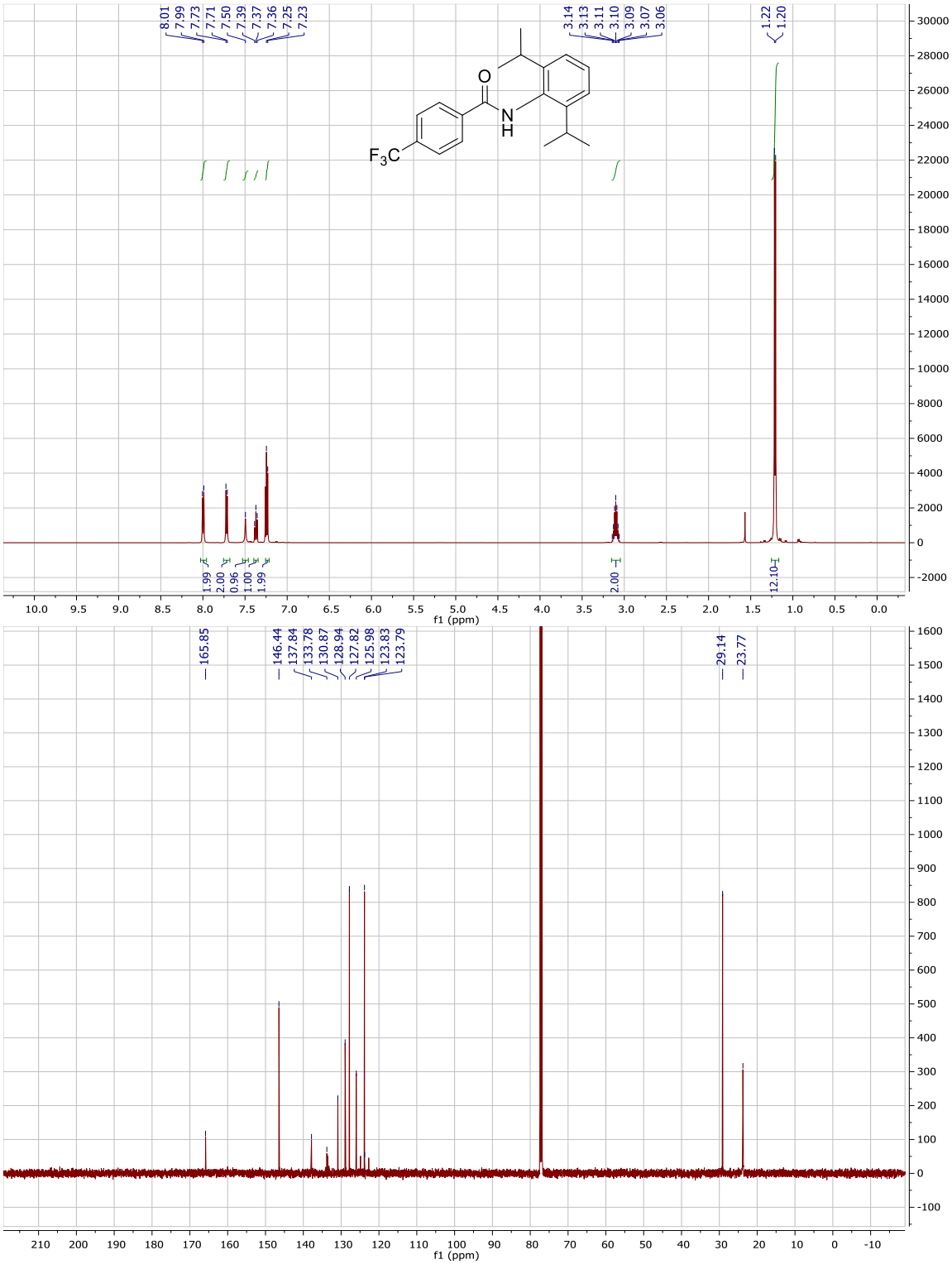

^{1}H and ^{13}C NMR data for 5.1h

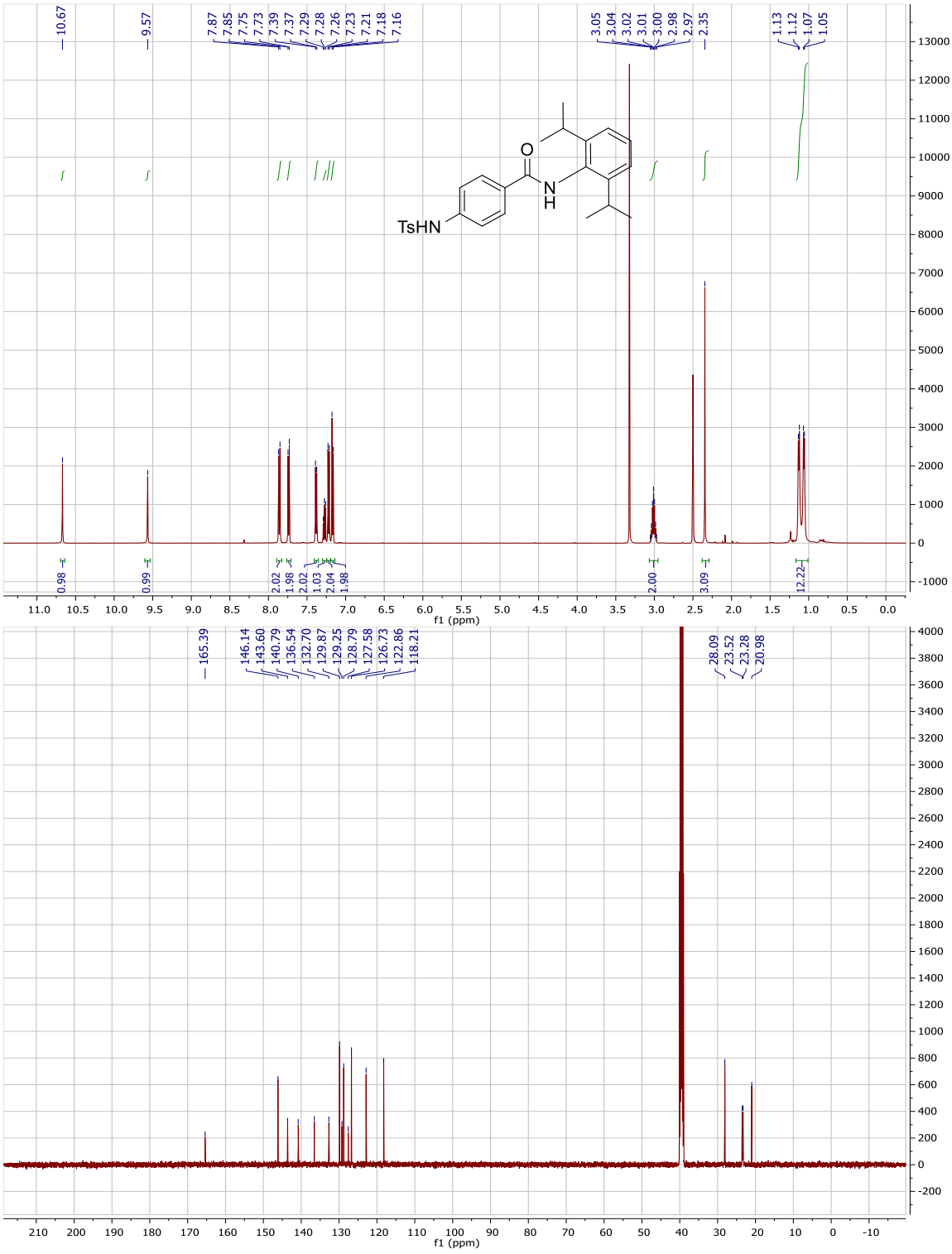

^{1}H and ^{13}C NMR data for 5.1i

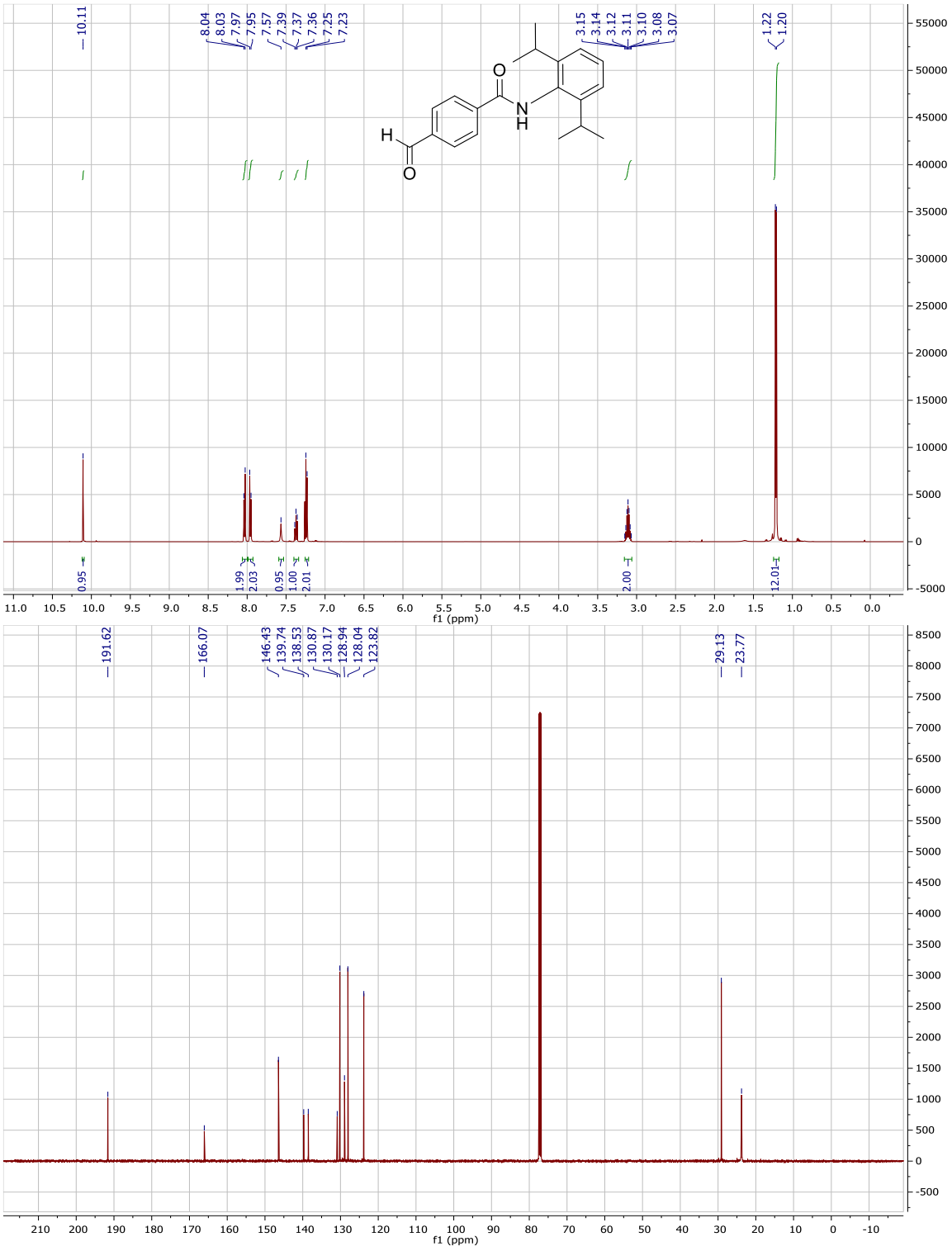

^{1}H and ^{13}C NMR data for 5.1j

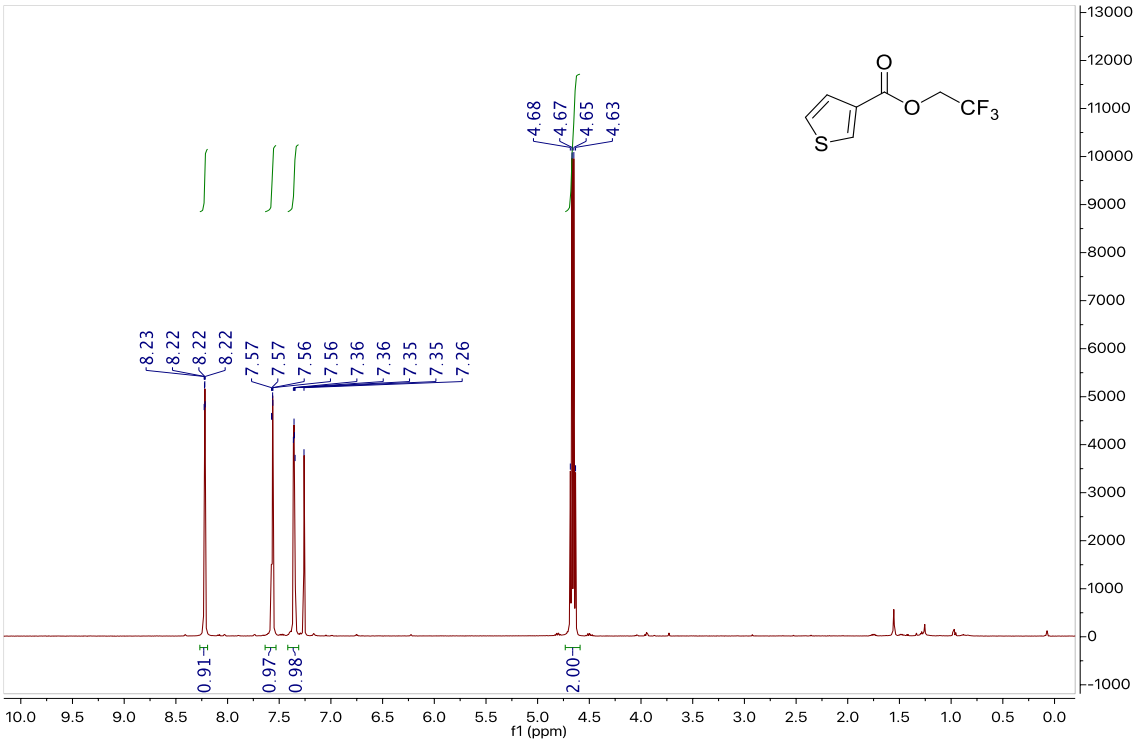

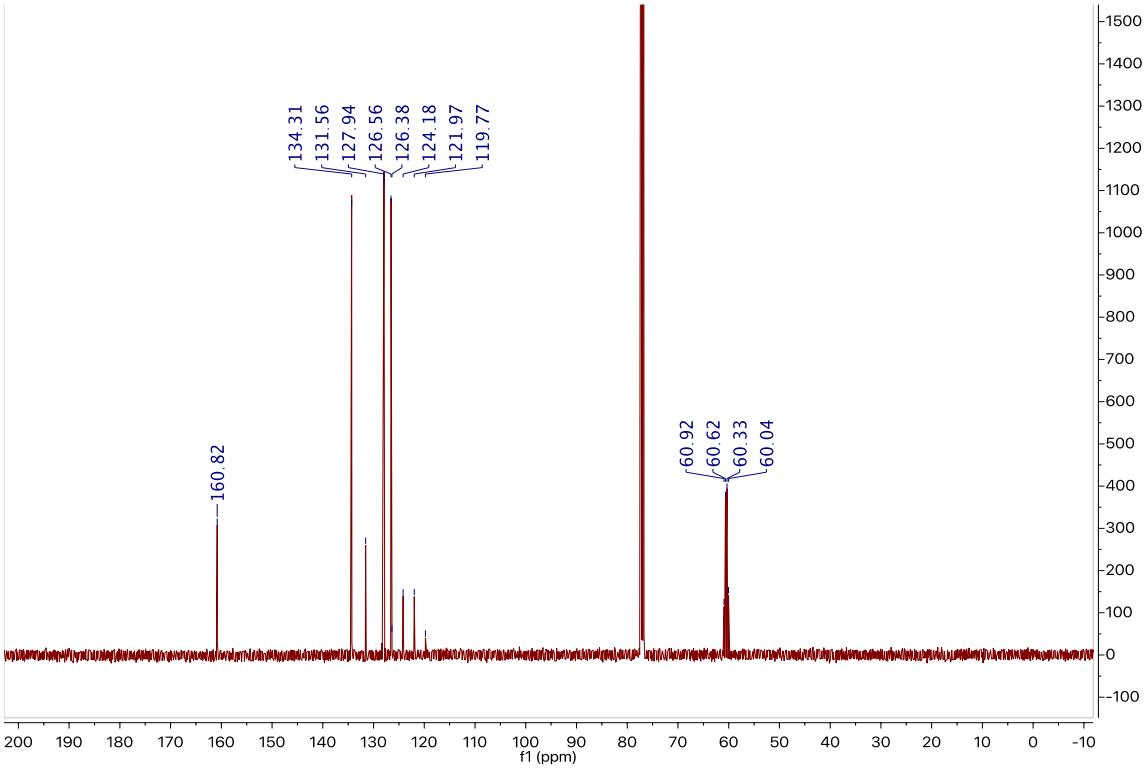

^{1}H and ^{13}C NMR data for 5.1k

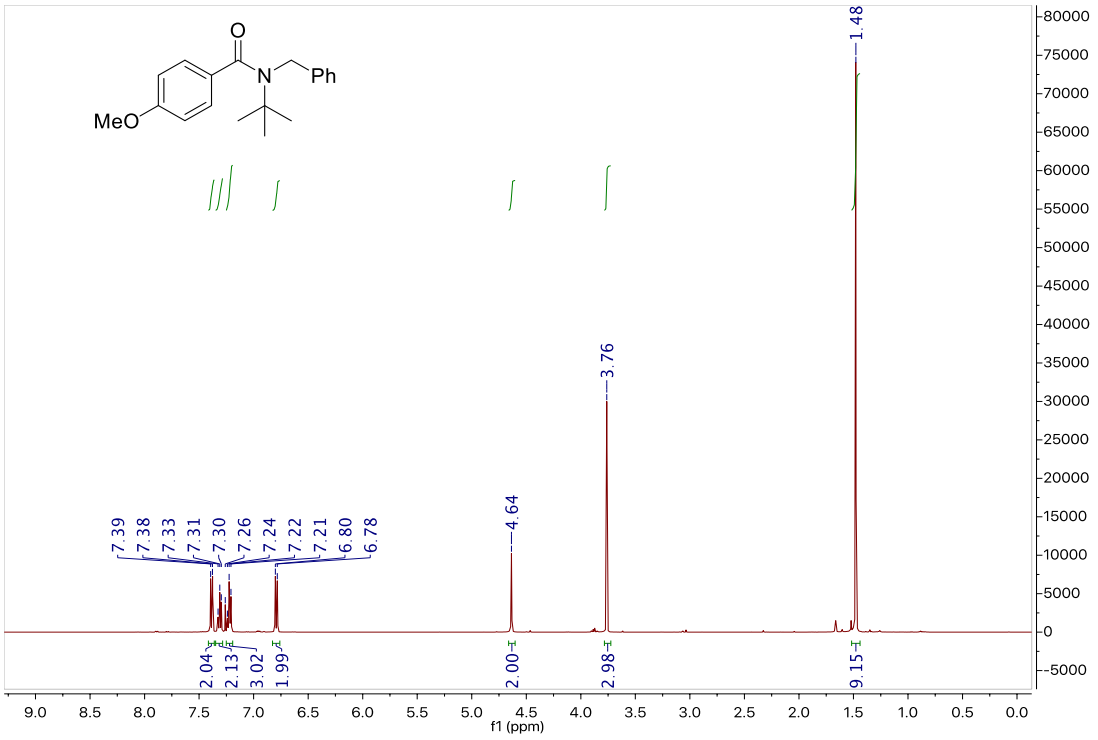

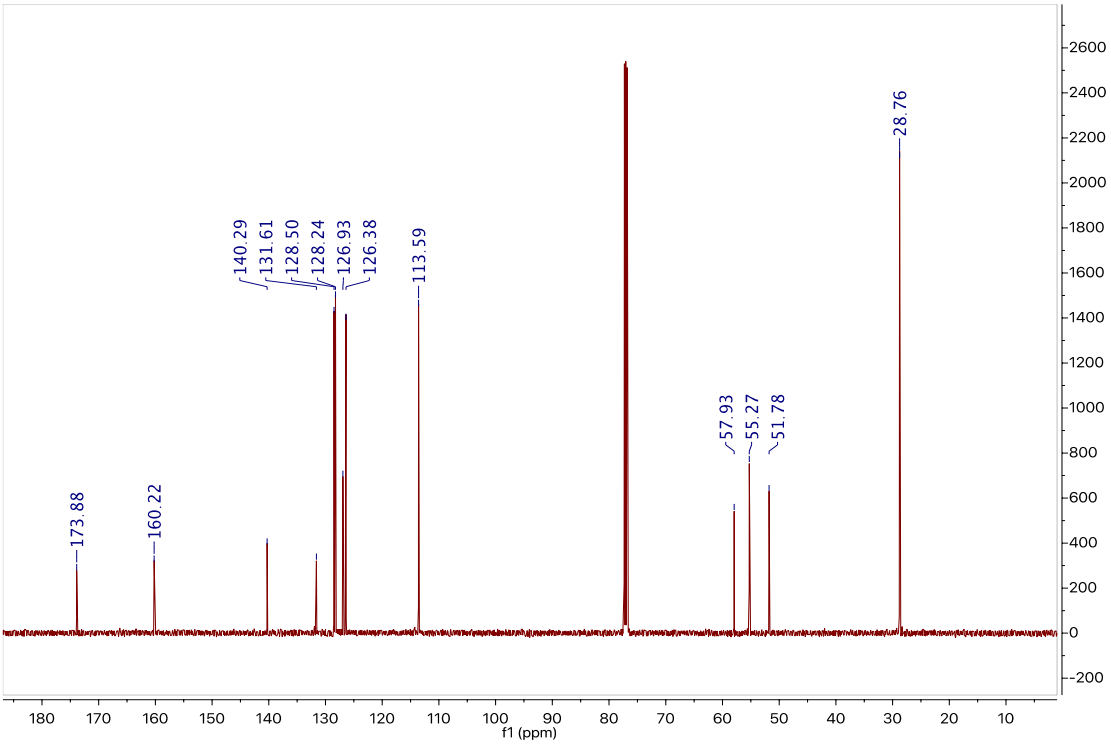

^{1}H and ^{13}C NMR data for 5.1l

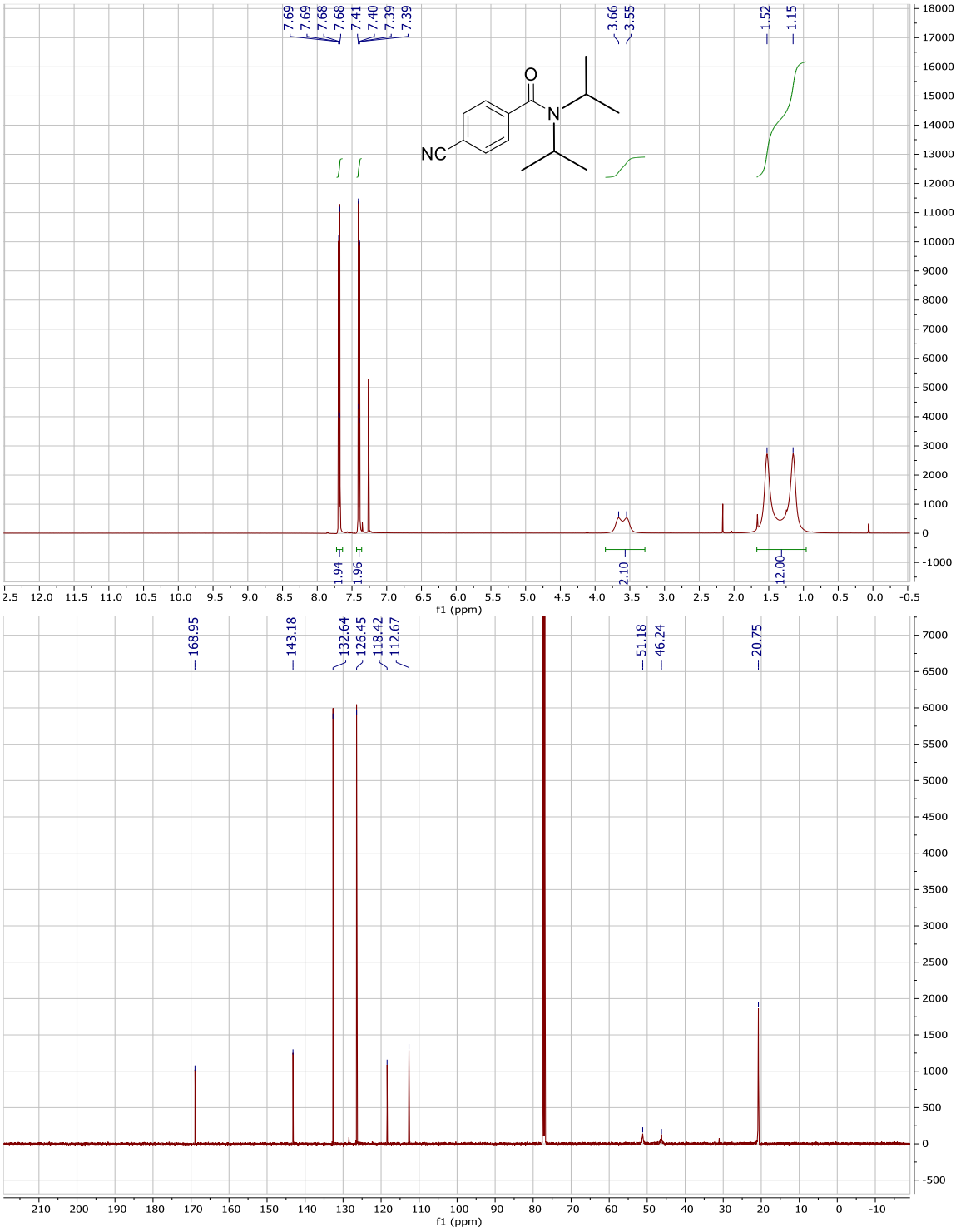

^{1}H and ^{13}C NMR data for 5.1m

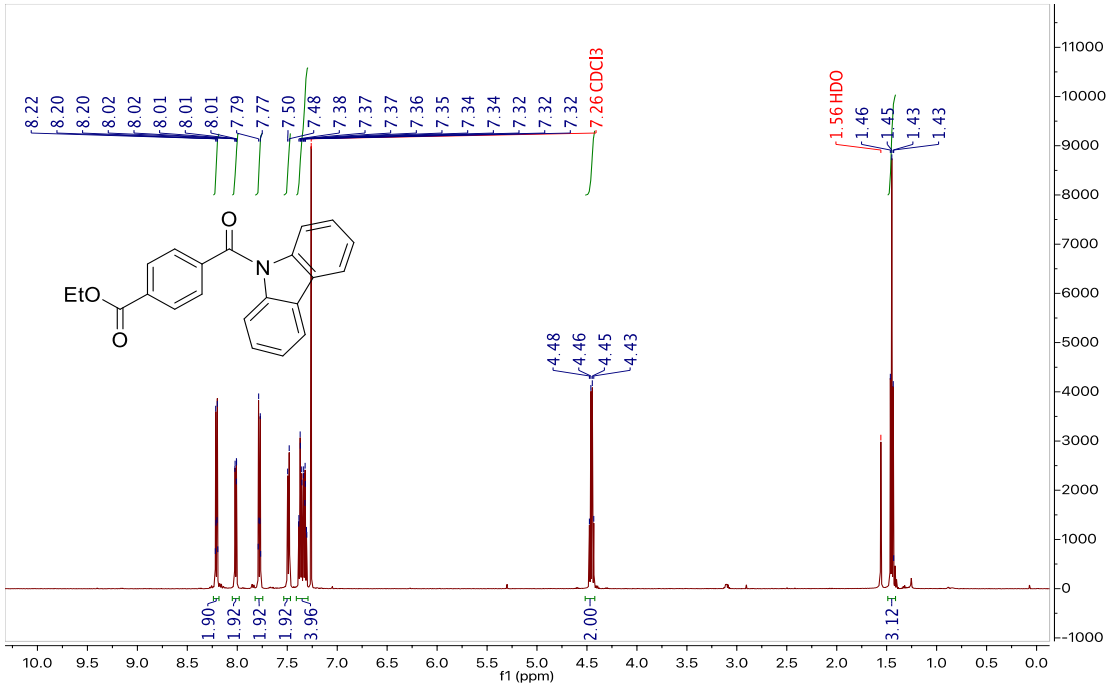

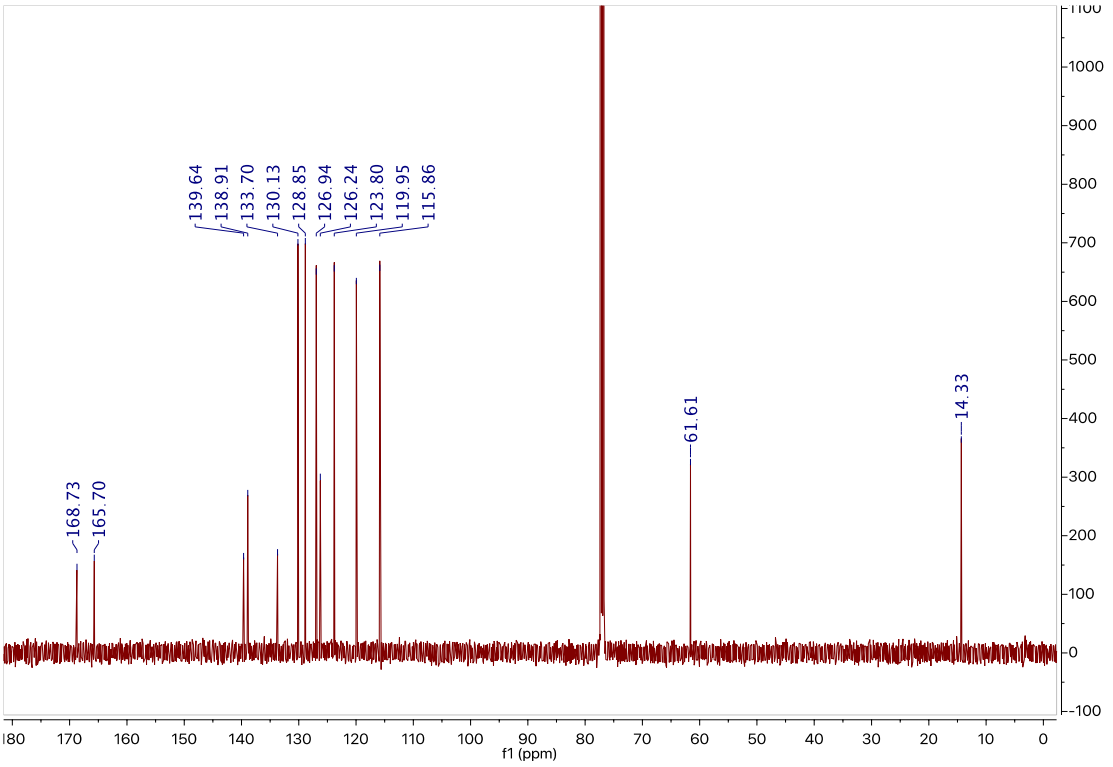

^{1}H and ^{13}C NMR data for 5.1n

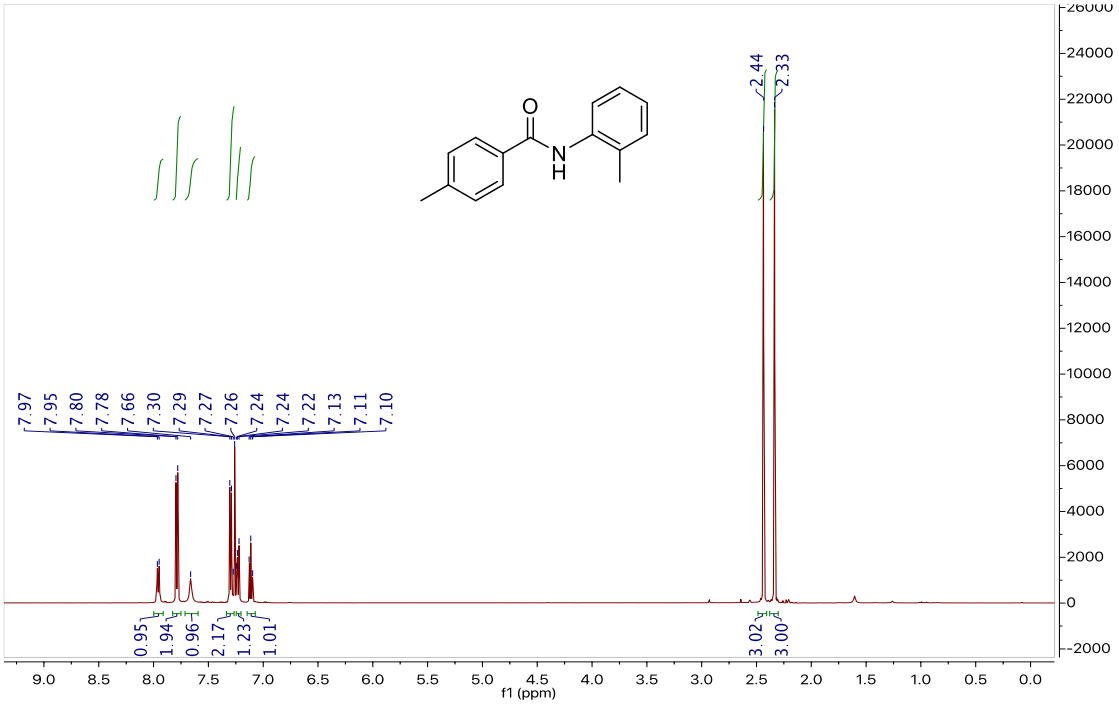

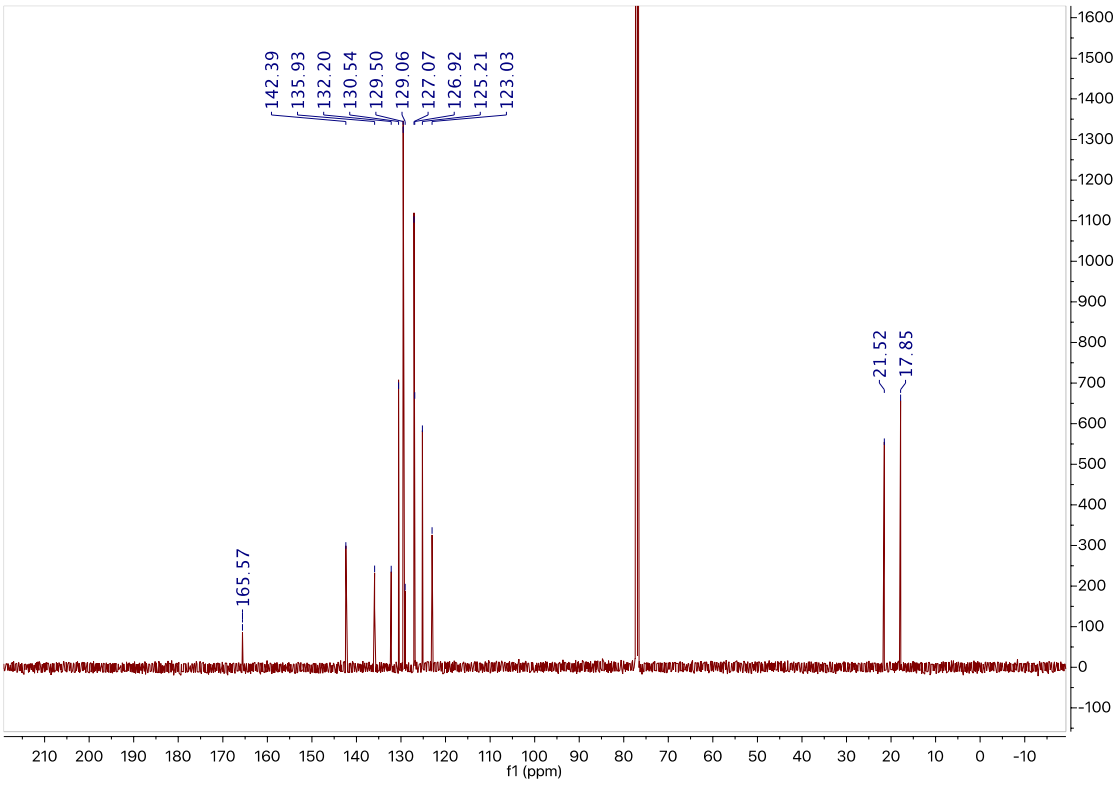

^{1}H and ^{13}C NMR data for 5.1o

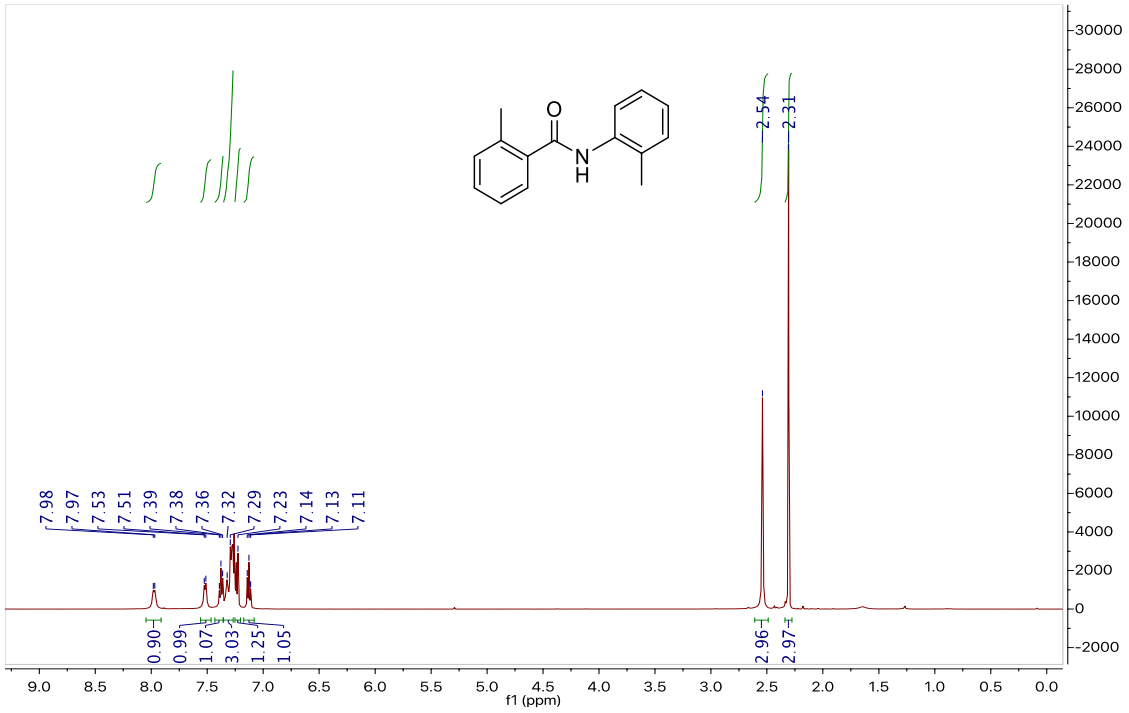

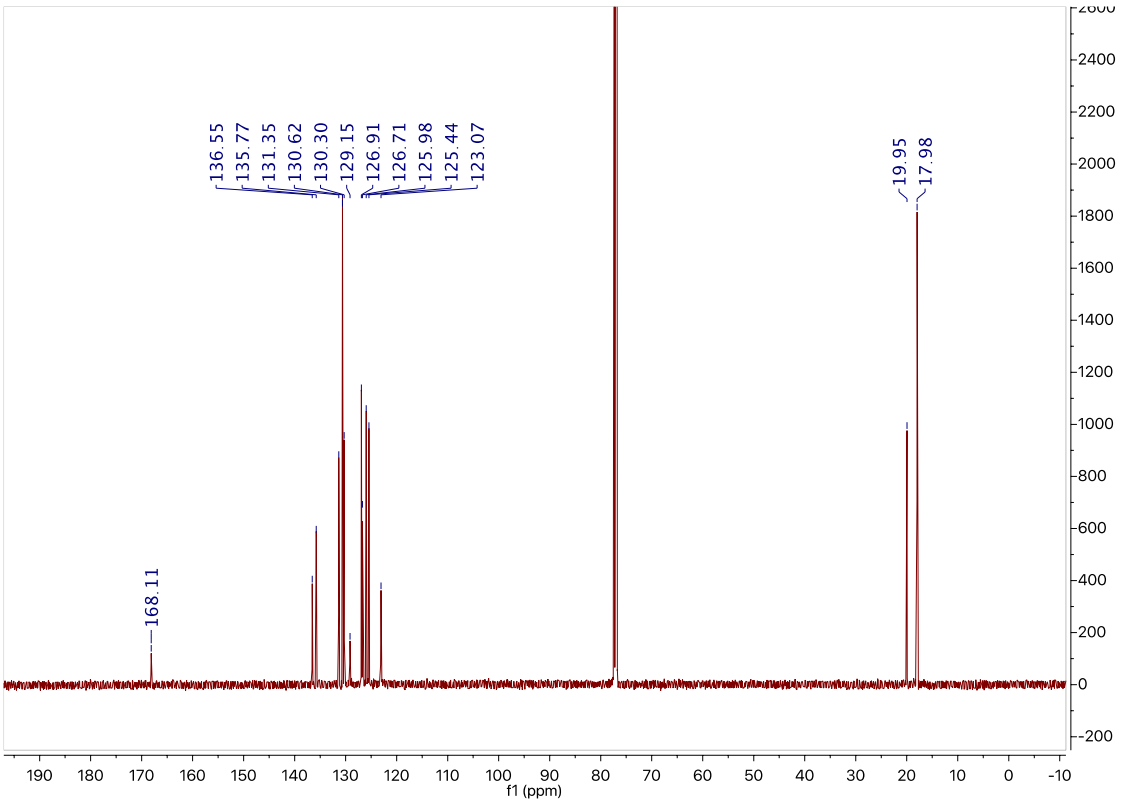

^{1}H and ^{13}C NMR data for 5.1p

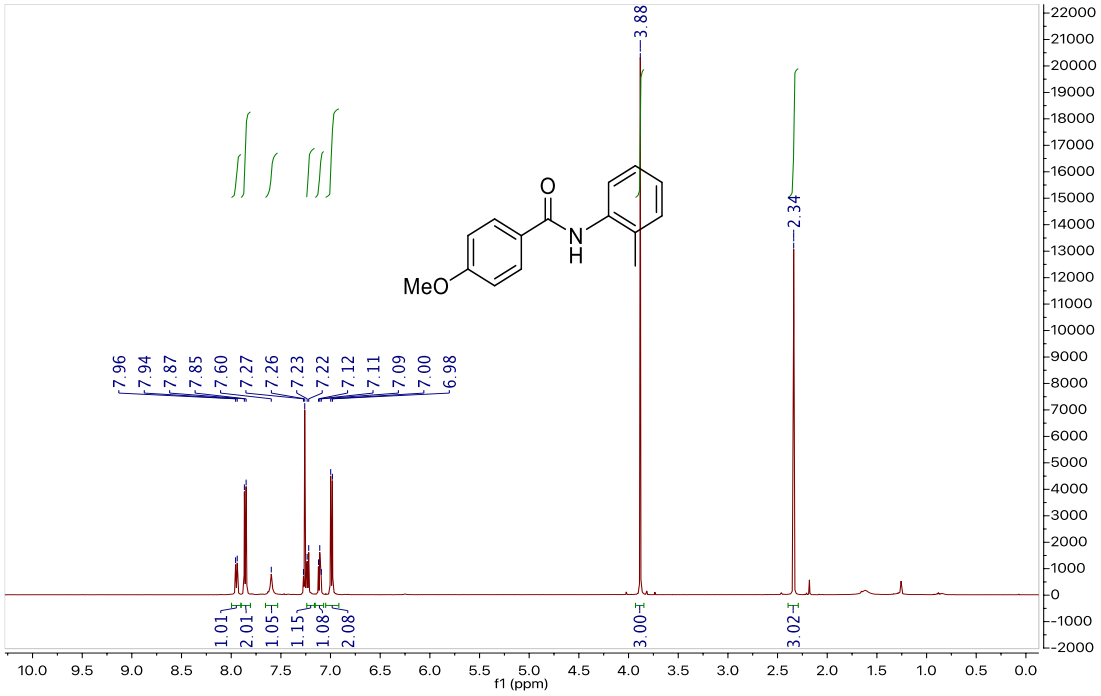

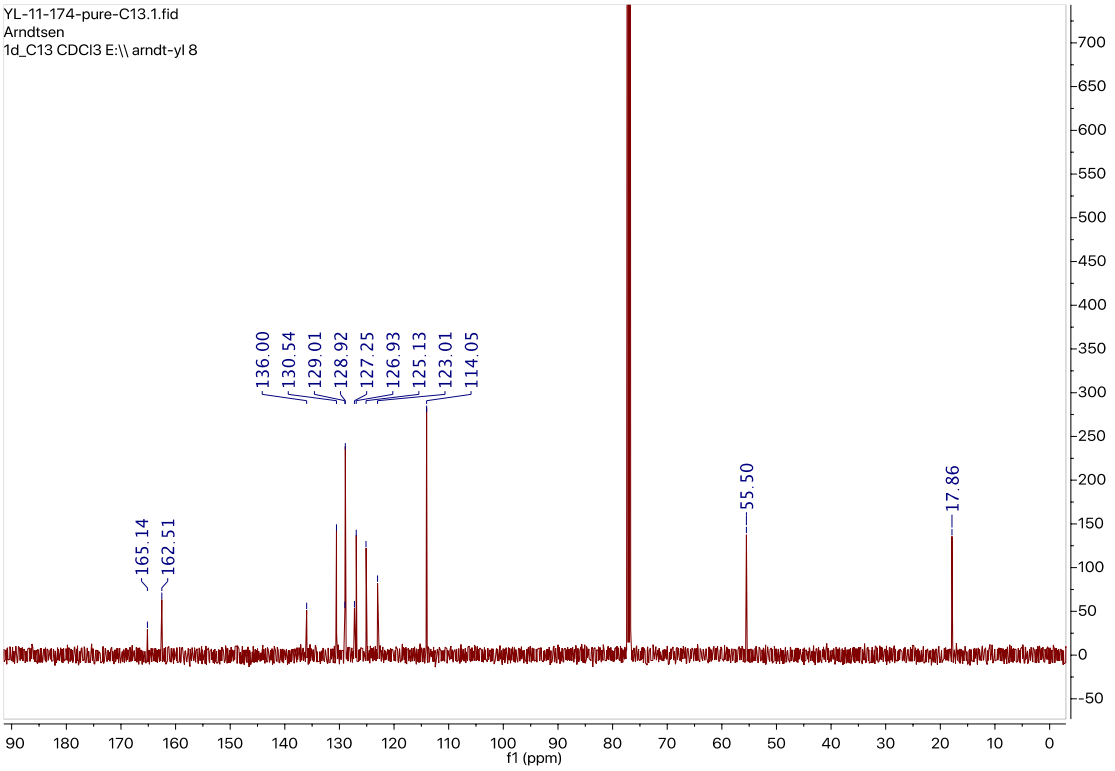

^{1}H and ^{13}C NMR data for 5.1q

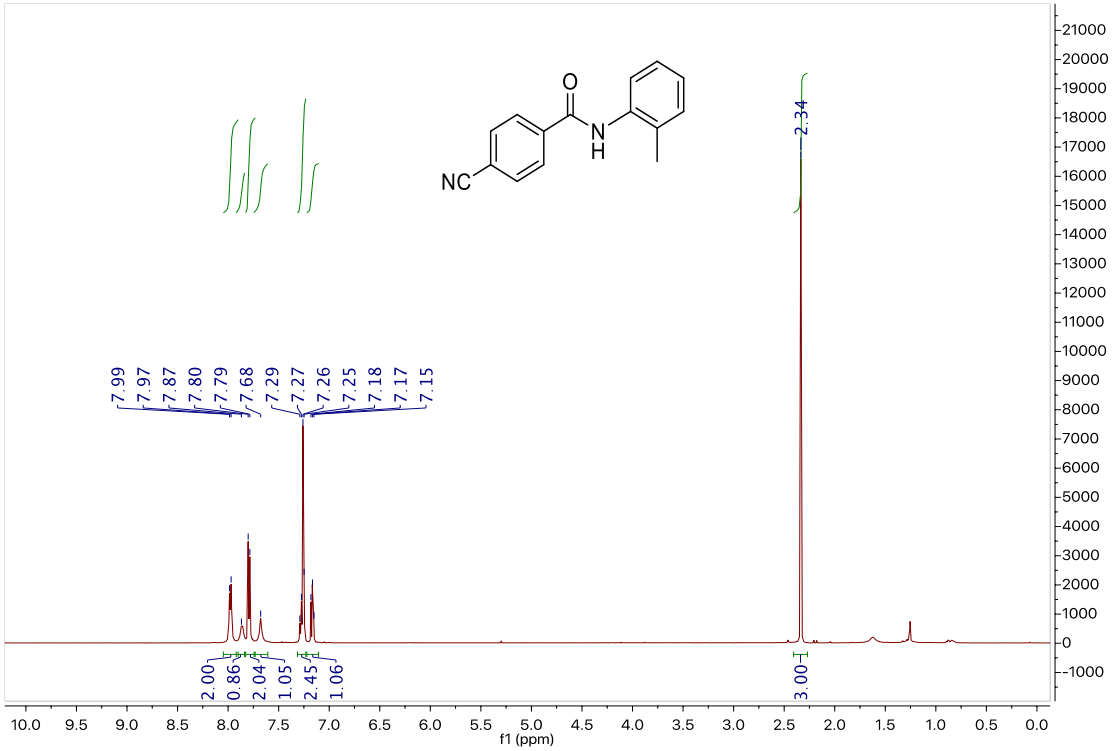

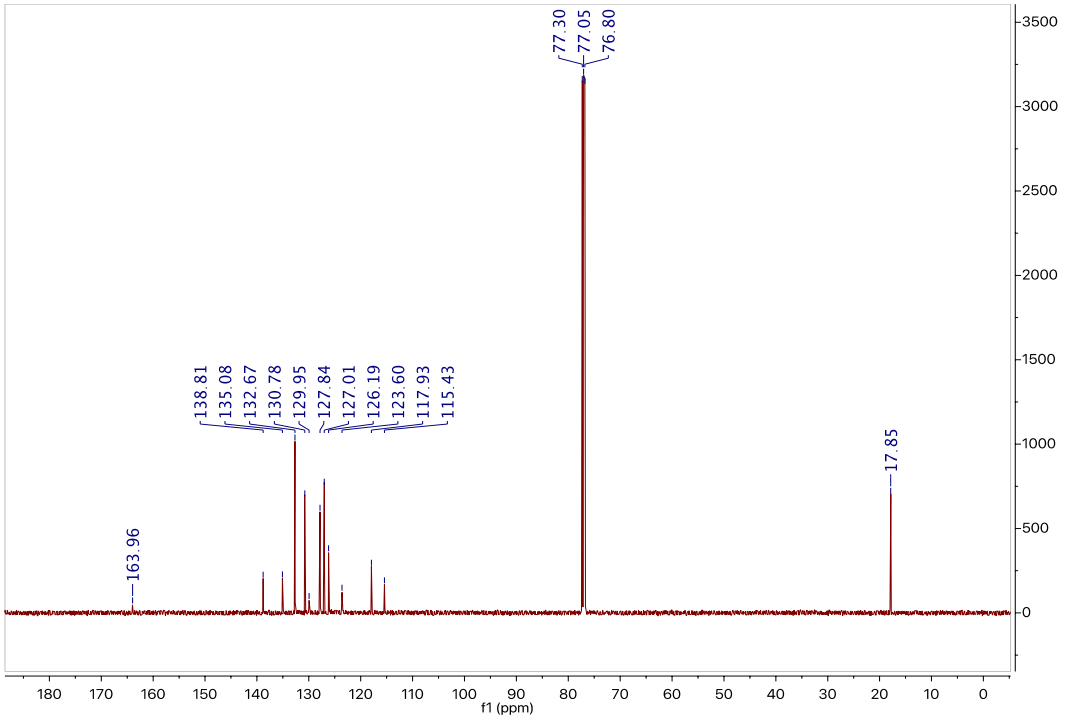

^{1}H and ^{13}C NMR data for 5.1r

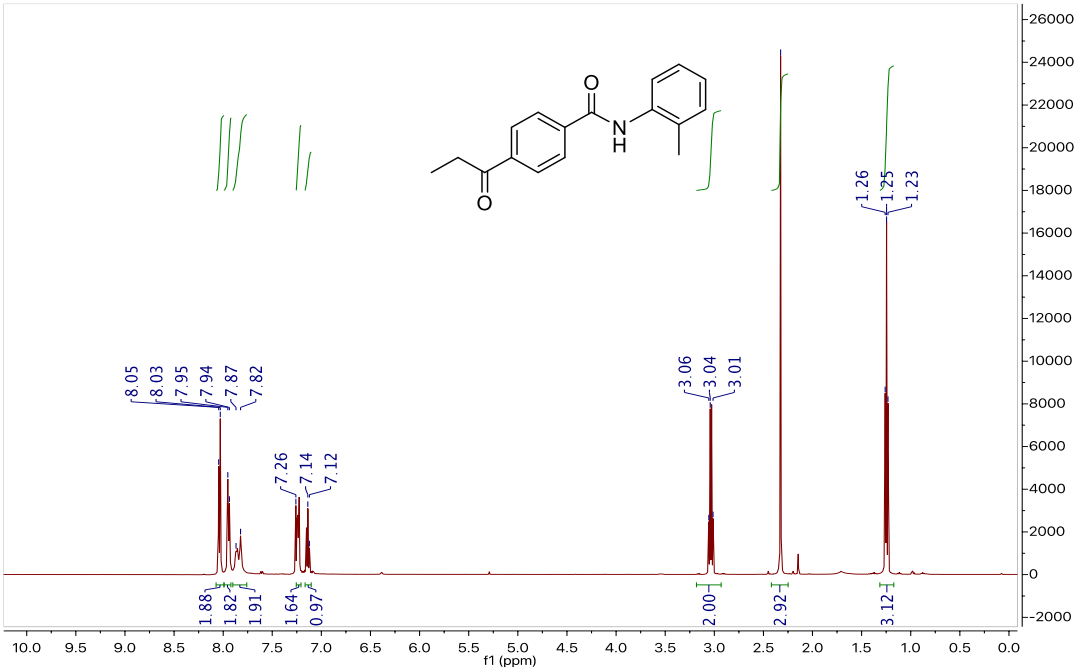

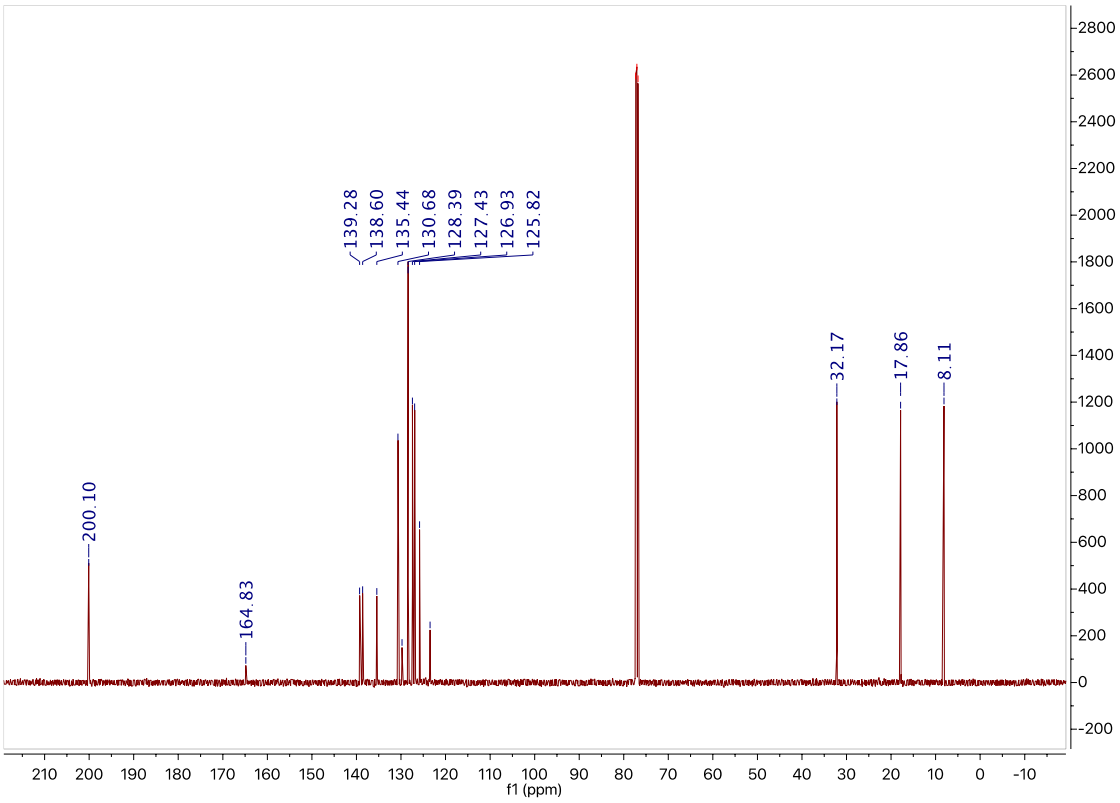

^{1}H and ^{13}C NMR data for 5.1s

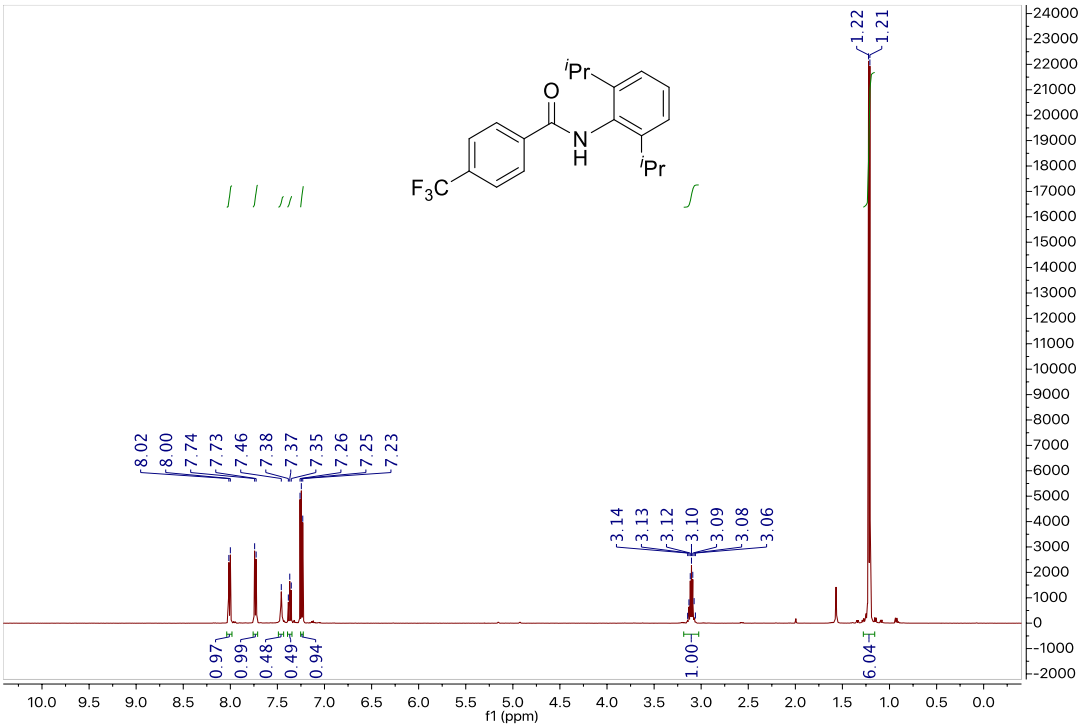

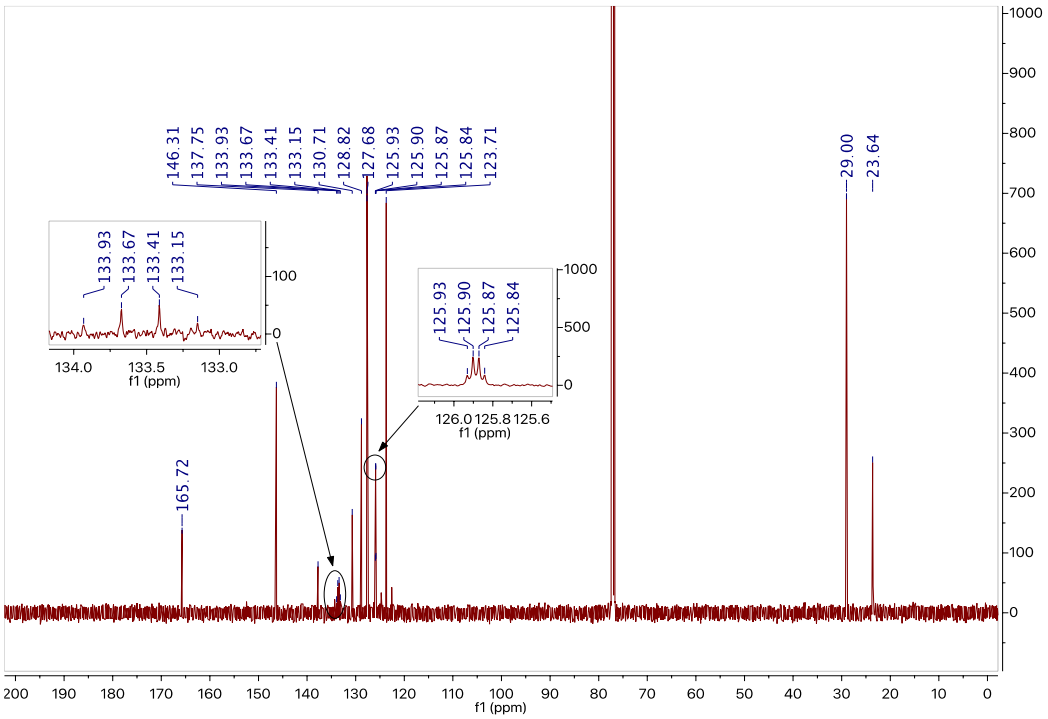

^{1}H and ^{13}C NMR data for 5.1t

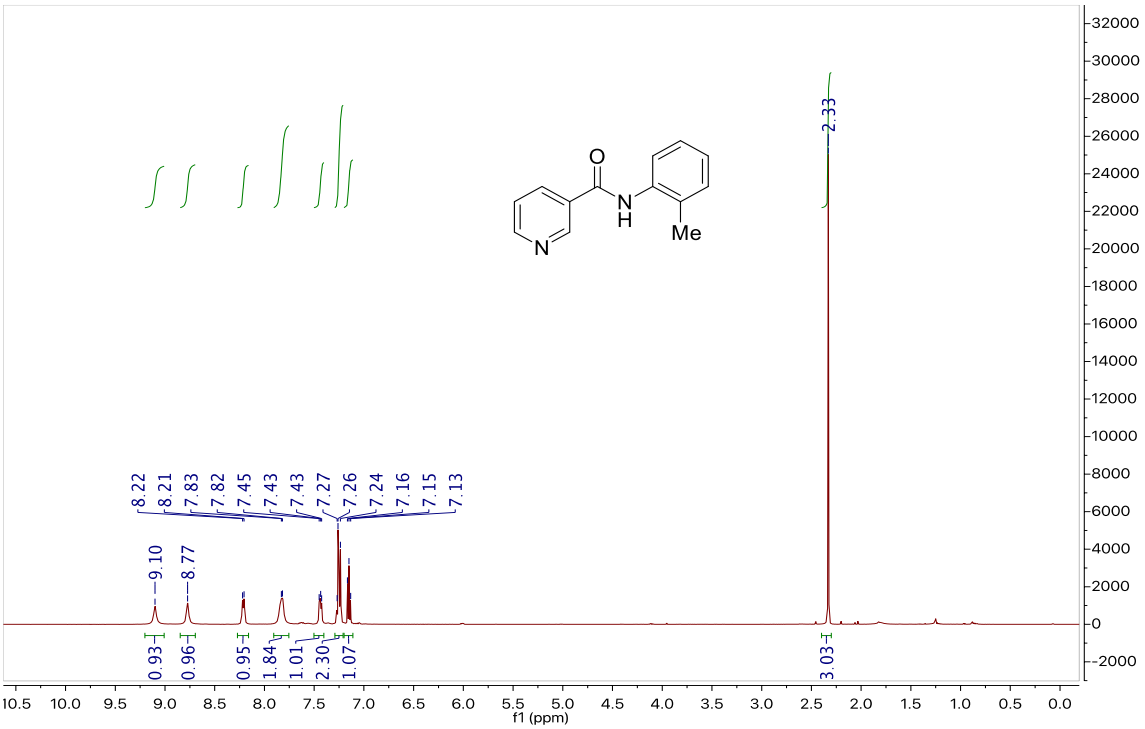

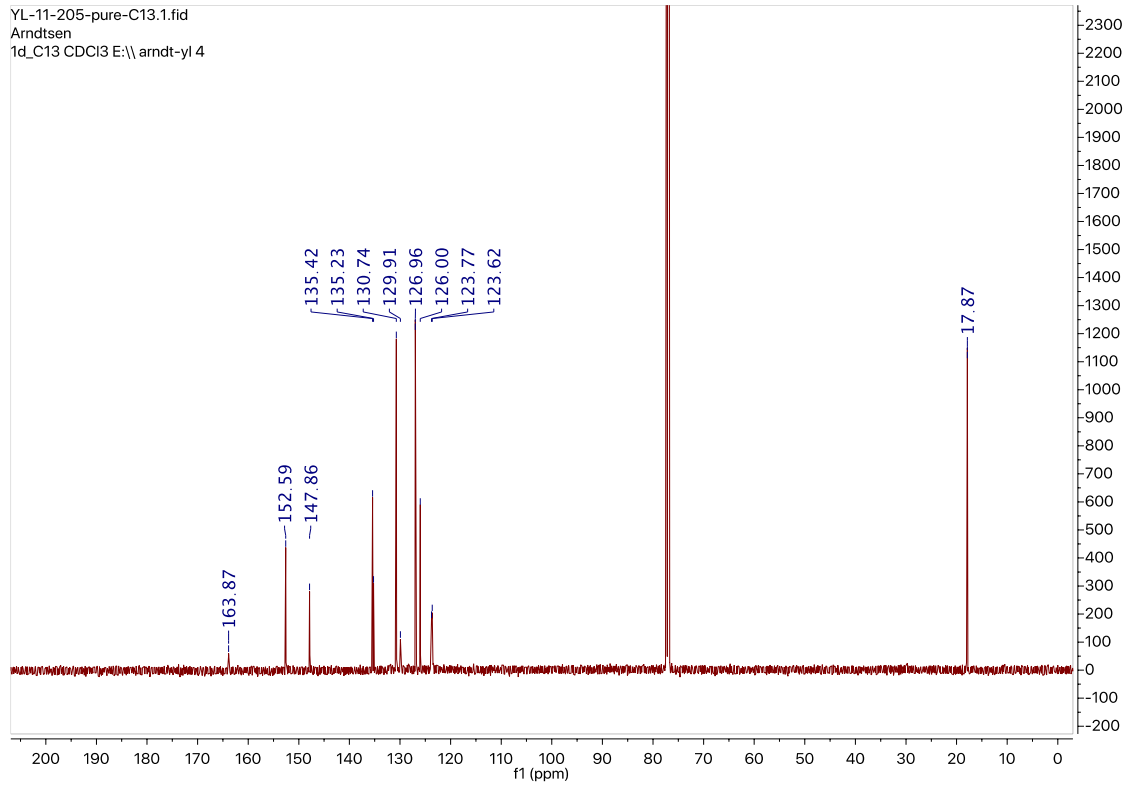

^{1}H and ^{13}C NMR data for 5.1u

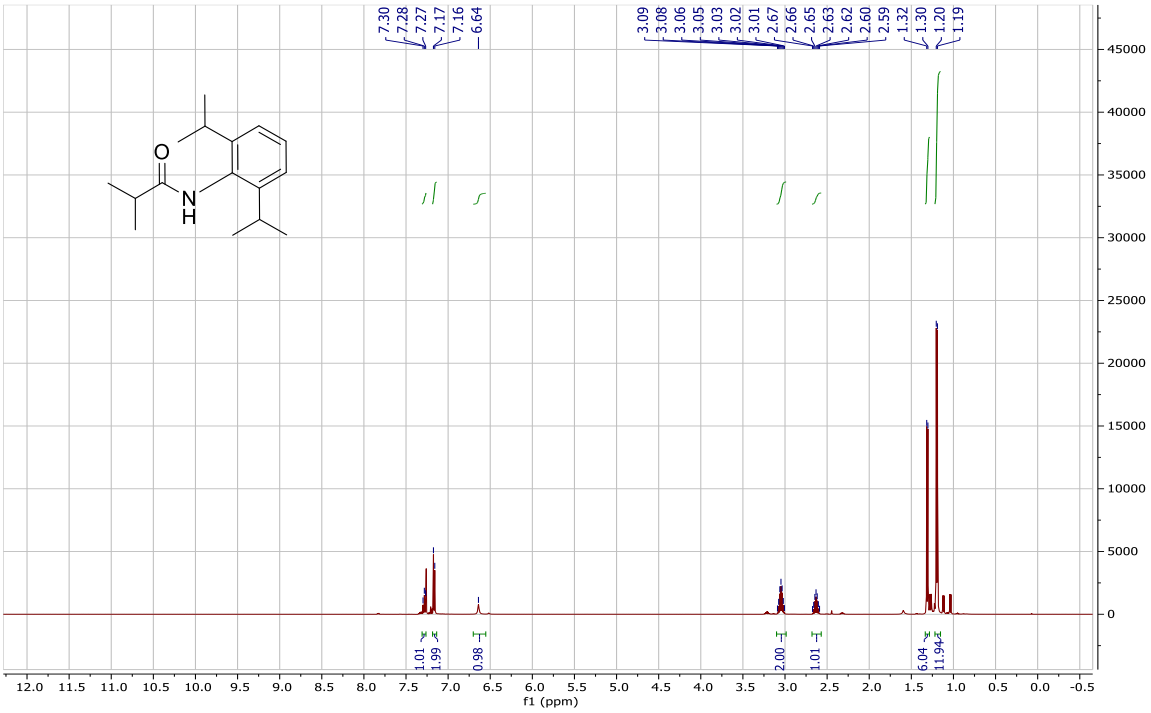

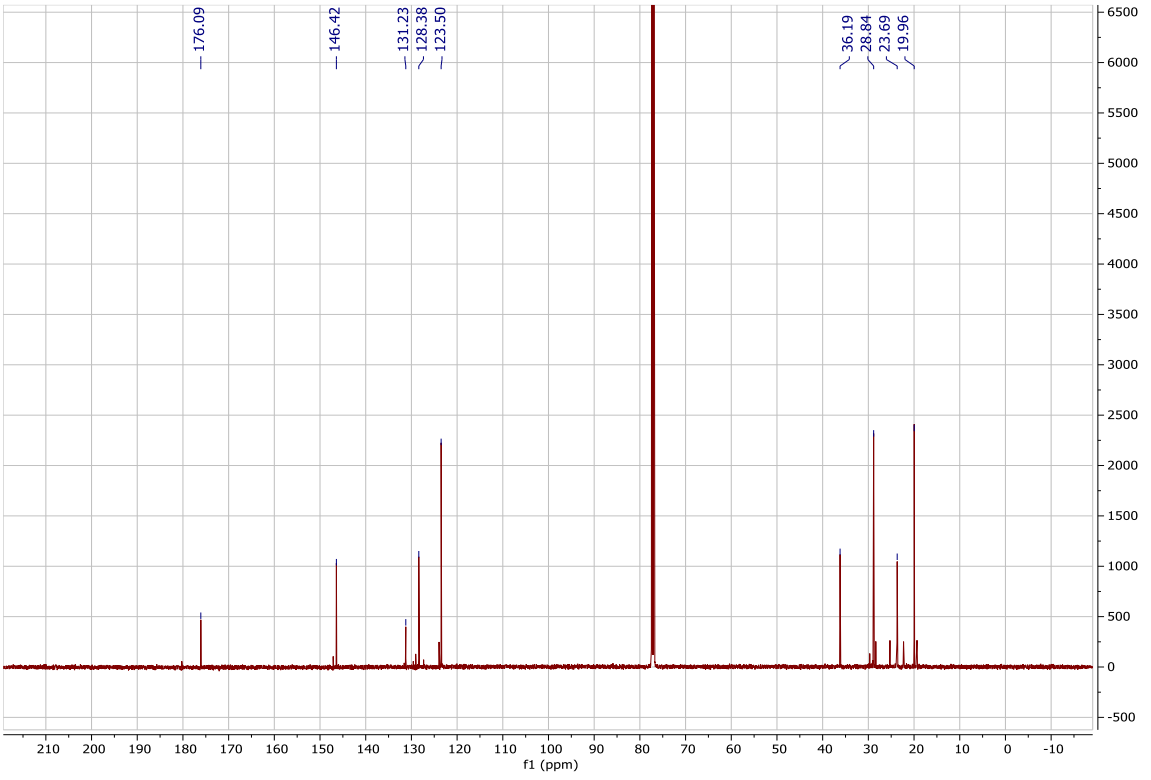

^{1}H and ^{13}C NMR data for 5.1v

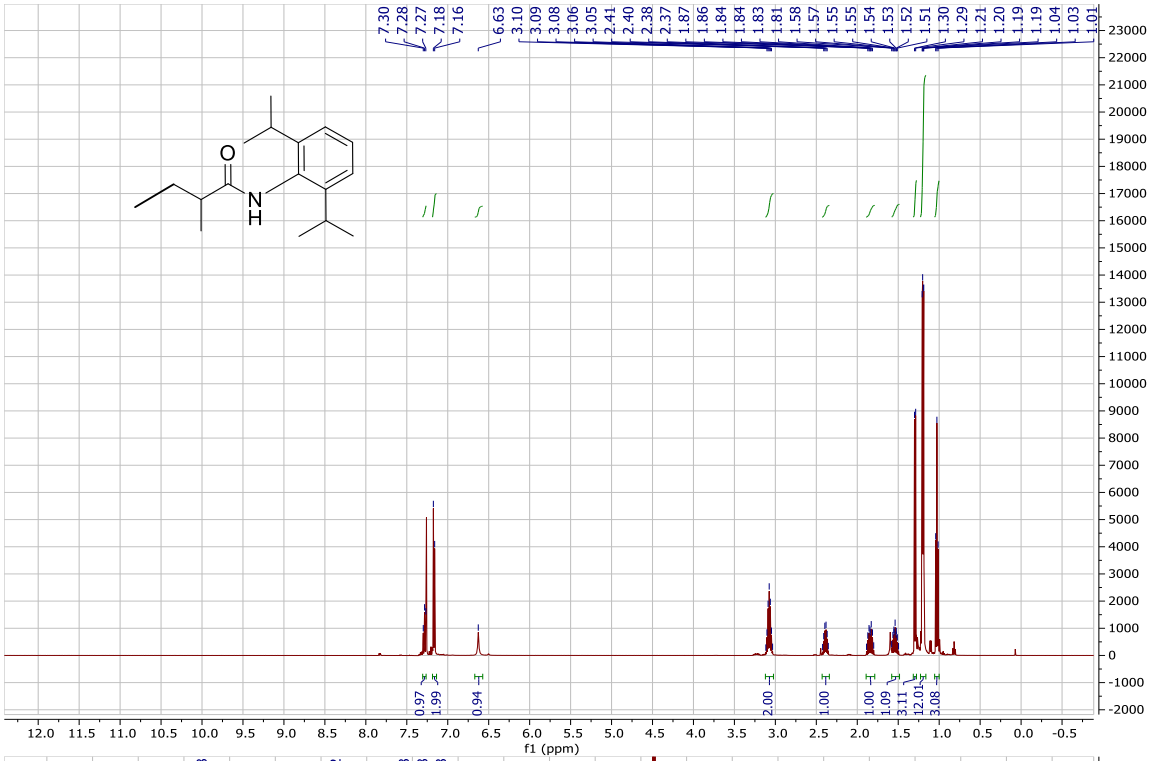

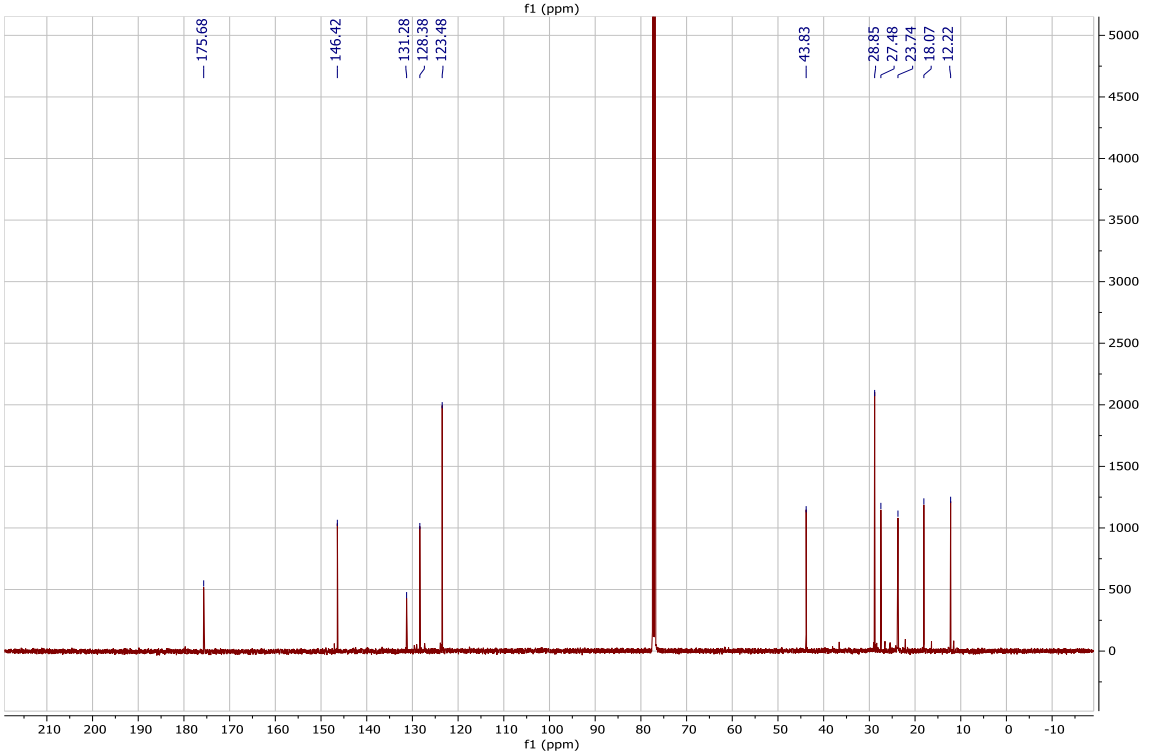

^{1}H and ^{13}C NMR data for 5.1w

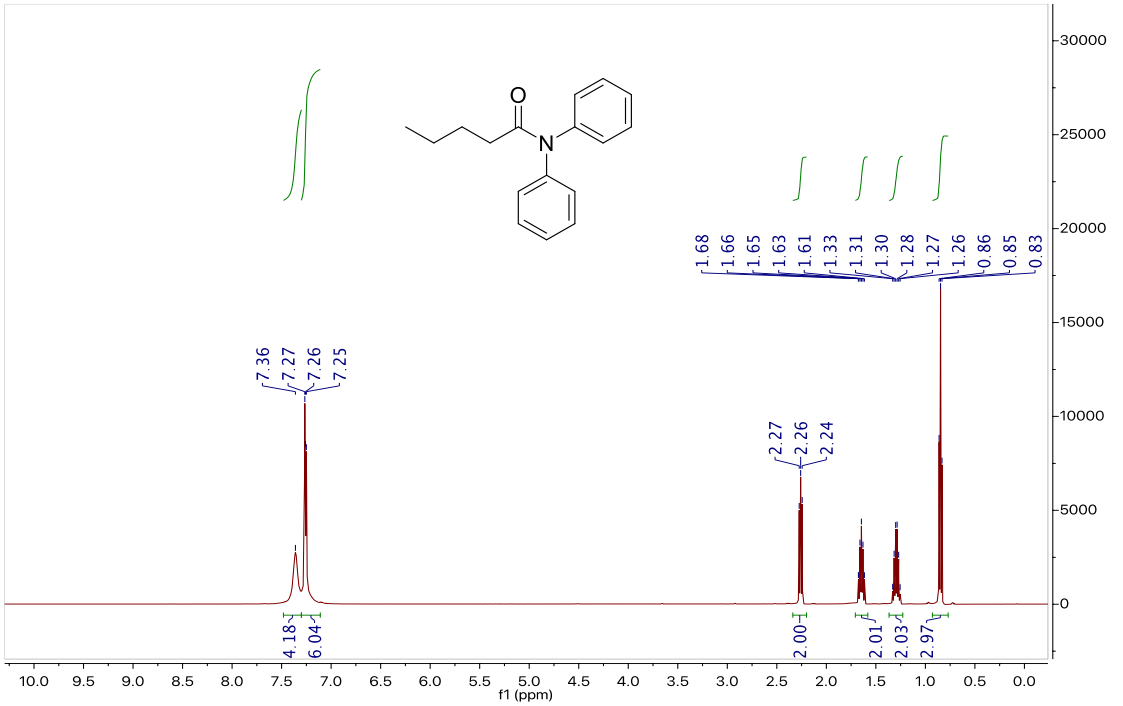

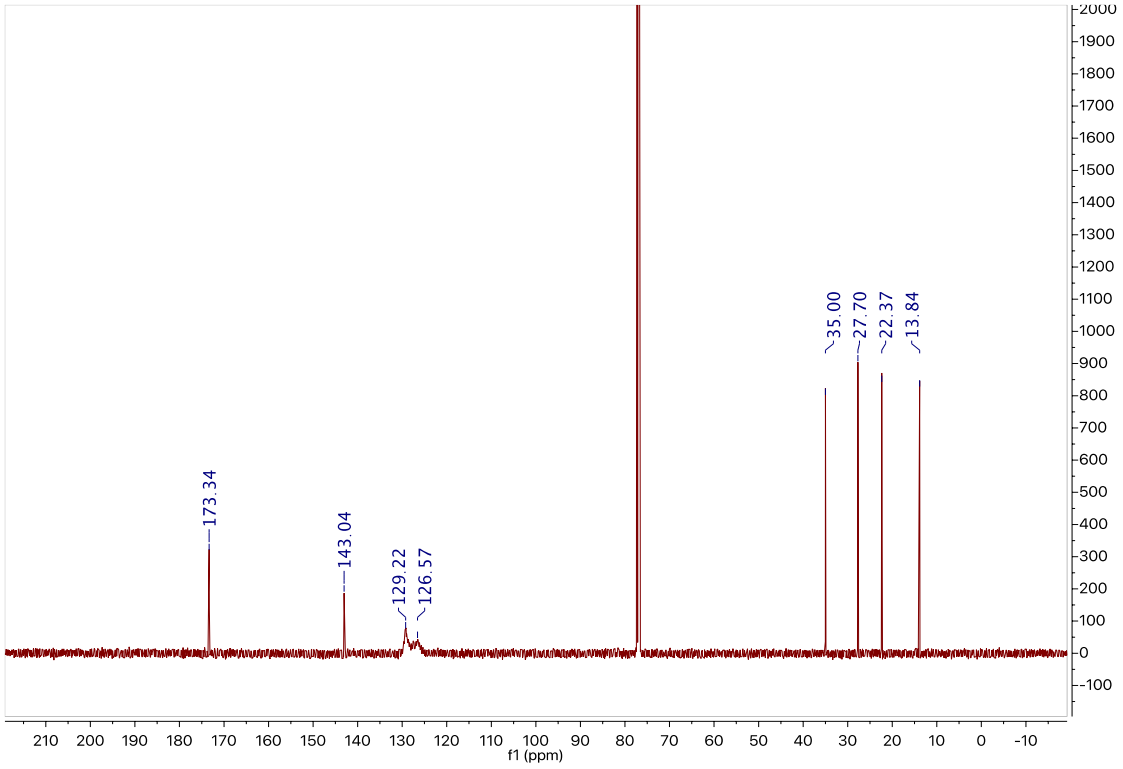

^{1}H and ^{13}C NMR data for 5.1x

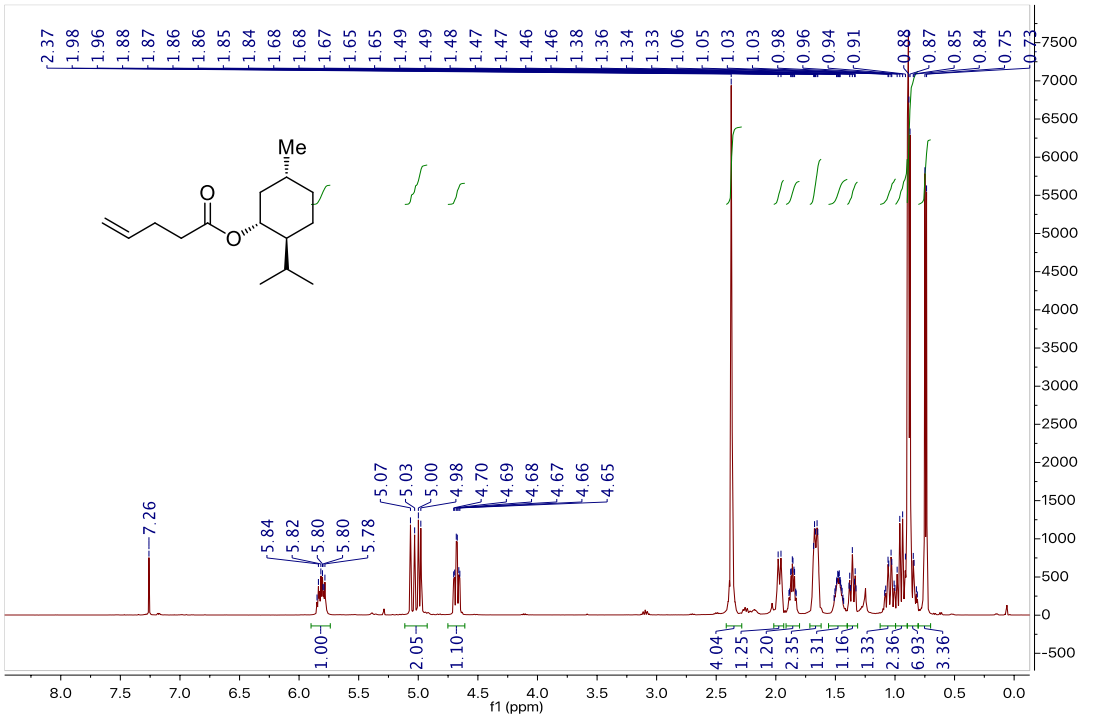

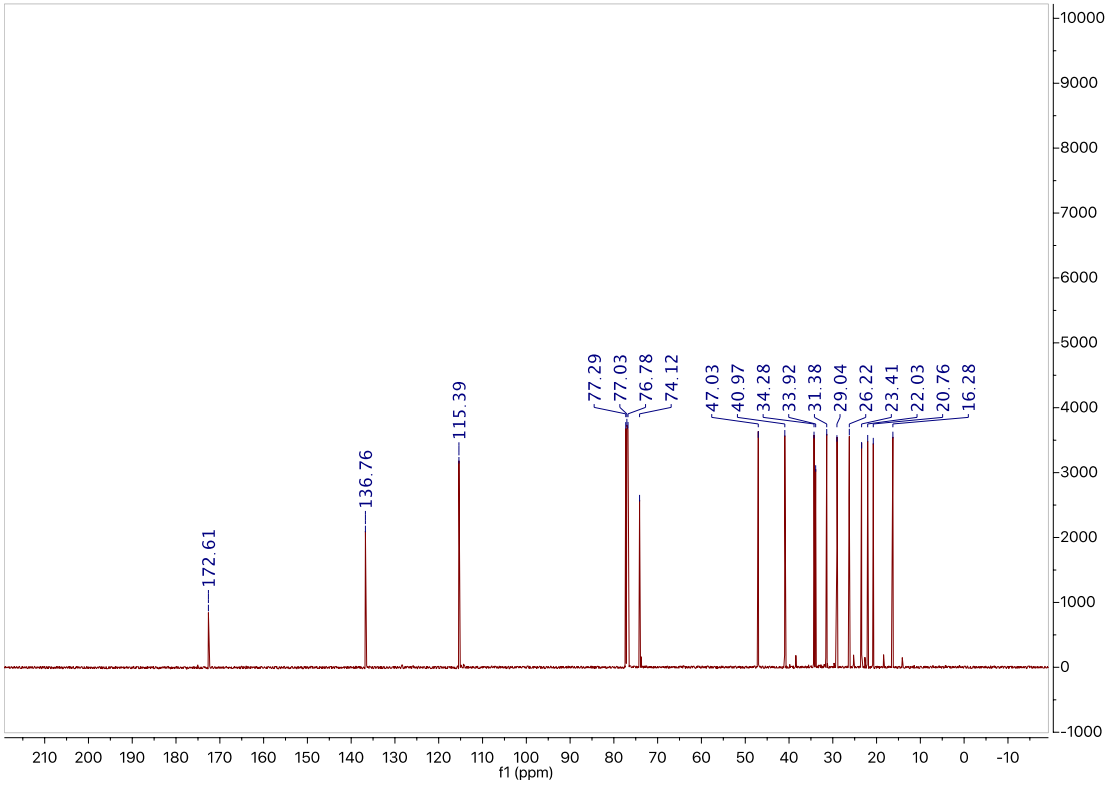

^{1}H and ^{13}C NMR data for 5.1y

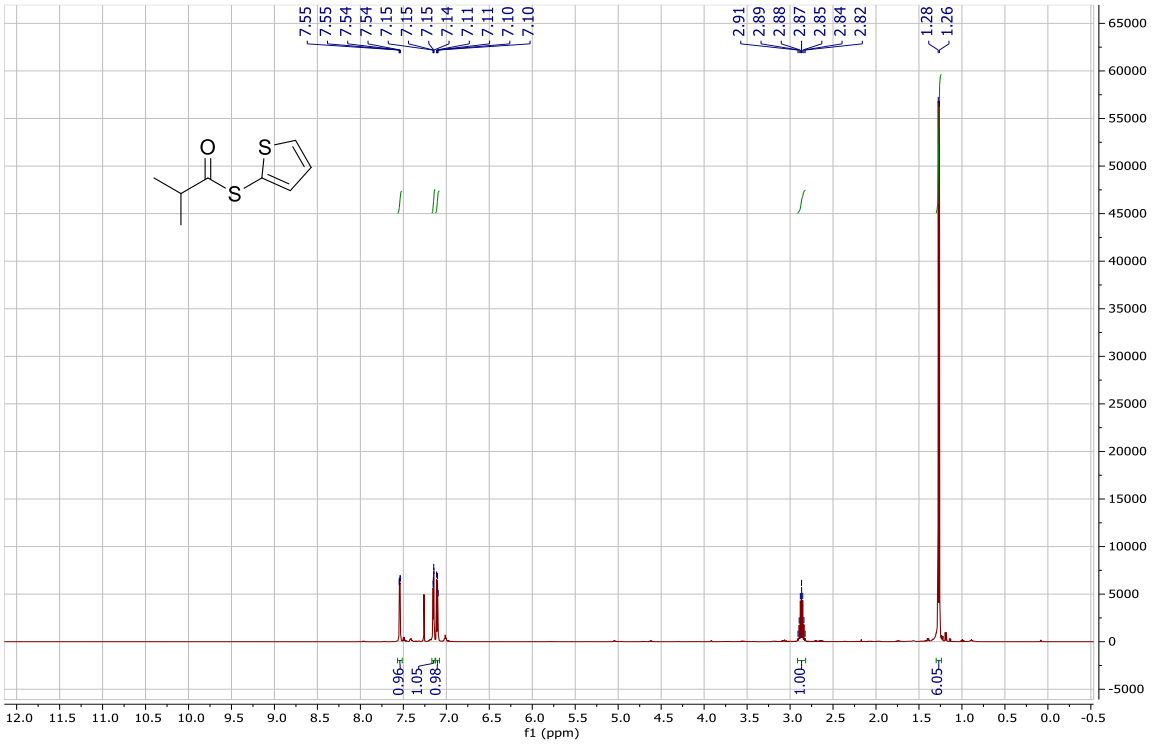

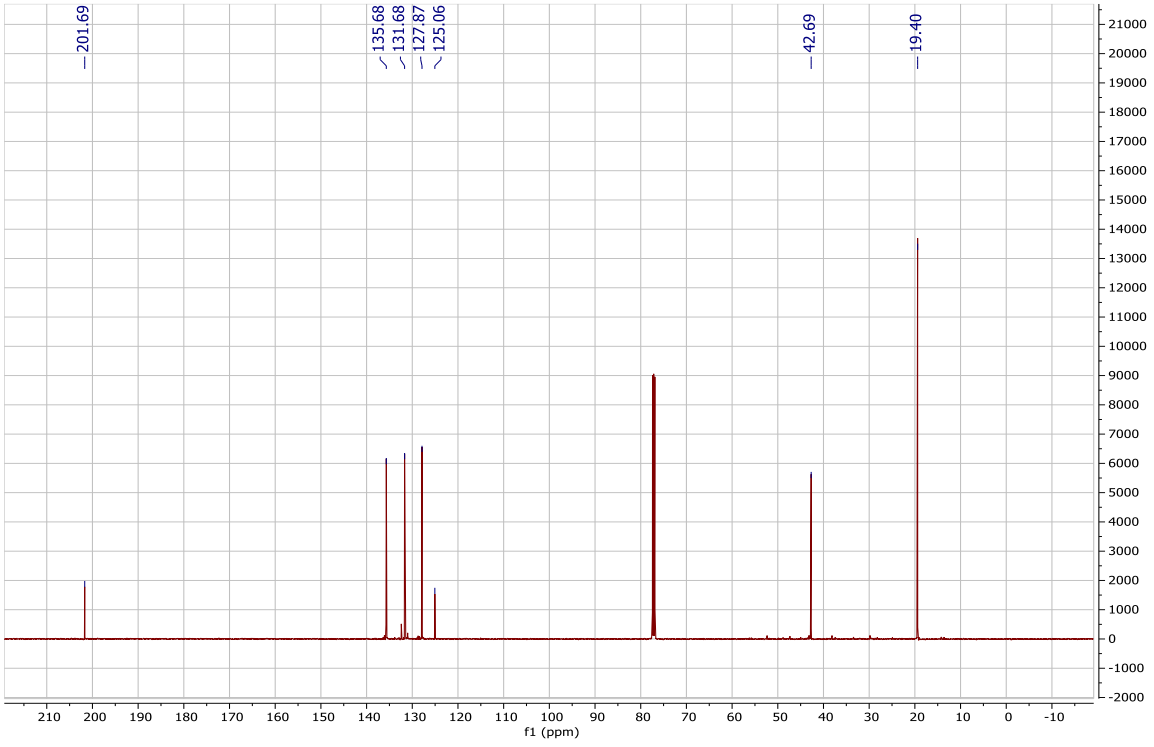

^{1}H and ^{13}C NMR data for 5.1z

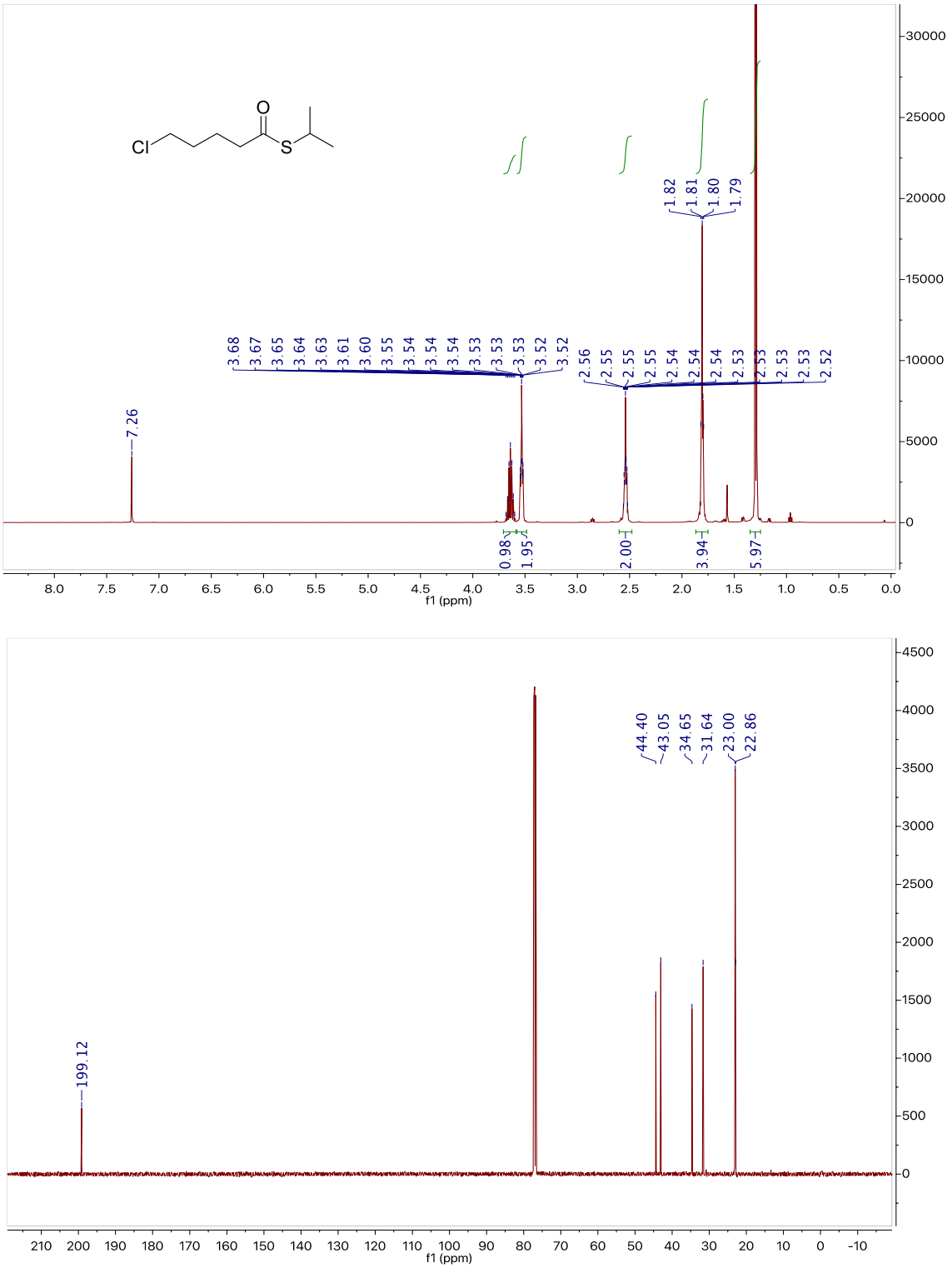

^{1}H and ^{13}C NMR data for 5.1aa

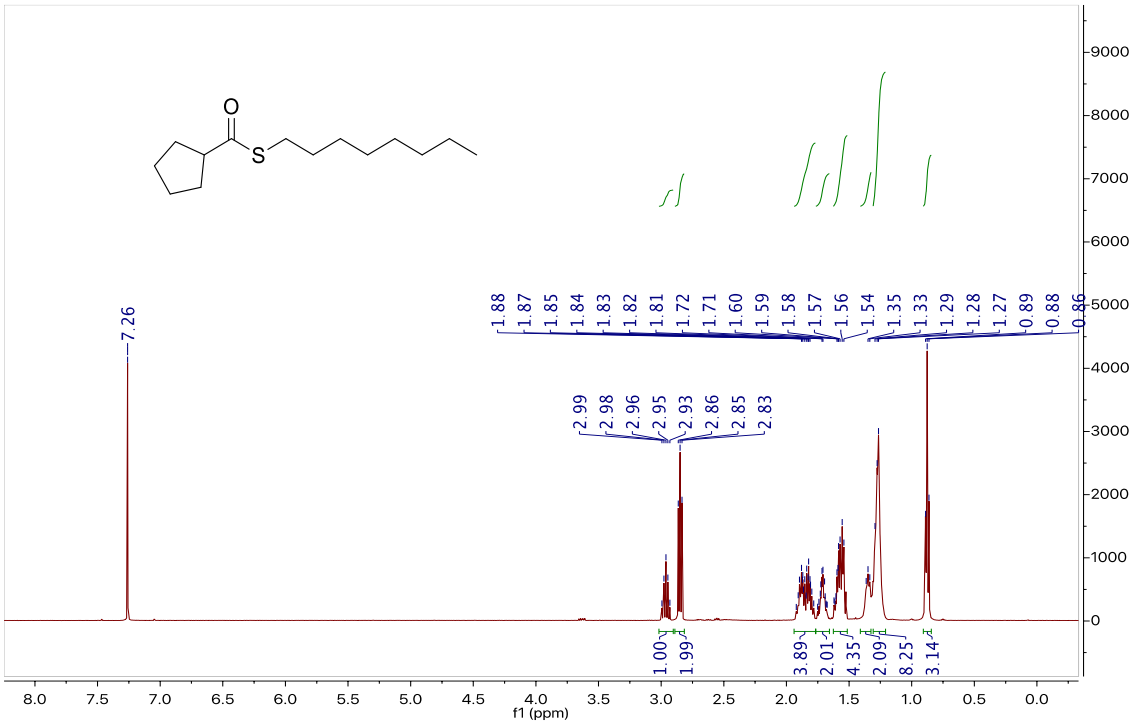

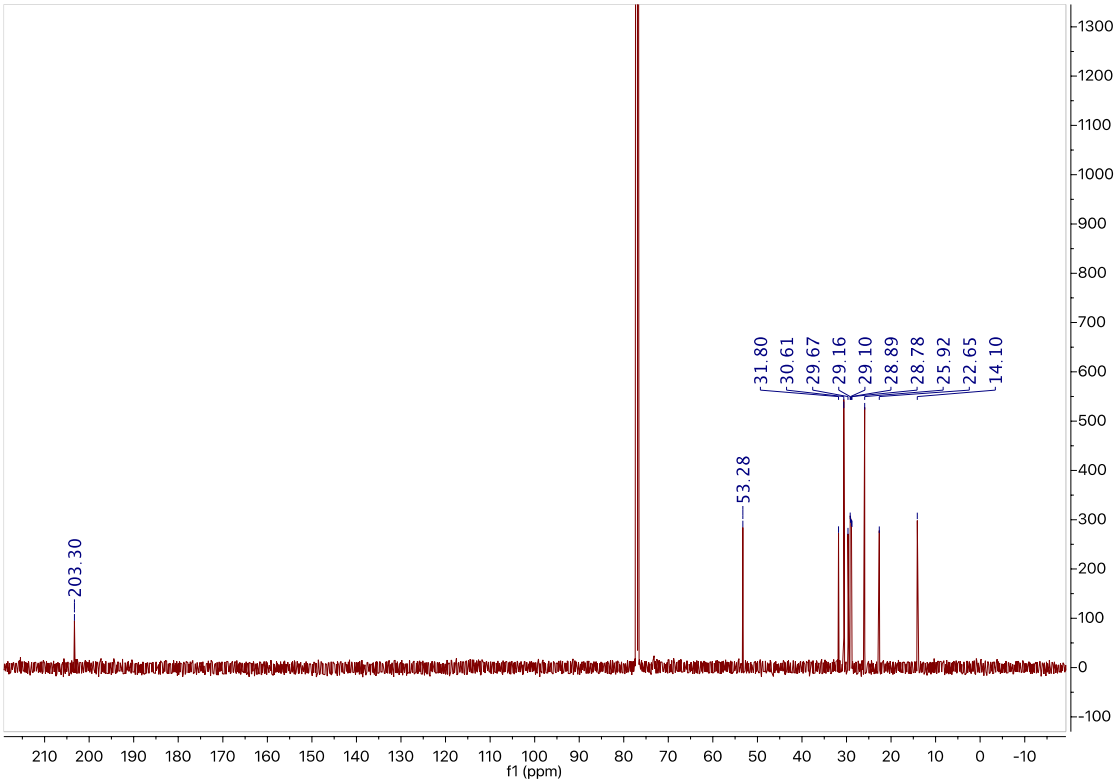

^{1}H and ^{13}C NMR data for 5.1bb

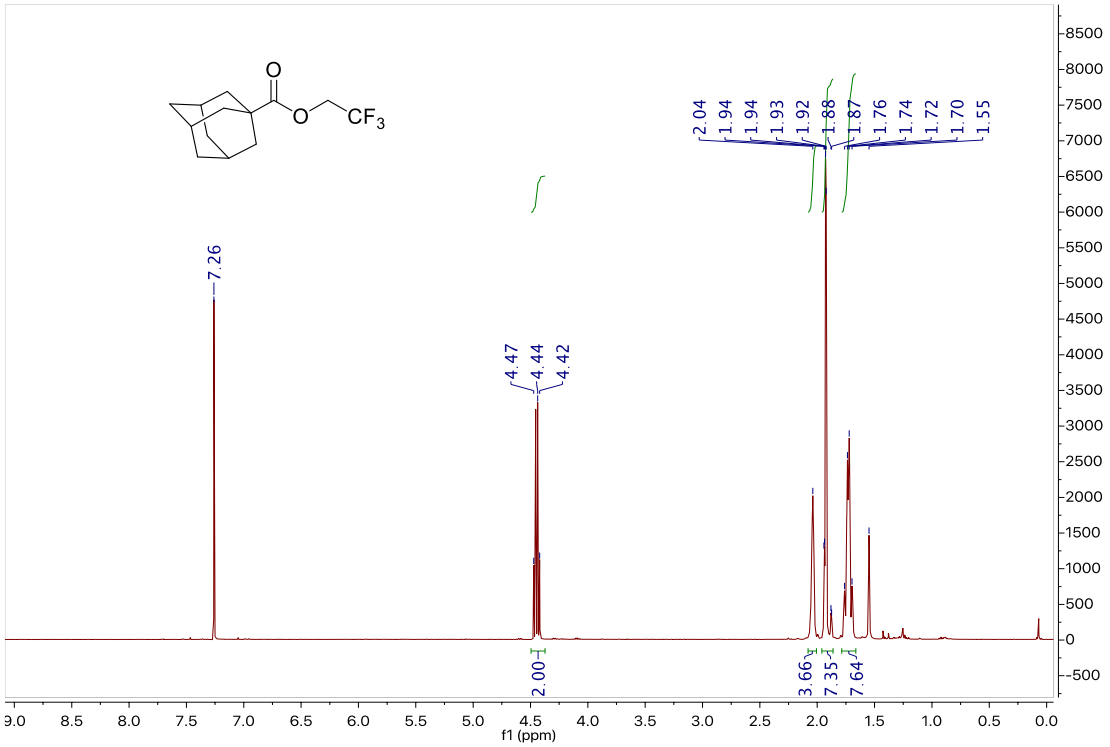

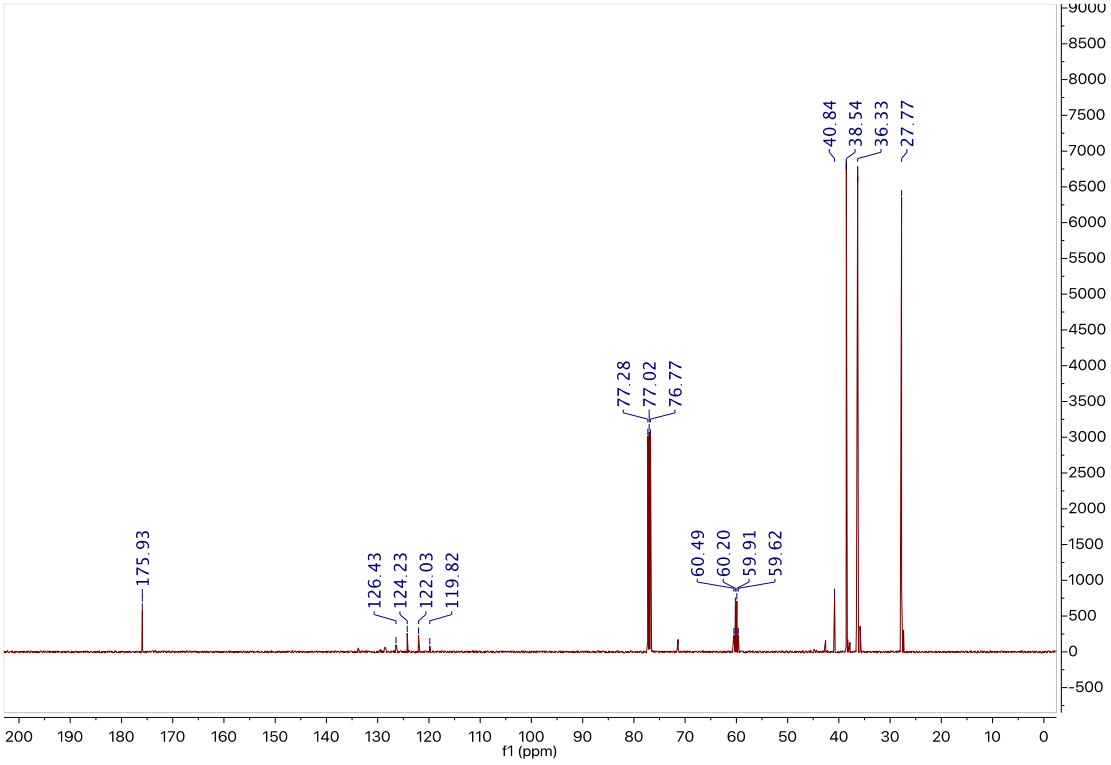

^{1}H and ^{13}C NMR data for 5.1cc

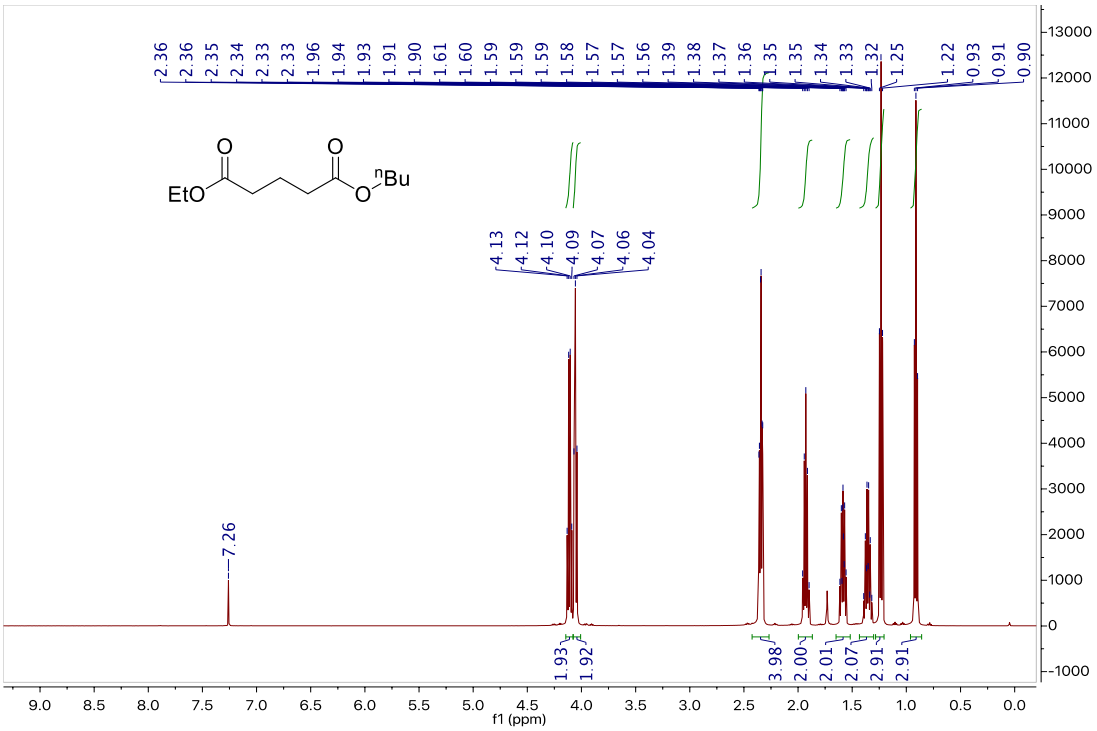

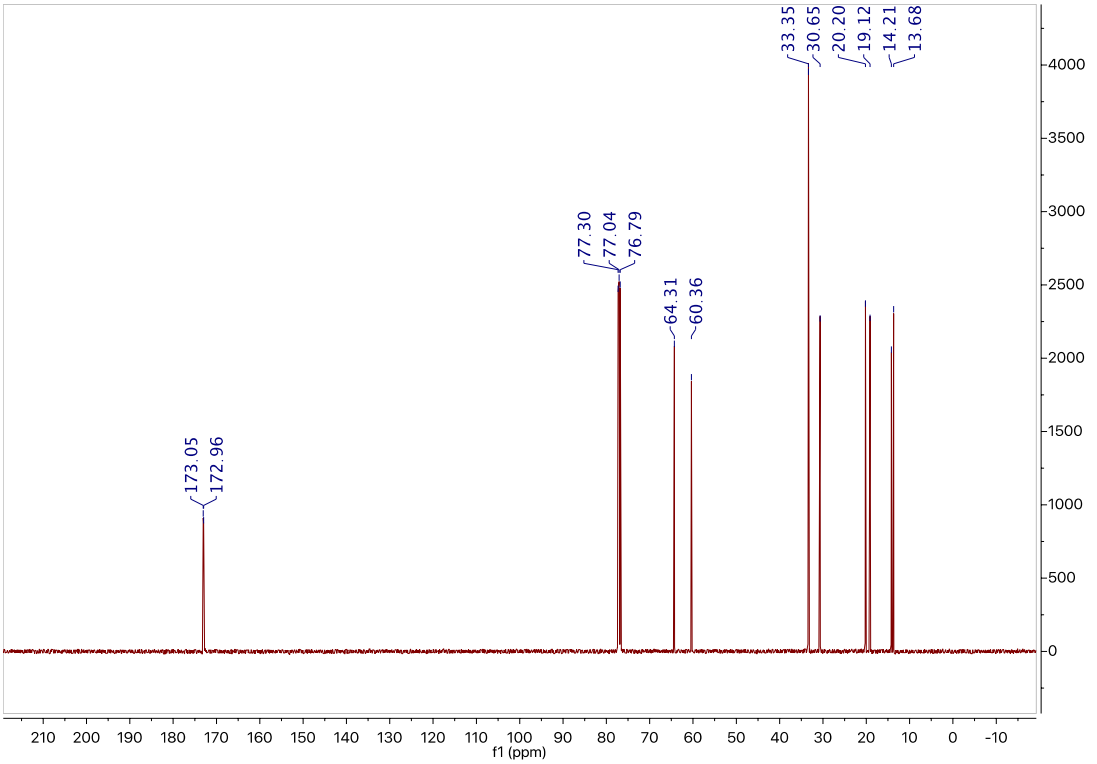

^{1}H and ^{13}C NMR data for 5.1dd

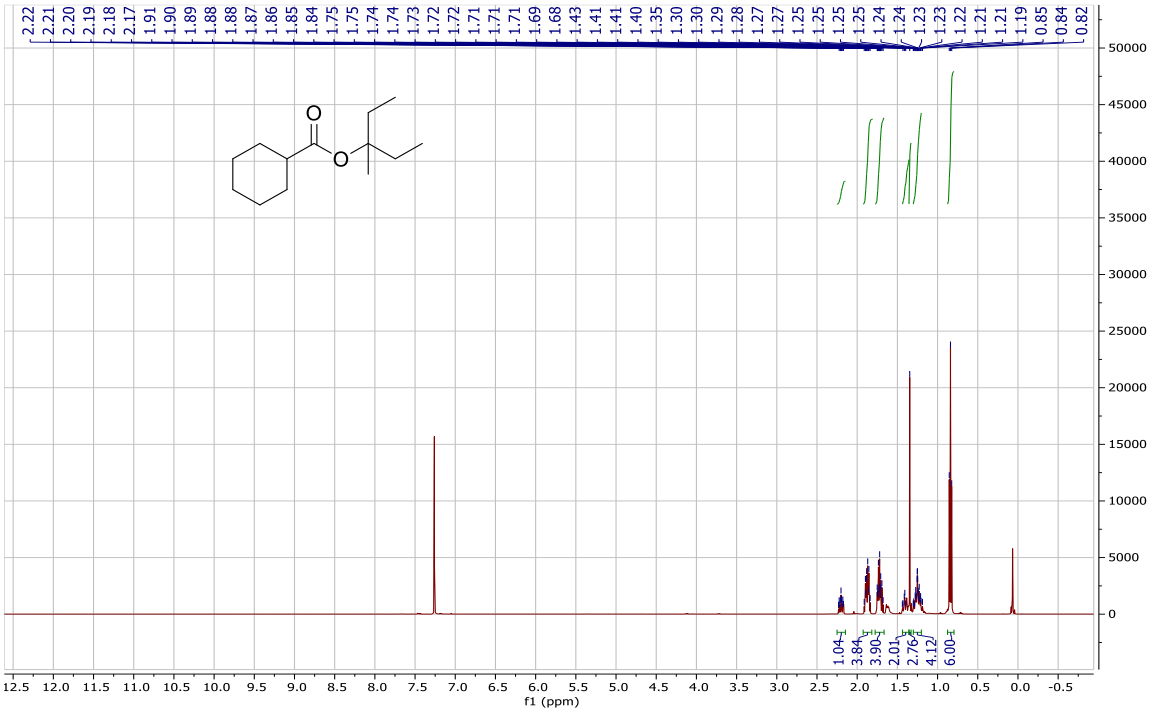

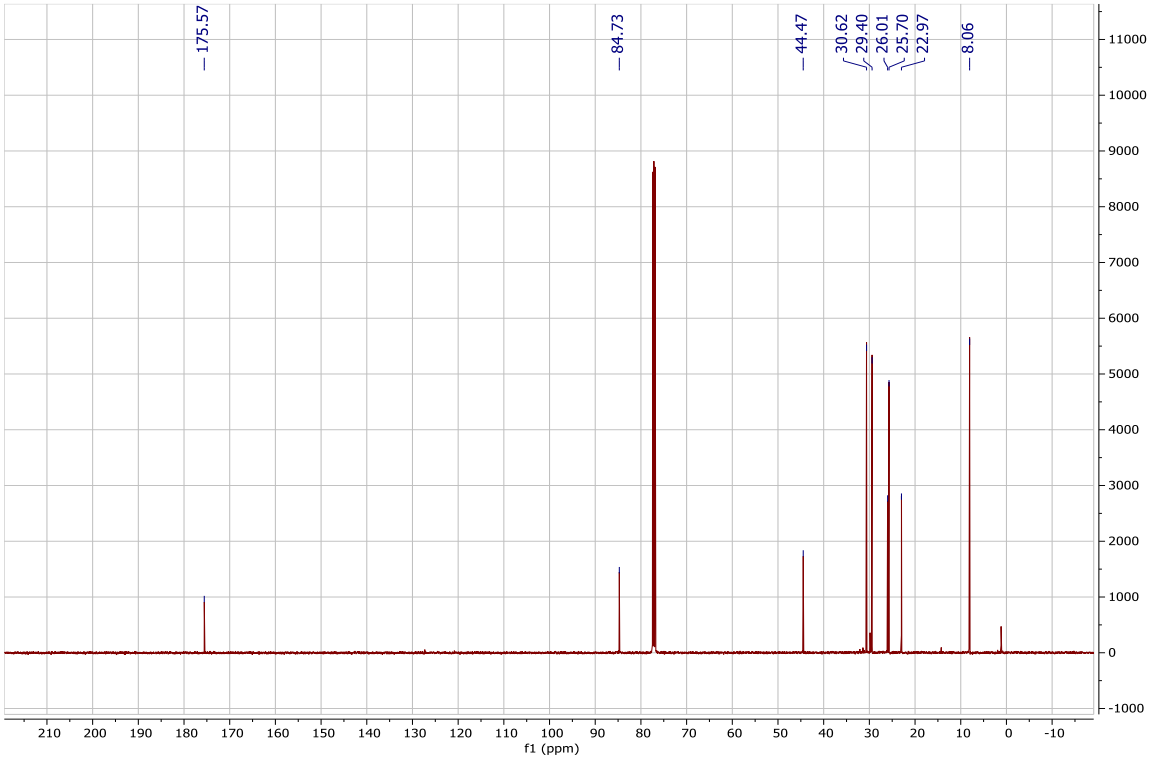

^{1}H and ^{13}C NMR data for 5.1ee

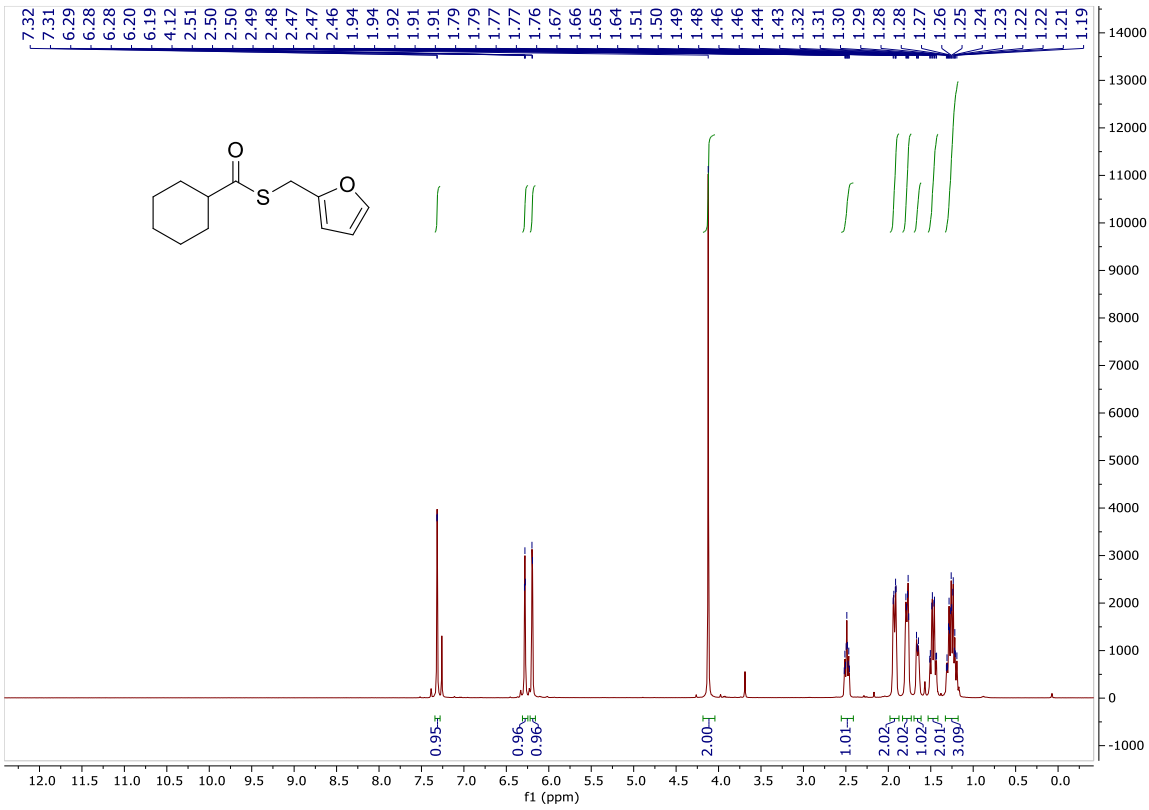

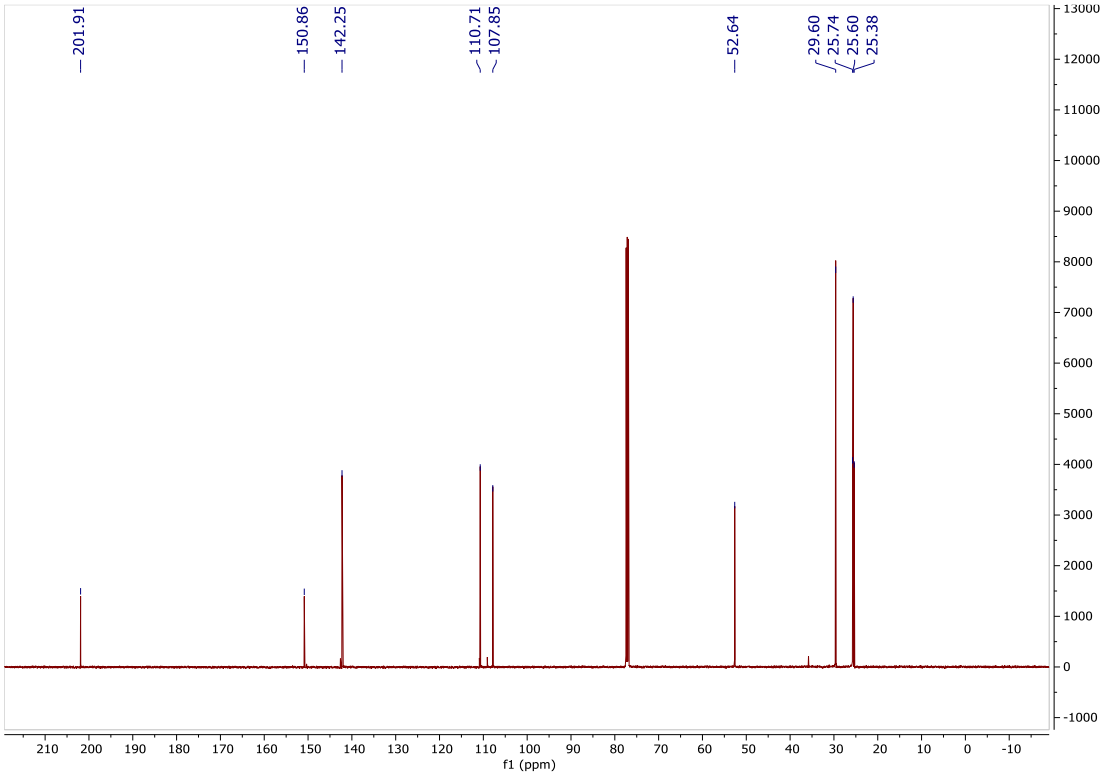

^{1}H and ^{13}C NMR data for 5.1ff

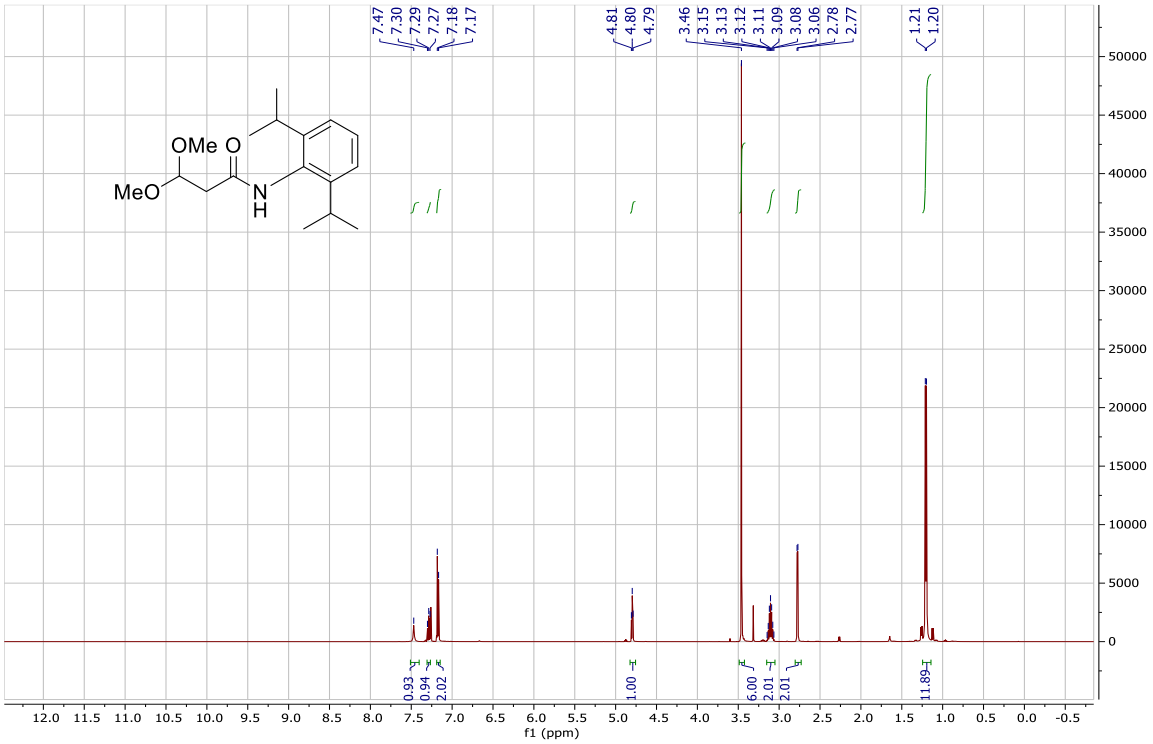

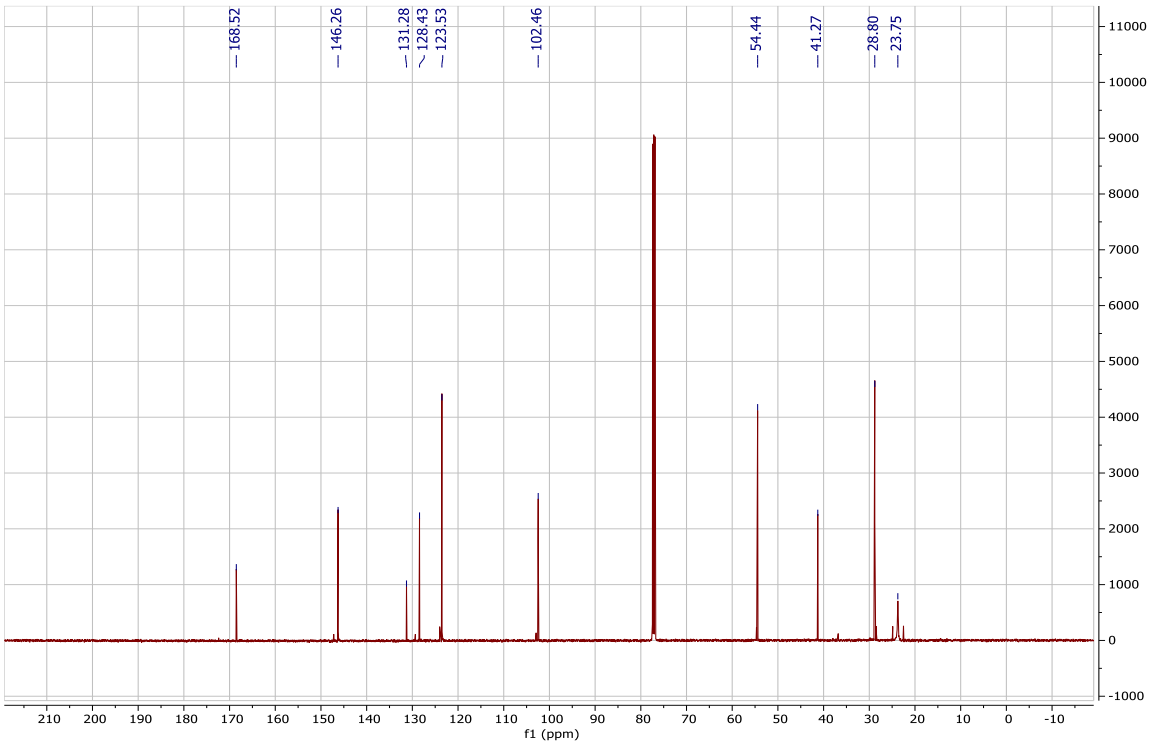

^{1}H and ^{13}C NMR data for 5.1gg

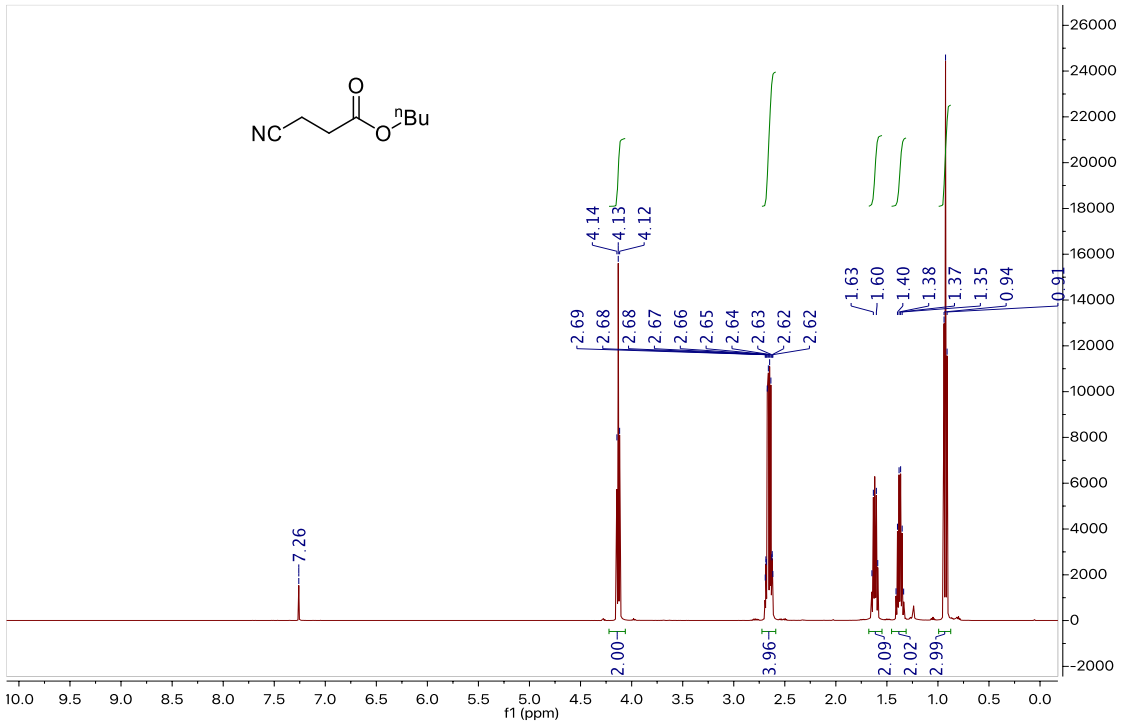

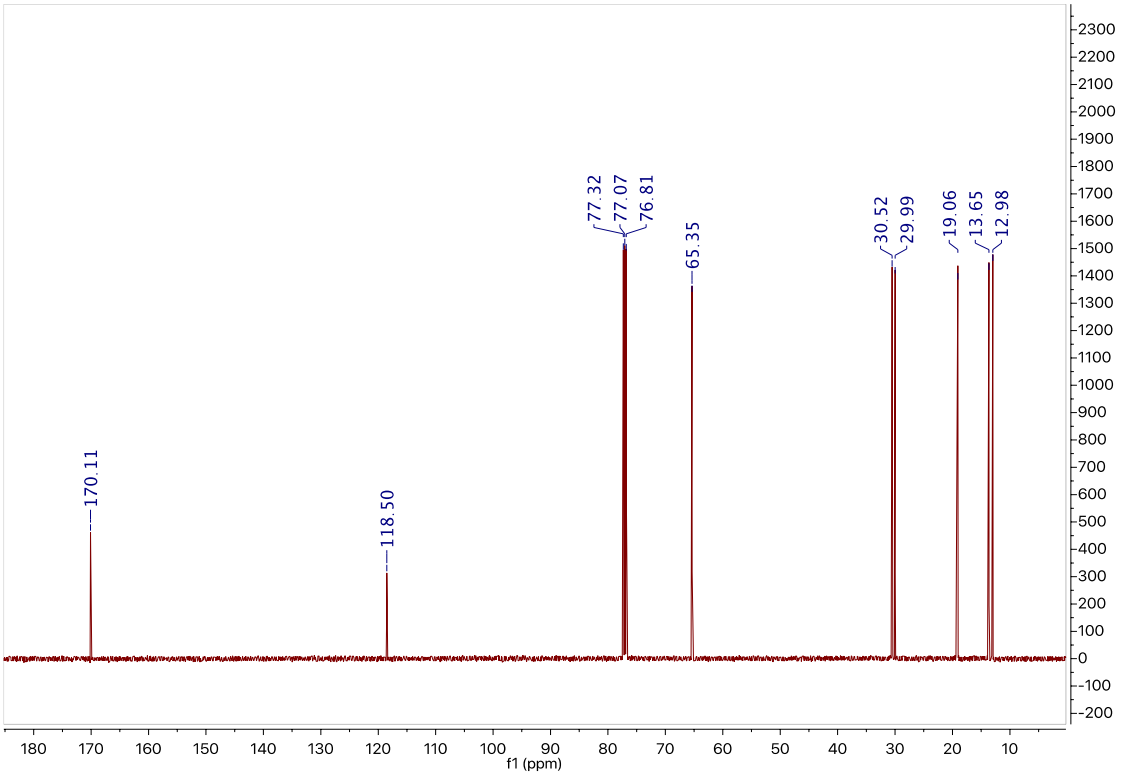

^{1}H and ^{13}C NMR data for 5.1hh

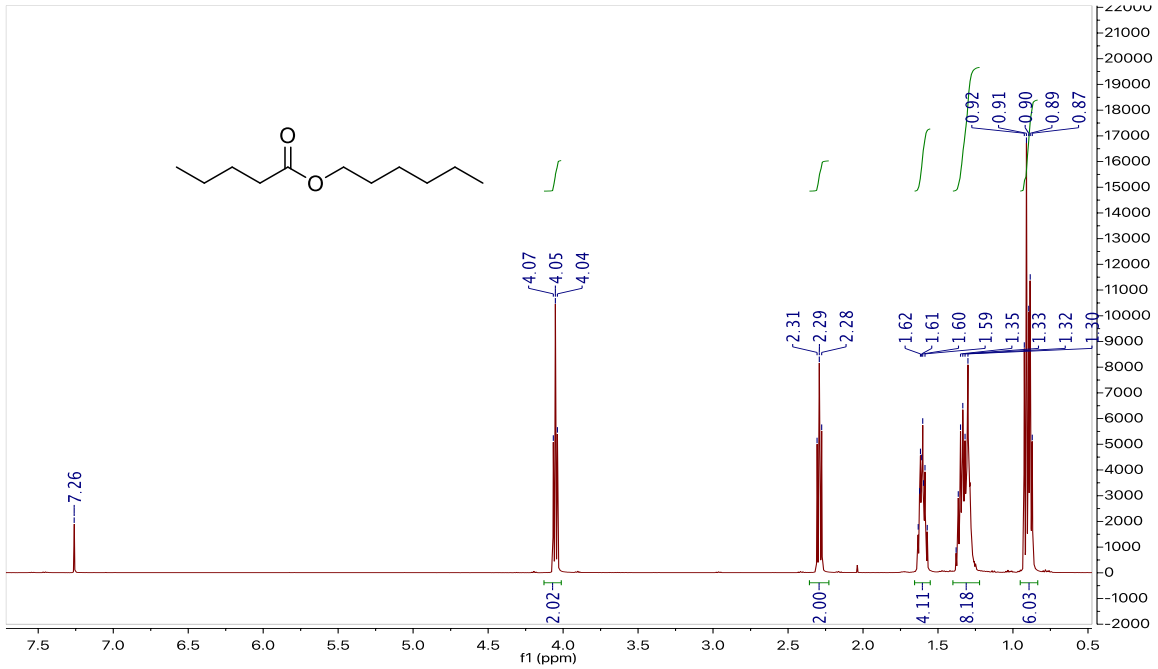

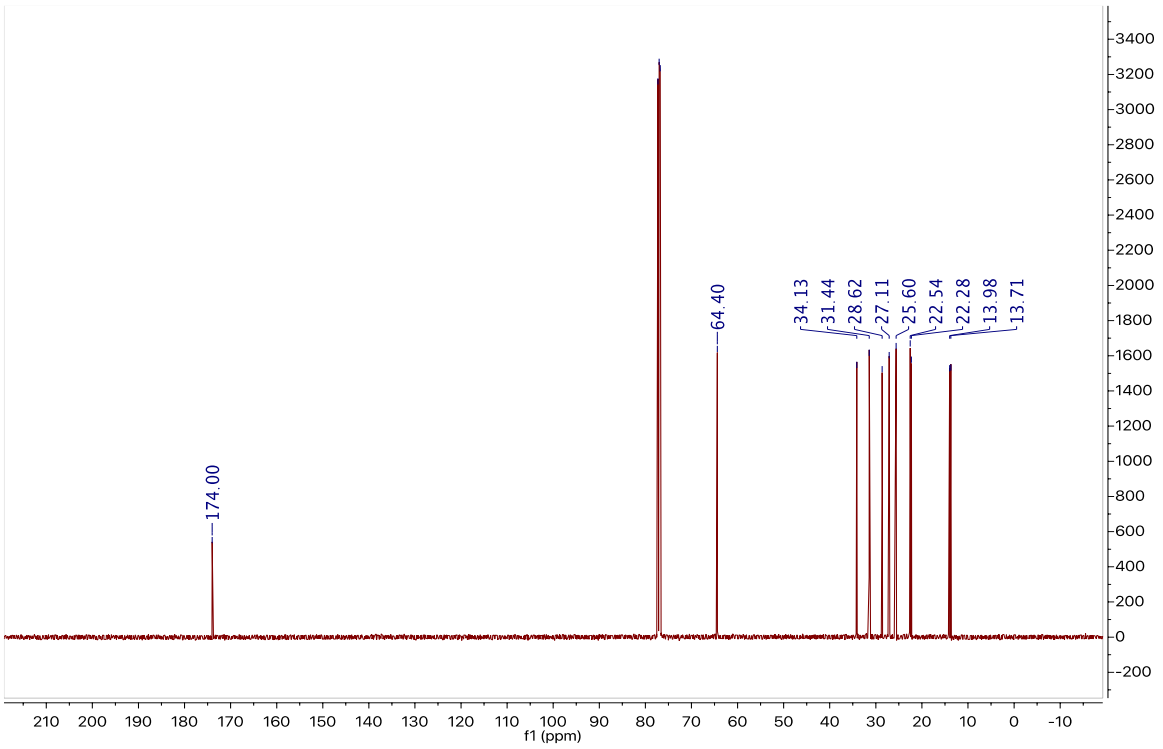

^{1}H and ^{13}C NMR data for 5.1ii

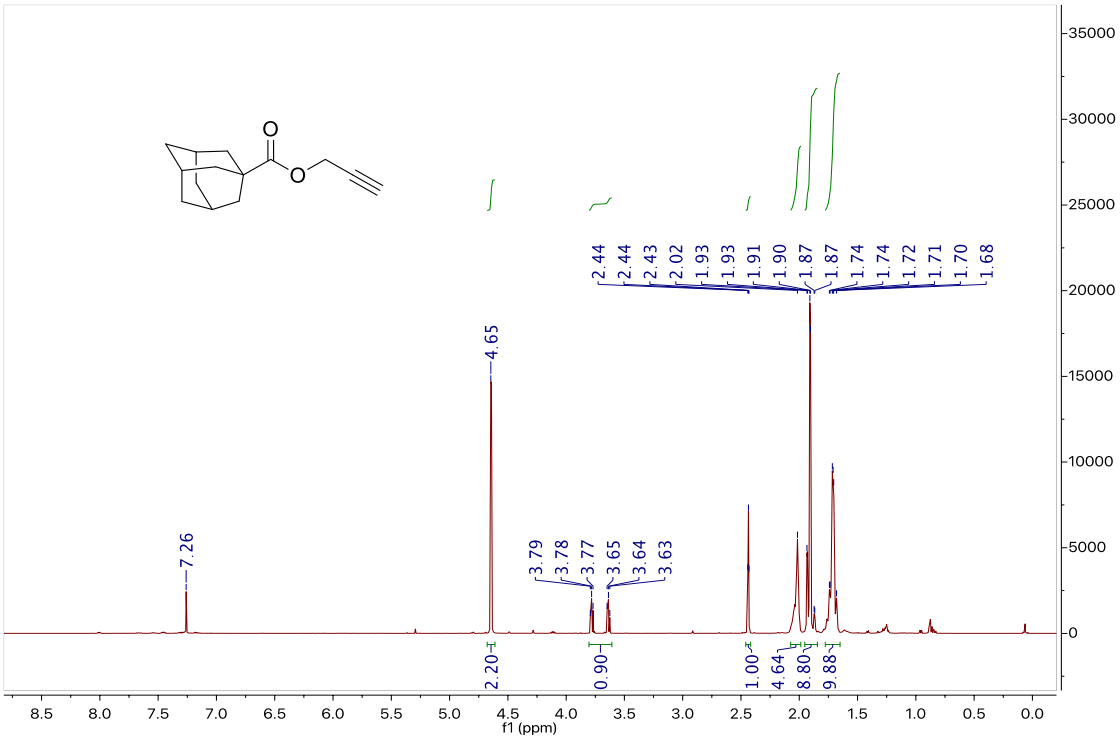

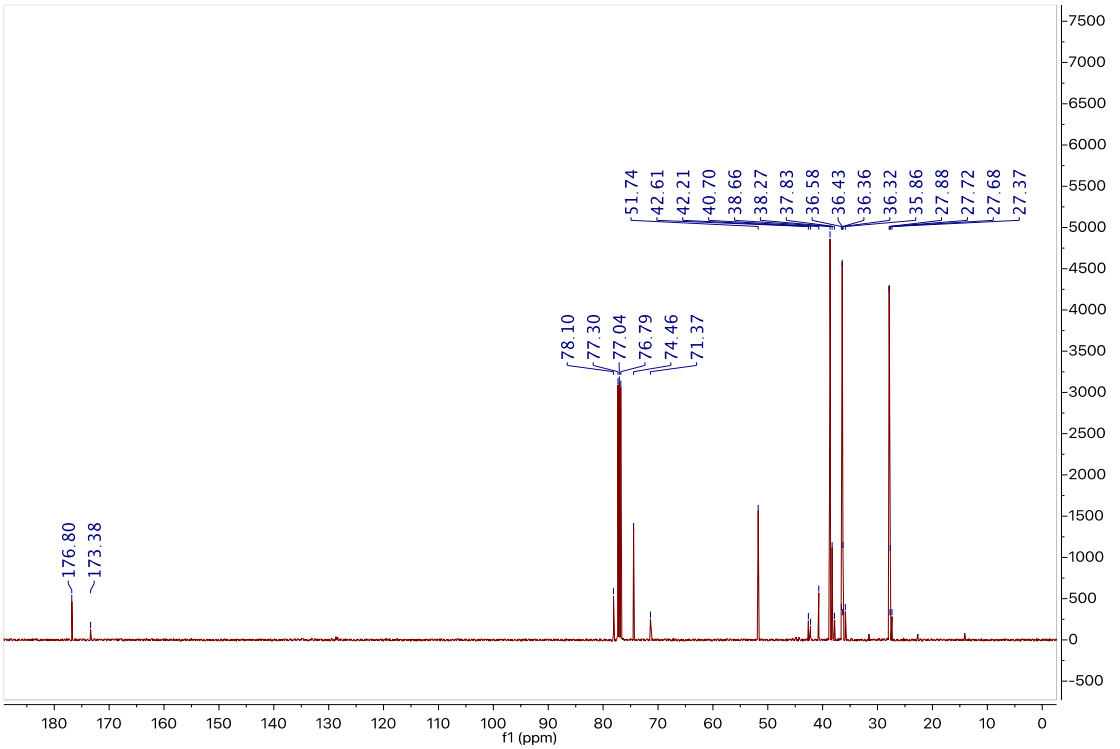

^{1}H and ^{13}C NMR data for 5.1jj

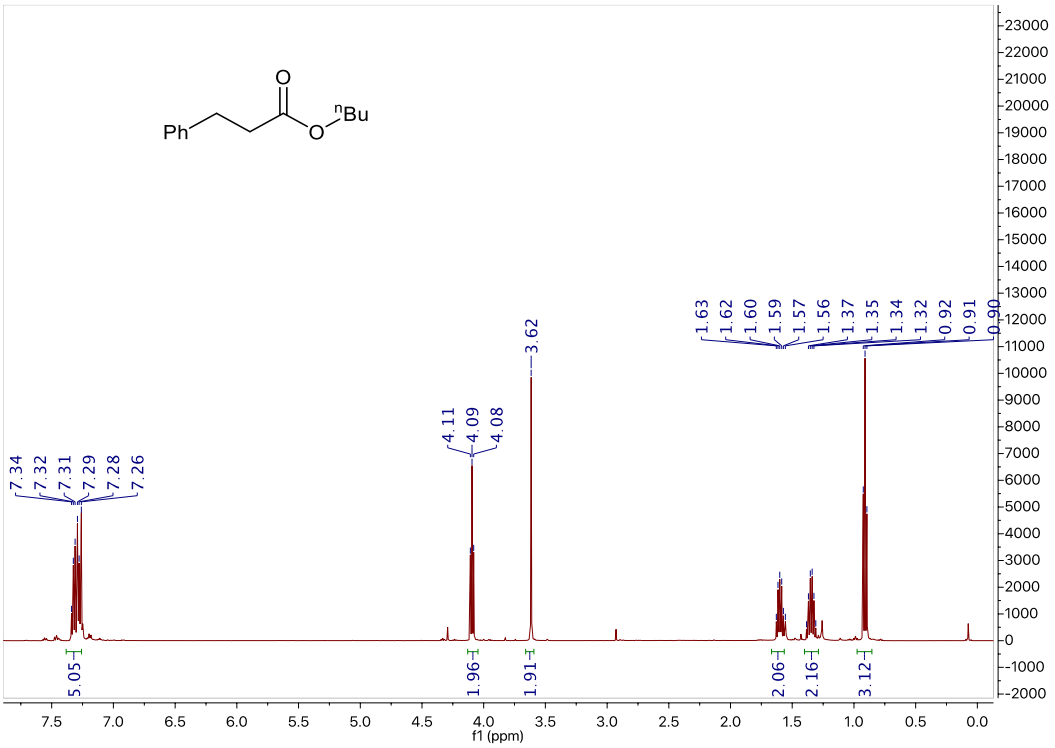

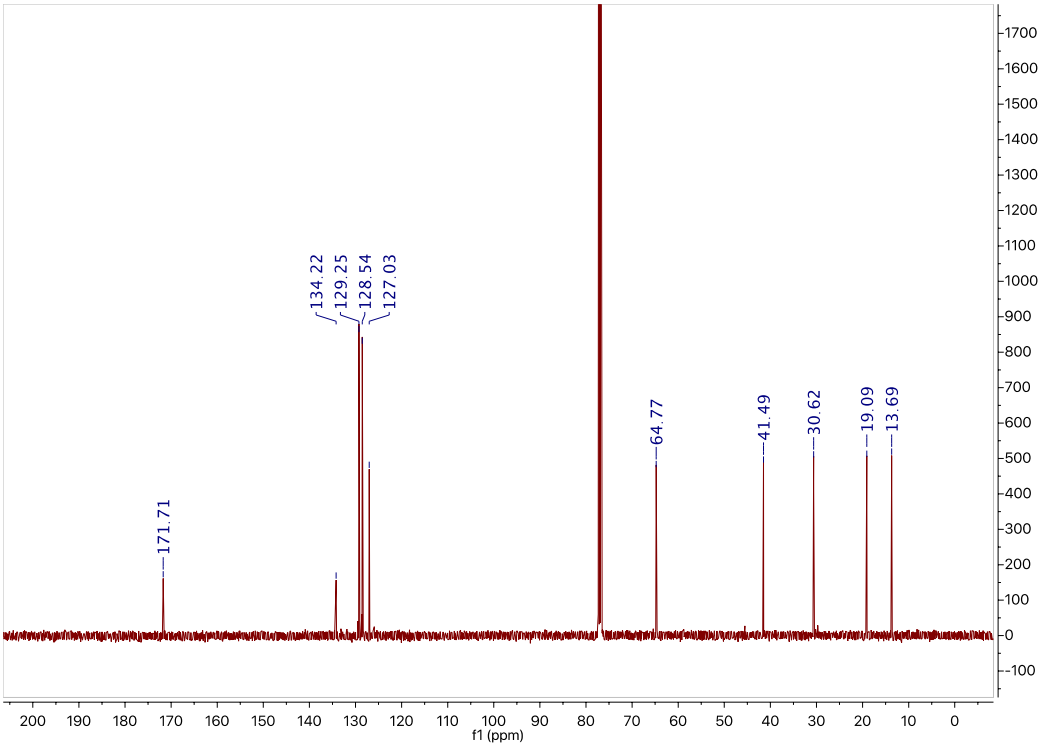

^{1}H and ^{13}C NMR data for 5.1kk

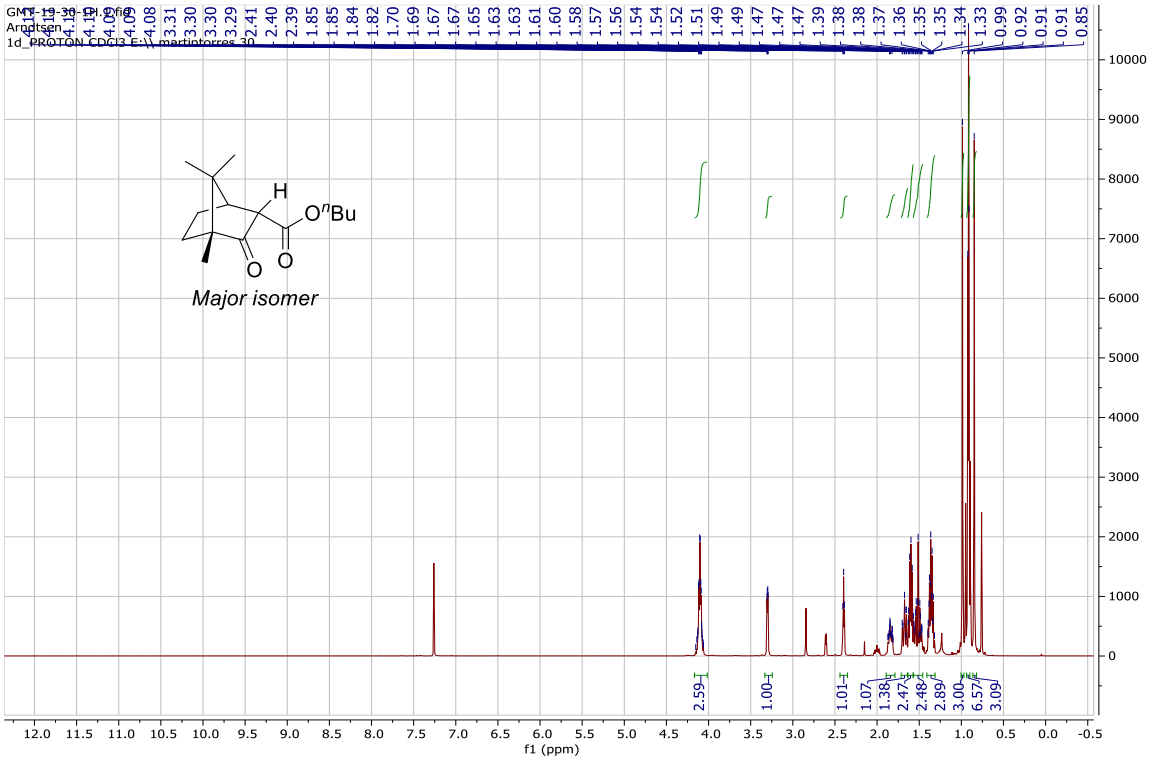

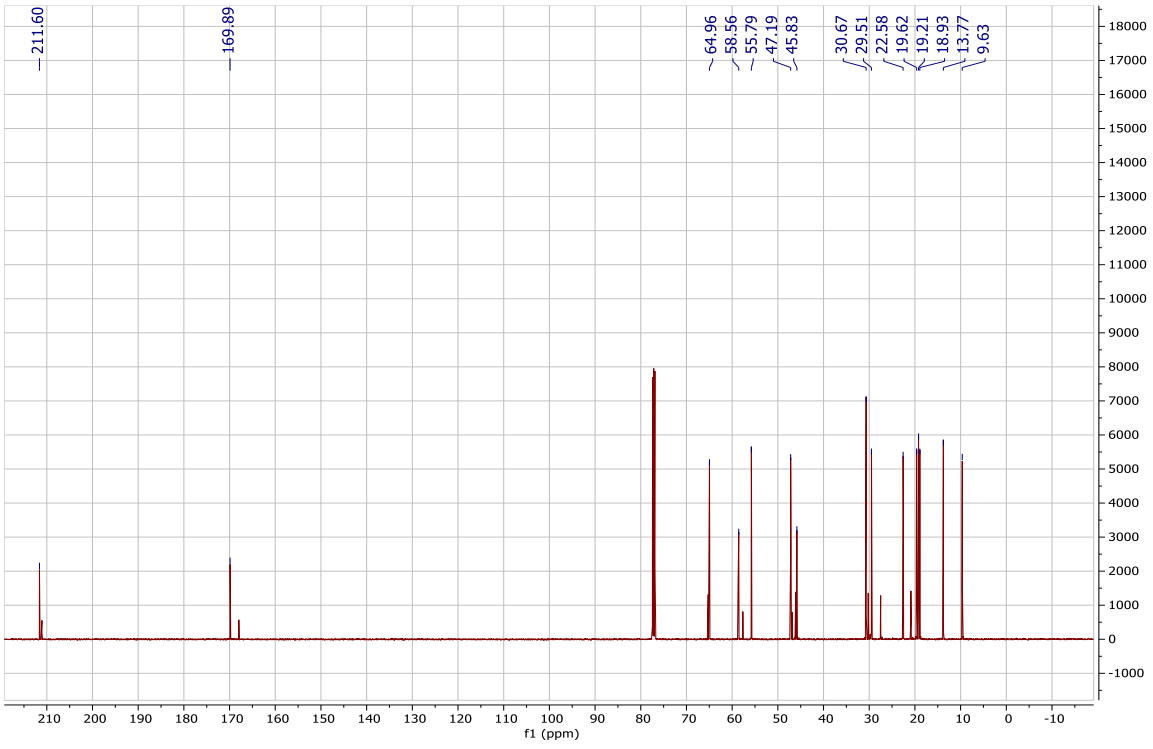

HSQC data for 5.1kk

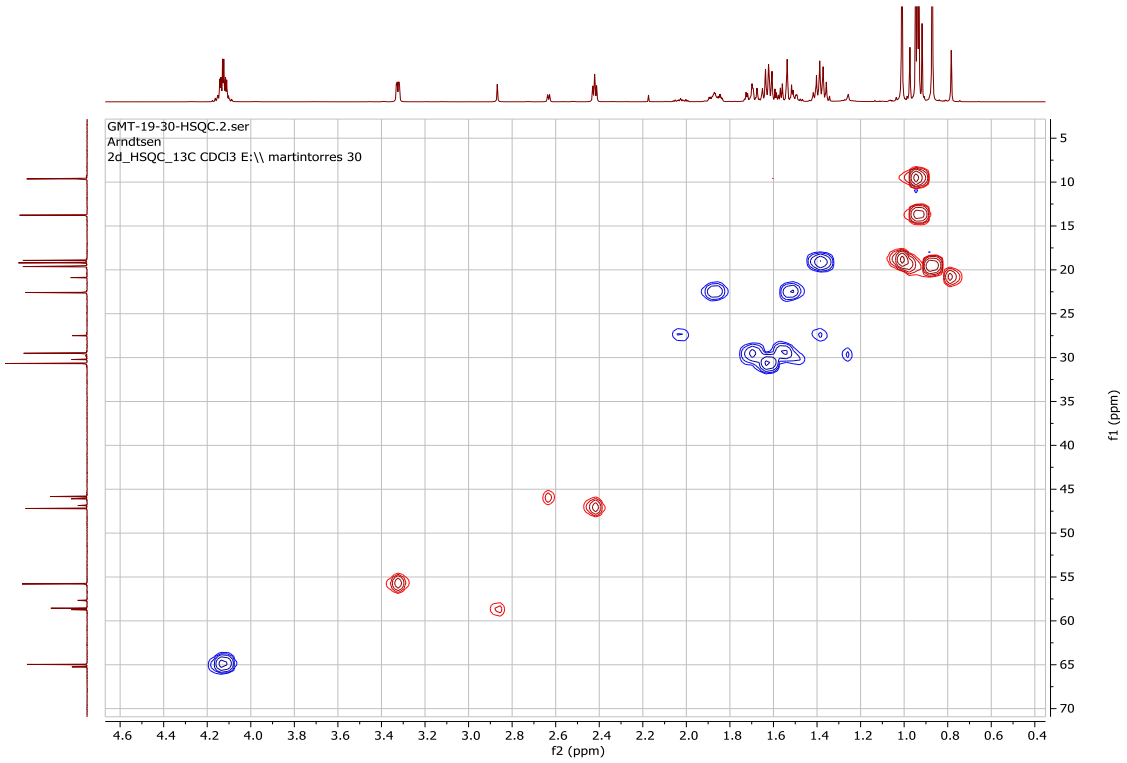

HMBC data for 5.1kk

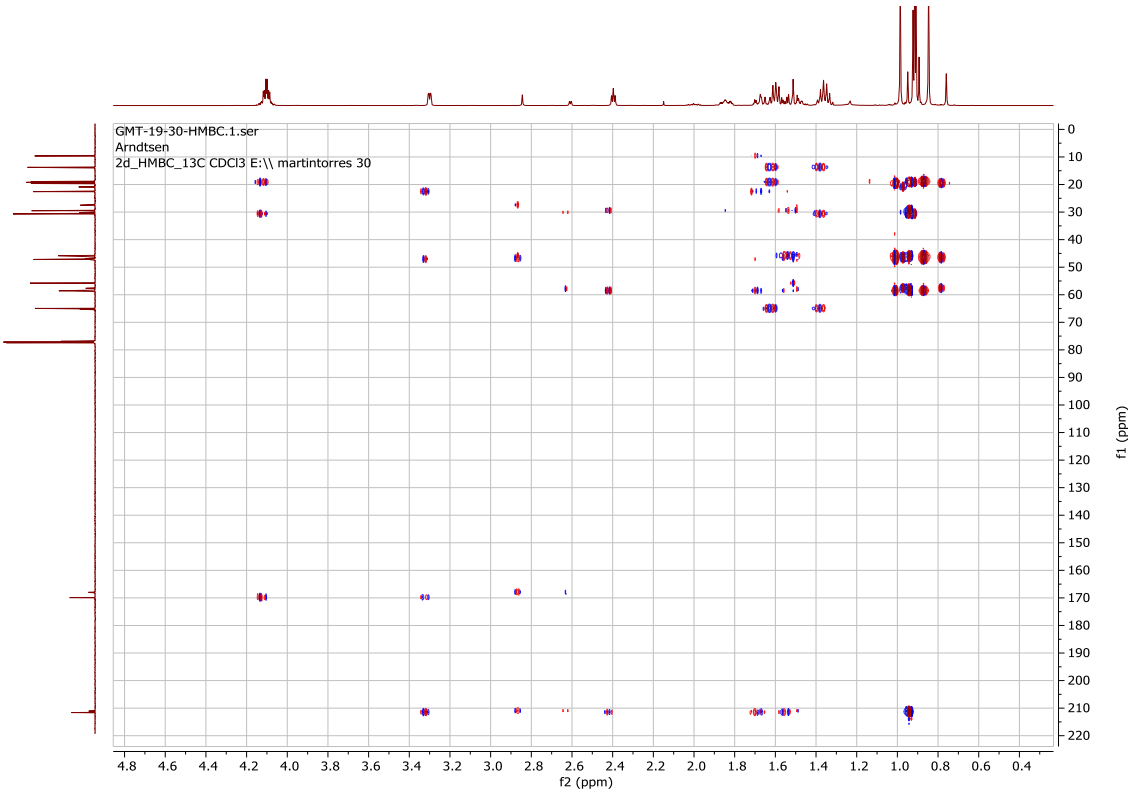

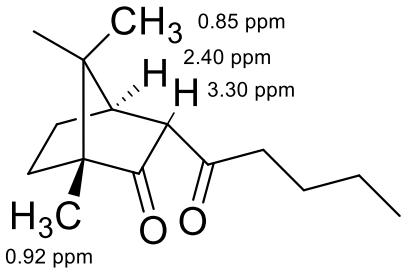

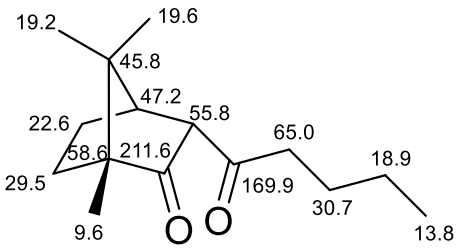

NOESY data for 5.1kk

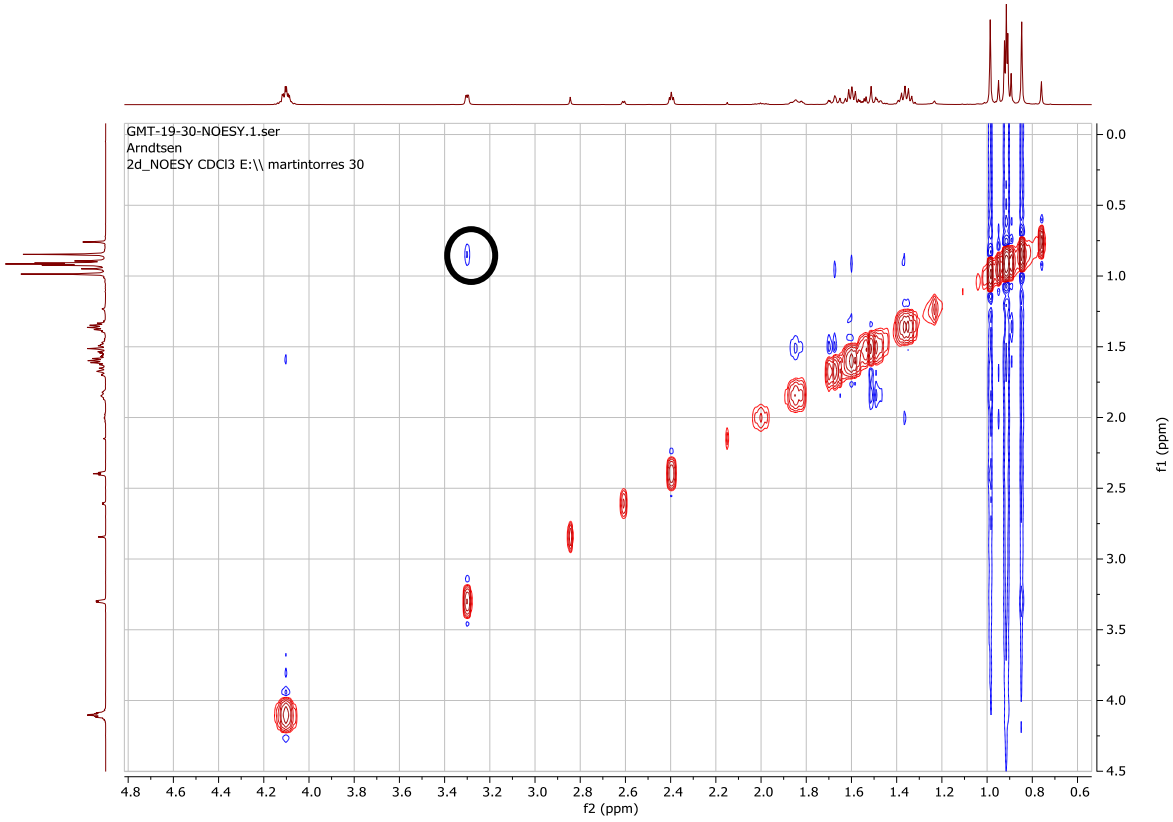

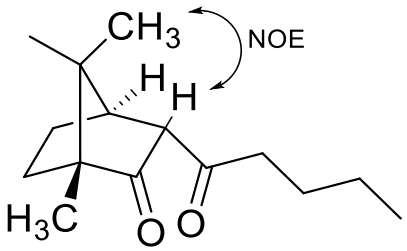

Major

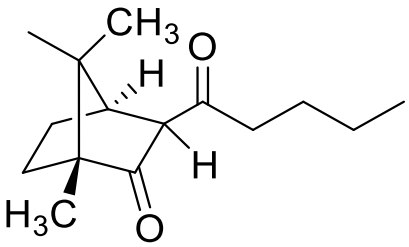

Minor

^{1}H and ^{13}C NMR data for 5.1ll

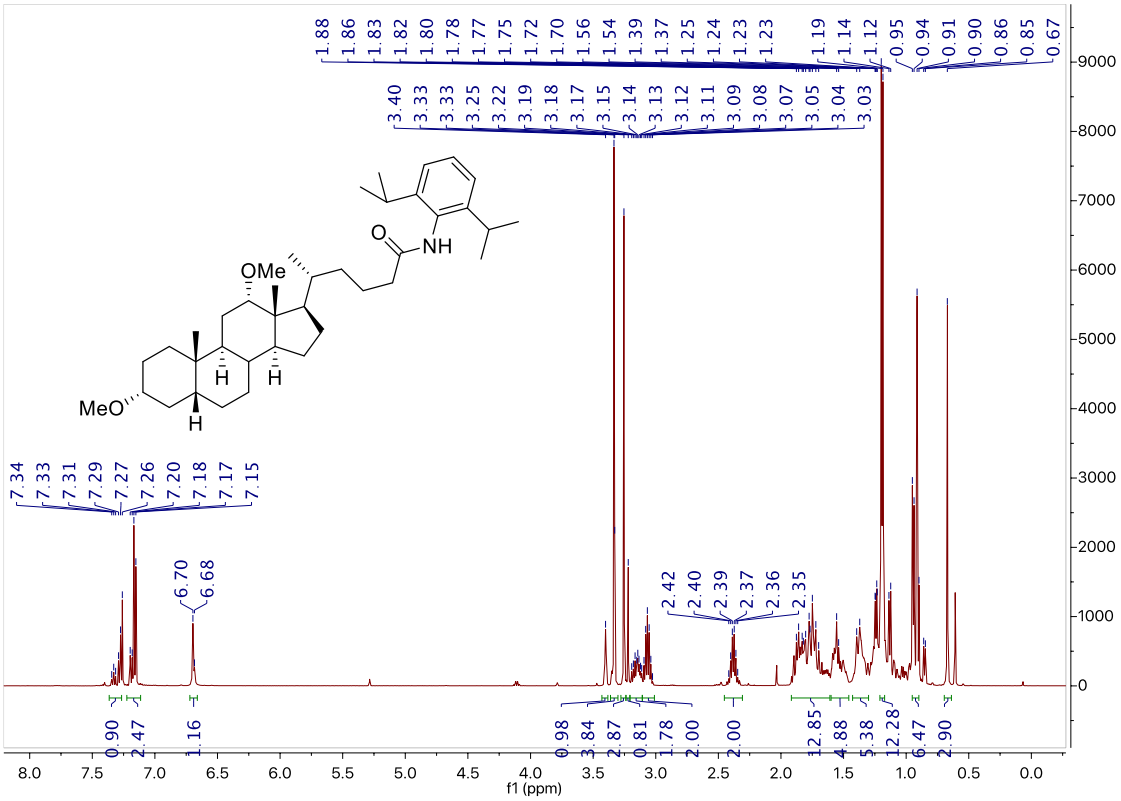

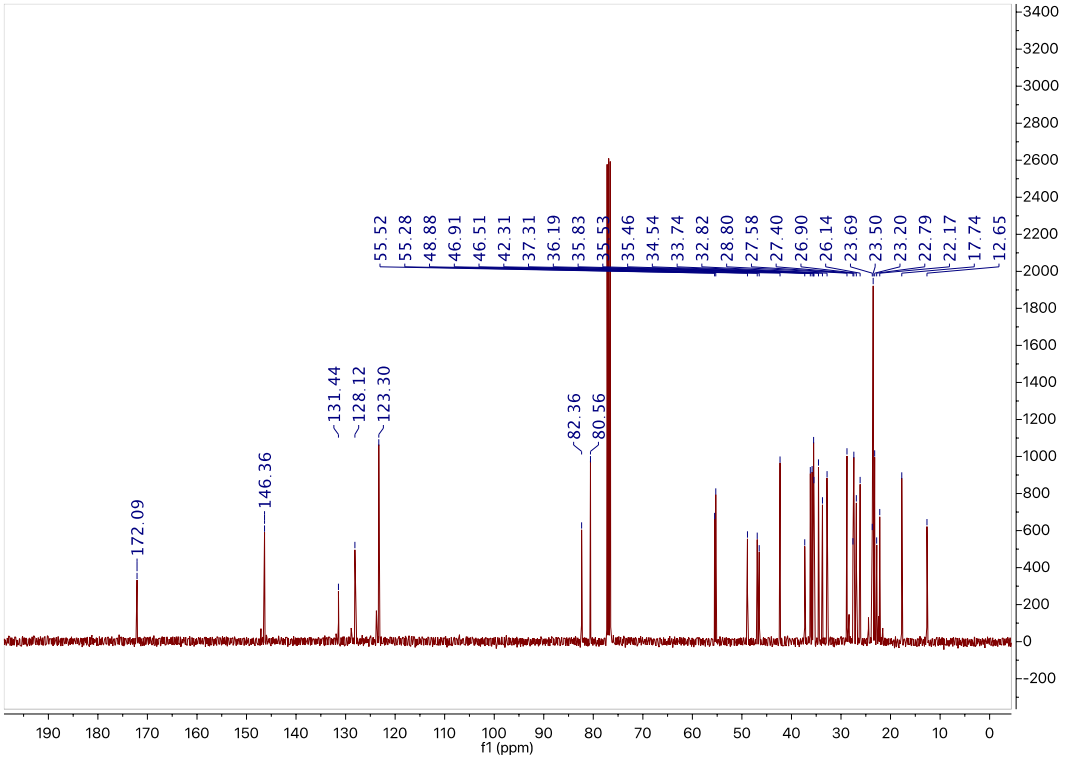

^{1}H and ^{13}C NMR data for 5.1mm-a

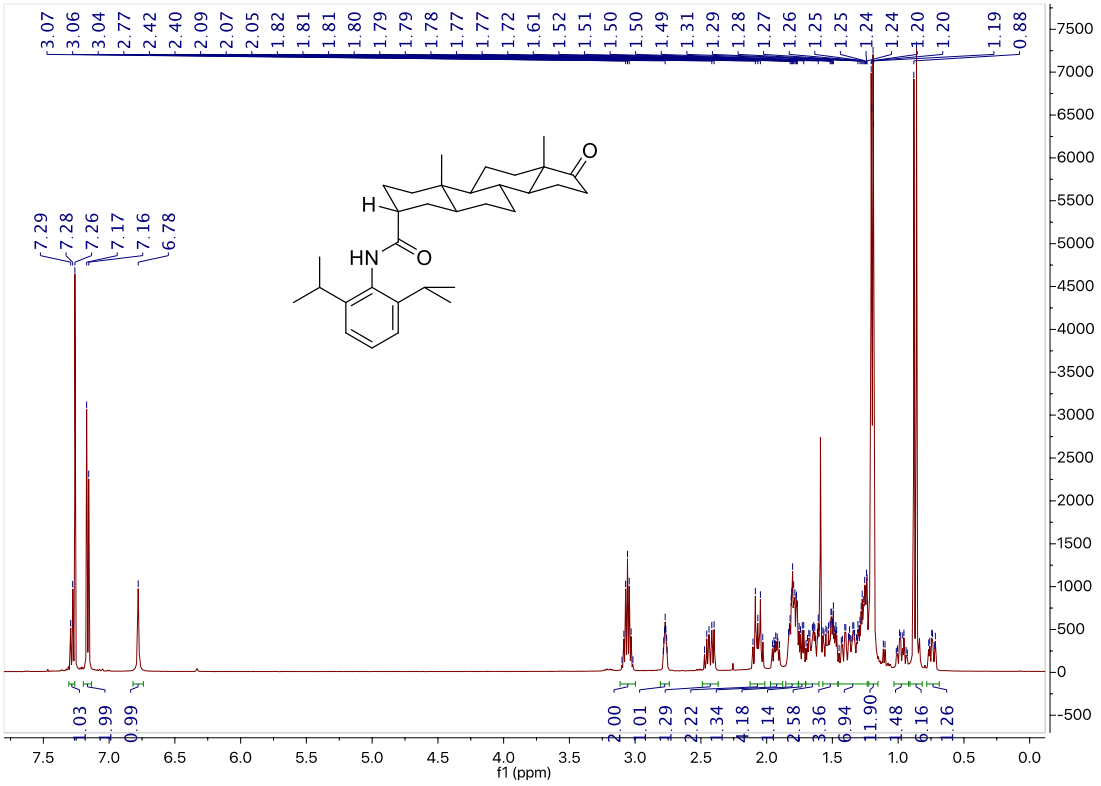

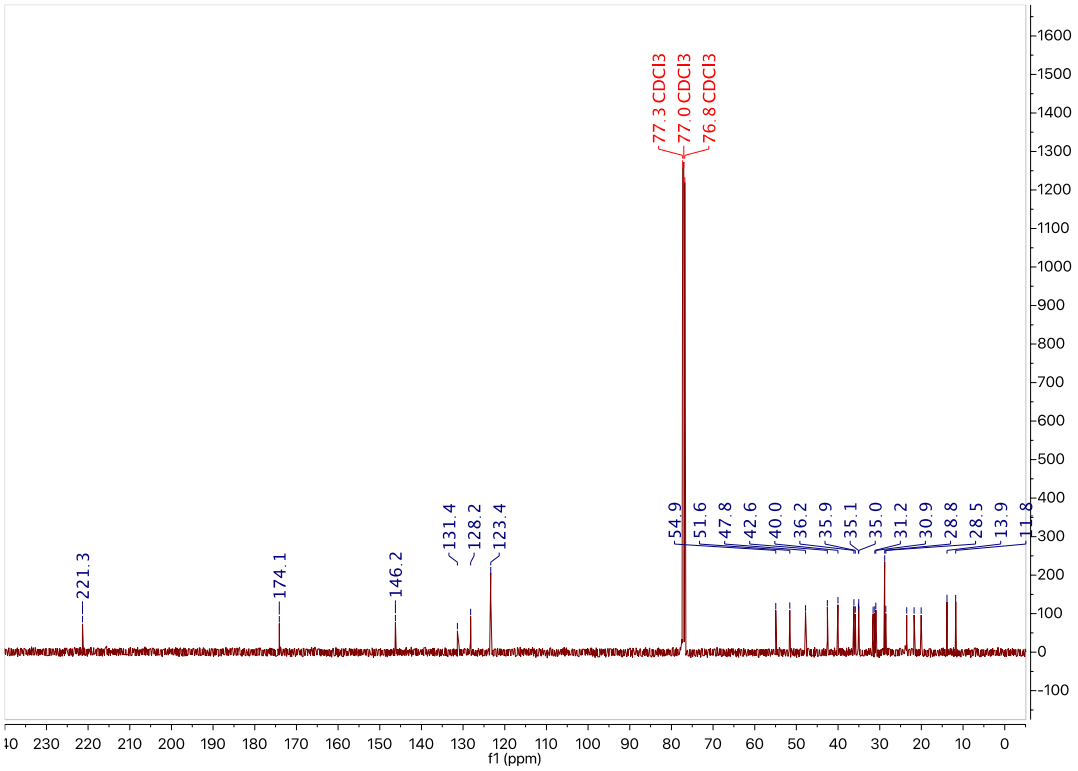

HMBC data for 5.1mm-a

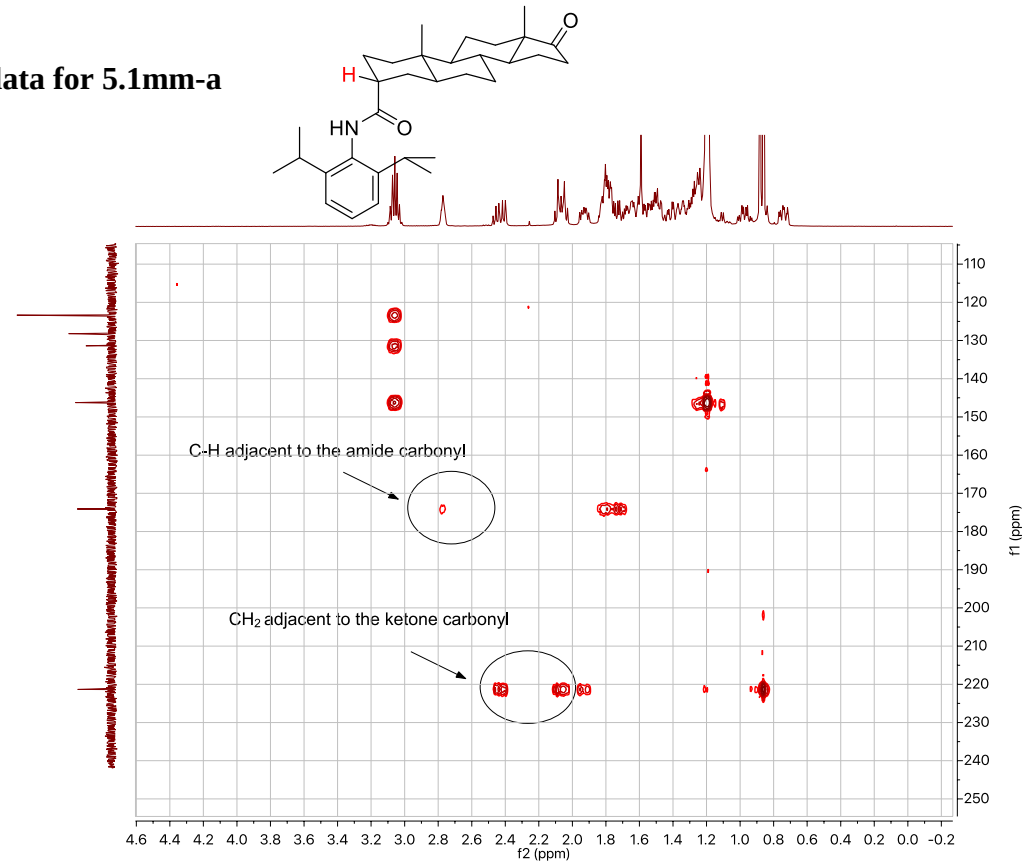

COSY data for 5.1mm-a

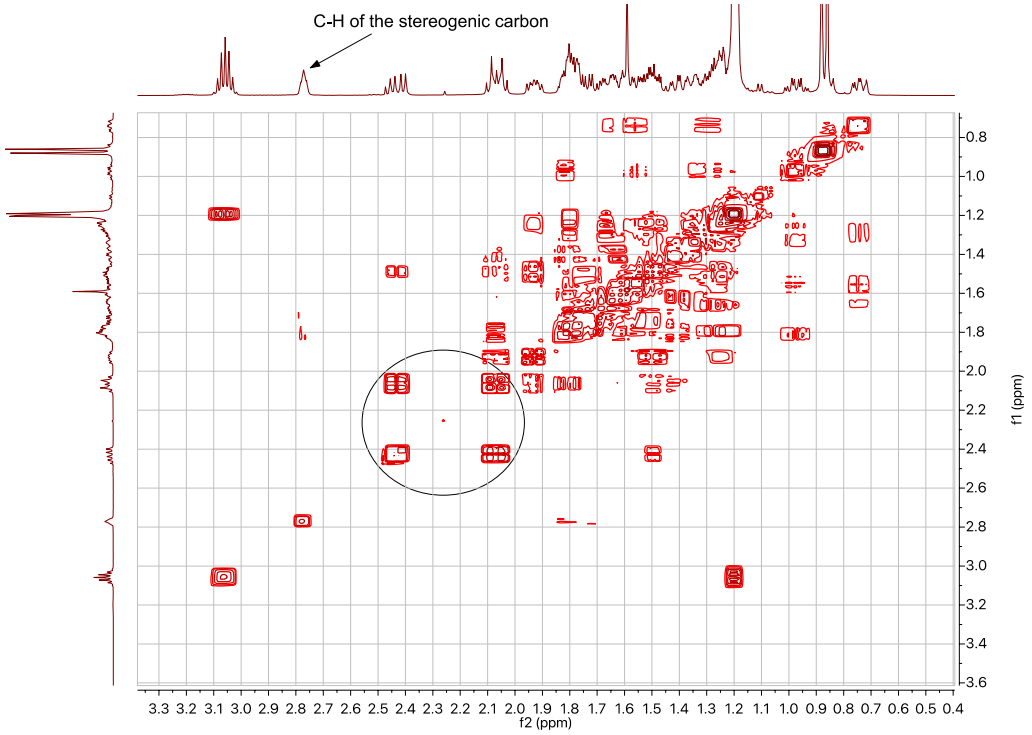

^{1}H and ^{13}C NMR data for 5.1mm-b

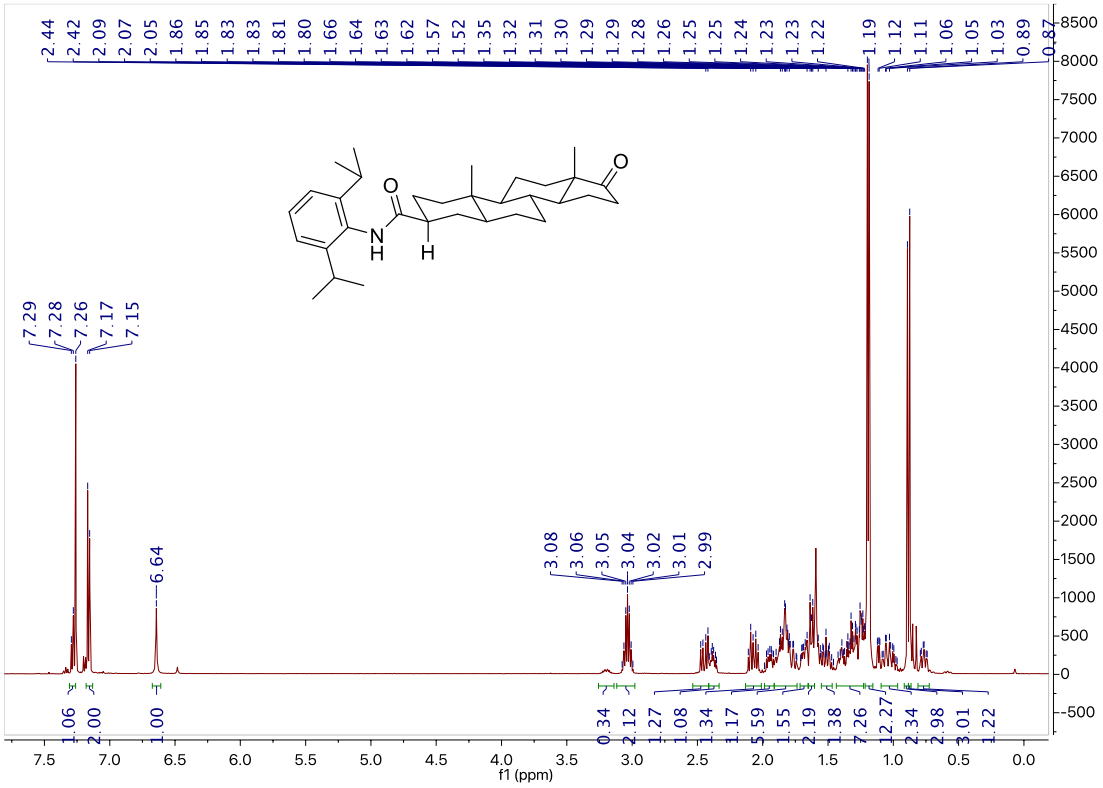

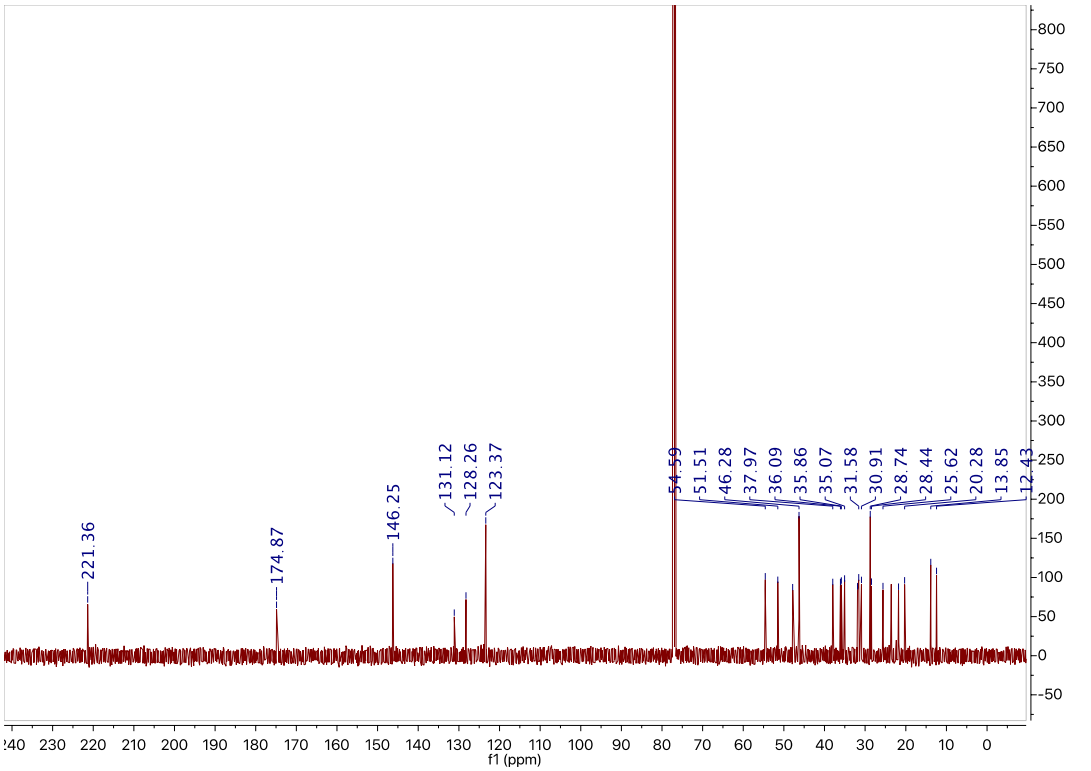

HMBC data for 5.1mm-b

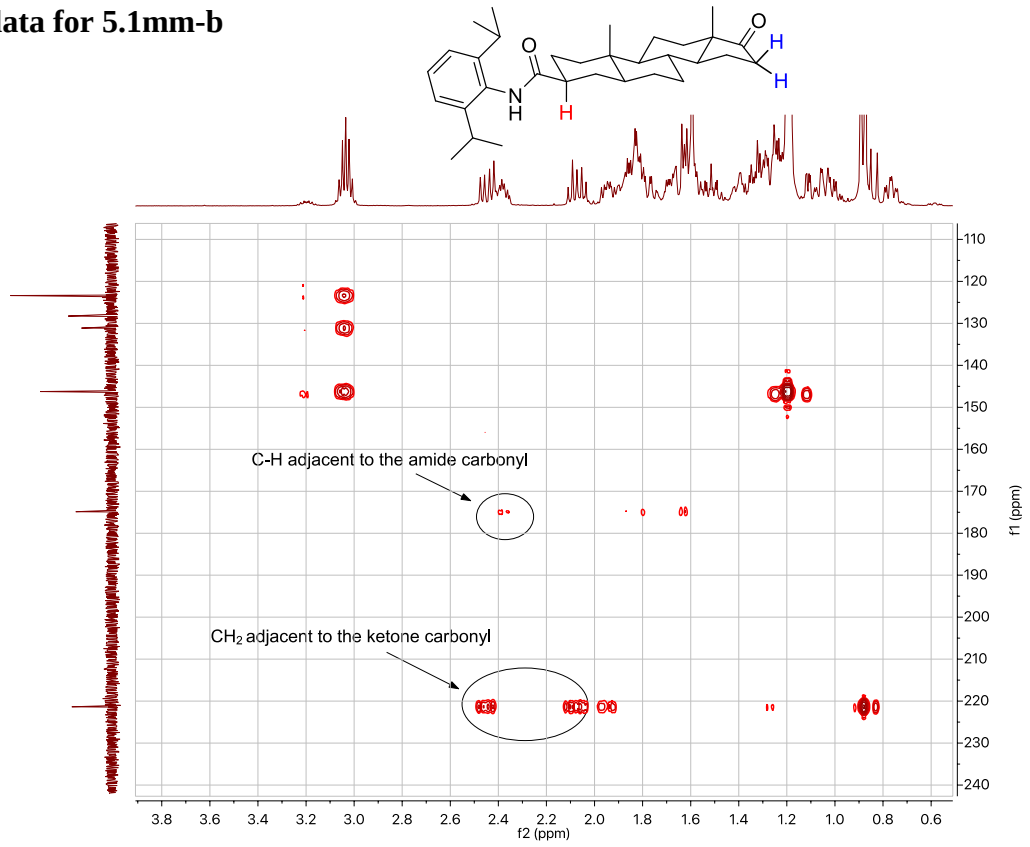

COSY data for 5.1mm-b

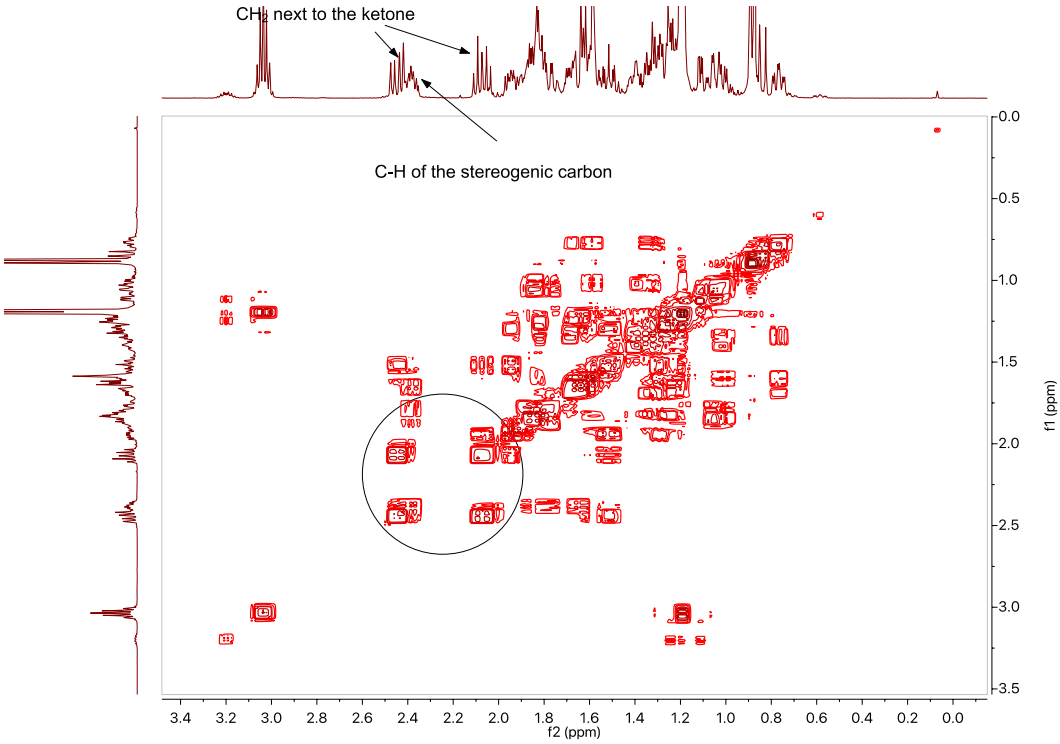

^{1}H and ^{13}C NMR data for 5.1nn

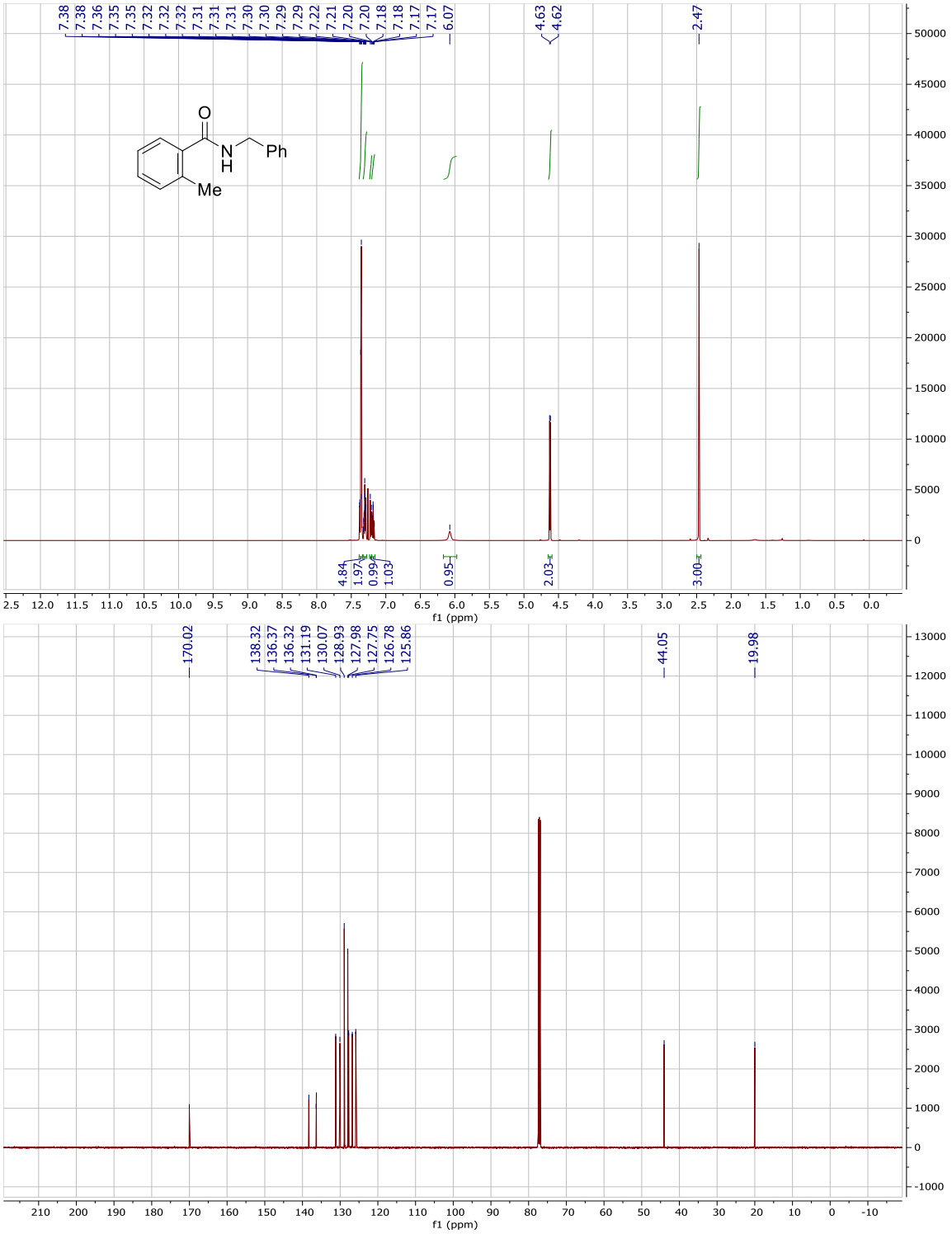

^{1}H and ^{13}C NMR data for 5.1oo

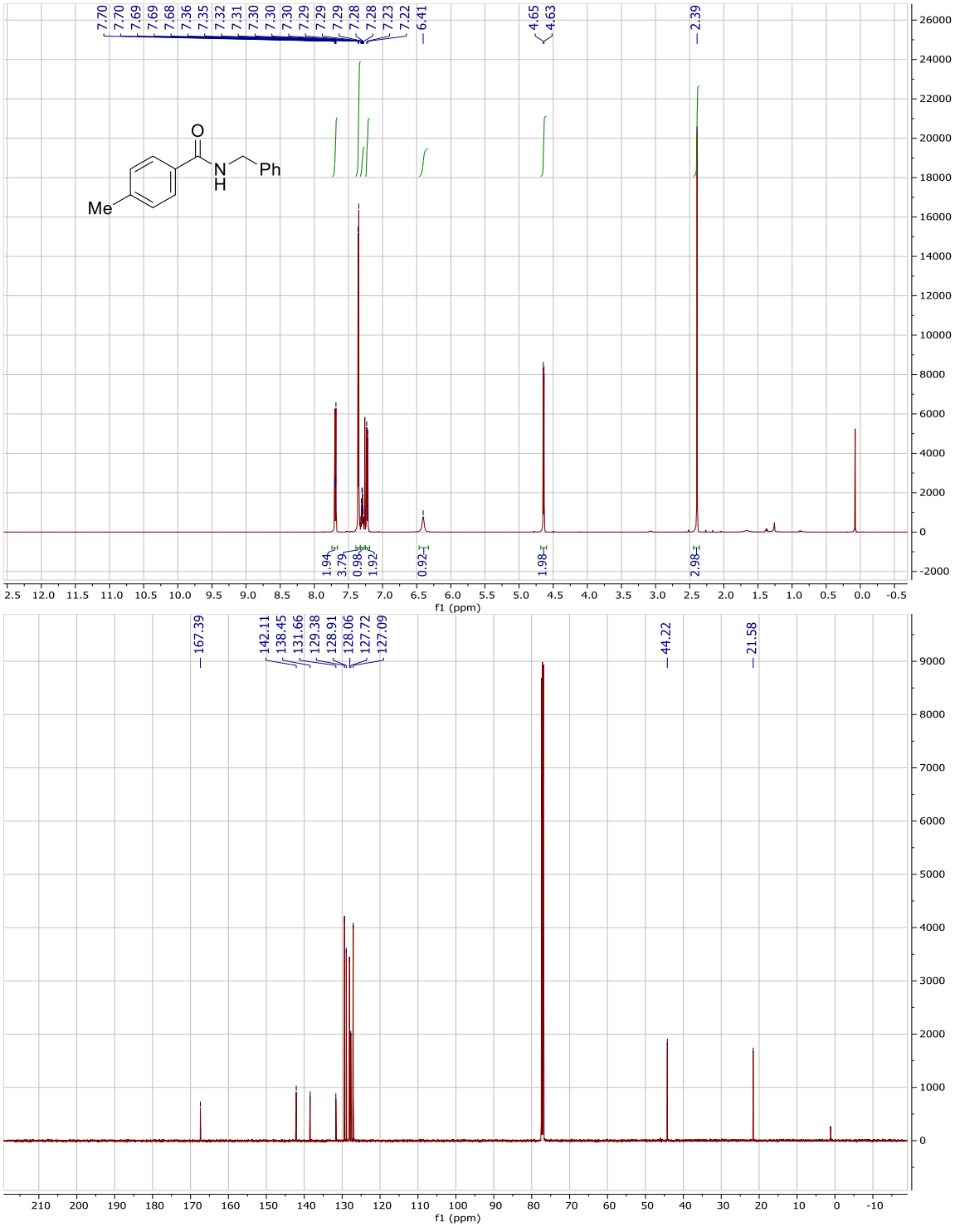

^{1}H and ^{13}C NMR data for 5.1pp

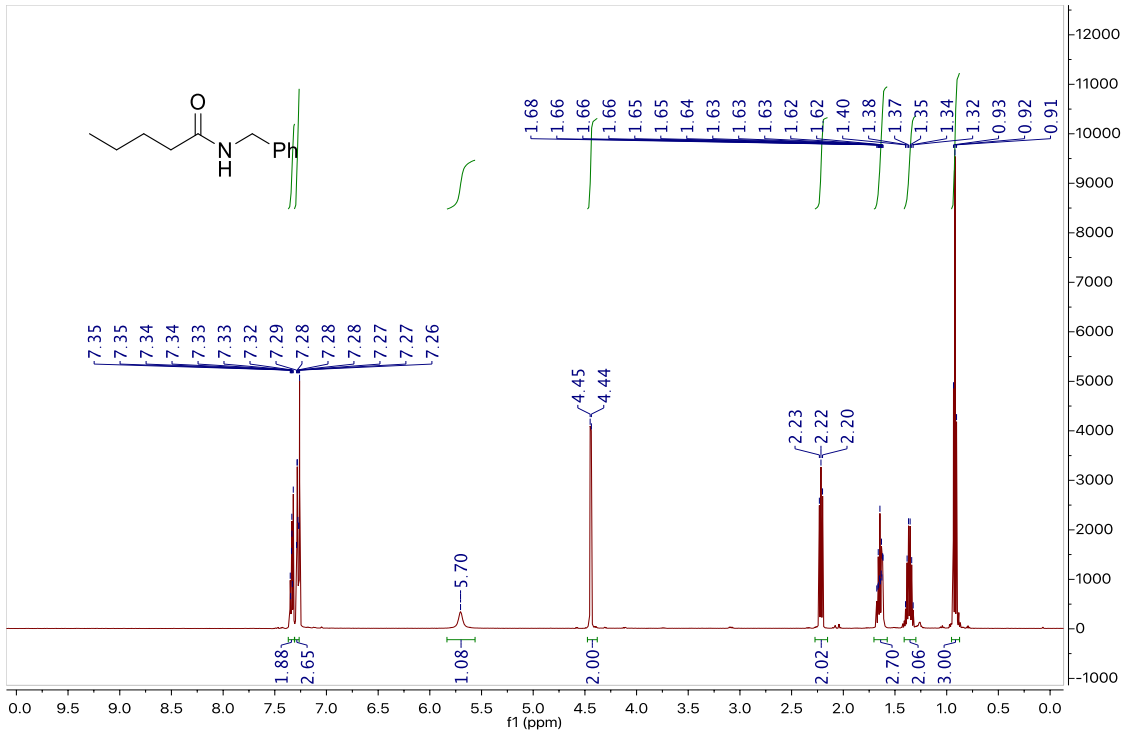

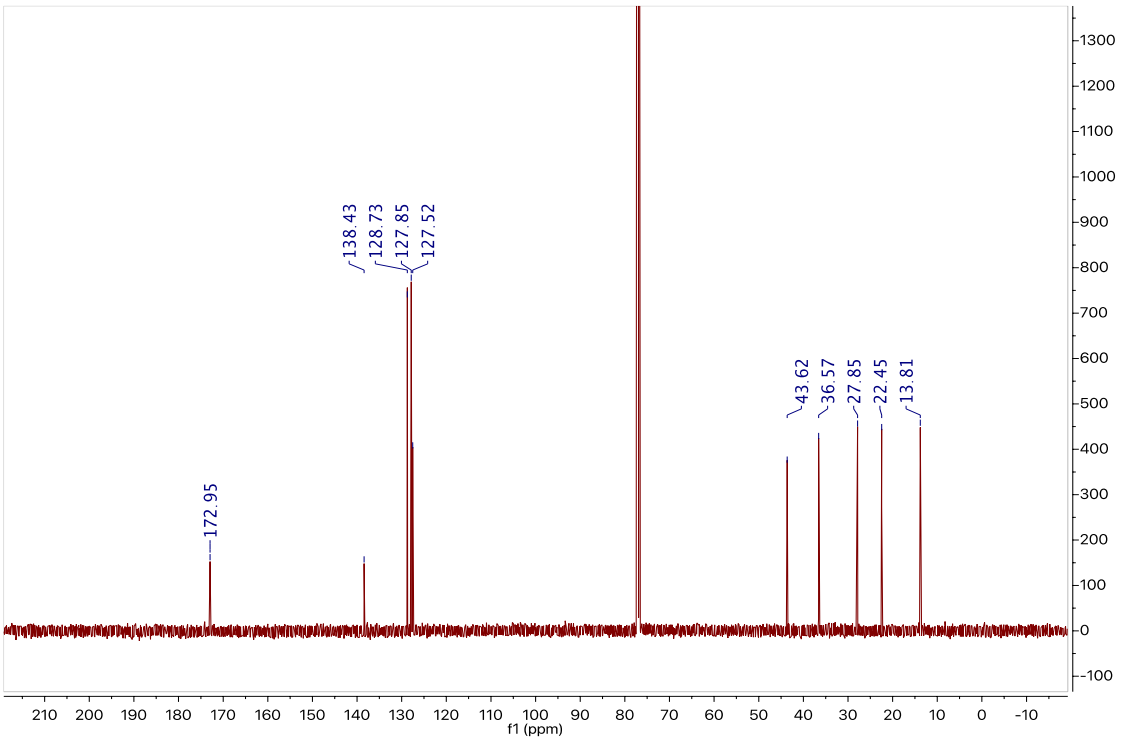

^{1}H and ^{13}C NMR data for 5.1qq

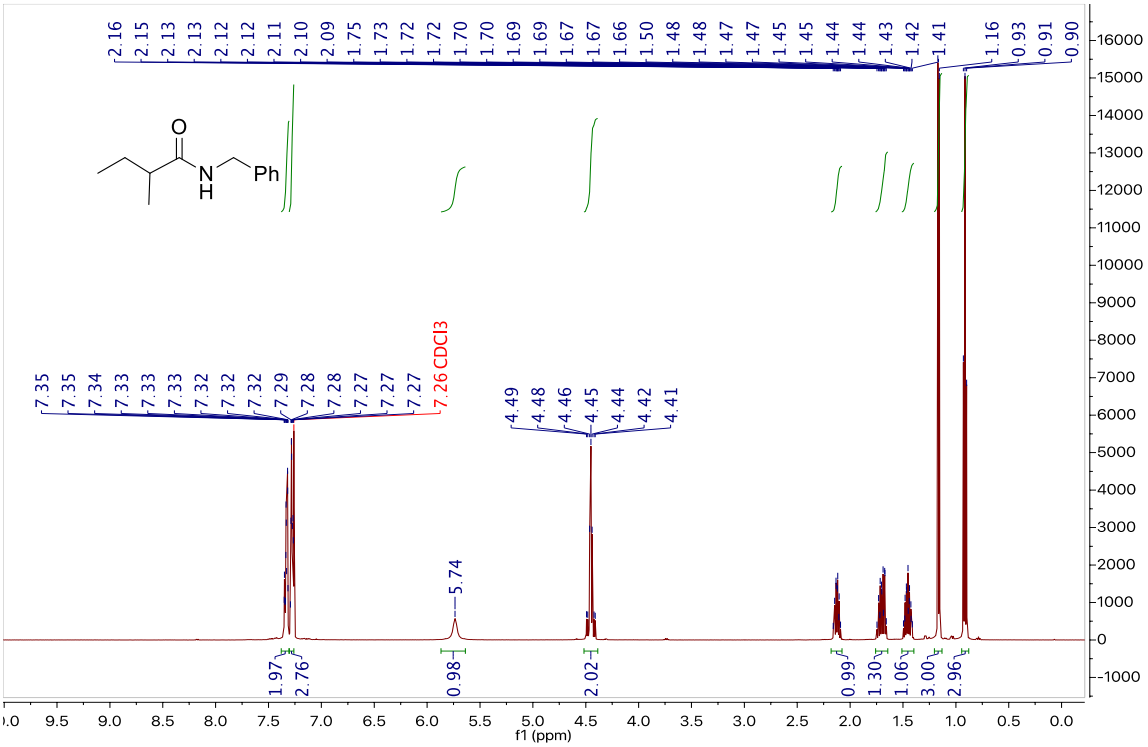

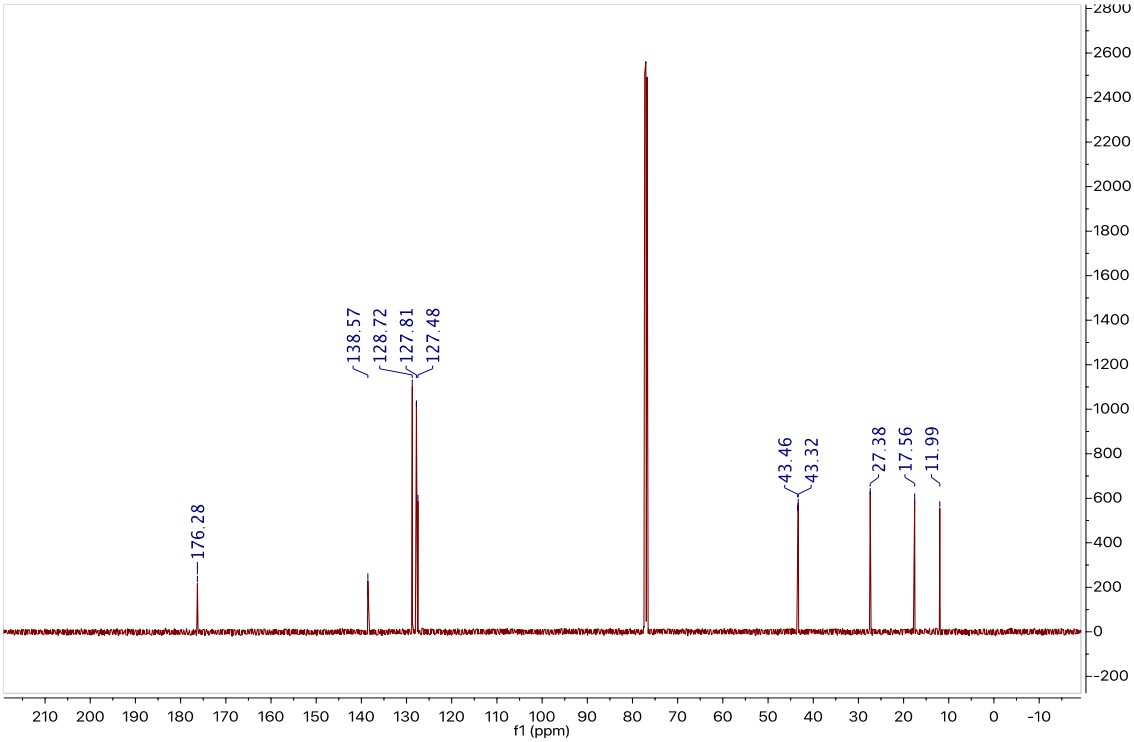

^{1}H and ^{13}C NMR data for 5.1rr

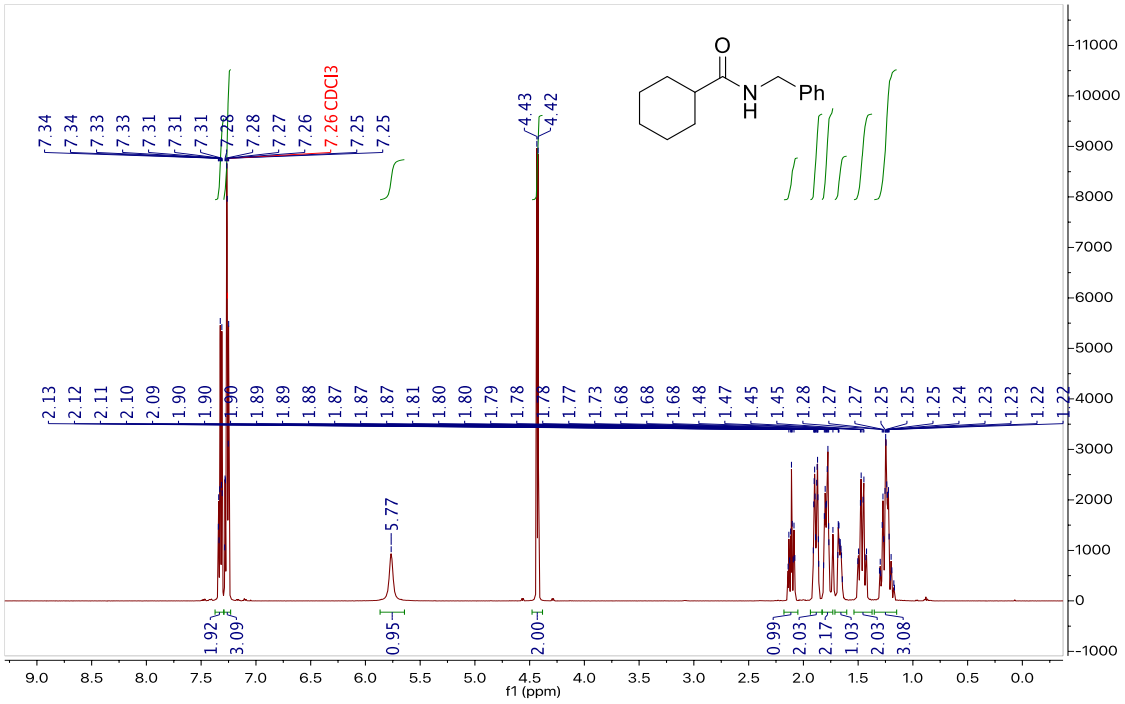

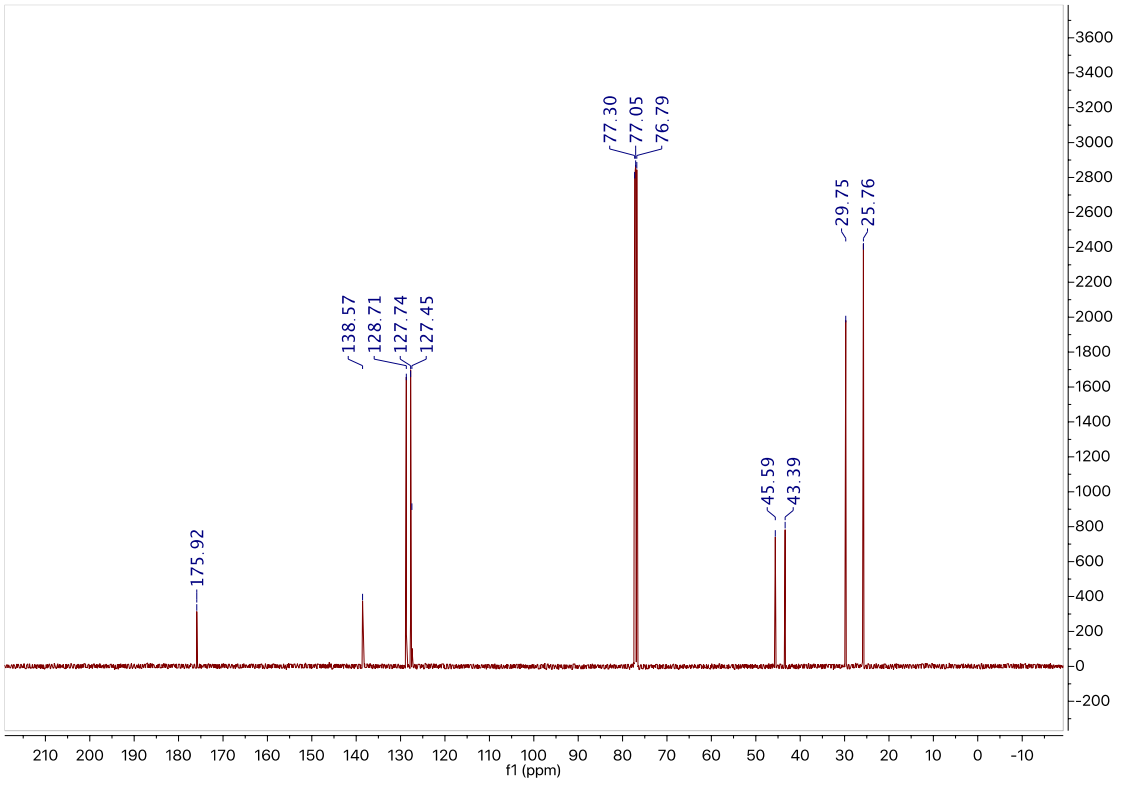

^{1}H and ^{13}C NMR data for 5.1ss

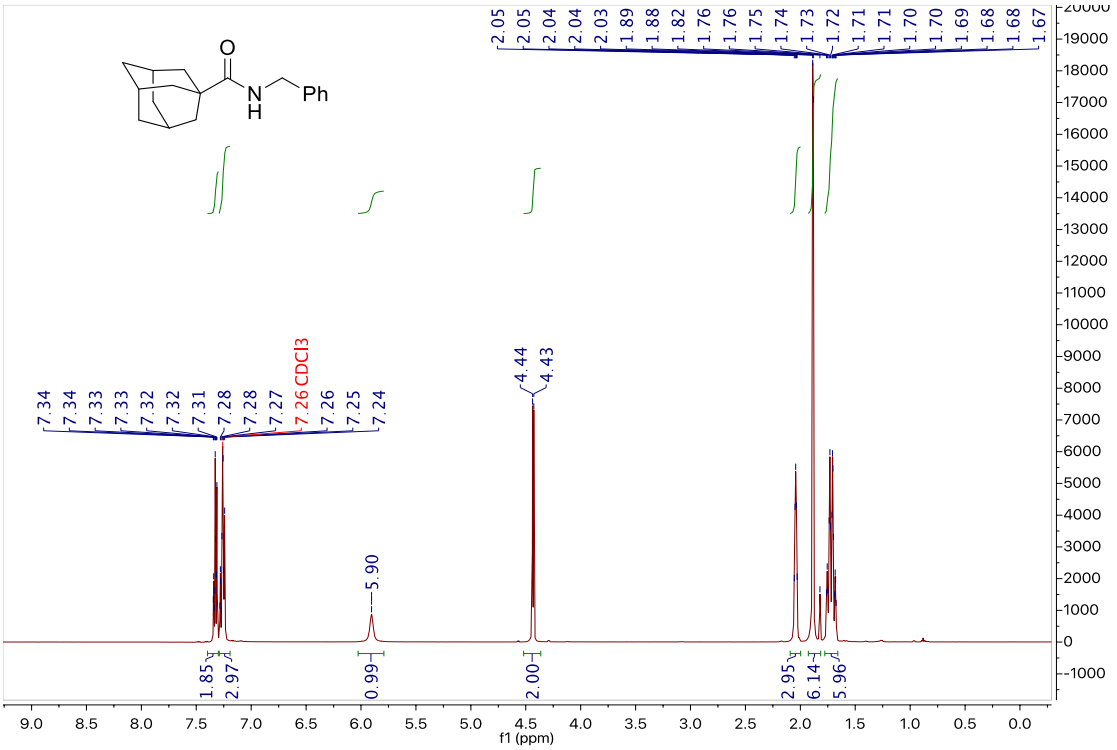

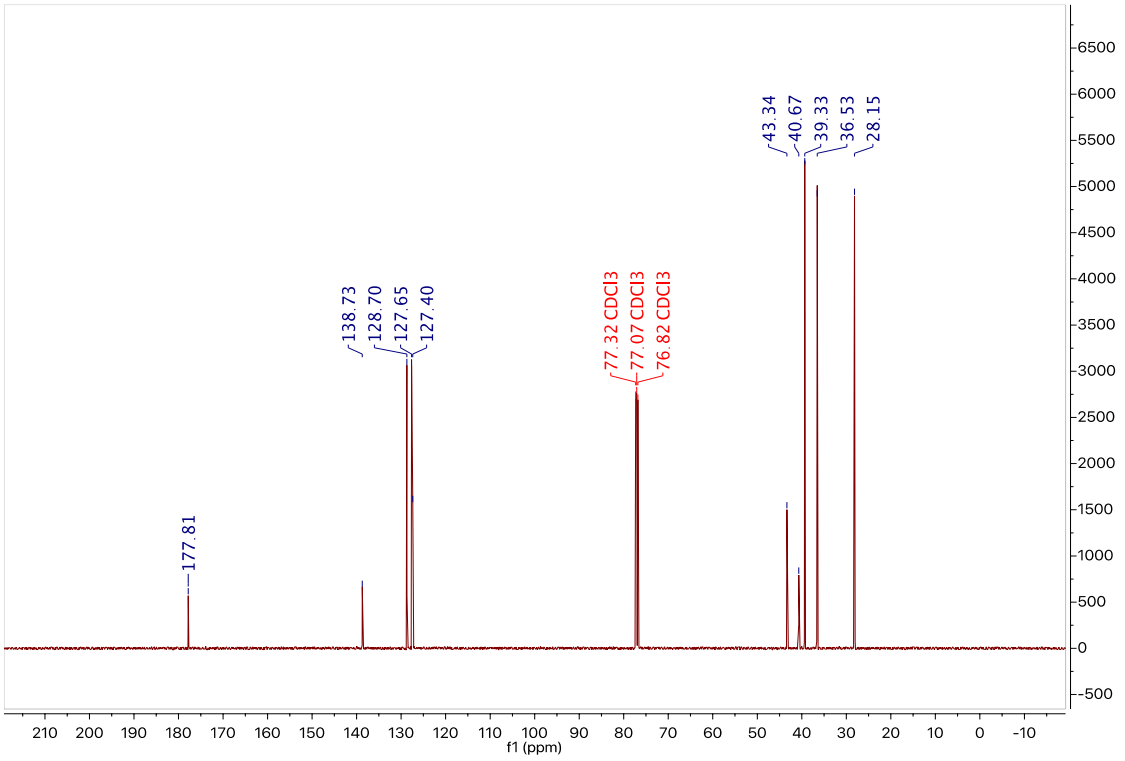

^{1}H and ^{13}C NMR data for 5.1tt

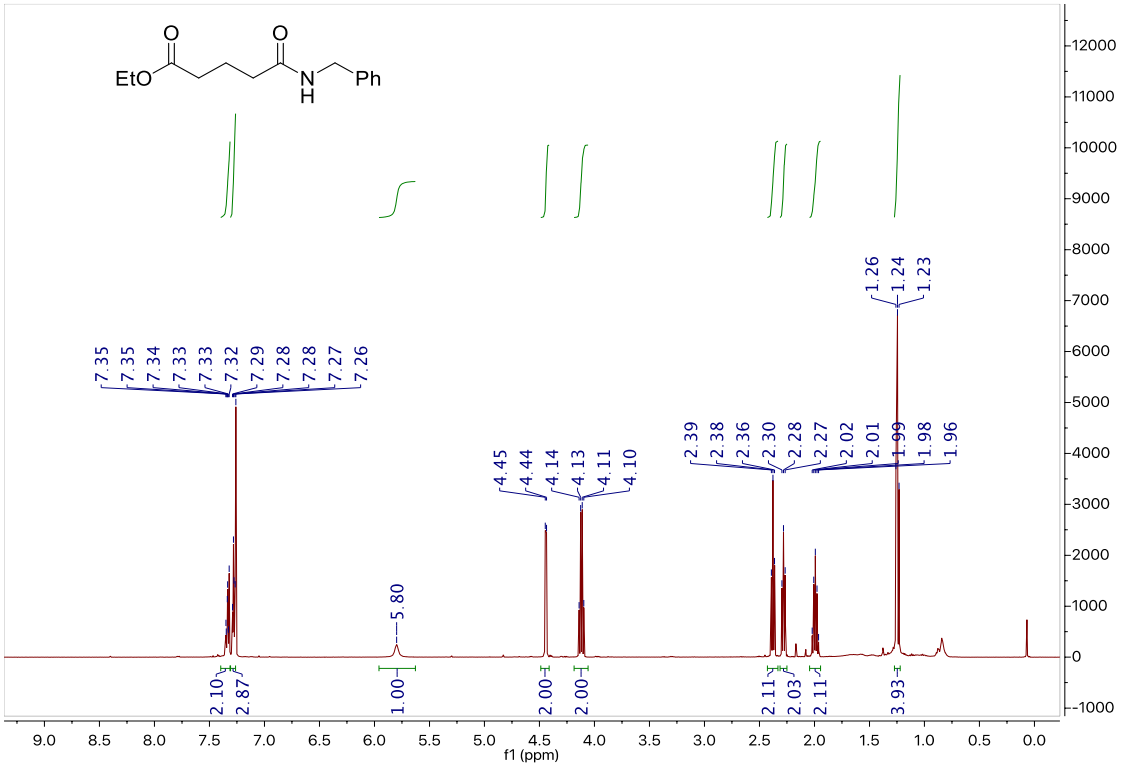

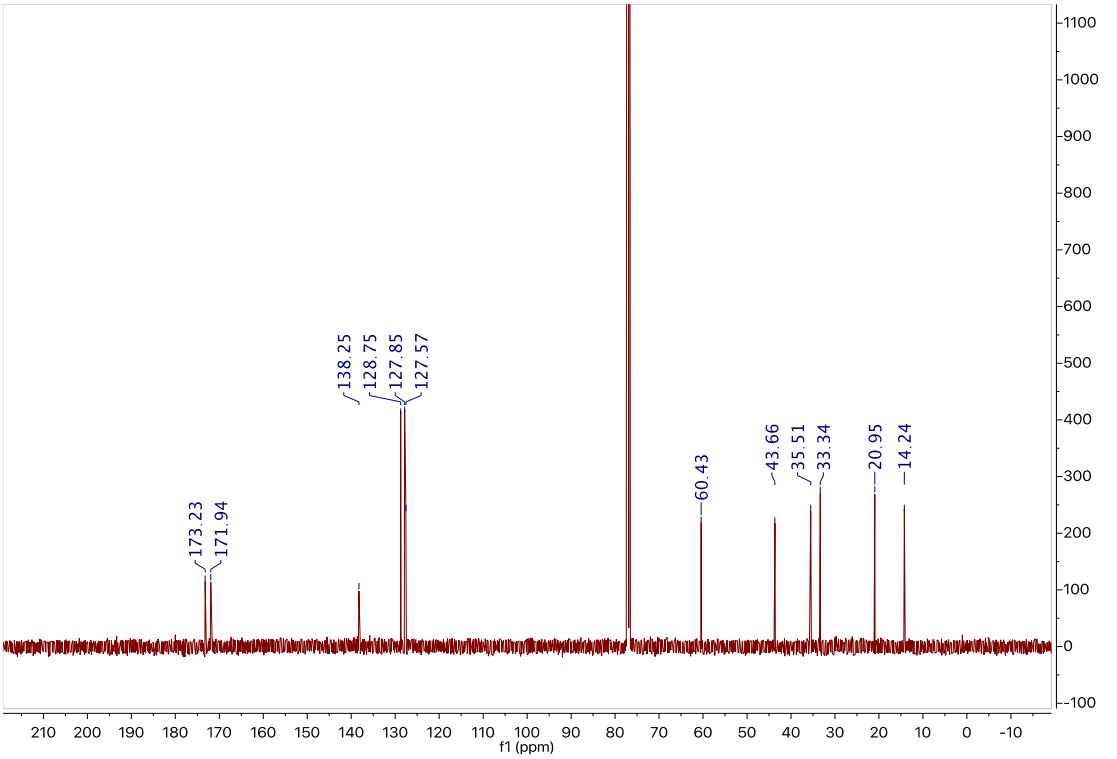

^{1}H and ^{13}C NMR data for S-octyl 4-methylbenzothioate (5.1uu)

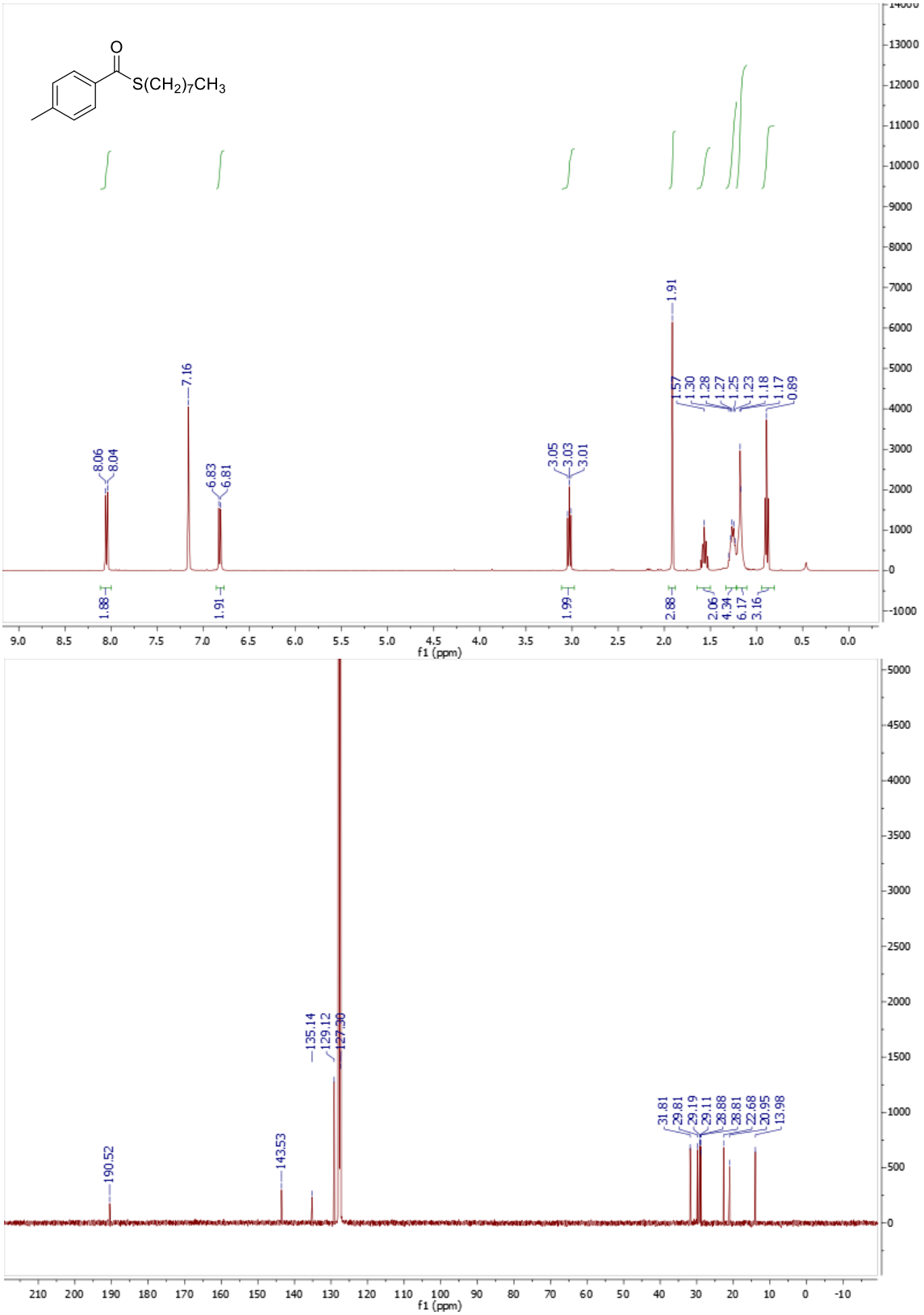

In-situ ^{1}H and ^{13}C NMR data for 5.2d

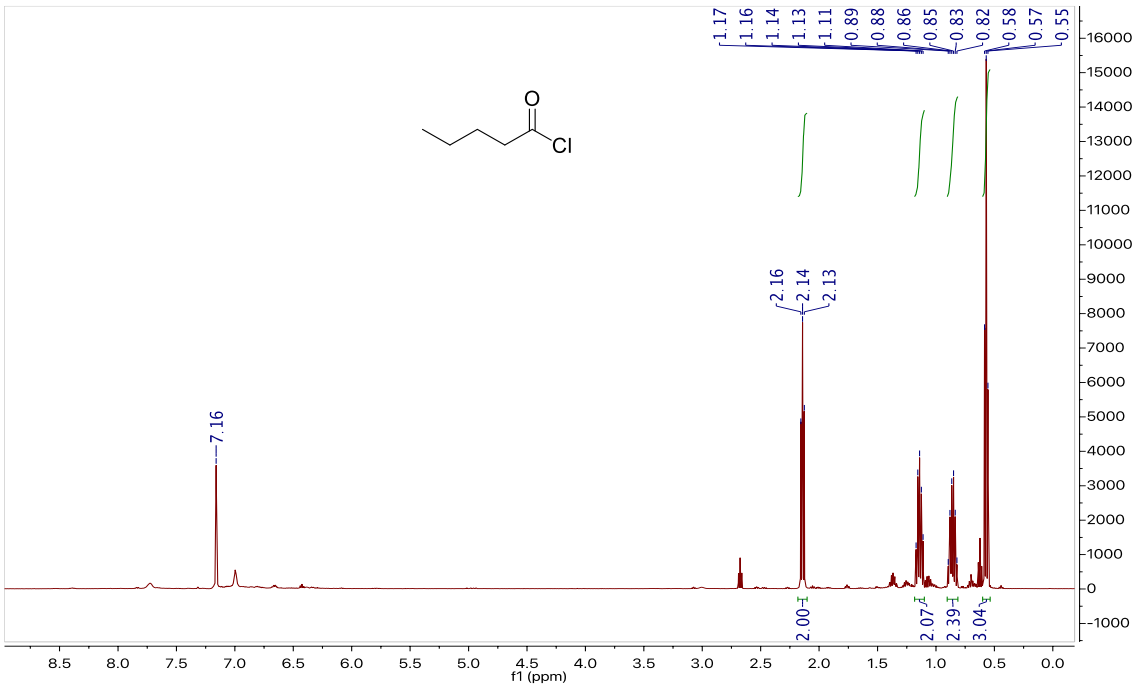

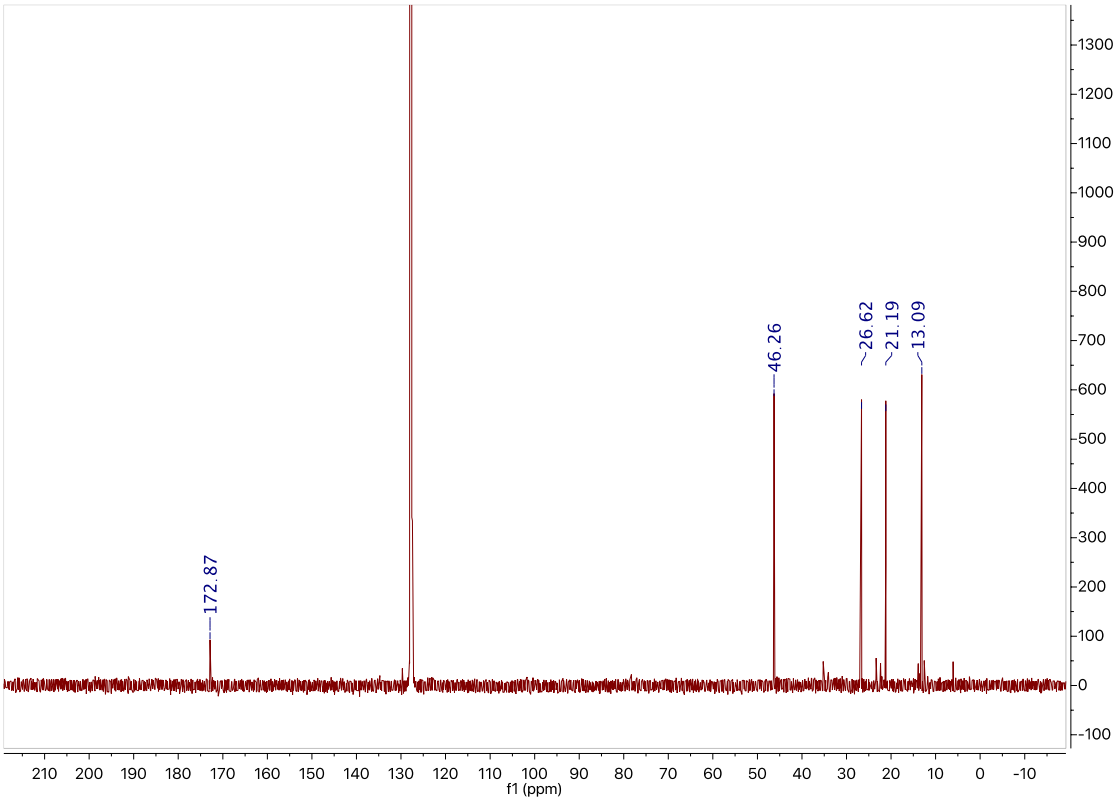

In-situ ^{1}H and ^{13}C NMR data for 5.2e

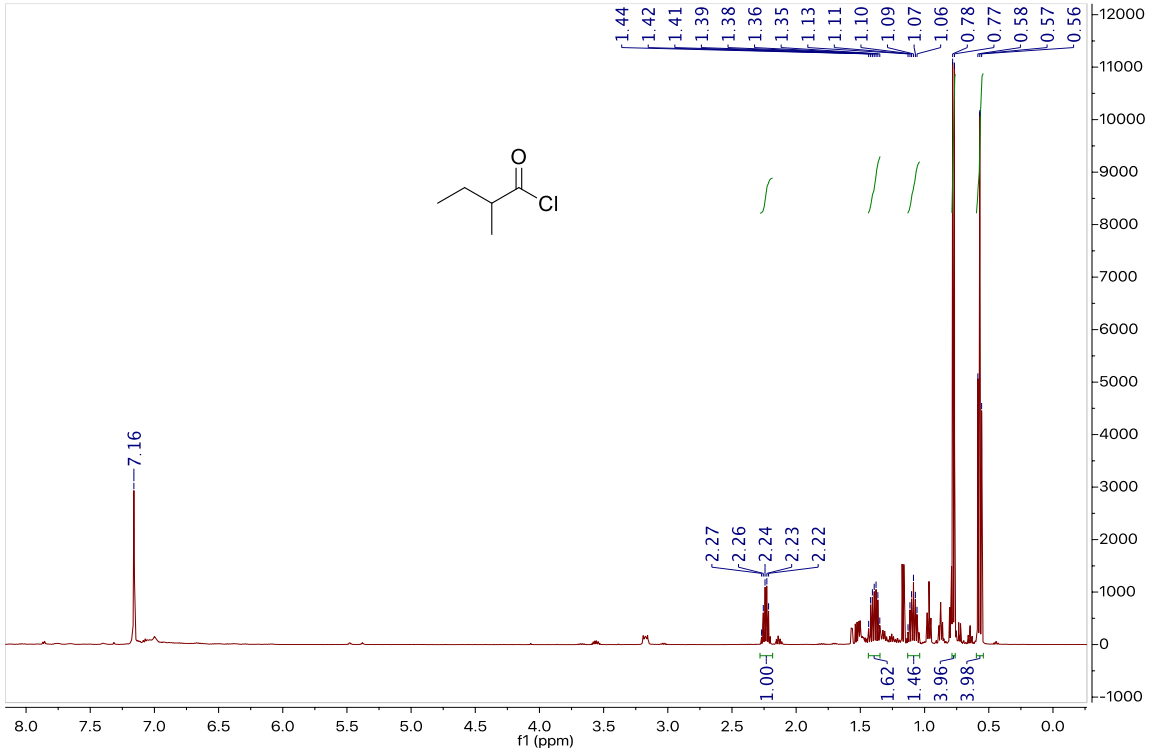

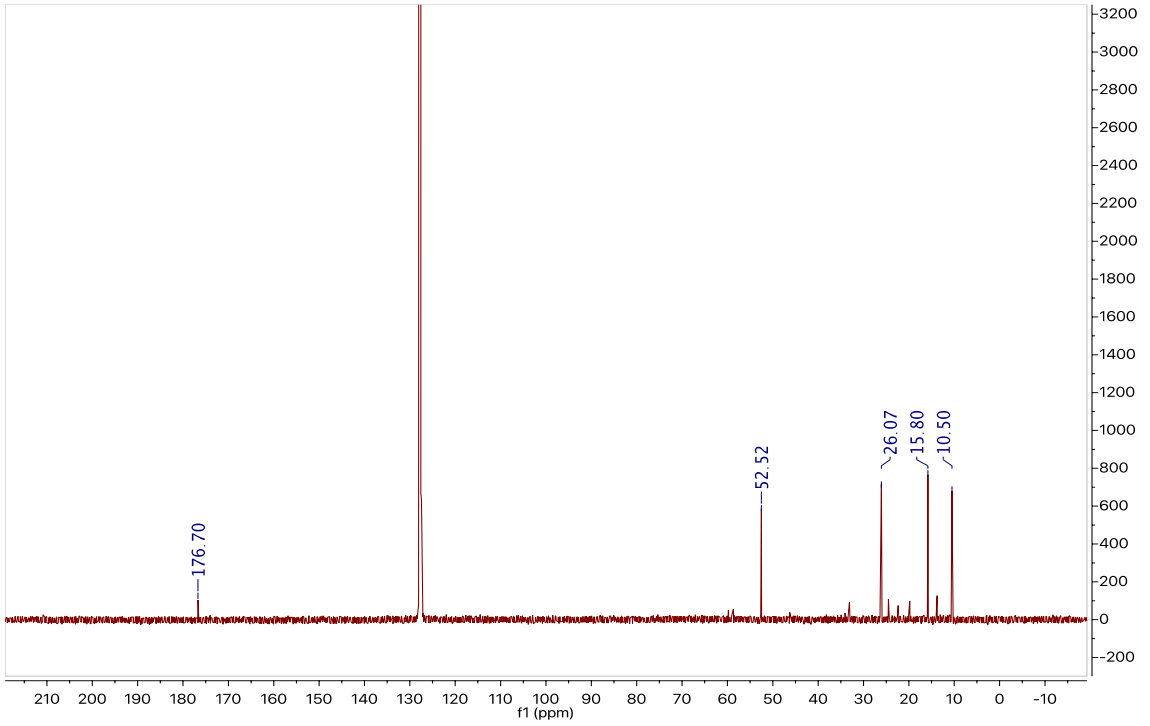

In-situ ^{1}H and ^{13}C NMR data for 5.2f

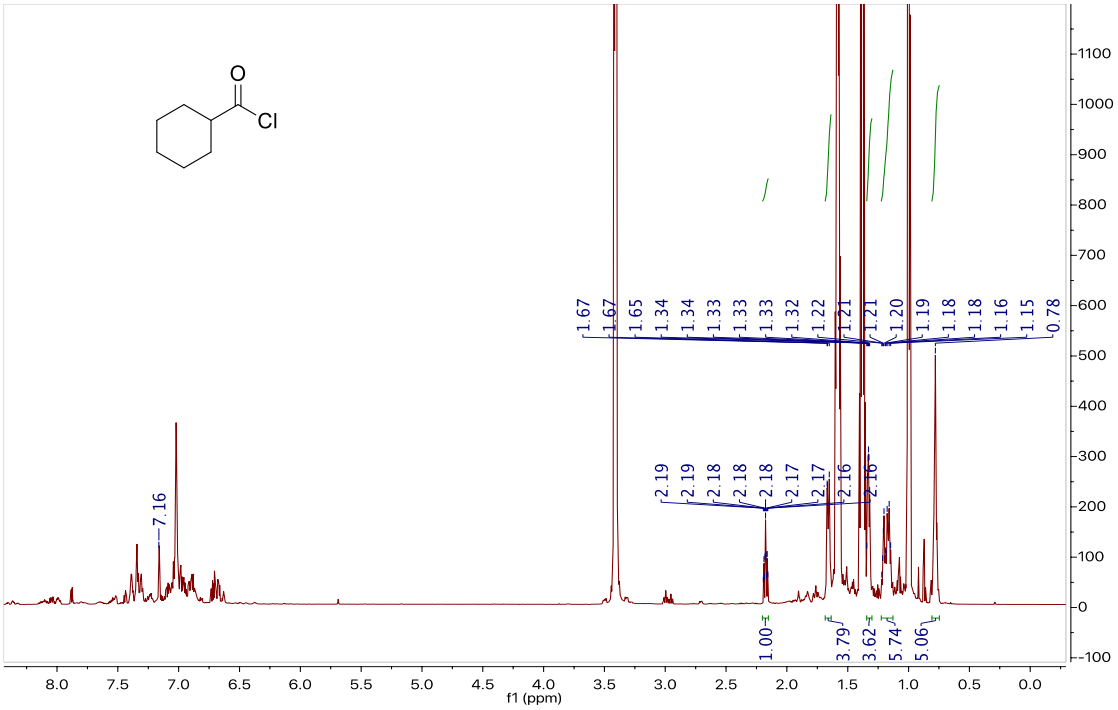

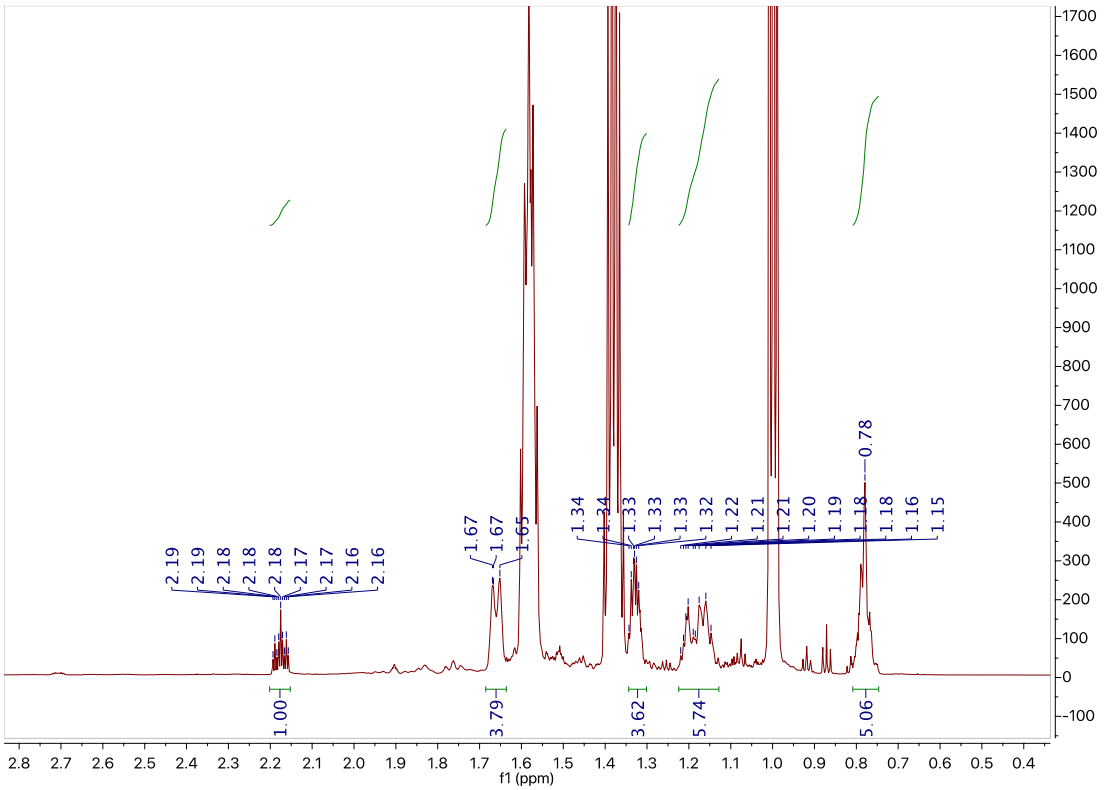

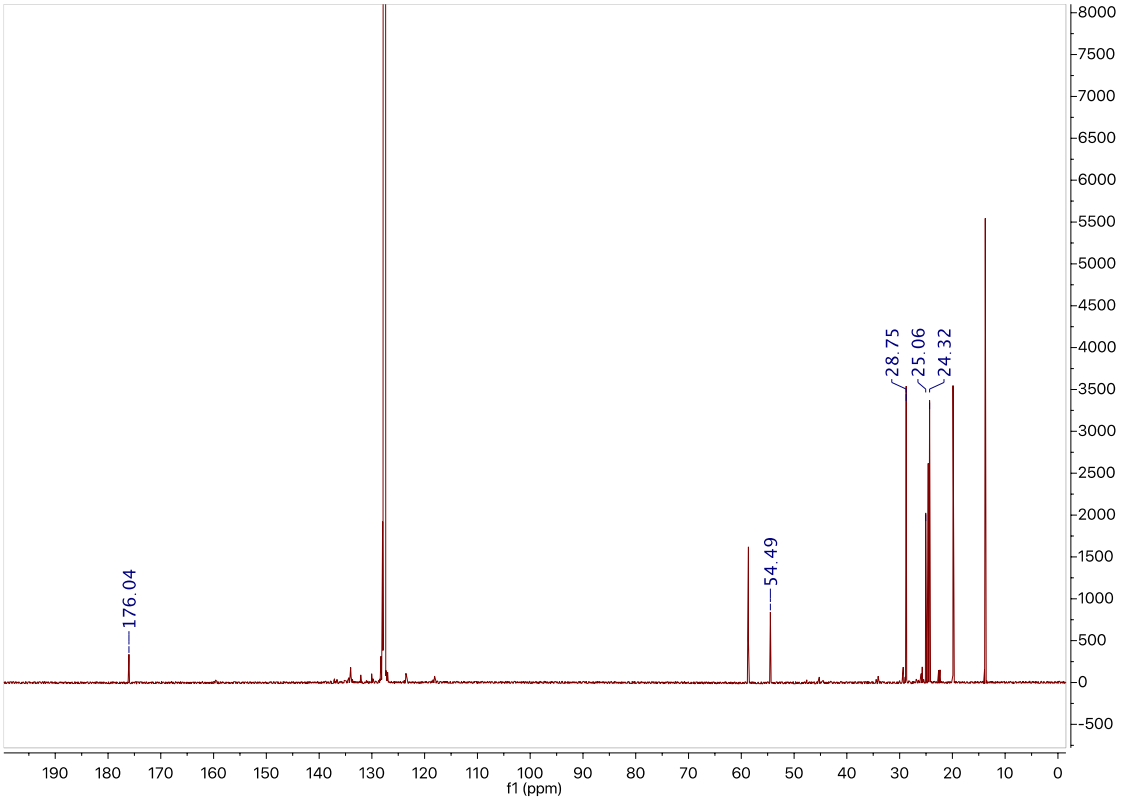
176.04
54.49
28.75
25.06
24.32
f1 (ppm)

In-situ ^{1}H and ^{13}C NMR data for 5.2g

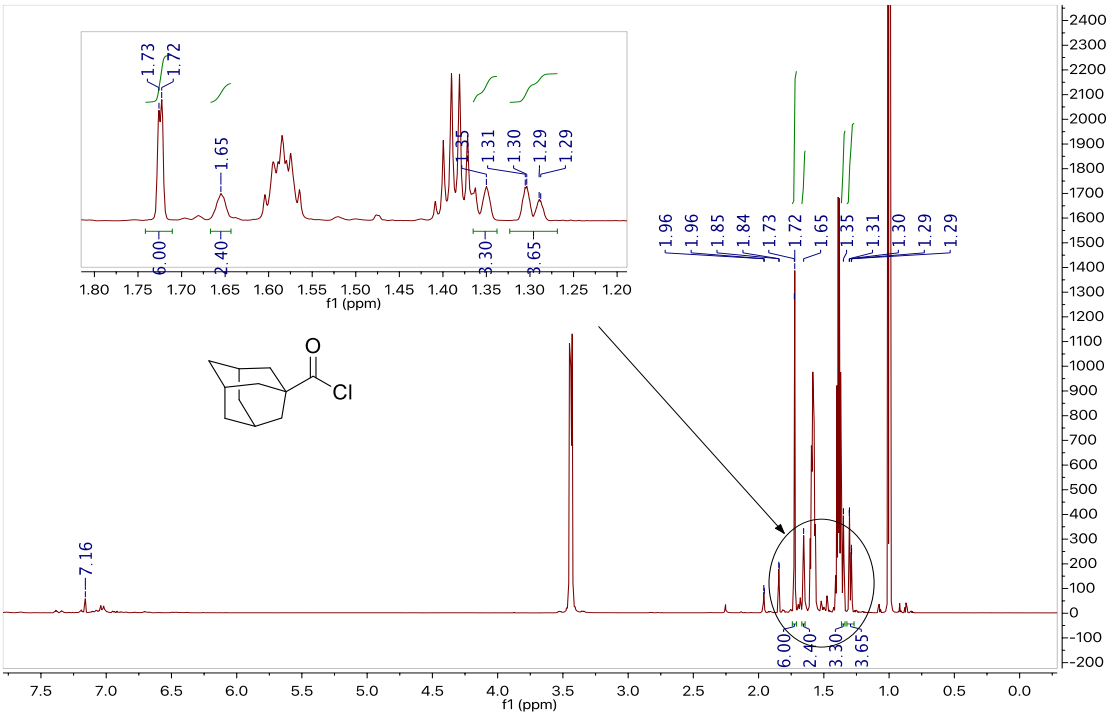

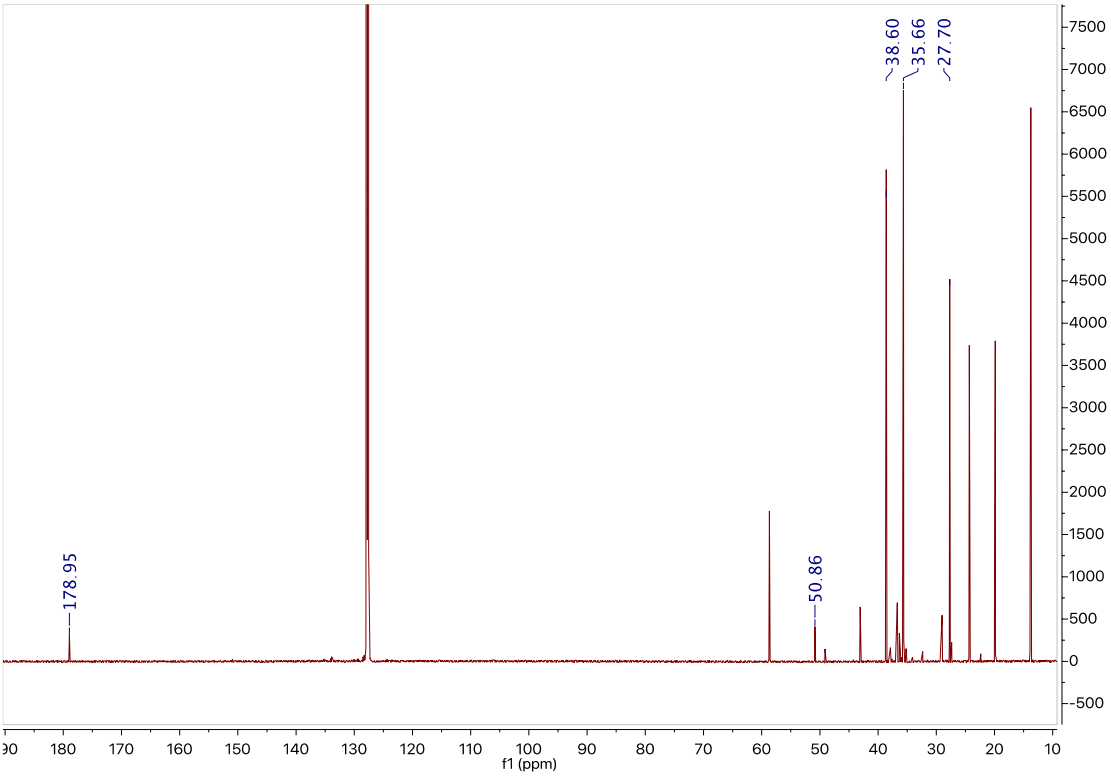

In-situ ^{1}H and ^{13}C NMR data for 5.2h

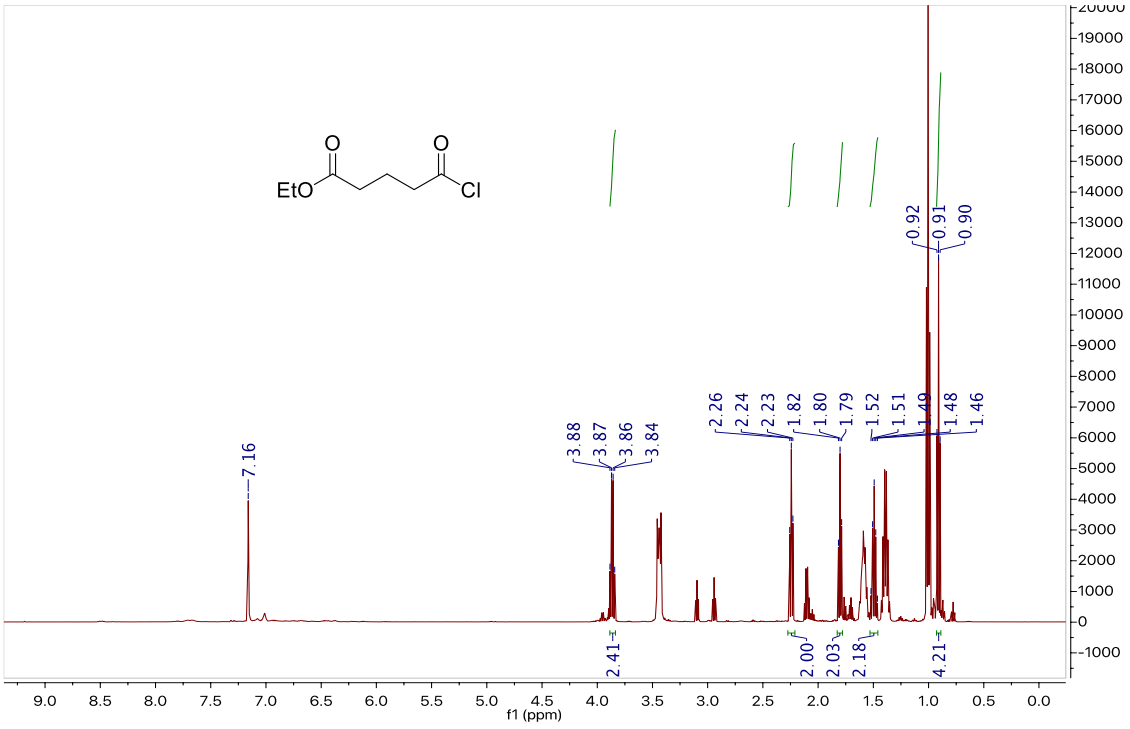

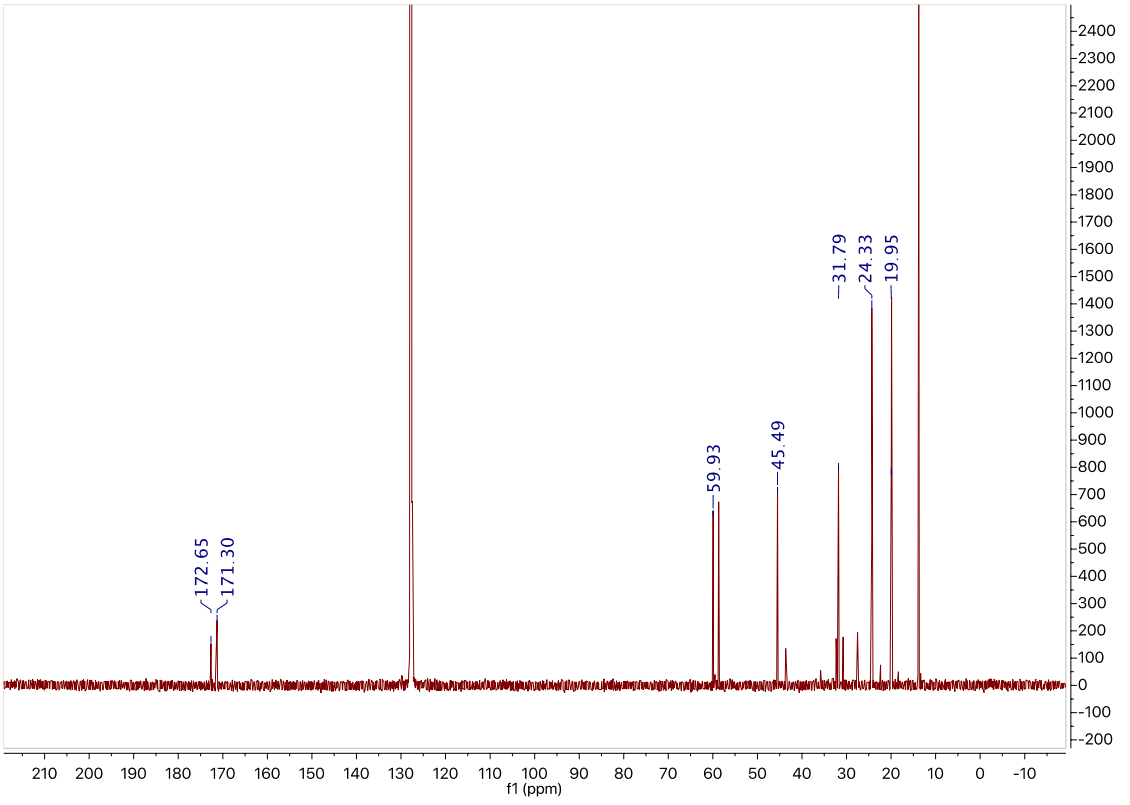

In-situ ^{1}H and ^{13}C NMR data for 5.2i

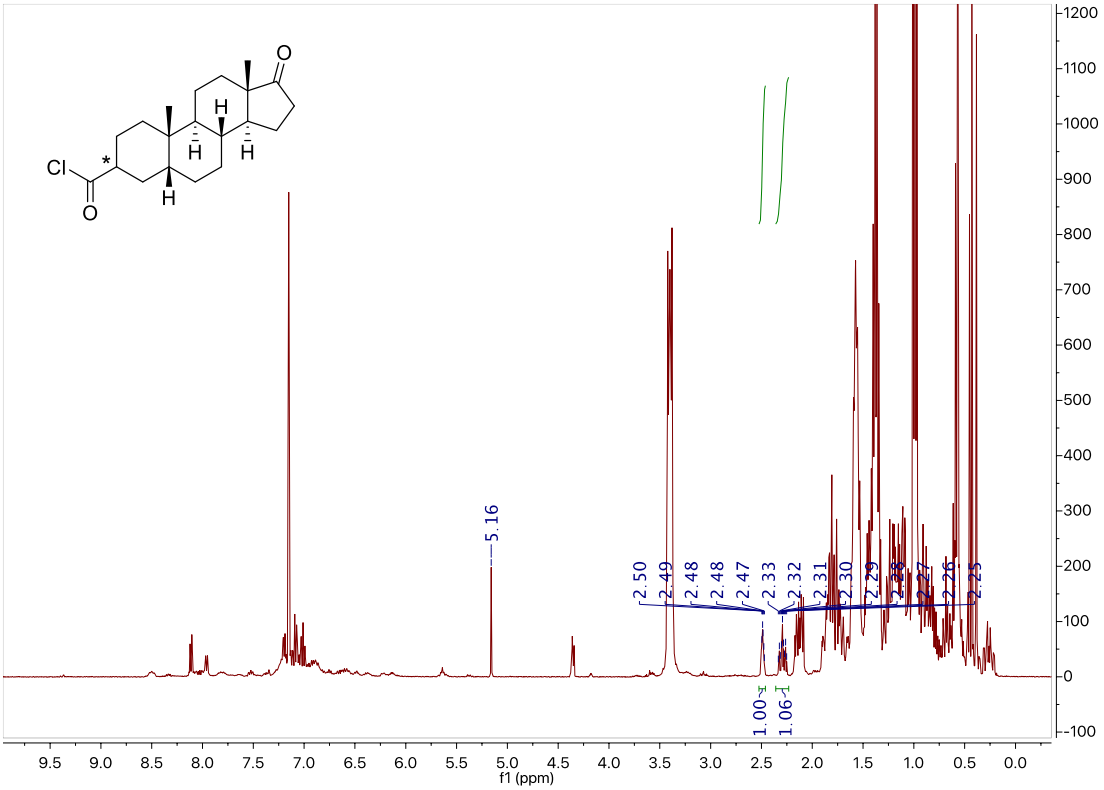

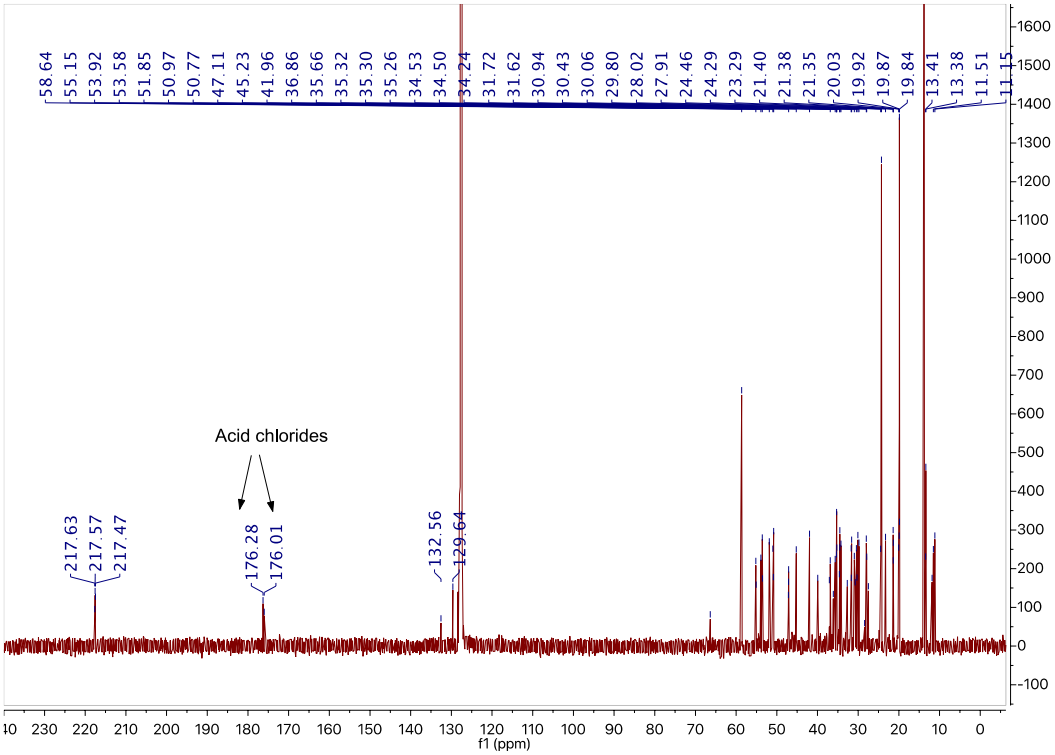

^{1}H, ^{13}C, and ^{31}P NMR data for 5.3b

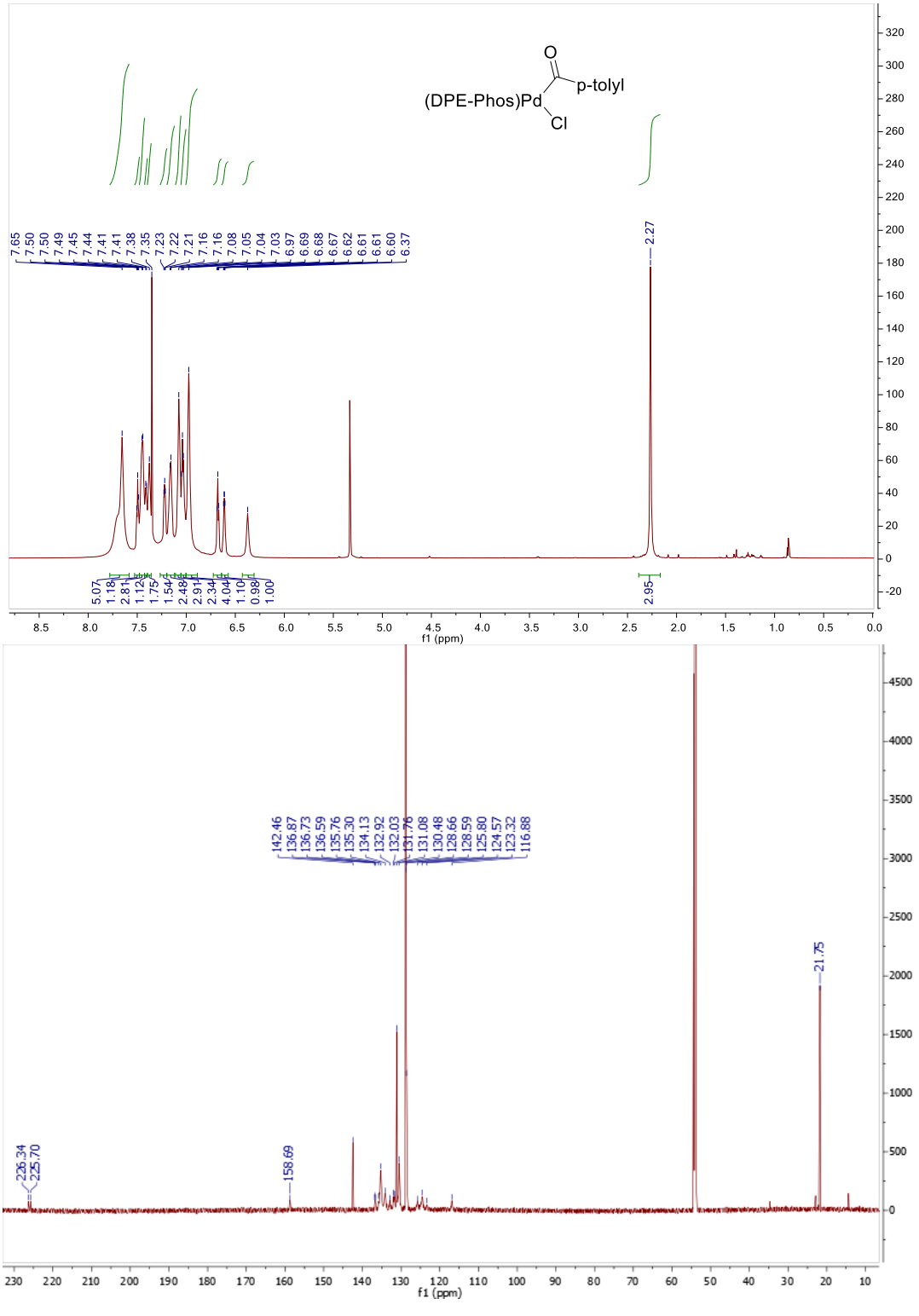

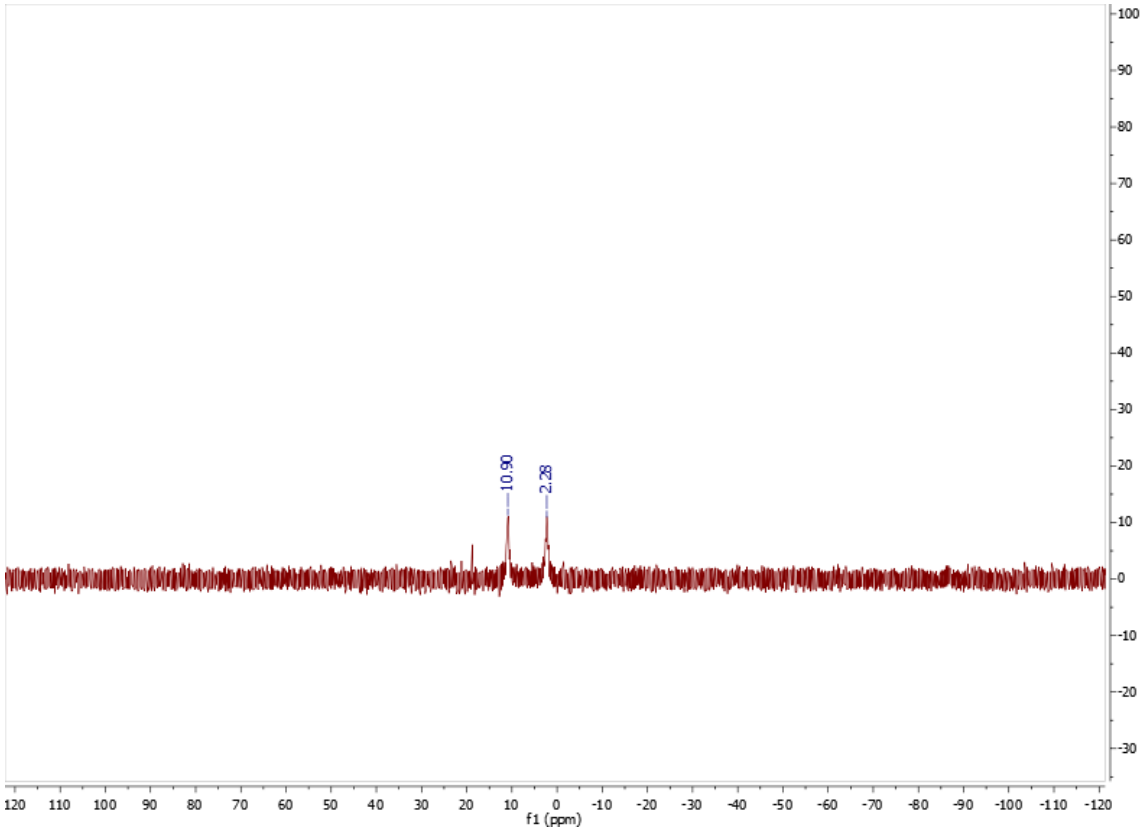
10.90
2.28
f1 (ppm)

^{1}H, ^{13}C, and ^{31}P NMR data for 5.3c

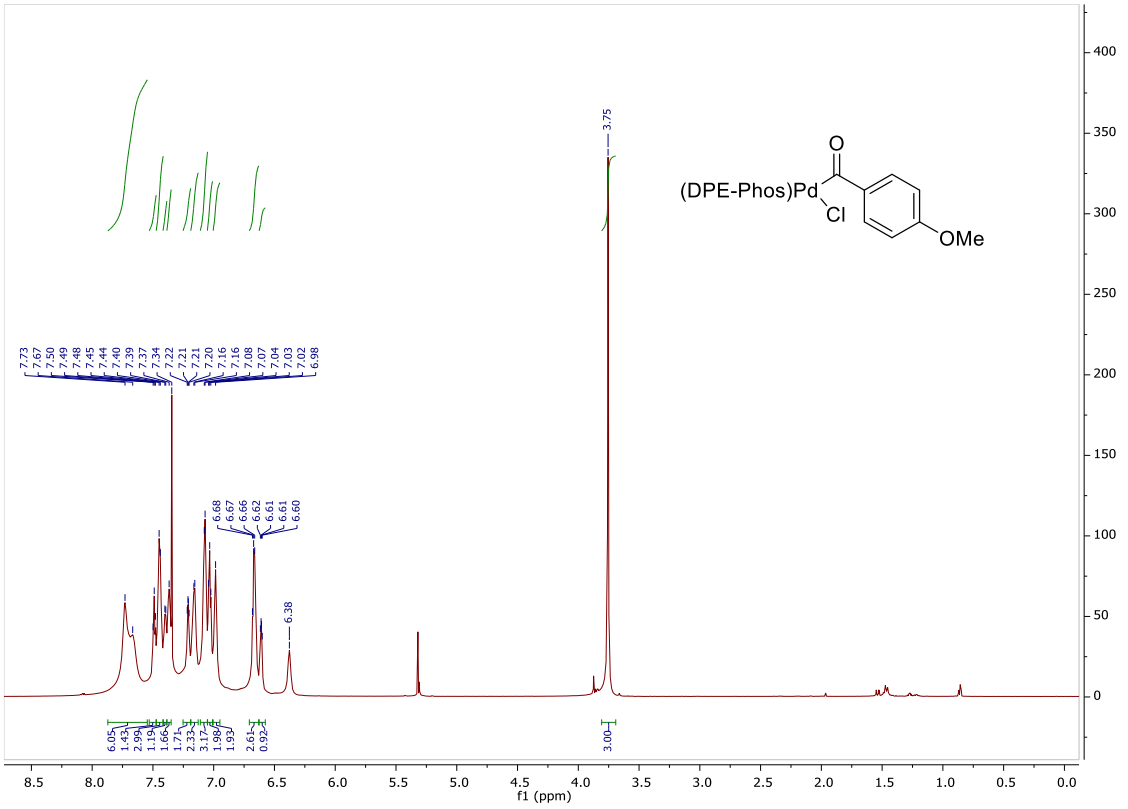

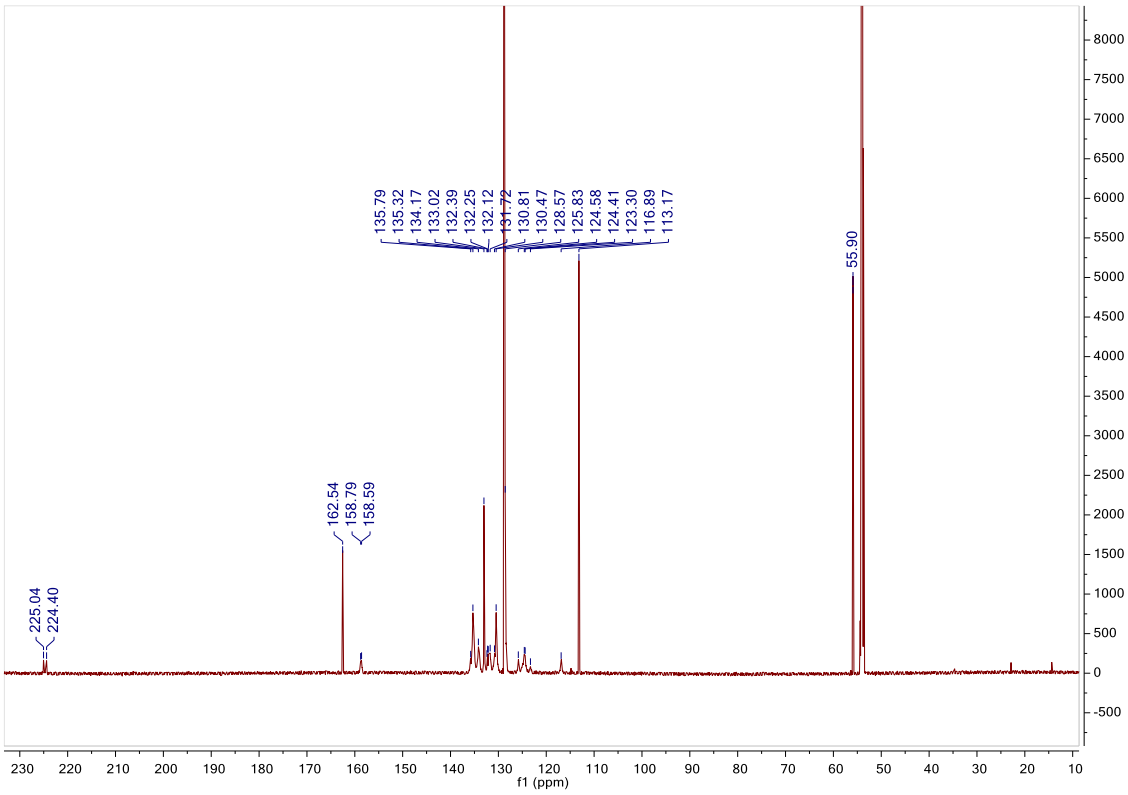

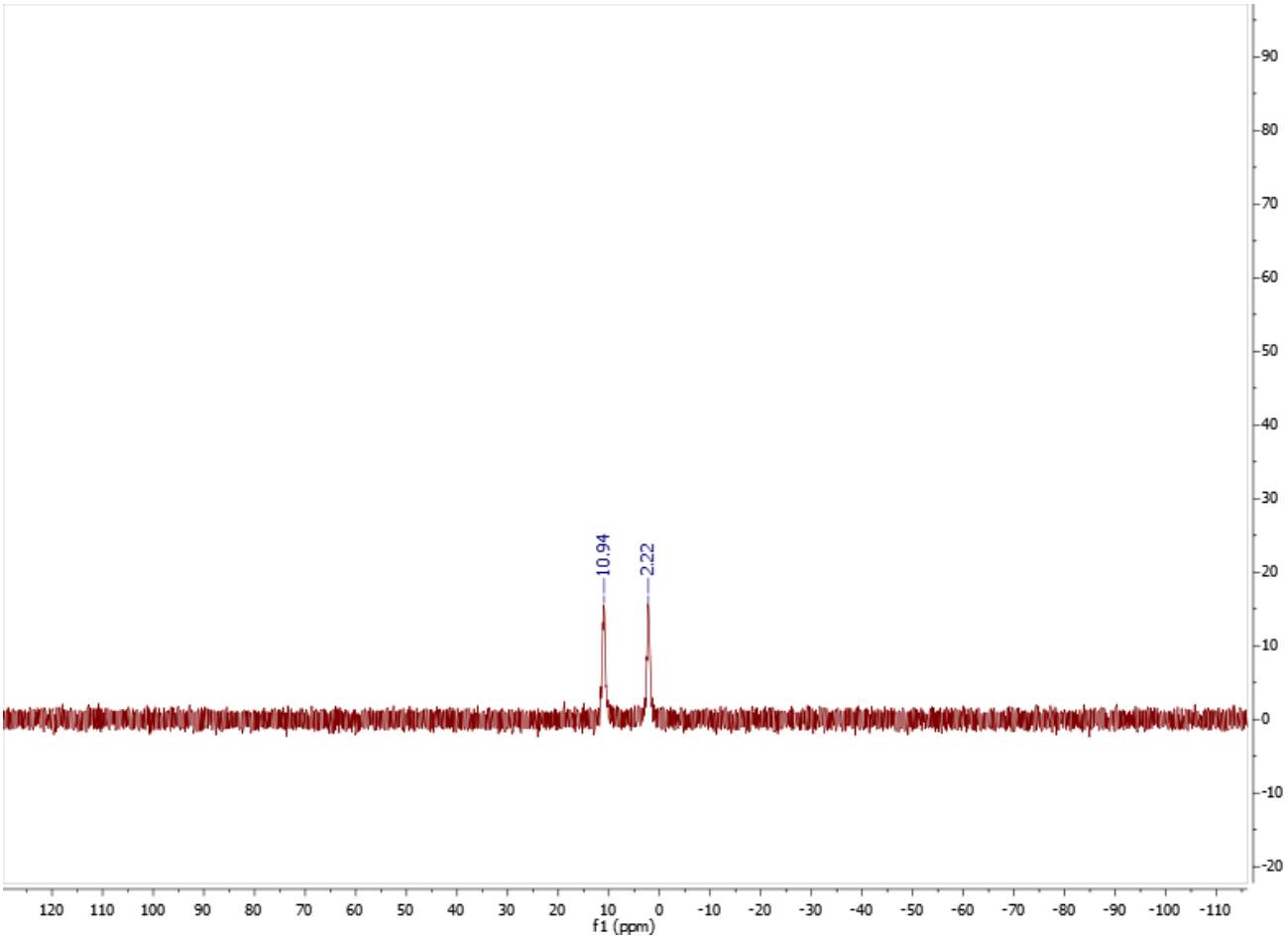
10.94
2.22
f1 (ppm)

^{1}H, ^{13}C, and ^{31}P NMR data for 5.3c-I

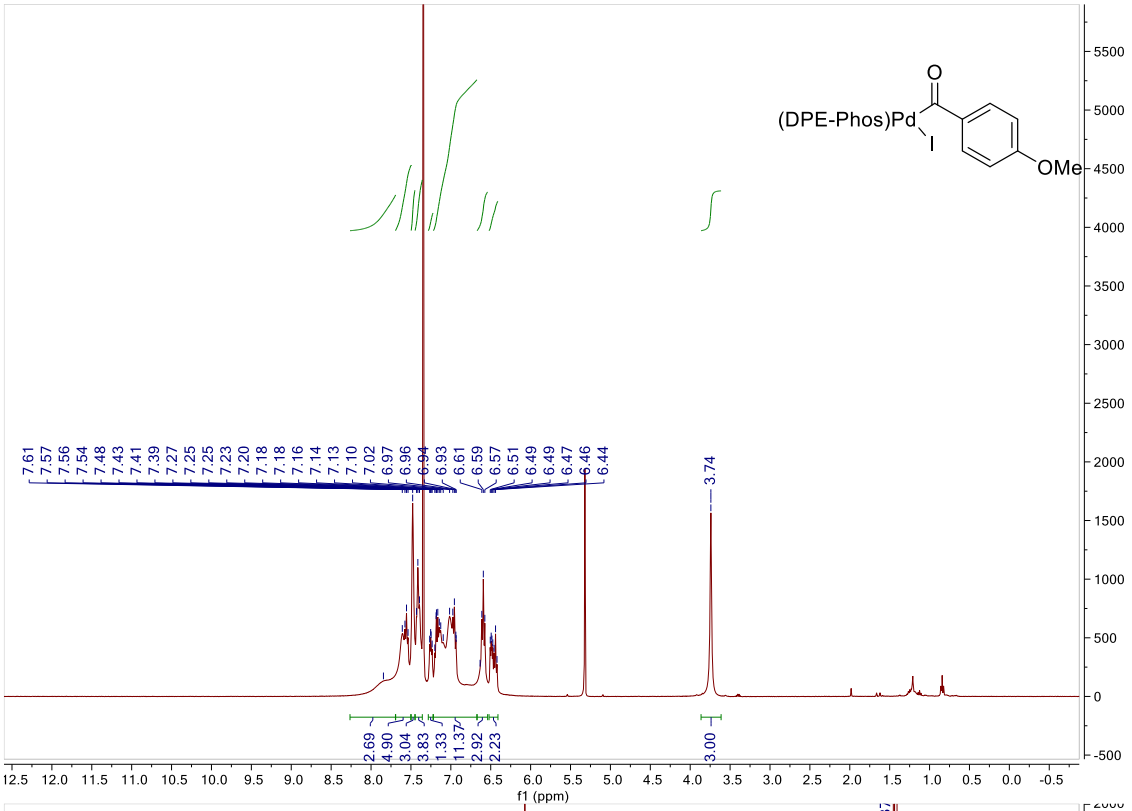

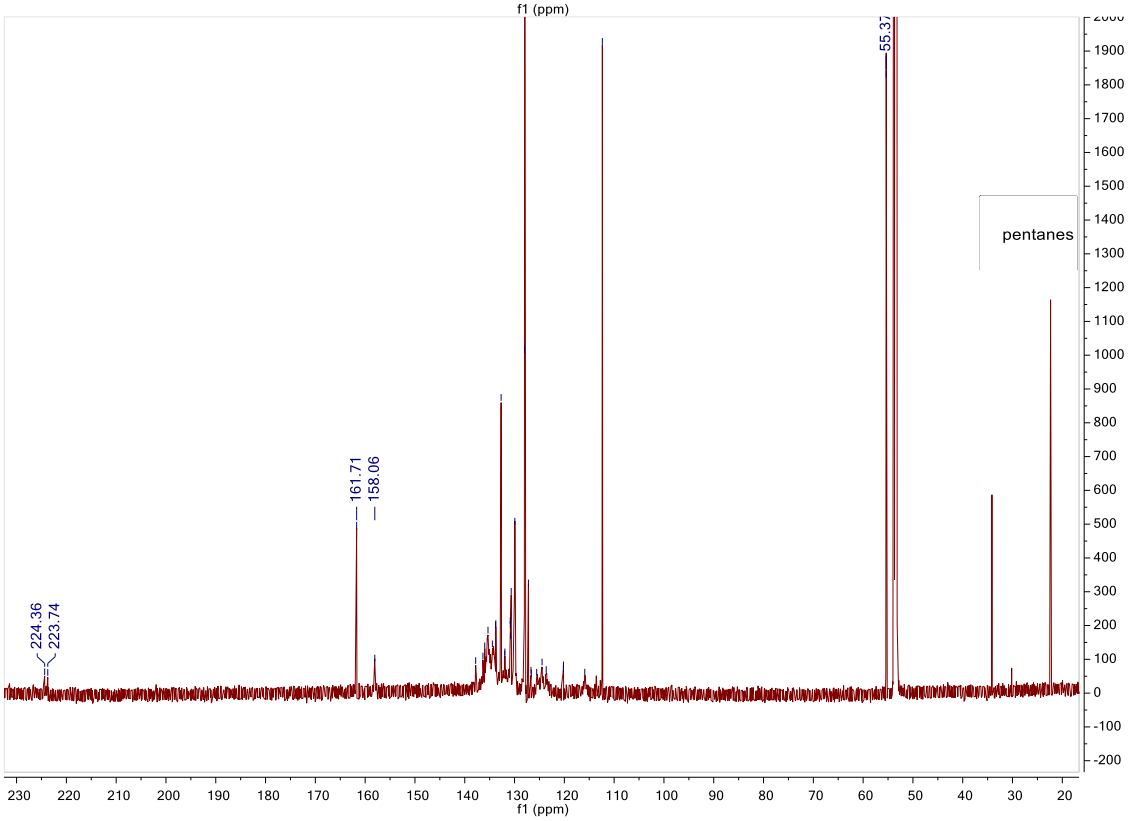

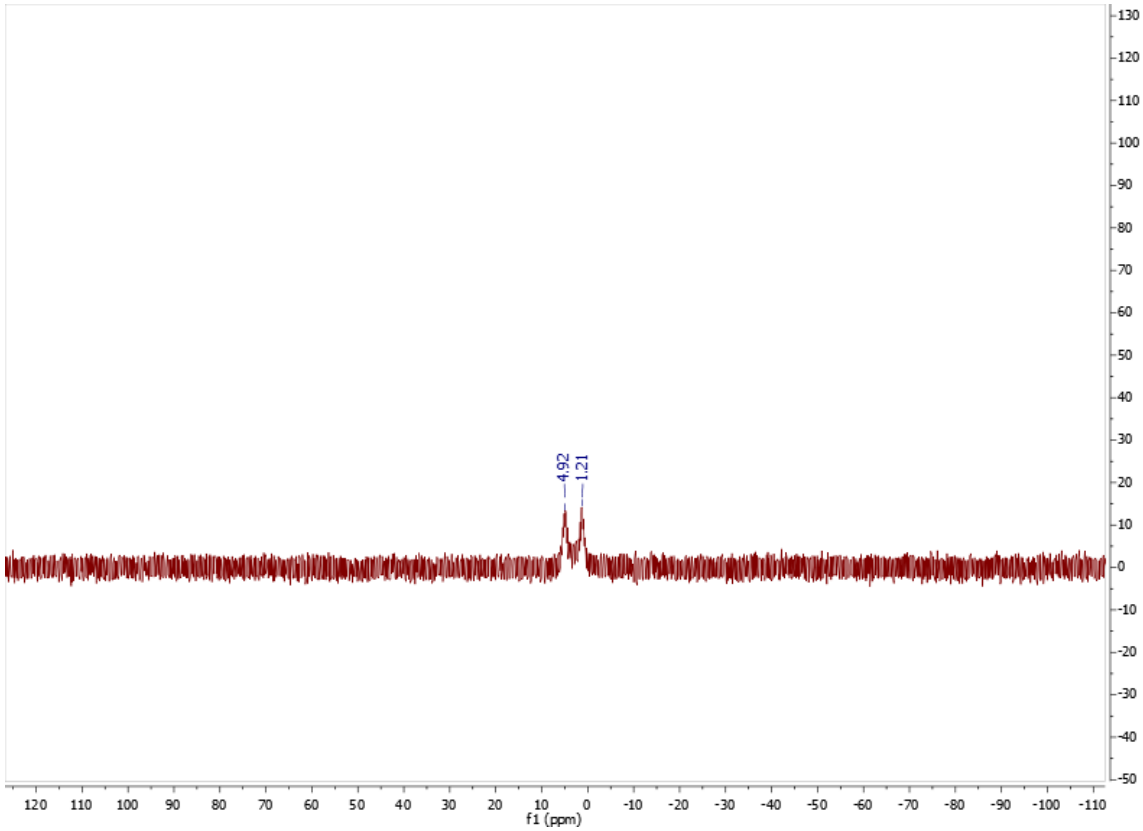
4.92
1.21
f1 (ppm)

^{1}H, ^{13}C, and ^{31}P NMR data for 5.3b-I

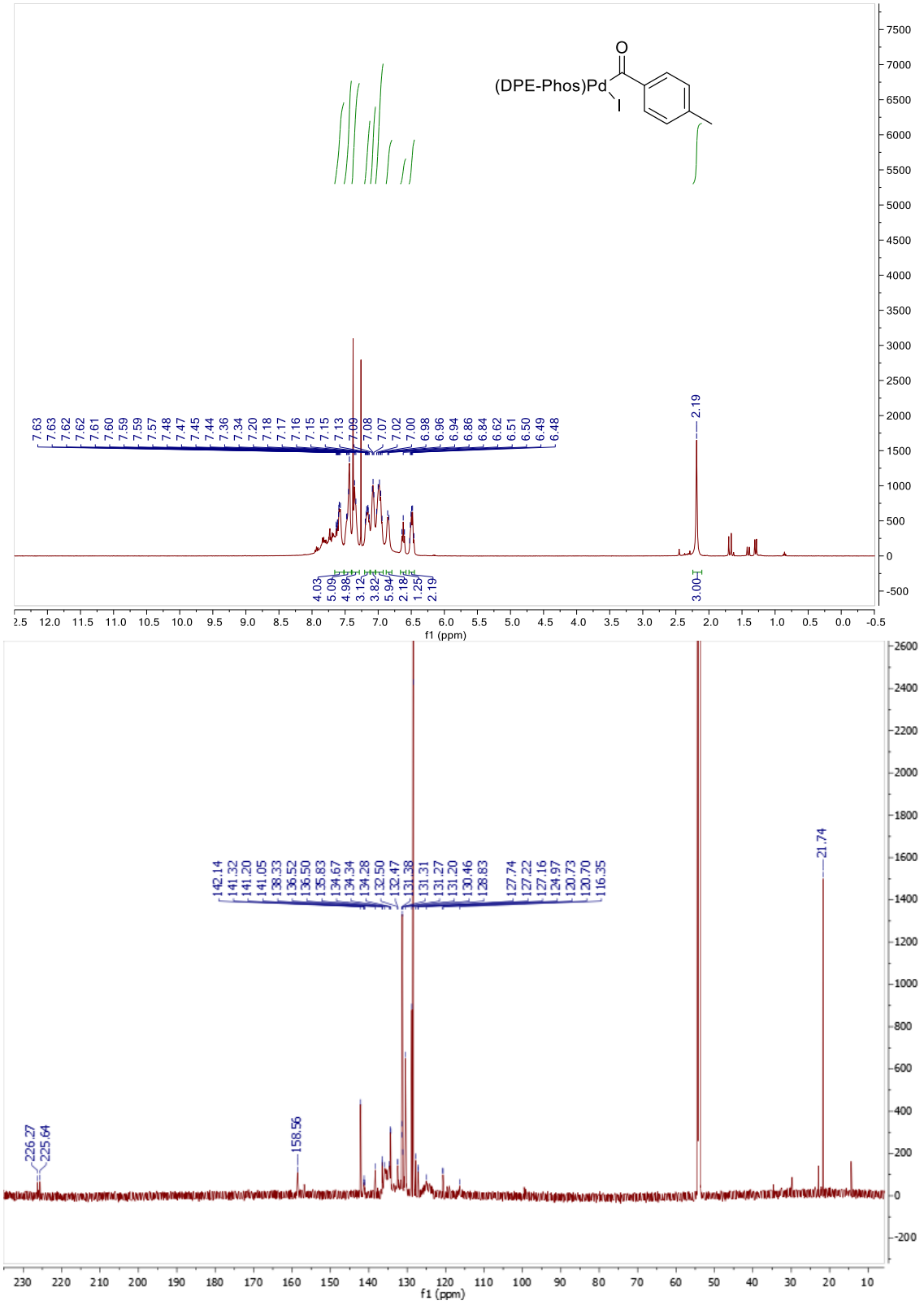

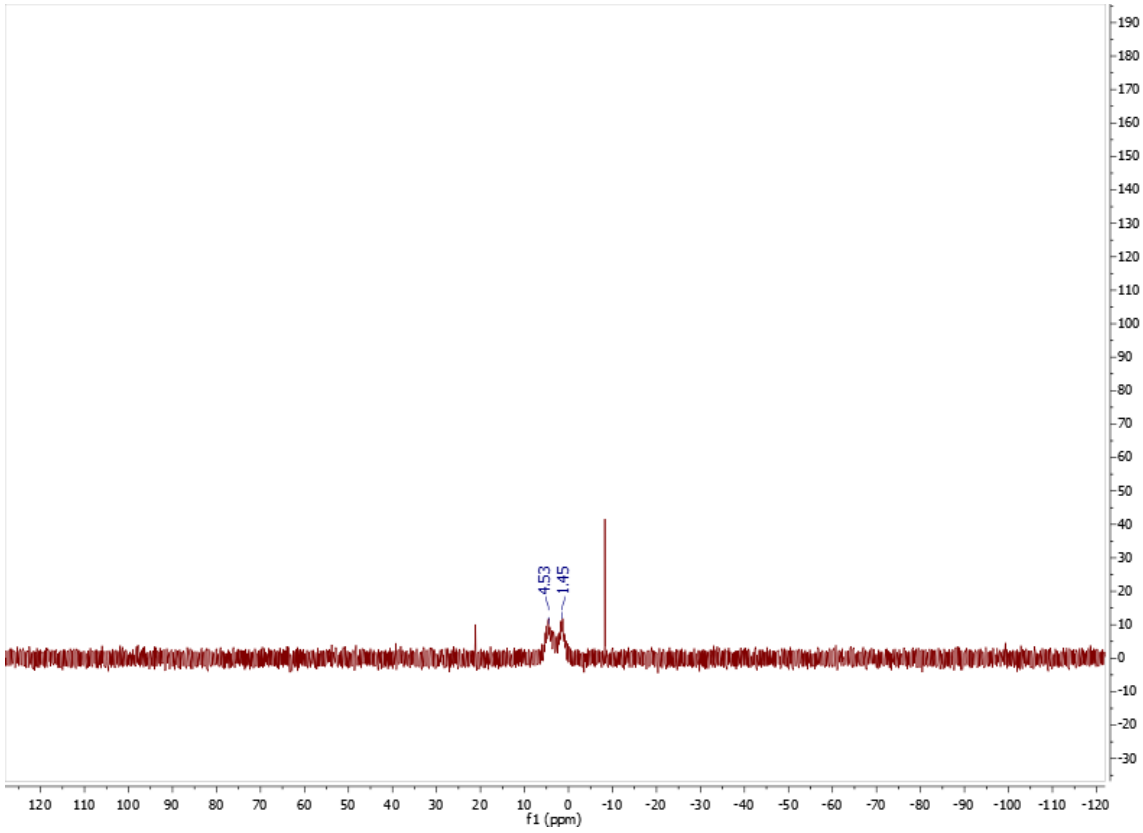
4.53
1.45
f1 (ppm)

^{1}H, ^{13}C, and ^{31}P NMR data for 5.3b-Br

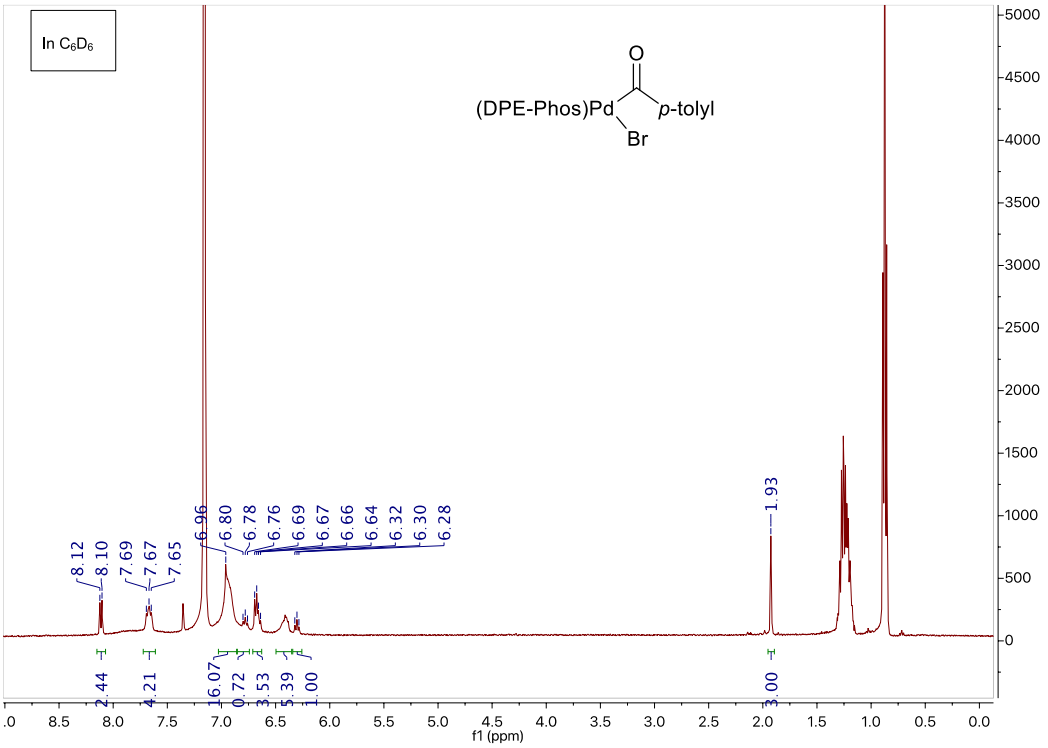

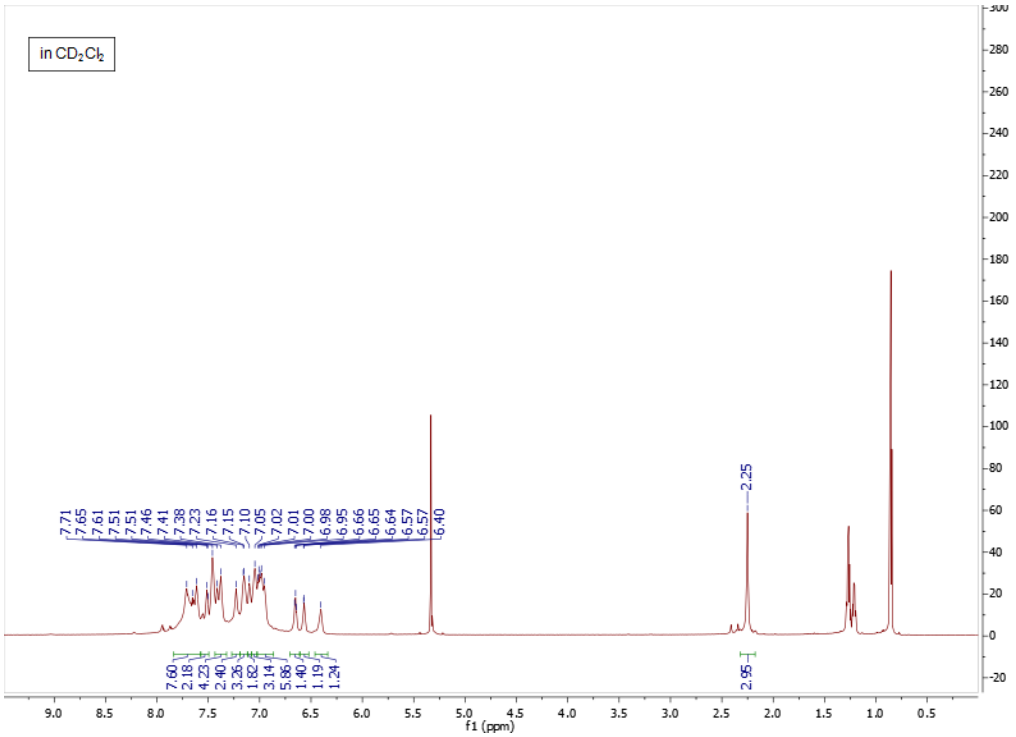

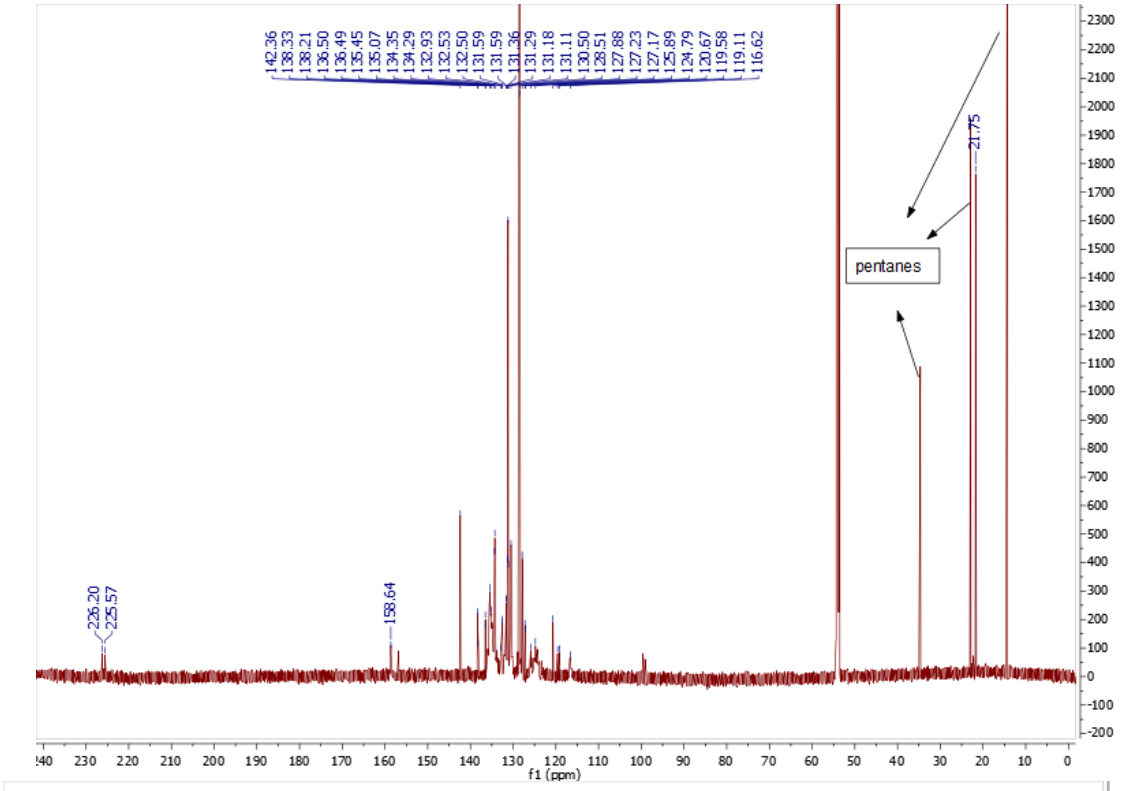
142.36
138.33
138.21
136.50
136.49
135.45
135.07
134.35
134.29
132.93
132.53
132.50
131.59
131.59
131.36
131.29
131.18
131.11
130.50
128.51
127.88
127.23
127.17
125.89
124.79
120.67
119.58
119.11
116.62
21.75
pentanes
226.20
225.57
158.64
f1 (ppm)

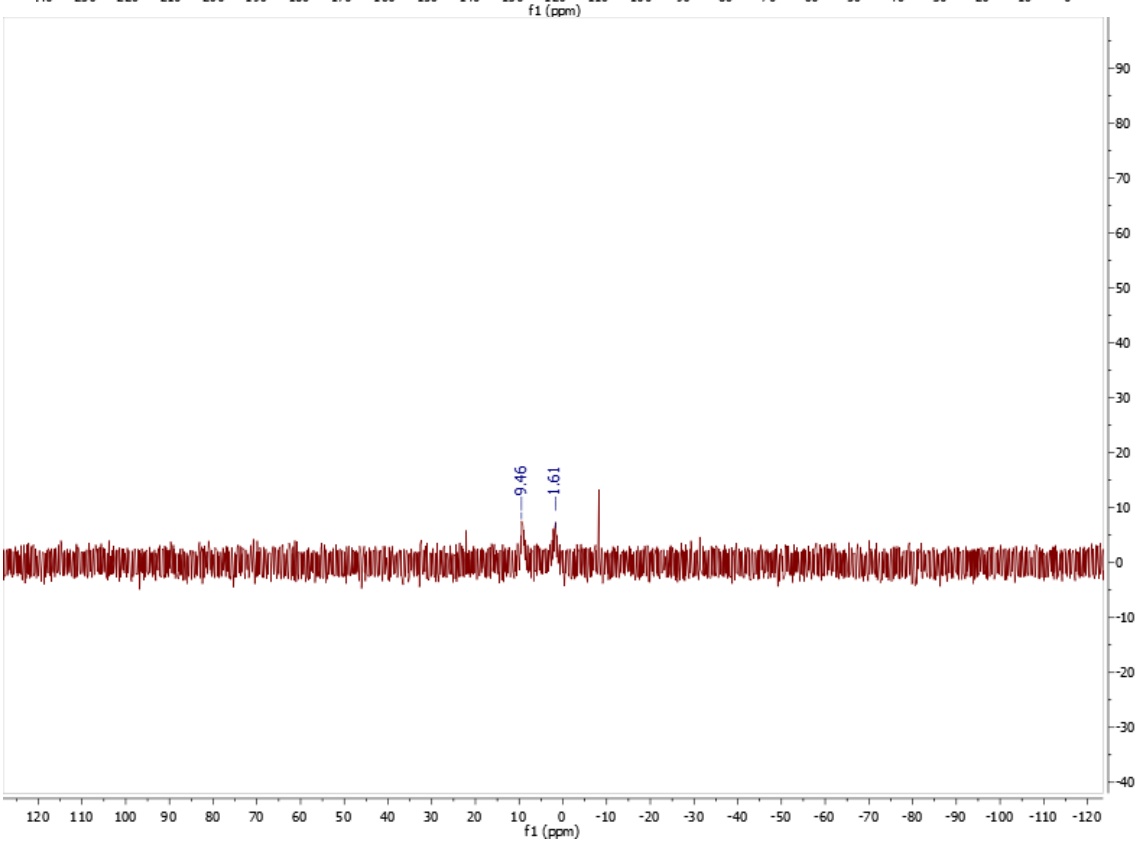
9.46
1.61
f1 (ppm)

^{1}H, ^{13}C, and ^{31}P NMR data for 5.3d

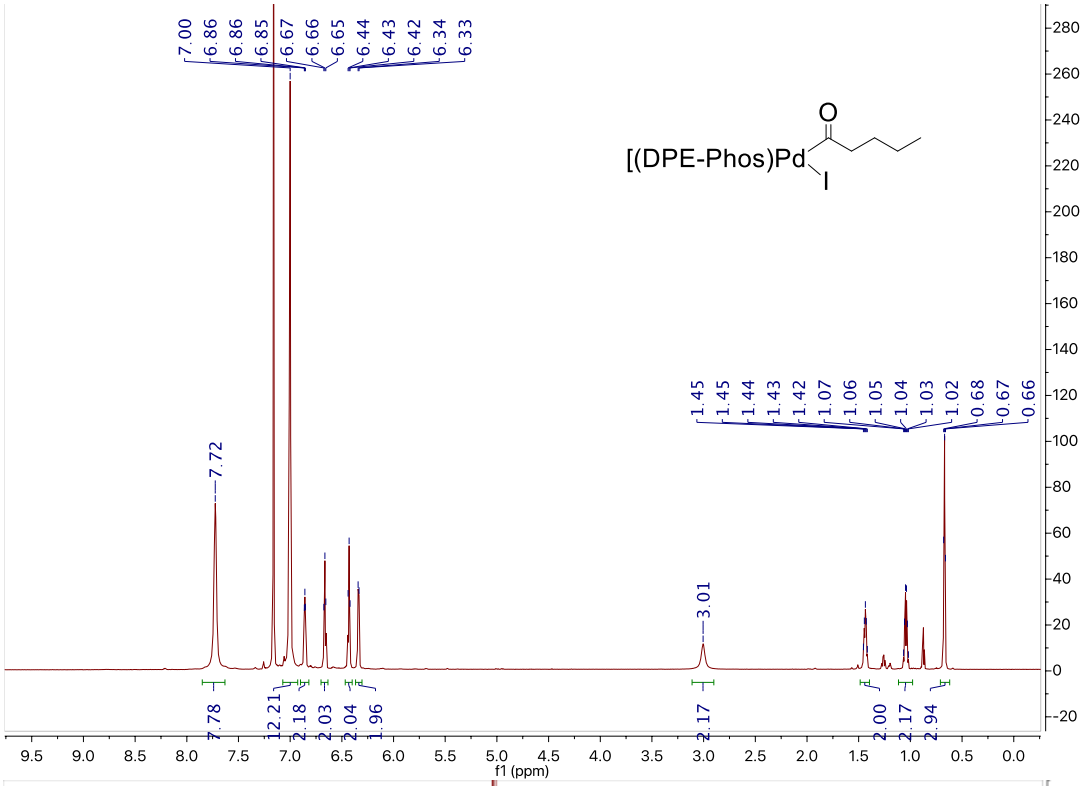

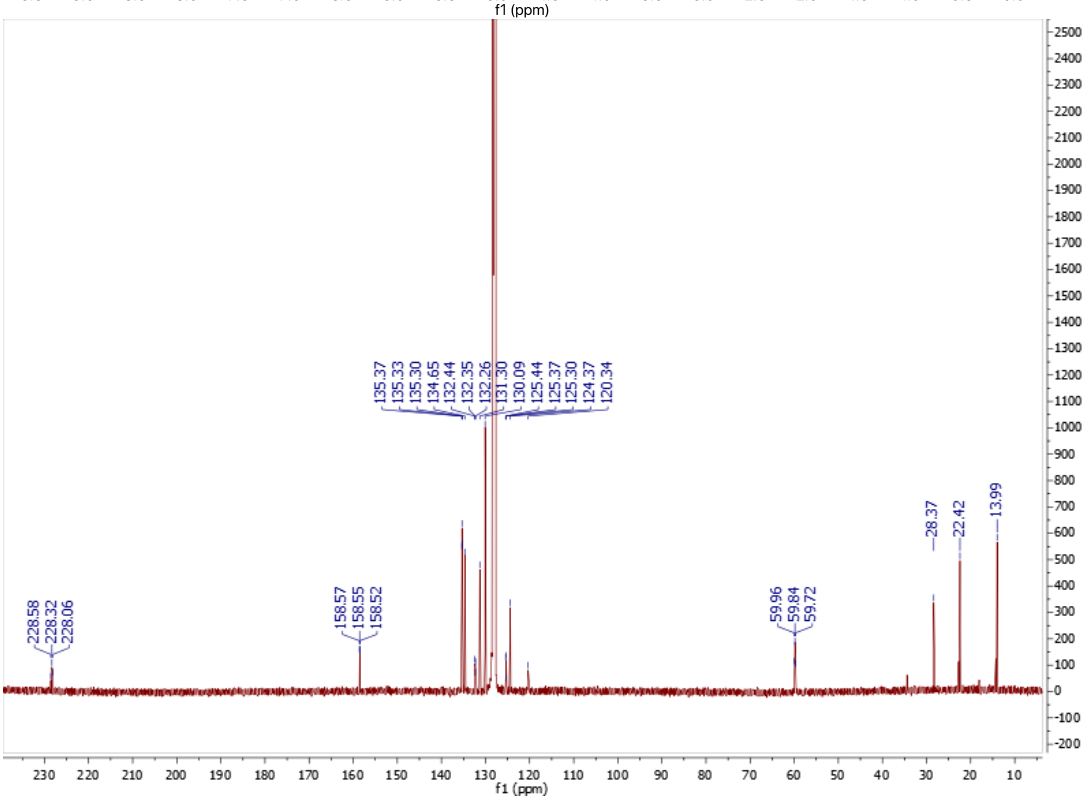

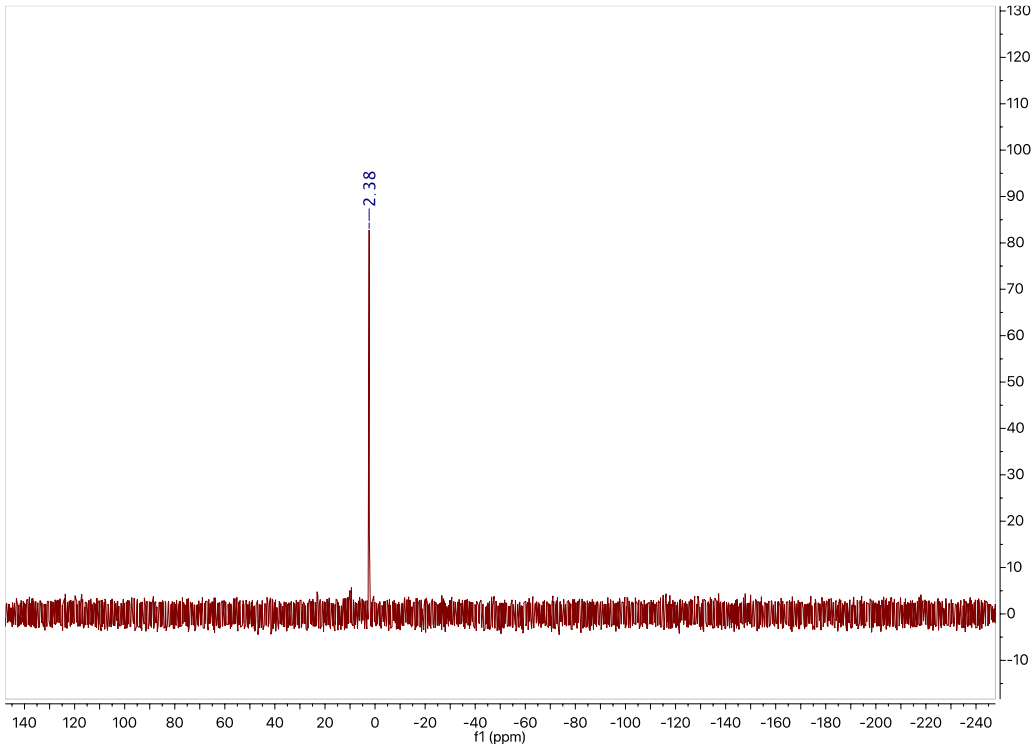
2.38
130
120
110
100
90
80
70
60
50
40
30
20
10
0
-10
140
120
100
80
60
40
20
0
-20
-40
-60
-80
-100
-120
-140
-160
-180
-200
-220
-240
f1 (ppm)

^{1}H and ^{13}C NMR data for 5.4b

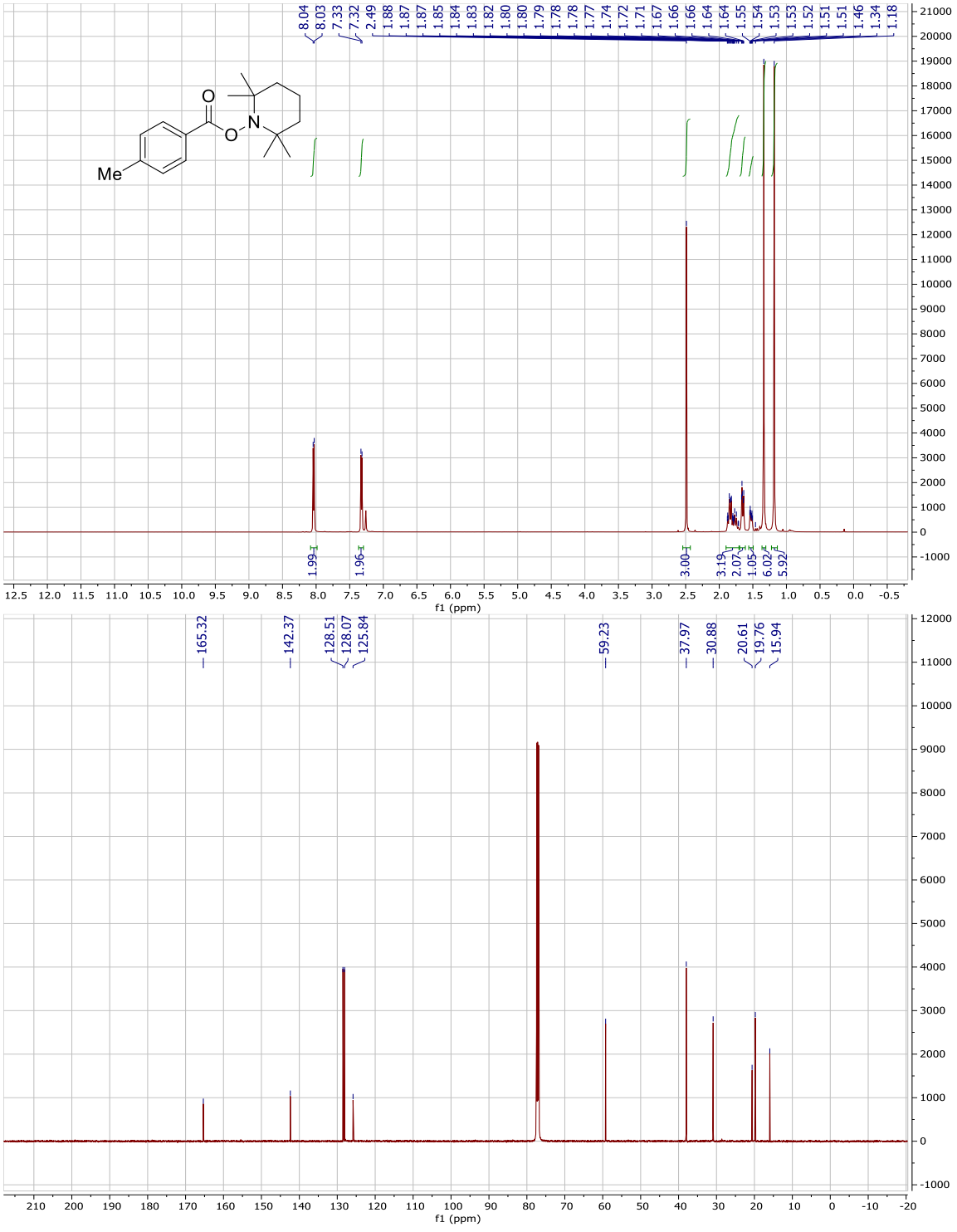

^{1}H and ^{13}C NMR data for 5.4c

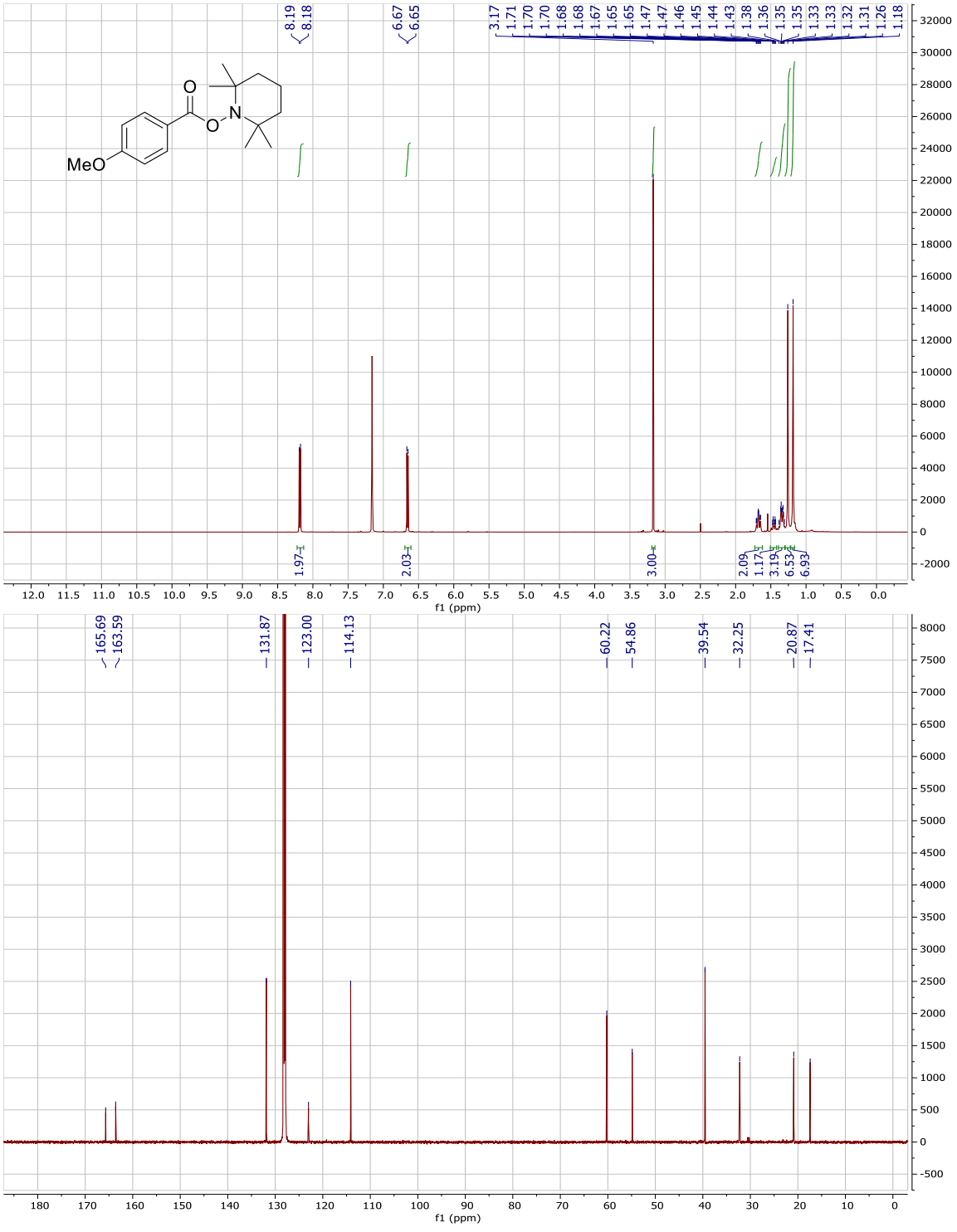

^{1}H and ^{13}C NMR data for 5.6a

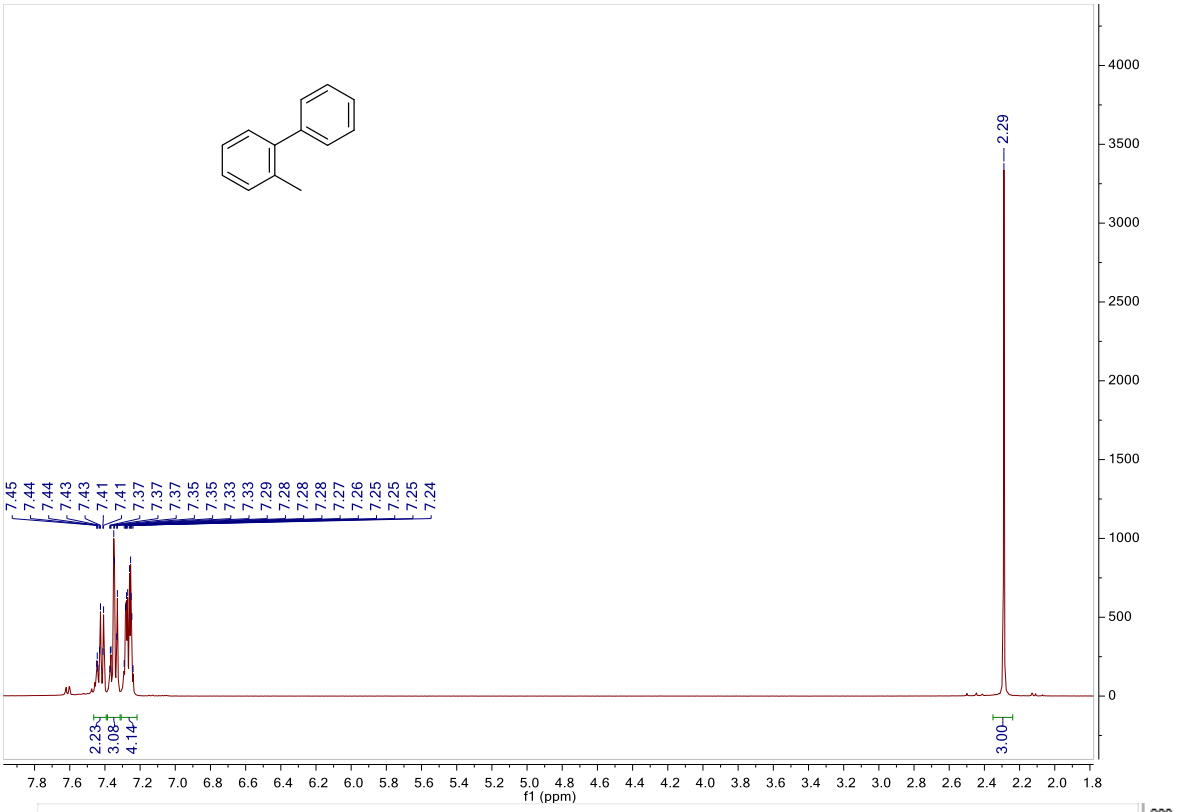

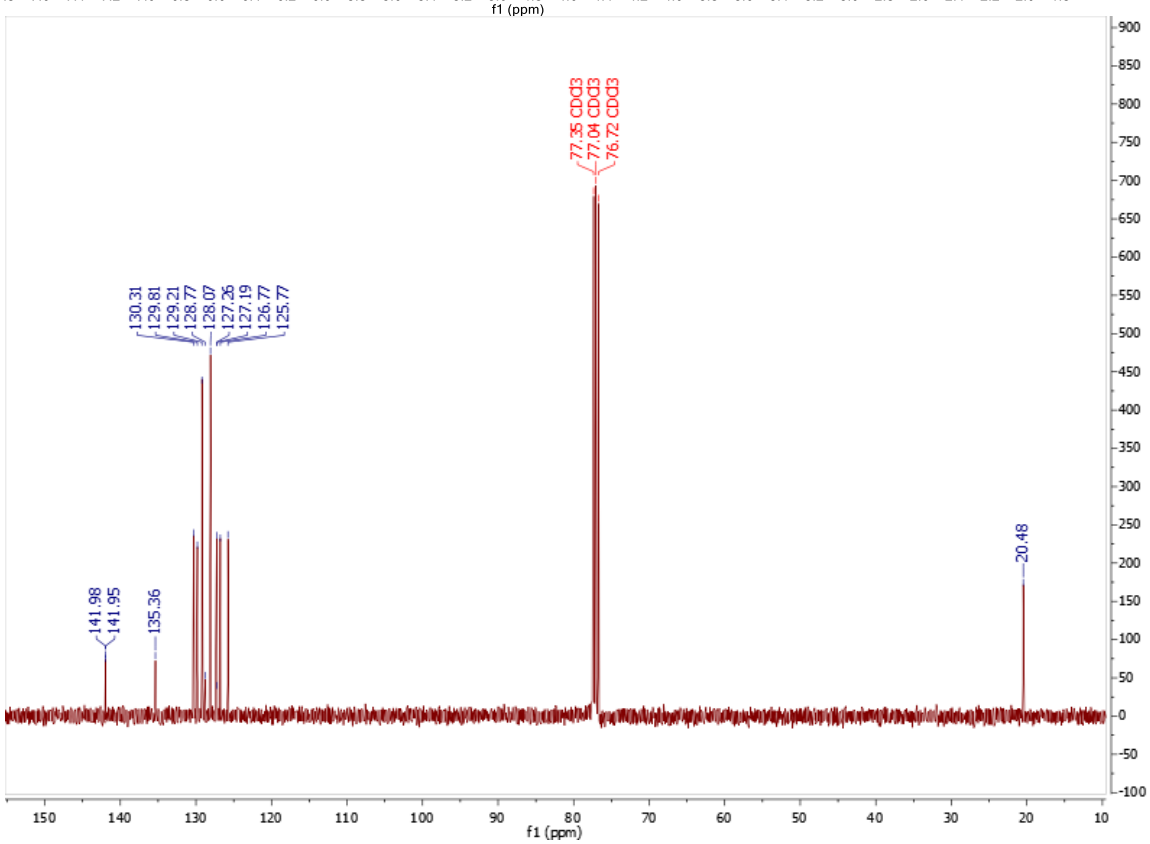

^{1}H and ^{13}C NMR data for 5.6b

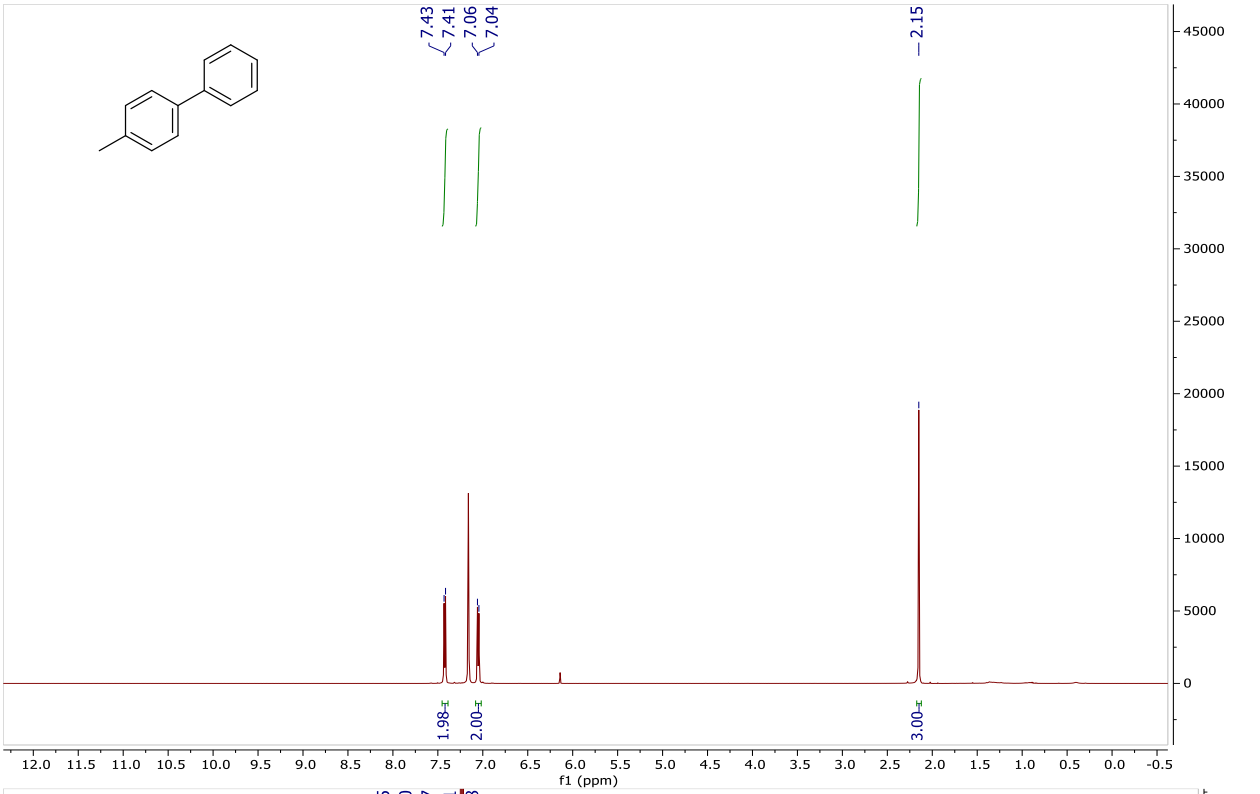

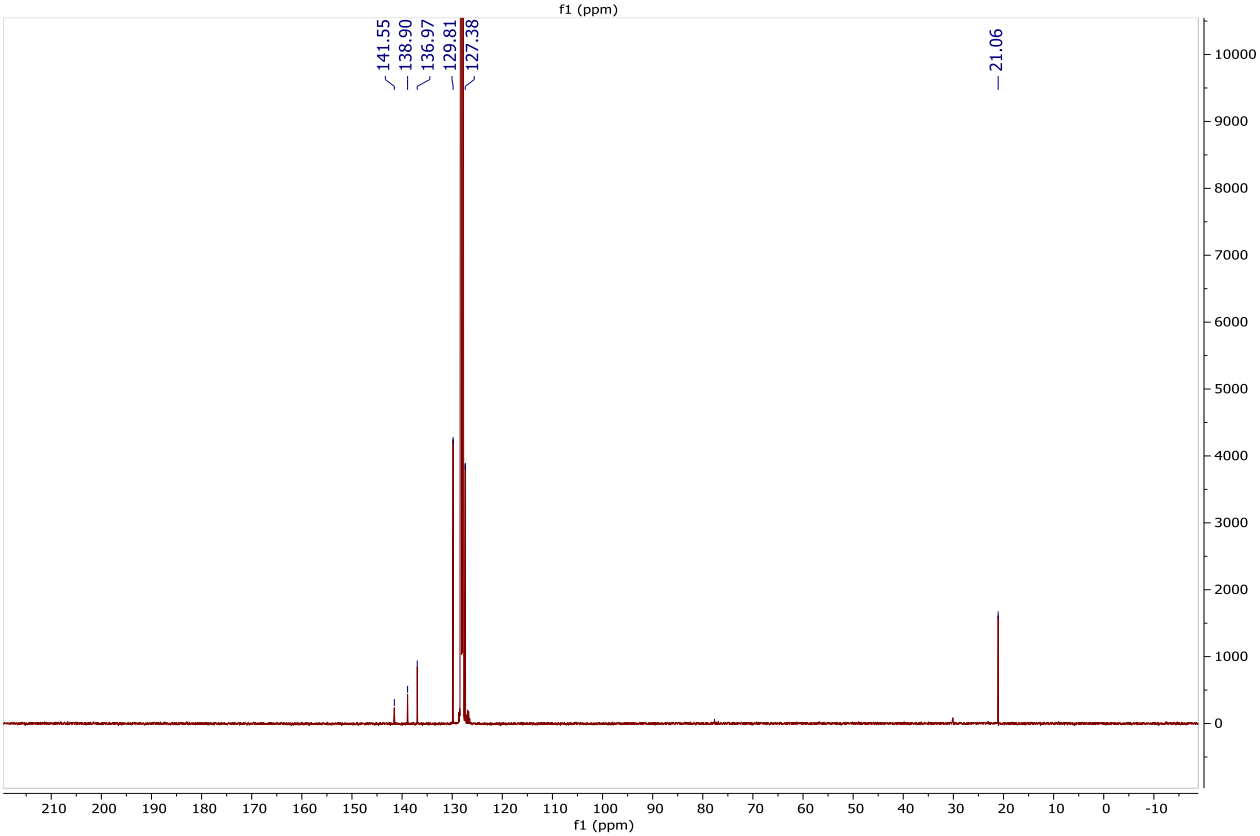

^{1}H and ^{13}C NMR data for 5.6c

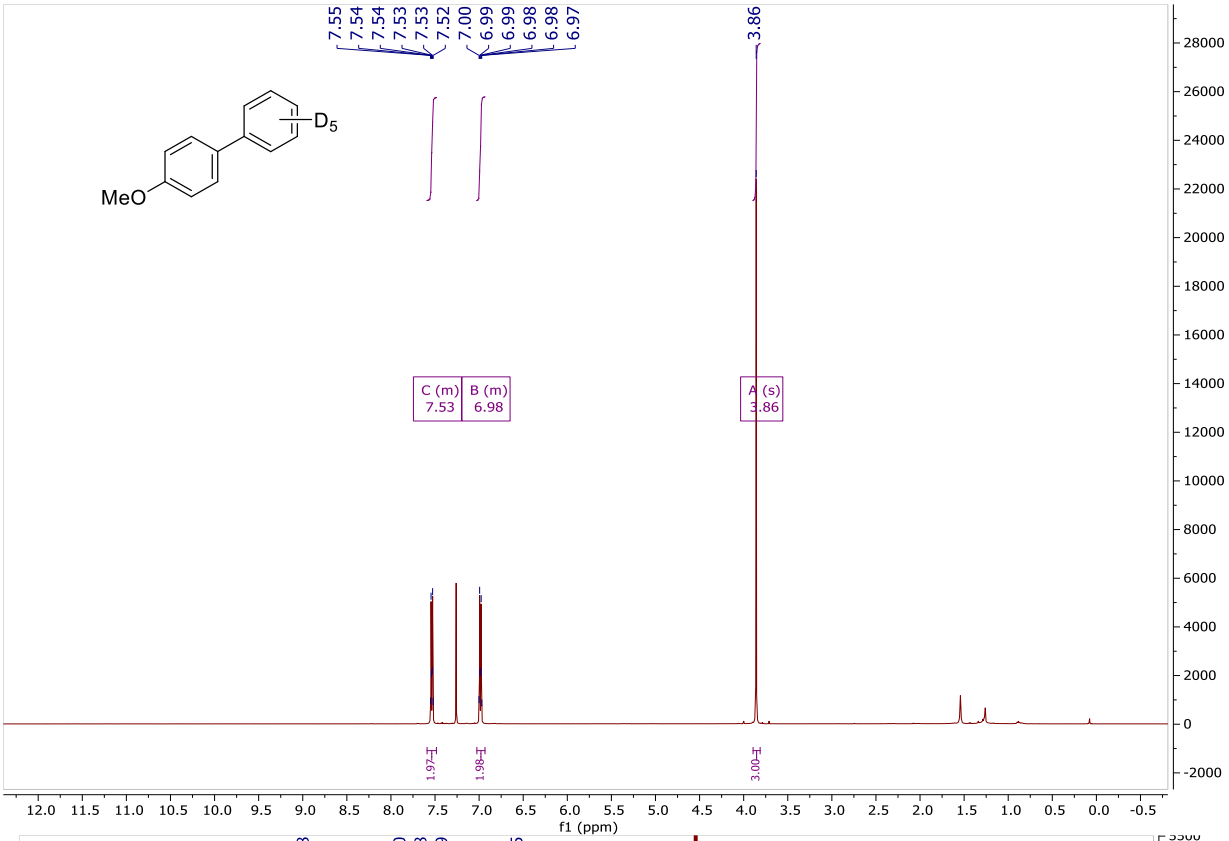

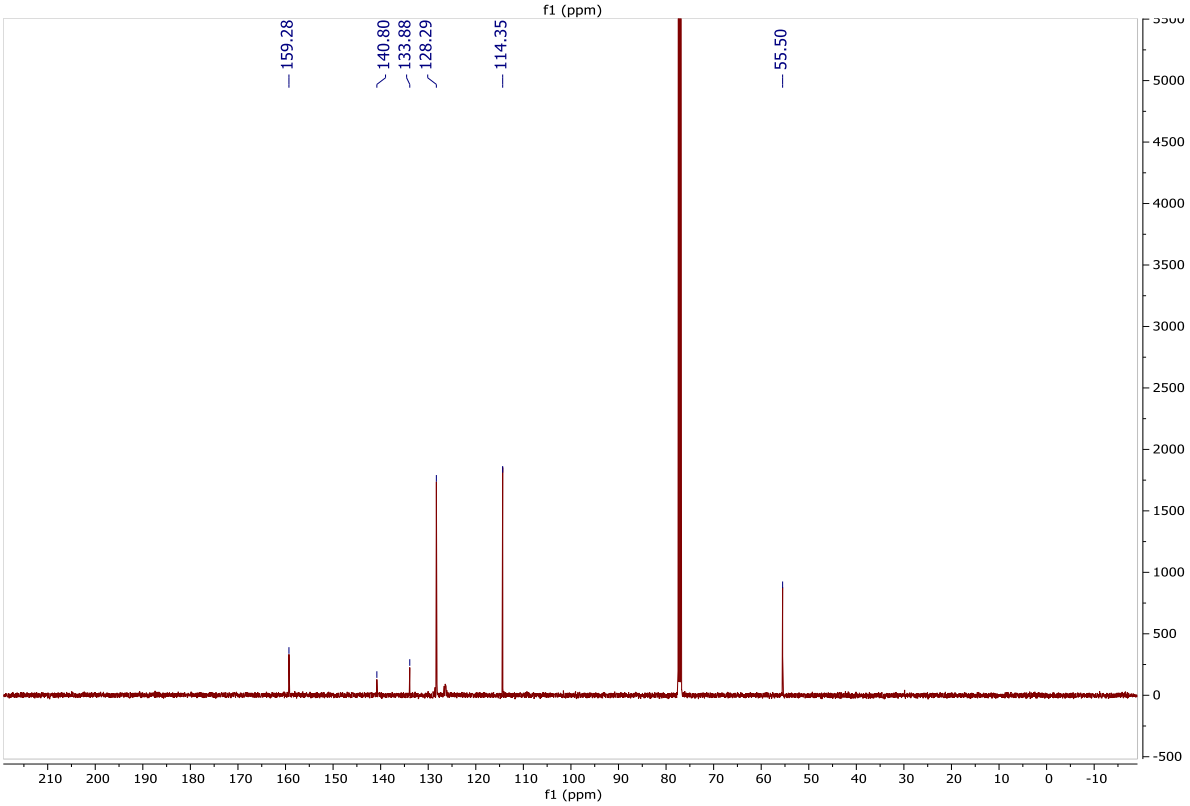

^{1}H and ^{31}P NMR data for 5.7a

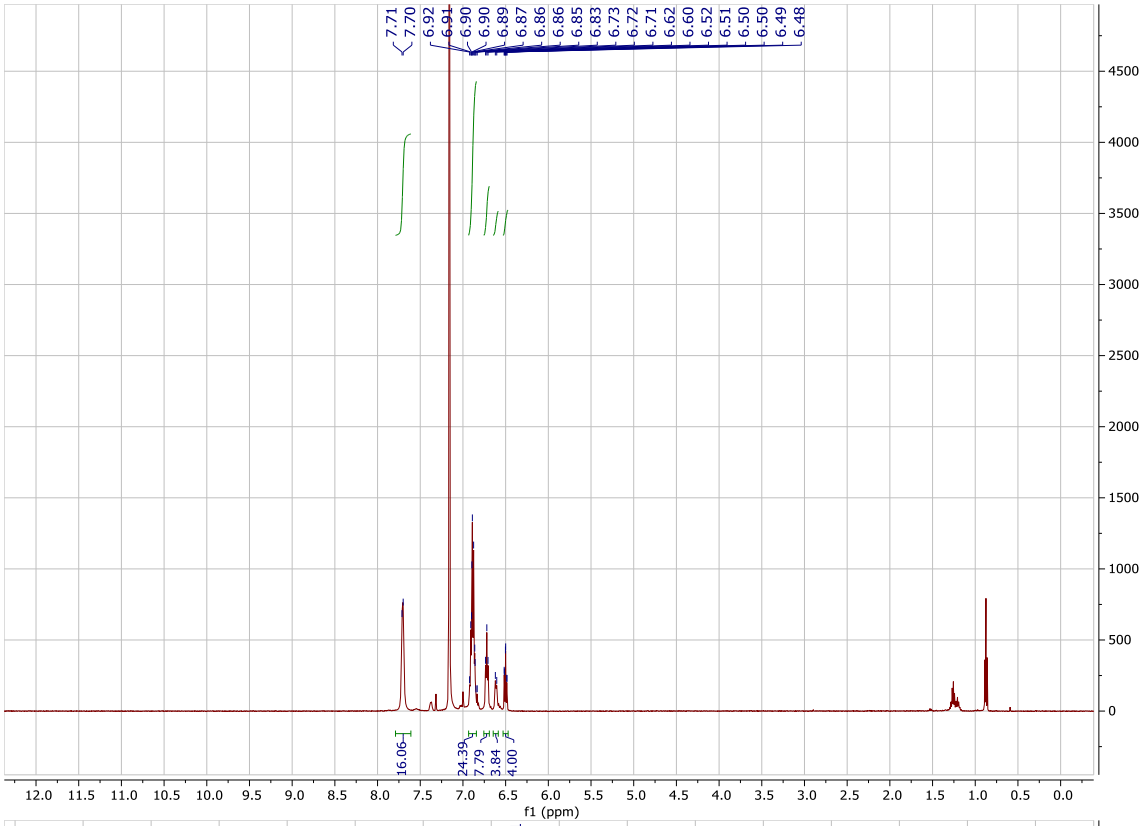

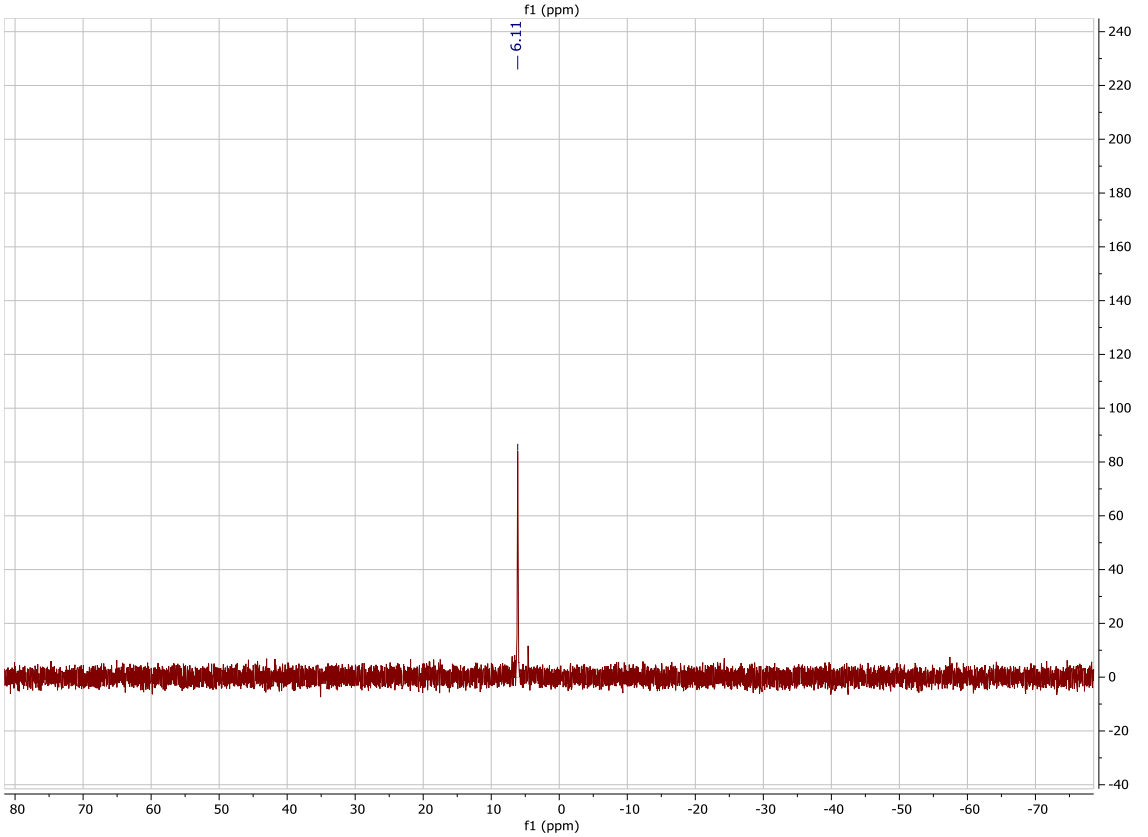

^{1}H, ^{13}C, and ^{31}P NMR data for 5.7 with ^{13}CO

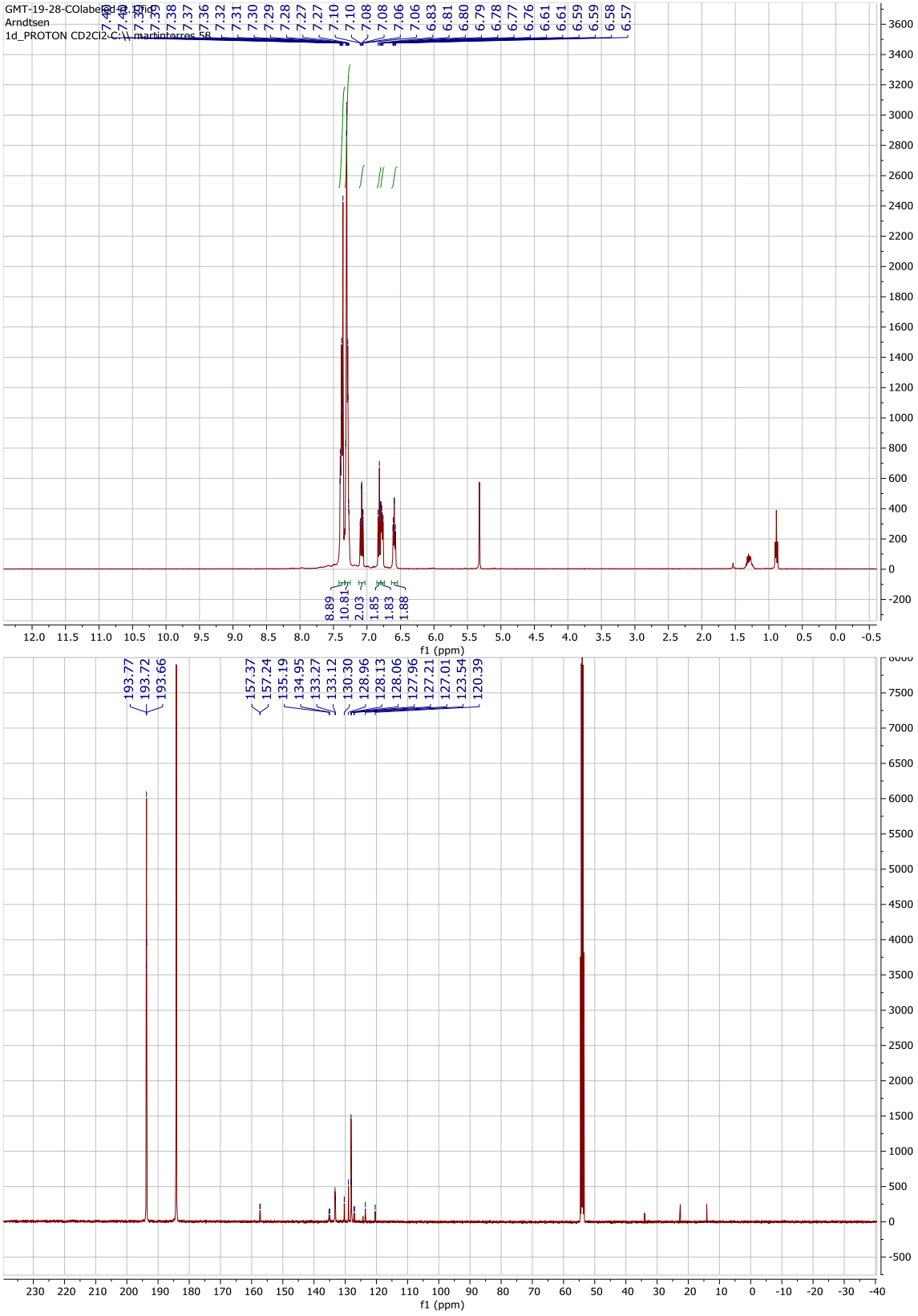

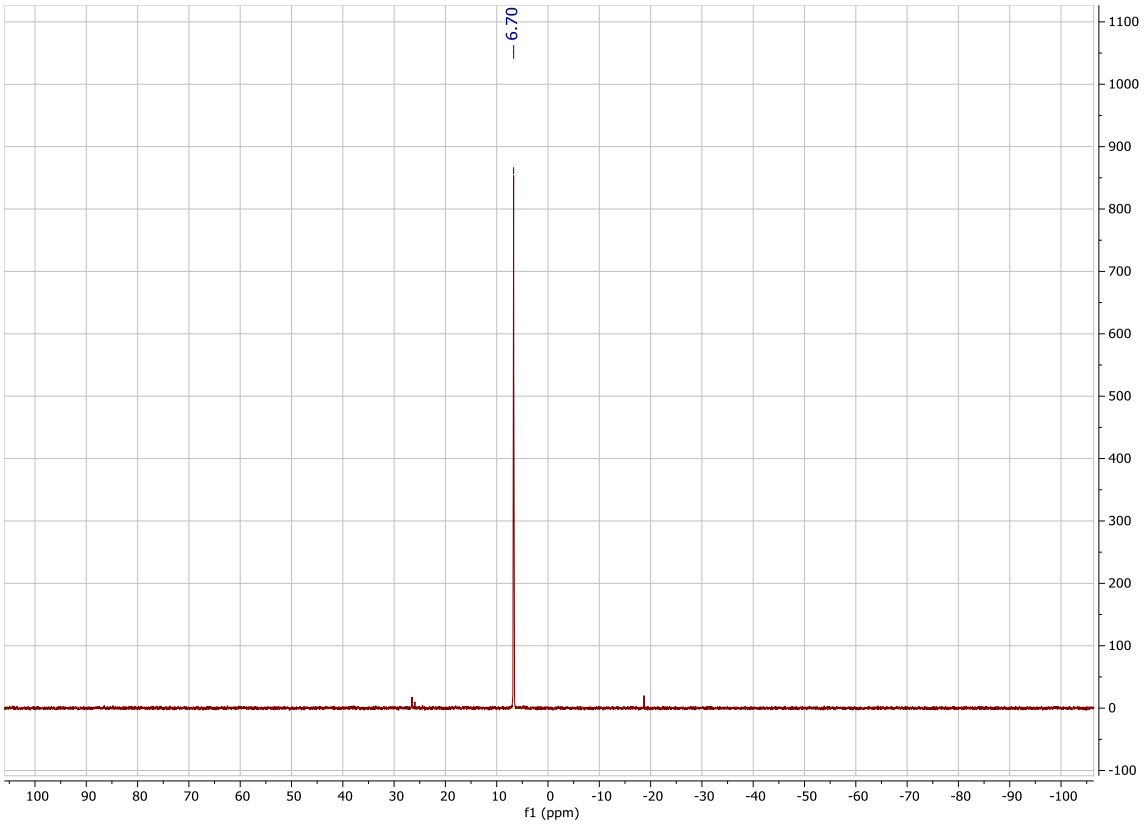
6.70
1100
1000
900
800
700
600
500
400
300
200
100
0
-100
100 90 80 70 60 50 40 30 20 10 0 -10 -20 -30 -40 -50 -60 -70 -80 -90 -100
f1 (ppm)

^{1}H and ^{13}C NMR data for 5.8

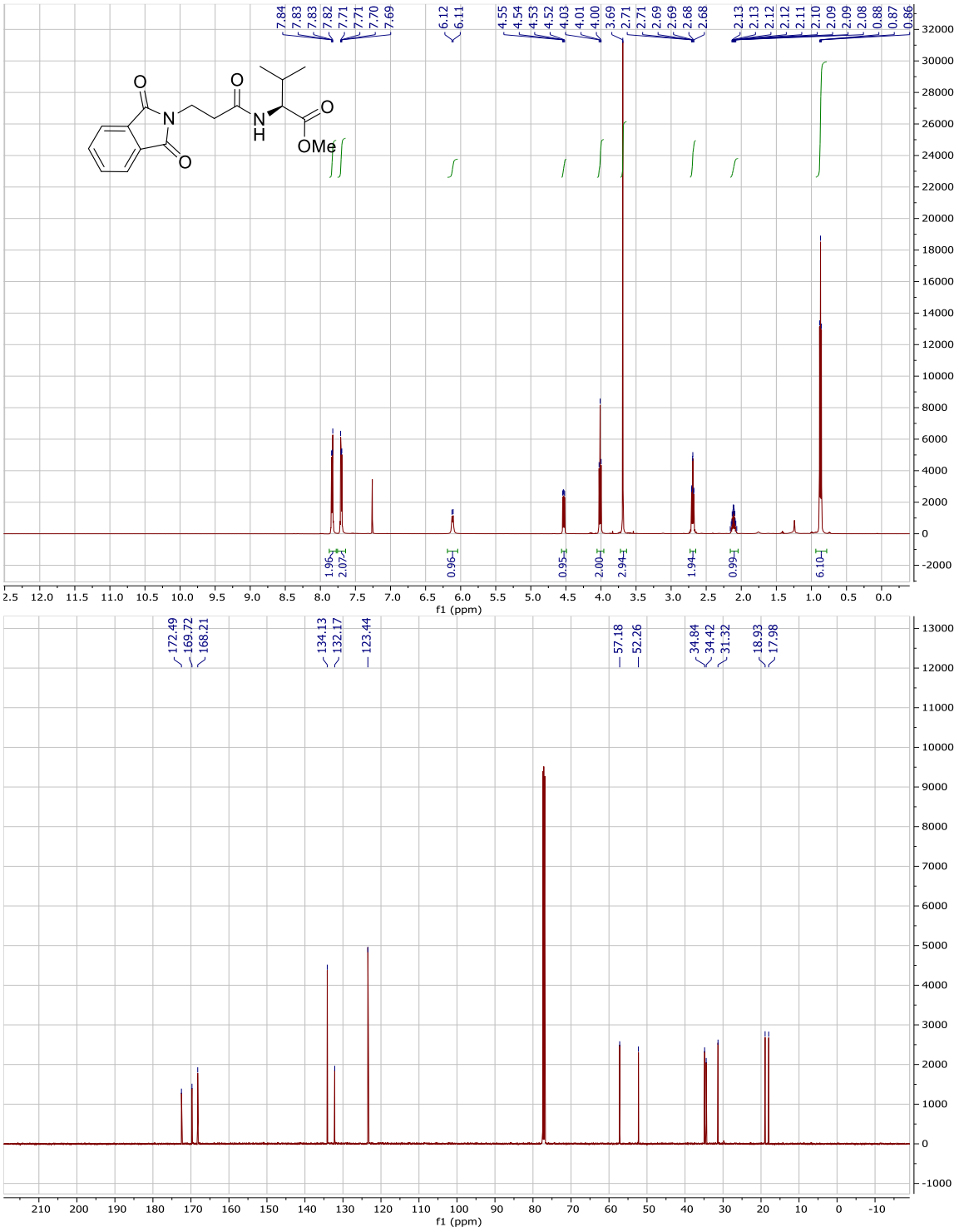

^{1}H and ^{13}C NMR data for 5.9a

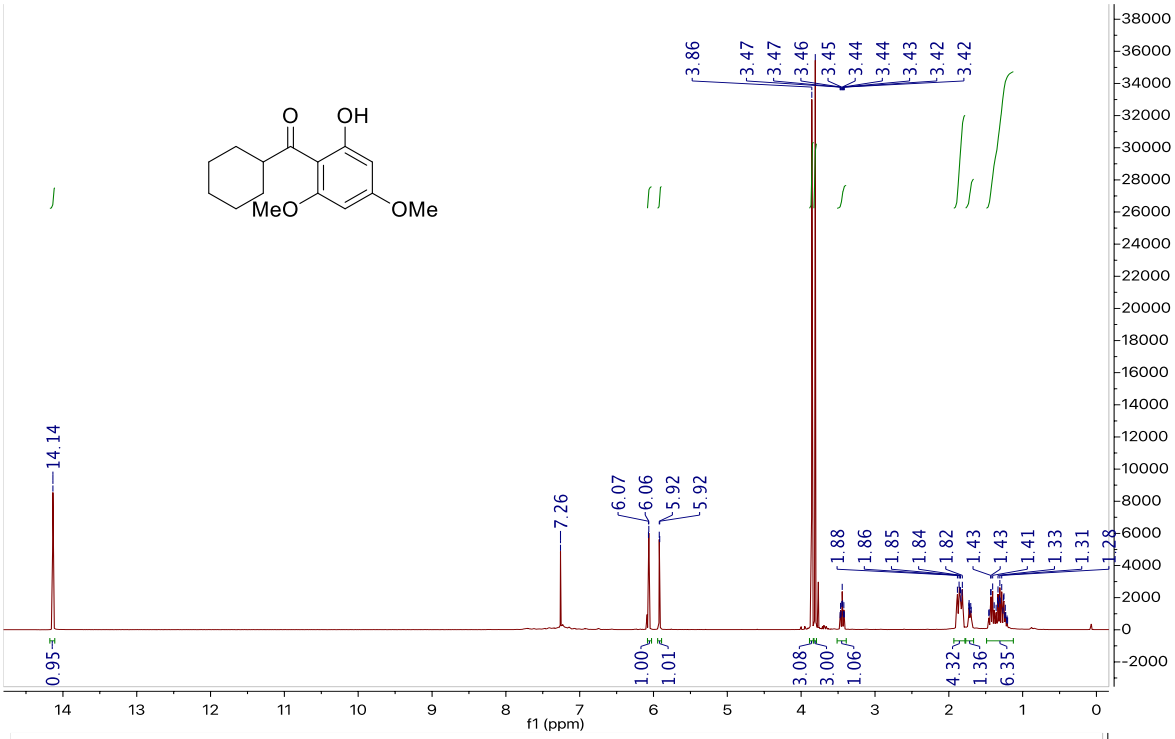

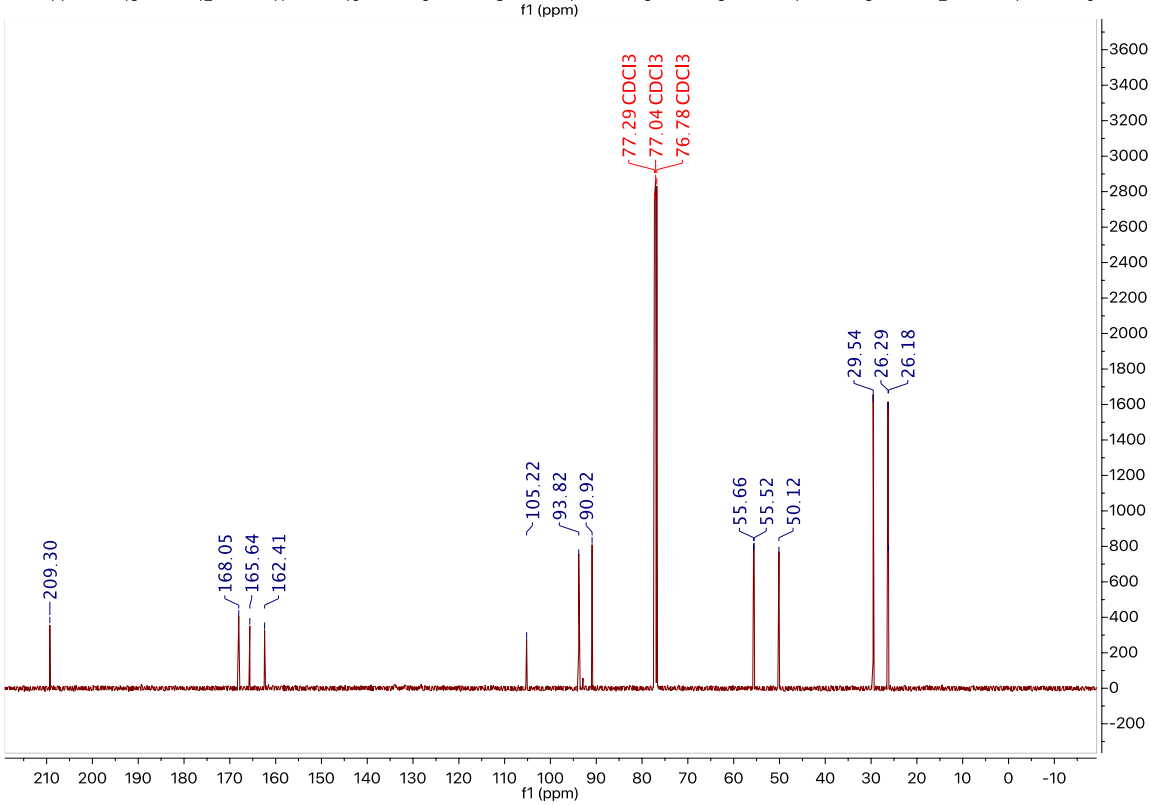

^{1}H and ^{13}C NMR data for 5.9b

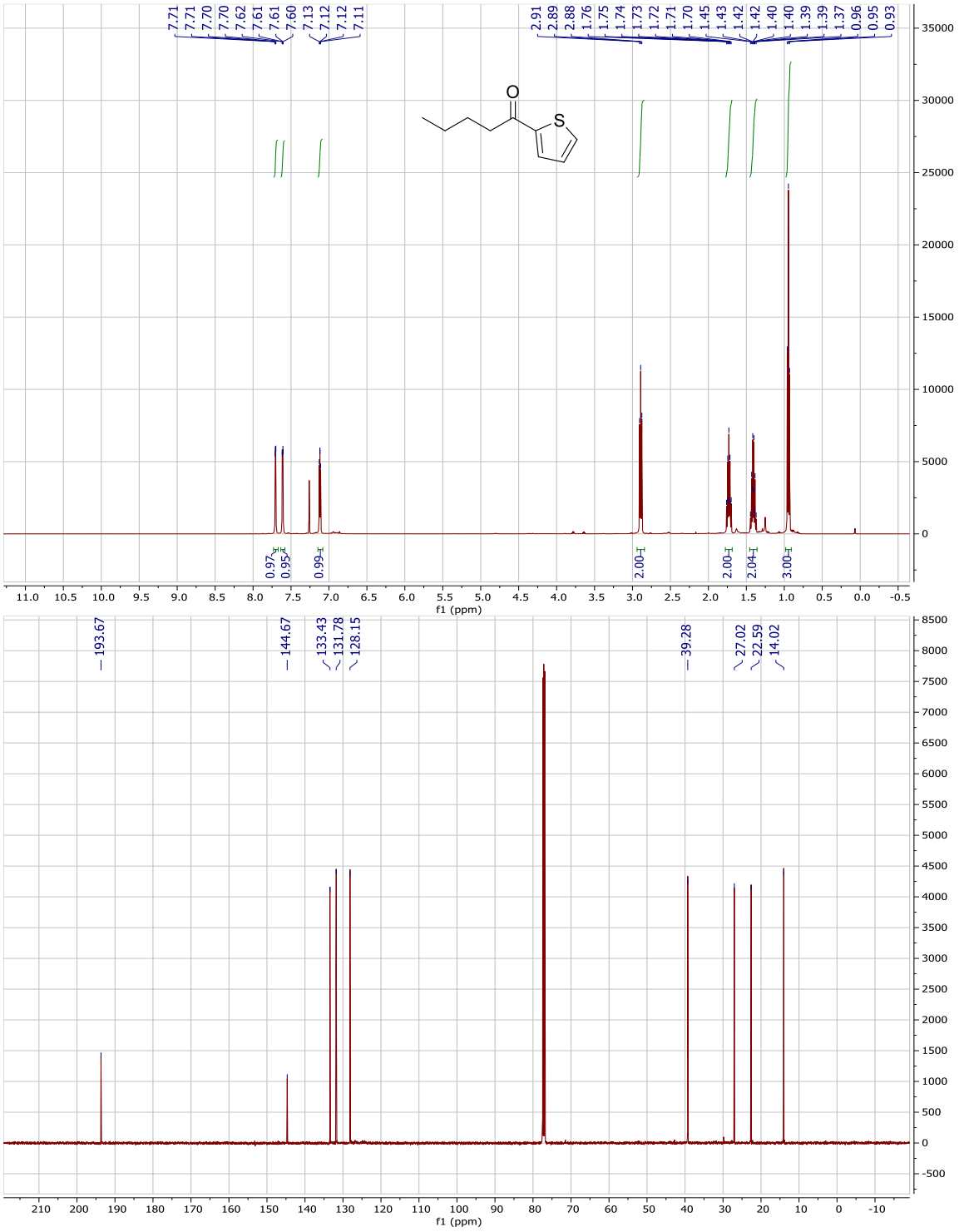

^{1}H and ^{13}C NMR data for 5.9c

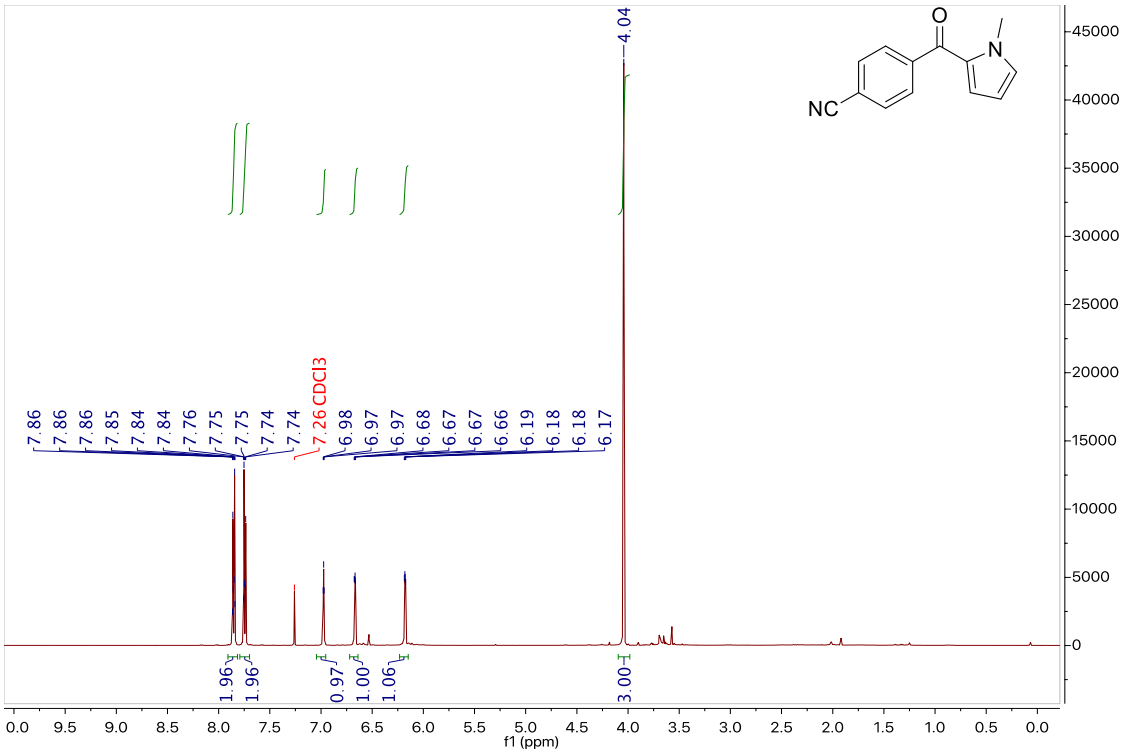

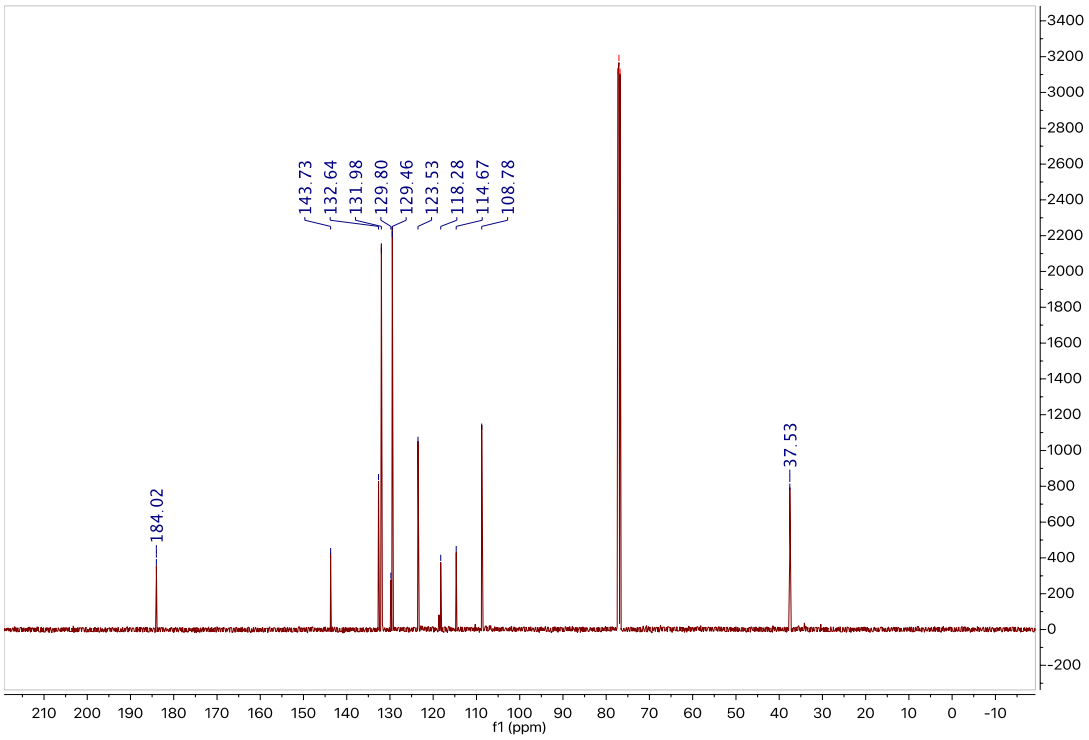

^{1}H and ^{13}C NMR data for 5.10a.

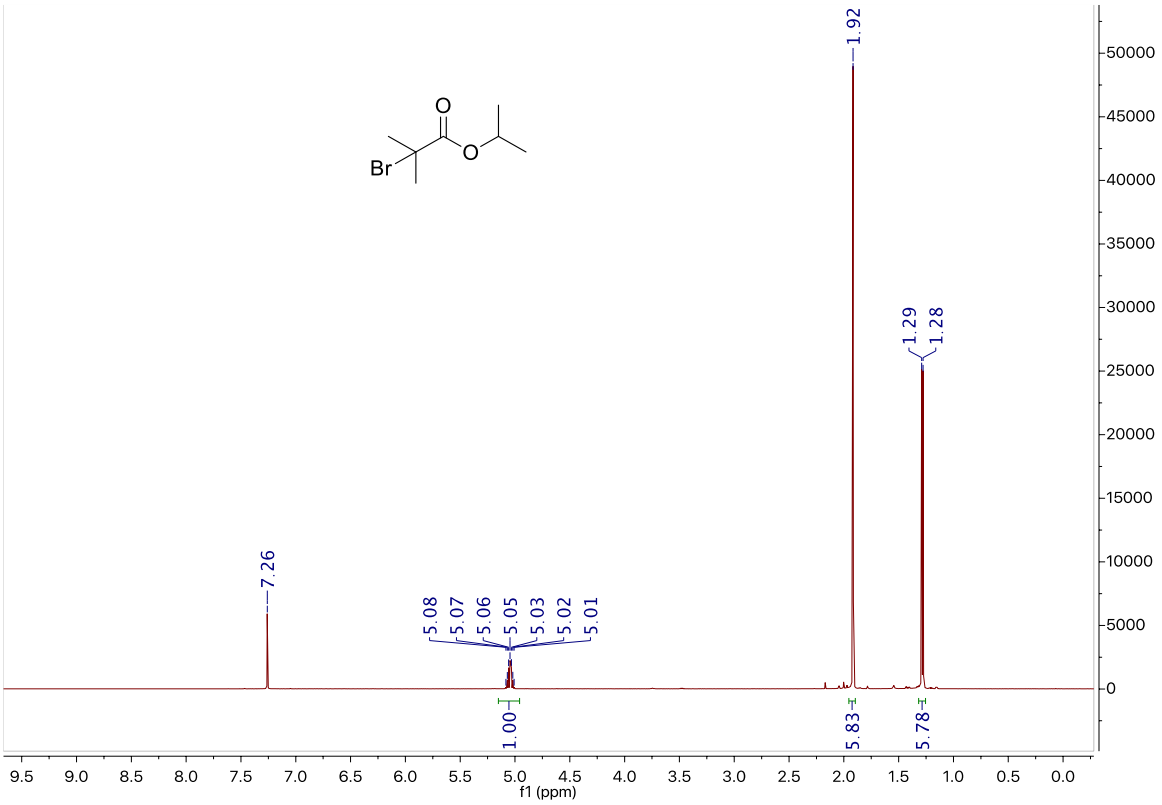

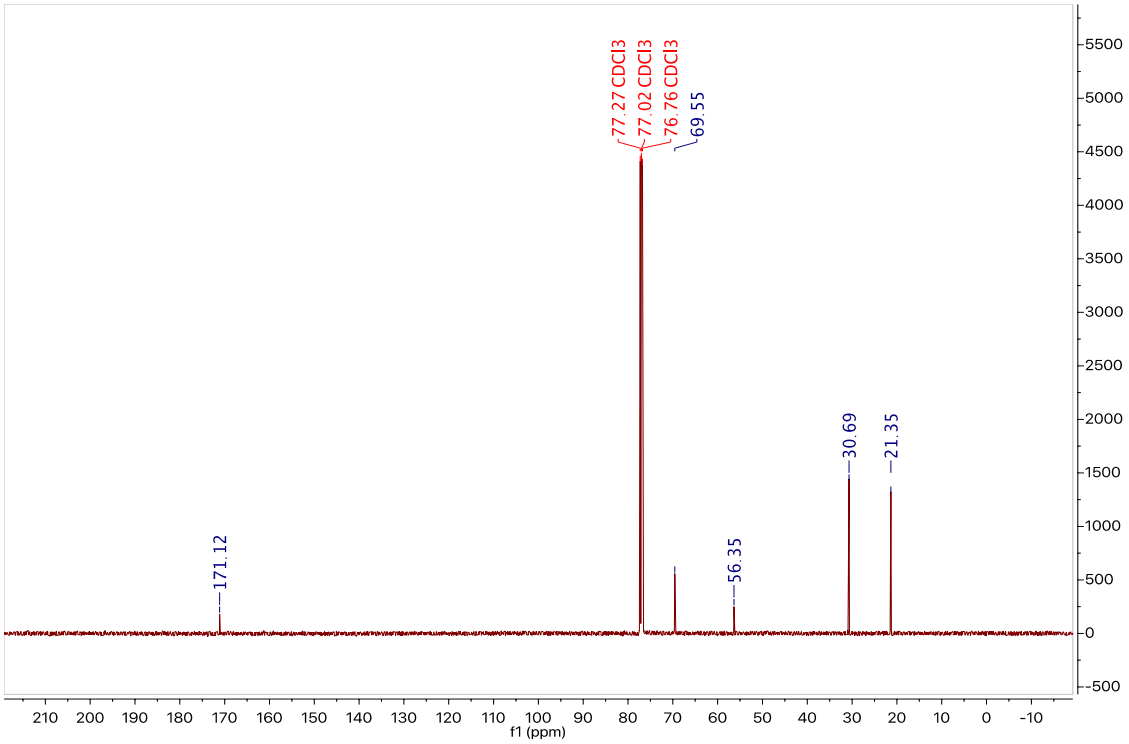

^{1}H and ^{13}C NMR data for 5.10b.

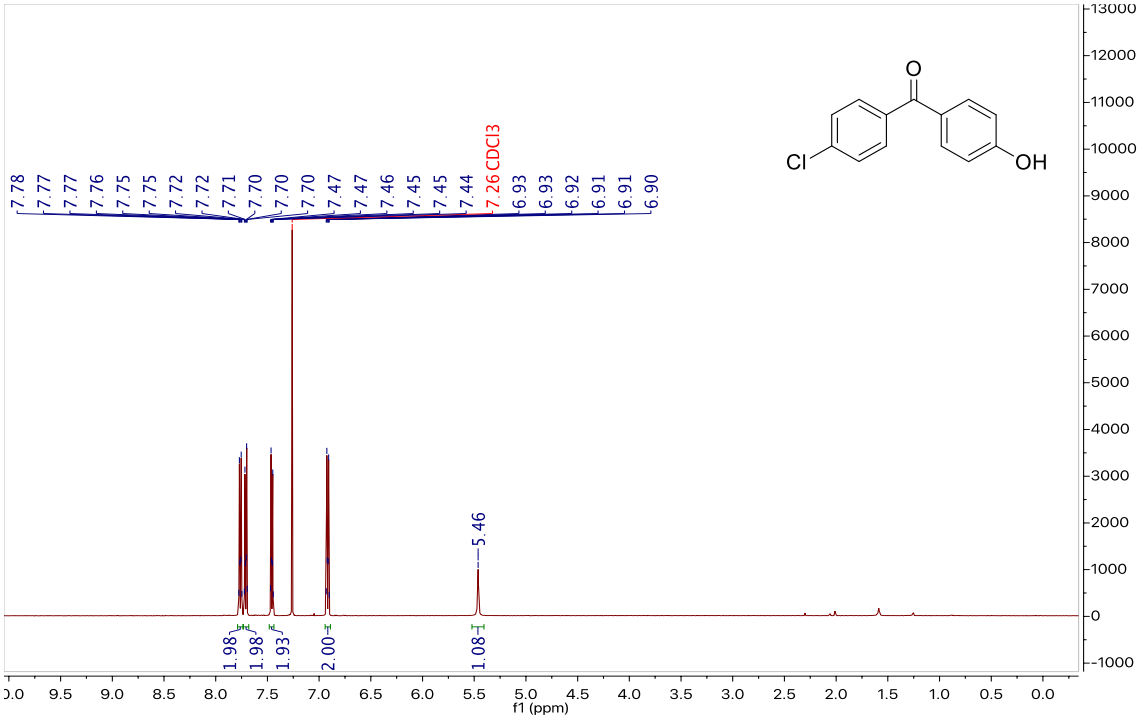

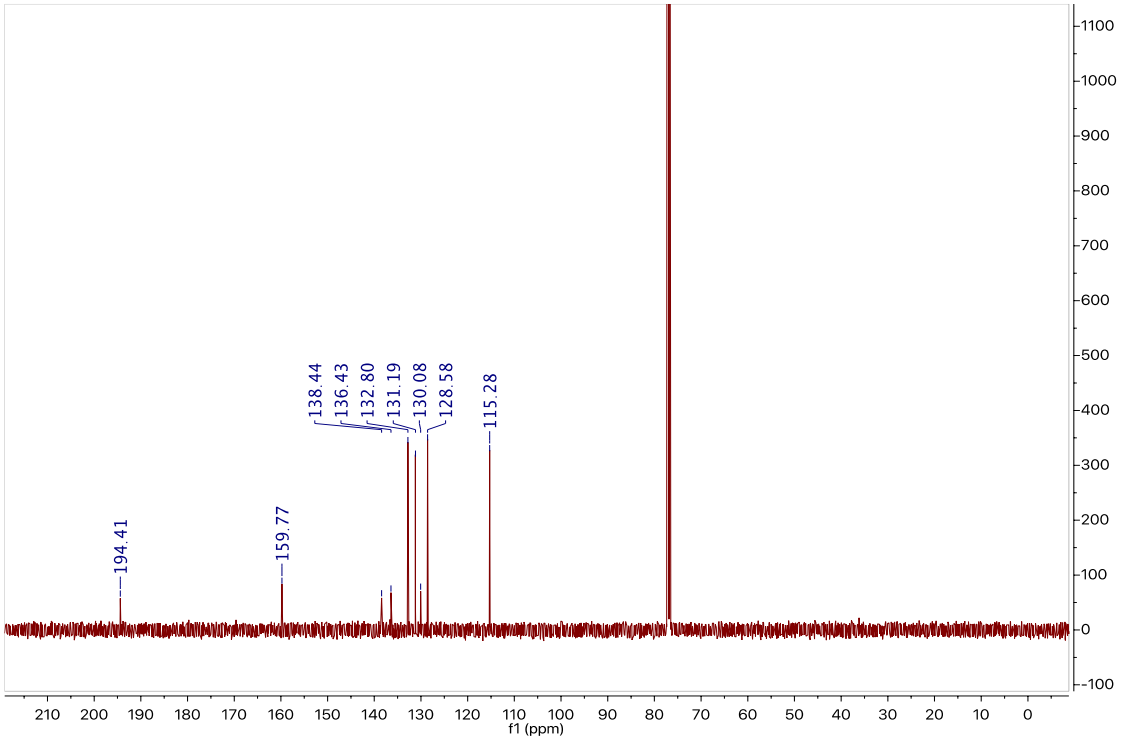

^{1}H and ^{13}C NMR data for 5.10c.

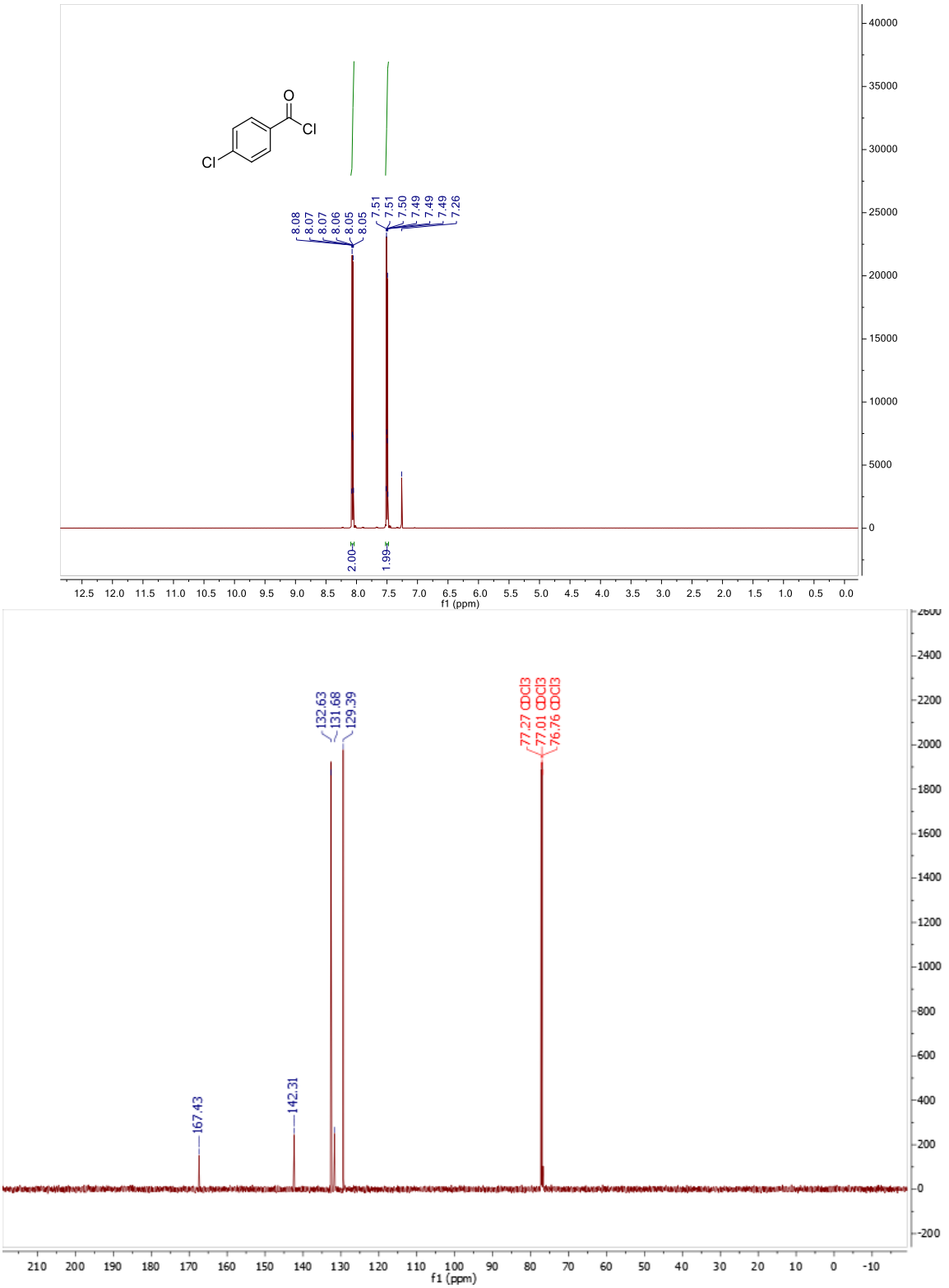

^{1}H and ^{13}C NMR data for fenofibrate, 5.10.

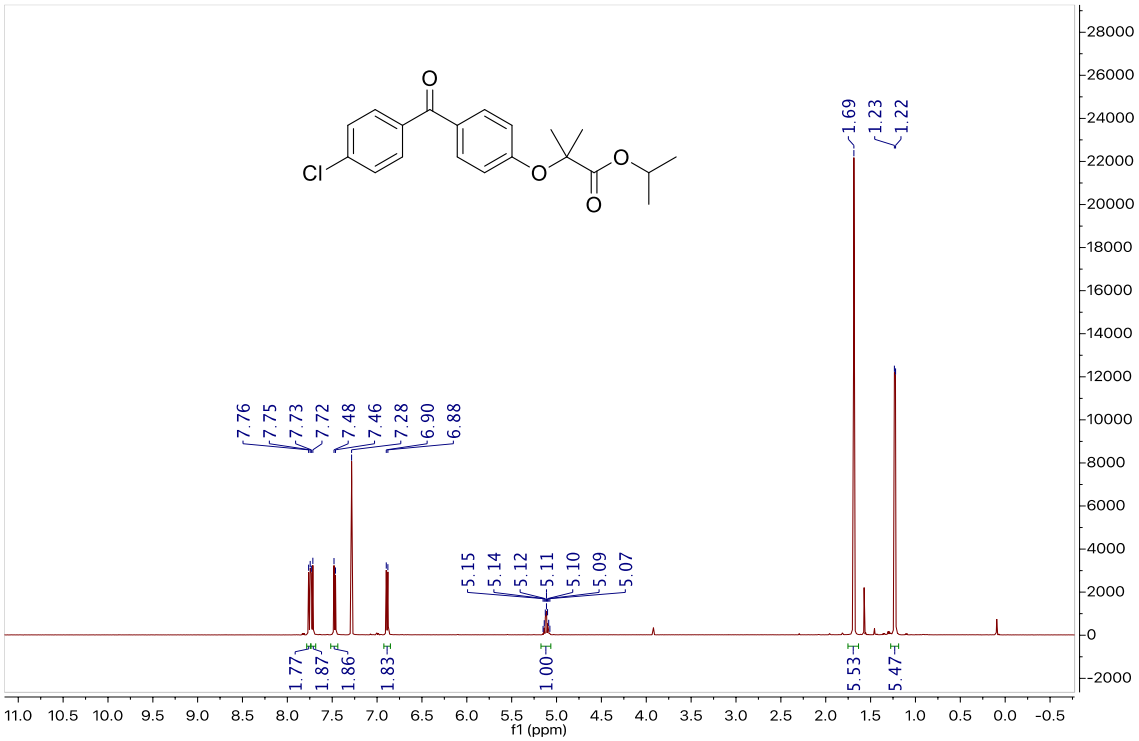

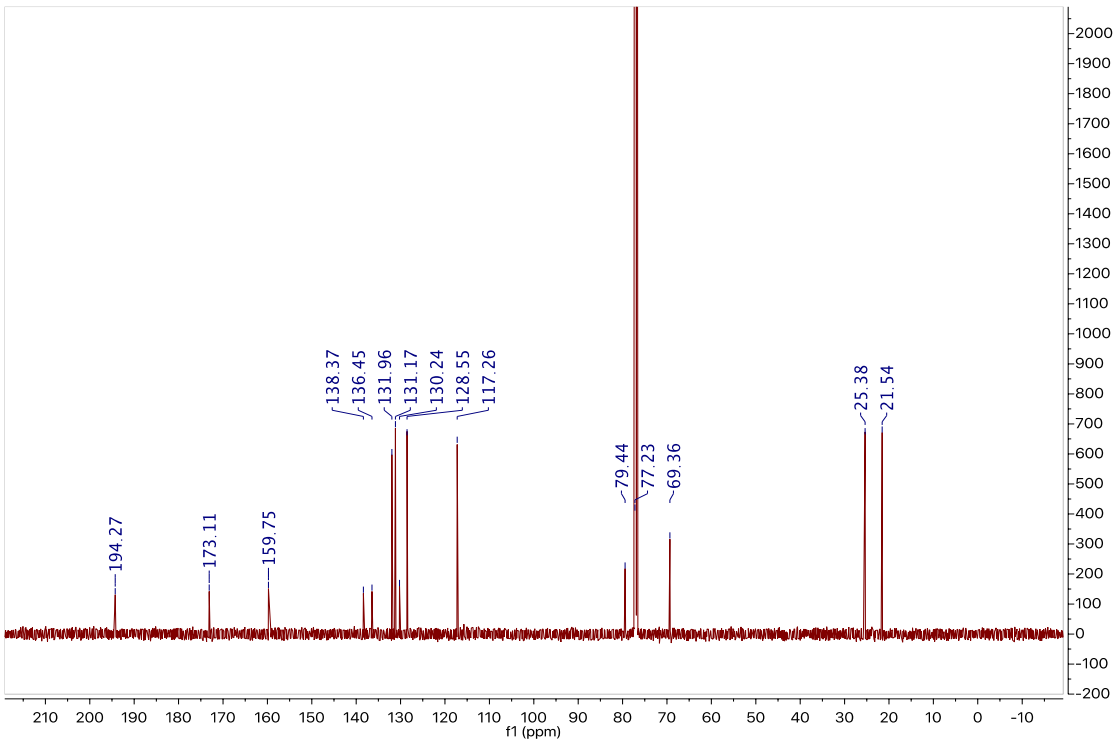

^{1}H and ^{13}C NMR data for 5.11.

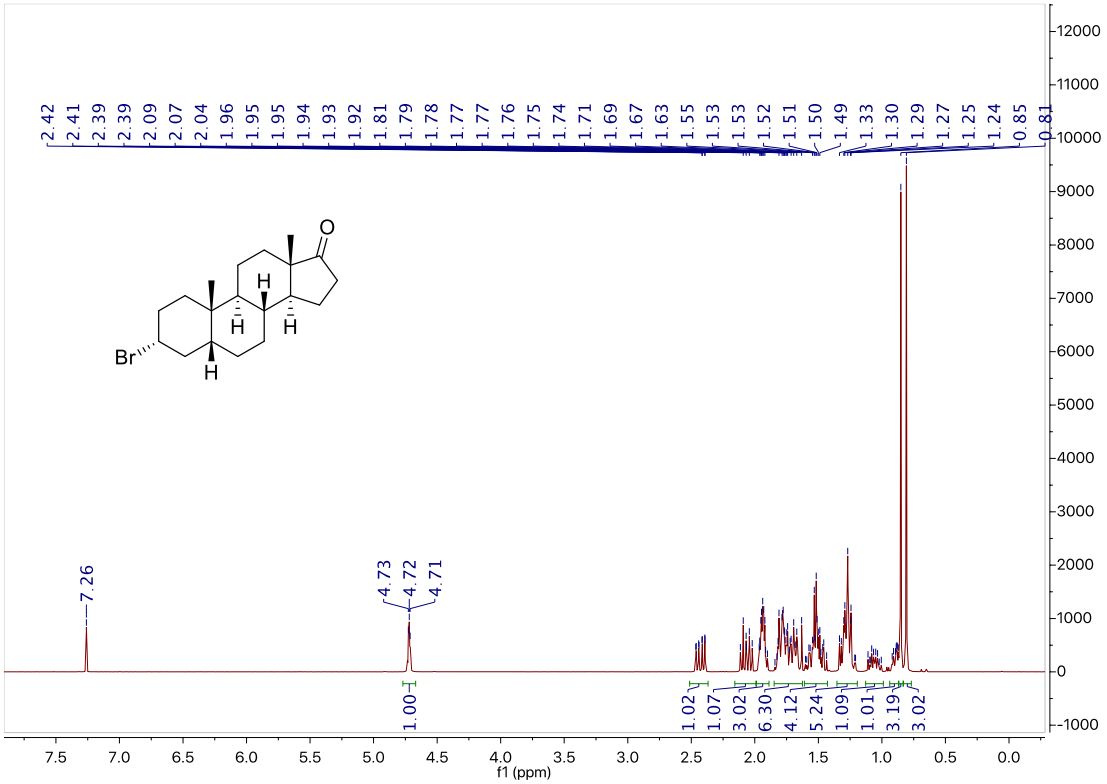

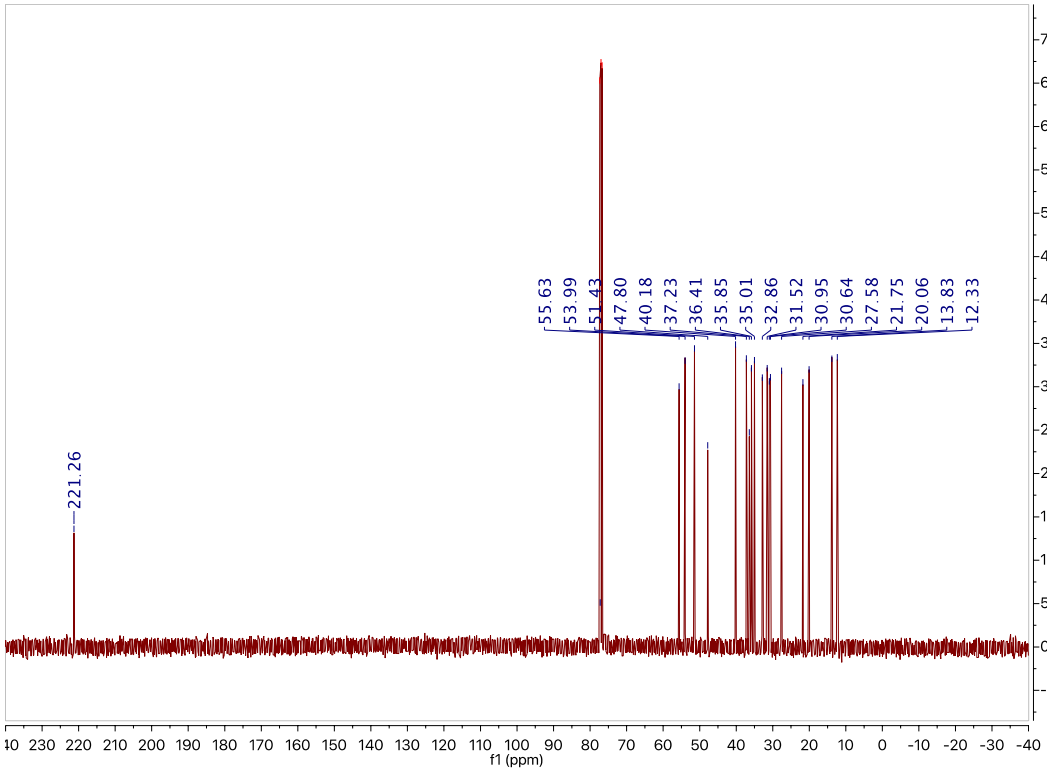

^{1}H and ^{13}C NMR data for 5.12.

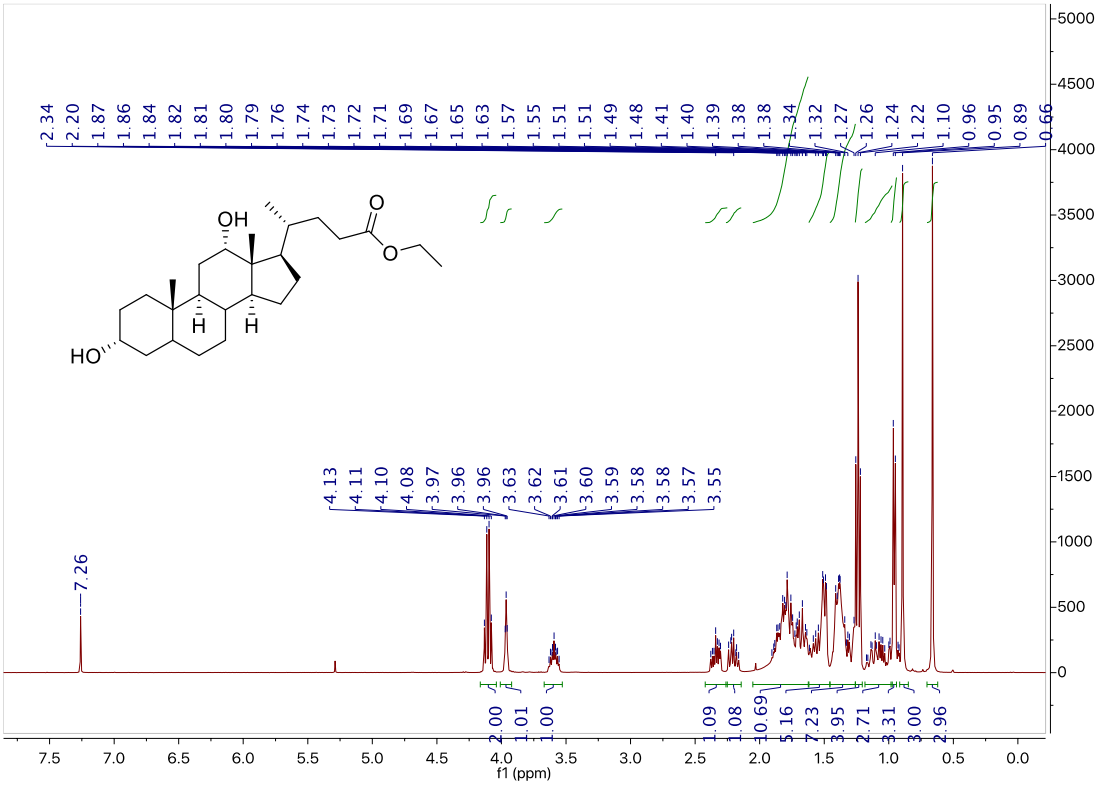

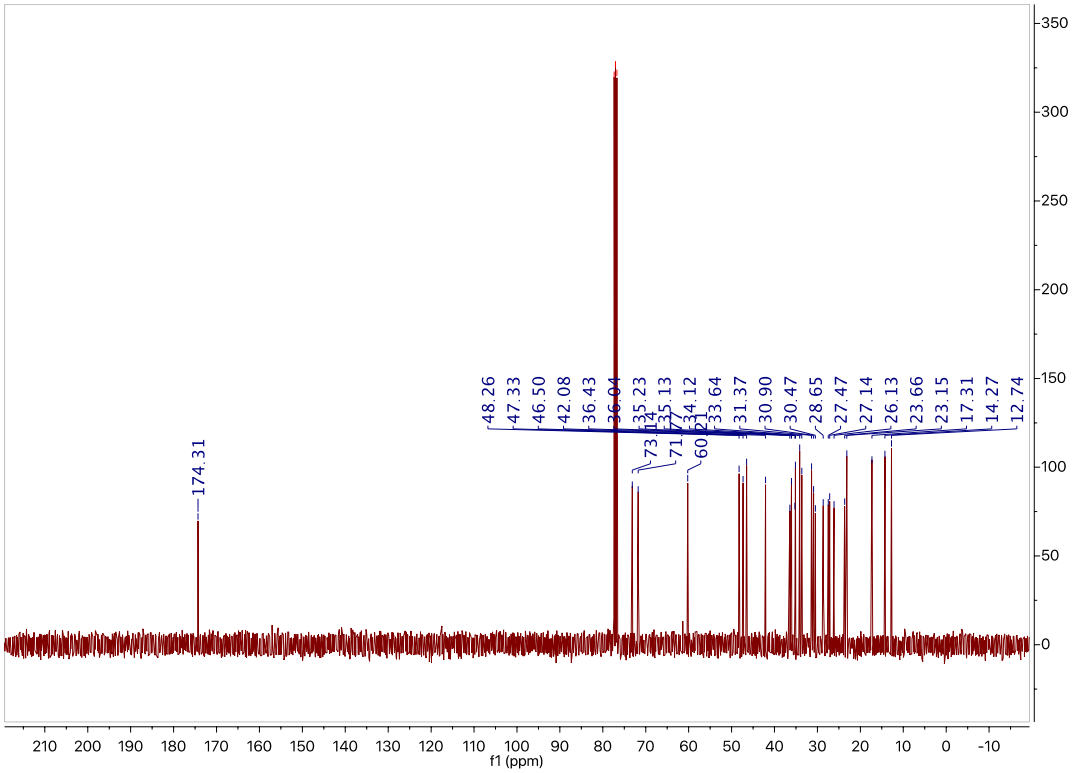

^{1}H and ^{13}C NMR data for 5.13.

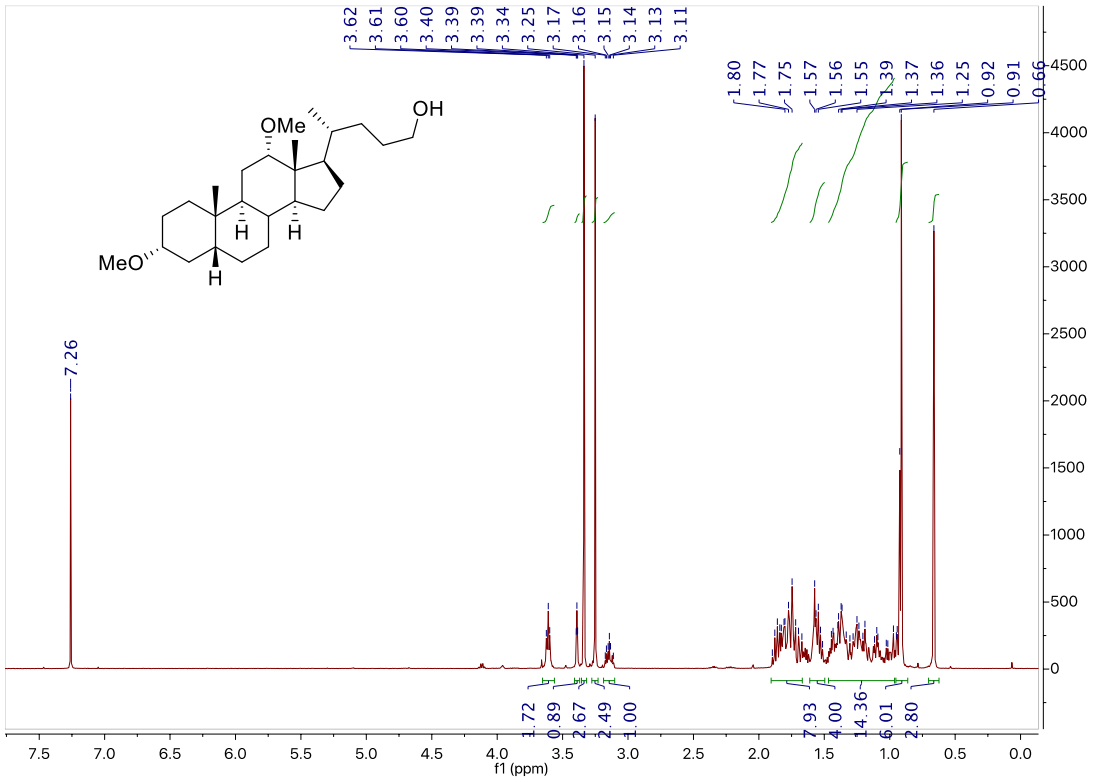

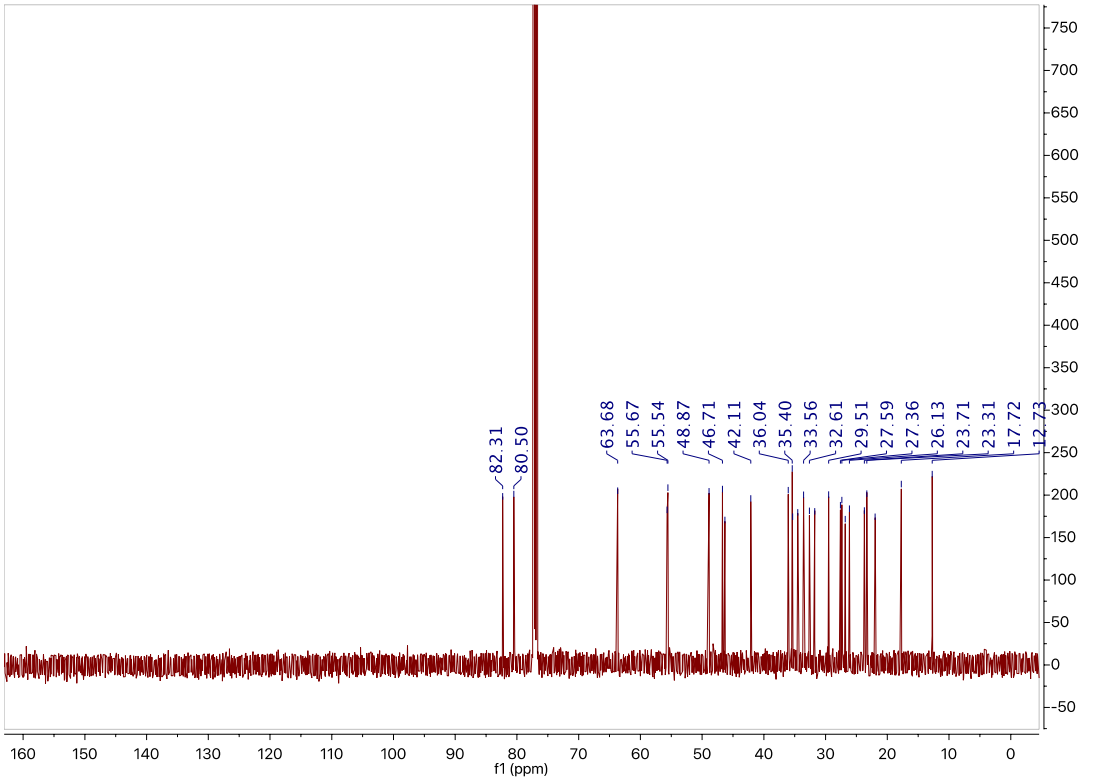

^{1}H and ^{13}C NMR data for 5.14.